



UNIVERSITAT DE  
BARCELONA

# Pushing peptides further: Novel methodologies for the synthesis of backbone-modified peptides

Ariadna Lobo Ruiz

**ADVERTIMENT.** La consulta d'aquesta tesi queda condicionada a l'acceptació de les següents condicions d'ús: La difusió d'aquesta tesi per mitjà del servei TDX ([www.tdx.cat](http://www.tdx.cat)) i a través del Dipòsit Digital de la UB ([diposit.ub.edu](http://diposit.ub.edu)) ha estat autoritzada pels titulars dels drets de propietat intel·lectual únicament per a usos privats emmarcats en activitats d'investigació i docència. No s'autoritza la seva reproducció amb finalitats de lucre ni la seva difusió i posada a disposició des d'un lloc aliè al servei TDX. No s'autoritza la presentació del seu contingut en una finestra o marc aliè a TDX (framing). Aquesta reserva de drets afecta tant al resum de presentació de la tesi com als seus continguts. En la utilització o cita de parts de la tesi és obligat indicar el nom de la persona autora.

**ADVERTENCIA.** La consulta de esta tesis queda condicionada a la aceptación de las siguientes condiciones de uso: La difusión de esta tesis por medio del servicio TDR ([www.tdx.cat](http://www.tdx.cat)) y a través del Repositorio Digital de la UB ([diposit.ub.edu](http://diposit.ub.edu)) ha sido autorizada por los titulares de los derechos de propiedad intelectual únicamente para usos privados enmarcados en actividades de investigación y docencia. No se autoriza su reproducción con finalidades de lucro ni su difusión y puesta a disposición desde un sitio ajeno al servicio TDR. No se autoriza la presentación de su contenido en una ventana o marco ajeno a TDR (framing). Esta reserva de derechos afecta tanto al resumen de presentación de la tesis como a sus contenidos. En la utilización o cita de partes de la tesis es obligado indicar el nombre de la persona autora.

**WARNING.** On having consulted this thesis you're accepting the following use conditions: Spreading this thesis by the TDX ([www.tdx.cat](http://www.tdx.cat)) service and by the UB Digital Repository ([diposit.ub.edu](http://diposit.ub.edu)) has been authorized by the titular of the intellectual property rights only for private uses placed in investigation and teaching activities. Reproduction with lucrative aims is not authorized neither its spreading and availability from a site foreign to the TDX service. Introducing its content in a window or frame foreign to the TDX service is not authorized (framing). This rights affect to the presentation summary of the thesis as well as to its contents. In the using or citation of parts of the thesis it's obliged to indicate the name of the author.



Tesi doctoral  
Programa de Doctorat en Química Orgànica

**Pushing peptides further: Novel methodologies for the  
synthesis of backbone-modified peptides**

**Ariadna Lobo Ruiz**

Dirigida i revisada per

**Dr. Judit Tulla Puche**

Universitat de Barcelona

Departament de Química Inorgànica i Orgànica  
Secció de Química Orgànica  
Universitat de Barcelona  
Març 2019



## AGRAÏMENTS

Encara recordo aquell estiu del 2012 en què vaig tenir el primer contacte amb el món de la recerca... Recordo les ganes i la il·lusió que tenia per donar el millor de mi mateixa, alhora que els nervis i la incertesa per si estaria a l'alçada. Gràcies Fernando per confiar en el meu potencial, per introduir-me en el món de la ciència i, sobretot, per estar sempre disposat a parlar amb mi i ajudar-me amb qualsevol cosa, ets un gran referent!

Des d'aleshores vaig tenir clar que volia fer la tesi. Així doncs, agraeixo a la Judit la confiança dipositada en mi i la oportunitat de fer-la. Aquests darrers anys han estat un gran aprenentatge en els quals m'he pogut desenvolupar com a científica. Als membres de la Comissió de Seguiment, en especial a la Miriam Royo i a l'Ernesto Nicolás, els volia agrair les bones idees i les converses científiques que m'han proporcionat durant aquests darrers anys, així com que hagin estat accessibles en qualsevol moment.

Aquests quatre anys no haguessin estat el mateix sense els grans companys (ara amics) del departament. Macarena, Cristina Cuscó, Marina, Javi, Alejandro, Stuart, Héctor, Roberto, Anna Rovira, Roser Segovia, Roser Tolrà... A tots vosaltres gràcies per fer les hores de dinar més amenes, per els berenars de "gordos", els sopars, les calçotades, etc. Sobretot gràcies per alegrar-me el dia a dia! Sou genials! No podia faltar un gran agraïment als membres del FUT, sense els quals no hagués estat possible realitzar aquesta tesi. Gràcies per el constant subministrament de dissolvents anhidres. A mi compañero de lab, Alexis gracias por introducirme en el departamento y por la ayuda y momentos compartidos.

Dins del departament, no ens oblidem dels estudiants de grau i màster que he tingut. En especial em dirigeixo a tu Pol, per ser tant dolç i per la amistat que m'emporto d'aquests mesos que vas estar al laboratori. Més que un estudiant, vas passar a ser un amic amb el que treballava! Espero continuar mantenint el contacte durant molt de temps! Janice, I loved your sweetness and your permanent smile! Mario grazie per tutti i momenti divertenti! Cristina i Laura, per estar sempre disposades a donar un cop de mà.

A la Laia i la Marta Pelay dir-vos que estic molt feliç que aquell estiu del 2012 entréssiu a la meva vida amb tanta força. Des d'aleshores sou un gran referent per mi (les meves germanetes grans!) Gràcies per els bons consells que em doneu sempre, la sinceritat, els moments divertits i especials que hem passat, els viatges, etc. Us estimo molt noies! A tu Anna-Iris dir-te que ets única i especial, alhora que una font de coneixement! Les teves converses són enriquidores! Judith tot i que estiguis lluny, continues estant present per parlar i compartir coses! Finalment dins la gent del PCB, dir-te Edgar, que m'alegro d'aquesta nova amistat que creix!

To my dear sweet polish friend... Magda thanks for all those shared experiences and for being such a good friend! Despite the distance, I am so happy that we grew so close and managed to meet every year. Love you! Isa, gracias por ser tan incondicional ese año en Glasgow, ¡me encantó compartir tantas experiencias contigo! Dani, que te voy a decir... que gracias por ser tan buen amigo, por estar siempre allí para hablar cuando te necesito aunque ahora vives en Manchester. Me encantan las eternas conversaciones filosóficas que tenemos. Yolán...Ay, ¡cómo me gustaría que fueras de BCN y no de Madrid! Gracias por los veranos tan maravillosos que hemos pasado desde pequeñas, por ser tan buena amiga, por los viajes, por estar en mi vida. ¡Te quiero! Al crack d'el Genís (o el "Bitxo"), dir-te que em fas riure moltíssim i que m'agradaria que aquesta amistat perdurés molts anys més!

A les coliflors, per compartir tants anys amb mi i per tots els plans i viatges! En especial a les Puxinel·lis Nàdia, Maria Campanyà i Roser... Gràcies per ser tant bones amigues i per la vostra alegria incondicional! Perquè, encara que ara algunes visquem a milers de kilòmetres, sé que aquesta amistat continuarà per sempre! Sou genials carallotes! Us estimo!

A tu Sally... Que hem compartit tantes coses des de petites i que t'estimo com si fossis la meva germana! Gràcies per estar sempre allà, per estimar-me incondicionalment, per aquesta amistat tant sincera i profunda! Recordo amb molta dolçor totes les hores dedicades a parlar infinitament, les coreografies i balls que fèiem de petites, així com les diverses tonteries que ens dedicàvem a fer! Em fa enormement feliç saber que sempre caminarem juntes i que estaràs present en totes les etapes de la meva vida! T'estimo molt!

A la Carla i el Ferran, els meus germans petitets (i ja no tant petitets), els volia donar les gràcies per acompanyar-me en les bones i en les dolentes, per les hores de jocs i converses infinites... Qui té un germà té un tresor!

A mis abuelos queridos, decirlos que os quiero más que a nada en este mundo. Todas las horas pasadas con vosotros han sido muy felices y me han curtido como persona. Muchas gracias por todo lo que habéis hecho y continuáis haciendo por mí, por estar siempre dispuestos a ayudarme en todo lo que necesite con una sonrisa de oreja a oreja y por ser un gran referente para mí. ¡Os quiero muchísimo!

A tu Omar, moltíssimes gràcies per haver aparegut a la meua vida, per donar-me tant amor i tant pur, per fer-ho tot més fàcil, en general per estar sempre allà! Gràcies per escoltar-me en qualsevol moment, especialment en els moments de crisi amb la tesi, i per proporcionar-me discussions científiques tant riques. Ets molt bon científic! Però sobretot ets una gran persona! T'estimo molt carinyo!

Finalment volia agrair als meus pares el seu suport incondicional, ja que sense ells no hagués estat possible arribar fins aquí. Estic molt agraïda per tot el que m'heu donat i em continueu donant. Gràcies per fer possible que hagi aconseguit tots els reptes que m'he proposat en aquesta vida. Us estimo molt!

## **CONTENTS**



## **ABOUT THE STRUCTURE OF THIS WORK**

### **ABBREVIATIONS AND ANNEXES**

|   |      |
|---|------|
| Annex I. Abbreviations and acronyms .....     | I    |
| Annex II. Natural amino acids.....            | IV   |
| Annex III. Non-proteogenic amino acids .....  | VI   |
| Annex IV. Protecting groups.....              | VIII |
| Annex V. Coupling reagents and additives..... | IX   |
| Annex VI. Polymeric supports.....             | I    |

### **INTRODUCTION ..... 1**

|                           |   |
|---------------------------|---|
| Introduction.....         | 3 |
| i. Depsipeptides.....     | 4 |
| ii. Stapled peptides..... | 5 |
| References .....          | 8 |

### **OBJECTIVES ..... 13**

|                  |    |
|------------------|----|
| Objectives ..... | 15 |
|------------------|----|

## **CHAPTER 1. DEVELOPMENT OF A ROBUST FMOC-BASED SOLID-PHASE**

### **METHODOLOGY FOR THE PREPARATION OF COMPLEX DEPSIPEPTIDES ..... 17**

|   |    |
|---|----|
| 1.1 Introduction.....   | 19 |
| 1.1.1 Biological importance of naturally-occurring depsipeptides .....              | 19 |
| 1.1.2 Chemical synthesis of depsipeptides .....                                     | 25 |
| 1.1.2.1 Synthetic approaches to prepare depsipeptides.....                          | 25 |
| 1.1.2.1.1 Total solution strategies.....  | 25 |
| 1.1.2.1.2 Full solid-phase strategies.....  | 26 |
| 1.1.2.1.3 Combined solid-phase and solution chemistry strategies.....               | 28 |
| 1.1.2.2 Ester bond formation methodologies .....                                    | 29 |
| 1.1.2.2.1 Steglich esterification.....  | 29 |
| 1.1.2.2.2 The Boc-AA <i>N</i> -hydroxysuccinimide ester bond formation method... 30 |    |
| 1.1.2.2.3 Mitsunobu esterification.....   | 31 |

|   |    |
|---|----|
| 1.1.2.2.4 Yamaguchi esterification.....   | 33 |
| 1.1.2.3 Hydroxyl functionalities protecting groups .....  | 34 |
| 1.1.2.4 Common drawbacks associated with depsipeptide synthesis .....   | 36 |
| 1.1.3 Naturally-occurring depsipeptide YM-254890: a synthetic challenge.....  | 37 |
| 1.2 Objectives of chapter 1.....  | 42 |
| 1.3 Results and discussion .....  | 43 |
| 1.3.1 Design of a model depsipeptide inspired by YM-254890 .....  | 43 |
| 1.3.2 Development of a fully solid-phase stepwise strategy .....  | 44 |
| 1.3.2.1 General synthetic considerations and retrosynthetic analysis .....  | 44 |
| 1.3.2.1.1 Ester moieties.....   | 45 |
| 1.3.2.1.2 DKP formation .....   | 46 |
| 1.3.2.1.3 Polymeric support .....   | 46 |
| 1.3.2.1.4 Macrolactamisation.....   | 47 |
| 1.3.2.1.5 Peptide chain elongation.....   | 47 |
| 1.3.2.1.6 Solid-phase reaction monitoring.....  | 48 |
| 1.3.2.1.7 Retrosynthetic analysis.....  | 48 |
| 1.3.2.2 Synthesis of the linear precursor of cyclodepsipeptide <b>1.1</b> : Ac-Thr(O(H <sub>2</sub> N-Thr(O(Ac-Thr(OH)-CO))-Fmoc- <i>N,O</i> -Me <sub>2</sub> Thr-CO))-COO-D-Pla-Pro-Ala- <i>N</i> -MeAla-COOH..... | 49 |
| 1.3.2.2.1 Peptide chain elongation .....  | 49 |
| 1.3.2.2.2 Study of the optimal Fmoc removal conditions to minimise DKP formation.....   | 50 |
| 1.3.2.2.3 Incorporation of the Ac-Thr-OH residue onto D-Pla-Pro-Ala- <i>N</i> -MeAla-CTC-resin ( <b>1.3</b> ) .....   | 52 |
| 1.3.2.2.3.1 Preparation of a series of R <sub>1</sub> -Thr( <sup>t</sup> Bu)-OH derivatives using different amine protecting groups.....  | 53 |
| 1.3.2.2.3.2 On-resin esterification using R <sub>1</sub> -Thr( <sup>t</sup> Bu)-OH derivatives with different amine protecting groups.....  | 55 |
| 1.3.2.2.3.3 Preparation of a series of Fmoc-Thr(R <sub>2</sub> )-OH derivatives using silyl protecting groups.....  | 59 |
| 1.3.2.2.3.4 On-resin esterification using Fmoc-Thr(R <sub>2</sub> )-OH derivatives containing silyl protecting groups.....  | 60 |

|   |    |
|---|----|
| 1.3.2.2.3.5 Fmoc and TBDMS removal studies of <b>Fmoc</b> -Thr( <b>TBDMS</b> )-COO-D-Pla-Pro-Ala- <i>N</i> -MeAla-CTC-resin ( <b>1.11</b> ) .....   | 61 |
| 1.3.2.2.3.6 Summary of the Ac-Thr-OH residue incorporation.....   | 64 |
| 1.3.2.2.4 Incorporation of the <i>N,O</i> -Me <sub>2</sub> Thr residue onto Ac-Thr(OH)-COO-D-Pla-Pro-Ala- <i>N</i> -MeAla-CTC-resin ( <b>1.14</b> ) and subsequent Boc-Thr-OH incorporation.....  | 65 |
| 1.3.2.2.4.1 Preparation of Alloc- <i>N,O</i> -Me <sub>2</sub> Thr-OH and Fmoc- <i>N,O</i> -Me <sub>2</sub> Thr-OH.....  | 66 |
| 1.3.2.2.4.2 On-resin esterification of Alloc- <i>N,O</i> -Me <sub>2</sub> Thr-OH ( <b>1.20</b> ) and Fmoc- <i>N,O</i> -Me <sub>2</sub> Thr-OH ( <b>1.24</b> ) and subsequent Boc-Thr-OH incorporation.....  | 69 |
| 1.3.2.2.4.3 Fmoc removal studies of Ac-Thr(O( <b>Fmoc</b> - <i>N,O</i> -Me <sub>2</sub> Thr-CO))-COO-D-Pla-Pro-Ala- <i>N</i> -MeAla-CTC-resin ( <b>1.26</b> ) .....   | 72 |
| 1.3.2.2.4.4 Summary of the <i>N,O</i> -Me <sub>2</sub> Thr-OH residue incorporation.....  | 75 |
| 1.3.2.2.5 Incorporation of the Ac-Thr( <sup>t</sup> Bu)-OH residue onto Ac-Thr(O(Boc-Thr(OH)-Fmoc- <i>N,O</i> -Me <sub>2</sub> Thr-CO))-COO-D-Pla-Pro-Ala- <i>N</i> -MeAla-CTC-resin ( <b>1.27</b> ).....   | 77 |
| 1.3.2.2.5.1 On-resin esterification of R <sub>1</sub> -Thr( <sup>t</sup> Bu)-OH .....   | 78 |
| 1.3.2.2.5.2 Fmoc removal studies of Ac-Thr(O(Boc-Thr(O( <b>Fmoc</b> -Thr( <sup>t</sup> Bu)-CO))-Fmoc- <i>N,O</i> -Me <sub>2</sub> Thr-CO))-COO-D-Pla-Pro-Ala- <i>N</i> -MeAla-CTC-resin ( <b>1.30</b> ).....  | 79 |
| 1.3.2.2.5.3 Summary of the Ac-Thr( <sup>t</sup> Bu)-OH incorporation .....  | 81 |
| 1.3.2.2.6 Final stepwise strategy to prepare the linear precursor of <b>1.1</b> : Synthesis of Ac-Thr(O(H <sub>2</sub> N-Thr(O(Ac-Thr(OH)-CO))-Fmoc- <i>N,O</i> -Me <sub>2</sub> Thr-CO))-COO-D-Pla-Pro-Ala- <i>N</i> -MeAla-COOH ( <b>1.32</b> ) ..... | 83 |
| 1.3.3 Efficiency of the stepwise synthetic strategy by comparison with segment condensation strategies .....  | 85 |
| 1.3.3.1 Development of a synthetic strategy containing one segment condensation.....  | 85 |
| 1.3.3.1.1 Initial synthetic approach.....   | 85 |

|  |   |            |
|--|---|------------|
| 1.3.3.1.1.1  | Preparation of dipeptide building block Ac-Thr(O(Alloc- <i>N,O</i> -Me <sub>2</sub> Thr-CO))-COOH (1.33).....   | 87         |
| 1.3.3.1.1.2  | Segment condensation of dipeptide Ac-Thr(O(Alloc- <i>N,O</i> -Me <sub>2</sub> Thr-CO))-COOH (1.33) .....  | 88         |
| 1.3.3.1.2  | Synthetic strategy containing one segment condensation:<br>Incorporation of the Ac-Thr(OH)-COO-D-Pla-COOH building block onto tripeptidyl-resin 1.2 ..... | 89         |
| 1.3.3.1.2.1  | Preparation of building block Ac-Thr(OH)-COO-D-Pla-COOH (1.37).....   | 89         |
| 1.3.3.1.2.2  | Segment condensation of dipeptide Ac-Thr(OH)-COO-D-Pla (1.37).....  | 90         |
| 1.3.3.1.2.3  | Synthetic strategy containing one segment condensation:<br>dipeptide chain elongation.....  | 91         |
| 1.3.3.2  | Development of a synthetic strategy containing two segment condensations.....   | 93         |
| 1.3.3.2.1  | Preparation of building block Boc-Thr(O(Ac-Thr( <sup>t</sup> Bu)-CO))-COOH (1.38).....  | 94         |
| 1.3.3.2.2  | Synthetic strategy containing two segment condensations:<br>dipeptide chain elongation.....   | 95         |
| 1.3.3.3  | Comparison of the three developed strategies.....   | 96         |
| 1.3.4  | Dipeptide macrolactamisation .....  | 97         |
| 1.3.5  | Overview of the Fmoc removal studies and selection of the appropriate protecting group scheme .....   | 99         |
| 1.3.5.1  | Overview of the Fmoc removal studies.....   | 99         |
| 1.3.5.2  | Overview of the appropriate protecting group scheme .....   | 102        |
| 1.5  | References .....  | 103        |
| <b>CHAPTER 2 . DEVELOPMENT OF A SYNTHETIC METHODOLOGY TO PREPARE HIGHLY <i>N</i>-METHYLATED STAPLED PEPTIDES .....</b> |   | <b>111</b> |
| 2.1  | Introduction.....   | 113        |
| 2.1.1  | Protein-Protein Interactions.....   | 113        |
| 2.1.2  | Protein mimicry: mimicking $\alpha$ -helix secondary structures .....   | 114        |

|   |     |
|---|-----|
| 2.1.2.1 Helix propensity of proteogenic amino acids.....  | 115 |
| 2.1.2.2 Insertion of $\alpha$ -amino acids with restricted conformation space.....                                  | 115 |
| 2.1.2.3 Electrostatic interactions to promote the $\alpha$ -helix conformation.....                                 | 116 |
| 2.1.2.4 Hydrophobic interactions to promote the $\alpha$ -helix conformation .....                                  | 117 |
| 2.1.2.5 Side-chain to side-chain cross-linking.....   | 117 |
| 2.1.2.5.1 $\alpha$ -Methylated hydrocarbon or all-hydrocarbon cross-linking .....                                   | 118 |
| 2.1.2.5.2 Thiol-based cross-linking.....  | 120 |
| 2.1.2.5.3 Lactam-based cross-linking .....  | 123 |
| 2.1.2.5.4 Triazole-based cross-linking .....  | 125 |
| 2.1.2.5.5 Other cross-linking approaches .....  | 127 |
| 2.1.2.5.6 Limitations of stapling techniques .....  | 127 |
| 2.1.2.5.7 Proposal of a novel stapling methodology.....   | 128 |
| 2.2 Objectives of chapter 2.....  | 131 |
| 2.3 Results and discussion .....  | 132 |
| 2.3.1 Development of a synthetic methodology to prepare highly <i>N</i> -methylated<br>stapled peptides (HMSP)..... | 132 |
| 2.3.1.1 General synthetic considerations .....  | 132 |
| 2.3.1.1.1 Low coupling rates and epimerisation .....  | 132 |
| 2.3.1.1.2 Deletion and over-incorporation of amino acids.....   | 133 |
| 2.3.1.1.3 DKP formation .....   | 133 |
| 2.3.1.1.4 Peptide fragmentation upon cleavage from the resin.....   | 134 |
| 2.3.1.2 General design of model HMSP .....  | 136 |
| 2.3.1.3 Preparation of a small library of Fmoc- <i>N</i> -MeAA .....  | 138 |
| 2.3.1.4 Lactam-based cross-linking approach .....   | 140 |
| 2.3.1.4.1 Chain elongation of a linear p53-based peptide.....   | 141 |
| 2.3.1.4.2 Evaluation of the best approach to insert <i>N</i> -methyl-rich peptide<br>linkers.....                   | 144 |
| 2.3.1.4.2.1 <i>Synthetic strategy A</i> : Stepwise incorporation of <i>N</i> -methylated<br>residues .....          | 144 |
| 2.3.1.4.2.2 <i>Synthetic strategy B</i> : On-resin Mitsunobu <i>N</i> -methylation of the<br>residues .....         | 146 |

|   |            |
|---|------------|
| 2.3.1.4.2.3 Evaluation of the best approach to insert <i>N</i> -methyl-rich peptide linkers ..... | 148        |
| 2.3.1.4.3 Scope of the lactam-based cross-link: macrolactamisation studies                        | 149        |
| 2.3.1.4.4 Cleavage and global deprotection of highly <i>N</i> -methylated peptide studies.....    | 154        |
| 2.3.1.5 Thioether-based cross-linking .....   | 161        |
| 2.3.1.5.1 Synthetic methodology development for single staples .....                              | 161        |
| 2.3.1.5.1.1 Preparation of “short “stapled peptides (i,i+4) .....                                 | 164        |
| 2.3.1.5.1.2 Preparation of “large “stapled peptides (i,i+7) .....                                 | 165        |
| 2.3.1.5.2 Synthetic methodology development for double staples .....                              | 168        |
| 2.3.1.5.2.1 Preparation of double stapled peptides (i,i+4 and i+8,i+12) ....                      | 171        |
| 2.3.2 Circular dichroism studies .....  | 174        |
| 2.3.2.1 CD studies of the HMSP library.....   | 174        |
| 2.4 References.....   | 182        |
| <b>CONCLUSIONS .....</b>  | <b>191</b> |
| Conclusions.....  | 193        |
| <b>EXPERIMENTAL SECTION .....</b>   | <b>199</b> |
| 3.1 Materials and methods .....   | 201        |
| 3.1.1 Solvents and reagents .....   | 201        |
| 3.1.1.1 Solvents.....   | 201        |
| 3.1.1.1.1 Anhydrous solvents.....   | 201        |
| 3.1.1.2 Reagents.....   | 201        |
| 3.1.2 Instrumentation .....   | 201        |
| 3.1.2.1 General basic instrumentation .....   | 201        |
| 3.1.2.2 Chromatography.....   | 202        |
| 3.1.2.2.1 Thin layer chromatography (TLC).....  | 202        |
| 3.1.2.2.2 Column chromatography on silica gel.....  | 202        |
| 3.1.2.2.3 High performance liquid chromatography (HPLC) .....                                     | 202        |
| 3.1.2.2.3.1 Analytical HPLC.....  | 202        |
| 3.1.2.2.3.2 Semi-analytical HPLC.....   | 203        |

|  |     |
|--|-----|
| 3.1.2.2.3.3 HPLC-MS .....  | 203 |
| 3.1.2.3 MALDI-TOF .....  | 204 |
| 3.1.2.4 Nuclear Magnetic Resonance (NMR) .....                             | 204 |
| 3.1.2.5 Circular dichroism spectroscopy .....                              | 204 |
| 3.1.3 Solid-Phase Peptide Synthesis (SPPS).....                            | 204 |
| 3.1.3.1 General considerations .....                                       | 204 |
| 3.1.3.2 Colorimetric test .....  | 205 |
| 3.1.3.2.1 Kaiser test.....   | 205 |
| 3.1.3.2.2 Chloranil test .....   | 205 |
| 3.1.3.3 Conditioning of the resin and first amino acid incorporation ..... | 206 |
| 3.1.3.3.1 Rink Amide Aminomethyl resin (Rink Amide AM) .....               | 206 |
| 3.1.3.3.2 2-Chlorotrityl chloride resin (2-CTC) .....                      | 206 |
| 3.1.3.3.2.1 Fmoc quantification and real loading determination.....        | 207 |
| 3.1.3.4 Cleavage from the resin and global deprotection protocols.....     | 207 |
| 3.1.3.4.1 Rink Amide Aminomethyl resin .....                               | 208 |
| 3.1.3.4.2 2-Chlorotrityl chloride resin .....                              | 208 |
| 3.1.3.4.3 Peptide “mini-cleavage” to monitor reaction conversion .....     | 209 |
| 3.1.4 Peptide purification .....   | 209 |
| 3.1.4.1 Semi-analytical reversed-phase equipment .....                     | 209 |
| 3.1.4.2 Porapak™ Rxn Cartridges .....                                      | 210 |
| 3.1.5 Peptide characterisation .....                                       | 210 |
| 3.2 Chapter 1.....   | 211 |
| 3.2.1 General protocols.....   | 211 |
| 3.2.1.1 Solid-phase synthesis protocols .....                              | 211 |
| 3.2.1.1.1 Peptide coupling protocols .....                                 | 211 |
| 3.2.1.1.2 On-resin Steglich esterification .....                           | 212 |
| 3.2.2 Preparation of the building blocks .....                             | 212 |
| 3.2.2.1 Synthesis of <b>1.5</b> .....                                      | 212 |
| 3.2.2.2 Synthesis of <b>1.6</b> .....                                      | 214 |
| 3.2.2.3 Synthesis of <b>1.9</b> .....                                      | 215 |
| 3.2.2.4 Synthesis of <b>1.10</b> .....                                     | 216 |

|  |     |
|--|-----|
| 3.2.2.5 Synthesis of <b>1.20</b> .....   | 217 |
| 3.2.2.6 Synthesis of <b>1.24</b> .....   | 219 |
| 3.2.2.7 Synthesis of <b>1.33</b> .....   | 221 |
| 3.2.2.8 Synthesis of <b>1.37</b> .....   | 223 |
| 3.2.2.9 Synthesis of <b>1.38</b> .....   | 224 |
| 3.2.3 Study of the optimal Fmoc removal conditions to minimise DKP formation   | 227 |
| 3.2.4 Ester bond formation studies by evaluation of the amino acid optimal<br>protecting group scheme .....                              | 234 |
| 3.2.5 Fmoc removal studies after formation of the three ester linkages .....   | 229 |
| 3.2.6 Assembly of linear depsipeptide <b>1.32</b> .....  | 242 |
| 3.2.6.1 Synthesis of <b>1.32</b> using a fully stepwise strategy .....   | 242 |
| 3.2.6.2 Synthesis of <b>1.32</b> using a synthetic strategy containing one depsipeptide<br>building block segment condensation.....      | 244 |
| 3.2.6.3 Synthesis of <b>1.32</b> by using a synthetic strategy containing two depsipeptide<br>building block segment condensations ..... | 246 |
| 3.2.6.4 <b>1.32</b> characterisation .....   | 248 |
| 3.2.7 Macrolactamisation of <b>1.32</b> to obtain cyclic depsipeptide <b>1.1</b> .....   | 249 |
| 3.2.7.1 Cyclisation of <b>1.32</b> .....   | 249 |
| 3.2.7.2 <b>1.1</b> characterisation .....  | 250 |
| 3.3 Chapter 2.....   | 251 |
| 3.3.1 General protocols.....   | 251 |
| 3.3.1.1 Solid-phase synthesis protocols .....  | 251 |
| 3.3.1.1.1 Peptide coupling protocols .....   | 251 |
| 3.3.1.1.2 Bromoacetic acid coupling protocol .....   | 252 |
| 3.3.1.1.3 Fmoc removal protocol .....  | 252 |
| 3.3.1.1.4 Dde removal protocol .....   | 252 |
| 3.3.1.1.5 Allyl and Alloc removal protocols.....   | 252 |
| 3.3.1.1.6 Mmt removal protocol .....   | 253 |
| 3.3.1.1.7 Acetylation protocols .....  | 253 |
| 3.3.1.1.8 Three-step Mitsunobu <i>N</i> -methylation protocol .....  | 253 |
| 3.3.1.1.9 Alloc protection protocol .....  | 254 |
| 3.3.1.1.10 Cyclisation through thioether cross-linking .....   | 254 |

|  |     |
|--|-----|
| 3.3.1.2 Solution phase synthesis protocols .....   | 255 |
| 3.3.1.2.1 Peptide cyclisation in solution through thioether cross-linking .....            | 255 |
| 3.3.2 Preparation of Fmoc- <i>N</i> -Me-amino acids.....                                   | 255 |
| 3.3.3 Chain elongation of a p53-based linear peptide.....                                  | 258 |
| 3.3.4 Evaluation of the best approach to insert the <i>N</i> -methyl-rich peptide linker   | 259 |
| 3.3.5 Scope of the lactam-based cross-link: Macrolactamisation studies.....                | 261 |
| 3.3.6 Cleavage and global deprotection of highly <i>N</i> -methylated peptides studies     | 263 |
| 3.3.7 Preparation of the peptide library .....   | 270 |
| 3.3.7.1 Preparation of single “short” HMSP (i,i+4) with the unblocked C-terminus.....      | 270 |
| 3.3.7.2 Preparation of single “large” HMSP (i,i+7) with the unblocked C-terminus.....      | 274 |
| 3.3.7.3 Preparation of single “large” HMSP (i,i+7) with the amidated C-terminus.....       | 279 |
| 3.3.7.4 Preparation of double HMSP (i,i+4, and i+8,i+12) with the amidated C-terminus..... | 289 |
| 3.3.7.5 Preparation of single HMSP (i,i+4) with the amidated C-terminus.....               | 294 |
| 3.3.7.6 Preparation of linear p53-based peptides .....                                     | 297 |



## ABOUT THE STRUCTURE OF THIS WORK

This work is divided into five sections.

The first section encloses a very brief introduction and general objectives of the present thesis, which mainly comprises two subjects: depsipeptides and stapled peptides

The second and third sections describe the *development of a robust Fmoc-based solid-phase strategy for the preparation of complex depsipeptides and a novel methodology to prepare highly N-methylated stapled peptides*, respectively. Both sections enclose: a comprehensive introduction on the subject, a results and discussion section, and the corresponding reference collection.

The fourth part comprises the conclusions reached during the intercourse of the work presented herein. The fifth part is the experimental section and contains all the necessary information to reproduce the experiments as well as the corresponding product characterisation.

For clarity, when showing relevant HPLC spectra to the discussion of the obtained results, the acronym "G20100t9T25" was used to describe the HPLC experiment conditions. "G20100t9T25" stands for "Linear HPLC gradient from 20%B to 100%B over 9 min at 25 °C, using as elution system A: 0.045%TFA in H<sub>2</sub>O and B: 0.036%TFA in ACN. In the third section, the acronym "HMSP", which stands for "Highly N-methylated stapled peptides", was used throughout the chapter to ease the writing and reading process.



## **ABBREVIATIONS AND ANNEXES**



**Annex I. Abbreviations and acronyms****A**

|       |                        |
|-------|------------------------|
| AA    | Amino acid             |
| Abs   | Absorbance             |
| Ac    | Acetyl                 |
| ACN   | Acetonitrile           |
| AcOH  | Acetic acid            |
| ADP   | Adenosine diphosphate  |
| Alloc | Allyloxycarbonyl       |
| AM    | Amino methyl           |
| aq    | Aqueous                |
| ATP   | Adenosine triphosphate |

**B**

|     |                               |
|-----|-------------------------------|
| Boc | <i>tert</i> -Butyloxycarbonyl |
| Bs  | broad signal                  |

**C**

|       |   |
|-------|---|
| CD    | Circular dichroism                          |
| COSY  | Correlation Spectroscopy                    |
| 2-CTC | 2-Chlorotriyl chloride resin                |
| CuAAc | Copper-catalysed azide-alkyne cycloaddition |

**D**

|          |  |
|----------|--|
| $\delta$ | Chemical shift                                       |
| d        | Doublet  |
| DBU      | 1,8-Diazabicyclo[5.4.0]undec-7-ene                   |
| DCC      | <i>N,N'</i> -Dicyclohexylcarbodiimide                |
| DCM      | Dichloromethane                                      |
| Dde      | 1-(4,4-Dimethyl-2,6-dioxocyclohex-1-ylidene)-3-ethyl |
| DEAD     | Diethyl azodicarboxylate                             |
| DIAD     | Diisopropyl azodicarboxylate                         |
| DIC      | <i>N,N'</i> -Diisopropylcarbodiimide                 |
| DIEA     | <i>N,N'</i> -Diisopropylethylamine                   |
| DKP      | Diketopiperazine                                     |
| DMAP     | 4-Dimethylaminopyridine                              |
| DMF      | Dimethylformamide                                    |
| DMSO     | Dimethyl sulfoxide                                   |

**E**

|                   |   |
|-------------------|---|
| EDC               | 1-Ethyl-3-(3-dimethylaminopropyl)carbodiimide |
| EDT               | 1,2-Ethanedithiol                             |
| eq                | Equivalents                                   |
| ESI               | Electrospray ionization mass spectrometry     |
| Et <sub>2</sub> N | Diethylamine                                  |

|                   |  |
|-------------------|--|
| Et <sub>3</sub> N | Triethylamine  |
| EtOAc             | Ethyl acetate  |
| EtOH              | Ethanol  |
| Et <sub>2</sub> O | Diethyl ether  |
| <b>F</b>          |  |
| Fmoc              | Fluorenylmethyloxycarbonyl   |
| <b>G</b>          |  |
| G20100t9T25       | Linear HPLC gradient from 20%B to 100%B over 9 min at 25 °C, using as elution system A: 0.045%TFA in H <sub>2</sub> O and B: 0.036%TFA in ACN                  |
| <b>H</b>          |  |
| HATU              | <i>N</i> -[(Dimethylamino)-1 <i>H</i> -1,2,3-triazolo[4,5- <i>b</i> ]pyridin-1-yl-methylene)- <i>N</i> -methylmethanaminiumhexafluorophosphate <i>N</i> -oxide |
| HFA               | Hexafluoroacetone  |
| HFIP              | Hexafluoro-2-propanol  |
| HMBC              | Heteronuclear multiple-bond correlation spectroscopy   |
| HMSP              | Highly <i>N</i> -methylated stapled peptides   |
| HMQC              | Heteronuclear multiple-quantum correlation   |
| HOAt              | 1-Hydroxy-7-azabenzotriazole   |
| HOBt              | Hydroxybenzotriazole   |
| HPLC-PDA          | High-performance liquid chromatography-photo diode array   |
| HPLC-MS           | High-performance liquid chromatography-mass spectrometry   |
| HRMS              | High-resolution mass spectrometry  |
| HSQC              | Heteronuclear single quantum coherence   |
| Hz                | Hertz  |
| <b>J</b>          |  |
| J                 | Coupling constant  |
| <b>M</b>          |  |
| m                 | Multiplet  |
| MALDI             | Matrix-assisted laser desorption/ionization  |
| MeOH              | Methanol   |
| Mmt               | Monomethoxytrityl  |
| MS                | Mass spectrometry  |
| MW                | Molecular weight   |
| <b>N</b>          |  |
| NMR               | Nuclear magnetic resonance   |
| NOESY             | Nuclear overhauser enhancement spectroscopy  |
| <b>O</b>          |  |
| <i>o</i> -NBS     | <i>o</i> -Nitrobenzenesulfonyl   |

**P**

|                  |   |
|------------------|---|
| PBS              | Phosphate buffered saline   |
| PG               | Protecting group  |
| PPh <sub>3</sub> | Triphenylphosphine  |
| ppm              | Parts per million   |
| PPIs             | Protein-Protein Interactions  |
| <i>p</i> -TsOH   | <i>p</i> -Toluenesulfonic acid                                      |
| PyBOP            | (Benzotriazol-1-yloxy)tripyrrolidinophosphonium hexafluorophosphate |
| PyBrop           | Bromotripyrrolidinophosphonium hexafluorophosphate                  |

**Q**

|    |                    |
|----|--------------------|
| q  | Quartet            |
| qt | Quintuplet/Quintet |

**R**

|       |  |
|-------|--|
| RCM   | Ring-closing metathesis                    |
| RM    | Reaction mixture                           |
| ROESY | Rotational nuclear overhauser spectroscopy |

**S**

|      |   |
|------|---|
| s    | Singlet                                 |
| SARs | Structure-activity relationship studies |
| SM   | Starting material                       |
| SPPS | Solid-phase peptide synthesis           |

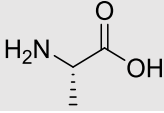
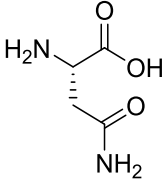
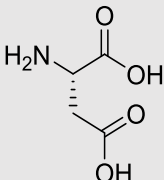
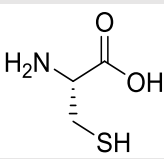
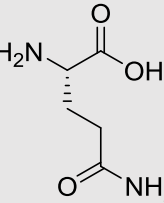
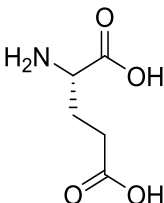
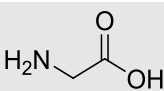
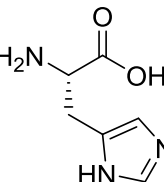
**T**

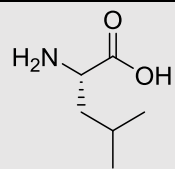
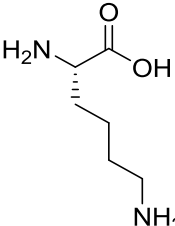
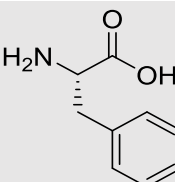
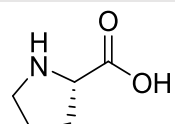
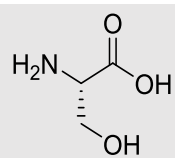
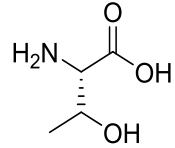
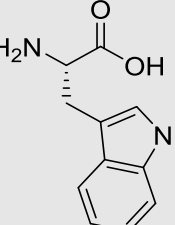
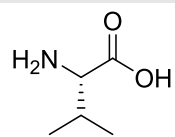
|                 |                                 |
|-----------------|---------------------------------|
| t               | triplet                         |
| TBAF            | Tetrabutylammonium fluoride     |
| TBDMS           | <i>tert</i> -Butyldimethylsilyl |
| TBDPS           | <i>tert</i> -Butyldiphenylsilyl |
| <sup>t</sup> Bu | <i>tert</i> -Butyl              |
| TFA             | Trifluoroacetic acid            |
| TFE             | Trifluoroethanol                |
| THF             | Tetrahydrofuran                 |
| THP             | Tetrahydropyranyl               |
| TIS             | Triisopropylsilane              |
| TLC             | Thin layer chromatography       |
| TOCSY           | Total correlated spectroscopy   |
| t <sub>R</sub>  | Retention time                  |
| Trt             | Trityl                          |

**U**

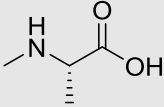
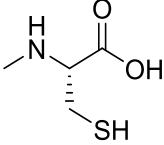
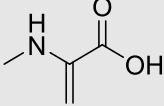
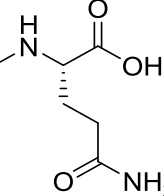
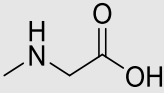
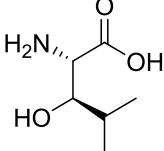
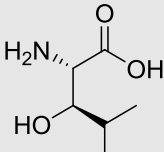
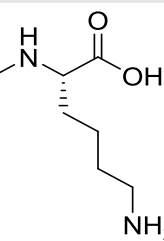
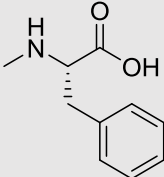
|    |             |
|----|-------------|
| UV | Ultraviolet |
|----|-------------|

## Annex II. Natural amino acids

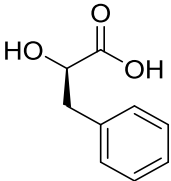
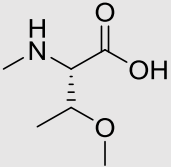
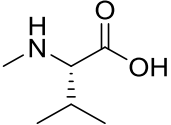
| Amino acid      | Code   | Structure   |
|-----------------|--------|---|
| L-Alanine       | Ala, A |    |
| L-Asparagine    | Asn, N |    |
| L-Aspartic acid | Asp, D |   |
| L-Cysteine      | Cys, C |  |
| L-Glutamine     | Gln, Q |  |
| L-Glutamic acid | Glu, E |  |
| L-Glycine       | Gly, G |  |
| L-Histidine     | His, H |  |

|                        |               |   |
|------------------------|---------------|---|
| <b>L-Leucine</b>       | <b>Leu, L</b> |    |
| <b>L-Lysine</b>        | <b>Lys, K</b> |    |
| <b>L-Phenylalanine</b> | <b>Phe, F</b> |    |
| <b>L-Proline</b>       | <b>Pro, P</b> |    |
| <b>L-Serine</b>        | <b>Ser, S</b> |   |
| <b>L-Threonine</b>     | <b>Thr, T</b> |  |
| <b>L-Tryptophan</b>    | <b>Trp, W</b> |  |
| <b>L-Valine</b>        | <b>Val, V</b> |  |

## Annex III. Non-proteogenic amino acids

| Amino acid            | Code    | Structure   |
|-----------------------|---------|---|
| L-N-Me-Alanine        | N-MeAla |    |
| L-N-Me-Cysteine       | N-MeCys |    |
| L-N-Me-Dehydroalanine | N-MeDha |    |
| L-N-Me-Glutamine      | N-MeGln |   |
| L-N-Me-Glycine        | N-MeGly |  |
| L-β-Hydroxyleucine    | β-HyLeu |  |
| L-N-Me-Leucine        | N-MeLeu |  |
| L-N-Me-Lysine         | N-MeLys |  |
| L-N-Me-Phenylalanine  | N-MePhe |  |

---

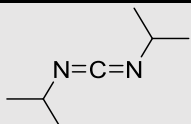
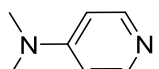
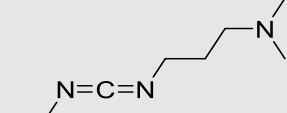
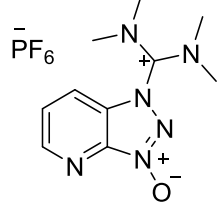
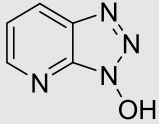
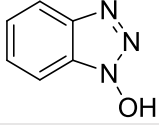
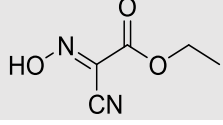
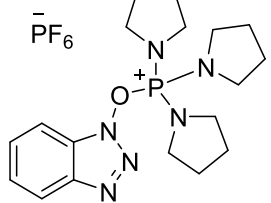
|                                       |                              |   |
|---------------------------------------|------------------------------|---|
| <b>D-Phenyllactic acid</b>            | <b>D-Pla</b>                 |  |
| <b>L-N,O-Me<sub>2</sub>-Threonine</b> | <b>N,O-Me<sub>2</sub>Thr</b> |  |
| <b>L-N-Me-Valine</b>                  | <b>N-MeVal</b>               |  |

---

## Annex IV. Protecting groups

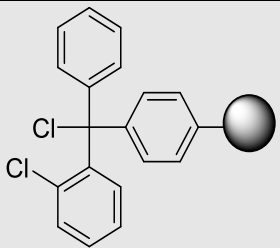
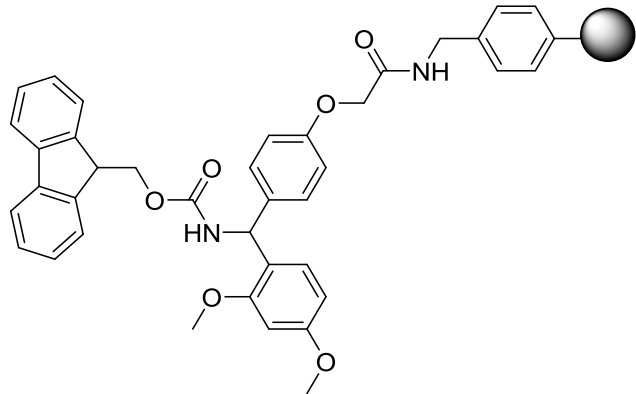
| Protecting group                                     | Symbol          | Structure |
|--|-----------------|-----------|
| Allyloxycarbonyl                                     | Alloc           |           |
| Allyl  | Allyl           |           |
| <i>tert</i> -Butyloxycarbonyl                        | Boc             |           |
| 1-(4,4-Dimethyl-2,6-dioxocyclohex-1-ylidene)-3-ethyl | Dde             |           |
| Fluorenylmethyloxycarbonyl                           | Fmoc            |           |
| Monomethoxytrityl                                    | Mmt             |           |
| <i>tert</i> -Butyldimethylsilyl                      | TBDMS           |           |
| <i>o</i> -Nitrobenzenesulfonyl                       | <i>o</i> -NBS   |           |
| <i>tert</i> -Butyl                                   | <sup>t</sup> Bu |           |
| Trityl   | Trt             |           |

## Annex V. Coupling reagents and additives

| Coupling reagent/additive   | Symbol    | Structure   |
|---|-----------|---|
| <i>N,N'</i> -Diisopropylcarbodiimide  | DIC       |    |
| 4-Dimethylaminopyridine   | DMAP      |    |
| 1-Ethyl-3-(3-dimethylaminopropyl)carbodiimide   | EDC       |    |
| <i>N</i> -[(Dimethylamino)-1 <i>H</i> -1,2,3-triazolo-[4,5- <i>b</i> ]-pyridin-1-yl-methylene)- <i>N</i> -methylmethanaminium hexafluorophosphate <i>N</i> -oxide | HATU      |   |
| 1-Hydroxy-7-azabenzotriazole  | HOAt      |  |
| 1-Hydroxybenzotriazole  | HOBt      |  |
| Ethyl(hydroxyimino)cynoacetate  | OxymaPure |  |
| (Benzotriazol-1-yloxy)tripyrrolidinophosphonium hexafluorophosphate   | PyBOP     |  |

## Annex VI. Polymeric supports

---

| Polymeric support                 | Symbol  | Structure   |
|-----------------------------------|---------|---|
| 2-Chlorotrityl chloride resin     | 2-CTC   |   |
| Fmoc-Rink Amide Aminomethyl resin | Rink AM |  |

---

## **INTRODUCTION**



## Introduction

Peptides and proteins are essential substances for living organisms, as they can be found in every cell and tissue and are involved in many biological and physiological processes.<sup>[1,2]</sup> Generally, peptides are selective and efficacious molecules that function as cell membrane transporters, hormones, enzyme inhibitors, growth promoters/inhibitors, neurotransmitters, among many other functions.<sup>[2,3]</sup> Given their intrinsic properties and their attractive pharmacological profile, peptides and proteins have emerged as potential tools for drug discovery.<sup>[4]</sup> However, *in vivo* instability due to protease degradation and poor bioavailability are the main drawbacks that have hampered their exploitation as therapeutic agents.<sup>[5-8]</sup> Nevertheless, there are nearly 200 peptide-based drugs currently in the market<sup>[9]</sup> and great advances have been made in the peptide-therapeutics field. Particularly, many drug discovery tools, new platforms and chemical modifications have been developed to tackle these hurdles and optimise their pharmacokinetic profile.

Peptide backbone modifications often result in improved pharmacological properties, such as greater stability and bioavailability, enhanced cell permeability and lower toxicity.<sup>[2,9,10]</sup> Among the most relevant types of bioactive backbone-modified

peptide families, cyclic peptides<sup>[11]</sup>, *N*-alkylated peptides,<sup>[12]</sup> depsipeptides<sup>[13]</sup>, lantibiotics<sup>[14]</sup> and stapled peptides<sup>[15]</sup> are included. Due to their growing interest in the pharmacological field, depsipeptides and stapled peptides have been the focus of the work presented herein, and therefore are reviewed in the following pages.

### i. Depsipeptides

Depsipeptides are biomolecules commonly found in nature that are characterised by the presence of at least one ester bond within the peptide backbone (Figure 1).<sup>[16–21]</sup> Naturally-occurring depsipeptides hold a complex structure and often present a head-to-side-chain cyclic arrangement and a high content of *N*-methylated residues. These features are responsible for their exceptional pharmacological properties and result in increased stability against proteases.<sup>[13,21–26]</sup> Although there is growing interest in their exploitation as therapeutic agents, the difficulties encountered during the isolation and purification of large quantities from natural sources, as well as their challenging chemical synthesis, have hampered their growth in the drug market.

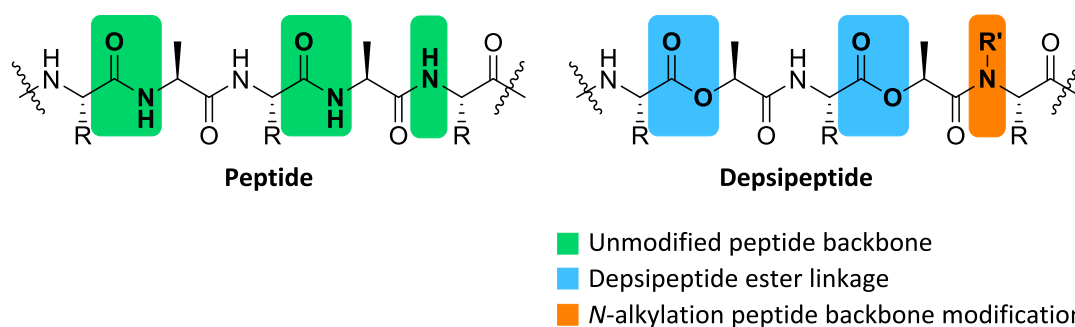


Figure 1. Comparison between peptide and depsipeptide backbones.

Up to date, the most general and effective strategy for the preparation of complex cyclodepsipeptides combines solid-phase synthesis and solution chemistry approaches. A general synthetic strategy can be outlined as follows. First, whereas common residues are assembled through amide bonds to the resin, the depsipeptide parts are prepared in solution as a peptide building blocks containing the ester moieties, followed by their incorporation to the polymeric support. Lastly, cyclisation, *via*, preferably, amide, or alternatively, ester bond formation, is carried out.<sup>[27–30]</sup> Although numerous depsipeptides have been prepared using *combined chemistry approaches*

(solid-phase and solution chemistry), this method presents some disadvantages. For instance, the synthetic route must be designed and optimised for each particular case, and therefore a versatile general synthetic method cannot be outlined. Additionally, preparation of the depsipeptide building blocks in solution often demands an isolation or purification step after each reaction, which limits the rapid preparation of synthetic analogues.

Development of a robust full solid-phase methodology would become a valuable chemical tool for both the preparation of naturally-occurring cyclodepsipeptides and the rapid generation of synthetic analogues. Unfortunately, this has been hindered by prevalent drawbacks encountered during solid-phase depsipeptide synthesis including: (i) DKP formation;<sup>[31–37]</sup> (ii) ester linkage instability upon basic and acid conditions;<sup>[38,39]</sup> (iii) formation of undesired  $\alpha,\beta$ -elimination side-products during Fmoc removal after ester bond formation,<sup>[40,41]</sup> among others. Additionally, depsipeptides of natural occurrence often hold multiple ester linkages, which results in extra synthetic complexity.

Hence, further research is needed to address the issues mentioned above and to open the door to the establishment of a general method. With that purpose, the first part of this thesis was focused on the development of a robust Fmoc-based solid-phase methodology for the preparation of complex depsipeptides that are composed of  $\beta$ -branched residues and present multiple and consecutive ester bonds.

## ii. Stapled peptides

The last years have witnessed increasing discoveries of naturally occurring peptide macrocycles with new structures and biological activities. The discovery and development of novel cyclic constrained peptides which are likely to combine the advantages of therapeutic proteins with those of small molecules is a topic of special interest. According to Arora *et al.*, over 60% of the protein-protein complexes in the Protein Data Bank possess  $\alpha$ -helical interfaces.<sup>[42]</sup> In nature,  $\alpha$ -helices are stabilised by intramolecular hydrogen bonds between the carbonyl oxygen and the amine proton at positions  $i,i+3$ ,  $i,i+4$  and  $i,i+7$ . Mimicking these  $\alpha$ -helices has become an appealing

approach to disrupt or promote protein-protein interactions. Short peptides, however, have little secondary structure in solution. Thus, it is not surprising that several methodologies have appeared over the years to favour or to stabilise  $\alpha$ -helices on short synthetic peptides.<sup>[43]</sup>

The concept “stapled peptide”, which is based on the peptide backbone modification by introduction of a chemical brace between positions  $i,i+4$ ,  $i,i+4$  or  $i,i+7$ , was introduced at the 80's of the XX century (Figure II).<sup>[44]</sup> In 2000, Verdine *et al.* coined the term of stapled peptide for C-C bridge helix stabilisation. Nowadays this term is commonly used for all kind of chemical bridges that favour the  $\alpha$ -helix conformation.<sup>[45]</sup>

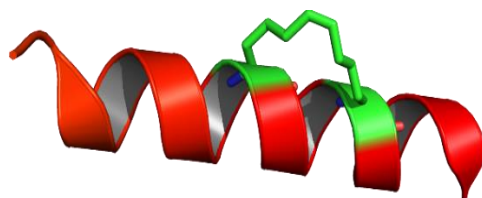


Figure II. Peptide backbone modification by insertion of a chemical staple to promote the helical conformation.

Verdine developed a molecular scaffold that contained functionalised amino acid side-chains at specific stapling positions (Figure III-A).<sup>[45]</sup> The peptide side-chains were cross-linked by using the well-established ruthenium-catalysed Ring-closing metathesis (RCM), being the  $\alpha$ -helix conformation induced (Figure III-B). This type of molecular architectures became exceptional drug candidates, since target recognition was improved (compared to the backbone unmodified peptide) whilst minimising protease degradation. In the past decades, several chemical approaches have been developed towards the generation of new  $\alpha$ -helix protein mimics including-, thiol-, lactam-, triazole-based cross-links, among many others.<sup>[46–52]</sup> Although extensive research has been carried out in the peptide stapling field, a single universal stapling technique cannot be established, since selection of the most suitable cross-linking approach highly depends on the nature of the PPI to be addressed.

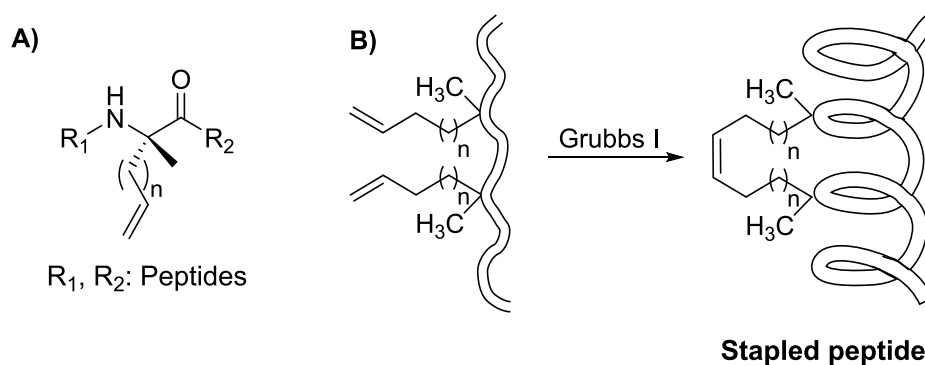


Figure III. A) Amino acid for RCM; B) Synthesis of a stapled peptide by formation of an  $\alpha$ -methylated hydrocarbon cross-link *via* RCM.

Nevertheless, the ability of stapled peptides to cross the cell membrane, increase *in vivo* stability and exhibit improved biological activity, has gained raising interest over the past years. It is well known, that backbone *N*-modified peptides exhibit greater lipophilicity, which ultimately results in enhanced cell internalisation. Additionally, *N*-modified peptides present higher resistance against proteolytic degradation.<sup>[12,53]</sup> Taking into account the benefits conferred by peptide backbone *N*-modification, we envisioned that insertion of *N*-methyl-rich peptide bridges as “staple entities” would be a good approach to develop peptides with an enhanced pharmacokinetic profile. In this context, the second part of this thesis was focused on the development of a synthetic methodology to access highly *N*-methylated stapled peptides.

## References

- [1] J. Deska, U. Kazmaier, *Curr. Org. Chem.* **2008**, *12*, 355–385.
- [2] A. Groß, C. Hashimoto, H. Sticht, J. Eichler, *Front. Bioeng. Biotechnol.* **2016**, *3*, 211.
- [3] I. Avan, C. D. Hall, A. R. Katritzky, *Chem. Soc. Rev.* **2014**, *43*, 3575–3594.
- [4] M. Erak, K. Bellmann-Sickert, S. Els-Heindl, A. G. Beck-Sickinger, *Bioorganic Med. Chem.* **2018**, *26*, 2759–2765.
- [5] P. Vlieghe, V. Lisowski, J. Martinez, M. Khrestchatisky, *Drug Discov. Today* **2010**, *15*, 40–56.
- [6] T. Kieber-Emmons, R. Murali, M. I. Greene, *Curr. Opin. Biotechnol.* **1997**, *8*, 435–441.
- [7] S. Lien, H. B. Lowman, *Trends Biotechnol.* **2003**, *21*, 556–562.
- [8] Z. Antosova, M. Mackova, V. Kral, T. Macek, *Trends Biotechnol.* **2009**, *27*, 628–635.
- [9] L. Nevola, E. Giralt, *Chem. Commun.* **2015**, *51*, 3302–3315.
- [10] A. Grauer, B. König, *Eur. J. Org. Chem.* **2009**, *2009*, 5099–5111.
- [11] S. H. Joo, *Biomol. Ther. (Seoul)*. **2012**, *20*, 19–26.
- [12] J. Chatterjee, C. Gilon, A. Hoffman, H. Kessler, *Acc. Chem. Res.* **2008**, *41*, 1331–1342.
- [13] R. Lemmens-Gruber, M. R. Kamyar, R. Dornetshuber, *Curr. Med. Chem.* **2009**, *16*, 1122–1137.
- [14] O. McAuliffe, R. P. Ross, C. Hill, *FEMS Microbiol. Rev.* **2001**, *25*, 285–308.
- [15] G. L. Verdine, G. J. Hilinski, *Methods Enzymol.* **2012**, *503*, 3–33.

- 
- [16] X. Ye, K. Anjum, T. Song, W. Wang, Y. Liang, M. Chen, H. Huang, X. Y. Lian, Z. Zhang, *Phytochemistry* **2017**, *135*, 151–159.
- [17] X. Wang, X. Gong, P. Li, D. Lai, L. Zhou, *Molecules* **2018**, *23*, 169.
- [18] M. Fujioka, S. Koda, Y. Morimoto, K. Biemann, *J. Org. Chem.* **1988**, *53*, 2820–2825.
- [19] G. Yang, Y. Li, *Helv. Chim. Acta* **2002**, *85*, 168–174.
- [20] A. Dmitrenok, T. Iwashita, T. Nakajima, B. Sakamoto, M. Namikoshi, H. Nagai, *Tetrahedron* **2006**, *62*, 1301–1308.
- [21] G. S. Andavan, R. Lemmens-Gruber, *Mar. Drugs* **2010**, *8*, 810–834.
- [22] G. M. Suarez-Jimenez, A. Burgos-Hernandez, J. M. Ezquerro-Brauer, *Mar. Drugs* **2012**, *10*, 963–986.
- [23] D. J. Newman, G. M. Cragg, *Mar. Drugs* **2014**, *12*, 255–278.
- [24] M. F. Mehbub, J. Lei, C. Franco, W. Zhang, *Mar. Drugs* **2014**, *12*, 4539–4577.
- [25] S. Sivanathan, J. Scherkenbeck, *Molecules* **2014**, *19*, 12368–12420.
- [26] J. Kitagaki, G. Shi, S. Miyauchi, S. Murakami, Y. Yang, *Anticancer Drugs* **2015**, *26*, 259–271.
- [27] T. Takahashi, H. Nagamiya, T. Doi, P. G. Griffiths, A. M. Bray, *J. Comb. Chem.* **2003**, *5*, 414–428.
- [28] Y. Lee, R. B. Silverman, *Org. Lett.* **2000**, *2*, 3743–3746.
- [29] T. Ast, E. Barron, L. Kinne, M. Schmidt, L. Germeroth, K. Simmons, H. Wenschuh, *J. Pept. Res.* **2001**, *58*, 1–11.
- [30] M. M. Nguyen, N. Ong, L. Suggs, *Org. Biomol. Chem.* **2013**, *11*, 1167–1170.
- [31] M. Stawikowski, P. Cudic, in *Methods Mol. Biol.* (Ed.: G.B. Fields), **2007**, vol. 386, pp. 321–339.

- [32] S. Capasso, A. Vergara, L. Mazzarella, *J. Am. Chem. Soc.* **1998**, *120*, 1990–1995.
- [33] J. D. Wade, M. N. Mathieu, M. Macris, G. W. Tregear, *Lett. Pept. Sci.* **2000**, *7*, 107–112.
- [34] B. F. Gisin, R. B. Merrifield, *J. Am. Chem. Soc.* **1972**, *94*, 3102–3106.
- [35] M. C. Khosla, R. R. Smeby, F. M. Bumpus, *J. Am. Chem. Soc.* **1972**, *94*, 4721–4724.
- [36] M. Rothe, J. Mazánek, *Angew. Chemie Int. Ed. Engl.* **1972**, *11*, 293–293.
- [37] J. M. Humphrey, A. R. Chamberlin, *Chem. Rev.* **1997**, *97*, 2243–2266.
- [38] J. Tulla-Puche, N. Bayó-Puxan, J. A. Moreno, A. M. Francesch, C. Cuevas, M. Álvarez, F. Albericio, *J. Am. Chem. Soc.* **2007**, *129*, 5322–5323.
- [39] Y. Sohma, Y. Hayashi, M. Kimura, Y. Chiyomori, A. Taniguchi, M. Sasaki, T. Kimura, Y. Kiso, *J. Pept. Sci.* **2005**, *11*, 441–451.
- [40] X. F. Xiong, H. Zhang, C. R. Underwood, K. Harpsøe, T. J. Gardella, M. F. Wöldike, M. Mannstadt, D. E. Gloriam, H. Bräuner-Osborne, K. Strømgaard, *Nat. Chem.* **2016**, *8*, 1035–1041.
- [41] H. Kaur, P. W. R. Harris, P. J. Little, M. A. Brimble, *Org. Lett.* **2015**, *17*, 492–495.
- [42] A. L. Jochim, P. S. Arora, *ACS Chem. Biol.* **2010**, *5*, 919–923.
- [43] K. Estieu-Gionnet, G. Guichard, *Expert Opin. Drug Discov.* **2011**, *6*, 937–963.
- [44] A. M. Felix, E. P. Heimer, C. T. Wang, T. J. Lambros, A. Fournier, T. F. Mowles, S. Maines, R. M. Campbell, B. B. Wegrzynski, V. Toome, et al., *Int. J. Pept. Protein Res.* **1988**, *32*, 441–454.
- [45] C. E. Schafmeister, J. Po, G. L. Verdine, *J. Am. Chem. Soc.* **2000**, *122*, 5891–5892.
- [46] A. M. Leduc, J. O. Trent, J. L. Wittliff, K. S. Bramlett, S. L. Briggs, N. Y. Chirgadze, Y. Wang, T. P. Burris, A. F. Spatola, *Proc. Natl. Acad. Sci. U.S.A.* **2003**, *100*, 11273–11278.

- 
- [47] H. Jo, N. Meinhardt, Y. Wu, S. Kulkarni, X. Hu, K. E. Low, P. L. Davies, W. F. Degrado, D. C. Greenbaum, *J. Am. Chem. Soc.* **2012**, *134*, 17704–17713.
- [48] M. Chorev, E. Roubini, R. L. Mckee, S. W. Gibbons, M. E. Goldman, M. P. Caulfield, M. Rosenblatt, *Biochemistry* **1991**, *30*, 5968–5974.
- [49] J. C. Phelan, N. J. Skelton, A. C. Braisted, R. S. Mcdowell, *J. Am. Chem. Soc.* **1997**, *119*, 455–460.
- [50] R. S. Harrison, N. E. Shepherd, H. N. Hoang, G. Ruiz-Gómez, T. A. Hill, R. W. Driver, V. S. Desai, P. R. Young, G. Abbenante, D. P. Fairlie, *Proc. Natl. Acad. Sci. U.S.A.* **2010**, *107*, 11686–11691.
- [51] H. C. Kolb, K. B. Sharpless, *Drug Discov. Today* **2003**, *8*, 1128–1137.
- [52] S. Cantel, C. Isaad Ale, M. Scrima, J. J. Levy, R. D. Dimarchi, P. Rovero, J. A. Halperin, A. M. D'Ursi, A. M. Papini, M. Chorev, *J. Org. Chem.* **2008**, 5663–5674.
- [53] M. Teixidó, F. Albericio, E. Giralt, *J. Pept. Res.* **2005**, *65*, 153–166.



## **OBJECTIVES**



## Objectives

The two main objectives of the present thesis were:

1. Development of a robust solid-phase methodology for the preparation of synthetically challenging cyclodepsipeptides that are composed of  $\beta$ -branched residues and present multiple and consecutive ester bonds. Evaluation of the fully stepwise strategy efficiency by comparison with traditional combinatorial solid-phase and solution chemistry approaches.
2. Development of a synthetic methodology to prepare highly *N*-methylated stapled peptides by insertion of short *N*-methyl-rich peptide bridges to the peptide linear sequence.



**CHAPTER 1 . DEVELOPMENT OF A ROBUST FMOC-  
BASED SOLID-PHASE METHODOLOGY FOR THE  
PREPARATION OF COMPLEX DEPSIPEPTIDES**



## 1.1 Introduction

### 1.1.1 Biological importance of naturally-occurring depsipeptides

Depsipeptides are biomolecules that incorporate at least one ester bond within the peptide backbone. Many naturally-occurring depsipeptides can be found in bacteria<sup>[1]</sup>, fungi<sup>[2]</sup>, plants<sup>[3,4]</sup>, algae<sup>[5]</sup>, sponges<sup>[6]</sup>, and other marine organisms<sup>[7–10]</sup> and have emerged as potential therapeutic agents. Depsipeptides readily found in nature present a complex structure and often display uncommon residues. These features are responsible for their outstanding biological properties including anticancer, antiviral, antimicrobial, anti-inflammatory, antimalarial, insecticidal, among other properties<sup>[6,10–15]</sup>. Substitution of amide bonds by ester bonds and the high content of *N*-methylated residues present within their structure account for increased stability against proteases.<sup>[13]</sup> Nevertheless, exploitation of natural bioactive depsipeptides has been limited by their synthetic complexity and the difficulties associated with the isolation and purification of large quantities from natural sources.

Kahalalides are a relevant family of depsipeptides that can be found in the green alga *Bryopsis* sp. and the molluscs *Elysia rufescens* and *Spisula polynyma*.<sup>[16]</sup> Among the natural members of the Kahalalide family are included linear, head-to-tail and head-to-side-chain depsipeptides. Additionally, all members of the Kahalalide family carry an aliphatic acid, mainly contain amino acids of common occurrence and are acetylated at the *N*-terminus. Kahalalides F and G hold the unusual dehydroaminobutyric acid residue within their sequence.<sup>[16,17]</sup> Although 24 linear and cyclic Kahalalides have been described, only seven members of the Kahalalide family exhibit exceptional biological activitiespotential therapeutic activities, including anti-tumoural, anti-microbial, anti-leishmanial and immunosuppressive properties.<sup>[18]</sup> Among the described Kahalalides, Kahalalide F shows the most interesting biological profile (Figure 1.1), and therefore it has been extensively studied over the past decades.

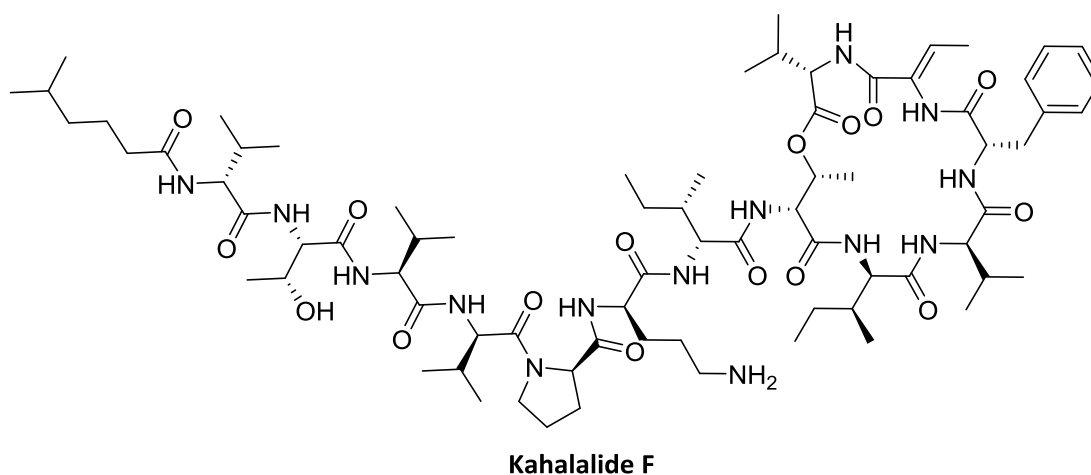


Figure 1.1. Structure of Kahalalide F.

Kahalalide F exhibits anticancer properties and shows relatively low toxicity to non-tumour cells compared to solid tumours, including prostate, breast and colon carcinomas, neuroblastomas, chondrosarcomas and osteosarcomas. Apart from its anticancer properties, Kahalalide F also presents antiviral activity against HSV II; antifungal activity against *Candida albicans*, *C. neoformans* and *Aspergillus fumigatus*; immunosuppressive activity; and anti-leishmanial activity against *Leishmania donovani* and *L. pifanoi*.<sup>[19]</sup>

Winiski and Foster first isolated HUN-7293 from a fungal broth during a screening for potent inhibitors of inducible cell adhesion molecule expression.<sup>[20]</sup> In parallel, another research group was able to isolate the depsipeptide from a different fungal specie.<sup>[21]</sup> HUN-7293 is a head-to-tail cyclodepsipeptide containing a total number of six L-amino acids and a D- $\alpha$ -hydroxy acid within its structure (Figure 1.2). The natural compound exhibits great biological activity against autoimmune diseases and anti-inflammatory disorders. Boger and co-workers reported the first total synthesis of the natural product and prepared a library of analogues consisting of an alanine scan and a *N*-methyl deletion of each residue.<sup>[21]</sup> Unfortunately, all synthetic analogues exhibited lower biological activity compared to their natural counterpart.

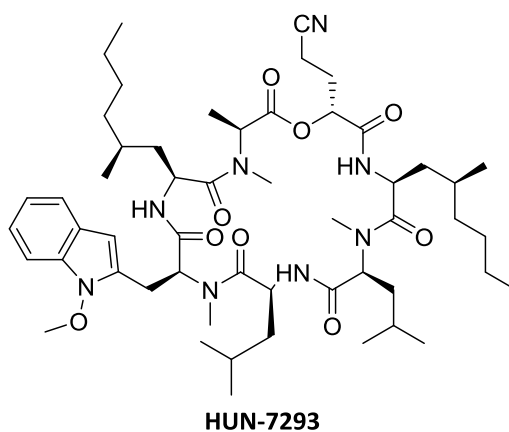


Figure 1.2. Structure of HUN-7293.

It is worth mentioning the importance of PF 1022A in the biomedical field. In 1992, Sasaki and collaborators first isolated this compound from the plant *Camellia japonica*.<sup>[22]</sup> PF 1022A is also a secondary metabolite of the fungus *imperfectus Mycelia sterilia* (*Rosellinia* sp.). This family of head-to-tail cyclooctadepsipeptides hold four alternating residues of 2-hydroxy-(*R*)-carboxylic acids, two *D*-phenyllactic acids and two *D*-lactic acids, and four *N*-methyl-(*S*)-amino acid residues. The eight residues are bound together in a regular pattern (Figure 1.3).<sup>[22,23]</sup> The cyclooctadepsipeptide became a lead structure in the search for novel anthelmintic agents due to its broad biological activity, since it presents great anthelmintic properties and low toxicity in animals. Peptide synthetase PFSYN, the enzyme responsible for PF 1022A's biosynthesis, was isolated and found capable of synthesising all the natural analogues of PF 10022. In this regard, several PF 1022A natural analogues have been isolated from the same culture.<sup>[24,25]</sup>

PF1022A's most relevant synthetic analogue, the so-called Emodepside, shows extraordinary anthelmintic properties, and was introduced in the drug market (Profender® and Procox®) in 2008 (Figure 1.3). Over the past decades, several synthetical analogues have been prepared and structure-activity relationship studies (SARs) carried out, which evidenced that the symmetric conformation of this family of depsipeptides plays an important role in its biological function.<sup>[26]</sup>

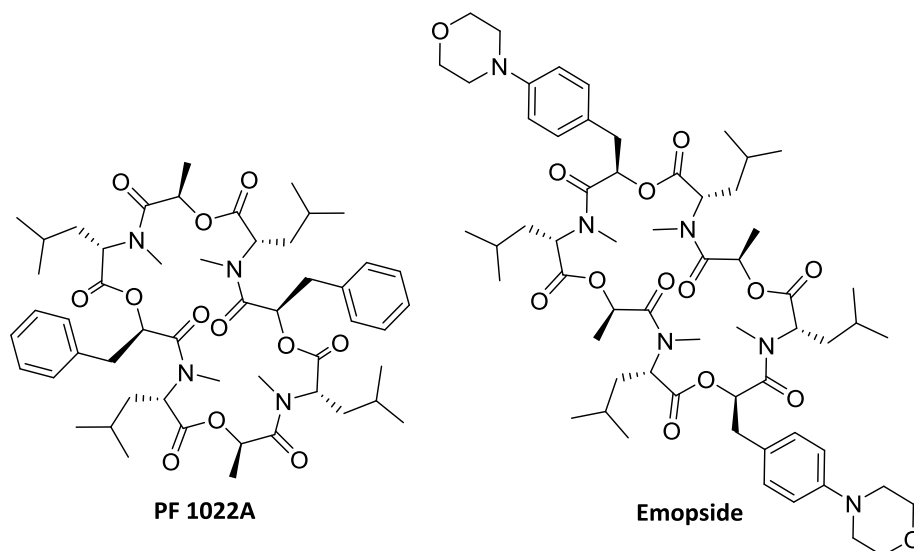


Figure 1.3. Structure of PF1022A and Emopside.

The so-called Romidepsin, also known as FK228, FR901228, NSC-630176, is a bicyclic depsipeptide present in the fermentation broth of *Chromabacterium violaceum* (Figure 1.4). Romidepsin is known to mediate growth arrest and apoptosis in lung cancer cells, and therefore it exhibits great anticancer properties. It can also act as a histone deacetylase (HDAC) inhibitor.<sup>[27–29]</sup> Several synthetic analogues of Romidepsin, consisting of simpler synthetic analogues containing a modification in the synthetically challenging unit: (3*S*,4*E*)-3-hydroxy-7-mercaptoheptenoic acid, also show great anticancer activity on various cancer cells.

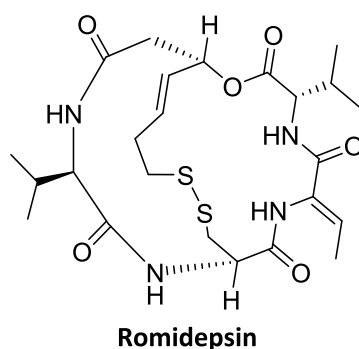


Figure 1.4. Structure of Romidepsin.

Isaridine and isariins, head-to-tail cyclodepsipeptides, are secondary metabolites that can be found in the *Isaria* strains. Members of the isaridine subgroup are extracted from the fungi *Isaria* sp. and *Nigrosabulum globosum*.<sup>[30,31]</sup> Their structure features one  $\alpha$ -hydroxy acid, four  $\alpha$ -amino acids and one  $\beta$ -amino acid, as well as a high content of *N*-alkylated residues. Depsipeptides comprised within the isariin subgroup inhibit insecticidal properties and display one  $\beta$ -hydroxy fatty acid and five  $\alpha$ -amino acids in their structure. Isaridin A and Isariin B are capable of affecting malarial parasites without causing lysis of the erythrocytes (Figure 1.5).

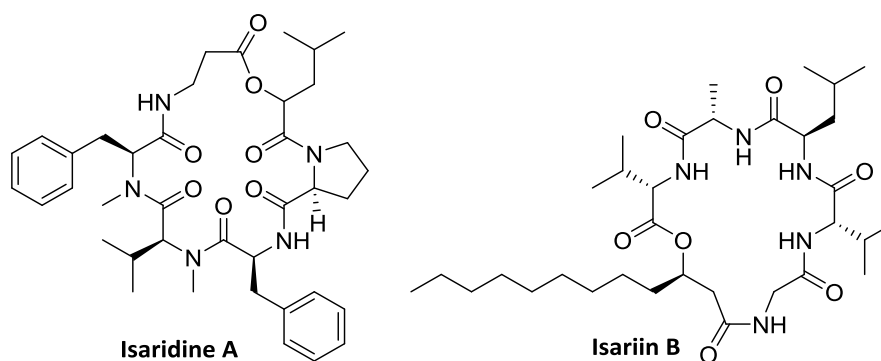


Figure 1.5. Structure of Isaridine A and Isariin B.

Destruxins can be found in fungus *Metarhizium anisoplae* and consist of head-to-tail cyclic hexadepsipeptides holding one  $\alpha$ -hydroxy acid and five amino acid residues (Figure 1.6). Within the destruxins family, several modifications in the hydroxy acid are observed, as well as different patterns in the  $\alpha$ -substituent and the *N*-methylation of the amino acid residues.<sup>[32]</sup> Remarkably, the presence of the ester moiety is crucial to preserve the biological activity, which include insecticidal and antiproliferative properties as well as cytotoxicity activity against mammalian cancer cells.<sup>[33]</sup>

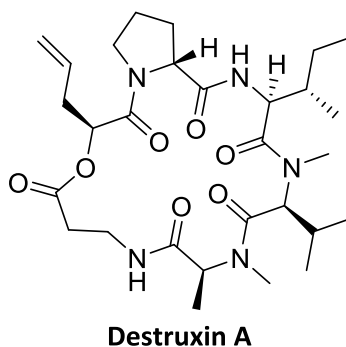


Figure 1.6. Structure of Destruxin A.

Symplocamide A is a depsipeptide of great interest and belongs to the Ahp (3-amino-6-hydroxy-2-piperidone)-containing class depsipeptide family. The core structure of this head-to-tail cyclodepsipeptide consists of a 19-membered ring containing six different amino acids, in which cyclisation takes place through the alcohol functionality of a threonine derivative (Figure 1.7). It presents uncommon residues within its structure such as the citrulline residue and the *N,O*-dimethyl-3-bromotyrosine moiety. The biological properties of Symplocamide A include inhibition of serine proteases and anticancer activity against H-460 lung cancer cells and neuro-2a neuroblastoma cells.<sup>[34]</sup>

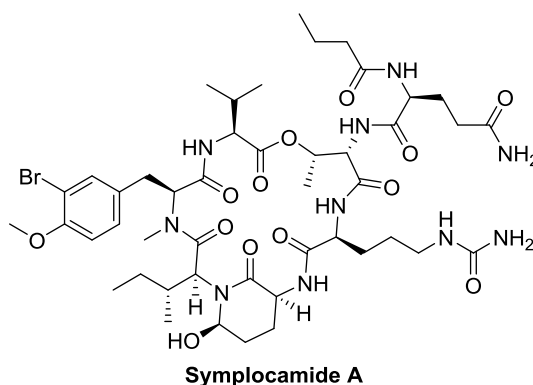


Figure 1.7. Structure of Symplocamide A.

The outstanding biological properties of some depsipeptides generate growing interest in the discovery and development of novel potential therapeutic agents based on depsipeptides. Thus, more efforts towards the development of efficient methodologies to access large quantities are necessary.

## 1.1.2 Chemical synthesis of depsipeptides

In the 60s, Merrifield introduced a novel methodology to efficiently synthesise peptides, nucleotides and oligosaccharides, which consists of the stepwise incorporation of monomer units onto a polymeric support.<sup>[35]</sup> The Merrifield method is not effective for ester bond formation, and therefore solid-phase synthesis of depsipeptides is by far not as established as it is for peptides. Development of solid-phase methodologies for depsipeptide synthesis has been hampered by prevalent drawbacks encountered during solid-phase depsipeptide synthesis including: (i) DKP formation;<sup>[36–42]</sup> (ii) ester linkage instability upon basic and acid conditions;<sup>[43,44]</sup> (ii) formation of undesired  $\alpha,\beta$ -elimination side-products during Fmoc removal after ester bond formation,<sup>[45,46]</sup> among others. Moreover, the use of large excesses of hydroxy acids in coupling reactions is hindered by their high prices and limited availability compared to proteogenic amino acids.

Although a general methodology for depsipeptide synthesis has not hitherto been established, several synthetic approaches can be considered when designing the total synthesis of a depsipeptide. The selection of the most suitable approach for each depsipeptide highly depends on the nature of the residues and the synthetic complexity of the target molecule, and among the described synthetic strategies are included (i) total solution strategies, (ii) fully solid-phase approaches, and (iii) combined chemistry approaches.

Other relevant parameters in depsipeptide synthesis are selection of the methodology to generate ester bonds and selection of the protecting groups for hydroxyl functionalities.

### 1.1.2.1 Synthetic approaches to prepare depsipeptides

#### 1.1.2.1.1 Total solution strategies

Many examples can be found in the literature describing the total synthesis of complex depsipeptides using a *total solution strategy*. Cyclodepsipeptide HUN-7293 was fully prepared in solution. A Mitsunobu reaction was used to incorporate the ester

linkage in a late stage of the synthesis.<sup>[21]</sup> A series of HUN-7293 analogues consisting of an alanine scan and a *N*-methyl delation of each residue were also prepared applying the same approach.<sup>[47]</sup>

Six analogues of natural cyclodepsipeptide PF 1022A were synthesised employing a solution chemistry approach. A Steglich esterification using the DCC/DMAP system was used for the ester bond formation.<sup>[48]</sup>

Many other total syntheses of naturally-occurring cyclodepsipeptides using a *total solution strategy* have been reported in the literature, including the synthesis of Destruins<sup>[33]</sup>, Enniatin B<sup>[49]</sup>, (-)-Tamandarin B<sup>[50]</sup>, among others.

Although many naturally-occurring depsipeptides have been prepared using a *total solution strategy*, this approach presents some limitations. The synthetic route must be designed and optimised for each particular case, and therefore a versatile general synthetic strategy cannot be outlined. Additionally, the rapid preparation of synthetic analogues is hampered by the required isolation or purification step after each reaction. Note that this is not the case for solid-phase peptide synthesis, where excess of reagents can be washed away by simple suction.

#### **1.1.2.1.2 Full solid-phase strategies**

Many groups have put great efforts into the development of a full *solid-phase depsipeptide methodology*.<sup>[51–54]</sup> This approach is based on incorporation and deprotection iterative cycles, which allows stepwise addition of each residue.

Davies and co-workers prepared a series of analogues of a relatively small cyclic pentadepsipeptide by using a fully solid-phase synthesis. Davies proposed a combination of TBDMS and Fmoc protecting groups for the hydroxy and amino functionalities, respectively. This approach mainly consisted of the stepwise incorporation of residues (Fmoc-amino acids and TBDMS-hydroxy acids) through amide or ester bond linkages, followed by the corresponding protecting group removal and subsequent chain elongation. Nevertheless, the obtained yields (52%) were rather moderate for the preparation of such a relatively small substrate, which contained two

standard peptide bonds and two ester bonds. Thus, the use of this strategy for the synthesis of longer depsipeptide chains might not be useful.<sup>[54]</sup>

Later on, Kuisle reported the total synthesis of depsides and depsipeptides by stepwise incorporation of THP-hydroxy acids through an amide/ester bond formation, and subsequent THP removal. In this case, the widely used Steglich esterification with the DIC/DMAP system successfully allowed the formation of ester moieties. This methodology became a versatile tool for the preparation of depsipeptides, however, it is limited to the use of  $\alpha$ -hydroxy acids and  $\alpha$ -amino acids.<sup>[55]</sup>

Spengler and co-workers published a detailed protocol for automated depsipeptide synthesis in a peptide synthesiser using THP-hydroxy acid monomers. Iterative cycles consisting of insertion of THP-hydroxy acid monomers and subsequent THP removal, furnished the target molecule. DCC/DMAP was the coupling system of choice to form ester linkages. The highest yields (30%) of the final product were seen with one or two ester substitutions on a sequence of 26 residues, while substitutions of six esters gave relatively low yields (7%).<sup>[53]</sup>

Albericio *et al.* reported the total synthesis of Kahalalide F using a fully solid-phase approach based on the well-known Fmoc/<sup>t</sup>Bu strategy. The cyclodepsipeptide presents a head-to-side-chain arrangement and contains an ester bond between two  $\beta$ -branched amino acids. A Thr residue was incorporated with the unprotected hydroxyl group *via* an amidation reaction. Subsequent on-resin Steglich esterification with DIC/DMAP afforded the ester bond product. Unfortunately, a low esterification yield was obtained (30 %).<sup>[56]</sup>

Another reported strategy describes the assembly of Fmoc-protected  $\gamma$ -amino- $\beta$ -hydroxy acids and THP-protected *syn*- $\beta$ -hydroxy acids units to obtain depsipeptide chains. This approach allowed the synthesis of a series of Hapalosin analogues, however, preparation of the protected amino acid residues was rather lengthy.<sup>[57]</sup>

Albericio and co-workers developed a convenient methodology by using recoverable and reusable  $\alpha$ -hydroxy acid building blocks. The  $\alpha$ -hydroxy acid units were protected with hexafluoroacetone (HFA) to afford the corresponding lactone, which is a

protected and activated specie that allows efficient solid-phase ester bond formation. This useful methodology is limited to the use of  $\alpha$ -hydroxy acids.<sup>[52]</sup>

Extensive research towards the development of a general *solid-phase depsipeptide methodology* for the synthesis of depsipeptides has been carried out in the past decades. However, up to date there is not a robust and versatile methodology to prepare complex depsipeptides in a systematic manner. The use of commercially available protected residues would be extremely useful for the preparation of complex depsipeptides as well as for the rapid generation of numerous synthetic analogues for SARs.

#### **1.1.2.1.3 Combined solid-phase and solution chemistry strategies**

*Combined chemistry approaches* are generally applied to depsipeptide synthesis.<sup>[58–61]</sup> These approaches mainly consist of the preparation of building blocks containing uncommon residues in solution, which often hold the depsipeptide moiety, followed by their incorporation onto the solid support.

For instance, Nguyen *et al.* applied this strategy to the synthesis of a family of depsipeptides presenting alternating ester and amide bonds. They used unique Fmoc-depsipeptide building blocks that were prepared in solution prior to its solid-phase assembly.<sup>[61]</sup>

Numerous depsipeptides have been prepared using *combined chemistry approaches*. However, this method presents some disadvantages. Preparation of the depsipeptide building blocks in solution often involves several synthetic steps, which are accompanied of their corresponding isolation or purification process. That, hinders the rapid generation of synthetic analogues, since preparation of numerous depsipeptide building blocks is rather time-consuming and laborious. In addition, segment condensation of depsipeptide building blocks onto the polymeric support is not as straightforward as assembly of single monomer units. In some cases, segment condensation might require strong coupling conditions, which can lead to side-reactions such as racemisation or ester linkage fragmentation.

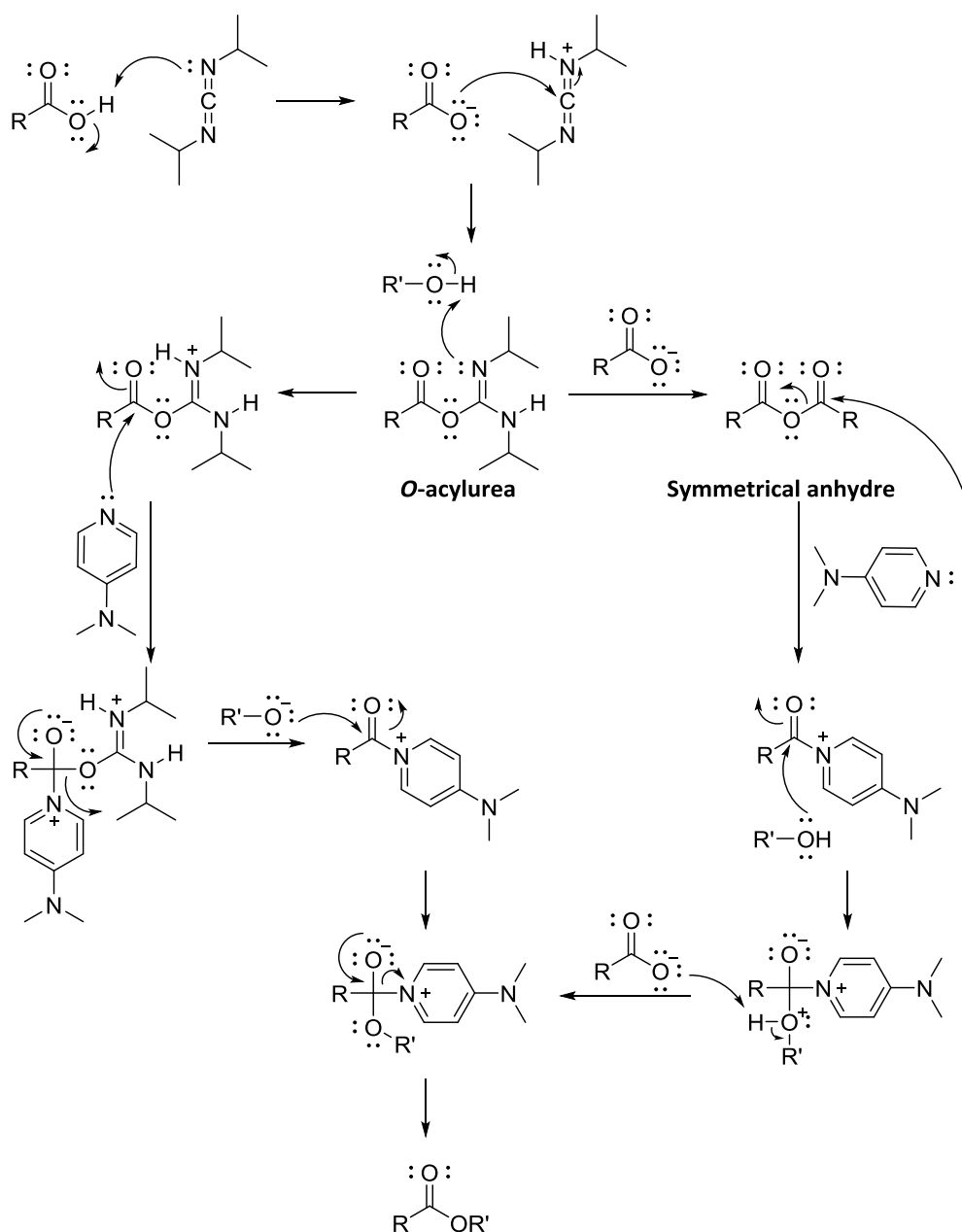
### 1.1.2.2 Ester bond formation methodologies

Several esterification procedures have been reported in the literature for depsipeptide synthesis including the Steglich esterification, the Boc-AA *N*-hydroxysuccinimide ester bond formation method, the Mitsunobu esterification and the Yamaguchi esterification.

#### 1.1.2.2.1 Steglich esterification

The so-called Steglich esterification or carbodiimide/DMAP coupling method is the most commonly used strategy for depsipeptide synthesis, since it usually performs properly and has a relative low cost.<sup>[51,55]</sup> The amino acid is activated with a carbodiimide, often with DIC, *via* the traditional *O*-acylurea mechanism (AA/DIC ratio 1:1) or the symmetrical anhydride formation mechanism (AA/DIC ratio 2:1) (Scheme 1.1). The activated specie reacts with the free alcohol in the presence of catalytic DMAP, being the corresponding ester product formed.<sup>[62]</sup>

The extensive use of aminium and phosphonium-salt based coupling reagents to activate amino acids in classic peptide synthesis led Riguera *et al.* to consider the effect of these reagents on the efficiency of ester bond formation. In an attempt to evaluate the best conditions, DIC, HBTU, HATU and PyBrop were tested (i) with no auxiliary, (ii) in the presence of HOBt and (iii) in combination with catalytic DMAP and different 2,4,6-trimethylpyridine (collidine) equivalents in relation to the phosphonium salt. Surprisingly, Riguera demonstrated that the best results were obtained with DIC/DMAP, being the highest conversion rates achieved within the first two hours.<sup>[55]</sup> Nowadays, the DIC/DMAP system is widely used for both solid-phase and solution chemistry approaches to form ester bonds, leading in most cases to exceptional conversion rates.<sup>[46,63,64]</sup>

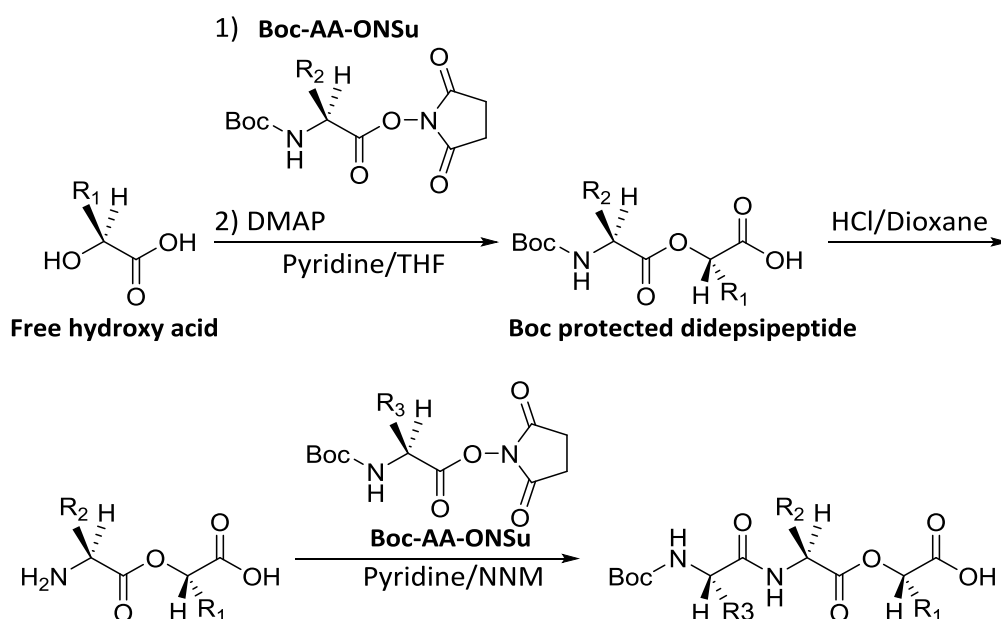


Scheme 1.1. Steglich esterification mechanism through the *O*-acylurea and the symmetrical anhydride intermediates.<sup>[65]</sup>

#### 1.1.2.2.2 The Boc-AA *N*-hydroxysuccinimide ester bond formation method

Katakai and coworkers reported a solution phase method for the preparation of Boc-protected depsipeptides by reaction of an  $\alpha$ -hydroxy acid with a Boc-amino acid *N*-hydroxysuccinimide ester (Boc-AA-ONSu). Boc-AA-ONSu, a commercially available reagent commonly used in peptide synthesis, serves as the activated amino acid specie that reacts with the hydroxyl functionality of a fully unprotected  $\alpha$ -hydroxy acid in the presence of catalytic amounts of DMAP to afford the corresponding Boc protected

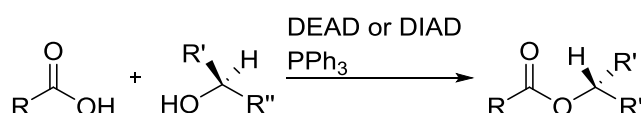
depsipeptide (Scheme 1.2).<sup>[66]</sup> Once the Boc protected didepsipeptide is formed, further chain elongation can be achieved by Boc removal upon treatment with hydrochloric acid in dioxane, followed by reaction with a Boc-AA-ONSu unit under basic conditions. Moreover, the non-aqueous organic solvent media prevents hydrolysis of the Boc-AA-ONSu building block, and therefore the Boc-AA *N*-hydroxysuccinimide ester bond formation method becomes a good approach to prepare depsipeptides in solution.



Scheme 1.2. General scheme of the Boc-AA *N*-hydroxysuccinimide esterification method.<sup>[66]</sup>

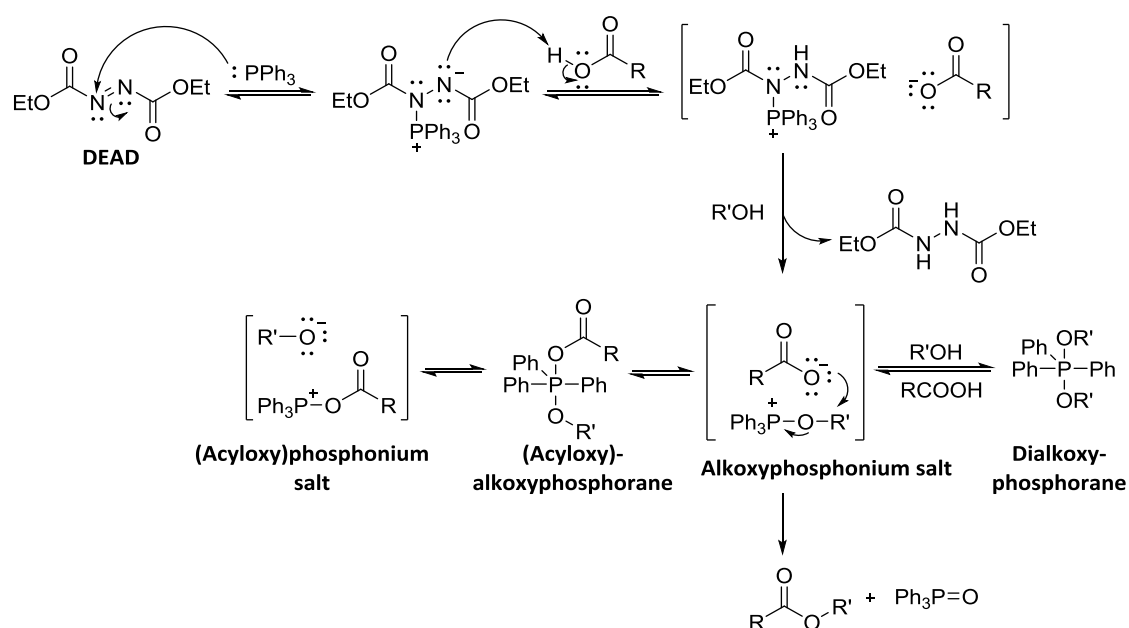
### 1.1.2.2.3 Mitsunobu esterification

Oyo Mitsunobu first reported the reaction between an alcohol and a carboxylic acid in the presence of the redox system DEAD/PPh<sub>3</sub> to form ester bonds with complete Walden inversion of the alcohol component (Scheme 1.3).<sup>[67,68]</sup> In addition to DEAD, the Mitsunobu esterification can also be performed with DIAD, leading to equivalent conversion rates. The versatility of the reaction allows its application to both solution chemistry and solid-phase synthesis.



Scheme 1.3. General scheme of the Mitsunobu esterification method.<sup>[21,67]</sup>

The Mitsunobu esterification mechanism gives an insight on how the inversion of the alcohol configuration occurs (Scheme 1.4). The initial stage is the activation of DEAD/DIAD with triphenylphosphine, followed by the capture of the carboxylic acid proton. Treatment with alcohols leads to the formation of alkoxyphosphonium and dialkoxyphosphorane species. Both species are involved intermediates in the esterification reaction and are in equilibrium with each other. The acid exerts a catalytic effect on the alkoxyphosphonium and dialkoxyphosphorane equilibrium rates, being the equilibrium shifted to the alkoxyphosphonium species.



Scheme 1.4. Mitsunobu esterification mechanism.<sup>[69]</sup>

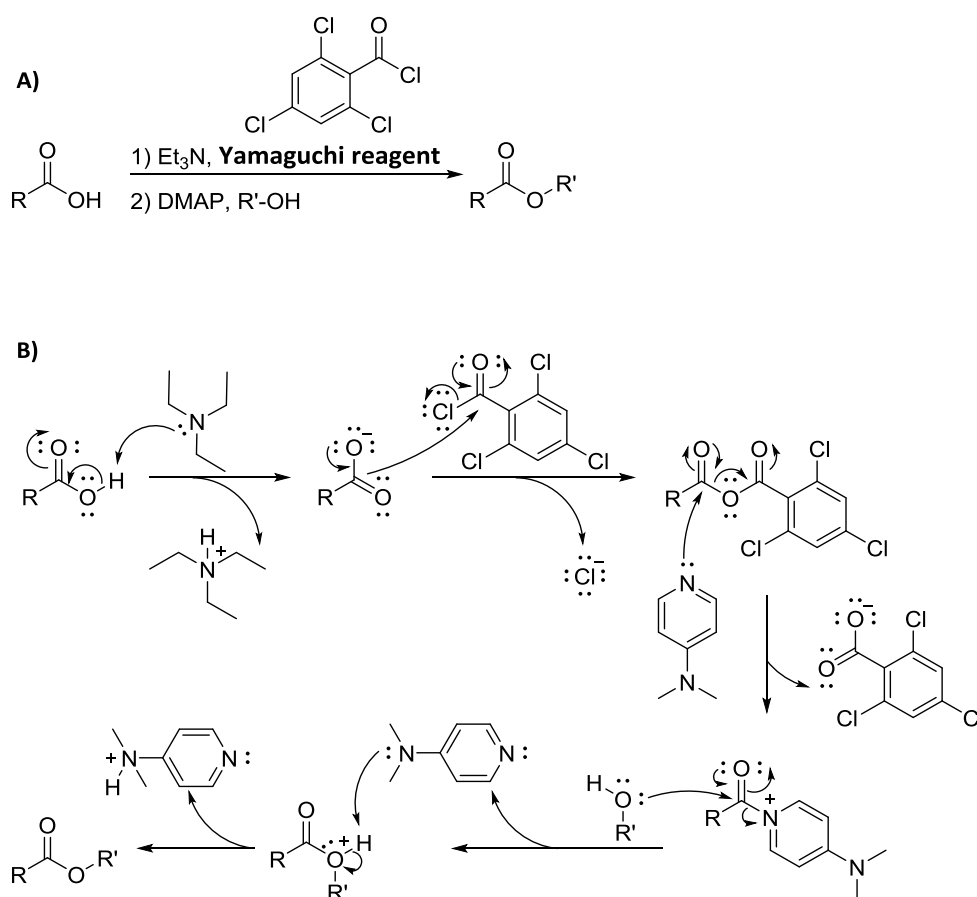
(Acyloxy)alkoxyphosphoranes are also intermediates involved in the Mitsunobu reaction and are in equilibrium with the corresponding (acyloxy)phosphonium salt. Nevertheless, the key intermediate that leads to inversion of the alcohol component configuration is the alkoxyphosphonium species. Hence, the favoured S<sub>N</sub>2 displacement at a primary carbon atom accounts for the regioselectivity of the Mitsunobu reaction.<sup>[69]</sup>

The Mitsunobu esterification applicability to depsipeptide synthesis was first reported by Boger *et al.*, who successfully applied this reaction to the total synthesis of cyclodepsipeptide HUN-7293.<sup>[21]</sup> Grab and collaborators also demonstrated that the Mitsunobu reaction was an efficient tool for the preparation of large depsipeptides, and

they observed that considerably better yields were obtained when performing the esterification reaction at initial stages of the synthesis rather than at the final assembly step.<sup>[67]</sup>

#### 1.1.2.2.4 Yamaguchi esterification

Yamaguchi *et al.* described the rapid and mild esterification reaction between an aliphatic acid and an alcohol using 2,4,6-trichlorobenzoyl chloride, namely the Yamaguchi reagent, as activating agent. The reaction requires the presence of DMAP and basic conditions (Scheme 1.5A).<sup>[70]</sup>



Scheme 1.5. A) General scheme of the Yamaguchi esterification method; B) Yamaguchi esterification mechanism.<sup>[70]</sup>

The first step of the esterification process is the reaction between a carboxylic acid and 2,4,6-trichlorobenzoyl chloride under basic conditions, where the 2,4,6-trichlorobenzoic carboxylic mixed anhydride is formed. The second step of the Yamaguchi esterification starts with the addition of the corresponding alcohol and

DMAP, which serves as catalyst, allowing alcoholysis of the mixed anhydride to afford the desired product (Scheme 1.5B). The Yamaguchi esterification has been used for ester bond formation of Palau'amide and Apratoxin A cyclodepsipeptides, among others, and it becomes an alternative efficient method for depsipeptide synthesis<sup>[71,72]</sup>

### 1.1.2.3 Hydroxyl functionalities protecting groups

Although unprotected hydroxy acids such as Ser or Thr can be used during peptide coupling reactions, protection of the hydroxyl group is required during ester bond formation to avoid side-reactions. Careful selection of appropriate protecting groups for hydroxyl functionalities becomes a crucial step during depsipeptide synthesis and the following considerations must be considered: (i) the protecting group must be stable to esterification reaction conditions, and (ii) the ester bond must be stable to protecting group elimination conditions. These two requirements limit the number of protecting groups for hydroxyl functionalities compatible with depsipeptide synthesis. Moreover, commercial availability of protected hydroxy acids meeting the requirements mentioned above is rather limited. Up to date three hydroxyl protecting groups are used in depsipeptide synthesis for  $\alpha$ -hydroxy acid protection, namely the TBDMS,<sup>[54]</sup> THP<sup>[51,55]</sup> and HFA<sup>[52]</sup> groups (Figure 1.8).

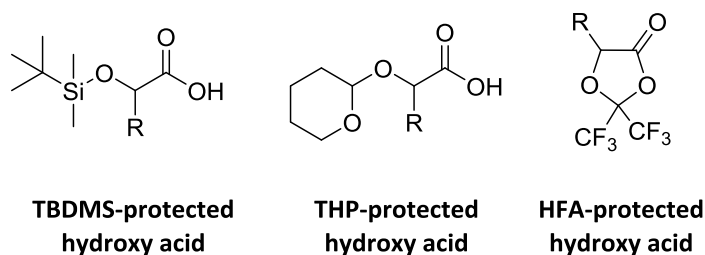


Figure 1.8. Protected  $\alpha$ -hydroxy acids.

Davies *et al.* first used the TBDMS group in depsipeptide synthesis. A proposed combination of TBDMS and Fmoc protection for hydroxy and amino groups, respectively, was applied to the solid-phase synthesis of a cyclic pentadepsipeptide.<sup>[54]</sup> The depsipeptide incorporated two non-consecutive esters moieties within the peptide backbone, and the target molecule was obtained with an overall 52% yield. Such a moderate yield for a relatively small molecule suggests that the use of this strategy

might not be effective for the preparation of longer depsipeptide chains. Later on, Kuisle and collaborators further studied the use of TBDMS in depsipeptide synthesis.<sup>[51,55]</sup> The esterification reaction was monitored by HPLC analysis and several side products were observed, suggesting that TBDMS might not be completely stable upon esterification conditions and that partial hydrolysis might take place. Kuisle then raised the possibility that the instability of the TBDMS group may be responsible for the moderate yields obtained by Davies. On further studies on the development of a robust general methodology for the preparation of depsipeptides, they selected THP as the protecting group of choice for hydroxyl functionalities.<sup>[51,55]</sup> Several depsides and depsipeptides were exclusively prepared on SPPS by using THP-protected hydroxy acids. The synthetic strategy comprised an esterification reaction and subsequent THP removal, being this cycle repeated as many times as required to furnish the linear depsipeptide sequence. In this case, good yields were obtained and therefore the synthesis of relatively large depsipeptides was accomplished. On the other hand, HFA was also described as a new type of recoverable and reusable  $\alpha$ -hydroxy acid building block for solid-phase synthesis and it was applied to the synthesis of a number of small cyclic depsipeptides.<sup>[52]</sup> HFA is a bidentate protecting and activating reagent suitable for  $\alpha$ -functionalised carboxylic acids such as  $\alpha$ -hydroxy,  $\alpha$ -amino and  $\alpha$ -mercapto acids. Protection is accomplished in one step, in which heterocyclisation of the carboxylic acid leads to the corresponding lactone. The carboxylic acid is then activated and the  $\alpha$ -functionality is protected. The lactone can undergo nucleophilic attack from a wide variety of nucleophiles (such as alcohols, among others) and consequently deblock the alpha functionality. The HFA protection/activation methodology can be applied to both solution chemistry and solid-phase approaches.<sup>[52,73]</sup>

Hydroxyl group protection procedures as well as on-resin protecting group removal conditions for the three protecting groups described above (TBDMS, THP and HFA) are summarised in Table 1.1. Thus, selection of a polymeric support compatible with the corresponding protecting group removal conditions carries significant importance and must be considered carefully.

| Protecting group                         | Protection conditions   | Protecting group removal                              | Ref        |
|--|---|---|------------|
| <i>tert</i> -butyl dimethylsilyl (TBDMS) | (a) TBDMS-Tf, 2,6-lutidine, DCM<br>or<br>(b) TBDMS-Cl, imidazole, DMF | (a) 3-4 eq. of TBAF in THF (1 h)                      | [54,74,75] |
| Tetrahydropyranil (THP)                  | (a) Dihydropyrane, <i>p</i> -TsOH, DCM                                | (a) <i>p</i> -TsOH (5 mg/mL) in DCM/MeOH (97:3) (1 h) | [51,55]    |
| Hexafluoroacetone (HFA)                  | (a) 2 eq. (CF <sub>3</sub> ) <sub>2</sub> CO, DMSO                    | Simultaneous incorporation and HFA elimination        | [76]       |

Table 1.1. Protection and deprotection conditions of  $\alpha$ -hydroxy acids protecting groups.

#### 1.1.2.4 Common drawbacks associated with depsipeptide synthesis

In addition to the described key parameters for the synthesis of depsipeptides other variables must be considered during the synthetic strategy design.<sup>[77]</sup> Many depsipeptides present a high content of *N*-methylated residues.<sup>[78]</sup> Incorporation of amino acids or hydroxy acids onto the secondary amine of *N*-methylated residues might result in lower *coupling rates*, and strong coupling conditions might be required to ensure full incorporation. The use of the HATU–HOAt–DIEA coupling system is highly recommended.<sup>[79]</sup>

A common drawback in depsipeptide synthesis is *diketopiperazine (DKP) formation* during Fmoc removal of the second residue. DKP formation is also observed at the second position following the ester linkage. *N*-alkyl, Proline or D-amino acids are likely to adopt *cis* conformation and therefore DKP formation is specially favoured.<sup>[37–42,80]</sup> However, DKP formation highly depends on the sequence and cannot be predicted in advance. The use of a sterically hindered resin, such as the 2-Chlorotrityl chloride (2-CTC) resin, is known to minimise DKP formation at the peptide *C*-terminus.<sup>[81]</sup> An alternative solution is replacement of the protecting group Fmoc by Alloc.<sup>[82]</sup> The latter is removed under neutral conditions, thus preventing base-promoted dipeptide loss. If Fmoc cannot be substituted, alternative protocols to the traditional piperidine–DMF (1:4 v/v) (1 x 1 min + 2 x 5 min) treatment can be used. Shortening of the piperidine–

DMF treatment<sup>[83]</sup> or the use of other bases such as DBU or TBAF might result in a decrease in DKP formation.<sup>[84,85]</sup>

*Ester bond instability* is a major concern in depsipeptide synthesis, and fragmentation can be observed upon treatment with acidic conditions, which are often required for depsipeptide cleavage from the resin.<sup>[43,44]</sup> The use of Fmoc-protected amino acids for ester bond formation is hampered by base-promoted fragmentation observed during Fmoc removal treatment. The use of alternative protecting groups such as Alloc must be considered.

*Aspartimide formation* is a prevalent side-reaction in peptide synthesis that occurs during Fmoc removal when the peptide sequence contains an *N*-terminal aspartic acid.<sup>[38,80]</sup> Addition of small percentages of an additive, such as HOBT<sup>[86]</sup>, OxymaPure<sup>[87]</sup> or formic acid<sup>[88]</sup>, to the piperidine–DMF cocktail has been reported to minimise the undesired side-reaction due to partial base neutralisation.<sup>[84]</sup> The use of other bases such as DBU instead of piperidine can also be helpful.<sup>[38]</sup>

Some residues such as Cys, Phe, D-amino acids and  $\beta$ -branched amino acids, are prone to *epimerisation*.<sup>[80]</sup> Assembly using the HATU–HOAt–DIEA coupling system when longer reactions are required is likely to decrease the reaction times and minimise epimerisation rates. Moreover, the use of HOBT instead of HOAt as coupling additive can be advantageous to minimise this undesired reaction.<sup>[79]</sup>

### 1.1.3 Naturally-occurring depsipeptide YM-254890: a synthetic challenge

Platelets aggregation, which is the main cause of several thromboembolic diseases, is mediated by ADP through G-protein coupled receptors (GPCR).<sup>[89–91]</sup> In 2003, Taniguchi *et al.* isolated and elucidated the structure of YM-254890 from the culture broth of *Chromobacterium* sp. QS3666 (Figure 1.9).<sup>[92]</sup> The cyclic depsipeptide acts as a selective inhibitor of protein  $G\alpha_{q/11}$ , being a potential therapeutic agent for the treatment of several  $G\alpha_{q/11}$  protein mediated diseases such as thromboembolic diseases.<sup>[93–95]</sup> YM-254890 is also a valuable tool for a better understanding of the biological function of GPCR. Over the last years, the pharmacological properties of YM-254890 have been evaluated. Although the cyclic depsipeptide exhibited low oral

bioavailability, inhibition of acute thrombosis and neointima formation was observed after systemic administration of YM-254890.<sup>[93,96]</sup> In addition to its biological interest, the cyclic depsipeptide is challenging from a synthetic point of view. YM-254890 is a head-to-side-chain cyclodepsipeptide that contains an overall of eight residues and presents a highly *N*-methylated structure. The natural compound holds an overall number of three ester bonds, being two of them consecutive (Figure 1.9). The consecutive ester linkages are located within the core ring and are composed of a *D*-phenyllactic acid (*D*-Pla) and a Thr residue, and a  $\beta$ -hydroxy branched Thr derivative and a *N,O*-dimethylthreonine (*N,O*-Me<sub>2</sub>Thr) residue, respectively. The third ester linkage between two unnatural  $\beta$ -hydroxyleucine ( $\beta$ -HyLeu) residues serves as the junction between the core ring and the branched linear chain. Additionally, the cyclodepsipeptide structure is based on uncommon residues such as (*2S,3R*)- $\beta$ -HyLeu, (*2S,3R*)-*N,O*-Me<sub>2</sub>Thr and *N*-methyldehydroalanine (*L-N*-MeDha).<sup>[92]</sup>

Until very recently, the total synthesis of the named depsipeptide remained undescribed. In fact, a \$100,000 reward was offered in a worldwide contest for the preparation of the naturally-occurring cyclodepsipeptide on a scale of at least 1 mg (<https://www.innocentive.com/ar/challenge/9933017>). Unfortunately, none of the 228 applicants succeeded in the synthesis of the target molecule.

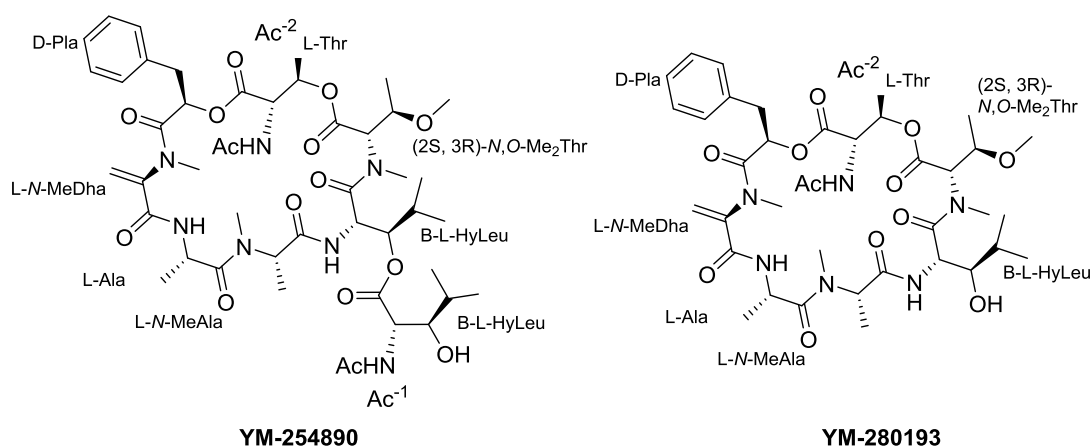


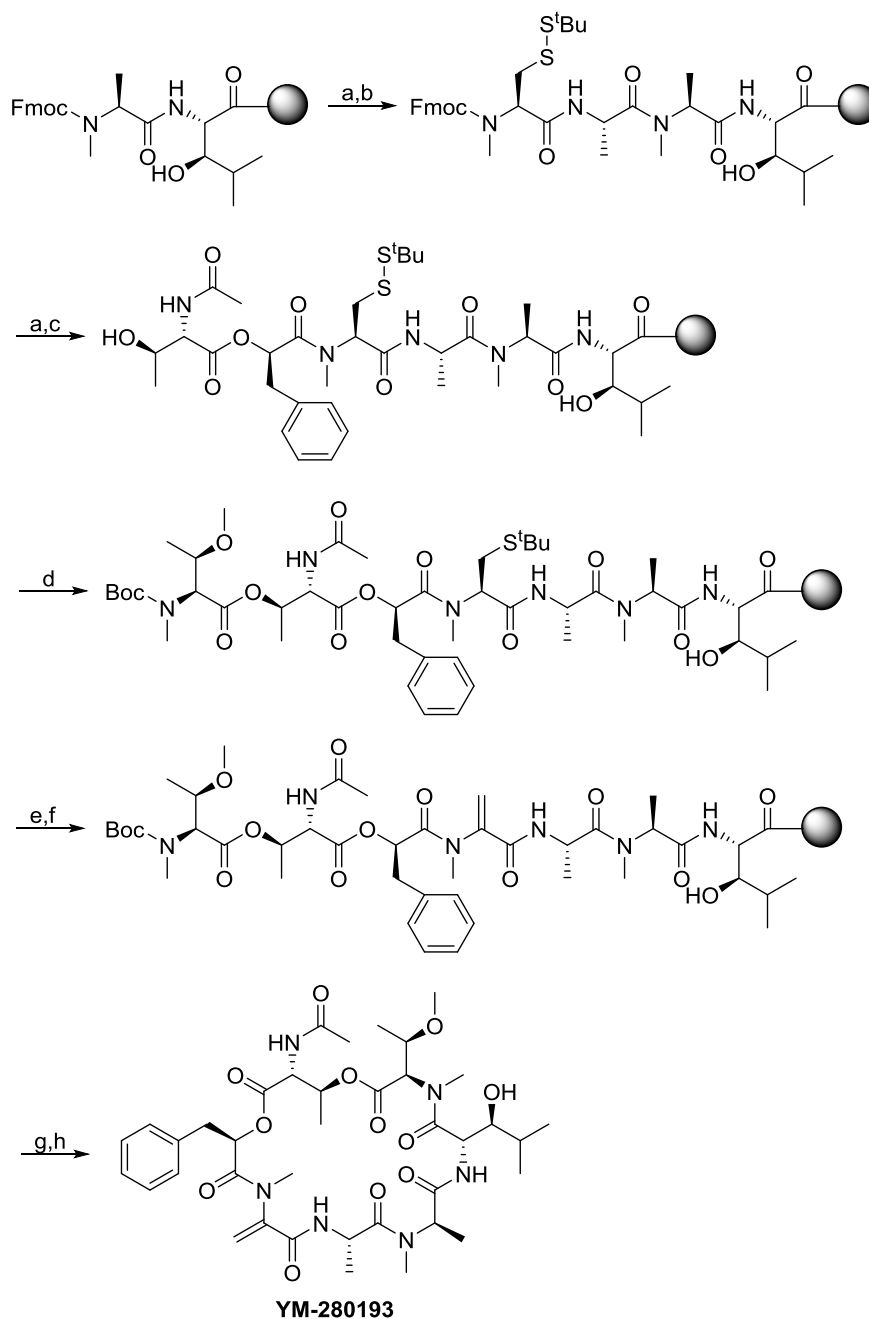
Figure 1.9. Structure of naturally-occurring depsipeptides YM-254890 and YM-280193.<sup>[46,92]</sup>

In an attempt to generate YM-254890, Harveen *et al.* reported the total synthesis of YM-280193 (Scheme 1.6),<sup>[46]</sup> a cyclic analogue of YM-254890 lacking the branched linear region ( $\beta$ -HyLeu residue) (Figure 1.9). Unsuccessful attempts towards the

development of a fully solid-phase strategy due to drawbacks associated with the low reactivity of the Ac-Thr-OH residue during on-resin esterification, led to the use of a combined solid-phase and solution chemistry approach. Thus, the well-known Fmoc/<sup>t</sup>Bu strategy was used for the chain elongation, which started with the incorporation of the  $\beta$ -HyLeu residue onto the 2-CTC resin. Due to the low reactivity of the Ac-Thr-OH during its incorporation *via* a Steglich esterification, this residue was inserted as the Ac-Thr(OH)-COO-D-Pla dipeptide building block using a segment condensation strategy. Assembly of the last residue, Fmoc-*N,O*-Me<sub>2</sub>Thr, was successfully accomplished through an on-resin Steglich esterification. Unfortunately, Fmoc removal completely failed to afford the desired product, and  $\alpha,\beta$ -elimination at the *N*-Ac-Thr residue afforded the dehydrobutyrine-pentapeptide instead. Incorporation of this residue was achieved using the Boc-*N,O*-Me<sub>2</sub>Thr building block instead, followed by dipeptide cleavage from the resin. Finally, cyclisation between the *N*-terminal *N,O*-Me<sub>2</sub>Thr and the steric hindered *C*-terminal  $\beta$ -HyLeu afforded the target molecule, YM-280193.

It was not until very recently that the total synthesis of YM-254890 was described for the first time (Scheme 1.7).<sup>[63]</sup> A combined solid-phase and solution chemistry approach was applied to prepare the so-called YM-254890 dipeptide. The ester moieties were incorporated by segment condensation of protected tripeptide Ac-Thr(O-(Fmoc-*N,O*-Me<sub>2</sub>Thr-CO))-D-Pla-COOH (**BB1a**, Figure 1.10) and dipeptide Boc- $\beta$ -HyLeu(O-(Ac- $\beta$ -HyLeu(Boc)-CO))-COOH (**BB2**, Figure 1.10) *via* amidation reactions (Scheme 1.7), being on-resin esterification reactions not required. Unfortunately, the same side-reaction encountered by Harveen *et al.* during Fmoc removal of the *N,O*-Me<sub>2</sub>Thr residue was observed. Although many conditions were tested, including shortening of Fmoc removal treatments with the traditional piperidine-DMF (1:4) cocktail and the use of other bases such as DBU or TBAF, none of them avoided the formation of the  $\alpha,\beta$ -elimination side-product and only traces of the desired product were obtained. Hence, Fmoc was replaced by Alloc for the protection of tripeptide Ac-Thr(O-(Alloc-*N,O*-Me<sub>2</sub>Thr-CO))-D-Pla-COOH (**BB1b**). The disconnection point between *N*-terminal  $\beta$ -HyLeu and *C*-terminal *N*-MeAla circumvented the presence of the *N*-methylated terminal amino group for the macrolactamisation reaction, which is a

poor nucleophile compared to primary amines. Lastly, head-to-side chain cyclisation yielded YM-254890. With this versatile strategy in hands, several groups have successfully prepared a series of synthetic analogues for structure-activity relationship studies purposes.<sup>[63,97,98]</sup>



**Scheme 1.6.** Synthesis of **YM-280193**. a) piperidine–DMF (1:4 v/v); b) Fmoc-*N*-MeAla-Cys(S<sup>t</sup>Bu)-OH, HATU, HOAt, DIEA, DMF; c) Ac-Thr(OH)-COO-D-Pla, HATU, HOAt, DIEA, DMF; d) Boc-*N,O*-Me<sub>2</sub>Thr-OH, DIC, DMAP, DCM–DMF (19:1 v/v); e) DTT, DIEA, DMF; f) 1,4-dibromobutane, K<sub>2</sub>CO<sub>3</sub>, DMF; g) TFA–H<sub>2</sub>O (19:1 v/v), 16% over 11 steps; h) HATU, HOAt, DIEA, DMF, 27%.<sup>[46]</sup>

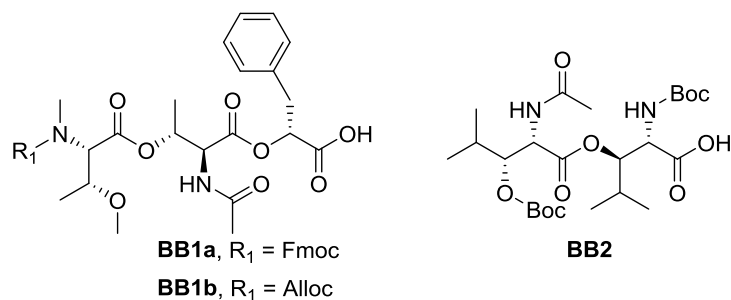
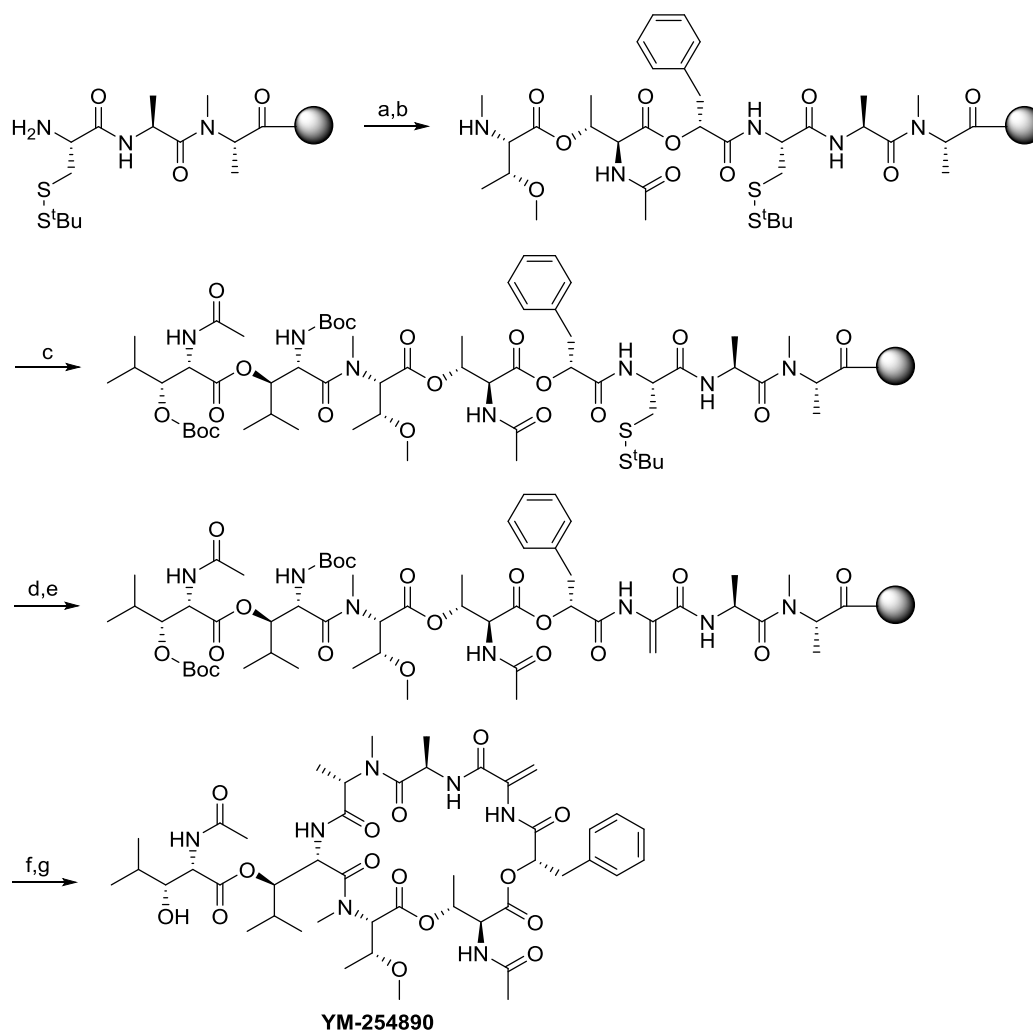


Figure 1.10. Structures of depsipeptide building blocks assembled via segment condensation.<sup>[63]</sup>



Scheme 1.7. Synthesis of YM-254890. a) **BB1**, HATU, collidine, DMF; b) Pd(PPh<sub>3</sub>)<sub>4</sub>, PhSiH<sub>3</sub>, N<sub>2</sub>, DCM; c) **BB2**, HATU, collidine, DMF; d) DTT, DIEA, DMF; e) 1,4-dibromobutane, K<sub>2</sub>CO<sub>3</sub>, DMF; f) TFA–TIS–DCM (19:0.5:0.5 v/v); g) HATU, collidine, DMF. Overall 1.5% yield.<sup>[63]</sup>

## 1.2 Objectives of chapter 1

1. Development of a robust Fmoc-based solid-phase methodology for the preparation of complex cyclodepsipeptides that are composed of  $\beta$ -branched residues and hold multiple and consecutive ester bonds. For that, a synthetic analogue of cyclodepsipeptide YM254890 was designed as a model of study.
2. Based on the previously mentioned synthetic challenges, study of the common drawbacks encountered during solid-phase depsipeptide synthesis, which include (i) problematic Fmoc protecting group removal due to DKP formation and  $\alpha,\beta$ -elimination side-reactions, and (ii) selection of the appropriate protecting group scheme for residue incorporation.
3. Comparison of the developed fully stepwise solid-phase strategy with traditional segment condensation approaches.

## 1.3 Results and discussion

### 1.3.1 Design of a model depsipeptide inspired by YM-254890

Combined solid-phase and solution chemistry approaches are widely used for the preparation of synthetically challenging depsipeptides containing multiple ester bonds.<sup>[58–61]</sup> An exclusive solid-phase Fmoc-based stepwise strategy for the synthesis of depsipeptides would become a valuable tool to access large quantities of naturally-occurring depsipeptides. Moreover, residue modification within the depsipeptide backbone would allow rapid and straightforward generation of numerous analogues for structure-activity relationship purposes. Other advantages of solid-phase synthesis include convenient purification after each step by simple washing and filtration processes, and stepwise incorporation of orthogonally protected amino acids and hydroxy acid monomer units.<sup>[80]</sup> The use of commercially available reagents such as Fmoc or TBDMS protected amino and hydroxy acids, respectively, would be extremely useful to avoid building block preparation in solution.

In sight of these advantages, we wished to address the problems mentioned earlier in this chapter in order to develop a versatile Fmoc-based solid-phase strategy for the synthesis of complex depsipeptides containing multiple and consecutive ester bonds.

Inspired by the structure complexity and features of naturally-occurring depsipeptide YM-254890<sup>[92]</sup>, we herein propose compound **1.1** (Figure 1.11), a simpler synthetic analogue of YM-254890, as a model peptide to address our research. The first logical modification was replacement of the two  $\beta$ -HyLeu residues by two Thr residues. Higher coupling rates were expected due to the less steric hindered environment provided by the Thr residues. Additionally, many commercially available Thr derivatives can be purchased at lower prices than  $\beta$ -HyLeu derivatives, which makes the present methodological study more viable. On the other hand, it is worth mentioning the additional synthetic complexity given by the dehydroalanine moiety, which must be introduced at a late stage of the synthesis to avoid Michael addition secondary reactions. In most cases, a masked residue is incorporated within the peptide sequence

and later converted to the corresponding dehydroalanine residue.<sup>[99–101]</sup> Selection of an orthogonal protecting group for the precursor of the L-N-Me-Dha residue would lead to an even more limited selection of available protecting groups for hydroxyl functionalities. Thus, replacement of L-N-Me-Dha by a likewise residue could facilitate the synthesis of the model depsipeptide analogue. Pro was a good candidate, since both L-N-Me-Dha and Pro are secondary amines and confer structure rigidity to the peptide backbone.

The sequence modifications proposed above preserve the synthetic challenges of YM-254890. The synthetic complexity conferred by the presence of two consecutive ester bonds and the overall chemical diversity provided by the depsipeptide, allowed Fmoc removal studies after ester bond formation upon diverse chemical environments. Additionally, optimal Fmoc elimination conditions to fully prevent or minimise DKP formation, the low reactivity associated with the Ac-Thr residue and selection of the optimal protecting group scheme were also studied.

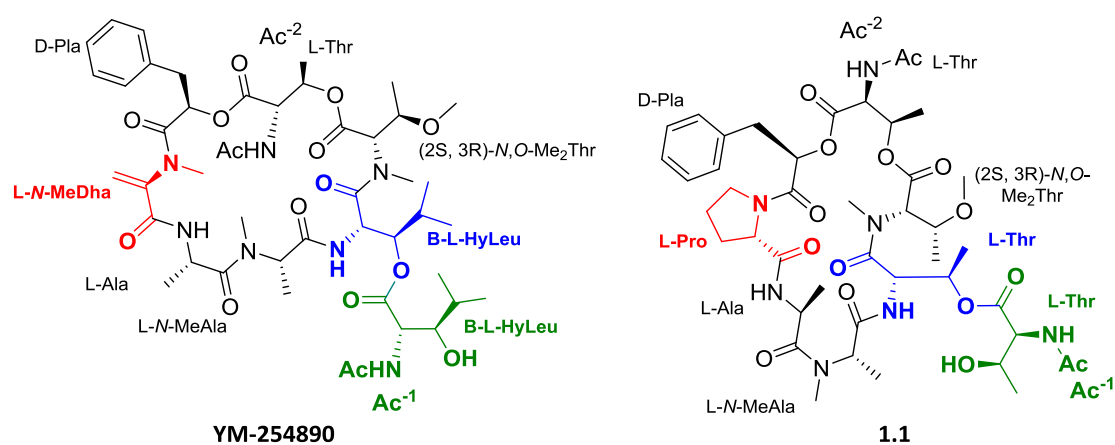


Figure 1.11. Chemical structure of YM-254890 and model depsipeptide 1.1.

### 1.3.2 Development of a fully solid-phase stepwise strategy

#### 1.3.2.1 General synthetic considerations and retrosynthetic analysis

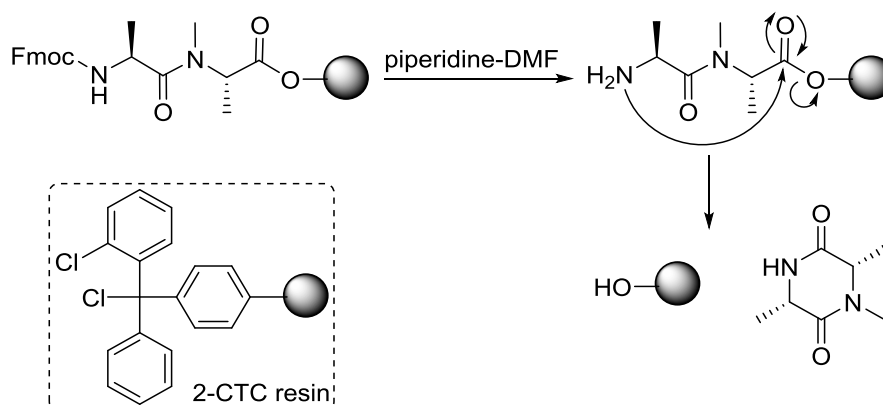
The key to a smart design of the synthetic strategy is based on the prediction of possible undesired reactions that are likely to occur.



functionalities. Stability of the ester linkages and racemisation were carefully considered along the synthesis.

### 1.3.2.1.2 DKP formation

As mentioned earlier in this chapter, a prevalent drawback in peptide synthesis is DKP formation during Fmoc removal, which ultimately leads to lower yields due to dipeptide loss.<sup>[37–42,80]</sup> Upon Fmoc removal of the second residue, the free amine can attack the carbonyl function to form the corresponding hexacyclic product (Scheme 1.9). DKP formation is also observed at the second position following the ester linkage. *N*-alkyl, Proline or D-amino acids are likely to adopt *cis* conformation and therefore DKP formation is specially favoured.<sup>[37–42,80]</sup> The following measures can be considered to diminish dipeptide loss: (i) the use of a steric hindered resin,<sup>[81]</sup> i.e. the 2-CTC resin (structure shown in Scheme 1.9); (ii) shortening the usual piperidine–DMF (1:4 v/v) treatment;<sup>[83]</sup> (iii) use other bases such as DBU or TBAF instead of piperidine.<sup>[84,85]</sup> DKP formation is highly sequence-dependent, and it was of special interest the percentage of DKP formed in the present system.



Scheme 1.9. DKP formation mechanism and structure of the 2-CTC resin.

### 1.3.2.1.3 Polymeric support

Solid-phase peptide synthesis was used for the chain elongation of the target molecule, being the 2-chlorotrityl (2-CTC or Barlos) resin the most suitable for the designed strategy. The Barlos resin is frequently used, since it minimises the most common drawbacks in peptide synthesis such as DKP formation and racemisation during incorporation of the first amino acid.<sup>[103]</sup> While other resins require stronger acidic

conditions when cleaving the peptide chain from the resin, the 2-CTC resin allows cleavage under very mild conditions such as 25% of HFIP or 1–2% of TFA. Moreover, the 2-CTC resin renders the C-terminus as a free carboxylic acid functionality, acting as protecting group of this moiety. The loading of the resin must be outlined previous to the first amino acid incorporation, and it is defined as mmol of functional groups per grams of resin. The loading values for common peptides range from 0.5–0.8 mmol/g resin, whereas a lower substitution level (0.1–0.2 mmol/g resin) is recommended to avoid aggregation problems during the synthesis of long or challenging peptides.<sup>[104]</sup> In this particular case, the loading was set up to 0.7 mmol/g resin.

#### 1.3.2.1.4 Macrolactamisation

Macrolactamisation carries significant importance when designing the synthetic strategy,<sup>[105–107]</sup> and therefore the cyclisation site must be chosen carefully according to several well-known rules. Sterically hindered amino acids such as *N*-alkyl,  $\alpha,\alpha$ -disubstituted or  $\beta$ -branched amino acids must be avoided at the *N*-terminus to obtain enhanced reactivity and minimised epimerisation rates.<sup>[108]</sup> High dilution conditions are essential to favour intramolecular cyclisation and prevent polymerisation.<sup>[109]</sup> Whereas ester bonds are easily hydrolysed, it is well known that amide bonds are stable, consequently, cyclisation must be undertaken by an amide bond if possible.<sup>[108]</sup> Following the above considerations, the preferred disconnection site for compound **1.1** was between the *N*-terminal L-Thr and C-terminal *N*-Me-Ala.

#### 1.3.2.1.5 Peptide chain elongation

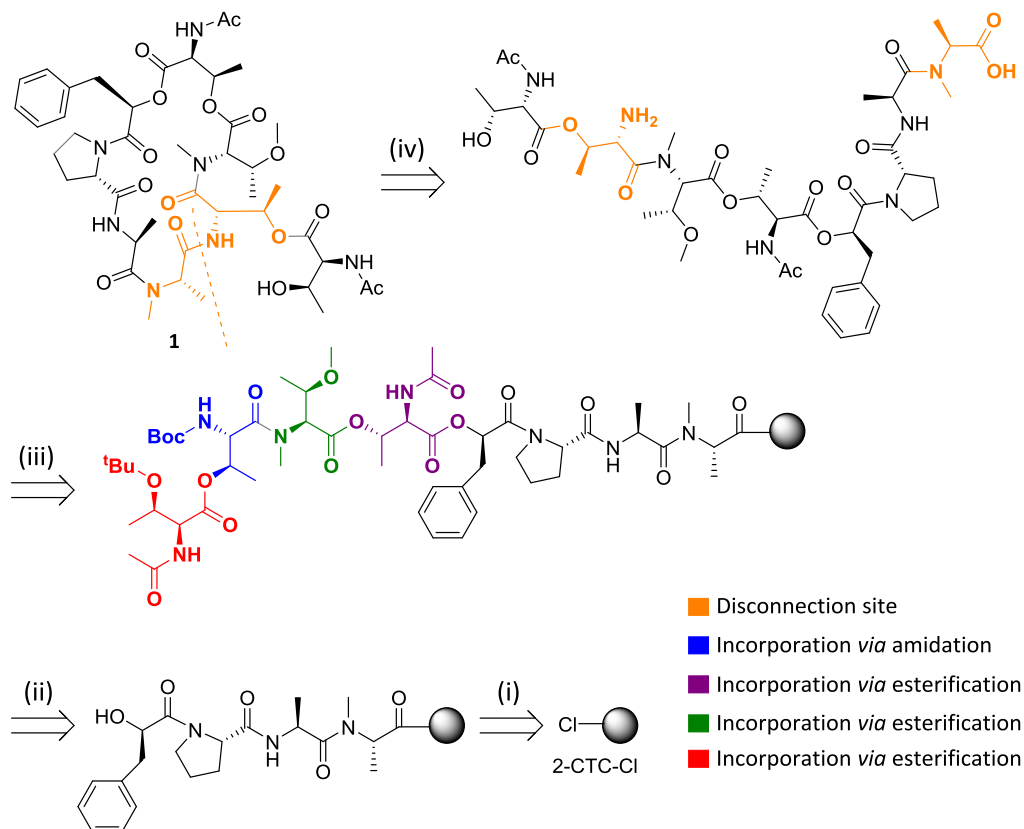
The peptide chain elongation consisted of coupling and deprotection repetitive cycles using the well-known Fmoc/<sup>t</sup>Bu strategy. Couplings were carried out using the AA–DIC–OxymaPure (3:3:3 eq) system, in which the residue was incorporated upon mild and neutral conditions, hence preventing epimerisation. Strong coupling conditions were required for residue incorporation onto secondary amines, which present a lower reactivity compared to primary amines. Couplings onto secondary amines such as Pro or *N*-methyl amino acids were performed using the AA–HATU–HOAt–DIEA (3:3:3:6 eq) system.<sup>[79]</sup>

### 1.3.2.1.6 Solid-phase reaction monitoring

Difficult steps during the synthesis of the target compound were monitored by acidolytic cleavage of a small aliquot of the peptidyl-resin using a mixture of HFIP–DCM (1:4 v/v) as cleavage cocktail during 45 min. The sample was subjected to HPLC-MS analysis.

### 1.3.2.1.7 Retrosynthetic analysis

The retrosynthetic analysis is herein described (Scheme 1.10). The general approach for the synthesis was a head-to-side-chain cyclisation once the depsipeptide linear chain was fully assembled on solid-phase. The peptide chain elongation (Scheme 1.10, (i)) was performed on solid-phase using the well-known Fmoc/<sup>t</sup>Bu strategy.



**Scheme 1.10.** Retrosynthetic analysis to prepare compound **1.1** using a fully stepwise strategy. (i) Chain elongation; (ii) Stepwise incorporation of the residues through amidation and esterification reactions; (iii) cleavage and global deprotection; (iv) Cyclisation.

As mentioned earlier, L-N-MeAla was the starting point of the linear chain elongation. A fully stepwise strategy was used for residue incorporation (Scheme 1.10,

(ii)) through both esterification and amidation reactions, followed by the corresponding deprotection step. Cleavage and global deprotection (Scheme 1.10, (iii)) rendered the linear depsipeptide chain. Lastly, head-to-side-chain cyclisation (Scheme 1.10, (iv)) was performed in solution.

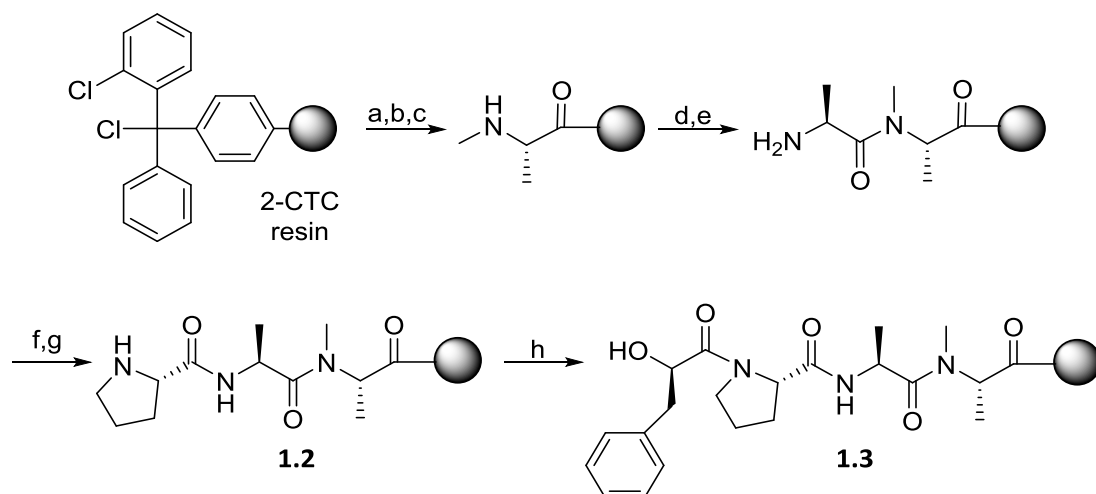
### 1.3.2.2 Synthesis of the linear precursor of cyclodepsipeptide **1.1**: Ac-Thr(O(H<sub>2</sub>N-Thr(O(Ac-Thr(OH)-CO))-Fmoc-N,O-Me<sub>2</sub>Thr-CO))-COO-D-Pla-Pro-Ala-N-MeAla-COOH

#### 1.3.2.2.1 Peptide chain elongation

The starting point of the synthesis was addition of commercially available Fmoc-MeAla-OH onto the resin by standard means through a nucleophilic attack of the carboxylate form of the corresponding Fmoc-protected amino acid to form an ester bond (Scheme 1.11). The real substitution level was determined by Fmoc UV quantification at  $\lambda = 290$  nm, being 0.70 mmol/g resin the experimental functionalisation.

The second residue, Fmoc-Ala-OH, was added to the resin under basic conditions using HATU–HOAt–DIEA as coupling reagents.<sup>[79]</sup> HPLC-MS analysis of the crude cleavage peptidyl-resin showed coupling completion. At this point of the synthesis, DKP formation was likely to occur during Fmoc protecting group elimination, and therefore the optimal Fmoc removal conditions to minimise DKP formation were studied. The obtained results are described in the following section (see section 1.3.2.2.2).

Incorporation of the third residue, Fmoc-Pro-OH, was carried out under neutral conditions using DIC–OxymaPure as coupling reagents. The Kaiser test was used to ensure full residue incorporation. Addition of D-Phenyllactic acid onto Pro was successfully accomplished using the HATU–HOAt–DIEA coupling system. Tetrapeptide formation was analysed by HPLC-MS analysis, being the peptidyl-resin **1.3** obtained as a single product.

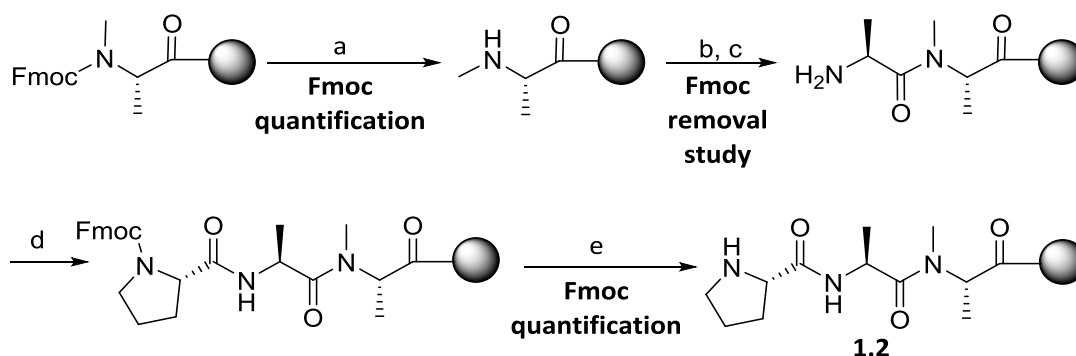


**Scheme 1.11.** Tetrapeptide chain elongation of **1.3** using the Fmoc/<sup>t</sup>Bu strategy. a) Fmoc-MeAla-OH (0.7 eq), DIEA (10 eq), DCM, 50 min; b) MeOH (800  $\mu$ L/g resin), 10 min; c) Piperidine-DMF (1:4 v/v) (1 x 1 min + 2 x 10 min); d) Fmoc-Ala-OH (3 eq), HATU (3 eq) HOAt (3 eq), DIEA (3 eq), DMF, 1 h; e) 0.1M HOBt in DBU-DMF (2:98 v/v) (2 x 1 min); f) Fmoc-Pro-OH (3 eq), OxymaPure (3 eq), DIC (3 eq), DMF, 40 min; g) Piperidine-DMF (1:4 v/v) (1 x 1 min + 2 x 5 min); h) D-Phenyllactic acid (3 eq), HATU (3 eq) HOAt (3 eq), DIEA (3 eq), DMF, 1 h.

#### 1.3.2.2.2 Study of the optimal Fmoc removal conditions to minimise DKP formation

As mentioned earlier, DKP formation is highly sequence-dependent. Considering that our model desipeptide holds an *N*-MeAla-OH residue at the C-terminal position, this sequence was expected to undergo DKP formation. A good approach to determine the extension of this secondary reaction is to estimate the resin loading after the third residue incorporation and compare it to the substitution level after the first amino acid incorporation. A dramatic decrease in this value implies dipeptide loss due to DKP formation. In this context, the loading level was determined after the first and third residue incorporation by Fmoc UV quantification of the dibenzofulvene-piperidine adduct formed during Fmoc removal at  $\lambda = 290$  nm (Scheme 1.12).

The six tested conditions for Fmoc removal of the second residue are summarised in Table 1.2. In all cases, a quick treatment (2 x 1 min), shorter than the conventional procedure, was performed. Removal of the Fmoc group with the usual piperidine-DMF (1:4 v/v) cocktail led to 18% of DKP formation (see entry #1 in Table 1.2). An improvement was observed when a DBU-DMF (2:98 v/v) solution was used instead, being 11% the chain loss (see entry #2 in Table 1.2).



*Scheme 1.12.* Study of the optimal Fmoc removal conditions to minimise DKP formation. a) Piperidine–DMF (1:4 v/v) (1 x 1 min + 2 x 10 min); b) Fmoc-Ala-OH (3 eq), HATU (3 eq) HOAt (3 eq), DIEA (3 eq), DMF, 1 h; c) **Evaluation of the best conditions to remove the Fmoc group** (see Table 1.2); d) Fmoc-Pro-OH (3 eq), OxymaPure (3 eq), DIC (3 eq), DMF, 40 min; e) Piperidine–DMF (1:4 v/v) (1 x 1 min + 2 x 5 min).

Addition of small percentages of organic acids, such as HOBt or OxymaPure, to both the piperidine and the DBU solutions proved effective to diminish aspartimide formation during Fmoc removal treatments.<sup>[83,87,88]</sup> In an attempt to minimise DKP formation, a source of protons was added to both cocktail mixtures (piperidine and DBU) to partially neutralise the base. Thus, the peptidyl-resin was treated with a solution of 0.1 M HOBt in piperidine–DMF (1:4 v/v) and a solution of 0.1 M OxymaPure in piperidine–DMF (1:4 v/v), and a dipeptide loss of 15% and 23% was observed, respectively (see entries #3-4 in Table 1.2). Treatment with a solution of 0.1 M HOBt in DBU–DMF (2:98 v/v) and a solution of 0.1M OxymaPure in DBU–DMF (2:98 v/v) resulted in 5% and 15% of DKP formation, respectively (see entries #5-6 in Table 1.2). Addition of OxymaPure to the piperidine–DMF (1:4 v/v) and DBU–DMF (2:98 v/v) cocktails did not exert a positive effect on the deprotection outcome.

Remarkably, Fmoc removal of the second residue with a 0.1 M HOBt in DBU–DMF (2:98 v/v) (2 x 1 min) solution seemed to be the most effective treatment, resulting in a small DKP formation compared to the DKP formed when using the traditional piperidine–DMF (1:4 v/v) or the alternative DBU–DMF (2:98 v/v) treatments. In fact, the 6% difference between 0.1 M in HOBt DBU–DMF (2:98 v/v) (2 x 1 min) and DBU–DMF (2:98 v/v) (2 x 1 min) might be comprised within the Fmoc UV quantification method error, and therefore it is not certain whether there was an actual DKP formation

decrease. However, these optimised conditions (0.1 M in HOBt DBU–DMF (2:98 v/v) (2 x 1 min)) become a good alternative to considerably reduce the undesired side-reaction.

| #        | Fmoc removal conditions of the second residue           | Loading (1 <sup>st</sup> AA Fmoc quantification) | Loading (3 <sup>rd</sup> AA Fmoc quantification) | DKP formation (%) |
|----------|---|--|--|-------------------|
| 1        | Piperidine–DMF (1:4 v/v) (2 x 1 min)                    | 0.65 mmol/g                                      | 0.57 mmol/g                                      | 18                |
| 2        | DBU–DMF (2:98 v/v) (2 x 1 min)                          | 0.66 mmol/g                                      | 0.59 mmol/g                                      | 11                |
| 3        | 0.1 M HOBt in Piperidine–DMF (1:4 v/v) (2 x 1 min)      | 0.67 mmol/g                                      | 0.57 mmol/g                                      | 15                |
| 4        | 0.1 M OxymaPure in Piperidine–DMF (1:4 v/v) (2 x 1 min) | 0.66 mmol/g                                      | 0.51 mmol/g                                      | 23                |
| <b>5</b> | <b>0.1 M HOBt in DBU–DMF (2:98 v/v) (2 x 1 min)</b>     | <b>0.62 mmol/g</b>                               | <b>0.59 mmol/g</b>                               | <b>5</b>          |
| 6        | 0.1 M OxymaPure in DBU–DMF (2:98 v/v) (2 x 1 min)       | 0.62 mmol/g                                      | 0.53 mmol/g                                      | 15                |

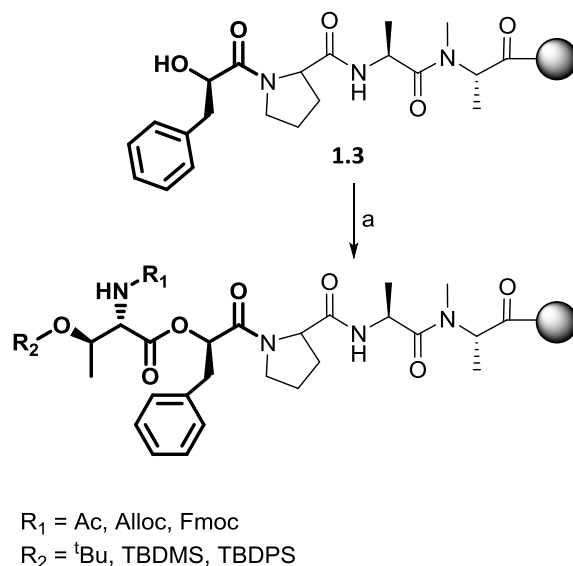
Table 1.2. Study of the optimal Fmoc removal conditions to minimise DKP formation.

### 1.3.2.2.3 Incorporation of the Ac-Thr-OH residue onto D-Pla-Pro-Ala-N-MeAla-CTC-resin (1.3)

Ester bond formation between the carboxylic acid of Ac-Thr-OH and the  $\alpha$ -hydroxyl group of D-phenyllactic acid was not foreseen facile. The  $\beta$ -hydroxyl moiety of the Thr residue must be protected to prevent polymerisation side-reactions. Selection of the alcohol protecting group entails significant importance, since the Barlos resin does not allow deprotection under acidic conditions. Moreover, the formed ester linkage must be stable to hydroxyl deprotecting conditions. On the basis of the above considerations, incorporation of the Thr derivative as Ac-Thr(Silyl)-OH turns into the smartest choice, since silyl groups are orthogonal to the Fmoc/tBu strategy and can be removed by treatment with TBAF.

However, Harveen *et al.* reported the low reactivity of the Ac-Thr(PG)-OH residue upon esterification conditions.<sup>[46]</sup> It was suggested that the acetyl moiety might deactivate the carbonyl function resulting in no residue incorporation. In order to develop a fully stepwise strategy, we studied this residue incorporation. The effect of the protecting group scheme on the esterification extent was evaluated by addition of

several Thr derivatives onto tetrapeptide **1.3** through the so-called Steglich esterification, which is readily used in depsipeptide synthesis and has proven effective in many cases (Scheme 1.13).<sup>[46,53,63,64]</sup> Accordingly, a series of Thr derivatives containing different amine and hydroxyl protecting groups were prepared and their reactivity was evaluated. Additionally, commercially available Thr derivatives were purchased and also tested.



*Scheme 1.13.* On-resin Steglich esterification of a series of Thr derivatives. a)  $R_1$ -Thr( $R_2$ )-OH (8 eq), DIC (8 eq), DMAP (0.5 eq), DCM–DMF (9:1 v/v), 35 °C, 2 h 30 min.

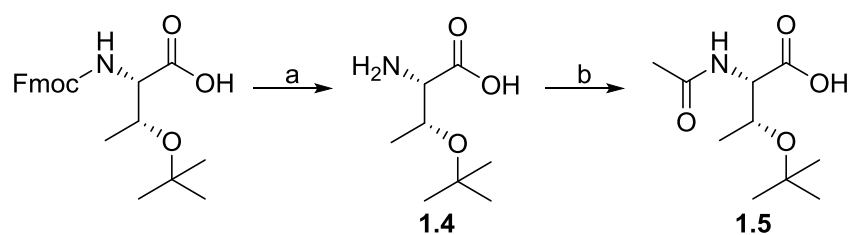
#### 1.3.2.2.3.1 Preparation of a series of $R_1$ -Thr( $t$ Bu)-OH derivatives using different amine protecting groups

As a first approach to considerably simplify the screening process,  $t$ Bu was selected as the hydroxyl functionality protecting group. On the other hand, three different orthogonal protecting groups (Fmoc, Ac and Alloc) for the  $\alpha$ -amino group of Thr were explored. Fmoc-Thr( $t$ Bu)-OH, which is readily used in peptide synthesis and can be purchased at low prices, was chosen as starting material for the rapid preparation Ac-Thr( $t$ Bu)-OH and Alloc-Thr( $t$ Bu)-OH.

##### Synthesis of Ac-Thr( $t$ Bu)-OH (**1.5**)

Fmoc-Thr( $t$ Bu)-OH was treated with a solution of  $\text{Et}_2\text{N}$ –DCM (4:6 v/v) and the resulting crude was purified with a C18 reversed-phase Porapak<sup>TM</sup> Rxn Cartridge, being

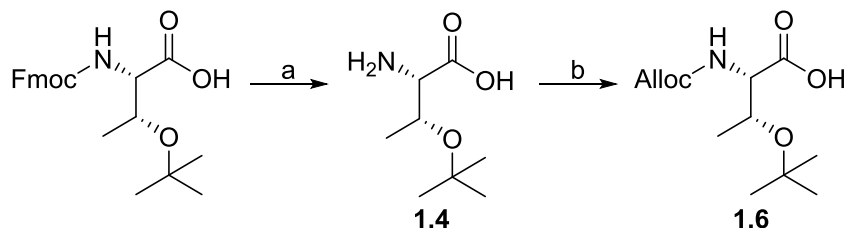
compound **1.4** obtained in good yields (85%) (Scheme 1.14). Compound **1.5** can be synthesised by amide bond formation between the free amine of **1.4** and AcOH using carbodiimide–DMAP as coupling system. EDC was the carbodiimide of choice, since the formed urea derivative can be washed away with acidic extractions and therefore the purification step can be avoided. The acetylation step allowed successful preparation of compound **1.5**, which was obtained in a quantitative yield and used without further purification.



*Scheme 1.14.* Synthesis of Ac-Thr(<sup>t</sup>Bu)-OH (**1.5**). a) Et<sub>2</sub>N–DCM (4:6 v/v), 25 °C, 4 h, 25 °C, 85%; b) AcOH (1 eq), EDC·HCl (1 eq), DIEA (1 eq), DMAP (0.1 eq), DCM–DMF (9:1 v/v), 25 °C, 3 h 30 min; Quantitative yield.

#### Synthesis of Alloc-Thr(<sup>t</sup>Bu)-OH (**1.6**)

This compound was synthesised by Alloc introduction after Fmoc removal of commercially available Fmoc-Thr(<sup>t</sup>Bu)-OH (Scheme 1.15). Traditional Alloc protection in solution through nucleophilic substitution of Alloc chloride (Alloc-Cl) can lead to dipeptide formation.<sup>[110]</sup> A common procedure used in our group to prevent this side-product formation is the one-pot reaction that proceeds through the Alloc azide (Alloc-N<sub>3</sub>) formation prior to nucleophilic attack of the amine.<sup>[110]</sup>



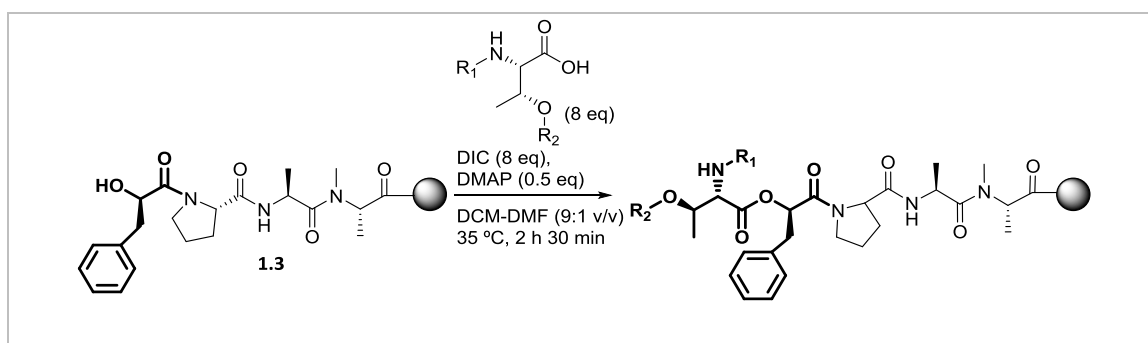
*Scheme 1.15.* Synthesis of Alloc-Thr(<sup>t</sup>Bu)-OH (**1.6**). a) Et<sub>2</sub>N–DCM (4:6 v/v), rt, 2 h, rt, 85%; b) Alloc-Cl (1 eq), NaN<sub>3</sub> (1.3 eq), H<sub>2</sub>O–Dioxane (1:1 v/v), rt, 18 h; Quantitative yield.

The poor leaving group character of the azide functionality allows milder substitution conditions and therefore successful protection of primary amines. Alloc-N<sub>3</sub>

was prepared *in situ*, followed by addition of H-Thr(<sup>t</sup>Bu)-OH (compound **1.4**) to afford the desired product **1.6** in a quantitative yield. **1.6** was used without further purification.

### 1.3.2.2.3.2 On-resin esterification using $R_1$ -Thr(<sup>t</sup>Bu)-OH derivatives with different amine protecting groups

With all the  $R_1$ -Thr(<sup>t</sup>Bu)-OH derivatives in hands, the on-resin Steglich esterification was studied. In all cases, the following incorporation conditions were used: AA–DIC–DMAP (8:8:0.5 eq), in which the carboxylic acid was pre-activated over 5 min prior to its on-resin incorporation, followed by addition of catalytic amounts of DMAP. All esterification reactions were performed at 35 °C under anhydrous conditions. The reaction was monitored by acidolytic cleavage of a small portion of the peptidyl-resin and subsequent HPLC-MS analysis of the resulting crude. Table 1.3 summarises the achieved results.



| # | Protected amino acid                          | R <sub>1</sub> | R <sub>2</sub>  | HPLC conversion (%) |
|---|---|----------------|-----------------|---------------------|
| 1 | Ac-Thr( <sup>t</sup> Bu)-OH ( <b>1.5</b> )    | Ac             | <sup>t</sup> Bu | 0                   |
| 2 | Alloc-Thr( <sup>t</sup> Bu)-OH ( <b>1.6</b> ) | Alloc          | <sup>t</sup> Bu | 0                   |
| 3 | Fmoc-Thr( <sup>t</sup> Bu)-OH                 | Fmoc           | <sup>t</sup> Bu | 100                 |

Table 1.3. Steglich esterification with different  $R_1$ -Thr(<sup>t</sup>Bu)-OH derivatives. HPLC data was processed at 220 nm.

#### On-resin esterification of Ac-Thr(<sup>t</sup>Bu)-OH (**1.5**) and Alloc-Thr(<sup>t</sup>Bu)-OH (**1.6**)

In an initial attempt to corroborate Harveen's hypothesis, tetrapeptide **1.3** was treated with Ac-Thr(<sup>t</sup>Bu)-OH (**1.5**) upon Steglich esterification conditions (see entry #1 in Table 1.3). Unfortunately, HPLC-MS analysis only showed one peak corresponding to the starting material (peptidyl-resin **1.3**). These results suggested that the acetyl group might deactivate the carbonyl function, thus hampering the on-resin esterification with

the conveniently acetylated Thr derivative. Hence, the amine function of the Thr derivative must be acetylated after residue incorporation. On the other hand, incorporation of Alloc-Thr(<sup>t</sup>Bu)-OH (**1.6**) gave the same unfortunate results, being 0% the esterification conversion (see entry #2 in Table 1.3).

#### On-resin esterification of Fmoc-Thr(<sup>t</sup>Bu)-OH: Initial Fmoc removal studies

To rapidly confirm whether the low reactivity was associated with the Thr residue itself or the amine protecting group, esterification with commercially available Fmoc-Thr(<sup>t</sup>Bu)-OH was carried out (see entry #3 in Table 1.3). Surprisingly, the esterification product (**1.7**, structure shown in Table 1.4) was obtained with a quantitative HPLC conversion according to HPLC-MS analysis (Figure 1.12A). These results suggest that the amine protecting group plays an important role in the reaction outcome. One would expect that both Alloc and Fmoc would lead to an equivalent esterification outcome, since the two protecting groups transform the amine into its carbamate form and therefore hold similar electron density at the N atom. Moreover, Alloc confers a less steric hindered environment than Fmoc, and therefore higher reactivity would be expected. However, Fmoc gave better results and was the only protecting group that afforded the desired esterification product so far.

With this promising result in hands, optimal Fmoc removal conditions of the model depsipeptide were extensively studied and are summarised in Table 1.4. In all cases, a short treatment of 1 min was performed and the deprotection efficiency was evaluated by HPLC-MS analysis. Although treatment of the peptidyl-resin with the conventional piperidine–DMF (1:4 v/v) cocktail over 1 min resulted in 95% of Fmoc removal to afford the desired product **1.8**, 54% of racemisation was observed by HPLC-MS analysis (see entry #1 in Table 1.4). In an attempt to optimise the elimination conditions, pentadepsipeptide **1.7** was treated with a DBU–DMF (2:98 v/v) solution resulting in complete Fmoc removal (see entry #4 in Table 1.4). Unfortunately, HPLC-MS analysis showed one broad peak indicating the presence of a racemic mixture. Remarkably, addition of small percentages of organic acids (HOBt or OxymaPure) to the Fmoc removal cocktail proved effective to diminish DKP formation (see section

1.3.2.2.2). Inspired by these results, we evaluated whether addition of HOBt and OxymaPure to the Fmoc removal cocktail could reduce racemisation of **1.8**.

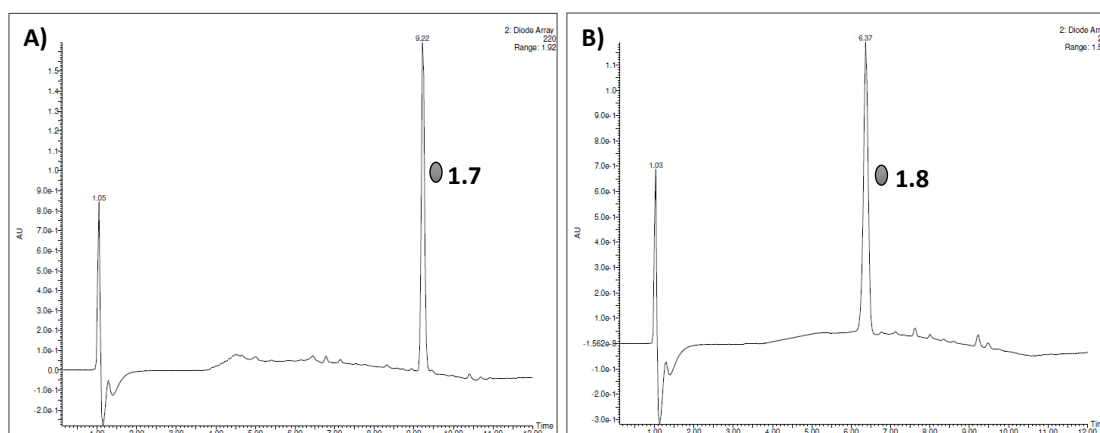


*Figure 1.12.* HPLC-MS chromatograms run at G0100t9T25 and processed at 220 nm (From now on G20100t9T25 stands for linear HPLC gradient from 20% to 100% of B over 9 min at 25 °C using as eluent system A: 0.045% TFA in H<sub>2</sub>O and B: 0.036% TFA in ACN). A) On-resin Steglich esterification between tetrapeptide **1.3** and Fmoc-Thr(<sup>t</sup>Bu)-OH to afford **1.7**; B) Fmoc removal of **1.7** with 0.1 M OxymaPure in a DBU–DMF (2:98 v/v) solution over 1 min to obtain **1.8**.

Treatment of the peptidyl-resin with a 0.1 M HOBt in piperidine–DMF (1:4 v/v) solution and a 0.2 M HOBt in piperidine–DMF (1:4 v/v) solution did not exert a positive effect on the racemisation extent (see entries #2-3 in Table 1.4). No Fmoc removal was observed when treating the peptidyl-resin with a 0.2 M HOBt in DBU–DMF (2:98 v/v) solution and a 0.2 M OxymaPure in DBU–DMF (2:98 v/v) solution (see #6 and #8 in Table 1.4). In this case, addition of an excess of the organic acids might result in complete DBU neutralisation, thus leading to no Fmoc elimination. Fmoc removal with a 0.1 M HOBt in DBU–DMF (2:98 v/v) solution was not effective, since 56% of racemisation was detected (see entry #5 in Table 1.4). Optimal Fmoc removal conditions were obtained using a 0.1 M OxymaPure in DBU–DMF (2:98 v/v) solution (see entry #7 in Table 1.4). In this case, all the starting material was successfully deprotected and racemisation of **1.8** was not observed by HPLC-MS analysis (Figure 1.12B).

Among all the tested conditions, stepwise introduction of the up to now unreactive Ac-Thr derivative as Fmoc-Thr(<sup>t</sup>Bu)-OH, and subsequent Fmoc removal with a 0.1 M OxymaPure in DBU–DMF (2:98 v/v) solution proved successful for the incorporation and subsequent deprotection of the named residue. A step further in the

development of a fully stepwise strategy for the preparation of **1.1** was made. Nevertheless, the <sup>t</sup>Bu protecting group was not orthogonal to the synthesis, and further studies with an orthogonal hydroxyl protecting group needed to be carried out.

**1.7**

↓ Fmoc removal assessment

**1.8**

| #        | Fmoc removal conditions                                  | Product/SM ratio               | Racemisation    |
|----------|--|--------------------------------|-----------------|
| 1        | Piperidine–DMF (1:4 v/v) (1 x 1 min)                     | <b>1.8/1.7</b><br>95:5         | 54%             |
| 2        | 0.1 M HOBT in Piperidine–DMF (1:4 v/v) (1 x 1 min)       | <b>1.8/1.7</b><br>95:5         | 60%             |
| 3        | 0.2 M HOBT in Piperidine–DMF (1:4 v/v) (1 x 1 min)       | <b>1.8/1.7</b><br>87:13        | Broad peak      |
| 4        | DBU–DMF (2:98 v/v) (1 x 1 min)                           | <b>1.8/1.7</b><br>100:0        | Broad peak      |
| 5        | 0.1 M HOBT in DBU–DMF (2:98 v/v) (1 x 1 min)             | <b>1.8/1.7</b><br>100:0        | 56%             |
| 6        | 0.2 M HOBT in DBU–DMF (2:98 v/v) (1 x 1 min)             | <b>1.8/1.7</b><br>0:100        | No Fmoc removal |
| <b>7</b> | <b>0.1 M OxymaPure in DBU–DMF (2:98 v/v) (1 x 1 min)</b> | <b>1.8/1.7</b><br><b>100:0</b> | <b>0%</b>       |
| 8        | 0.2 M OxymaPure in DBU–DMF (2:98 v/v) (1 x 1 min)        | <b>1.8/1.7</b><br>0:100        | No Fmoc removal |

*Table 1.4.* Study of the optimal Fmoc removal conditions to deprotect pentadepsipeptide **1.7**. The racemisation extent was determined by HPLC–MS analysis. HPLC data was processed at 220 nm.

### 1.3.2.2.3.3 Preparation of a series of Fmoc-Thr(R<sub>2</sub>)-OH derivatives using silyl protecting groups

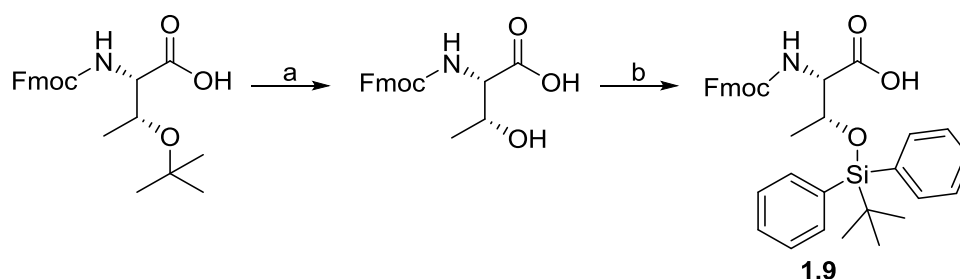
Once Fmoc was selected as the optimal protecting group for the amine moiety, evaluation of an appropriate protecting group for the hydroxyl function was carried out.

Silyl protecting groups can be selectively removed by treatment with catalytic fluorides such as TBAF. TBDMS removal can be carried out in the presence of acid-labile protecting groups.<sup>[54,111]</sup> Therefore, protection of the hydroxyl functionality with a silyl protecting group becomes a good approach to the synthesis. In this context, the hydroxyl group was protected with TBDMS and TBDPS, which allowed evaluation of the bulkiness effect on the esterification rates.

#### Synthesis of Fmoc-Thr(TBDPS)-OH (**1.9**)

Commercially available Fmoc-Thr(<sup>t</sup>Bu)-OH was treated with a TFA–DCM (6:4 v/v) mixture to afford Fmoc-Thr-OH. Introduction of the TBDPS group can be achieved by reaction of alcohol moieties with TBDPS-Cl using DBU as base (Scheme 1.16).<sup>[112]</sup>

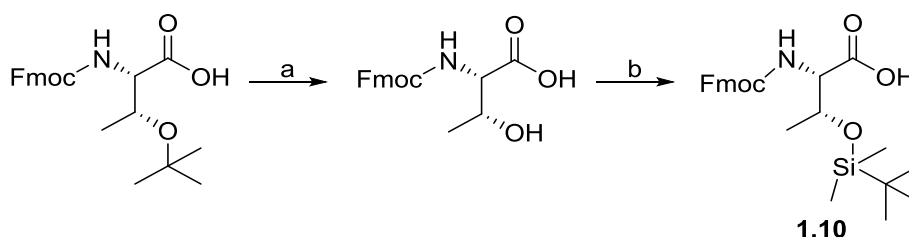
Protection of the hydroxyl group was monitored by HPLC-MS, being the SM/Product HPLC conversion 4:6. Although the reaction time and the reagents excesses were increased, a conversion improvement was not observed. The crude product was purified by flash chromatography on silica gel to afford pure **1.9** in a low yield (12%).



*Scheme 1.16.* Synthesis of Fmoc-Thr(TBDPS)-OH (**1.9**). a) TFA–DCM (6:4 v/v), 25 °C, 2 h, Quantitative yield; b) TBDPS-Cl (1.5 eq), DBU (1.5 eq), ACN, 0–20 °C, 20 h, 12%.

Synthesis of Fmoc-Thr(TBDMS)-OH (**1.10**)

Preparation of Fmoc-Thr(TBDMS)-OH started with <sup>t</sup>Bu removal of Fmoc-Thr(<sup>t</sup>Bu)-OH by treatment with a TFA–DCM (6:4 v/v) mixture. Protection of the hydroxyl group with TBDMS can be accomplished by treatment with TBDMS-Cl and imidazole (Scheme 1.17).<sup>[113]</sup> The reaction was monitored by HPLC-MS, being the SM/Product conversion 55:45. Full conversion was not accomplished, and compound **1.10** was obtained in a moderate yield (54%) after flash chromatography purification.



Scheme 1.17. Synthesis of Fmoc-Thr(TBDMS)-OH (**1.10**). a) TFA–DCM (6:4 v/v), 25 °C, 2 h, Quantitative yield; b) TBDMS-Cl (3 eq), imidazole (4 eq), DCM, 0-20 °C, 24 h, 54%.

#### 1.3.2.2.3.4 *On-resin esterification using Fmoc-Thr(R<sub>2</sub>)-OH derivatives containing silyl protecting groups*

With all Fmoc-Thr(R<sub>2</sub>)-OH derivatives in hands, the on-resin Steglich esterification was studied. In all cases, the following incorporation conditions were used: AA–DIC–DMAP (8:8:0.5 eq), in which the carboxylic acid was pre-activated over 5 min prior to its on-resin incorporation, followed by addition of catalytic amounts of DMAP. All esterification reactions were performed at 35 °C under anhydrous conditions. The reaction was monitored by HPLC-MS analysis of a small portion of the peptidyl-resin cleavage crude, and the obtained results are summarised in Table 1.5.

The outcome of the on-resin Steglich esterification with Fmoc-Thr(TBDPS)-OH (**1.9**) and Fmoc-Thr(TBDMS)-OH (**1.10**) was determined, and whereas incorporation of Fmoc-Thr(TBDPS)-OH resulted in failed attempts to introduce the Thr derivative (see entry #1 in Table 1.5), incorporation of Fmoc-Thr(TBDMS)-OH was successfully achieved with a quantitative incorporation yield (determined by HPLC see entry #2 in Table 1.5 and Figure 1.13A). These results suggest that the steric hindrance provided by the bulky TBDPS group might hamper the esterification reaction between D-Pla and the Thr

derivative. Although incorporation of Fmoc-Thr(TBDMS)-OH was a good starting point, further studies on TBDMS and Fmoc removal optimal conditions needed to be carried out.

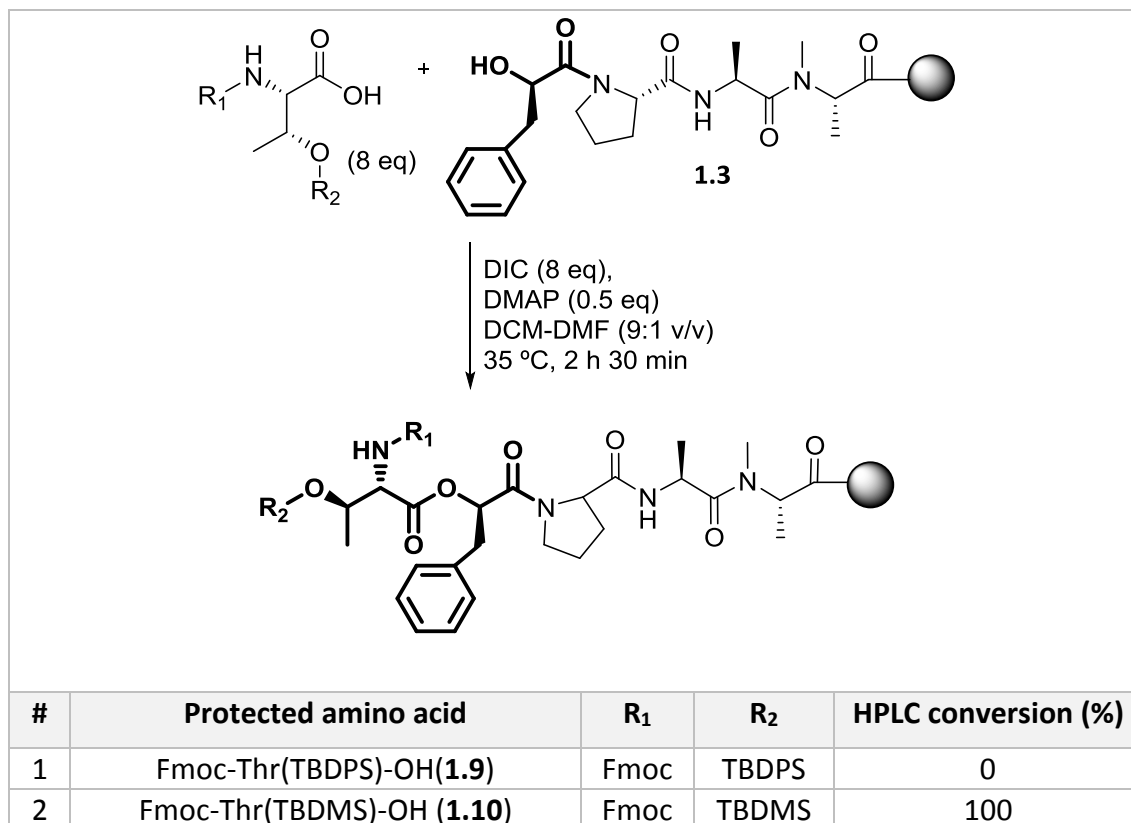
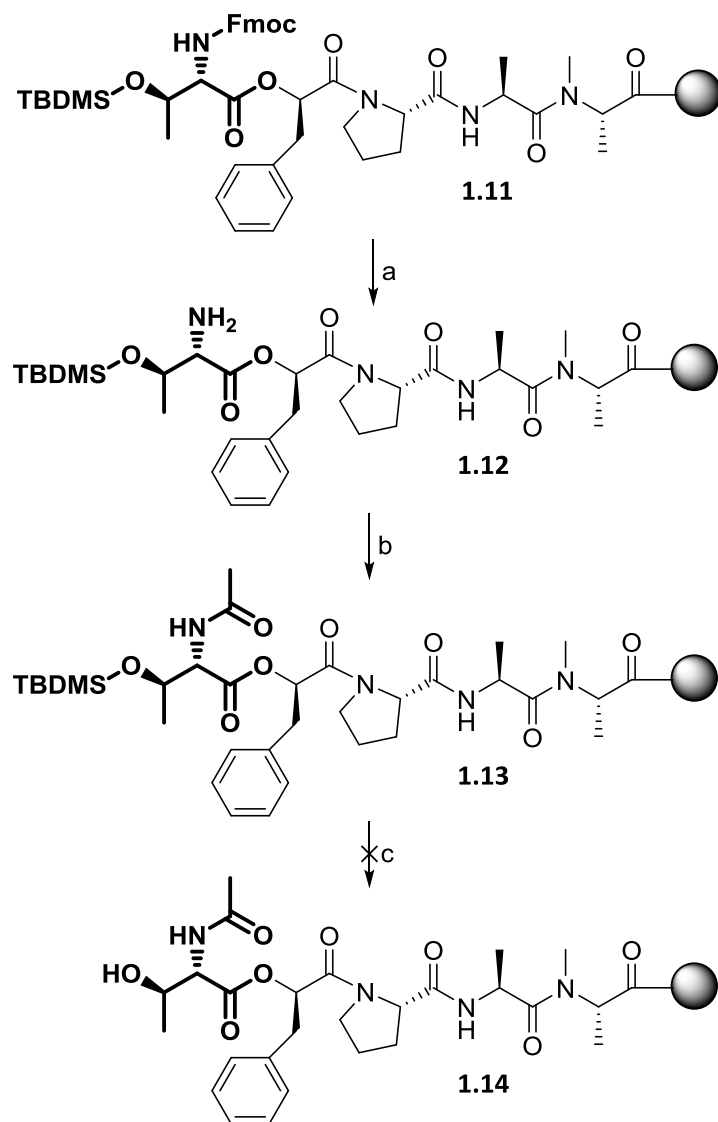


Table 1.5. Steglich esterification of Fmoc-Thr(R<sub>2</sub>)-OH derivatives to study the reactivity of the Ac-Thr-OH esterification reaction. HPLC data was processed at 220 nm.

#### 1.3.2.2.3.5 Fmoc and TBDMS removal studies of Fmoc-Thr(TBDMS)-COO-D-Pla-Pro-Ala-N-MeAla-CTC-resin (**1.11**)

Initial attempts to remove Fmoc and TBDMS of **1.11** are described in Scheme 1.18. The first step consisted of Fmoc elimination with the already optimised conditions (treatment with a 0.1 M OxymaPure in DBU-DMF (2:98 v/v) solution for 1 min). The corresponding unprotected depsipeptide (**1.12**, Figure 1.14) was detected by HPLC-analysis of a small portion of the peptidyl-resin cleavage crude (Figure 1.13B). Subsequent acetylation with the AcOH-OxymaPure-DIC (3:3:3 eq) coupling system afforded the acetylated derivative (**1.13**) in good HPLC yields (Figure 1.13C).



*Scheme 1.18.* Initial attempts to remove Fmoc and TBDMS of **1.11**. a) 0.1 M OxymaPure in a DBU-DMF (2:98 v/v) solution (1 x 1 min); b) AcOH (3 eq), OxymaPure (3 eq), DIC (3 eq), DMF, rt, 30 min; c) 1.0 M TBAF in THF (1 eq), 10 min, N<sub>2</sub> atm., 25 °C.

Next, stability of the ester linkage upon TBDMS removal conditions was evaluated. The peptidyl-resin **1.13** was treated with a 1.0 M TBAF solution in THF under anhydrous conditions for 10 min. Unfortunately, treatment of the peptidyl-resin with TBAF failed to afford the desired product (**1.14**), and depsipeptide fragmentation was observed instead. According to HPLC-MS analysis, one single product corresponding to starting material **1.3** was detected, thus indicating Ac-Thr-OH residue loss. We hypothesise that the acetyl function is responsible for **1.13** instability upon TBDMS removal conditions, triggering ester linkage fragmentation.

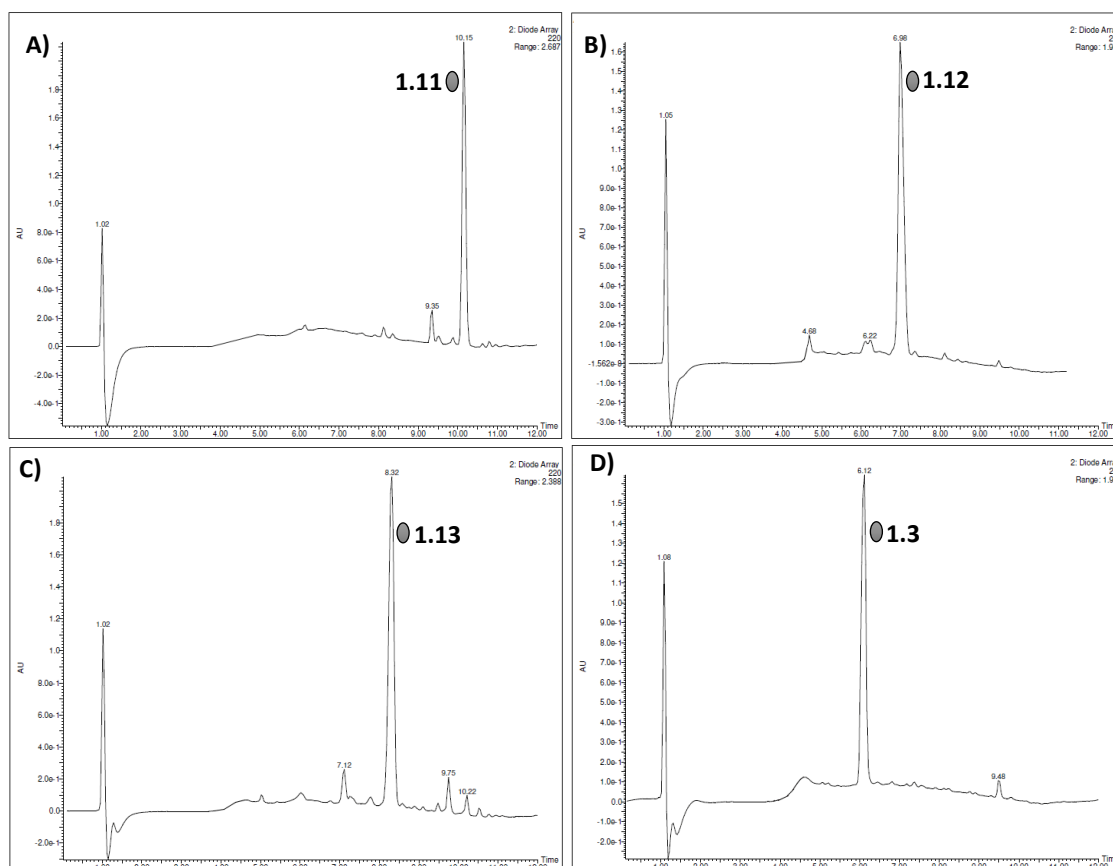
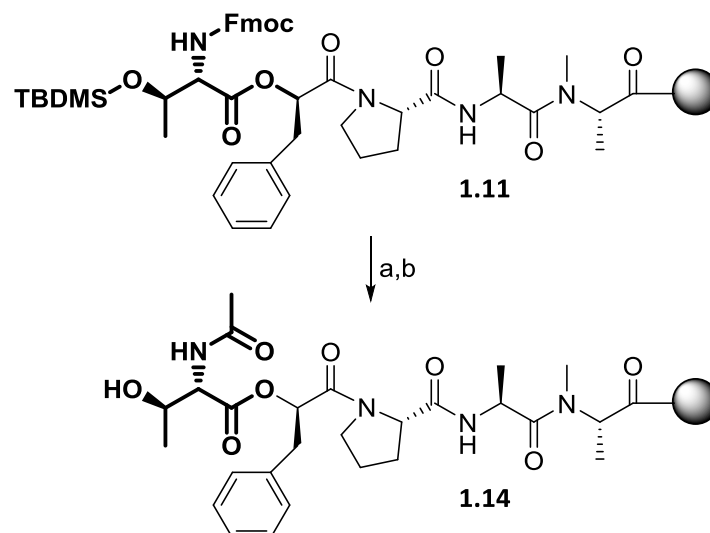


**Figure 1.13.** HPLC-MS chromatograms run at G0100t9T25 and processed at 220 nm. A) On-resin Steglich esterification between tetrapeptide **1.3** and Fmoc-Thr(TBDMS)-OH to afford **1.11**; B) Fmoc removal of **1.11** with 0.1 M OxymaPure in a DBU–DMF (2:98 v/v) solution over 1 min to obtain **1.12**, C) Amine acetylation to afford **1.13**; D) Treatment of **1.13** with a 1.0 M TBAF in THF (1 eq) solution over 10 minutes.

In order to avoid depsipeptide fragmentation, TBDMS removal prior to amine acetylation was attempted with the peptidyl-resin **1.11**. This strategy led to partial elimination of the Fmoc and TBDMS protecting groups.

Although piperidine is generally used for Fmoc removal, TBAF has proven useful to obtain the unprotected amine function.<sup>[54,111]</sup> Taking advantage of this and in order to avoid one deprotection step, we explored simultaneous Fmoc and TBDMS removal using TBAF. Thus, **1.11** was treated with a 1.0 M TBAF solution in THF for 10 min under anhydrous conditions (Scheme 1.19). We were happy to observe simultaneous Fmoc and TBDMS removal, being intermediates **1.15** and **1.16** formed (Figure 1.14A). Moreover, fragmentation of the ester linkage was not observed. An additional TBAF treatment was required to fully remove both protecting groups.



*Scheme 1.19.* Simultaneous Fmoc and TBDMS removal of **1.11** to afford pentadepsipeptide **1.3**. a) 1.0 M TBAF in THF (1 eq), 10 min, N<sub>2</sub> atm., 25 °C, this step was repeated twice; b) AcOH (3 eq), OxymaPure (3 eq), DIC (3 eq), DMF, 25 °C, 40 min.

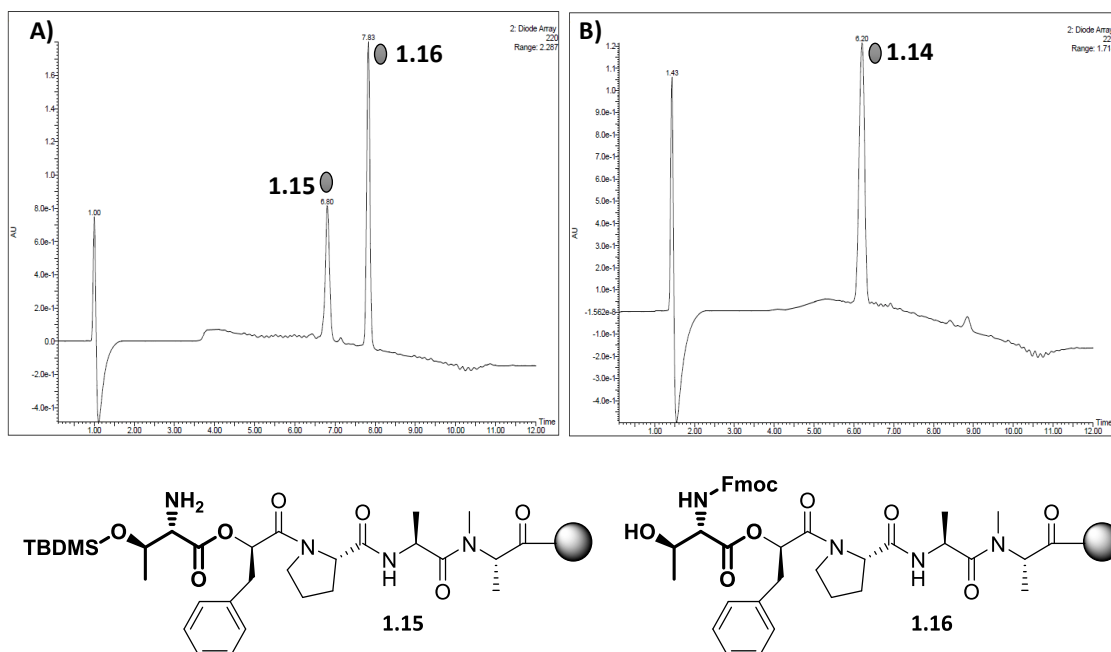


*Figure 1.14.* HPLC-MS chromatograms run at G0100t9T25 and processed at 220 nm. A) First treatment of pentadepsipeptide **1.11** with a 1.0 M TBAF in THF (1 eq) solution over 10 minutes; B) Acetylated and unprotected pentadepsipeptide **1.14**.

#### 1.3.2.2.3.6 Summary of the Ac-Thr-OH residue incorporation

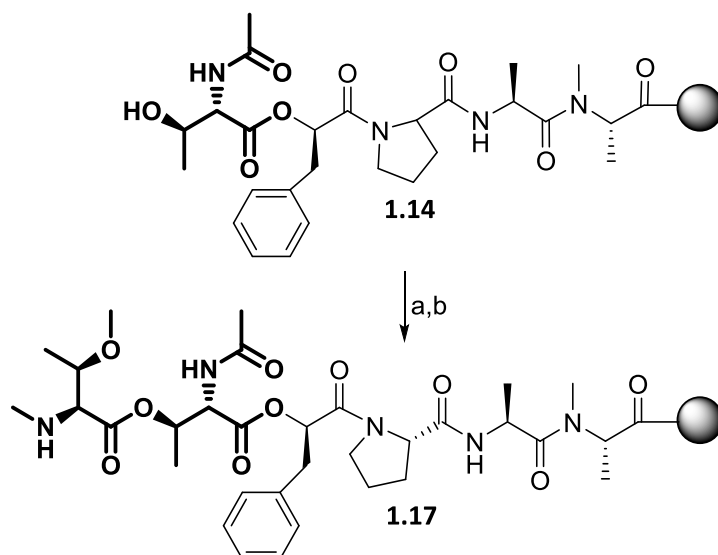
A step further in the development of a fully-stepwise strategy was made. We were able to introduce the until now unreactive Ac-Thr-OH derivative in a stepwise manner. Furthermore, the derivative was provided with appropriate and orthogonal

protecting groups for the amine and the hydroxyl functions (Fmoc and TBDMS, respectively). Optimal protecting group removal conditions and subsequent acetylation of the amine group were studied, being Fmoc and TBDMS simultaneously removed by treatment with TBAF.

#### 1.3.2.2.4 Incorporation of the *N,O*-Me<sub>2</sub>Thr residue onto Ac-Thr(OH)-COO-D-Pla-Pro-Ala-N-MeAla-CTC-resin (1.14) and subsequent Boc-Thr-OH incorporation

Although on-resin esterification of the *N*-protected *N,O*-Me<sub>2</sub>Thr residue is foreseen facile, selection of the appropriate protecting group for the amine function is not straightforward. Previous attempts reported in the literature to remove the Fmoc protecting group failed to afford the unprotected product due to undesired  $\alpha,\beta$ -elimination at the *N*-Ac-Thr residue.<sup>[46,63]</sup> In fact, only traces of the desired unprotected product could be obtained.

Attempts to circumvent this major drawback were carried out and are described in the present section. Furthermore, assembly of this residue with the amine functionality protected with Alloc was also carried out, and the best incorporation conditions were determined (Scheme 1.20).

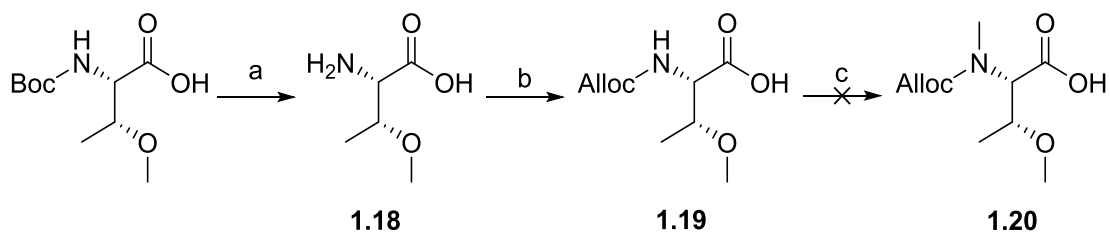


Scheme 1.20. Assembly of *N,O*-Me<sub>2</sub>Thr-OH through on-resin Steglich esterification. a) Steglich esterification of R<sub>1</sub>-*N,O*-Me<sub>2</sub>Thr-OH; b) Amine protecting group removal.

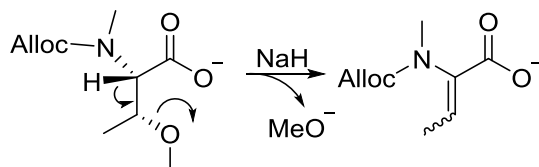
1.3.2.2.4.1 Preparation of Alloc-*N,O*-Me<sub>2</sub>Thr-OH and Fmoc-*N,O*-Me<sub>2</sub>Thr-OHPreparation of Alloc-*N,O*-Me<sub>2</sub>Thr-OH (1.20)

As a first approach to synthesise building block **1.20**, the three-step synthesis of Alloc-*N,O*-Me<sub>2</sub>Thr-OH was attempted (Scheme 1.21). Boc removal from commercially available Boc-Thr(Me)-OH was successfully accomplished by treatment with TFA. Again, the Alloc-azide (Alloc-N<sub>3</sub>) intermediate was used to avoid dipeptide formation during Alloc protection of the free amine.<sup>[110]</sup> Alloc-N<sub>3</sub> preparation *in situ*, followed by addition of H-Thr(Me)-OH (**1.18**) afforded the desired product (**1.19**) in a quantitative yield.

Benoiton and coworkers first reported the selective *N*-methylation procedure with MeI and NaH in the presence of free carboxyl groups.<sup>[114]</sup> The high selectivity is attributed to the protection of the carboxylate by chelation to Na<sup>+</sup> ions.<sup>[115]</sup> The reaction must be performed under anhydrous atmosphere. Although amino acid **1.19** was successfully *N*-methylated, the methoxide group underwent elimination due to the high basicity provided by NaH (Scheme 1.22). According to <sup>1</sup>H-NMR and HPLC-MS analysis, the corresponding β-elimination undesired product was obtained instead.



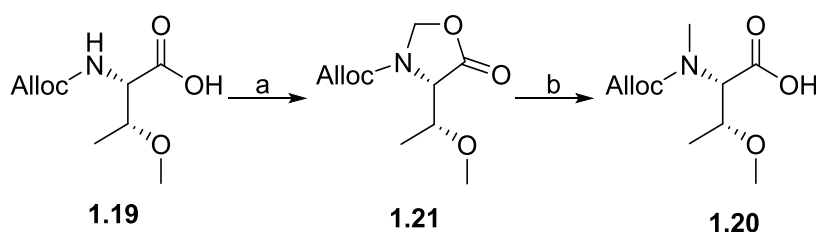
Scheme 1.21. Attempts to prepare Alloc-*N,O*-Me<sub>2</sub>Thr-OH (**1.20**). a) TFA–DCM (4:6 v/v), 25 °C, 2h, Quantitative yield; b) Alloc-Cl (1 eq), NaN<sub>3</sub> (1.3 eq), H<sub>2</sub>O–Dioxane (1:1 v/v), rt, 18 h; 97%.; c) MeI (4 eq), NaH (3 eq), THF, 0 °C, 8 h, β-elimination.



Scheme 1.22. Formation of the β-elimination side-product during *N*-methylation of **1.19** with MeI and NaH.

A good alternative to overcome elimination is the preparation of the *N*-methylated amino acid *via* the 5-oxazolidine intermediate.<sup>[116,117]</sup> Ben-Ishai first proposed the reaction between *N*-protected amino acids and *p*-formaldehyde in the presence of catalytic *p*-TsOH to form the corresponding 5-oxazolidine intermediate.<sup>[118]</sup> Reduction of 5-oxazolidine with TIS and a great excess of TFA renders the desired *N*-methylated residue (Scheme 1.23).<sup>[119]</sup> Among other advantages, this procedure allows *N*-methylation under very mild conditions, being racemisation prevented. Additionally, *N*-methylation of Fmoc and Alloc *N*-protected amino acids is feasible and the protocol is compatible with many amino acid side chains. However, large amounts of silane and TFA are required for the ring opening. Replacement of these reagents by other hydride donors led to carbamate elimination and were discarded.<sup>[116]</sup>

Preparation of Alloc-*N,O*-Me<sub>2</sub>Thr-OH (**1.20**) started with the formation of the corresponding 5-oxazolidine by reaction of previously prepared **1.19** with *p*-formaldehyde in the presence of catalytic *p*-TsOH acid (Scheme 1.23). The reaction was brought to reflux and a Dean Stark apparatus was used to remove the water formed during the reaction.



Scheme 1.23. Synthesis of Alloc-*N,O*-Me<sub>2</sub>Thr-OH (**1.20**). a) *p*-TsOH (0.12 eq), *p*-formaldehyde (1.1 eq), toluene, reflux, 3 h, 89%; b) TIS (4 eq), TFA (76 eq), DCM, 25 °C. N<sub>2</sub> atmosphere, 14 h, 82%.

Reaction conditions were optimised and are summarised in Table 1.6. In all cases catalytic amounts of *p*-TsOH acid (0.12 eq.) were kept constant. Since solubility problems were detected when dissolving the Alloc-protected amino acid in pure toluene, a yield improvement was attempted by running the reaction in a toluene–DMF (8:2 v/v) mixture (see entries #2-4 in Table 1.6). Effect of longer reaction times as well as addition of a greater excess of *p*-formaldehyde were also evaluated. However, low to moderate yields (15-50%) were obtained in most of the cases (see entries #1–6 in Table

1.6). The work up process of conditions #1–6 consisted of washes with an aqueous saturated NaHCO<sub>3</sub> solution to isolate the desired product. HPLC-MS analysis showed that most of the product remained in the aqueous layer, leading to product loss. A drastic yield improvement was observed when basic washes were carried out with an aqueous 5% NaHCO<sub>3</sub> solution instead (see entry #7 in Table 1.6), being the product finally obtained in good yields (90%).

| #        | <i>p</i> -TsOH | <i>p</i> -formaldehyde | Solvent               | Reaction time | Work up                              | Yield (%) |
|----------|----------------|------------------------|-----------------------|---------------|--------------------------------------|-----------|
| 1        | 0.12 eq        | 1.1 eq                 | Toluene               | 3 h           | Aq. Sat NaHCO <sub>3</sub> sol.      | 33        |
| 2        | 0.12 eq        | 25 eq                  | Toluene/DMF (8:2 v/v) | 3 h           | Aq. Sat NaHCO <sub>3</sub> sol.      | 50        |
| 3        | 0.12 eq        | 25 eq                  | Toluene/DMF (8:2 v/v) | 20 h          | Aq. Sat NaHCO <sub>3</sub> sol.      | 27        |
| 4        | 0.12 eq        | 1.1 eq                 | Toluene/DMF (8:2 v/v) | 3 h           | Aq. Sat NaHCO <sub>3</sub> sol.      | 25        |
| 5        | 0.12 eq        | 1.1 eq                 | Toluene               | 20 h          | Aq. Sat NaHCO <sub>3</sub> sol.      | 32        |
| 6        | 0.12 eq        | 25 eq                  | Toluene               | 3 h           | Aq. Sat NaHCO <sub>3</sub> sol.      | 15        |
| <b>7</b> | <b>0.12 eq</b> | <b>1.1 eq</b>          | <b>Toluene</b>        | <b>3 h</b>    | <b>Aq. 5% NaHCO<sub>3</sub> sol.</b> | <b>90</b> |

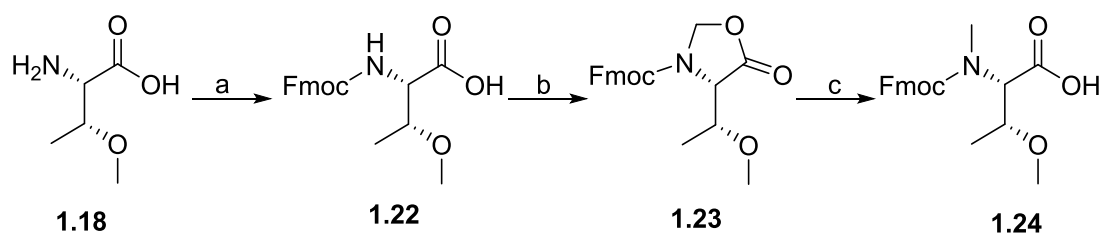
Table 1.6. Optimisation of the 5-oxazolidine intermediate (**1.21**) formation.

Ring opening of **1.21** was accomplished by treatment with TIS and a great excess of TFA (Scheme 1.23). The crude product was subjected to flash chromatography on silica gel and pure **1.20** was obtained in good yields (82%).

#### Preparation of Fmoc-*N,O*-Me<sub>2</sub>Thr-OH (**1.24**)

Preparation of Fmoc-*N,O*-Me<sub>2</sub>Thr-OH started with the amine protection with Fmoc by treatment of **1.18** with Fmoc-OSu in an aqueous NaHCO<sub>3</sub>-Dioxane (2:3 v/v)

mixture (Scheme 1.24). Purification by flash chromatography afforded the desired product in a moderate yield (60%). Next, synthesis of the 5-oxazolidine derivative was carried out following the same conditions as the ones used for the synthesis of the Alloc protected counterpart, and the crude product **1.23** was obtained as a pure compound (56%) and therefore it was used without further purification. Lastly, reduction of 5-oxazolidine with TIS and a great excess of TFA afforded the desired *N*-methylated residue **1.24** in good yields (82%) after flash chromatography purification.

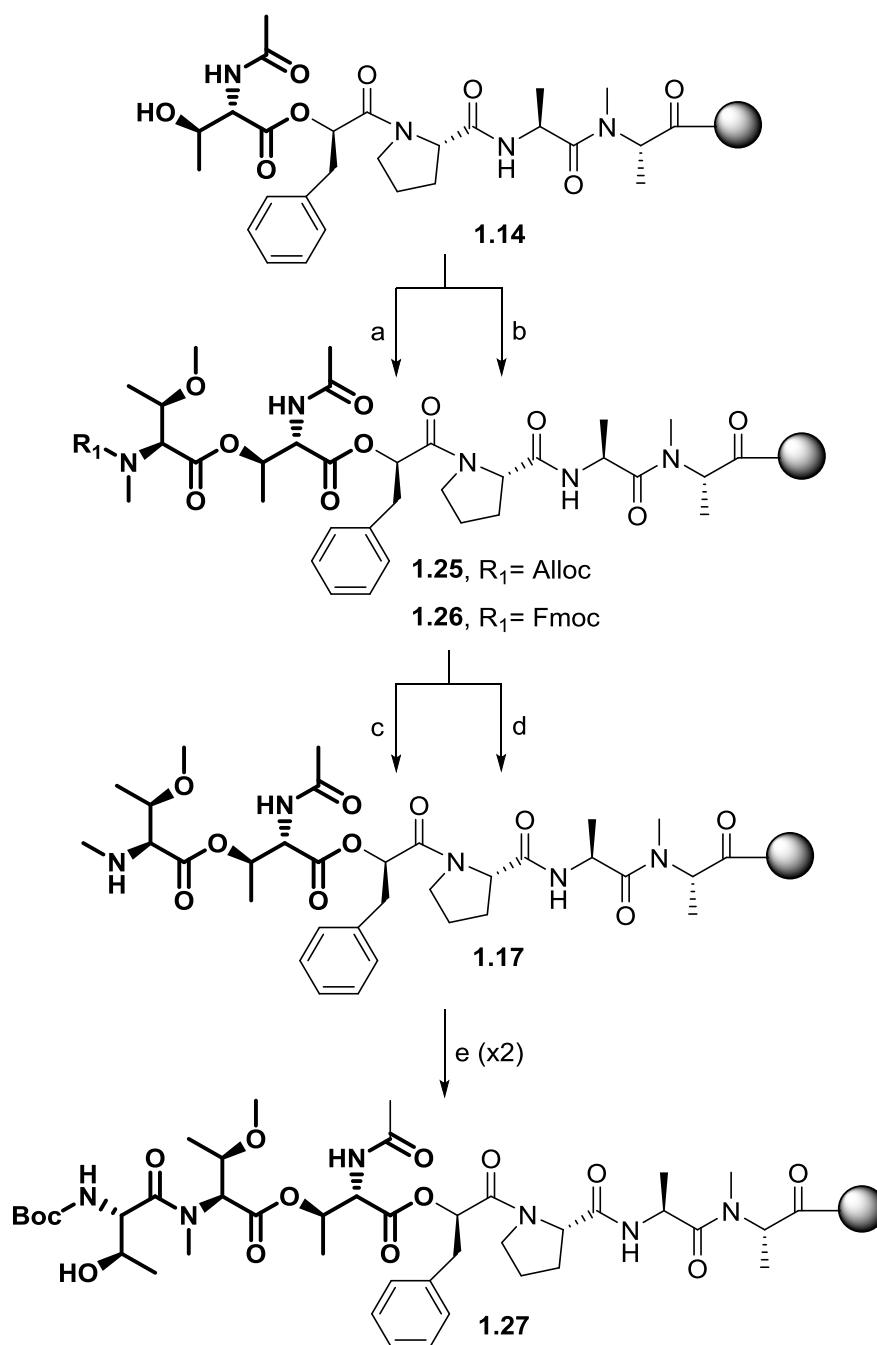


*Scheme 1.24.* Preparation of Fmoc-*N,O*-Me<sub>2</sub>Thr-OH (**1.24**). a) Fmoc-OSu (1.3 eq), aq NaHCO<sub>3</sub>-Dioxane (2:3 v/v), 22 h, 25 °C, 60%; b) *p*-TsOH (0.12 eq), *p*-formaldehyde (1.1 eq), toluene, reflux, 3 h, 56%; c) TIS (4 eq), TFA (76 eq), DCM, 25°C, N<sub>2</sub> atmosphere, 14 h, 82%.

#### 1.3.2.2.4.2 *On-resin esterification of Alloc-N,O-Me<sub>2</sub>Thr-OH (1.20) and Fmoc-N,O-Me<sub>2</sub>Thr-OH (1.24) and subsequent Boc-Thr-OH incorporation*

Introduction of the *N,O*-Me<sub>2</sub>Thr-OH residue through on-resin Steglich esterification of Alloc-*N,O*-Me<sub>2</sub>Thr-OH (**1.20**) and Fmoc-*N,O*-Me<sub>2</sub>Thr-OH (**1.24**) onto **1.14** was successfully accomplished (Scheme 1.25). A mixture of AA-DIC (8:8 eq) was pre-activated over 5 min before it was added to the peptide-resin. Next, addition of DMAP (0.5 eq) was carried out. All esterification reactions were performed at 35 °C under anhydrous conditions.

According to HPLC-MS analysis of a small portion of the peptidyl-resin cleavage crude of **1.25** and **1.26**, the incorporation yield was quantitative in both cases. However, esterification of Alloc-*N,O*-Me<sub>2</sub>Thr-OH and Fmoc-*N,O*-Me<sub>2</sub>Thr-OH resulted in 23% and 22% of racemisation, respectively (Figure 1.15A and Figure 1.15B). *N*-alkylated amino acids are more susceptible to epimerisation at the α-carbon upon amino acid activation, and racemisation might be attributed to this moiety (see racemisation mechanism in section 1.3.2.1.1).<sup>[117]</sup> Unfortunately, further optimisation experiments led similar or less satisfactory results.



*Scheme 1.25.* a) Alloc-*N,O*-Me<sub>2</sub>Thr-OH (**1.20**) (8 eq), DIC (8 eq), DMAP (0.5 eq), DCM–DMF (9:1 v/v), 35 °C, 2 h 30 min; b) Fmoc-*N,O*-Me<sub>2</sub>Thr-OH (**1.24**) (8 eq), DIC (8 eq), DMAP (0.5 eq), DCM–DMF (9:1 v/v), 35 °C, 2 h 30 min; c) Pd(PPh<sub>3</sub>)<sub>4</sub> (0.1 eq), PhSiH<sub>3</sub> (10 eq), DCM, 15 min; d) DBU–DMF (2:98 v/v) (1 x 1 min); e) Boc-Thr-OH (3 eq), HATU (3 eq), HOAt (3 eq), DIEA (6 eq), 25 °C, 1 h.

Next, removal of the amine protecting group of the two derivatives was studied. Alloc removal was accomplished by treatment of the peptidyl-resin with catalytic amounts of palladium and phenylsilane, which served as scavenger. Subsequent incorporation of the seventh residue, Boc-Thr-OH, through an amidation reaction onto

a secondary amine was performed with the AA–HATU–HOAt–DIEA (3:3:3:6 eq) coupling system. HPLC-MS analysis of the peptidyl-resin cleavage crude of **1.27** showed excellent conversion rates (Figure 1.15C). The Boc-Thr-OH residue was assembled with the free hydroxyl group to later on perform the last on-resin esterification. At a later stage of the synthesis, the Boc protecting group was removed upon cleavage to perform the cyclisation in solution.

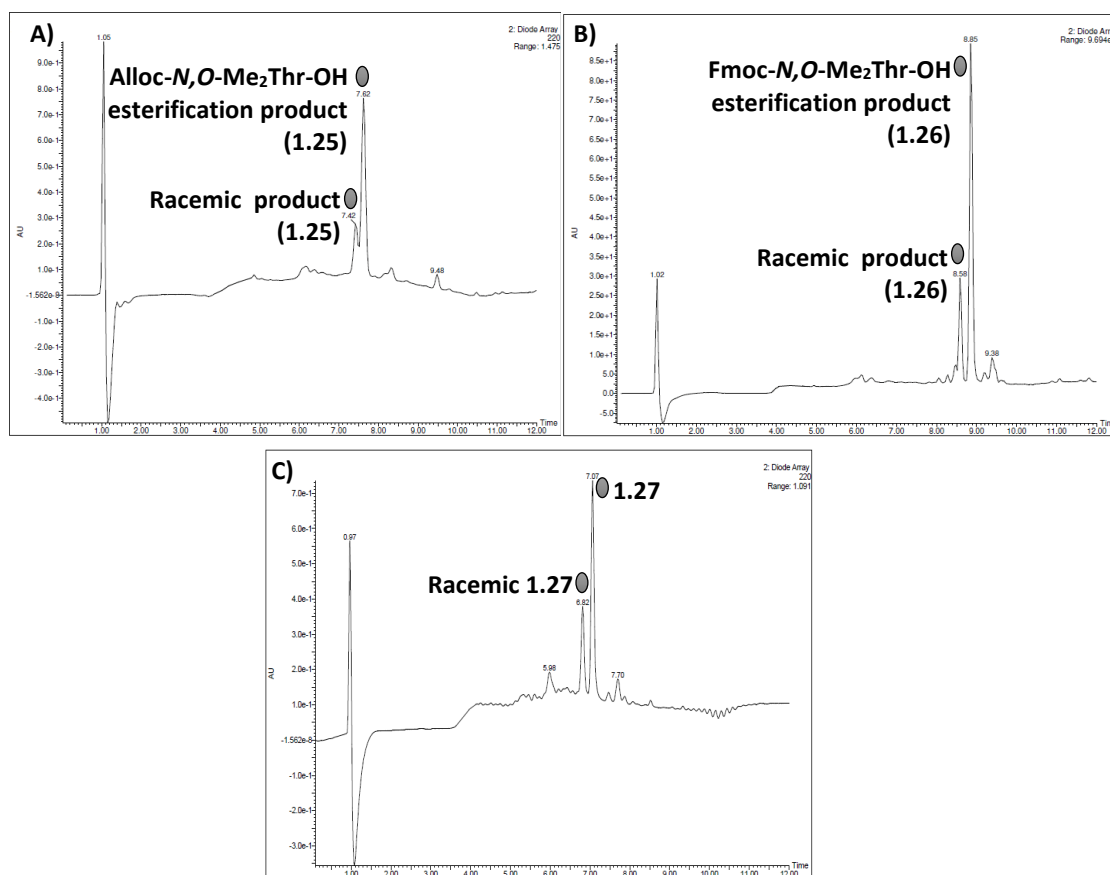


Figure 1.15. HPLC-MS chromatograms run at G0100t9T25 and processed at 220 nm. A) On-resin Steglich esterification of **1.20** where 23% of racemisation is observed. B) On-resin Steglich esterification of **1.24** where 22% of racemisation is observed. C) Coupling of Boc-Thr-OH after Alloc removal to afford **1.27**.

Although a fully stepwise strategy for the preparation of the target molecule (**1.1**) could be developed with the Alloc protected *N,O*-Me<sub>2</sub>Thr-OH residue, we wanted to further study Fmoc removal of this residue. A major aim of this project was optimisation of Fmoc removal after formation of all three ester linkages. Evaluation of Fmoc removal of the Fmoc-*N,O*-Me<sub>2</sub>Thr-OH residue, together with Fmoc removal studies after the first and third ester bond formation (see section 1.3.2.2.3 and

1.3.2.2.5.2, respectively), allowed the development of a robust Fmoc-based methodology for the preparation of complex depsipeptides following a fully stepwise approach.

1.3.2.2.4.3 *Fmoc removal studies of Ac-Thr(O(Fmoc-N,O-Me<sub>2</sub>Thr-CO))-COO-D-Pla-Pro-Ala-N-MeAla-CTC-resin (1.26)*

According to previous studies reported in the literature, Fmoc removal at this point mostly leads to formation of the  $\alpha,\beta$ -elimination side-product.<sup>[46,63]</sup> We hypothesised that the presence of two consecutive ester bonds enhanced the formation of the  $\alpha,\beta$ -elimination side-product at this point of the synthesis. Successful Fmoc removal would lead to the development of a versatile stepwise strategy for the preparation of complex depsipeptides and would allow rapid access to numerous depsipeptide synthetic analogues, since many Fmoc-protected derivatives are commercially available. Thus, the previously tested Fmoc removal conditions (see section 1.3.2.2.3) were applied to the present system to evaluate the effect of different chemical environments in the deprotection outcome, as well as to establish the best conditions for this particular deprotection step.

In all cases, a short treatment of 1 min with the corresponding deprotection cocktail was performed, as previously tested for Fmoc removal after the first ester bond formation. The HPLC traces as well as the structures of the peptidyl-resin cleavage crude of the desired product (**1.17**) and the two main side-products corresponding to *N,O*-Me<sub>2</sub>Thr-OH residue loss (**1.14**) and the  $\alpha,\beta$ -elimination product (**1.28**) are shown in Table 1.7.

As expected, Fmoc removal with the traditional piperidine–DMF (1:4 v/v) cocktail mainly led to the formation of the  $\alpha,\beta$ -elimination product (**1.27**), but also to *N,O*-Me<sub>2</sub>Thr-OH residue loss (**1.14**) and racemisation of the desired product (**1.17**) (see entry #1 in Table 1.7 and HPLC chromatogram in Figure 1.16A).

Previous positive results suggested that addition of small percentages of HOBt or OxymaPure can improve the outcome of the deprotection step by lessening racemisation and formation of undesired products. Thus, the peptidyl-resin was treated

with a 0.1 M HOBT in piperidine–DMF (1:4 v/v) solution, a 0.2 M HOBT in piperidine–DMF (1:4 v/v) solution, a 0.1M OxymaPure in piperidine–DMF (1:4 v/v) solution and a 0.2 M OxymaPure in piperidine–DMF (1:4 v/v) solution (see entries #2-5 in in Table 1.7). None of these four conditions resulted in improved Fmoc removal conditions compared to the results obtained when no additive was added. Whereas 10-11% of *N,O*-Me<sub>2</sub>Thr-OH (**1.14**) loss was observed, the undesired  $\alpha,\beta$ -elimination product (**1.28**) was formed in high percentages (43-57%). Note that complete Fmoc removal was not accomplished. However, it was expected that additional treatments to achieve full deprotection would lead to even higher percentages of the undesired side products compared to the formation of the desired product, and therefore no extra treatments were carried out and these deprotection conditions were discarded.

Encouraged by previous positive results obtained during Fmoc removal after the first ester bond formation, the peptidyl-resin was treated with a DBU–DMF (2:98 v/v) solution (see entry #6 in in Table 1.7). Remarkably, the desired product was obtained with a 57% conversion determined by HPLC, and we were able to significantly decrease the formation of the  $\alpha,\beta$ -elimination product (**1.28**) and *N,O*-Me<sub>2</sub>Thr-OH (**1.14**) loss to 19% and 23%, respectively (Figure 1.16B). Moreover, a source of protons was added to the DBU–DMF (2:98 v/v) solution, and Fmoc removal was evaluated (see entries #7-10 in Table 1.7). Unfortunately, addition of HOBT and OxymaPure to the DBU–DMF (2:98 v/v) solution accounted for poorer results compared to the ones obtained with no additive.

Whereas treatment with a 0.1 M HOBT in DBU–DMF (2:98 v/v) solution led to complete Fmoc removal, a high percentage of the Fmoc-protected depsipeptide was observed (51-60%) after treatment with a 0.1 M OxymaPure in DBU–DMF (2:98 v/v) solution, a 0.2 M OxymaPure in DBU–DMF (2:98 v/v) solution and a 0.2 M HOBT in DBU–DMF (2:98 v/v) solution. Since relatively good desired/undesired product ratios were obtained with the 0.2 M HOBT in DBU–DMF (2:98 v/v) solution (see entry #10 in Table 1.7), an additional treatment was carried out to attempt full deprotection. Unfortunately, further Fmoc removal was not achieved.

| #  | Fmoc removal conditions                                 | 1.26 (%) | 1.17 (%)  | 1.14 (%)  | 1.28 (%)  |
|----|---|----------|-----------|-----------|-----------|
| 1  | Piperidine–DMF (1:4 v/v) (1 x 1 min)                    | 0        | 37        | 15        | 48        |
| 2  | 0.1 M HOBT in Piperidine–DMF (1:4 v/v) (1 x 1 min)      | 32       | 8         | 11        | 49        |
| 3  | 0.2 M HOBT in Piperidine–DMF (1:4 v/v) (1 x 1 min)      | 26       | 9         | 10        | 57        |
| 4  | 0.1 M OxymaPure in Piperidine–DMF (1:4 v/v) (1 x 1 min) | 38       | 9         | 10        | 43        |
| 5  | 0.2 M OxymaPure in Piperidine–DMF (1:4 v/v) (1 x 1 min) | 8        | 25        | 10        | 57        |
| 6  | <b>DBU–DMF (2:98 v/v) (1 x 1 min)</b>                   | <b>0</b> | <b>57</b> | <b>23</b> | <b>19</b> |
| 7  | 0.1 M HOBT in DBU–DMF (2:98 v/v) (1 x 1 min)            | 0        | 43        | 36        | 21        |
| 8  | 0.2 M HOBT in DBU–DMF (2:98 v/v) (1 x 1 min)            | 60       | 16        | 16        | 8         |
| 9  | 0.1 M OxymaPure in DBU–DMF (2:98 v/v) (1 x 1 min)       | 51       | 22        | 18        | 9         |
| 10 | 0.2 M OxymaPure in DBU–DMF (2:98 v/v) (1 x 1 min)       | 54       | 30        | 11        | 5         |

Table 1.7. Fmoc removal studies of Fmoc-*N,O*-Me<sub>2</sub>Thr-O-Ac-Thr-O-D-Pla-Pro-Ala-N-Me-Ala-CTC-resin (**1.26**). HPLC data was processed at 220 nm.

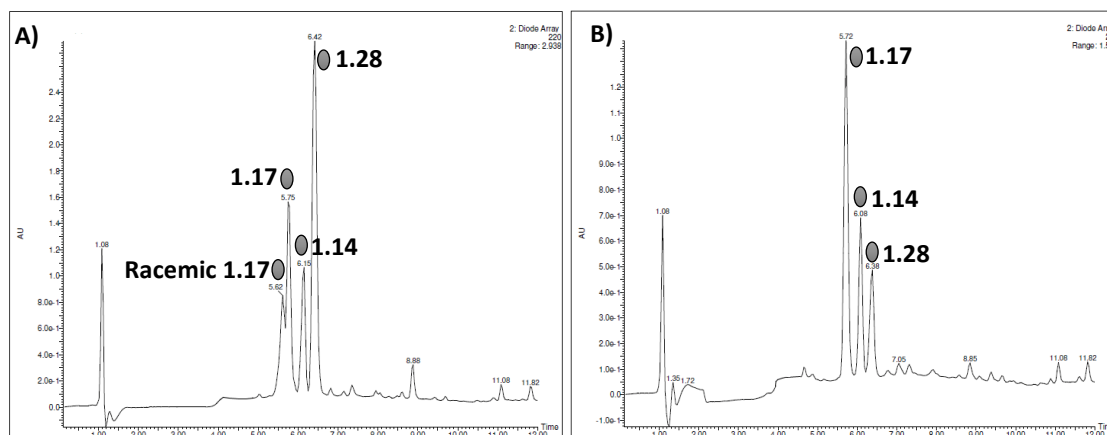


Figure 1.16. HPLC-MS chromatograms run at G0100t9T25 and processed at 220 nm. A) Fmoc removal with piperidine–DMF (1:4 v/v) (1 x 1 min); B) Fmoc removal with DBU–DMF (2:98 v/v) (1 x 1 min).

We were happy to considerably minimise  $\alpha,\beta$ -elimination and obtain the desired unprotected depsipeptide (**1.17**) with a good enough conversion (57% determined by HPLC-MS) to carry on with the synthesis. In fact, a remarkable improvement compared to the results described by other groups was made. Note that Harveen *et al.* completely failed to prepare the unprotected depsipeptide, being  $\alpha,\beta$ -elimination observed instead (with a quantitative conversion determined by HPLC).<sup>[46]</sup> Efforts of another group to perform this  $N^\alpha$ -Fmoc-deprotection also led to the formation of the  $\alpha,\beta$ -elimination side-product, however, 40% of the desired unprotected peptide could be obtained using a piperidine–DMF (1:99 v/v) solution. Unfortunately, further optimisation using other bases such as TBAF or Et<sub>2</sub>N, led to poorer deprotection outcomes.<sup>[63]</sup>

Although there is room for improvement, our results are a big step forward compared to those reported in the recent literature<sup>[46,63]</sup> and open the door to the development of a fully Fmoc-based stepwise strategy for the preparation of complex depsipeptides containing multiple and consecutive ester linkages.

#### 1.3.2.2.4.4 Summary of the *N,O*-Me<sub>2</sub>Thr-OH residue incorporation

A step further in the development of a fully-stepwise strategy was made. We were able to introduce the *N,O*-Me<sub>2</sub>Thr-OH residue *via* on-resin Steglich esterification of either Alloc-*N,O*-Me<sub>2</sub>Thr-OH or Fmoc-*N,O*-Me<sub>2</sub>Thr-OH. *N*-alkylated amino acids are more susceptible to epimerisation at the  $\alpha$ -carbon, and the observed racemisation

might be attributed to this moiety.<sup>[117]</sup> Alloc removal and subsequent Boc-Thr-OH incorporation through an amidation reactions were successfully accomplished, being **1.27** obtained with good HPLC conversions (Figure 1.17A).

For the first time, Fmoc removal at this point of the synthesis with a DBU–DMF (2:98 v/v) solution successfully afforded the desired product in a fairly good enough HPLC yield (57%) to carry on with the synthesis, being complete formation of the undesired  $\alpha,\beta$ -elimination side-product significantly minimised.<sup>[46,63]</sup> Subsequently, introduction of the Boc-Thr-OH residue through an amidation reaction was performed (Figure 1.17B). Considering the synthetic complexity of the target molecule, the presence of 43% of impurities (Figure 1.17B) at this late stage of the synthesis was considered good enough to follow up with the assembly the last residue.

To conclude, a fully stepwise strategy for the preparation of the target molecule could be developed with either the Alloc or the Fmoc protected *N,O*-Me<sub>2</sub>Thr-OH residue. Although Fmoc removal led to lower HPLC yields (compare Figure 1.17A and Figure 1.17B), the Fmoc protecting group might be very useful for the rapid preparation of a series of synthetic depsipeptide analogues.

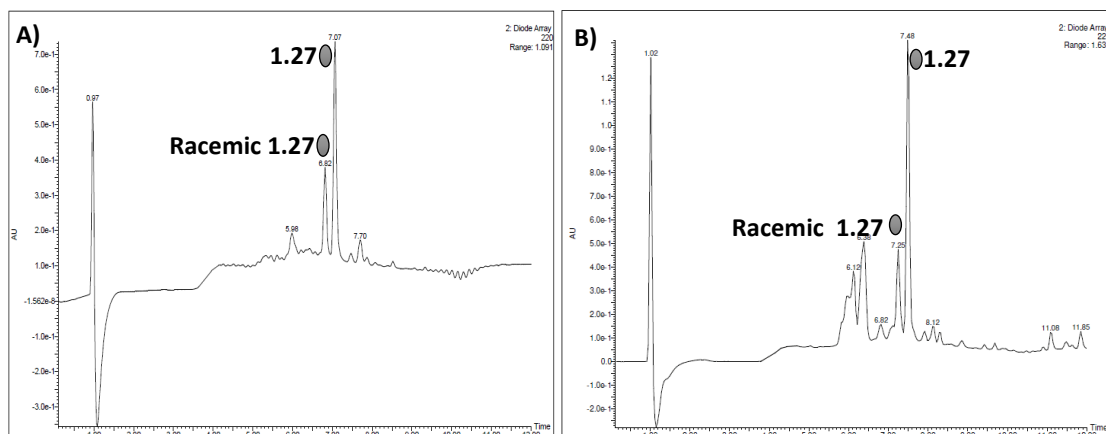
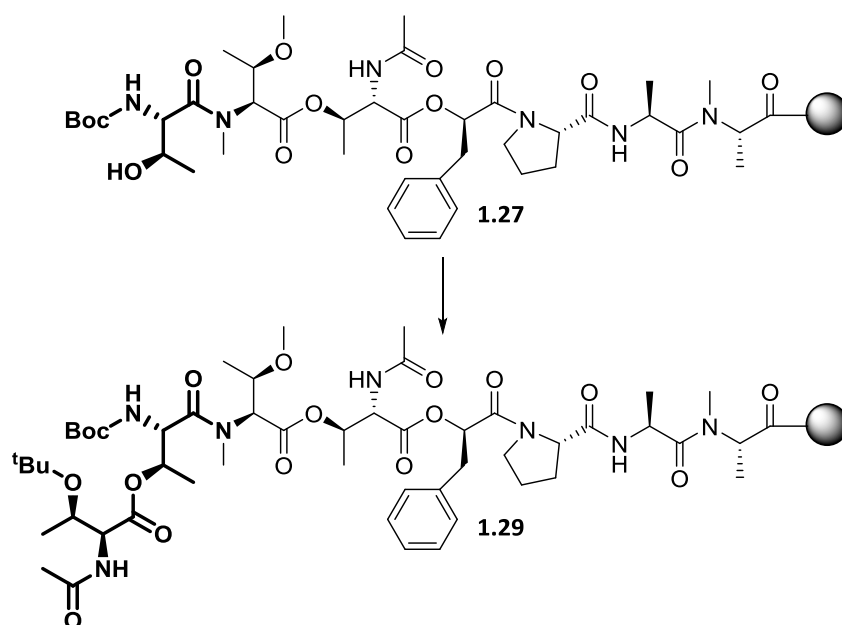


Figure 1.17. HPLC-MS chromatograms run at G0100t9T25 and processed at 220 nm of Boc-Thr-OH incorporation after the A) on-resin Steglich esterification of Alloc-*N,O*-Me<sub>2</sub>Thr-OH (**1.20**), Alloc removal and subsequent Boc-Thr-OH incorporation to afford **1.27**; or B) on-resin Steglich esterification of Fmoc-*N,O*-Me<sub>2</sub>Thr-OH (**1.24**), Fmoc removal and subsequent Boc-Thr-OH incorporation to afford **1.27**.

Next, assembly of the last residue was accomplished through an on-resin Steglich esterification. Esterification studies were carried out with the peptidyl-resin **1.27** derived from the Alloc-*N,O*-Me<sub>2</sub>Thr-OH incorporation strategy, which contained a lower content of impurities compared to the ones obtained with the Fmoc-*N,O*-Me<sub>2</sub>Thr-OH incorporation route (Figure 1.17A).

### 1.3.2.2.5 Incorporation of the Ac-Thr(<sup>t</sup>Bu)-OH residue onto Ac-Thr(O(Boc-Thr(OH)-Fmoc-*N,O*-Me<sub>2</sub>Thr-CO))-COO-D-Pla-Pro-Ala-*N*-MeAla-CTC-resin (**1.27**)

The last step for the preparation of the linear precursor of **1.1** was assembly of the Ac-Thr(<sup>t</sup>Bu)-OH residue *via* an ester bond formation between the carboxylic acid of Ac-Thr(<sup>t</sup>Bu)-OH and the β-hydroxyl group present in compound **1.27** (Scheme 1.26). Esterification of Ac-Thr(<sup>t</sup>Bu)-OH was foreseen troublesome due to the presence of the acetyl moiety, which might deactivate the residue according to previous obtained results (see section 1.3.2.2.3.2). However, esterification rates were evaluated by introduction of the previously prepared residues Ac-Thr(<sup>t</sup>Bu)-OH (**1.5**) and Alloc-Thr(<sup>t</sup>Bu)-OH (**1.6**) as well as commercially available Fmoc-Thr(<sup>t</sup>Bu)-OH. As a part of the Fmoc removal studies, optimal Fmoc removal conditions were assessed.



Scheme 1.26. Assembly of Ac-Thr(<sup>t</sup>Bu)-OH through an on-resin Steglich esterification. R<sub>1</sub>-Thr(<sup>t</sup>Bu)-OH (8 eq), DIC (8 eq), DMAP (0.5 eq), DCM-DMF (9:1 v/v), 35 °C, 2 h 30 min.

1.3.2.2.5.1 On-resin esterification of  $R_1$ -Thr(<sup>t</sup>Bu)-OH

On-resin Steglich esterification was performed as follows. A mixture of AA–DIC–DMAP (8:8:0.5 eq), in which the carboxylic acid was pre-activated over 5 min, was added to the peptide-resin, followed by addition of DMAP. All esterification reactions were performed at 35 °C under anhydrous conditions. Reaction monitoring was performed by HPLC-MS analysis of a small portion of the corresponding cleaved peptidyl-resin. The observed esterification conversions determined by HPLC are shown in Table 1.8.

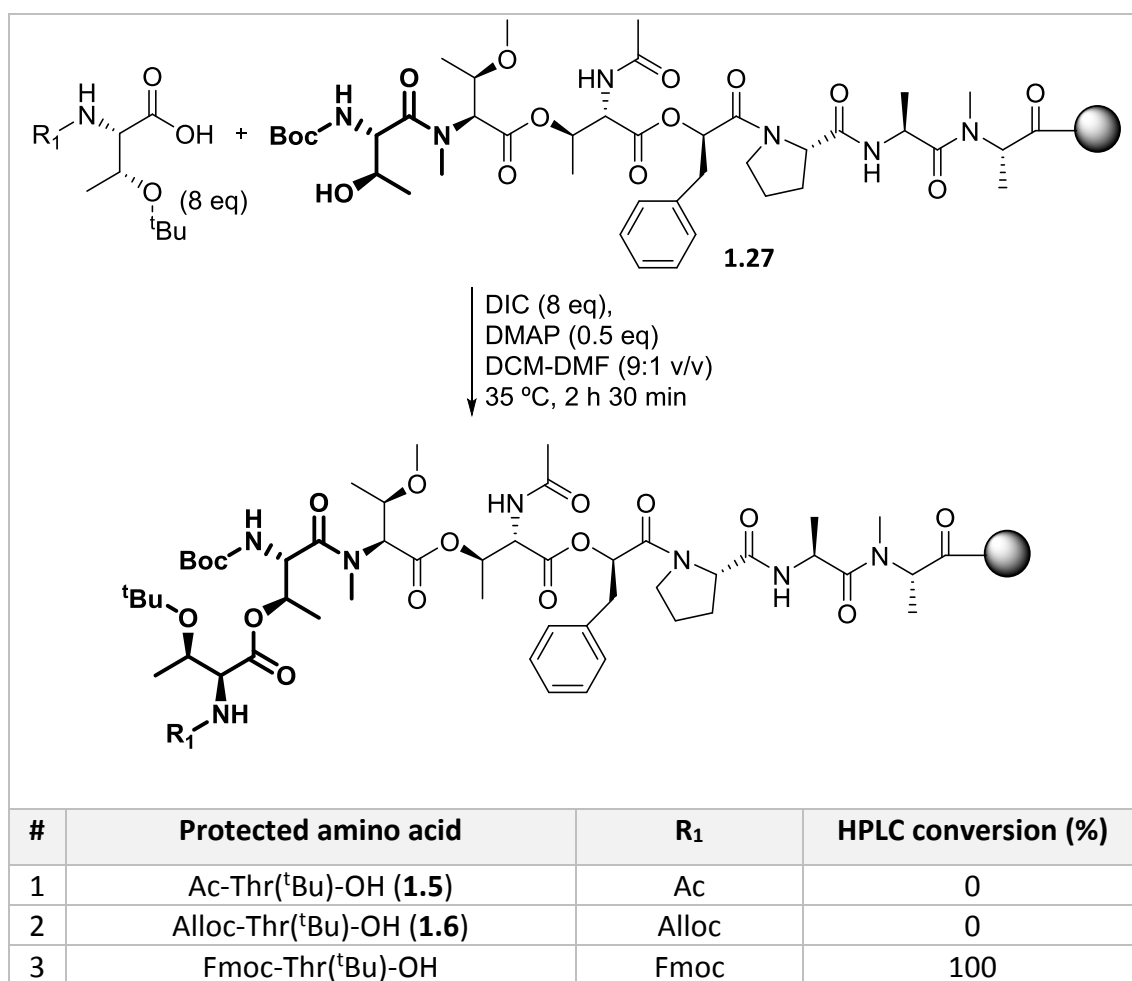


Table 1.8. Steglich esterification of a series of Thr derivatives to study the reactivity of the Ac-Thr(<sup>t</sup>Bu)-OH esterification reaction. HPLC data was processed at 220 nm.

Unfortunately, Steglich esterification of Ac-Thr(<sup>t</sup>Bu)-OH (**1.5**) and Alloc-Thr(<sup>t</sup>Bu)-OH (**1.6**) resulted in no product formation (see entries #1-2 in Table 1.8). On the other hand, esterification with Fmoc-Thr(<sup>t</sup>Bu)-OH was successfully accomplished. Complete incorporation of commercially available Fmoc-Thr(<sup>t</sup>Bu)-OH was determined by HPLC-MS analysis (see entry #3 in Table 1.8). These experiments comply with previously obtained

results, in which formation of the first ester linkage could not be accomplished with the corresponding Ac and Alloc protected residues and was only successful when using the Fmoc protecting group.

1.3.2.2.5.2 *Fmoc removal studies of Ac-Thr(O(Boc-Thr(O(Fmoc-Thr(<sup>t</sup>Bu)-CO))-Fmoc-N,O-Me<sub>2</sub>Thr-CO))-COO-D-Pla-Pro-Ala-N-MeAla-CTC-resin (1.30)*

Efficient Fmoc removal of the last residue incorporation was extensively studied. In all cases, treatments of 1 min were performed and the deprotection efficiency was determined by HPLC-MS analysis. As for Fmoc removal after formation of the first and second ester linkage, combination of different bases (piperidine and DBU) as well as various additives (no additive, HOBt and OxymaPure) and different additive concentrations were tested. All tested conditions are summarised in Table 1.9.

To start up with, the peptidyl-resin was treated with the conventional piperidine–DMF (1:4 v/v) solution (see entry #1 in Table 1.9). HPLC-MS analysis showed formation of the undesired  $\alpha,\beta$ -elimination product (**1.28**) in 90% HPLC yield, and only 10% of the desired unprotected depsipeptide (**1.31**) was obtained (Figure 1.18A). As previously observed, addition of small percentages of organic acids to the Fmoc removal solution proved effective to improve the Fmoc removal outcome. Inspired by these results, the peptidyl-resin was treated with a 0.1 M HOBt in piperidine–DMF (1:4 v/v) solution and a 0.2 M HOBt in piperidine–DMF (1:4 v/v) solution (see entries #2-3 in Table 1.9). Unfortunately, treatment with a 0.1 M HOBt in piperidine–DMF (1:4 v/v) solution did not exert a positive effect on the deprotection step, leading to equivalent ratios (12:88) of the unprotected depsipeptide (**1.31**): $\alpha,\beta$ -elimination product (**1.28**) as the ones observed when no additive was added. Treatment of the peptidyl-resin with a 0.2 M HOBt in piperidine–DMF (1:4 v/v) solution resulted in improved unprotected depsipeptide (**1.31**): $\alpha,\beta$ -elimination product (**1.28**) ratios (44:15), however, complete Fmoc removal was not accomplished.

In an attempt to optimise the deprotection conditions, pentadepsipeptide **1.30** was treated with a DBU–DMF (2:98) solution (see entry #4 in Table 1.9). Although HPLC-MS analysis showed 15% of remaining protected depsipeptide (**1.30**), the unprotected depsipeptide (**1.31**): $\alpha,\beta$ -elimination product (**1.28**) ratio was improved to 45:22.

| # | Fmoc removal conditions                             | 1.30 (%) | 1.31 (%)   | 1.28 (%) |
|---|---|----------|------------|----------|
| 1 | Piperidine–DMF (1:4 v/v) (1 x 1 min)                | 0        | 10         | 90       |
| 2 | 0.1 M HOBT in Piperidine–DMF (1:4 v/v) (1 x 1 min)  | 0        | 12         | 88       |
| 3 | 0.2 M HOBT in Piperidine–DMF (1:4 v/v) (1 x 1 min)  | 41       | 44         | 15       |
| 4 | DBU–DMF (2:98 v/v) (1 x 1 min)                      | 15       | 45         | 22       |
| 5 | 0.1 M OxymaPure in DBU–DMF (2:98 v/v) (1 x 1 min)   | 30       | 26         | 9        |
| 6 | 0.2 M OxymaPure in DBU–DMF (2:98 v/v) (1 x 1 min)   | 100      | 0          | 0        |
| 7 | <b>0.1 M HOBT in DBU–DMF (2:98 v/v) (1 x 1 min)</b> | <b>0</b> | <b>100</b> | <b>0</b> |
| 8 | 0.2 M HOBT in DBU–DMF (2:98 v/v) (1 x 1 min)        | 63       | 32         | 5        |

Table 1.9. Fmoc removal studies of **Fmoc**-Thr(<sup>t</sup>Bu)-O-Boc-Thr-*N,O*-Me<sub>2</sub>Thr-O-Ac-Thr-O-D-Pla-Pro-Ala-*N*-Me-Ala-CTC-resin (**1.30**). HPLC data was processed at 220 nm.

Treatment of the peptidyl-resin with 0.1 M OxymaPure in DBU–DMF (2:98) solution resulted in an unprotected depsipeptide (**1.31**): $\alpha,\beta$ -elimination product **1.28**) 26:9 ratio (see entry #5 in Table 1.9). However, 30% of the protected peptide (**1.30**) was detected. Additionally, the HPLC-MS spectrum was rather dirty and many unidentified

side-products (in an overall 35% percentage) arising from the deprotection step were observed. No Fmoc removal was observed when treating the peptidyl-resin with a 0.2 M OxymaPure in DBU–DMF (2:98 v/v) solution, and only 37% of Fmoc removal was observed upon treatment with a 0.2 M HOBt in DBU–DMF (2:98 v/v) solution (see entry #6 and entry #8 in Table 1.9). In agreement with previous observations, addition of a 0.2 M concentration of acidic additives was prone to partially or completely suppress the effect of the base. Successful Fmoc removal was achieved by treatment of the peptidyl-resin with a 0.1 M HOBt in DBU–DMF (2:98) solution, which led to complete Fmoc removal to afford the desired unprotected depsipeptide **1.31** (see entry #7 in Table 1.9 and Figure 1.18B).

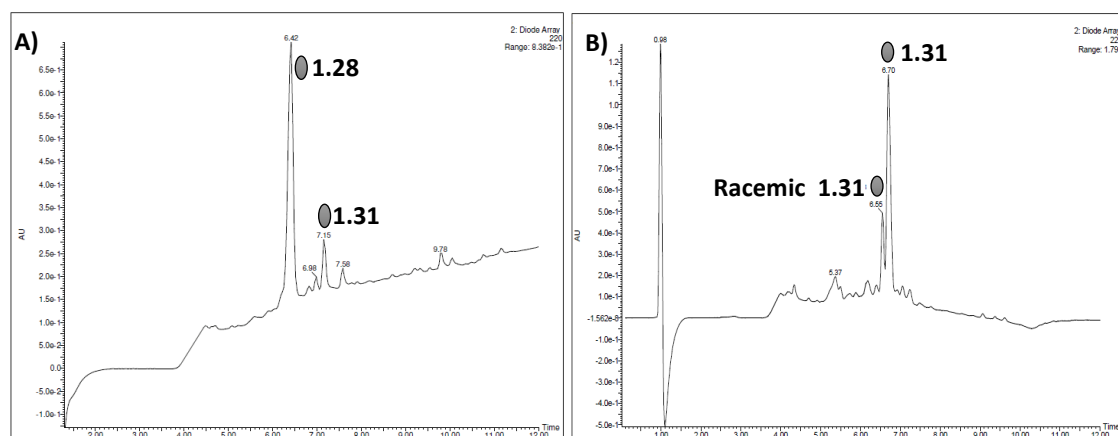
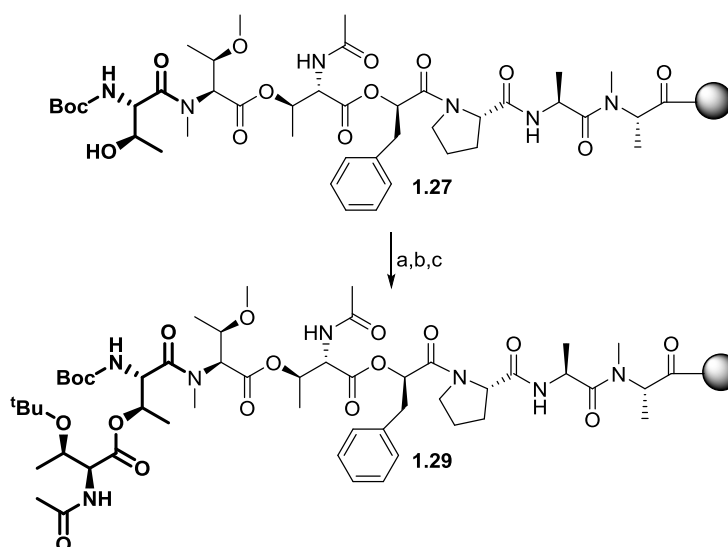


Figure 1.18. HPLC-MS chromatograms run at G0100t9T25 and processed at 220 nm of Fmoc removal studies after Fmoc-Thr(<sup>t</sup>Bu)-OH assembly. A) Fmoc removal with a piperidine–DMF (1:4 v/v) (1 x 1 min) solution to mainly afford **1.28**; B) Fmoc removal with a 0.1M HOBt in DBU–DMF (2:98 v/v) (1 x 1 min) solution to mainly afford **1.31**.

#### 1.3.2.2.5.3 Summary of the Ac-Thr(<sup>t</sup>Bu)-OH incorporation

Stepwise incorporation of the last residue to fully assemble the linear depsipeptide chain was successfully accomplished (Scheme 1.27). First, commercially available Fmoc-Thr(<sup>t</sup>Bu)-OH was introduced upon on-resin Steglich esterification conditions (Figure 1.19A). Formation of the undesired  $\alpha,\beta$ -elimination side-product upon Fmoc removal was completely circumvented by treatment of the peptidyl-resin with a 0.1 M HOBt in DBU–DMF (2:98 v/v) solution (Figure 1.19B). Acetylation of the free amine of **1.31** was performed using the AcOH–OxymaPure–DIC coupling system to render the final depsipeptide linear chain **1.29** (Figure 1.19C).



Scheme 1.27. Assembly of the Ac-Thr(<sup>t</sup>Bu)-OH residue. a) Fmoc-Thr(<sup>t</sup>Bu)-OH (8 eq), DIC (8 eq), DMAP (0.5 eq), DCM-DMF (9:1 v/v), 35 °C, 2 h 30 min; b) 0.1M HOBT in DBU-DMF (2:98 v/v) (1 x 1 min); c) AcOH (3 eq), OxymaPure (3 eq), DIC (3 eq), 25 °C, 40 min.

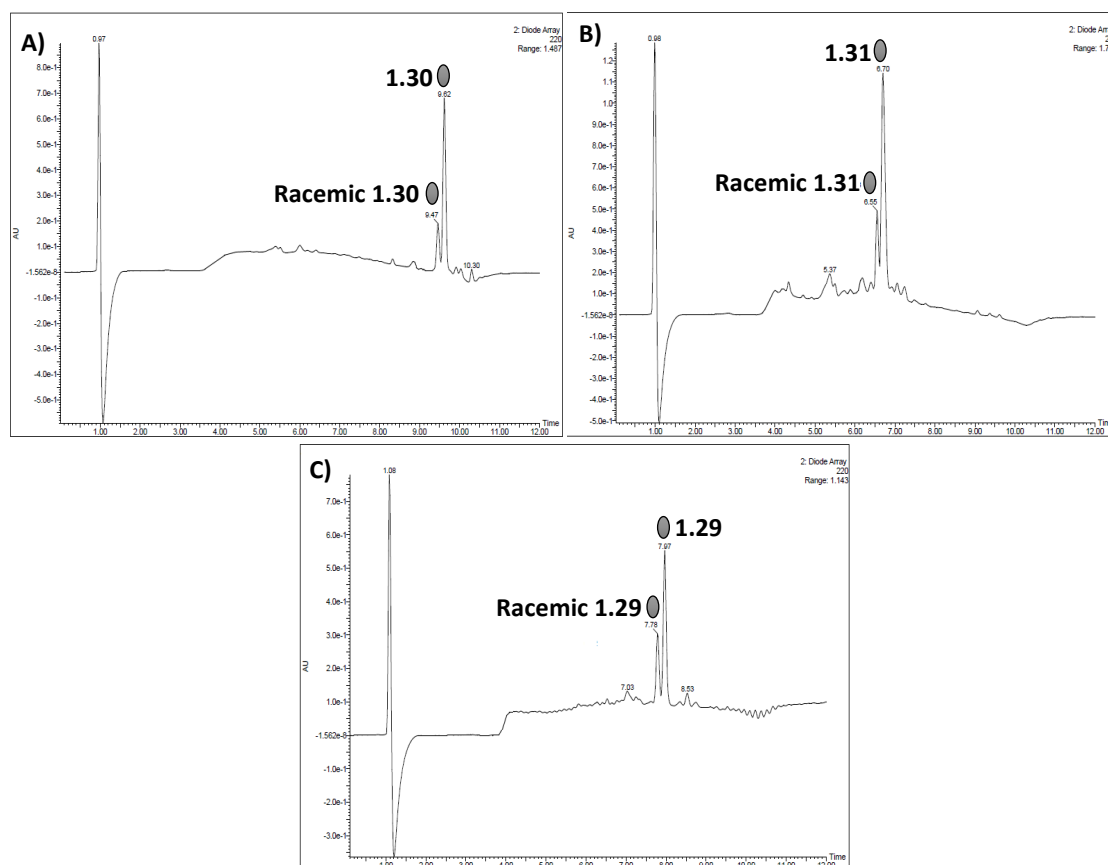
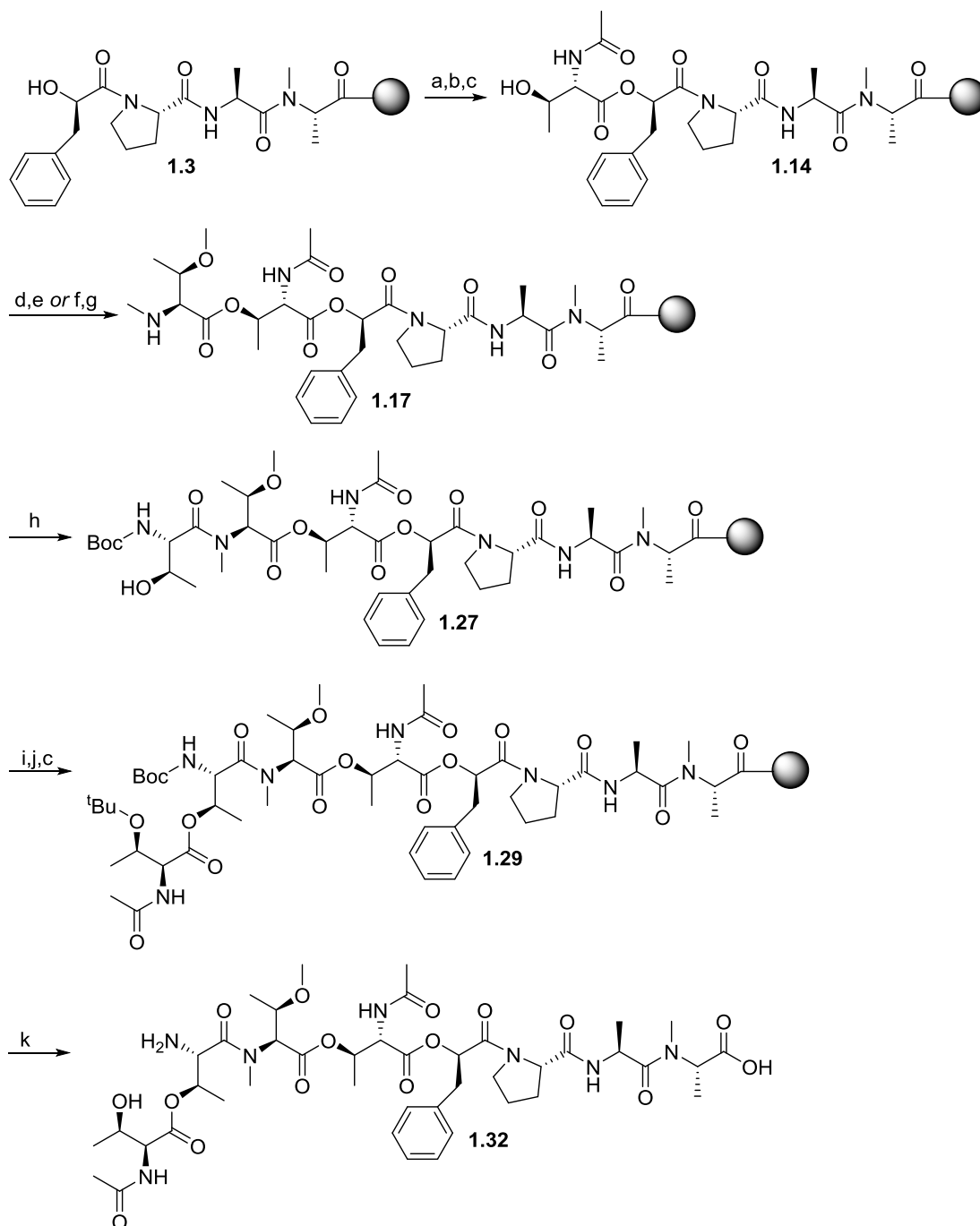


Figure 1.19. HPLC-MS chromatograms run at G0100t9T25 and processed at 220 nm of Ac-Thr(<sup>t</sup>Bu)-OH assembly. A) on-resin Steglich esterification of Fmoc-Thr(<sup>t</sup>Bu)-OH to render **1.30**; B) Fmoc removal with a 0.1M HOBT in DBU-DMF (2:98 v/v) (1 x 1 min) solution to afford **1.31**; C) Acetylation of the free amine to afford the linear protected depsipeptide **1.29**.

### 1.3.2.2.6 Final stepwise strategy to prepare the linear precursor of **1.1**: Synthesis of Ac-Thr(O(H<sub>2</sub>N-Thr(O(Ac-Thr(OH)-CO))-Fmoc-*N,O*-Me<sub>2</sub>Thr-CO))-COO-D-Pla-Pro-Ala-*N*-MeAla-COOH (**1.32**)

For the first time, a fully Fmoc-based stepwise strategy to prepare complex depsipeptides that are composed of  $\beta$ -branched residues and hold multiple and consecutive ester linkages was developed (Scheme 1.28). Synthesis of linear tetrapeptide **1.3** was accomplished by SPPS standard means. We were able to introduce the until now unreactive Ac-Thr-OH derivative in a stepwise manner. The Thr derivative was introduced as Fmoc-Thr(TBDMS)-OH, being Fmoc and TBDMS simultaneously removed by treatment with TBAF. Next, the free amine function was selectively acetylated in the presence of a free hydroxyl functionality to afford **1.14**. Consecutive ester bond formation between the free hydroxyl group of **1.14** and either Alloc-*N,O*-Me<sub>2</sub>Thr-OH (**1.20**) or Fmoc- *N,O*-Me<sub>2</sub>Thr-OH (**1.24**) was successfully accomplished, followed by corresponding Alloc or Fmoc removal. However, 22-23% of racemisation was observed upon esterification conditions. *N*-alkylated amino acid are more susceptible to epimerisation at the  $\alpha$ -carbon, and racemisation might be attributed to this moiety.<sup>[117]</sup> Remarkably, Fmoc removal at this point of the synthesis with a DBU–DMF (2:98 v/v) solution successfully afforded the desired product in a 57% HPLC yield, being formation of the undesired  $\alpha,\beta$ -elimination side-product significantly minimised for the first time.<sup>[46,63]</sup> The fully stepwise strategy for the preparation of the target molecule can be developed with both the Alloc and the Fmoc protected *N,O*-Me<sub>2</sub>Thr-OH residues. Although Fmoc removal led to lower HPLC yields, it becomes a very useful strategy for the rapid preparation of numerous **1.1** analogues, since many Fmoc-protected amino acid derivatives are commercially available. Next, Boc-Thr-OH incorporation *via* an amidation reaction was performed with the unprotected hydroxyl group to afford compound **1.27**. Full assembly of the linear depsipeptide chain **1.29** was achieved by introduction of commercially available Fmoc-Thr(<sup>t</sup>Bu)-OH through a Steglich esterification with the hydroxyl group of **1.27**. Fmoc removal conditions were optimised (0.1 M HOBT in DBU–DMF (2:98 v/v) (1 x 1 min)), being the formation of the undesired  $\alpha,\beta$ -elimination side-product fully circumvented.



**Scheme 1.28.** Final stepwise strategy to prepare the linear precursor of **1.1**. a) Fmoc-Thr(TBDMS)-OH (**1.10**) (8 eq), DIC (8 eq), DMAP (0.5 eq), DCM-DMF (9:1 v/v), 35 °C, 2 h 30 min; b) 1.0 M TBAF in THF (1 eq), 10 min, N<sub>2</sub> atm., 25 °C; c) AcOH (3 eq), OxymaPure (3 eq), DIC (3 eq), 25 °C, 40 min; d) Alloc-*N,O*-Me<sub>2</sub>Thr-OH (**1.20**) (8 eq), DIC (8 eq), DMAP (0.5 eq), DCM-DMF (9:1 v/v), 35 °C, 2 h 30 min; e) Pd(PPh<sub>3</sub>)<sub>4</sub> (0.1 eq), PhSiH<sub>3</sub> (10 eq), DCM, 15 min; f) Fmoc-*N,O*-Me<sub>2</sub>Thr-OH (**1.24**) (8 eq), DIC (8 eq), DMAP (0.5 eq), DCM-DMF (9:1 v/v), 35 °C, 2 h 30 min; g) DBU-DMF (2:98 v/v) (1 x 1 min); h) Boc-Thr-OH (3 eq), HATU (3 eq), HOAt (3 eq), DIEA (6 eq), rt, 1 h; i) Fmoc-Thr(<sup>t</sup>Bu)-OH (8 eq), DIC (8 eq), DMAP (0.5 eq), DCM-DMF (9:1 v/v), 35 °C, 2 h 30 min; j) 0.1M HOBT in a DBU-DMF (2:98 v/v) solution (1 x 1 min); k) TFA-TIS-DCM (90:5:5 v/v), 25 °C, 30 min, anhydrous conditions; 25% overall yield after HPLC purification.

Lastly, acetylation of the free amine was carried out prior to depsipeptide **1.29** cleavage and global deprotection with a TFA–TIS–DCM (90:5:5 v/v) cocktail under anhydrous conditions. The linear precursor **1.32** was subjected to HPLC purification and obtained with an overall yield of 25%. Considering the synthetic complexity of the target molecule and the numerous steps required for the preparation, **1.32** was prepared with an outstanding overall yield after HPLC purification.

### **1.3.3 Efficiency of the stepwise synthetic strategy by comparison with segment condensation strategies**

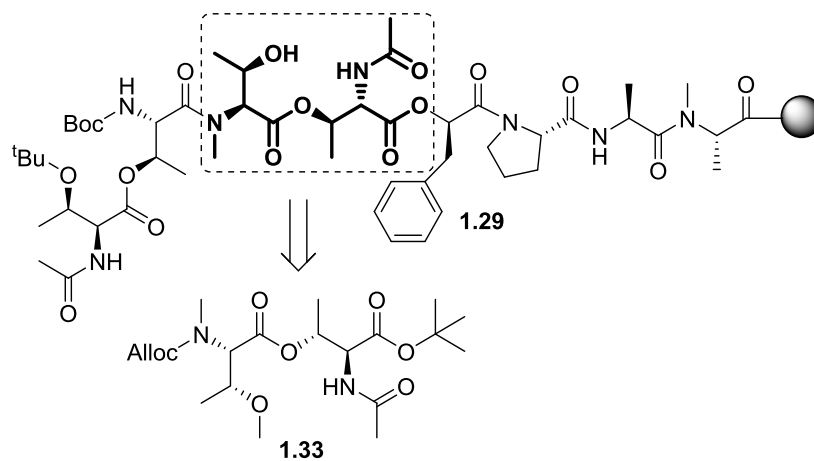
A readily used approach in depsipeptide synthesis is segment condensation, in which the segment containing the ester bond is synthesised in solution and incorporated onto the peptide chain through an amide bond formation.<sup>[61]</sup> Up to date, segment condensation is the most efficient strategy for depsipeptide synthesis.

We wished to evaluate the efficiency of our recently developed stepwise strategy by its comparison with a traditional segment condensation approach. In order to evaluate whether it is more efficient to incorporate the residues in an exclusive stepwise manner or following a traditional segment condensation approach, two synthetic strategies incorporating either one or two depsipeptide segments, respectively, were developed.

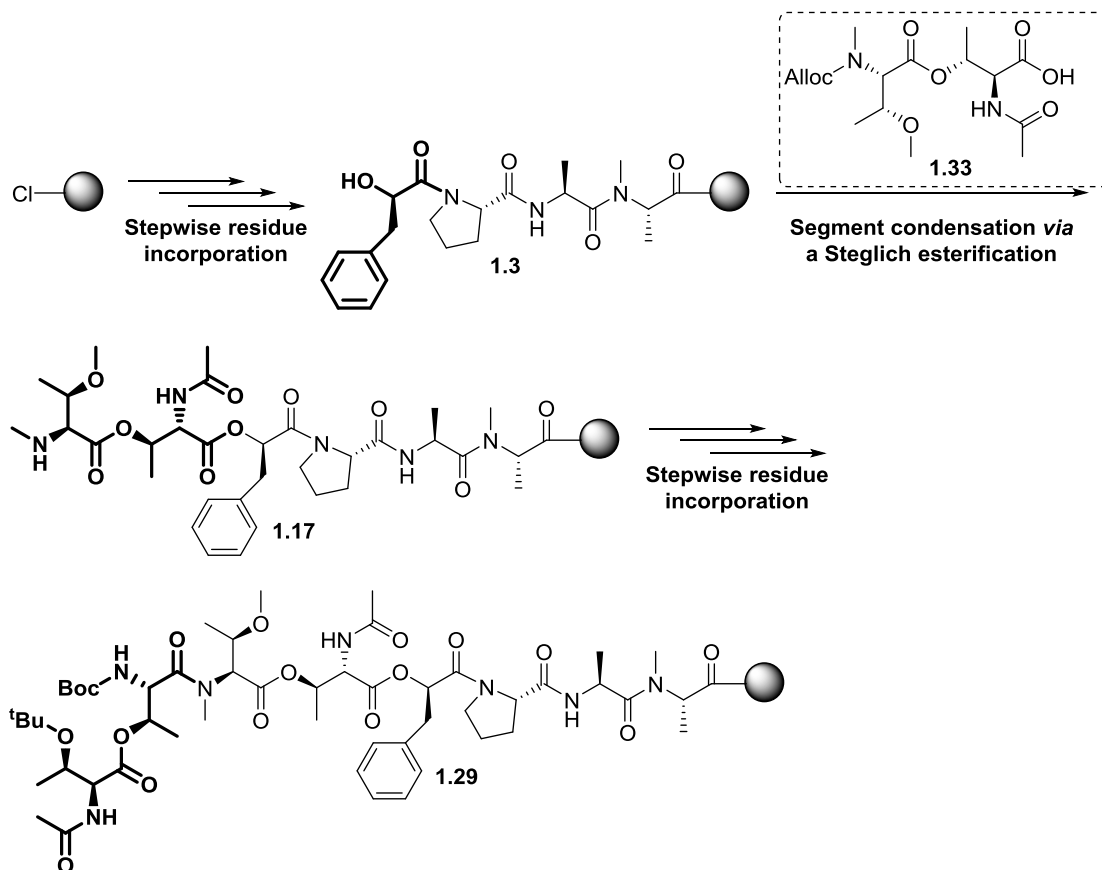
#### **1.3.3.1 Development of a synthetic strategy containing one segment condensation**

##### **1.3.3.1.1 Initial synthetic approach**

According to our synthetic approach, the Ac-Thr-OH residue was the first one to be assembled through an ester linkage. Thus, the first logical segment condensation that came to mind was insertion of the depsipeptide building Ac-Thr(O(Alloc-*N,O*-Me<sub>2</sub>Thr-CO))-COOH (**1.33**, Scheme 1.29) onto tetrapeptide **1.3**. In this context, the synthetic strategy described in Scheme 1.30 was pursued.



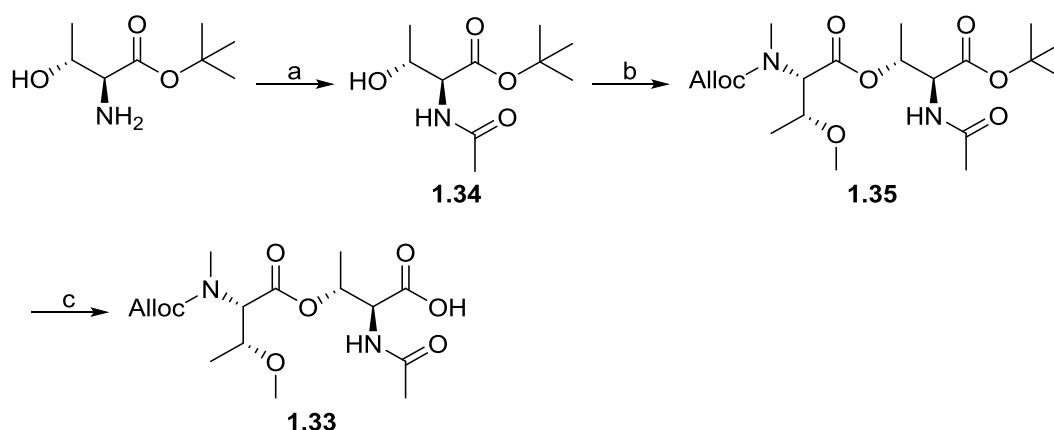
Scheme 1.29. Depsipeptide building block containing the Ac-Thr-OH and the *N,O*-Me<sub>2</sub>Thr-OH residues.



Scheme 1.30. Initial proposal of a synthetic strategy containing one depsipeptide building block segment condensation.

### 1.3.3.1.1.1 Preparation of dipeptide building block Ac-Thr(O(Alloc-N,O-Me<sub>2</sub>Thr-CO)-COOH (**1.33**)

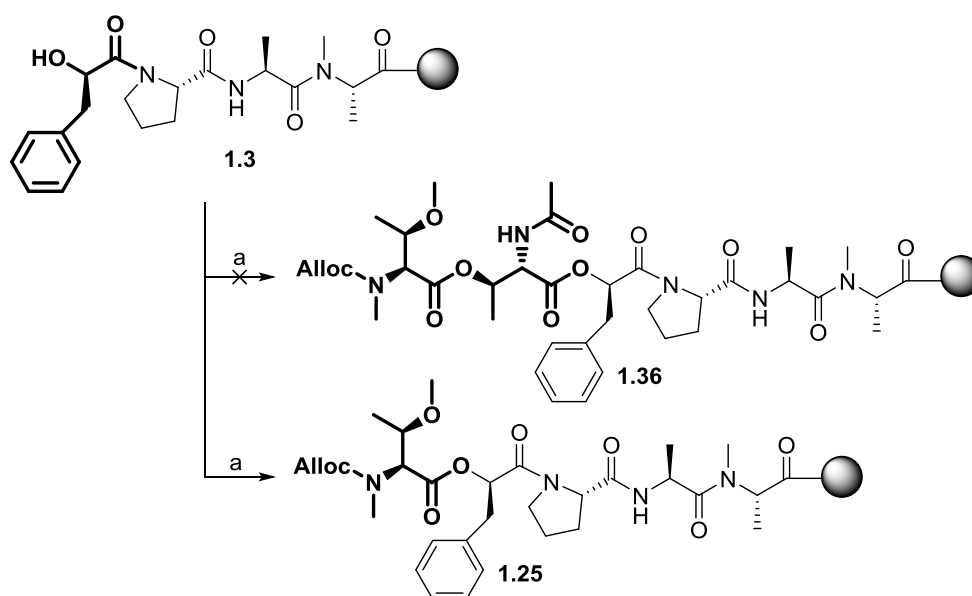
Synthesis of building block **1.33** was carried out as follows. Compound **1.34** can be obtained in the presence of free hydroxyl functionalities by amide bond formation between threonine *tert*-butyl ester and AcOH using DIC/DMAP as coupling agents (Scheme 1.31). DIC is widely used in peptide chemistry because of its high reactivity and low cost. In this case, full conversion of starting material was reached after 3 h 30 min. Purification was required to fully eliminate the corresponding formed urea, and compound **1.34** was obtained with a 97% yield after flash chromatography purification. Acetylation was also evaluated using carbodiimide EDC instead of DIC, since its urea derivate can be washed away with acidic extractions and therefore the purification step would be avoided. Nevertheless, acetylation with EDC led to longer reaction times and low yields (28%). Thus, acetylation was performed with the DIC/DMAP system. Next, esterification between **1.34** with previously prepared Alloc-*N,O*-Me<sub>2</sub>Thr-OH (**1.20**) was performed in solution phase upon Steglich esterification conditions, being compound **1.35** obtained in a 46% yield after purification with a C18 reversed-phase Porapak™ Rxn Cartridge. Carboxylic acid deprotection was successfully accomplished by treatment with a TFA–DCM (9:1 v/v) mixture. Pure **1.33** was obtained in quantitative yields and used without further purification.



*Scheme 1.31.* Synthesis of dipeptide **1.33**. a) AcOH (1.2 eq), DIC (1.2 eq), DIEA (1 eq), DMAP (0.1 eq), DMF, rt, 3 h 30 min, 97%; b) Alloc-*N,O*-Me<sub>2</sub>Thr-OH (**1.20**) (1.5 eq), DIC (1.5 eq), DMAP (0.1 eq), DCM–DMF (9:1 v/v), 0–20 °C, 24 h, 46%; c) TFA–DCM (9:1 v/v), 2 h, N<sub>2</sub> atmosphere, Quantitative yield.

### 1.3.3.1.1.2 Segment condensation of didesipeptide *Ac-Thr(O(Alloc-N,O-Me<sub>2</sub>Thr-CO))-COOH (1.33)*

Segment condensation of building block **1.33** onto tetrapeptidyl-resin **1.3** was performed upon Steglich esterification conditions (Scheme 1.32). The following incorporation conditions were used AA–DIC–DMAP (8:8:0.5 eq), in which the carboxylic acid was pre-activated over 5 min prior to its on-resin incorporation, followed by addition of catalytic amounts of DMAP. The reaction was performed at 35 °C under anhydrous conditions.



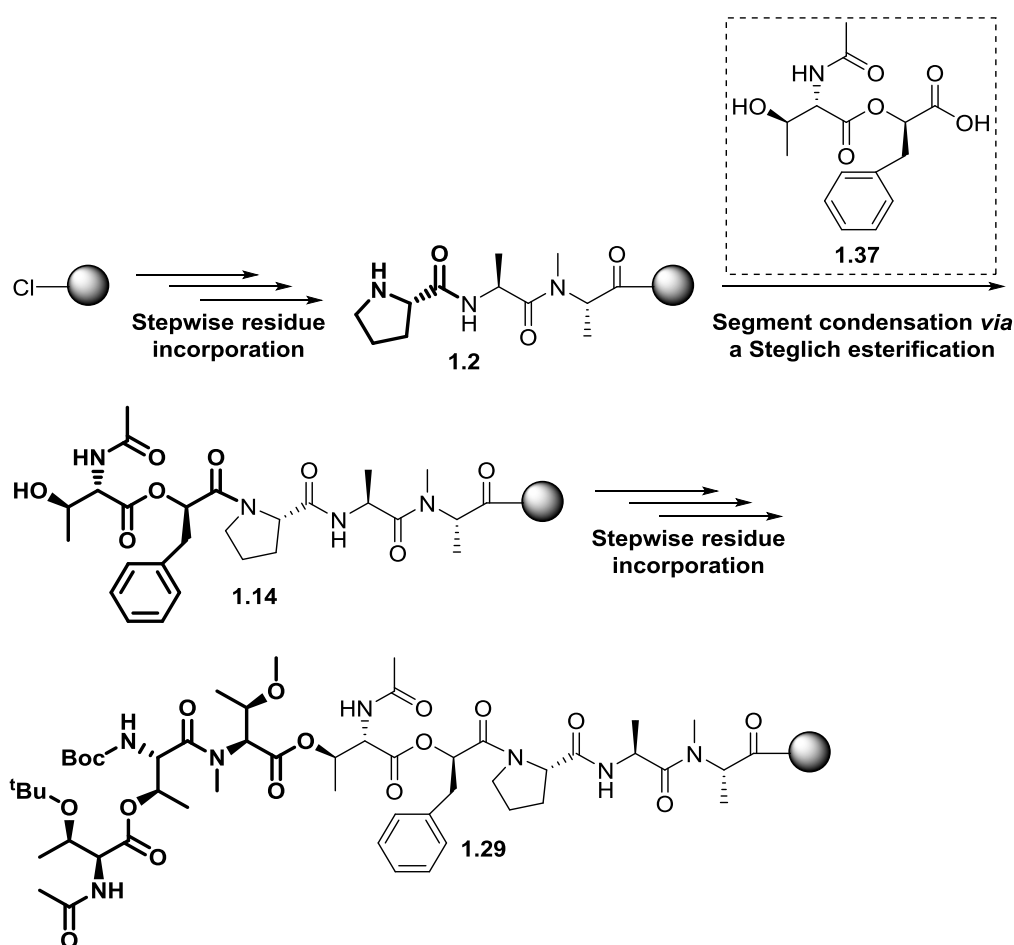
*Scheme 1.32.* Segment condensation of **1.33** via an on-resin Steglich esterification failed to afford **1.25** and **1.36** was obtained instead. a) **1.33** (8 eq), DIC (8 eq), DMAP (0.5 eq), DCM–DMF (9:1 v/v), 35 °C, 2 h 30 min.

HPLC-MS analysis of the hexadepsipeptidyl-resin cleavage crude showed complete formation of compound **1.36** and formation of the desired product (**1.25**) was not detected. We hypothesised that the acetyl moiety might account for deactivation of the carboxylic acid function of **1.33** (see below), thus leading to poor esterification outcome. In this context, desipeptide fragmentation might take place upon activation conditions, and activation of the Alloc-*N,O*-Me<sub>2</sub>Thr-OH residue resulted in complete formation of **1.36**. These results comply with previous experiments carried out in this project and reported in the literature,<sup>[46,63]</sup> in which incorporation of acetylated Ac-Thr(<sup>t</sup>Bu)-OH residue through an on-resin Steglich esterification was not accomplished.

### 1.3.3.1.2 Synthetic strategy containing one segment condensation: Incorporation of the Ac-Thr(OH)-COO-D-Pla-COOH building block onto tripeptidyl-resin **1.2**

Since assembly of **1.33** complete failed to afford the desired product, segment condensation was attempted with the depsipeptide moiety containing the Ac-Thr(OH)-COO-D-Pla-COOH building block instead (**1.37**, Scheme 1.33).

In this case, depsipeptide building block **1.37** was first synthesised to be later on inserted to the depsipeptide chain by segment condensation *via* an amide bond formation.

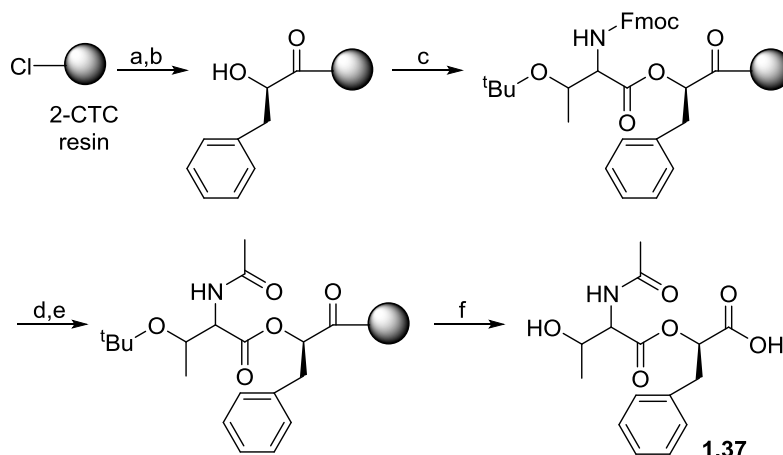


Scheme 1.33. Final synthetic strategy containing one depsipeptide building block segment condensation.

#### 1.3.3.1.2.1 Preparation of building block Ac-Thr(OH)-COO-D-Pla-COOH (**1.37**)

Synthesis of building block **1.37** was carried out on solid-phase, being 2-CTC the resin of choice. The 2-CTC renders the C-terminus as a free carboxylic acid function upon

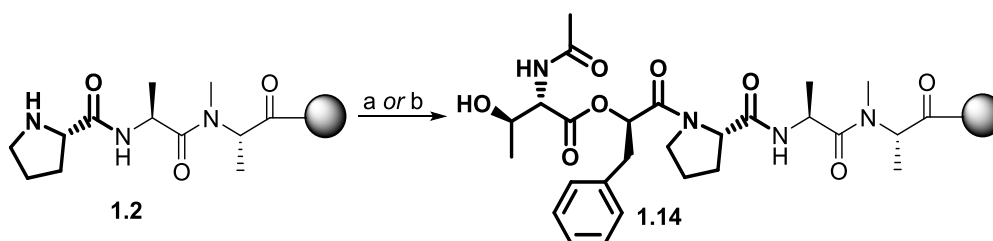
cleavage conditions. Incorporation of D-Pla-OH was performed by standard SPPS means (Scheme 1.34), followed by on-resin Steglich esterification of commercially available Fmoc-Thr(<sup>t</sup>Bu)-OH. HPLC-MS analysis of the cleavage crude showed complete depsipeptide formation. Fmoc removal with the traditional piperidine–DMF (1:4 v/v) (2 x 1 min) cocktail successfully afforded the free amine. Quickly after Fmoc elimination, acetylation of the free amine was performed with the AcOH–OxymaPure–DIC (3:3:3 eq) coupling system. The reaction conversion was monitored by HPLC-MS analysis. Depsipeptide cleavage from the resin and <sup>t</sup>Bu removal were accomplished by treatment with a TFA–TIS–DCM (90:5:5 v/v) mixture. The crude product was purified with a C18 reversed-phase Porapak™ Rxn Cartridge and pure **1.37** was obtained with an overall yield of 31% over 5 steps.



*Scheme 1.34.* Preparation of the **1.37** building block. a) D-Pla-OH (0.8 eq), DIEA (10 eq), DCM, 50 min; b) MeOH (800  $\mu$ L/g resin), 10 min; c) Fmoc-Thr(<sup>t</sup>Bu)-OH (8 eq), DIC (8 eq), DMAP (0.5 eq), DCM–DMF (9:1 v/v), 2 h 30 min; d) piperidine–DMF (1:4 v/v) (2 x 1 min); e) AcOH (3 eq), OxymaPure (3 eq), DIC (3 eq), DMF, 20 min; TFA–TIS–DCM (90:5:5 v/v), 40 min, anhydrous conditions. Overall yield after purification: 31% over 5 steps.

#### 1.3.3.1.2.2 Segment condensation of depsipeptide Ac-Thr(OH)-COO-D-Pla (**1.37**)

With tripeptidyl-resin **1.2** and building block **1.37** in hands, the best conditions to perform the segment condensation *via* an amidation reaction were evaluated (Scheme 1.35).



*Scheme 1.35.* Segment condensation of **1.37** via an amidation reaction. a) **1.37** (3 eq), PyBOP (3 eq), HOAt (3 eq), DIEA (6 eq), 25 °C, 24 h; b) **1.37** (3 eq), HATU (3 eq), HOAt (3 eq), DIEA (6 eq), 25 °C, 2 h.

Segment condensation was tested with the **1.37**–HATU–HOAt–DIEA (3:3:3:6 eq) and the **1.37**–PyBOP–HOAt–DIEA (3:3:3:6 eq) coupling systems. The latter led to a better incorporation outcome, being pentadepsipeptide **1.2** obtained with excellent conversion according to HPLC-MS analysis (Figure 1.20).

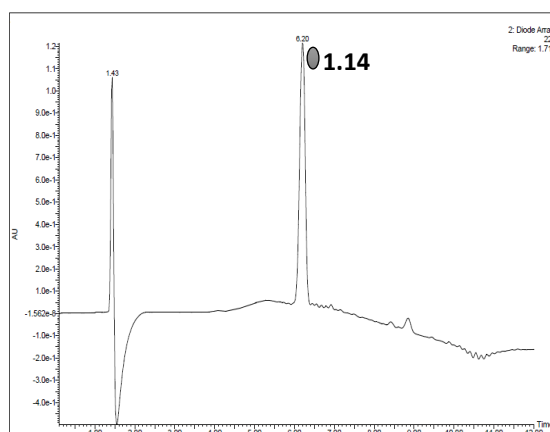
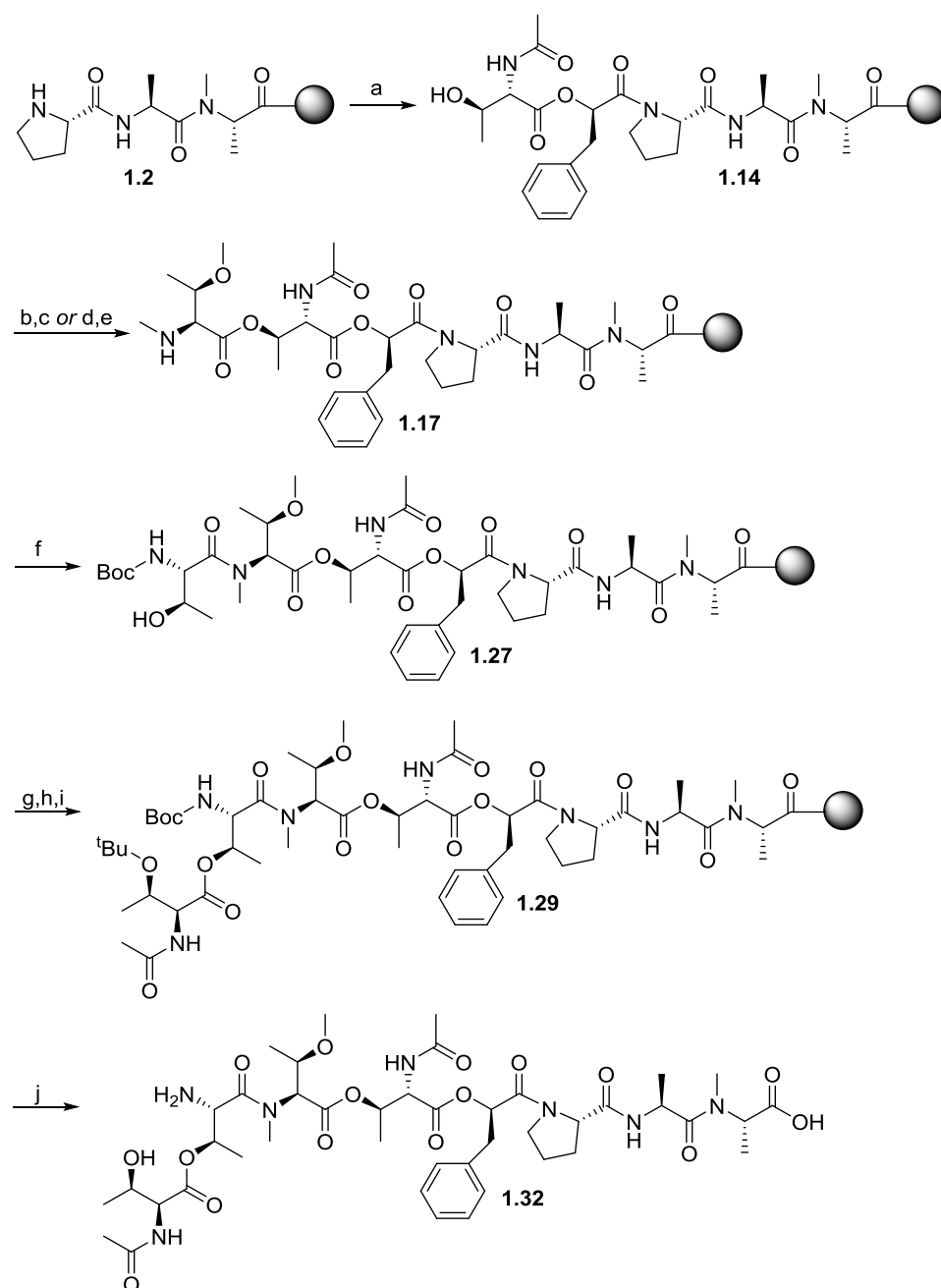


*Figure 1.20.* HPLC-MS chromatograms run at G0100t9T25 and processed at 220 nm. **1.37** incorporation onto **1.2** through an amidation reaction.

#### 1.3.3.1.2.3 Synthetic strategy containing one segment condensation: depsipeptide chain elongation

Once segment condensation of **1.37** was accomplished, assembly of the remaining residues, namely *N,O*-Me<sub>2</sub>Thr-OH, Boc-Thr-OH and Ac-Thr(<sup>t</sup>Bu)-OH, was carried out in a stepwise manner following the already developed fully stepwise strategy (Scheme 1.36). Thus, on-resin Steglich esterification between the hydroxyl group of **1.2** and the *N*-protected *N,O*-Me<sub>2</sub>Thr carboxylic acid was carried out. In this case, 22-23% of racemisation upon ester bond formation was also observed.

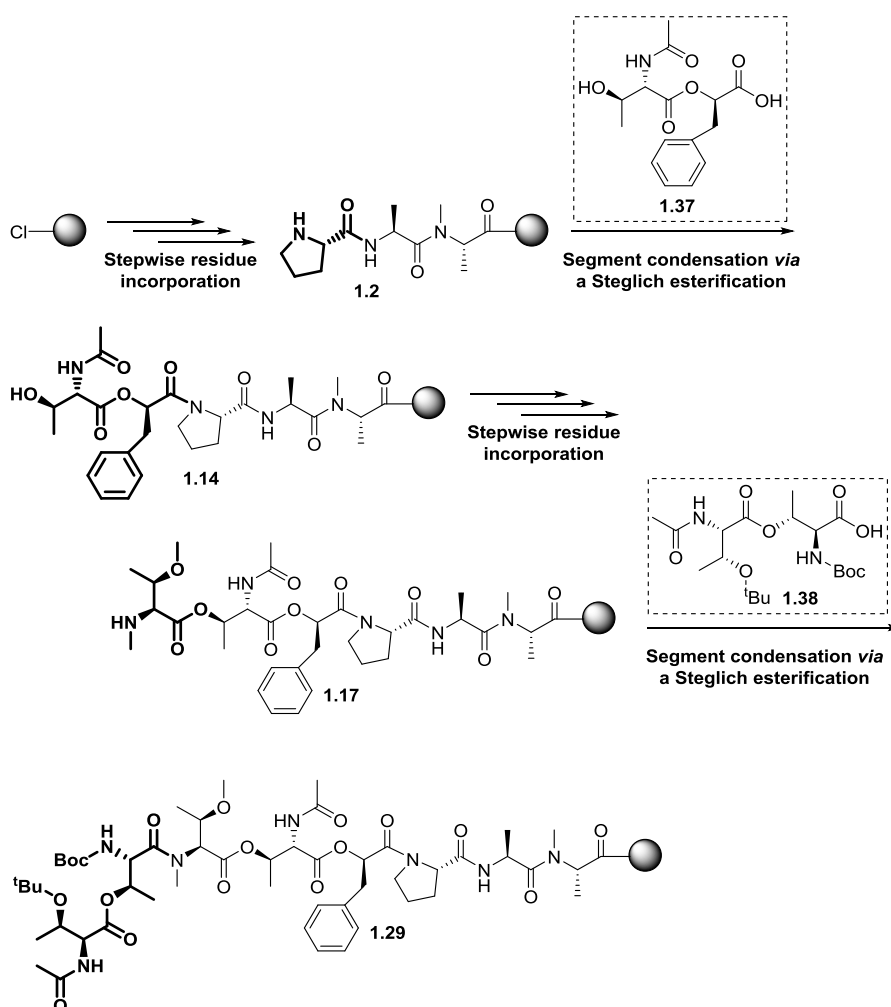


**Scheme 1.36.** Final strategy containing one segment condensation to prepare the linear precursor of **1.1**. a) **1.37** (3 eq), PyBOP (3 eq), HOAt (3 eq), DIEA (6 eq), DMF, 25 °C, 24 h; b) Alloc-*N,O*-Me<sub>2</sub>Thr-OH (**1.20**) (8 eq), DIC (8 eq), DMAP (0.5 eq), DCM–DMF (9:1 v/v), 35 °C, 2 h 30 min; c) Pd(PPh<sub>3</sub>)<sub>4</sub> (0.1 eq), PhSiH<sub>3</sub> (10 eq), DCM, 15 min; d) Fmoc-*N,O*-Me<sub>2</sub>Thr-OH (**1.24**) (8 eq), DIC (8 eq), DMAP (0.5 eq), DCM–DMF (9:1 v/v), 35 °C, 2 h 30 min; e) DBU–DMF (2:98) (1 x 1 min); f) Boc-Thr-OH (3 eq), HATU (3 eq), HOAt (3 eq), DIEA (6 eq), 25 °C, 1 h; g) Fmoc-Thr(<sup>t</sup>Bu)-OH (8 eq), DIC (8 eq), DMAP (0.5 eq), DCM–DMF (9:1 v/v), 35 °C, 2 h 30 min; h) 0.1M HOBT in a DBU–DMF (2:98 v/v) solution (1 x 1 min); i) AcOH (3 eq), OxymaPure (3 eq), DIC (3 eq); j) TFA–TIS–DCM (90:5:5 v/v), 25 °C, 30 min, anhydrous conditions; 24% overall yield after HPLC purification.

Amine removal protecting group, Alloc, was required prior to Boc-Thr-OH residue coupling with the HATU-HOAt-DIEA coupling system. Lastly, Steglich esterification of commercially available Fmoc-Thr(<sup>t</sup>Bu)-OH was carried out, followed by Fmoc removal and subsequent acetylation. The linear depsipeptide was released from the resin and subjected to HPLC purification. HPLC purification of the crude product furnished the linear peptide **1.32** with a 24% overall yield. Remarkably, a comparable overall yield was obtained with our convenient fully stepwise strategy.

### 1.3.3.2 Development of a synthetic strategy containing two segment condensations

A synthetic strategy containing two depsipeptide building blocks segment condensations was designed as follows (Scheme 1.37).



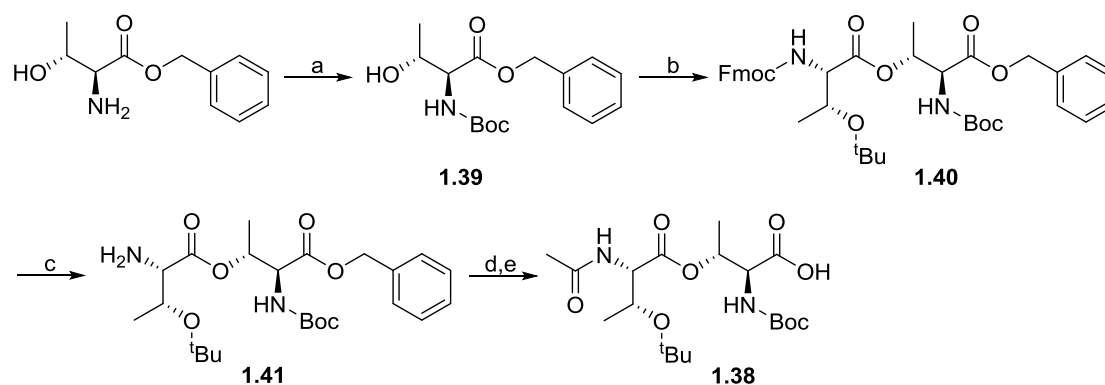
Scheme 1.37. Proposal of a synthetic strategy containing two segment condensations.

Two building blocks corresponding to dipeptides Ac-Thr(OH)-COO-D-Pla-COOH (**1.37**) and Boc-Thr(O(Ac-Thr(<sup>t</sup>Bu)-CO))-COOH (**1.38**) were assembled to the linear chain upon an amide bond formation.

Since building block Ac-Thr(OH)-COO-D-Pla-COOH (**1.37**) assembly was already optimised as described in the previous section, the synthesis of the Boc-Thr(O(Ac-Thr(<sup>t</sup>Bu)-CO))-COOH dipeptide (**1.38**) and its subsequent incorporation to the linear chain is described in the present section.

### 1.3.3.2.1 Preparation of building block Boc-Thr(O(Ac-Thr(<sup>t</sup>Bu)-CO))-COOH (**1.38**)

Synthesis of **1.38** started with commercially available threonine benzyl ester (Scheme 1.38). The amine function was selectively protected with the Boc group in the presence of a free hydroxyl group by treatment with Boc<sub>2</sub>O and Et<sub>3</sub>N. Compound **1.39** was obtained in moderate yields (56%) after column chromatography purification. Next, esterification between **1.39** and commercially available Fmoc-Thr(<sup>t</sup>Bu)-OH was carried out in solution phase upon Steglich esterification conditions, being dipeptide **1.40** obtained in good yields (86%) after column chromatography purification. Fmoc group removal was accomplished by treatment with Et<sub>2</sub>N, and the free amine was subjected to column chromatography purification to afford pure **1.41** with a 46% yield.



*Scheme 1.38.* Synthesis of dipeptide **1.38** a) Boc<sub>2</sub>O (1.1 eq), Et<sub>3</sub>N (2.1 eq), DCM, 25 °C, 2 h, 56%; b) Fmoc-Thr(<sup>t</sup>Bu)-OH (1.5 eq), DIC (1.5 eq), DMAP (0.1 eq), DCM-DMF (9:1 v/v), 0 °C, 1 h, 86%; c) Et<sub>2</sub>N-DCM (4:6 v/v), 25 °C, 2 h, 46%; d) CH<sub>3</sub>COCl (1.2 eq), Et<sub>3</sub>N (1.4 eq), 25 °C, 1 h; e) H<sub>2</sub> Pd/C, MeOH 47% over two steps.

Acetylation was accomplished by reaction of **1.41** with CH<sub>3</sub>COCl and Et<sub>3</sub>N, followed by benzyl protecting group removal under catalytic hydrogenation conditions.

Flash chromatography purification afforded compound **1.38** with a 47% yield over two steps.

#### **1.3.3.2.2 Synthetic strategy containing two segment condensations: depsipeptide chain elongation**

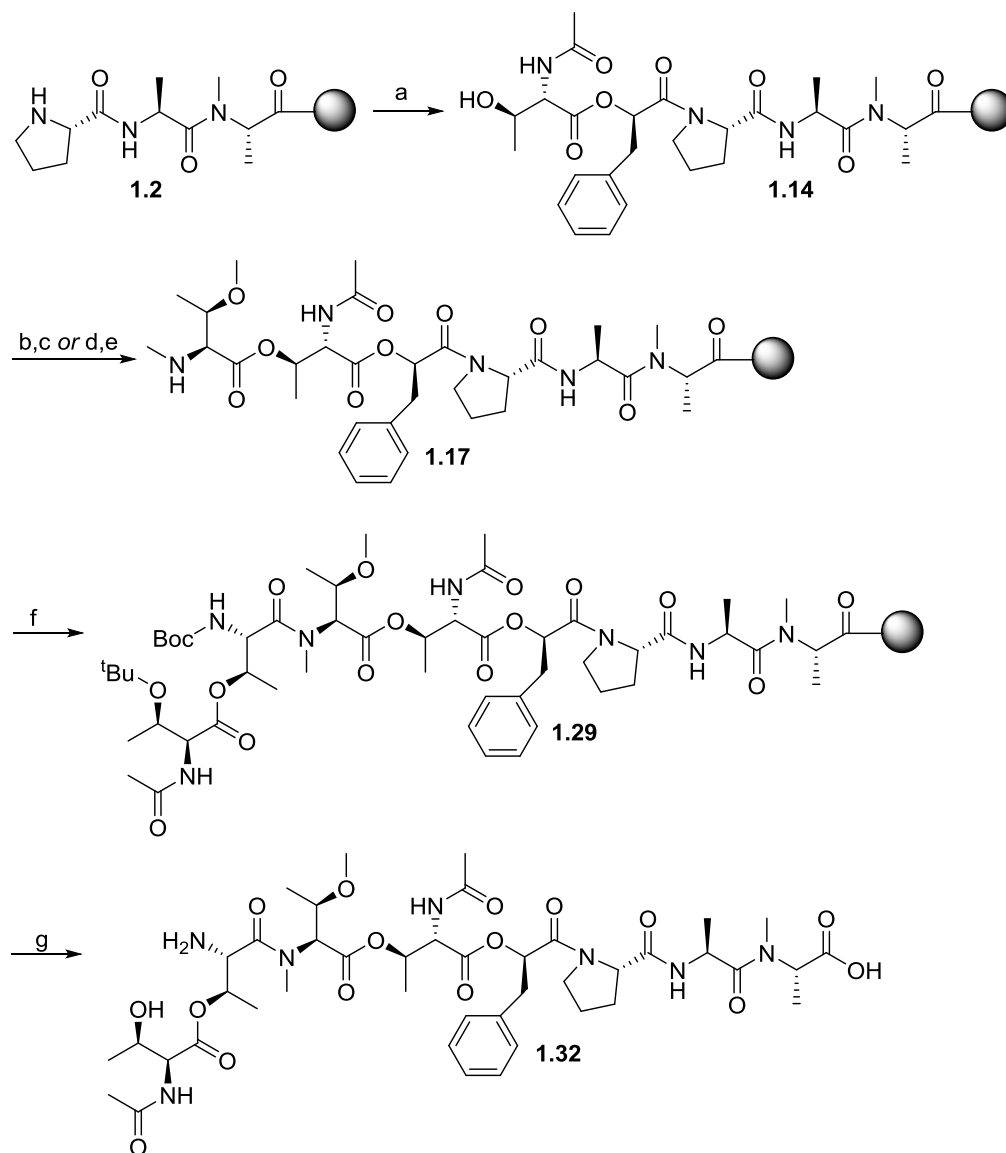
The general synthetic strategy to prepare the linear precursor of **1.1** through a strategy containing two segment condensations is described as follows (Scheme 1.39).

Linear tripeptide **1.2** was prepared by standard SPPS means. Segment condensation of Ac-Thr-O-D-Pla-OH building block was successfully accomplished with the **1.37**–PyBOP–HOAt–DIEA (3:3:3:6 eq) coupling system. As previously mentioned, HPLC-MS analysis showed the formation of a single product corresponding to the desired product (**1.14**).

Next, on-resin Steglich esterification between the free alcohol group of **1.14** and either the Alloc or the Fmoc protected *N,O*-Me<sub>2</sub>Thr-OH residue was carried out. Amine protecting group removal was followed by incorporation of the last depsipeptide segment (**1.38**). Segment condensation of **1.38** was successfully accomplished by treatment of the peptidyl-resin **1.17** with the **1.38**–HATU–collidine (3:3:6 eq) coupling system. HPLC-MS analysis showed the presence of one single peak corresponding to the desired product (**1.29**).

Finally, global deprotection and depsipeptide release from the resin was performed under anhydrous conditions by using a TFA–TIS–DCM mixture. The crude linear product was subjected to HPLC purification to furnish **1.32** in a 26% overall yield.

Remarkably, a comparable overall yield was obtained with our convenient fully stepwise strategy and the synthetic strategy containing one depsipeptide building block segment condensation.



**Scheme 1.39.** Final synthetic strategy containing two depsipeptide building blocks segment condensations to prepare the linear precursor of **1.1**. a) **1.37** (3 eq), PyBOP (3 eq), HOAt (3 eq), DIEA (6 eq), DMF, 25 °C, 24 h; b) Alloc-*N,O*-Me<sub>2</sub>Thr-OH (**1.20**) (8 eq), DIC (8 eq), DMAP (0.5 eq), DCM-DMF (9:1 v/v), 35 °C, 2 h 30 min; c) Pd(PPh<sub>3</sub>)<sub>4</sub> (0.1 eq), PhSiH<sub>3</sub> (10 eq), DCM, 15 min; d) Fmoc-*N,O*-Me<sub>2</sub>Thr-OH (**1.24**) (8 eq), DIC (8 eq), DMAP (0.5 eq), DCM-DMF (9:1 v/v), 35 °C, 2 h 30 min; e) DBU-DMF (2:98 v/v) (1 x 1 min); f) **1.38** (3 eq), HATU (3 eq), collidine (6 eq), DMF, 25 °C, 2 h; g) TFA-TIS-DCM (90:5:5 v/v), 25 °C, 30 min, anhydrous conditions; 26% overall yield after HPLC purification.

### 1.3.3.3 Comparison of the three developed strategies

Three synthetic strategies have been developed and optimised for the preparation of the linear precursor of depsipeptide **1.1** including (i) a fully stepwise strategy, (ii) a strategy containing one depsipeptide segment condensation and (iii) a strategy containing two depsipeptide segment condensations. Evaluation of the best

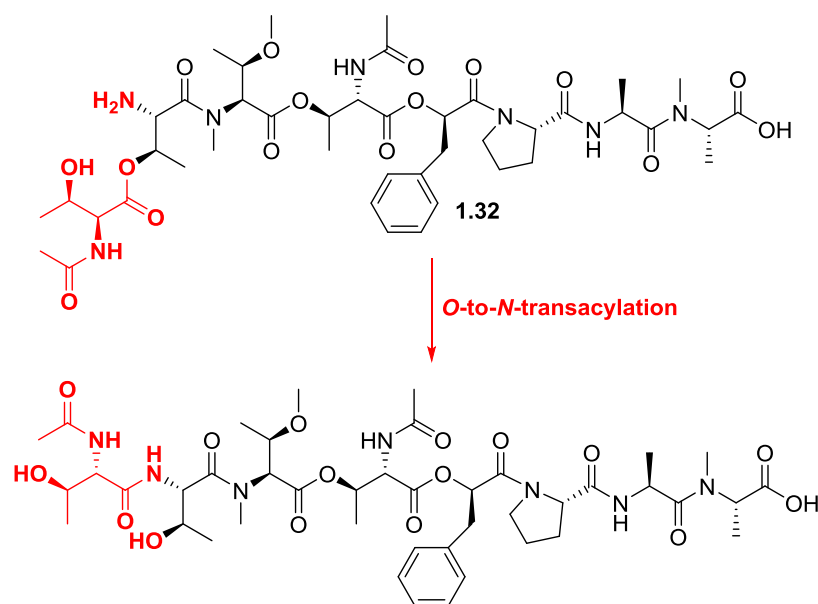
approach to the total synthesis of the target molecule was undertaken, and all three strategies proved effective for the preparation of complex depsipeptides that are composed of  $\beta$ -branched residues and contain multiple and consecutive ester linkages. Although one would think that the fully stepwise strategy would lead to higher percentages of side-products (since more steps are carried out along the solid-phase synthesis), HPLC analysis of all three crude linear products showed similar HPLC traces. In fact, comparable yields after HPLC purification of the crude linear depsipeptide **1.32** were obtained (between 24-26%).

However, the fully stepwise strategy presents some advantages over segment condensation strategies. A major advantage of this strategy is that the excesses of reagents can be washed away by simple suction, and therefore only one purification step throughout the synthesis is required. Additionally, the numerous commercially available Fmoc-protected amino acid derivatives facilitate the synthetic process. Contrary, segment condensation strategies demand numerous purifications, since preparation of depsipeptide building blocks often comprises several reaction and purification steps. Thus, segment condensation approaches are ultimately more time-consuming and laborious.

It is worth highlighting the versatility of the fully stepwise strategy, as the prevalent drawbacks encountered during depsipeptide synthesis associated with (i) the Fmoc protecting group and (ii) the protecting group scheme for residue incorporation, were extensively studied and solved. In fact, the Fmoc-based stepwise strategy becomes a valuable tool for the rapid preparation of many synthetic analogues.

#### 1.3.4 Depsipeptide macrolactamisation

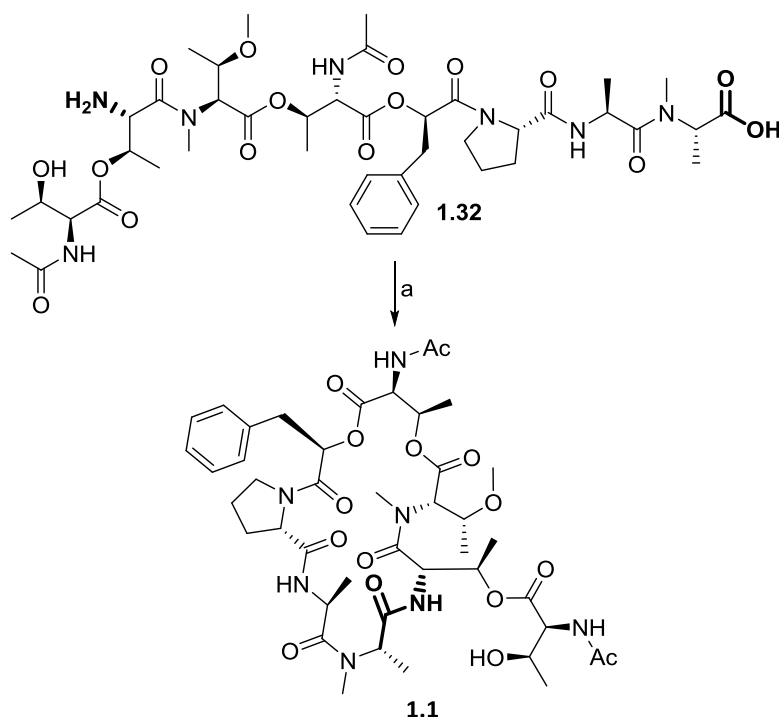
The disconnection site for compound **1.1** was chosen between the *N*-terminal L-Thr and *C*-terminal *N*-MeAla. Cyclisation in solution can be undertaken in the presence of free hydroxyl functionalities. Nevertheless, the linear depsipeptide can undergo *O*-to-*N*-transacylation (see Scheme 1.40), and therefore special attention was put into this when carrying out the reaction.



Scheme 1.40. Possible *O-to-N*-transacylation side-reaction.

High dilution conditions were required to favour intramolecular cyclisation and prevent polymerisation,<sup>[109]</sup> and therefore the linear depsipeptide concentration was set up to 1.0 mM. Macrolactamisation of **1.32** was carried out in solution using the HATU–collidine coupling system (Scheme 1.41). According to HPLC-MS analysis, full consumption of the starting material was not accomplished, being the highest conversion rates achieved within the first two hours. Neither *O-to-N*-transacylation nor racemisation were observed. HPLC purification of the crude product furnished the target molecule **1.1** with a 22% yield. These results comply with literature, being the yields for cyclisation of YM-254890 and their synthetic analogues comprised within this range.<sup>[63]</sup>

Nevertheless, this cyclisation extent is rather low, and future work should be addressed at the optimisation of this step. A good starting point would be evaluation of the optimal coupling reagents system as well as selection of a different disconnection point for cyclodepsipeptide **1.1**.



Scheme 1.41. Depsipeptide **1.32** cyclisation in solution to afford **1.1**. a) HATU (1 eq), collidine (3 eq), DMF, 25 °C, 2 h, 22%.

### 1.3.5 Overview of the Fmoc removal studies and selection of the appropriate protecting group scheme

This section encloses a brief summary on the obtained results regarding extensive Fmoc removal studies. Additionally, a brief summary on the selection of the appropriate protecting group scheme for stepwise residue incorporation is also given.

#### 1.3.5.1 Overview of the Fmoc removal studies

Fmoc removal after formation of ester linkages *via* assembly of Fmoc-protected residues at the *N*-terminus, as well as incorporation of the second residue of the peptide sequence, were extensively studied. Whilst the first led to racemisation and formation of undesired  $\alpha,\beta$ -elimination side-products, the latter led to DKP formation. As previous studies had already shown, addition of small percentages of organic acids to both the piperidine and the DBU solutions has proven effective to diminish aspartimide formation during Fmoc removal treatments.<sup>[83,87,88]</sup> Inspired by this principle, a source of protons (HOBt or OxymaPure) was added to both cocktail mixtures to partially neutralise the

base and improve the deprotection outcome. Thus, optimal conditions to prevent or minimise these drawbacks are summarised in the present section.

#### Overview of the Fmoc removal studies regarding DKP formation

1. For the first time, addition of small percentages of organic acids to the Fmoc removal cocktail considerably minimised DKP formation.
2. An improvement in the Fmoc removal outcome was observed when replacing the traditional piperidine–DMF (1:4 v/v) system by the DBU–DMF (2:98 v/v) cocktail.
3. Although addition of OxymaPure did not exert a positive effect on the deprotection step, addition of HOBt to both the piperidine and the DBU solutions resulted in minimised DKP formation rates. DKP formation could be reduced to a more than acceptable 5% percentage.
4. Among all tested conditions, the optimal treatment to minimise DKP formation was found to be the following: 0.1 M HOBt in DBU–DMF (2:98 v/v) (2 x 1 min).

#### Overview of the Fmoc removal studies after ester bond formation

General conclusions for Fmoc removal after formation of the three ester linkages are drawn as follows.

1. For the first time, addition of small percentages of organic acids to the Fmoc removal cocktail resulted, in most of the cases, in an improvement in the deprotection step after assembly of Fmoc-protected residues *via* ester bond formation.
2. In all cases, an improvement in the Fmoc removal step was observed when replacing the traditional piperidine–based mixture by the DBU–DMF (2:98 v/v) cocktail.
3. In most cases, addition of HOBt or OxymaPure in a 0.1 M concentration improved the Fmoc removal outcome. Generally, addition of higher percentages of both organic acids (in a 0.2 M concentration) accounted for poorer results, probably due to the base being neutralised in excess.

Next, an overview on the evaluation of the optimal Fmoc removal conditions after formation of each ester linkage is given. Note that the overall chemical diversity provided by the model peptide **1.1**, allowed Fmoc removal studies upon diverse chemical environments after ester bond formation.

1. Optimal Fmoc removal conditions after formation of the *first ester linkage* were accomplished by treatment of the peptidyl-resin with either a 0.1 M OxymaPure in DBU–DMF (2:98 v/v) solution (1 x 1 min) or a 1.0 M TBAF solution in THF (2 x 15 min). In this case, epimerisation (50–60%) was fully circumvented.
2. Optimal Fmoc removal conditions after formation of the *second ester linkage* were accomplished by treatment of the peptidyl-resin with a DBU–DMF (2:98 v/v) solution (1 x 1 min), in which the desired product was obtained with a 57% conversion. In this case, addition of small percentages of organic acids did not improve the deprotection outcome. For the first time, a big step forward was made since formation of the  $\alpha,\beta$ -elimination side-product was considerably minimised, however, there is still room for improvement and further research is needed. Future studies could focus on attempting the complete prevention of the undesired side-product formation. For that, other additives such as formic acid could be used. Additionally, compounds with less acidic protons like phenols or polyphenols could be assessed.
3. Optimal Fmoc removal conditions after formation of the *third ester linkage* were accomplished by treatment of the peptidyl-resin with a 0.1 M HOBT in DBU–DMF (2:98 v/v) solution (1 x 1 min). Whereas treatment with the traditional piperidine-based mixture accounted for the formation of the undesired  $\alpha,\beta$ -elimination side-product in high percentages (90%), the conditions mentioned above fully prevented this undesired side-reaction. In this last Fmoc removal step, we were happy to observed quantitative formation of the desired unprotected product.

### 1.3.5.2 Overview of the appropriate protecting group scheme

Next, an overview on the appropriate protecting group scheme for residue assembly *via* ester bond formation is given. Note that the overall chemical diversity provided by the model peptide **1.1**, allowed development of the optimal protection scheme for each residue incorporation upon diverse chemical environments.

1. Formation of the *first ester linkage* was accomplished by assembly of Fmoc-Thr(TBDMS)-OH. Surprisingly, introduction of the until now unreactive Ac-Thr-OH derivative in a stepwise manner was only accomplished with the amine function protected with Fmoc, and protection with Ac or Alloc resulted in no incorporation. The Thr derivative was provided with appropriate and orthogonal protecting groups for the amine and the hydroxyl functions (Fmoc and TBDMS, respectively), being Fmoc and TBDMS simultaneously removed by treatment with TBAF after residue incorporation.
2. Formation of the *second ester linkage* was accomplished by assembly of either Alloc-*N,O*-Me<sub>2</sub>Thr-OH or Fmoc-*N,O*-Me<sub>2</sub>Thr-OH. Whereas Alloc removal was successfully accomplished, Fmoc elimination afforded the desired product in a more modest HPLC conversion (57%). Although Fmoc removal led to lower HPLC yields, the Fmoc protecting group might be very useful for the rapid preparation of a series of analogues. In fact, the presence of 43% of impurities at this late stage of the synthesis was considered good enough to carry on with the assembly of the last two residues. Most importantly, these results represent a huge step forward compared to previously described results, since prior studies that aimed at Fmoc removal of this residue, mostly resulted in  $\alpha,\beta$ -elimination.
3. Formation of the *third ester linkage* was accomplished by assembly of commercially available Fmoc-Thr(<sup>t</sup>Bu)-OH. In agreement with previous results, incorporation of this residue was only accomplished with the amine function protected with Fmoc, and protection with Ac or Alloc resulted in no incorporation.

## 1.5 References

- [1] X. Ye, K. Anjum, T. Song, W. Wang, Y. Liang, M. Chen, H. Huang, X. Y. Lian, Z. Zhang, *Phytochemistry* **2017**, *135*, 151–159.
- [2] X. Wang, X. Gong, P. Li, D. Lai, L. Zhou, *Molecules* **2018**, *23*, 169.
- [3] M. Fujioka, S. Koda, Y. Morimoto, K. Biemann, *J. Org. Chem.* **1988**, *53*, 2820–2825.
- [4] G. Yang, Y. Li, *Helv. Chim. Acta* **2002**, *85*, 168–174.
- [5] A. Dmitrenok, T. Iwashita, T. Nakajima, B. Sakamoto, M. Namikoshi, H. Nagai, *Tetrahedron* **2006**, *62*, 1301–1308.
- [6] G. S. B. Andavan, R. Lemmens-Gruber, *Mar. Drugs* **2010**, *8*, 810–834.
- [7] V. Gogineni, M. T. Hamann, *Biochim. Biophys. Acta - Gen. Subj.* **2018**, *1862*, 81–196.
- [8] A. Aneiros, A. Garateix, *J. Chromatogr. B Anal. Technol. Biomed. Life Sci.* **2004**, *803*, 41–53.
- [9] Y. Lee, C. Phat, S. C. Hong, *Peptides* **2017**, *95*, 94–105.
- [10] G. M. Suarez-Jimenez, A. Burgos-Hernandez, J.-M. Ezquerra-Brauer, *Mar. Drugs* **2012**, *10*, 963–986.
- [11] D. J. Newman, G. M. Cragg, *Mar. Drugs* **2014**, *12*, 255–278.
- [12] M. F. Mehbub, J. Lei, C. Franco, W. Zhang, *Mar. Drugs* **2014**, *12*, 4539–4577.
- [13] S. Sivanathan, J. Scherckenbeck, *Molecules* **2014**, *19*, 12368–12420.
- [14] J. Kitagaki, G. Shi, S. Miyauchi, S. Murakami, Y. Yang, *Anticancer. Drugs* **2015**, *26*, 259–271.
- [15] R. Lemmens-Gruber, M. Kamyar, R. Dornetshuber, *Curr. Med. Chem.* **2009**, *16*, 1122–1137.

- [16] M. T. Hamann, C. S. Otto, P. J. Scheuer, *J. Org. Chem.* **1996**, *61*, 6594–6600.
- [17] I. Bonnard, I. Manzanares, K. L. Rinehart, *J. Nat. Prod.* **2003**, *66*, 1466–70.
- [18] J. Gao, M. T. Hamann, *Chem. Rev.* **2011**, *111*, 3208–3235.
- [19] M. Pelay-Gimeno, J. Tulla-Puche, F. Albericio, *Mar. Drugs* **2013**, *11*, 1693–1717.
- [20] U. Hommel, H. P. Weber, L. Oberer, H. U. Naegeli, B. Oberhauser, C. A. Foster, *FEBS Lett.* **1996**, *379*, 69–73.
- [21] D. L. Boger, H. Keim, B. Oberhauser, E. P. Schreiner, C. A. Foster, *J. Am. Chem. Soc.* **1999**, *121*, 6197–6205.
- [22] T. Sasaki, M. Takagi, T. Yaguchi, S. Miyadoh, T. Okada, M. Koyama, *J. Antibiot. (Tokyo)*. **1992**, *45*, 692–697.
- [23] G. Von Samson-Himmelstjerna, A. Harder, T. Schnieder, J. Kalbe, N. Mencke, *Parasitol. Res.* **2000**, *86*, 194–199.
- [24] W. Weckwerth, K. Miyamoto, K. Iinuma, M. Krause, M. Glinski, T. Storm, G. Bonse, H. Kleinkauf, R. Zocher, *J. Biol. Chem.* **2000**, *275*, 17909–17915.
- [25] J. Müller, S. C. Feifel, T. Schmiederer, R. Zocher, R. D. Süßmuth, *ChemBioChem* **2009**, *10*, 323–328.
- [26] K. Yanai, N. Sumida, K. Okakura, T. Moriya, M. Watanabe, T. Murakami, *Nat. Biotechnol.* **2004**, *22*, 848–855.
- [27] R. L. Piekarz, R. Robey, V. Sandor, S. Bakke, W. H. Wilson, L. Dahmouh, D. M. Kingma, M. L. Turner, R. Altemus, S. E. Bates, *Blood* **2001**, *98*, 2865–2868.
- [28] R. Thiel, E. Engineering, M. Ave, E. Engineering, M. Ave, Ê. S, S. Z. Khan, S. Suman, M. Pavani, S. K. Das, et al., *J. Geotech. Geoenvironmental Eng.* **2013**, *1*, 1–11.
- [29] A. N. A. Bicyclic, *J. Antibiot. (Tokyo)*. **1993**, *47*, 301–310.
- [30] G. Ravindra, R. S. Ranganayaki, S. Raghothama, M. C. Srinivasan, R. D. Gilardi, I. L.

- Karle, P. Balaram, *Chem. Biodivers.* **2004**, *1*, 489–504.
- [31] V. Sabareesh, R. S. Ranganayaki, S. Raghothama, M. P. Bopanna, H. Balaram, M. C. Srinivasan, P. Balaram, *J. Nat. Prod.* **2007**, *70*, 715–729.
- [32] F. Cavelier, R. Jacquier, J. L. Mercadier, J. Verducci, M. Traris, A. Vey, *J. Pept. Res.* **1997**, *50*, 94–101.
- [33] M. S. C. Pedras, L. I. Zaharia, D. E. Ward, *Phytochemistry* **2002**, *59*, 579–596.
- [34] R. G. Linington, D. J. Edwards, C. F. Shuman, K. L. McPhail, T. Matainaho, W. H. Gerwick, *J. Nat. Prod.* **2008**, *71*, 22–27.
- [35] R. B. Merrifield, *J. Am. Chem. Soc.* **1963**, *85*, 2149–2154.
- [36] M. Stawikowski, P. Cudic, in *Pept. Charact. Appl. Protoc.* (Ed.: G.B. Fields), **2007**, pp. 321–339.
- [37] S. Capasso, A. Vergara, L. Mazzarella, *J. Am. Chem. Soc.* **1998**, *120*, 1990–1995.
- [38] J. D. Wade, M. N. Mathieu, M. Macris, G. W. Tregear, *Int. J. Pept. Res. Ther.* **2000**, *7*, 107–112.
- [39] B. F. Gisin, R. B. Merrifield, *J. Am. Chem. Soc.* **1972**, *94*, 3102–3106.
- [40] M. C. Khosla, R. R. Smeby, F. M. Bumpus, *J. Am. Chem. Soc.* **1972**, *94*, 4721–4724.
- [41] M. Rothe, J. Mazánek, *Angew. Chemie Int. Ed. English* **1972**, *11*, 293–293.
- [42] J. M. Humphrey, A. R. Chamberlin, *Chem. Rev.* **1997**, *97*, 2243–2266.
- [43] J. Tulla-Puche, N. Bayó-Puxan, J. A. Moreno, A. M. Francesch, C. Cuevas, M. Álvarez, F. Albericio, *J. Am. Chem. Soc.* **2007**, *129*, 5322–5323.
- [44] Y. Sohma, Y. Hayashi, M. Kimura, Y. Chiyomori, A. Taniguchi, M. Sasaki, T. Kimura, Y. Kiso, *J. Pept. Sci.* **2005**, *11*, 441–451.
- [45] X. F. Xiong, H. Zhang, C. R. Underwood, K. Harpsøe, T. J. Gardella, M. F. Wöldike,

- M. Mannstadt, D. E. Gloriam, H. Bräuner-Osborne, K. Strømgaard, *Nat. Chem.* **2016**, *8*, 1035–1041.
- [46] H. Kaur, P. W. R. Harris, P. J. Little, M. A. Brimble, *Org. Lett.* **2015**, *17*, 492–495.
- [47] Y. Chen, M. Bilban, C. A. Foster, D. L. Boger, *J. Am. Chem. Soc.* **2002**, *124*, 5431–5440.
- [48] F. E. Dutton, B. H. Lee, S. S. Johnson, E. M. Coscarelli, P. H. Lee, *J. Med. Chem.* **2003**, *46*, 2057–2073.
- [49] A. M. Sefler, M. C. Kozlowski, T. Guo, P. A. Bartlett, *J. Org. Chem.* **1997**, *62*, 93–102.
- [50] M. M. Joullié, P. Portonovo, B. Liang, D. J. Richard, *Tetrahedron Lett.* **2000**, *41*, 9373–9376.
- [51] O. Kuisle, E. Quinoa, R. Riguera, *Tetrahedron Lett.* **1999**, *40*, 1203–1206.
- [52] F. Albericio, K. Burger, J. Ruíz-Rodríguez, J. Spengler, *Org. Lett.* **2005**, *7*, 597–600.
- [53] J. Spengler, B. Kokschi, F. Albericio, *Biopolym. - Pept. Sci. Sect.* **2007**, *88*, 823–828.
- [54] J. S. Davies, J. Howe, J. Jayatilake, T. Riley, *Lett. Pept. Sci.* **1997**, *4*, 441–445.
- [55] O. Kuisle, E. Quiñoá, R. Riguera, *J. Org. Chem.* **1999**, *64*, 8063–8075.
- [56] A. López-Macià, J. C. Jiménez, M. Royo, E. Giralt, F. Albericio, *J. Am. Chem. Soc.* **2001**, *123*, 11398–11401.
- [57] C. Hermann, C. Giammasi, A. Geyer, M. E. Maier, *Tetrahedron* **2001**, *57*, 8999–9010.
- [58] T. Takahashi, H. Nagamiya, T. Doi, P. G. Griffiths, A. M. Bray, *J. Comb. Chem.* **2003**, *5*, 414–428.
- [59] Y. Lee, R. B. Silverman, *Org. Lett.* **2000**, *2*, 3743–3746.

- [60] T. Ast, E. Barron, L. Kinne, M. Schmidt, L. Germeroth, K. Simmons, H. Wenschuh, *J. Pept. Res.* **2001**, *58*, 1–11.
- [61] M. M. Nguyen, N. Ong, L. Suggs, *Org. Biomol. Chem.* **2013**, *11*, 1167–1170.
- [62] D. J. Berry, C. V. DiGiovanna, S. S. Metrick, R. Murugan, *Arkivoc* **2005**, *2001*, 201–226.
- [63] X. F. Xiong, H. Zhang, C. R. Underwood, K. Harpsøe, T. J. Gardella, M. F. Wöldike, M. Mannstadt, D. E. Gloriam, H. Bräuner-Osborne, K. Strømgaard, *Nat. Chem.* **2016**, *8*, 1035–1041.
- [64] M. Pelay-Gimeno, Y. García-Ramos, M. Jesús Martín, J. Spengler, J. M. Molina-Guijarro, S. Munt, A. M. Francesch, C. Cuevas, J. Tulla-Puche, F. Albericio, *Nat. Commun.* **2013**, *4*, 1–10.
- [65] B. Neises, W. Steglich, *Angew. Chemie Int. Ed. English* **1978**, *17*, 522–524.
- [66] R. Katakai, K. Kobayashi, K. Yamada, H. Oku, N. Emori, *Biopolymers* **2004**, *73*, 641–644.
- [67] T. Grab, S. Bräse, *Adv. Synth. Catal.* **2005**, *347*, 1765–1768.
- [68] O. Mitsunobu, M. Yamada, *Bull. Chem. Soc. Jpn.* **1967**, *40*, 2380–2382.
- [69] D. Camp, I. D. Jenkins, *J. Org. Chem.* **1989**, *54*, 3045–3049.
- [70] J. Inanaga, K. Hirata, H. Saeki, T. Katsuki, M. Yamaguchi, *Bull. Chem. Soc. Jpn.* **1979**, *52*, 1989–1193.
- [71] B. Zou, K. Long, D. Ma, *Org. Lett.* **2005**, *7*, 4237–4240.
- [72] J. Chen, C. J. Forsyth, *Proc. Natl. Acad. Sci. U. S. A.* **2004**, *101*, 12067–12072.
- [73] F. Albericio, K. Burger, T. Cupido, J. Ruiz, J. Spengler, *Arkivoc* **2005**, *vi*, 191–199.
- [74] W. Yuan, Y. Jia, J. Tian, K. D. Snell, U. Müh, A. J. Sinskey, R. H. Lambalot, C. T. Walsh, J. Stubbe, *Arch. Biochem. Biophys.* **2001**, *394*, 87–98.

- [75] E. J. Corey, A. Venkateswarlu, *J. Am. Chem. Soc.* **1972**, *94*, 6190–6191.
- [76] K. Burger, E. Windeisen, R. Pires, *J. Org. Chem.* **1995**, *60*, 7641–7645.
- [77] M. Pelay-Gimeno, F. Albericio, J. Tulla-Puche, *Nat. Protoc.* **2016**, *11*, 1924–1947.
- [78] E. Marcucci, J. Tulla-Puche, F. Albericio, *Org. Lett.* **2012**, *14*, 612–615.
- [79] L. A. Carpino, *J. Am. Chem. Soc.* **1993**, *115*, 4397–4398.
- [80] M. Stawikowski, G. B. Fields, in *Curr. Protoc. Protein Sci.*, **2002**, p. Chapter 18, Unit 18.1.
- [81] F. Albericio, *Curr. Opin. Chem. Biol.* **2004**, *8*, 211–221.
- [82] F. Guibé, *Tetrahedron* **1998**, *54*, 2967–3042.
- [83] M. J. Martin, R. Rodriguez-Acebes, Y. Garcia-Ramos, V. Martinez, C. Murcia, I. Digon, I. Marco, M. Pelay-Gimeno, R. Fernández, F. Reyes, et al., *J. Am. Chem. Soc.* **2014**, *136*, 6754–6762.
- [84] J. D. Wade, J. Bedford, R. C. Sheppard, G. W. Tregear, *Pept. Res.* **1991**, *4*, 194–199.
- [85] I. Coin, M. Beerbaum, P. Schmieder, M. Bienert, M. Beyermann, *Org. Lett.* **2008**, *10*, 3857–3860.
- [86] R. Dölling, M. Beyermann, J. Haenel, F. Kernchen, E. Krause, P. Franke, M. Brudel, M. Bienert, *J. Chem. Soc. Chem. Commun.* **1994**, *20*, 853–854.
- [87] R. Subirós-Funosas, A. El-Faham, F. Albericio, *Biopolymers* **2012**, *98*, 89–97.
- [88] T. Michels, R. Dölling, U. Haberkorn, W. Mier, *Org. Lett.* **2012**, *14*, 5218–5221.
- [89] M. Taniguchi, K. I. Suzumura, K. Nagai, T. Kawasaki, J. Takasaki, M. Sekiguchi, Y. Moritani, T. Saito, K. Hayashi, S. Fujita, et al., *Bioorganic Med. Chem.* **2004**, *12*, 3125–3133.
- [90] S. Kim, J. Jin, S. P. Kunapuli, *Blood* **2006**, *107*, 947–954.

- [91] F. Campus, P. Lova, A. Bertoni, F. Sinigaglia, C. Balduini, M. Torti, *J. Biol. Chem.* **2005**, *280*, 24386–24395.
- [92] M. Taniguchi, K. I. Suzumura, K. Nagai, T. Kawasaki, T. Saito, J. Takasaki, K. I. Suzuki, S. Fujita, S. I. Tsukamoto, *Tetrahedron* **2003**, *59*, 4533–4538.
- [93] T. Uemura, H. Takamatsu, T. Kawasaki, M. Taniguchi, E. Yamamoto, Y. Tomura, W. Uchida, K. Miyata, *Eur. J. Pharmacol.* **2006**, *536*, 154–161.
- [94] J. Takasaki, T. Saito, M. Taniguchi, T. Kawasaki, Y. Moritani, K. Hayashi, M. Kobori, *J. Biol. Chem.* **2004**, *279*, 47438–47445.
- [95] A. Nishimura, K. Kitano, J. Takasaki, M. Taniguchi, N. Mizuno, K. Tago, T. Hakoshima, H. Itoh, *Proc. Natl. Acad. Sci.* **2010**, *107*, 13666–13671.
- [96] T. Kawasaki, M. Taniguchi, Y. Moritani, T. Uemura, T. Shigenaga, H. Takamatsu, K. Hayashi, J. Takasaki, T. Saito, K. Nagai, *Thromb. Haemost.* **2005**, *94*, 184–192.
- [97] H. Zhang, X. F. Xiong, M. W. Boesgaard, C. R. Underwood, H. Bräuner-Osborne, K. Strømgaard, *ChemMedChem* **2017**, *12*, 830–834.
- [98] H. Zhang, A. L. Nielsen, M. W. Boesgaard, K. Harpsøe, N. L. Daly, X. F. Xiong, C. R. Underwood, L. M. Haugaard-Kedström, H. Bräuner-Osborne, D. E. Gloriam, et al., *Eur. J. Med. Chem.* **2018**, *156*, 847–860.
- [99] N. M. Okeley, Y. Zhu, W. A. van der Donk, *Org. Lett.* **2000**, *2*, 3603–3606.
- [100] J. C. Jiménez, N. Bayó, B. Chavarría, À. López-Macià, M. Royo, E. Nicolás, E. Giralt, F. Albericio, *Lett. Pept. Sci.* **2003**, *9*, 135–141.
- [101] B. N. Naidu, M. E. Sorenson, T. P. Connolly, Y. Ueda, *J. Org. Chem.* **2003**, *68*, 10098–10102.
- [102] A. El-Faham, F. Albericio, *Chem. Rev.* **2011**, *111*, 6557–6602.
- [103] F. García-Martín, N. Bayó-Puxan, L. J. Cruz, J. C. Bohling, F. Albericio, *QSAR Comb. Sci.* **2007**, *26*, 1027–1035.

- [104] M. Amblard, J. Fehrentz, J. Martinez, G. Subra, *Mol. Biotechnol.* **2006**, *33*, 229–254.
- [105] C. J. White, A. K. Yudin, *Nat. Chem.* **2011**, *3*, 509–524.
- [106] E. Marsault, M. L. Peterson, *J. Med. Chem.* **2011**, *54*, 1961–2004.
- [107] D. Borja-Cacho, J. Matthews, *ACS Comb sci* **2013**, *15*, 120–129.
- [108] J. S. Davies, *J. Pept. Sci.* **2003**, *9*, 471–501.
- [109] M. Malesevic, U. Strijowski, D. Bächle, N. Sewald, *J. Biotechnol.* **2004**, *112*, 73–77.
- [110] L. J. Cruz, N. G. Beteta, A. Ewenson, F. Albericio, *Org. Process Res. Dev.* **2004**, *8*, 920–924.
- [111] A. J. Pearson, W. R. Roush, *Activating Agents and Protecting Groups*, **1999**.
- [112] X. Wu, Z. Jiang, H. M. Shen, Y. Lu, *Adv. Synth. Catal.* **2007**, *349*, 812–816.
- [113] G. Stork, D. Niu, A. Fujimoto, E. R. Koft, J. M. Balkovec, J. R. Tata, G. R. Dake, *J. Am. Chem. Soc.* **2001**, *123*, 3239–3242.
- [114] J. R. Coggins, N. L. Benoiton, *Can. J. Chem.* **1971**, *49*, 1968–1971.
- [115] A. V. Malkov, K. Vranková, M. Černý, P. Kočovský, *J. Org. Chem.* **2009**, *74*, 8425–8427.
- [116] S. Zhang, T. Govender, T. Norström, P. I. Arvidsson, *J. Org. Chem.* **2005**, *70*, 6918–6920.
- [117] L. Aurelio, R. T. C. Brownlee, A. B. Hughes, *Chem. Rev.* **2004**, *104*, 5823–5846.
- [118] D. Ben-ishai, *J. Am. Chem. Soc.* **1957**, *79*, 5736–5738.
- [119] R. M. Freidinger, J. S. Hinkle, D. S. Perlow, B. H. Arison, *J. Org. Chem.* **1983**, *48*, 77–81.

**CHAPTER 2 . DEVELOPMENT OF A SYNTHETIC  
METHODOLOGY TO PREPARE HIGHLY  
*N*-METHYLATED STAPLED PEPTIDES**



## 2.1 Introduction

### 2.1.1 Protein-Protein Interactions

Protein-Protein Interactions (PPIs) play an important role in all virtually cellular processes. Communication between proteins mediate many biological functions such as enzymatic activity, subcellular localisation, binding properties, among others.<sup>[1-4]</sup> Of great interest is the stabilisation or disruption of these interactions for the modulation of the protein function within the cell, thus, great efforts have been put into developing new modulators for PPIs, becoming an important breakthrough towards the generation of new drugs. PPIs are divided into two major classes that involve either two globular proteins (domain-domain) or the interaction between a linear sequence of amino acids and a globular domain of the other partner (peptide-domain). In the latter, amino acid residues responsible for peptide-protein interactions, namely hot-spot regions, typically adopt a secondary structure.<sup>[1,4,5]</sup>

Generally, PPIs interfaces comprise a large contact area of 1500–3000 Å<sup>2</sup> and exhibit a flat surface.<sup>[6]</sup> In order to achieve good affinity and competitive binding, PPIs inhibitors/activators should display a significantly large area to interact with the so-called hot-spots.<sup>[1-3,5,7]</sup> It is not surprising, therefore, that peptides serve as a good

starting point for the design of PPIs modulators, since they are typically larger in size than most of the common small molecule drugs.<sup>[6]</sup>

Constrained peptides<sup>[8]</sup> combine the advantages of therapeutic proteins with those of small molecules, such as (i) high specificity and binding affinity; (ii) lower toxicity, as peptides can degrade into amino acids; and (iii) easy modulation by incorporation of diverse chemical modifications.<sup>[1,4,6]</sup> However, *in vivo* instability due to protease degradation and poor bioavailability are the main drawbacks that have hampered their exploitation as therapeutic drugs. Nevertheless, great advances have been made in the peptide therapeutics field to optimise their pharmacokinetic profile,<sup>[1,9–12]</sup> including the following peptide backbone modifications: peptide cyclisation, *N*-alkylation, carbonyl replacement,  $\alpha$ -carbon replacement,  $\alpha$ -carbon substitution, backbone extension among others.<sup>[13]</sup>

### 2.1.2 Protein mimicry: mimicking $\alpha$ -helix secondary structures

$\alpha$ -Helix, or the so-called Pauling-Corey-Branson alpha helix structure, is the most prevalent secondary structure in proteins, being the most regular and predictable conformation.<sup>[14]</sup> It is a right-handed-coiled or spiral conformation structure in which each amino group (N-H) donates a hydrogen bond to the backbone C = O group of the amino acid located four residues earlier (Figure 2.1).<sup>[14,15]</sup>

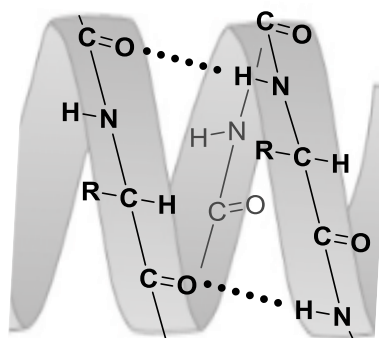


Figure 2.1.  $\alpha$ -helix conformation.

Moreover, according to Arora *et al.*, over 60% of the protein-protein complexes in the Protein Data Bank possess  $\alpha$ -helical interfaces.<sup>[16]</sup> Thus, mimicking these  $\alpha$ -helices

has become an appealing approach to generate molecules that disrupt or promote PPIs. However, short peptides usually have little structure in solution. In this context, several approaches have appeared over the years to favour or to stabilise an  $\alpha$ -helix, such as: (i) to insert proteogenic amino acids that show more propensity to form  $\alpha$ -helices (e.g. Ala, Met and Leu);<sup>[17]</sup> (ii) to insert constrained amino acids such as  $\alpha,\alpha$ -disubstituted residues (e.g.  $\alpha$ -aminoisobutyric acid (Aib));<sup>[18,19]</sup> (iii) to promote electrostatic interactions by H-bonding, dipole formation or salt bridges interactions;<sup>[20,21]</sup> (iv) to promote side-chain to side-chain hydrophobic interactions with aromatic residues;<sup>[22]</sup> (v) to introduce side-chain to side-chain cross-linking of amino acids located on the same face of the helix;<sup>[23-27]</sup> and (vi) combinations thereof. Following, these approaches are reviewed in more detail.

### 2.1.2.1 Helix propensity of proteogenic amino acids

The helix propensity of proteogenic amino acids is crucial to determine the contribution of each residue to the overall secondary structure of a peptide or a protein.<sup>[17]</sup> The propensity to stabilise helical conformations is associated with short interactions between the amino acid side chain and both the peptide backbone and the solvent. This value can be experimentally determined,<sup>[17]</sup> and accordingly, amino acids can be classified into three different families, including: helix forming, helix indifferent and helix breaking residues. This data becomes useful for the prediction of the optimal location of amino acid residues within the peptide backbone to induce the desired secondary structure. Extensive studies concluded that insertion of Ala, Met and Leu to the peptide chain promotes and stabilises the  $\alpha$ -helical conformation.<sup>[17]</sup> Contrary, Val, Ile and Gly are prone to break  $\alpha$ -helix turns and are likely to induce  $\beta$ -sheet conformations instead.<sup>[28]</sup>

### 2.1.2.2 Insertion of $\alpha$ -amino acids with restricted conformation space

A useful approach to promote the formation of the helical turn is the insertion of  $\alpha,\alpha$ -disubstituted residues (e.g. Aib). The Aib and Aib-like amino acids present a restricted space conformation that results in stabilisation of helical secondary structure.<sup>[18,19]</sup> Not surprisingly, the ratio of the  $\alpha,\alpha$ -disubstituted residues as well as the

solvent polarity play a crucial role in the helical stabilisation.<sup>[29–31]</sup> In polar solvents, helicity is maintained as long as the Aib percentage does not exceed 50%. Although peptide couplings onto Aib residues is hampered by the sterically hindered environment provided by  $\alpha,\alpha$ -disubstituted amino acids, several SPPS methodologies have appeared over the past years to circumvent these difficulties.<sup>[32,33]</sup> Up to date, numerous non-proteogenic  $\alpha,\alpha$ -disubstituted amino acids have been used to promote the helical conformation of a series of biologically active relevant short helical peptides.<sup>[34,35]</sup>

### 2.1.2.3 Electrostatic interactions to promote the $\alpha$ -helix conformation

It is well known that  $\alpha$ -helical structures are stabilised by H-bonds between residue side-chains and both the *N*- and the *C*-terminus. As an example, a negatively charged side-chain such as the one provided by the carboxylic acid present in Asp or Glu residues located at adequate positions can form H-bonds with the free *N*-terminus amine, resulting in  $\alpha$ -helix stabilisation.<sup>[36]</sup> Concomitantly, since the helical conformation is polarised from the *N*- to the *C*-terminus, side-chain–dipole interactions can be promoted by placing favourable charged residues within close proximity to both ends.<sup>[37]</sup>

Additionally, creation of ion pairs or salt bridges between oppositely charged side-chains at positions  $i,i+3$  or  $i,i+4$  (within one helical turn distance) promotes the  $\alpha$ -helix conformation (Figure 2.2). In fact, dipolar interactions between a negatively charged side-chain (e.g.; Glu or Asp) and a positively charged side-chain containing a free amine (e.g.; Lys or Arg) separated by one helical turn becomes an efficient approach to induce and stabilise the  $\alpha$ -helical structure.<sup>[21,38]</sup>

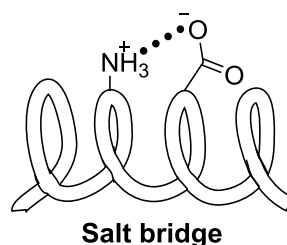


Figure 2.2. Salt bridge to promote  $\alpha$ -helix conformation.

#### 2.1.2.4 Hydrophobic interactions to promote the $\alpha$ -helix conformation

$\alpha$ -helix secondary structures can as well be stabilised by hydrophobic interactions by insertion of two hydrophobic groups.<sup>[22]</sup> Insertion of two highly electron-deficient aromatic rings separated by one or two helical turns promotes  $\pi$ - $\pi$  interactions,<sup>[39]</sup> which ultimately leads to stabilised  $\alpha$ -helix conformations (Figure 2.3).

In this context, Albert *et al.* evaluated the effect of the solvent and the location of the two aromatic groups on the helical content.<sup>[22]</sup> With that purpose, a series of  $i,i+4$ ,  $i,i+7$  and  $i,i+13$  stapled peptides were prepared and their structural features were extensively studied. Location of the two aromatic groups at positions  $i$  and  $i+4$ , respectively, accounted for the highest helicity. These results are not surprising, since the  $i,i+4$  staple presents the closest arrangement of these groups and consequently  $\pi$ - $\pi$  interactions exert a greater impact on the secondary structure stabilisation. Additionally, Albert and co-workers demonstrated that the nature of the solvent and the solvent concentration play a key role in  $\alpha$ -helical stabilisation. Maximum helicity was observed in intermediate  $H_2O$ /methanol mixtures, as well as high percentages of  $H_2O$  in TFE.

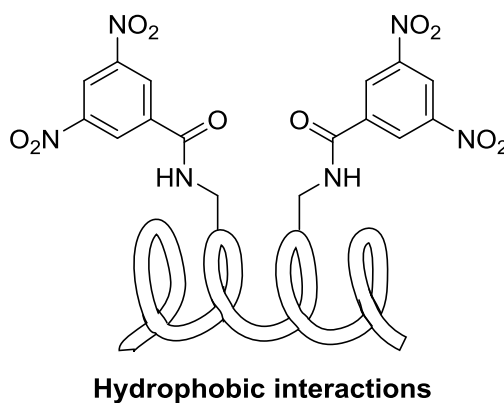


Figure 2.3. Hydrophobic interactions to promote  $\alpha$ -helix conformation.

#### 2.1.2.5 Side-chain to side-chain crosslinking

As mentioned earlier,  $\alpha$ -helices are stabilised by intramolecular hydrogen bonds between the carbonyl oxygen and the amine proton at positions  $i,i+3$ ,  $i,i+4$  and  $i,i+7$ . Thus, it is not surprising, that covalent cross-links were designed to act as the bridge

between positions  $i,i+3$  and positions  $i,i+4$  to favour the  $\alpha$ -helix turn, and between positions  $i,i+7$  for two helical turns (Figure 2.4).<sup>[40–45]</sup> Longer helical peptide sequences might require the insertion of multiple covalent bridges. For that, multiple individual staples or a stitched-tandem staple can be inserted to stabilise the  $\alpha$ -helix conformation (Figure 2.4).<sup>[44,46–48]</sup> The relative location of the cross-link/s and the length of the bridges must be selected with careful consideration whilst designing the cross-linker in order to achieve the desired 3D structure without interfering with the binding site.<sup>[49]</sup> Additionally, the cross-linked residues must be located on the same face of the  $\alpha$ -helix.

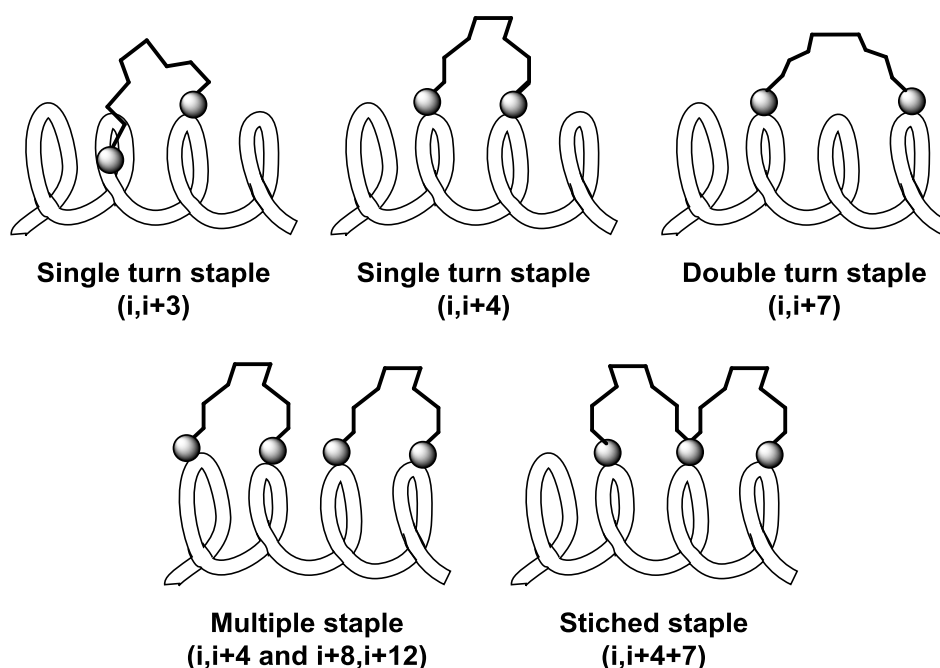


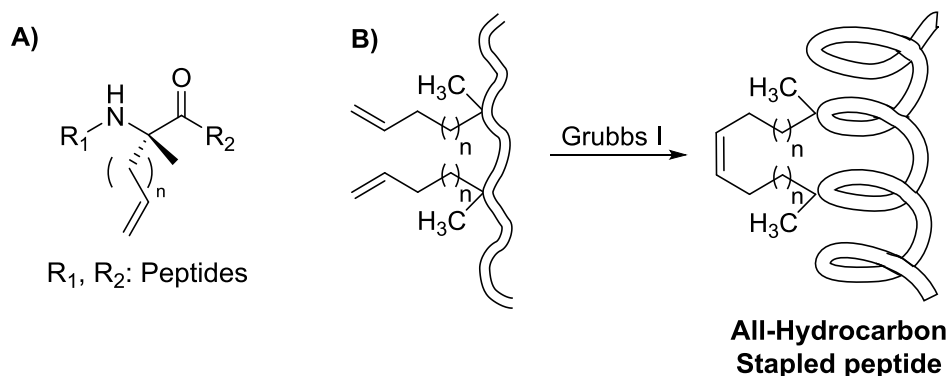
Figure 2.4. Types of staple.

Several chemical approaches have been developed towards the generation of new  $\alpha$ -helix protein mimics such as  $\alpha$ -methylated hydrocarbon-,<sup>[50]</sup> thiol-,<sup>[43]</sup> lactam-,<sup>[51]</sup> triazole-based cross-links,<sup>[52]</sup> among others.<sup>[23]</sup> Following, a non-comprehensive review on the most common peptide stapling techniques is given.

#### 2.1.2.5.1 $\alpha$ -Methylated hydrocarbon or all-hydrocarbon cross-linking

In 2000, Verdine *et al.* coined the term of stapled peptide for C-C bridge helix stabilisation. A molecular scaffold, in which the amino acid side-chains at specific positions  $i,i+4$  were functionalised with an alkene moiety as shown in Scheme 2.1A, was developed.<sup>[53]</sup> By using the well-established Ring-closing metathesis reaction (RCM),

the peptide side-chains were cross-linked, being the  $\alpha$ -helix conformation induced (Scheme 2.1B). These particular molecular constructs, or the so-called  $\alpha$ -methylated hydrocarbon stapled peptides, turn into exceptional drug candidates, since target recognition is retained whilst protease degradation is minimised.<sup>[53]</sup>



*Scheme 2.1.* A) Alkene functionalised amino acid scaffold; B) Synthetic scheme of a stapled peptide by formation of the  $\alpha$ -methylated hydrocarbon bridge through RCM cross-linking.

Extensive research was carried out to determine the optimal stereochemistry of the two  $\alpha$ -methyl, $\alpha$ -alkenylglycine residues (structure shown in Scheme 2.1A) as well as the corresponding alkene chain length.<sup>[53–55]</sup> Following, the X<sub>Y</sub> convention is used, in which X defines the  $\alpha$ -carbon stereochemistry (S or R) and Y determines the side-chain length of the  $\alpha$ -methyl, $\alpha$ -alkenylglycine residues. The highest helicity of peptide stapling at positions  $i, i+3$  was observed when placing R<sub>5</sub> and S<sub>5</sub> cross-linking amino acids at positions  $i$  and  $i+3$ , respectively. Contrary, for  $i, i+4$  cross-linking, optimal conditions were observed when using S<sub>5</sub> amino acid at both the  $i$  and the  $i+4$  positions. For peptide stapling at positions  $i, i+7$ , the greater helicity was observed when a R<sub>8</sub> cross-linking amino acid was placed at position  $i$  and a S<sub>5</sub> amino acid was located at position  $i+7$  instead. As previously mentioned, the relative position of the so-called all-hydrocarbon staple within the peptide backbone cannot be predicted beforehand and must be optimised for each particular peptide. Importantly, the cross-link must not interfere with the binding side motif.

Chemical synthesis of all hydrocarbon stapled peptides is by far optimised and a general synthetic strategy can be outlined as follows. First, stepwise incorporation of Fmoc-protected amino acid can be accomplished on SPPS by using the well-established

Fmoc/<sup>t</sup>Bu strategy.<sup>[56–58]</sup> Note that the sterically hindered environment provided by the  $\alpha$ -disubstituted residues might require strong coupling conditions and involve several coupling steps. Additionally, aggregation problems might be encountered. Often, lowering the resin functionalisation proves effective to circumvent aggregation issues. Nevertheless, once the linear chain is assembled, RCM can be performed on solid-phase either before or after *N*-terminus derivatisation. If needed, the *N*-terminus can be derivatised with a fluorescent tag (for biological studies and binding assays), biotin (for affinity capture assays) or benzophenone (for photo-cross-linking and mass-spectrometry-based identification).<sup>[59–63]</sup> Finally, peptide cleavage from the resin and HPLC purification renders the target molecule. It is worth mentioning that  $\alpha$ -methyl, $\alpha$ -alkenylglycine building blocks can be easily accessed. In fact, the olefin-bearing residues can be purchased from commercial suppliers at relatively low prices. Chemical synthesis of unnatural olefin-bearing amino acids is also feasible and can be accomplished by using several methodologies, including: (i) the use of an oxazinone chiral auxiliary based on the method developed by Williams and co-workers;<sup>[64]</sup> or (ii) the use of a benzylproplylaminobenzophenone (BPB) based chiral auxiliary.<sup>[65,66]</sup>

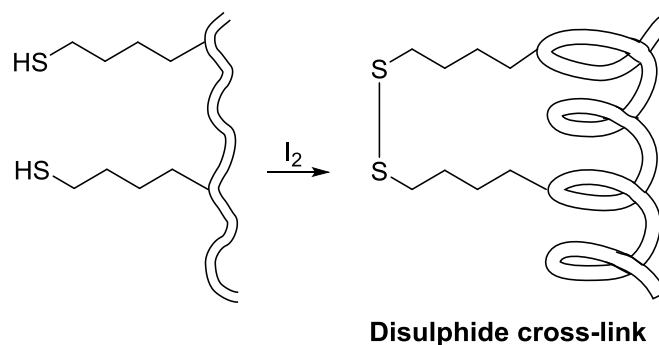
Over the past decades, numerous bioactive  $\alpha$ -methylated hydrocarbon stapled peptides have been prepared and successfully applied to diverse human diseases such as cancer, diabetes, HIV, atherosclerosis, among others.<sup>[67–69]</sup> Moreover, up to date hydrocarbon stapling of the peptide backbone is the most widely used approach for the preparation of constrained helical peptides.

#### **2.1.2.5.2 Thiol-based cross-linking**

In the literature, the first reported thiol-based cross-link to promote the helical structure was based on the disulphide bond formation between two 2-amino-6-mercaptohexanoic acids at positions *i* and *i*+7, respectively (Scheme 2.2).<sup>[70]</sup> This approach benefits from the selectivity of the oxidation reaction, since the bridge formation can be achieved in the presence of many functional groups, thus allowing the use of unprotected peptide side-chains. Jackson *et al.* evaluated the effect of the amino acid stereochemistry at positions *i* and *i*+7, concluding that the  $\alpha$ -helix turn was promoted when placing *L*-amino acid isomers at both positions.<sup>[70]</sup>

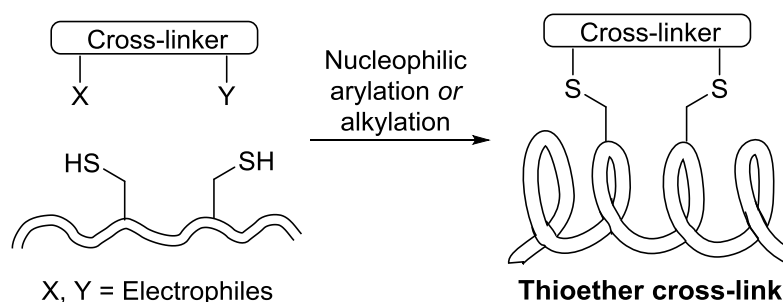
Later on, Leduc and colleagues demonstrated that cross-linking of the same residues (2-amino-6-mercaptohexanoic acid) separated by one helical turn ( $i, i+4$ ) also led to high  $\alpha$ -helical content structures.<sup>[43]</sup>

Unfortunately, applicability of disulphide bridges to promote and stabilise the helical structure has been limited by the instability of the disulphide cross-links, which are prone to be reduced upon the reducing conditions found in the cytosol.



*Scheme 2.2.* Oxidation of two thiols located at positions  $i, i+7$  to form a disulphide bridge, which ultimately leads to  $\alpha$ -helix structure stabilisation.

Cysteine derivatisation by alkylation and arylation reactions turned into a versatile and inexpensive method to prepare novel thiol-based constrained helical peptides with enhanced chemical stability. Given the unique reactivity properties of cysteine, which is able to react with a wide variety of electrophiles, as well as its exceptional chemical selectivity, it is not surprising that thioether moieties came up as a good alternative to replace disulphide bridges. In this context, preparation of thioether cross-linked stapled peptides can generally be accomplished by simple and neat nucleophilic arylation or alkylation of bis-electrophilic cross-linkers (Scheme 2.3). Following, just a few of the many available examples of cysteine alkylation and arylation cross-linking strategies are reviewed.



*Scheme 2.3.* Thioether cross-linking *via* nucleophilic displacement of bis-electrophilic cross-linkers.

Jo *et al.* evaluated the  $\alpha$ -helical secondary structure stabilisation by simple cross linking of a peptide bearing two cysteine residues through the double nucleophilic substitution of halides or maleimide-based cross-linkers.<sup>[71]</sup> Thus, a series of 24 commercially available bis-electrophilic cross-linkers were screened for cys-thioether side-chain to side-chain macrocyclisations, in which nucleophilic displacement was accomplished under slightly basic aqueous conditions (buffer at pH = 7.5). Out of the 24 tested cross-linkers, only five led to  $\alpha$ -helix stabilisation. The highest helicity was observed for peptide stapling at positions  $i, i+4$ , using a dibromo-*m*-xylene linker (Figure 2.5A).

Brunel and co-workers developed a one-component stapling methodology based on the nucleophilic substitution of an  $\alpha$ -bromo amide group (Figure 2.5B).<sup>[72]</sup> With that purpose, the peptide linear chain was provided with an alpha-bromo amide side-chain at position  $i$ , and a free thiol cys was located at either position  $i+3$  or position  $i+4$ . Nucleophilic displacement was accomplished at pH = 8.4, being the  $\alpha$ -helix secondary structure successfully stabilised.

Chou *et al.* developed a novel class of stapled peptides, in which two cysteine residues were cross-linked *via* the well-known thiol-ene click reaction.<sup>[73]</sup> In the presence of UV light, the thiol-ene click reaction between cysteine thiols and  $\alpha, \omega$ -dienes is highly specific, thus allowing cross-linking of unprotected peptides. The  $\alpha$ -helical conformation was stabilised by insertion of either an eight-carbon cross-linker or a nine-carbon cross-linker at positions  $i, i+4$  and  $i, i+7$ , respectively (Figure 2.5C).

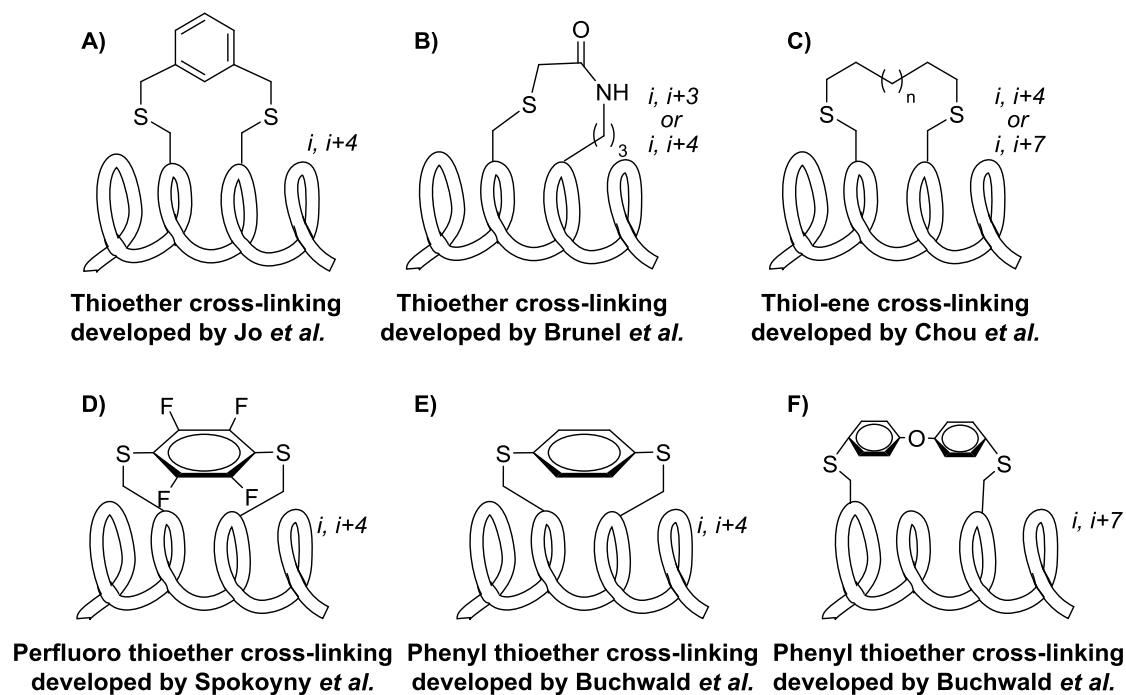


Figure 2.5. Thiol-based cross-linking to promote the  $\alpha$ -helix secondary structure.

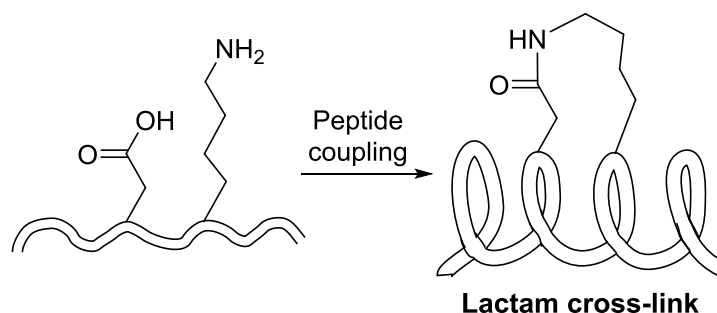
An example of cysteine arylation was the one reported by Spokoyny and co-workers. Cysteine thiols were successfully arylated with perfluoro-aromatic molecules, in which the reaction regioselectivity led to the formation of a single product corresponding to the *para*-disubstituted isomer. Thus, this method allowed the development of a novel class of perfluoro thioether cross-linked peptides exhibiting  $\alpha$ -helical conformation (Figure 2.5D).<sup>[74]</sup>

Another example of cysteine arylation to generate stapled peptides is the one described by the Buchwald group.<sup>[75]</sup> Inspired by a palladium-mediated methodology for cysteine arylation previously developed in their group,<sup>[76]</sup> phenyl thioether cross-links were inserted to a series of peptides. In this context, aryl or diaryl linkers were introduced for  $i, i+4$  and  $i, i+7$  cross-linking, respectively (Figure 2.5E and Figure 2.5F, respectively).

### 2.1.2.5.3 Lactam-based cross-linking

Felix *et al.* first applied lactam-based peptide stapling techniques for the generation of short constrained helical peptides.<sup>[77]</sup> Peptide coupling between the side-chains of Lys

and Asp residues located at positions  $i$  and  $i+4$ , respectively, resulted in a lactam-based cross-links that induced the  $\alpha$ -helical turn (Scheme 2.4).<sup>[78]</sup>



*Scheme 2.4.* Lactam cross-linking *via* peptide coupling to promote the  $\alpha$ -helical conformation.

Whereas further developments were made in this field, just a few are reviewed in the present section. Within the lactam-based cross-linking group, the reaction between a diamino-functionalised building block and the side-chain of two Glu residues at positions  $i$  and  $i+7$ , respectively, resulted in the formation of two amide bonds (Figure 2.6A).<sup>[14]</sup> A similar approach that involves two lactam-based cross-links resulted in highly helical peptide structures (Figure 2.6B).<sup>[79]</sup>

Synthetic access to lactam-based stapled peptides is relatively easy. Whilst many other stapling techniques require the preparation of non-proteogenic modified amino acids, lactam-based cross-linking is generally based on natural amino acid residues. A general synthetic strategy can be outlined as follows.<sup>[41,43]</sup> First, linear peptide chain elongation is carried out on SPPS by standard means, followed by selective protecting group removal of the residues to be cross-linked and a final on-resin macrolactamisation step. Note that orthogonal protecting groups for the side-chain functionalities to be cross-linked are required.

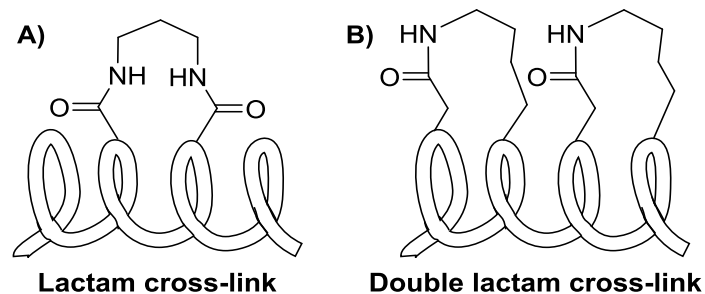
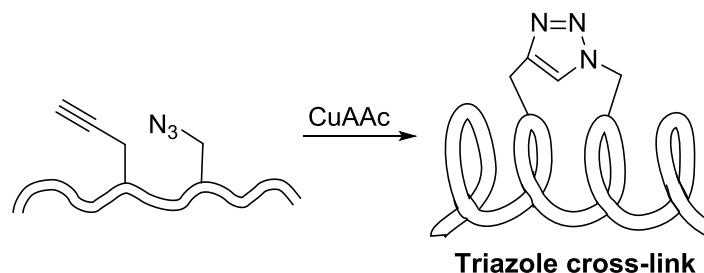


Figure 2.6. Examples of lactam-based cross-links to promote the  $\alpha$ -helix secondary structure.

Although there are many reported examples describing the generation of short helical constrained peptides using lactam-based peptide stapling techniques, there is a lack in literature regarding their capability to cross the cell membrane. Up to date, it is still unclear whether these molecular constructs exhibit a poorer cellular uptake than the so-called all-hydrocarbon stapled peptides analogues.

#### 2.1.2.5.4 Triazole-based cross-linking

In 2002, Sharpless first developed the so-called Huisgen cycloaddition or copper-catalysed azide-alkyne cycloaddition (CuAAC). The reaction between an alkyne and an azide in the presence of a copper catalyst is high yielding and leads to a single triazole product.<sup>[80]</sup> CuAAC is widely used in drug discovery, and increasingly applied to the stabilization of  $\alpha$ -helices *via* peptide stapling (Scheme 2.5).<sup>[52]</sup> Triazole-based cross-links provide peptides with similar properties as the ones given by  $\alpha$ -methylated hydrocarbon-, thiol and lactam-based cross-links, and therefore the  $\alpha$ -helicity is induced whilst retaining the biological activity.<sup>[81,82]</sup> Formation of triazole bridges between an alkyne located at position  $i$  and an azide placed at position  $i+4$  has proven effective to stabilise  $\alpha$ -helical secondary structures (Figure 2.7A).<sup>[83]</sup> Additionally, ditriazole-based cross-link scaffolds have been successfully developed, in which a double-click reaction between a 3,5-dialkynyl benzene linker and two azide groups placed at positions  $i$  and  $i+4$  or  $i+7$  was carried out (Figure 2.7B).<sup>[82]</sup>



*Scheme 2.5.* Triazole cross-linking to promote the  $\alpha$ -helical conformation.

Given the synthetic ease of the Huisgen cycloaddition, chemical synthesis of triazole-based stapled peptides is foreseen facile. Nevertheless, preparation of side-chain azide- and/or alkyne- functionalised residues is required. A good approach for the synthesis of  $N_3$ -derivatised amino acids used by many researches is the transformation of the amine group of a Lys residue into the corresponding azide moiety. In fact, protected Lys( $N_3$ ) residues can nowadays be purchased from commercial suppliers if desired. On the other hand, incorporation of the alkyne moieties can be easily accomplished by using commercially available propargyl amino acids. Synthesis of these molecular architectures can be accomplished using SPPS by standard means, in which the azide and alkene moieties are located at key stapling positions ( $i, i+4$  or  $i, i+7$ ). The click reaction can be performed either on the polymeric support or in solution with the unprotected peptide side-chains.<sup>[83,84]</sup> This stapling technique becomes a versatile approach to prepare  $\alpha$ -helical constrained peptides.

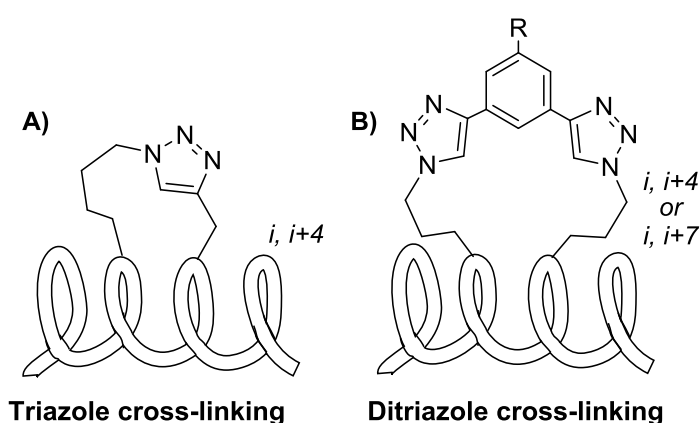


*Figure 2.7.* Triazole-based cross-linking to promote the  $\alpha$ -helix secondary structure.

### 2.1.2.5.5 Other cross-linking approaches

Many other stapling techniques have been developed over the past years to promote the  $\alpha$ -helix conformation of short peptides, including photo-switchable-based,<sup>[85]</sup> oxime-based,<sup>[86]</sup> 1,3-dinyl-based,<sup>[87]</sup> ether-based,<sup>[88]</sup> dihydroxylated-based cross-linking,<sup>[88]</sup> among others (Figure 2.8). Although extensive research has been carried out in the peptide stapling field, further efforts towards the generation of intracellular drug targets are required. In the following section, limitations of the up to date available side-chain to side-chain cross-linking methodologies are reviewed.

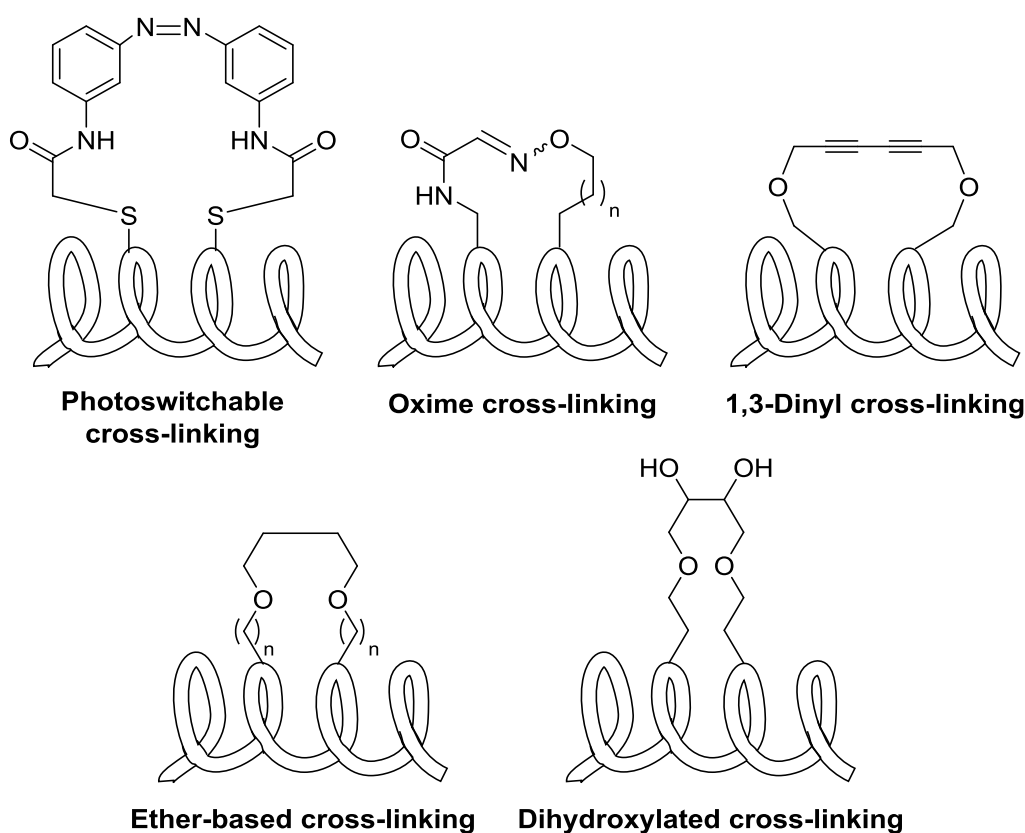


Figure 2.8. Other cross-linking techniques to promote the  $\alpha$ -helix secondary structure.

### 2.1.2.5.6 Limitations of stapling techniques

Among the many stapling methodologies that have appeared over the last years, the well-known all-hydrocarbon stapling technique is currently the most popular method for the preparation of constrained helical peptides.<sup>[25,26,47,57]</sup> Often, hydrocarbon cross-linking results in enhanced *in vitro* binding affinity, however, cellular uptake and improved bioavailability are not always accomplished, which make post-stapling

modifications necessary.<sup>[69,89–91]</sup> In this regard, one of the major limitations of the all-hydrocarbon stapling approach is the lack of versatility, since this technique is limited to the use of one specific derivatised amino acid ( $\alpha$ -methyl, $\alpha$ -alkenylglycine).

Concurrently, there is a lack in the literature regarding the ability of lactam-based, thioether-based and triazole-based stapled peptides to cross the cell membrane, and further research is necessary to determine their biological applicability. In fact, it is still unknown whether these other stapling techniques exhibit a poorer cellular uptake character compared to the all-hydrocarbon stapled peptides analogues.

A single universal stapling technique cannot be established, since selection of the most suitable cross-linking approach highly depends on the nature of the PPIs to be addressed. Nevertheless, the ability of stapled peptides to cross the cell membrane, increase *in vivo* stability and exhibit improved biological activity, has gained raising interest over the past years. Thus, a major challenge to be addressed is the development of novel stapled peptides meeting these requirements.

#### **2.1.2.5.7 Proposal of a novel stapling methodology**

In the present thesis, we envisaged the construction of stapled peptides containing an *N*-methyl-rich peptide that acts as a bridge between key stapling positions (Figure 2.9). With that purpose, we took advantage of the beneficial properties conferred by *N*-methylated residues, which include: (i) greater lipophilicity, (ii) enhanced proteolytic stability; (iii) enhanced rigidity by the conformational restriction of *N*-methyl amino acids; and (iv) enhanced cell internalisation.<sup>[92–95]</sup> We believe that this novel stapling approach would become a good alternative to overcome the limitations mentioned earlier.

In the work presented herein, these molecular architectures will be designated as “HMSP”, which stands for highly *N*-methylated stapled peptides. The proposed novel molecular architectures were expected to display  $\alpha$ -helical conformation with an improved pharmacological profile. In fact, *N*-methylated staples are highly versatile, as the length and flexibility of the staple can be modulated by (i) the number of *N*Me-amino acids; (ii) the nature of the staple can be modified by playing with the hydrophobicity of

the *N*Me-amino acids; and (iii) the flexibility of the staple can be modulated by introducing also  $\beta$ - and  $\gamma$ -*N*Me-amino acids.

Hence, the present chapter of the thesis was focused on the development of a synthetic methodology for the preparation of highly *N*-methylated stapled peptides (Figure 2.9).

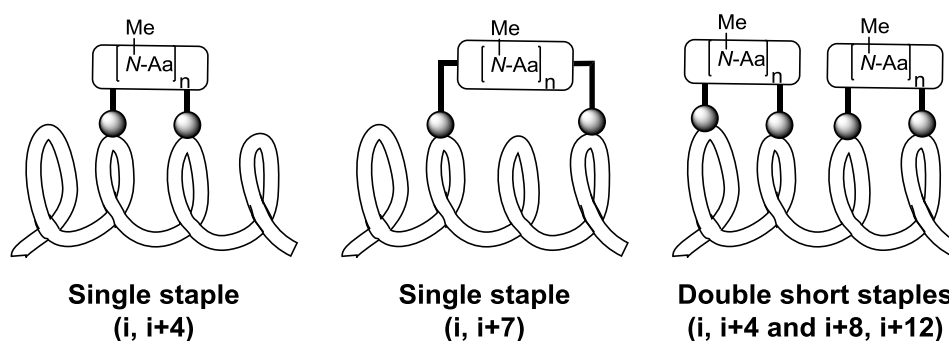


Figure 2.9. Single and double HMSP.

The p53-MDM2 protein-protein interaction was the focus in the development of our synthetic methodology.<sup>[96]</sup> Protein p53 is a tumour suppressor that helps maintaining the genomic integrity of the cell by inducing cell arrest or apoptosis of damaged DNA. Its biological function is modulated by protein murine double minute 2 homolog (MDM2). MDM2 blocks p53's transactivation domain and therefore represses its transcriptional activity once its biological function has been accomplished. However, overproduction of MDM2 is observed in tumour cells, where consecutive inhibition of p53 results in complete blockage of p53.<sup>[97]</sup> This MDM2 amplification has been reported mostly in soft tissue sarcomas, and also in other well-known types of cancer, including leukaemia and breast cancer.<sup>[96]</sup>

The p53-MDM2 PPI involves binding between the amphipathic  $\alpha$ -helix that adopts p53 and the cleft present in MDM2 conformation (Figure 2.10). The binding takes place through Van der Waals interactions and steric complementarity, where p53 introduces not all but one of its five hydrophobic amino acid side-chains in the interface between the two proteins. This interaction relies mostly on three of the amino acids present in the p53 bioactive sequence, which are Phe<sup>19</sup>, Trp<sup>23</sup> and Leu<sup>26</sup>.

A PPI modulator able to inhibit overproduction of MDM2 turns into a promising drug candidate for cancer treatment. With that purpose, HMSP based on the p53 wild-type peptide bioactive sequence was envisioned. These novel molecular architectures were designed to exhibit higher affinity for MDM2 than the parental p53 peptide.

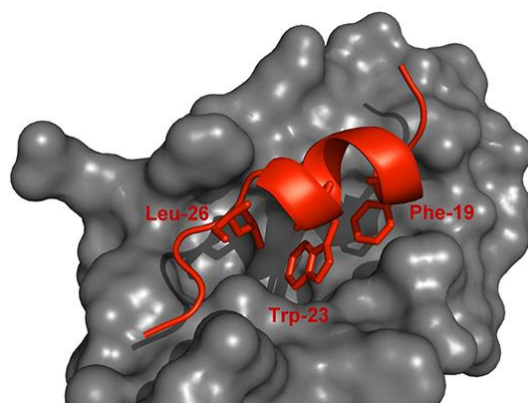


Figure 2.10. p53-MDM2 interaction.<sup>[98]</sup>

## 2.2 Objectives of chapter 2

1. Development of a novel synthetic methodology for the preparation of HMSP, in which short *N*-methyl-rich peptide bridge/s were inserted at key stapling positions to stabilise the  $\alpha$ -helical conformation. We envisioned that the developed approach could also be applied to the preparation of complex *N*-methyl-rich peptides. The p53-MDM2 protein-protein interaction was the focus in the development of the synthetic methodology, where potential inhibitors for this interaction, which were based on a fragment of the p53 wild-type protein, were generated.
2. Assessment of the developed strategy applicability by preparation of a library of HMSP where the *N*-methyl-rich peptide bridge/s were inserted at positions: (i) *i,i+4* (short staple); (ii) *i,i+7* (long staple); and (iii) *i,i+4* and *i+8,i+12* (double staple).
3. Study of the effect of the *N*-methyl-rich peptide bridges on the  $\alpha$ -helical conformation stabilisation. The length and the flexibility of the staple was modulated by the number and nature of *N*-methylated amino acids. Evaluation of the secondary structure of a library of short, long and double highly *N*-methylated stapled peptides by circular dichroism experiments.

## 2.3 Results and discussion

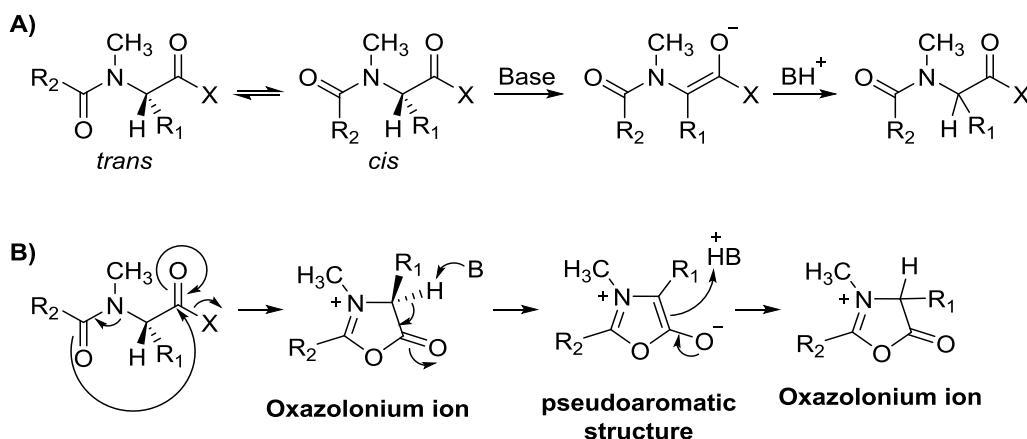
### 2.3.1 Development of a synthetic methodology to prepare highly *N*-methylated stapled peptides (HMSP)

#### 2.3.1.1 General synthetic considerations

Synthesis of highly *N*-methylated peptides is not a facile task, since many complications can be encountered throughout the synthesis. Following, these issues are described.

##### 2.3.1.1.1 Low coupling rates and epimerisation

Due to steric hindrance, peptide coupling rates onto secondary amines are rather low and generally require strong coupling conditions. Moreover, repetitive coupling cycles are often necessary to ensure full residue incorporation. The use of either HATU or PyBOP in combination with HOAt has proven useful for peptide coupling onto secondary amines.<sup>[99]</sup>



Scheme 2.6. Epimerisation upon activation of *N*-methyl amino acids *via* A) Direct base-catalysed enolization; and B) Tautomerization of the pseudoaromatic oxazolonium ion.

On the other hand, *N*-alkylated amino acids are prone to undergo racemisation upon activation conditions. In fact, epimerisation can occur through the direct base-catalysed enolization (Scheme 2.6A) or tautomerization of the pseudoaromatic

oxazolonium mechanism,<sup>[100]</sup> which resembles the corresponding oxazolone anion formed upon activation of common non-*N*-alkylated amino acids (Scheme 2.6B).<sup>[101]</sup>

Several guidelines can be considered to prevent or minimise the undesired side-reaction. First, amino acid epimerisation that proceeds through tautomerization of pseudoaromatic oxazolonium ions can be fully prevented by carbamate-protection at the  $\alpha$ -amino group. Contrary,  $N^\alpha$ -acyl protection should be avoided, since it has been found to enhance epimerisation.<sup>[101]</sup> It is worth mentioning that the presence of coupling additives such as HOBt, HOAt or OxymaPure when using carbodiimide coupling reagents results in minimised epimerisation rates.<sup>[101]</sup> On the other hand, sterically hindered bases are preferred over non-bulky amines, since they are less prone to abstract the  $\alpha$ -proton.<sup>[102]</sup> Additionally, stepwise residue incorporation rather than segment coupling has proven effective to prevent or diminish racemisation at the carboxy-termini upon *N*-alkylated amino acid activation.

#### 2.3.1.1.2 Deletion and over-incorporation of amino acids

Incomplete peptide couplings can lead to amino acid deletion, which ultimately lowers the overall yield and hampers the purification process. Peptide couplings onto *N*-alkylated residues can be especially low-yielding. In order to prevent growth of the undesired peptide chain, capping of the free amine prior to deprotection of the *N*-terminal is highly recommended.

Over-incorporation of amino acids displaying a less bulky side-chain can take place due to premature Fmoc elimination. The undesired side-reaction generally occurs upon amino acid activation *via* the symmetrical anhydride intermediate.<sup>[103]</sup>

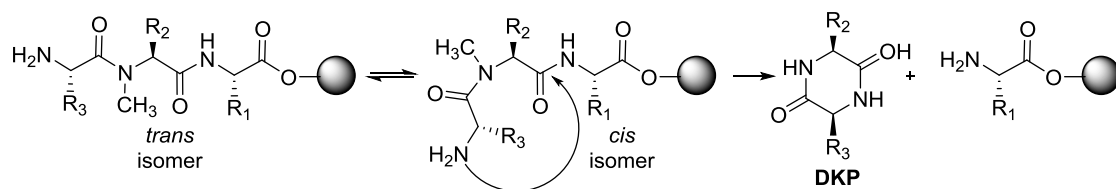
Special attention will be put into these issues throughout the synthesis.

#### 2.3.1.1.3 DKP formation

As mentioned earlier in this thesis, a common undesired reaction in peptide synthesis is DKP formation during Fmoc removal, which ultimately leads to lower yields due to dipeptide loss.<sup>[104,105]</sup> DKP is a base- and acid-catalysed side-reaction that is

specially favoured in the presence of *N*-alkyl amino acids, which are prone to adopt a *cis* conformation, thus enhancing the side-reaction (Scheme 2.7).<sup>[106]</sup>

Note that DKP formation is generally observed at the second residue of the peptide chain, however, it can also occur along the peptide sequence as well as upon cleavage of peptides containing a high content of *N*-methyl residues.<sup>[93]</sup> Several approaches have appeared over the years to prevent or minimise DKP formation, which include i) the use of a steric hindered resin, i.e. the 2-CTC resin<sup>[107]</sup>; (ii) shortening the usual piperidine–DMF (1:4) treatment;<sup>[108]</sup> (iii) use other bases such as DBU or TBAF instead of piperidine.<sup>[109,110]</sup>

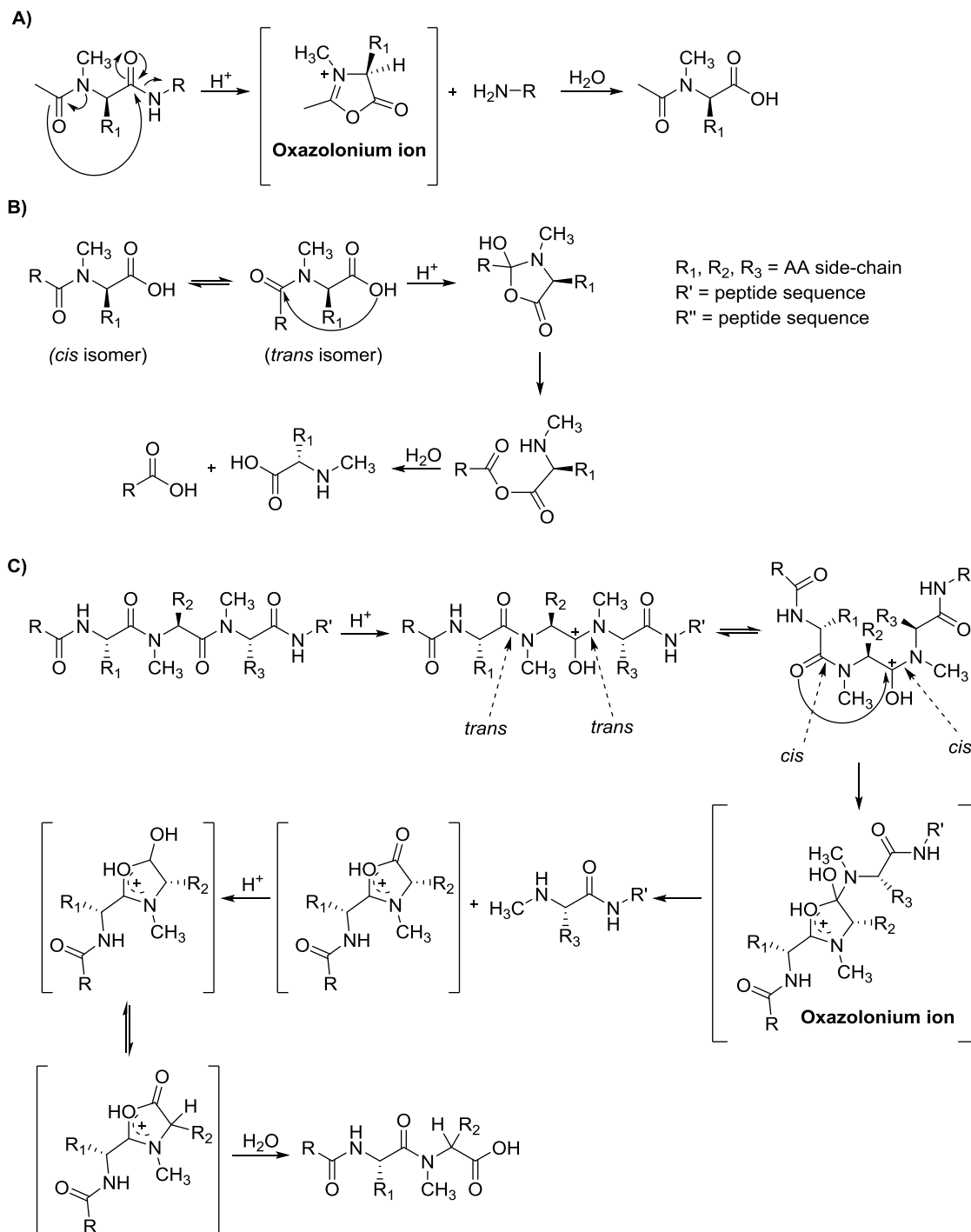


Scheme 2.7. DKP formation mechanism of *N*-methyl-containing peptides.

#### 2.3.1.1.4 Peptide fragmentation upon cleavage from the resin

Peptides presenting a high content of *N*-methyl residues are very unstable upon treatment with acidic conditions. It is not surprising that many side-reactions arise from peptide cleavage from the resin, which is accomplished by treatment with TFA and the appropriate scavengers cocktail based on the peptide side-chains. Some of the most common side-reactions include: (i) loss of *N*-terminal Ac-*N*-methyl amino acid residue *via* the oxazolonium ion intermediate (see mechanism in Scheme 2.8A);<sup>[111]</sup> and (ii) loss of the *C*-terminal *N*-methyl amino acid residue *via* the DKP formation mechanism (see mechanism in Scheme 2.8B).<sup>[112]</sup> The latter proceeds slowly and it is only detected in small percentages. One relevant drawback for this project was peptide fragmentation involving consecutive *N*-methylated residues, since construction of highly *N*-methylated stapled peptides was a major goal of this chapter. In this context, the lability of the amide bond between consecutive *N*-methylated residues upon cleavage conditions has been described.<sup>[93]</sup> Urban *et al.* hypothesised that fragmentation between consecutive *N*-methyl amino acids proceeds through the oxazolonium ion mechanism (Scheme 2.8C).<sup>[93]</sup> Interestingly, fragmentation rates can be minimised or prevented by

shortening the cleavage times. Additionally, evaluation of the optimal cleavage mixture composition must be undertaken for each particular case in order to get the least fragmentation.<sup>[93]</sup>



**Scheme 2.8.** Acid-catalysed side-reactions of highly *N*-methylated peptides. A) Loss of the *N*-terminal Ac-*N*-methyl residue; B) loss of the *C*-terminal *N*-methyl amino acid; C) Peptide fragmentation between two consecutive *N*-methyl residues.

Development of a synthetic strategy to avoid or minimise the drawbacks mentioned before can not only be useful for HMSP compound's synthesis, but also for the preparation of *N*-methyl rich peptides.

In this thesis, we designed *de novo* HMSP compounds as models for the development of the synthetic strategy.

### 2.3.1.2 General design of model HMSP

The design of the model HMSP was carried out as follows. Three possibilities were envisioned: insertion of i) a single "short" *N*-methyl-rich peptide bridge between positions  $i, i+4$ ; ii) a single "large" *N*-methyl-rich peptide bridge between positions  $i, i+7$ ; and iii) a double "short" *N*-methyl-rich peptide bridge between positions  $i+8, i+12$  (Figure 2.11).

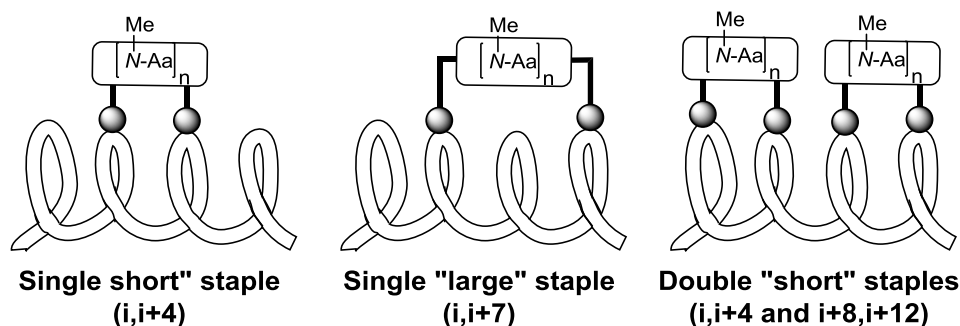


Figure 2.11. Designed single and double HMSP.

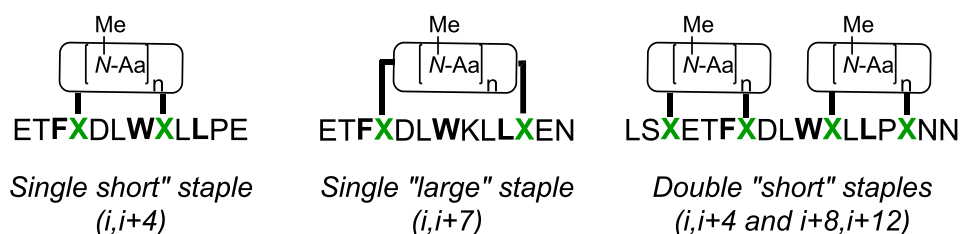
#### Proposed parental p53 peptide to be stapled

As mentioned earlier, the p53-MDM2 protein-protein interaction was the focus in the development of our synthetic methodology. The wild-type p53 peptide comprises the following amino acid sequence: LSQETF<sup>19</sup>SDLW<sup>23</sup>KLL<sup>26</sup>PENN, where Phe<sup>19</sup>, Trp<sup>23</sup> and Leu<sup>26</sup> are key residues for the p53-MDM2 interaction (shown in bold).<sup>[96]</sup> Parental peptide p53, which presents a random coil secondary structure, was taken as starting point of the synthesis to insert the chemical brace.

Location of the staple

Location of the staple was selected according to previous bioactive p53-stapled peptides reported in the literature, in which different stapling techniques such as all-hydrocarbon and triazole-based cross-links were used to accommodate the helical conformation.<sup>[60,82,84,113]</sup> In this context, a 12-mer, a 13-mer and a 17-mer p53-based peptide were selected for the preparation of single “short” HMSP, single “large” HMSP and double HMSP, respectively (Figure 2.12). Whereas the key residues for protein-protein interaction were maintained, selected amino acids (see **X** in Figure 2.12) were modified to insert the *N*-methylated chemical brace.

*p53 wild-type*: LSQETFSDLWKLLEN



X = modified residues to insert the chemical brace

Figure 2.12. Different staple location of p53-based HMSP.

Amino acid sequence of the *N*-methyl-rich peptide bridges

Ala scanning has been widely employed as a method of identifying the contribution of a specific residue to the stability or function of a given peptide or protein.<sup>[114]</sup> Ala is used because of its non-bulky, chemically inert, methyl functional group that mimics the secondary structure preferences that many of the other amino acids possess. Sometimes bulky amino acids such as Val or Leu are used in cases where conservation of the size of mutated residues is needed.

Bearing in mind these considerations, optimisation of the synthetic strategy was carried out with *N*-MeAla residues. Thus, once the synthetic methodology was established, several *N*-methyl amino acid combinations were prepared. It is well-known that hydrophobic *N*-methyl amino acids favour cell internalisation. Thus, various

combinations of hydrophobic *N*-methyl amino acids such as *N*-MePhe, *N*-MeLeu, and  $\beta$ -branched residues such as *N*-Val were inserted. Additionally, effect of other residues was also evaluated. For instance, *N*-MeGly and Pro, which are known to destabilise the helical turn, were inserted to assess their effect on secondary structure stability. Insertion of hydrophilic residues, such as *N*-MeLys and *N*-MeGln, was also carried out and studied.

### Length of the staple

Length of the chemical brace plays an important role in the secondary structure stabilisation. In addition, the staple ring size is crucial to side-chain to side-chain cyclisation success.<sup>[115]</sup> In general, cyclisation of peptides displaying seven or more residues within the core ring is foreseen straightforward. Contrary, cyclisation of smaller peptides can be very problematic, being in some cases not even accomplished. Moreover, *N*-terminal *N*-methyl residues are known to hamper the cyclisation step due to steric hindrance issues. As mentioned earlier, the use of strong coupling conditions has proven effective to enhance the cyclisation rates.<sup>[99]</sup>

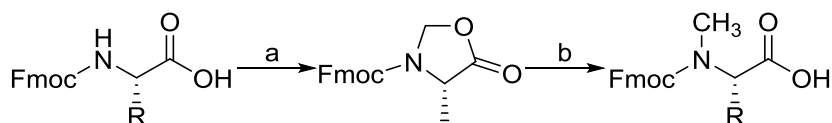
Considering the above factors, selection of the optimal staple length to simultaneously favour cyclisation and promote the  $\alpha$ -helical turn is, *a priori*, a challenging task. However, this key point needed to be established at an early stage of the synthetic methodology development. We considered that a good starting point was screening of *N*-methyl-rich peptide bridges containing two to four residues for peptide stapling at positions *i,i*+4, where the ring size presents at least seven residues.

#### **2.3.1.3 Preparation of a small library of Fmoc-*N*-MeAA**

For SPPS purposes, *N*-protected *N*-MeAA were prepared following the strategy proposed by Ben-Ishai *et al.*, in which *N*-methylation of amino acid proceeds *via* the oxazolidine intermediate.<sup>[116]</sup> Reduction of 5-oxazolidine with TIS and a great excess of TFA renders the desired *N*-methylated residue.<sup>[117]</sup> Among other advantages, this procedure allows *N*-methylation under very mild conditions, where racemisation is prevented. Additionally, *N*-methylation of Fmoc-*N*-protected amino acids is feasible and

the protocol is compatible with amino acid side-chain protecting groups as long as they are not acid-labile. However, large amounts of silane and TFA are required for the ring opening.

A small library of Fmoc-*N*-MeAA (Table 2.1) was prepared *via* the 5-oxazolidine intermediate (Scheme 2.9). In all cases, the first step of the synthesis started with formation of the 5-oxazolidine intermediate by reaction of the corresponding commercially available Fmoc-AA(PG)-OH and *p*-formaldehyde in the presence of catalytic amounts of *p*-TsOH acid. The reaction was brought to reflux, being a Dean Stark apparatus required to remove the water formed in the system and therefore shift the equilibrium to the formation of the 5-membered ring. A basic aqueous work-up to get rid of possible unreacted starting material (Fmoc-AA(PG)-OH) and *p*-TsOH acid was performed. Without further purification, the ring opening of the crude product was achieved by treatment of the corresponding 5-oxazolidine with a great excess of TFA and TIS.



Scheme 2.9. Synthesis of Fmoc-*N*-MeAA. a) *p*-TsOH (0.12 eq), *p*-formaldehyde (1.1 eq), toluene, reflux, 3 h; b) TIS (4 eq), TFA (76 eq), DCM, rt. N<sub>2</sub> atmosphere, 14 h.

The yields for all residues after column chromatography purification are summarised in Table 2.1. Synthesis of all five Fmoc-*N*-MeAA residues proceeded smoothly and good-excellent yields were obtained in all cases.

| Preparation of Fmoc- <i>N</i> -Me amino acids |            |                          |                          |
|---|------------|--------------------------|--------------------------|
| #   | Compound   | Fmoc- <i>N</i> -MeAA     | Yield over two steps (%) |
| 1   | <b>2.1</b> | Fmoc- <i>N</i> -MeAla-OH | 82                       |
| 2   | <b>2.2</b> | Fmoc- <i>N</i> -MeGly-OH | 72                       |
| 3   | <b>2.3</b> | Fmoc- <i>N</i> -MePhe-OH | 91                       |
| 4   | <b>2.4</b> | Fmoc- <i>N</i> -MeVal-OH | 82                       |
| 5   | <b>2.5</b> | Fmoc- <i>N</i> -MeLeu-OH | 88                       |

Table 2.1. Preparation of a small library of Fmoc-*N*-Me-AA.

All five residues were prepared in large amounts, and were further used for the development and optimisation of the synthetic strategy to construct *N*-methyl-bridged stapled peptides.

### 2.3.1.4 Lactam-based cross-linking approach

In order to optimise the synthetic strategy, single “short” HMSP (stapling position  $i,i+4$ ) were pursued. We envisioned that at a later stage, the same methodology could be applied to access “large” or “double” stapled peptides.

The initial approach to insert *N*-methyl-rich peptide bridges was through a lactam-based cyclisation. Lys and Glu acids were selected as the stapling points (Figure 2.13). Their relative position,  $i,i+4$ , was expected to promote the  $\alpha$ -helical conformation. As mentioned earlier, a 12-mer peptide based on the p53 wild-type sequence was used for the preparation of single “short” stapled peptides, in which the key residues for the interaction were maintained and are shown in bold.

The best approach to incorporate the *N*-methyl-rich peptide staples was evaluated. With that purpose, two strategies were envisioned. The bridge was constructed by either stepwise incorporation of *N*-methylated residues previously synthesised in solution (*Strategy A*) or sequential Fmoc-Ala-OH residues assembly and subsequent on-resin Mitsunobu *N*-Methylation (*Strategy B*). Once this was established, scope of the macrolactamisation was assessed with different *N*-methyl-rich peptide staple combinations. Finally, selection of the optimal cleavage and global deprotection conditions was carried out. Note that highly *N*-methylated peptides are very unstable upon treatment with acidic conditions, and therefore fragmentation studies were necessary at this point.

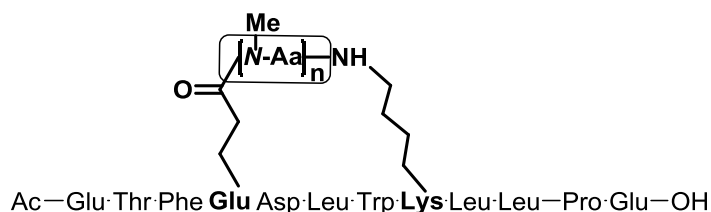


Figure 2.13. Lactam-based cross-link.

#### 2.3.1.4.1 Chain elongation of a linear p53-based peptide

A solid-phase approach combined with an Fmoc/tBu strategy was pursued (Scheme 2.10). The 2-chlorotrityl (2-CTC) resin was the solid support of choice, which renders the C-terminus as a free carboxylic acid function upon peptide cleavage from the resin. Since on-resin macrolactamisation was envisaged, a low resin functionalisation was needed to avoid interchain reactions. Therefore, the loading of the resin was set up to 0.30 mmol/g resin. The chain elongation was carried out by standard means, with successive cycles of coupling and deprotection steps. Couplings were generally carried out with the AA–OxymaPure–Dic (3:3:3 eq) coupling system, in which the amino acid was pre-activated for 5 min before it was added to the resin. The Kaiser test was run to monitor coupling completion.

For couplings onto secondary amines such as Pro, stronger conditions were used. Thus, the peptidyl-resin was treated with the AA–HATU–HOAt–DIEA (3:3:3:6 eq) coupling mixture. At position 5 starting from the C-terminus, a Lys residue was introduced, conveniently protected with the Dde group, which is orthogonal to the Fmoc group (see structure in Scheme 2.10). Next, four positions further from the Lys residue, a Glu residue was placed, with the side-chain protected with the allyl group, which is orthogonal to both the Fmoc and the Dde protecting groups.

In order to avoid undesired elongation at the N-terminus upon construction of the staple, acetylation was carried out with the traditional Ac<sub>2</sub>O–DIEA (3:9 eq) mixture. Next, the Dde group was selectively removed by treatment with a freshly prepared hydrazine–DMF solution. Although Dde removal is generally accomplished by treatment with a hydrazine–DMF (2:98 v/v) solution, in this particular system full Dde removal was only accomplished with a more concentrated solution (hydrazine–DMF (1:9 v/v) solution).

Throughout all this chapter, on-resin reaction monitoring of difficult steps was carried out by HPLC-MS analysis. The following procedure, designated as “*mini-cleavage*” was used: cleavage of a small aliquot of the peptidyl-resin was carried out with either (i) a TFA–TIS–H<sub>2</sub>O (90:5:5 v/v) mixture for one hour, which resulted in peptide cleavage and global deprotection; or (ii) a HFIP–DCM (1:4 v/v) mixture for 45



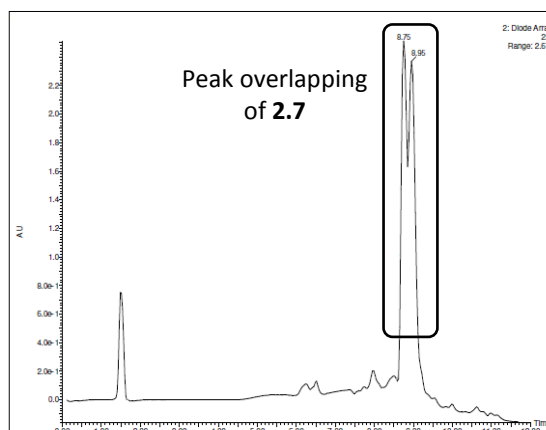
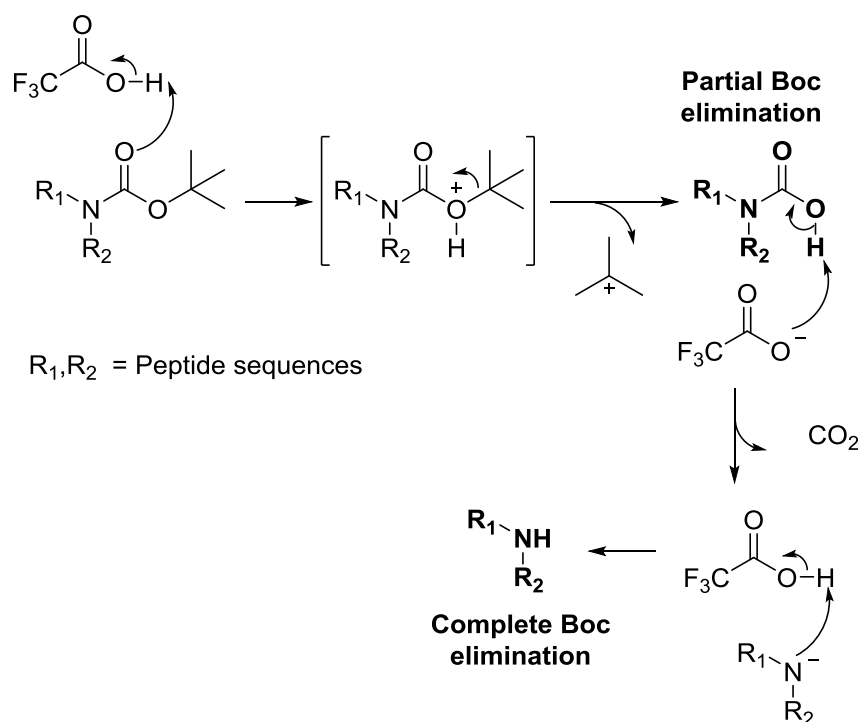


Figure 2.14. HPLC-MS chromatogram run at G20100t9T25 and processed at 220 nm (From now on G20100t9T25 stands for linear HPLC gradient from 20% to 100% of B over 9 min at 25 °C using as eluent system A: 0.045% TFA in H<sub>2</sub>O and B: 0.036% TFA in ACN). HPLC-MS analysis showed two peaks overlapping corresponding to full and partial Boc removal of peptide **2.7**.



Scheme 2.11. Boc removal mechanism.

Partial Boc removal is a reaction of common occurrence in Trp-containing peptides (see mechanism in Scheme 2.11). In fact, complete carbamate elimination can be accomplished by successive lyophilisation cycles, which leads to an equilibrium shift towards complete Boc removal. Thus, partial Boc removal did not represent a problem at this stage of the synthesis. It is worth mentioning that peak overlapping

corresponding to full and partial Boc unprotected peptides was occasionally observed throughout all the synthetic strategy development.

Apart from this rather anecdotic fact, the linear peptide sequence was successfully synthesised with a 96% HPLC purity. The next step of the synthetic methodology development was the evaluation of the best approach for the construction of short *N*-methyl-bridged peptides.

#### **2.3.1.4.2 Evaluation of the best approach to insert *N*-methyl-rich peptide linkers**

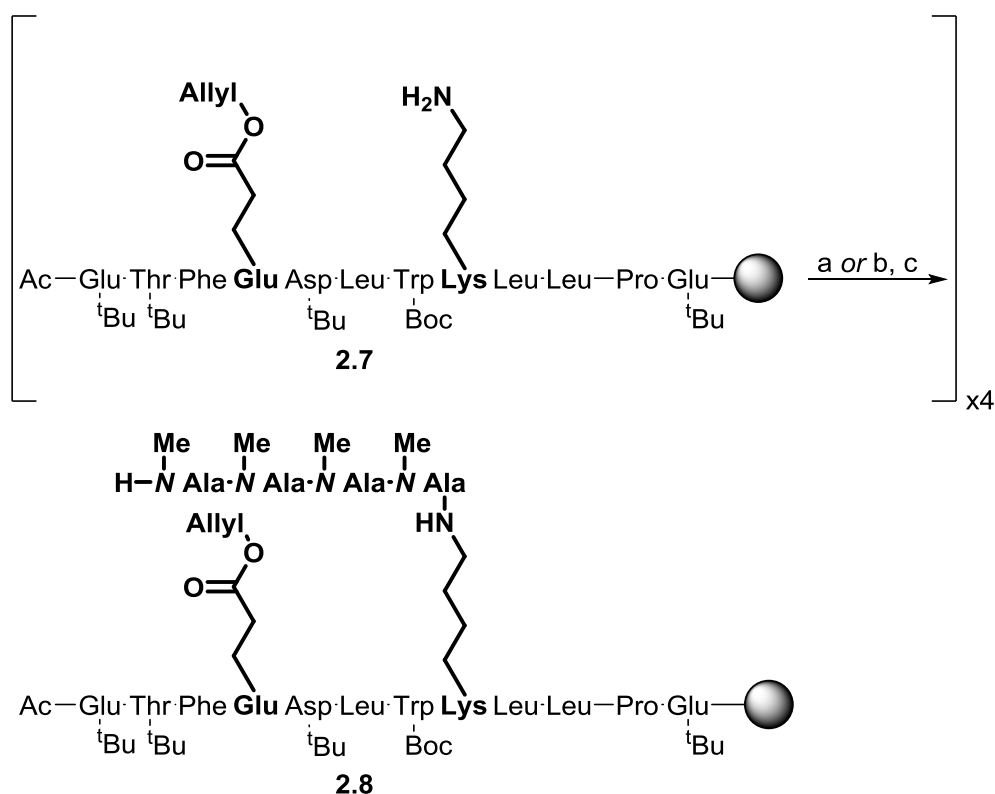
As we mentioned before, two strategies for the incorporation of the *N*-methyl-rich peptide linkers were evaluated. The linker was constructed by either stepwise incorporation of *N*-methylated residues previously synthesised in solution (*Strategy A*) or sequential Fmoc-Ala-OH residues assembly and subsequent on-resin Mitsunobu *N*-Methylation (*Strategy B*). For that, *N*-MeAla residues were exclusively used (review the advantages of using Ala for the optimisation process in section 2.3.1.2). Since a long enough peptide staple was necessary for the evaluation of the best approach to insert highly *N*-methylated peptide bridges, the staple length was set up to four residues. Thus, a sequence of four *N*-MeAla residues was selected to serve as the chemical brace between relative positions  $i, i+4$ .

##### *2.3.1.4.2.1 Synthetic strategy A: Stepwise incorporation of *N*-methylated residues*

The starting point of the staple chain elongation was the Lys residue located at the fifth position starting from the *C*-terminus. With the Fmoc-*N*-MeAla-OH residue in hands (previously prepared in solution), a general approach for stepwise *N*-MeAla residue incorporation consisted of successive cycles of coupling and deprotection steps (Scheme 2.12).

Assembly of the first *N*-methylated residue through amide bond formation was accomplished by treatment of the peptidyl-resin **2.7** with the AA–OxymaPure–Dic (3:3:3 eq) coupling system. In this case re-coupling was required to achieve full residue incorporation, which was checked by means of the Kaiser test. After Fmoc removal, stronger conditions were used for amino acid couplings onto secondary amines, and

therefore the remaining residues were incorporated by using the AA–HATU–HOAt–DIEA (3:3:3:6 eq) coupling conditions.



*Scheme 2.12.* Construction of the branched *N*-methylated peptide **2.8**, an intermediate of stapled peptide **2.9**, via Strategy A. Protocol a) was used for couplings onto primary amines, and protocol B was used for couplings onto secondary amines. a) Fmoc-*N*-MeAla-OH (3 eq), OxymaPure (3 eq), DIC (3 eq), DMF, 40 min; b) Fmoc-*N*-MeAla-OH (3 eq), HATU (3 eq) HOAt (3 eq), DIEA (3 eq), DMF, 1 h. c) piperidine–DMF (1:4 v/v) (1 x 1 min + 2 x 5 min).

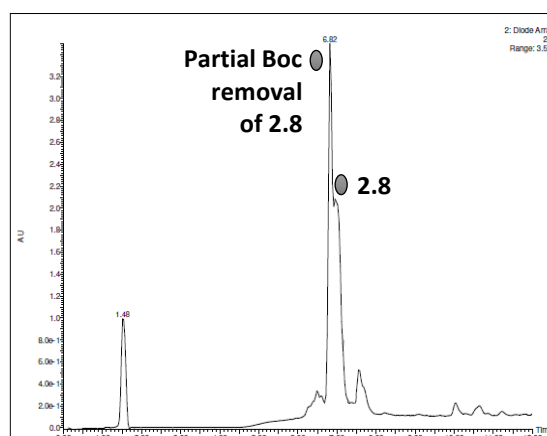


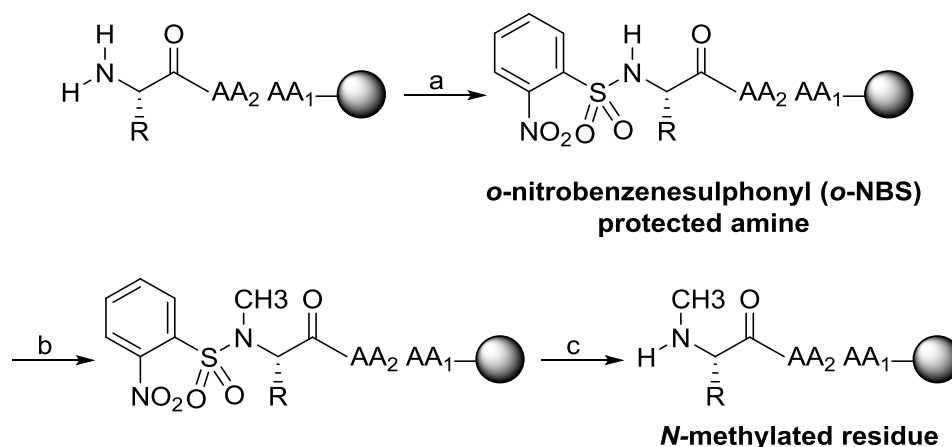
*Figure 2.15.* HPLC-MS chromatogram run at G20100t9T25 and processed at 220 nm. Branched *N*-methylated linker elongation via Strategy A, in which peak overlapping due to partial and complete Boc removal was observed.

A “mini-cleavage” after each step was carried out to monitor the synthesis. In most cases, a single treatment was not enough to achieve full conversion, and therefore re-coupling was carried out by default.

Preparation of compound **2.8** was successfully accomplished according to HPLC-MS analysis of a peptidyl-resin cleavage crude, in which peak overlapping due to partial and complete Boc elimination was again observed (Figure 2.15). In fact, considering the synthetic complexity of peptide **2.8**, the highly *N*-methylated linker elongation proceeded smoothly and a very clean HPLC chromatogram was observed at this late stage of the synthesis. Although multiple re-coupling steps were required, construction of the linker by insertion of Fmoc-*N*-Me-amino acids became a good alternative to furnish the staple peptide chain.

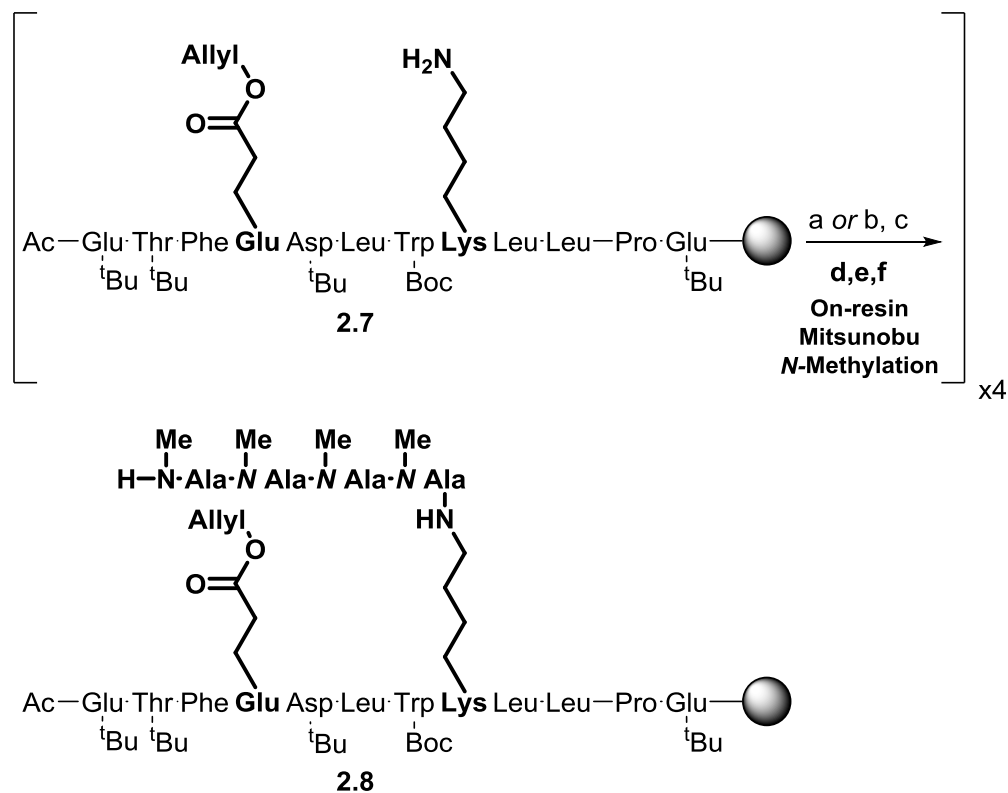
#### 2.3.1.4.2.2 Synthetic strategy B: On-resin Mitsunobu *N*-methylation of the residues

Mitsunobu first reported the three-step effective *N*-methylation that can be performed either on solid-phase or in solution (Scheme 2.13). The first step is protection of the primary amine and activation of the NH proton with the *o*-nitrobenzenesulfonyl (*o*-NBS) group, which allows mild *N*-methylation conditions with MeOH, PPh<sub>3</sub> and DIAD. Once the residue has been *N*-methylated, *o*-NBS removal can be accomplished by treatment with DBU and 2-mercaptoethanol.<sup>[118]</sup> This site-selective *N*-methylation was used for the development of *Strategy B*.



Scheme 2.13. On-resin Mitsunobu *N*-methylation protocol. a) *o*-NBS-Cl, DIEA, DCM; b) MeOH, PPh<sub>3</sub>, DIAD; c) DBU, HOCH<sub>2</sub>CH<sub>2</sub>SH.

A general approach for *Strategy B* was outlined as follows. The *N*-methylated linker elongation was accomplished by successive cycles of Fmoc-Ala-OH incorporation, followed by Fmoc removal and subsequent on-resin Mitsunobu *N*-methylation (Scheme 2.14).



*Scheme 2.14.* Construction of the branched *N*-methylated peptide **2.8**, an intermediate of stapled peptide **2.9**, via *Strategy B*. a) Fmoc-Ala-OH (3 eq), OxymaPure (3 eq), DIC (3 eq), DMF, 40 min; b) Fmoc-Ala-OH (3 eq), HATU (3 eq) HOAt (3 eq), DIEA (3 eq), DMF, 1 h; c) piperidine–DMF (1:4 v/v) (1 x 1 min + 2 x 5 min); d) *o*-NBS (4 eq), DIEA (10 eq), DCM, 30 min; e) MeOH (10 eq), PPh<sub>3</sub> (5 eq), DIAD (5 eq), THF<sub>dry</sub>, 1 h; f) DBU (5 eq), HOCH<sub>2</sub>CH<sub>2</sub>SH (10 eq), DMF, (1 x 1 min + 2 x 10 min).

Mitsunobu *N*-methylation of the Ala residue started with protection of the free amine with the *o*-NBS group to form the corresponding sulphonamide. This was accomplished by treatment of the peptidyl-resin with *o*-NBS-Cl and DIEA. Full protection was confirmed by means of the Kaiser test. Once the amine was protected, treatment with MeOH–PPh<sub>3</sub>–DIAD resulted in residue *N*-methylation. Addition of the reagents plays an important role in the reaction success. Thus, the amine was first reacted with MeOH/PPh<sub>3</sub>, followed by the dropwise addition of DIAD. A “*mini-cleavage*” was used to monitor the reaction by HPLC-MS, being a double treatment required to reach full

conversion. Lastly, *o*-NBS removal was accomplished by addition of DBU and 2-mercaptoethanol.

Assembly of the second residue, Fmoc-Ala-OH, was accomplished using the same conditions as the ones used for *Strategy A*. Thus, the HATU–HOAt–DIEA (3:3:3:6 eq) mixture was added to the peptide-bound. Again, a double treatment was performed after each coupling. The cycle involving coupling of Fmoc-Ala-OH and subsequent Mitsunobu *N*-methylation was successively repeated to furnish compound **2.8**.

*Strategy B* turned out effective for the linker elongation. As shown in the HPLC analysis, synthesis of the corresponding peptide staple proceeded smoothly and the desired product was obtained in excellent HPLC yields (Figure 2.16).

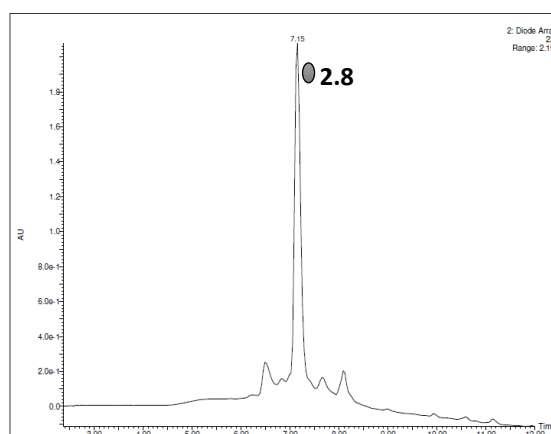


Figure 2.16. HPLC-MS chromatogram run at G20100t9T25 and processed at 220 nm. Branched *N*-methylated linker elongation via *Strategy B*.

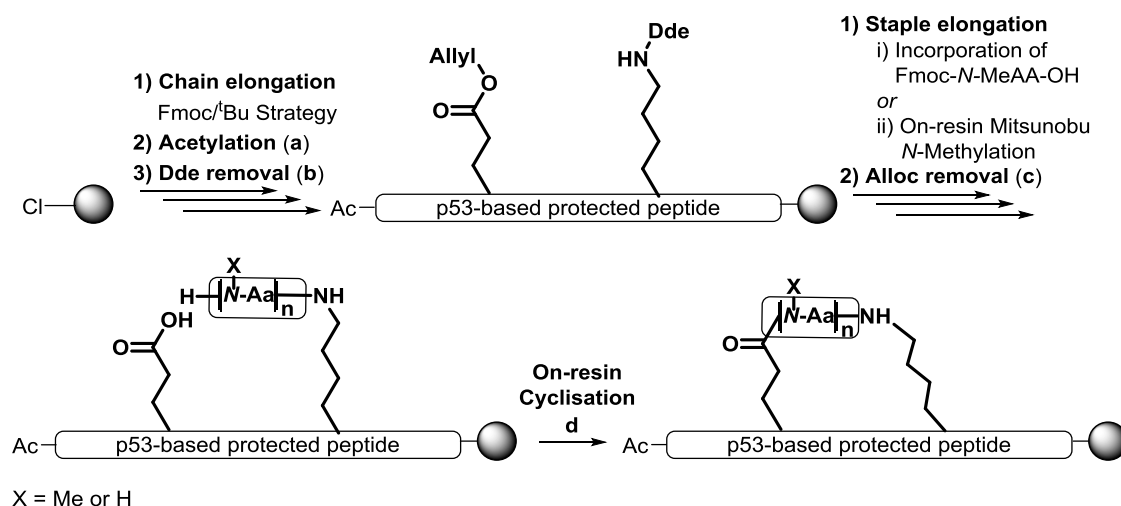
#### 2.3.1.4.2.3 Evaluation of the best approach to insert *N*-methyl-rich peptide linkers

Both approaches turned out efficient for the construction of the highly *N*-methylated tetrapeptide (Figure 2.15 and Figure 2.16). Conveniently, either method can be used based on the staple length and nature of the amino acids. For instance, preparation of large amounts of Fmoc-*N*-Me-amino acids (*Strategy A*) for frequent use results less time-consuming than repeatedly *N*-methylate the residues on solid-phase. On the other hand, at a later stage of the project, insertion of residues of occasional use for screening of the optimal staple sequence can be facilitated by simple on-resin Mitsunobu *N*-methylation of those particular residues. Another scenario where *Strategy*

*B* becomes useful is for the incorporation of *N*-methylated residues presenting acid-labile side-chain protecting groups, since their preparation *via* the 5-oxazolidine intermediate is not feasible due to the use of TFA.

### 2.3.1.4.3 Scope of the lactam-based cross-link: macrolactamisation studies

Scope of the lactam-based cross-link was evaluated with staple sequence combinations of various lengths containing both *N*-methylated and non-*N*-methylated residues at the *N*-terminal position (Table 2.2). In this context, the staple/linker length and sequence effect on the cyclisation extent was the focus on the study. The general lactam-based synthetic approach for the preparation of the peptide library is described in Scheme 2.15. In all cases, the *N*-methyl-rich peptide linker was inserted following previously developed *Strategy A* (see section 2.3.1.4.2.3).



*Scheme 2.15.* General synthetic strategy to prepare highly *N*-methylated lactam-based stapled peptides. **Chain elongation:** Couplings onto primary amines: Fmoc-AA(PG)-OH (3 eq), OxymaPure (3 eq), DIC (3 eq), DMF, 40 min; peptide couplings onto secondary amines: Fmoc-AA(PG)-OH (3 eq). **Staple elongation:** *Strategy A* (repetitive cycles of: 1) Fmoc-*N*-MeAla-OH (3 eq), HATU (3 eq) HOAt (3 eq), DIEA (3 eq), DMF, 1 h; and 2) piperidine-DMF (1:4 v/v) (1 x 1 min + 2 x 5 min)) or *Strategy B* (repetitive cycles of 1) Fmoc-Ala-OH (3 eq), HATU (3 eq) HOAt (3 eq), DIEA (3 eq), DMF, 1 h; 2) piperidine-DMF (1:4 v/v) (1 x 1 min + 2 x 5 min); 3) *o*-NBS (4 eq), DIEA (10 eq), DCM, 30 min; 4) MeOH (10 eq), PPh<sub>3</sub> (5 eq), DIAD (5 eq), THF<sub>dry</sub>, 1 h; 5) DBU (5 eq), HOCH<sub>2</sub>CH<sub>2</sub>SH (10 eq), DMF, (1 x 1 min + 2 x 10 min)). a) **Acetylation:** Ac<sub>2</sub>O (3 eq), DIEA (9 eq), DCM, 20 min; b) **Dde removal:** Hydrazine-DMF (1:9 v/v) (1 x 1 min + 2 x 15 min); c) **Alloc removal:** Pd(PH<sub>3</sub>)<sub>4</sub> (0.1 eq), Phenylsilane (10 eq), DMF, (3 x 15 min); d) **On-resin cyclisation:** HATU (3 eq) HOAt (3 eq), DIEA (3 eq), DMF, 12 h.

Next, the allyl group was removed by using a Pd-based catalyst in the presence of phenylsilane, which serves as scavenger. With both unprotected binding points, cyclisation trials were performed. A “mini-cleavage” with the HFIP–DCM (1:4 v/v) cocktail was carried out and the sample was further analysed by HPLC. “Mini-cleavage” upon very mild conditions furnished the protected cleaved linear branched peptide, thus possible peptide fragmentation between *N*-methylated residues was prevented. The cyclisation outcomes are summarised in Table 2.2.

**Branched peptide**

**On-resin Cyclisation**

HATU (3 eq),  
HOAt (3 eq),  
DIEA (6 eq),  
DMF, rt, 12 h

**Stapled peptide**

X = Me or H

| # | Branched peptide | Stapled peptide | Staple sequence   | On-resin cyclisation (% HPLC conversion) |
|---|------------------|-----------------|---|--|
| 1 | 2.8              | 2.9             | – <i>N</i> -MeAla– <i>N</i> -MeAla– <i>N</i> -MeAla– <i>N</i> -MeAla– | 0  |
| 2 | 2.10             | 2.11            | – <i>N</i> -MeAla– <i>N</i> -MeAla– <i>N</i> -MeAla–                  | 0  |
| 3 | 2.12             | 2.13            | – <i>N</i> -MeAla– <i>N</i> -MeAla–                                   | 0  |
| 4 | 2.14             | 2.15            | – <i>N</i> -MePhe– <i>N</i> -MeAla– <i>N</i> -MeAla– <i>N</i> -MeAla– | 0  |
| 5 | 2.16             | 2.17            | – <i>N</i> -MeGly– <i>N</i> -MeAla– <i>N</i> -MeAla– <i>N</i> -MeAla– | 30                                       |
| 6 | 2.18             | 2.19            | – <i>N</i> -MeGly–Phe– <i>N</i> -MeAla– <i>N</i> -MeAla–              | 0  |
| 7 | 2.20             | 2.21            | –Ala– <i>N</i> -MeAla– <i>N</i> -MeAla– <i>N</i> -MeAla–              | 100                                      |
| 8 | 2.22             | 2.23            | –Phe– <i>N</i> -MeAla– <i>N</i> -MeAla– <i>N</i> -MeAla–              | 0  |
| 9 | 2.24             | 2.25            | –Gly– <i>N</i> -MeAla– <i>N</i> -MeAla– <i>N</i> -MeAla–              | 55                                       |

Table 2.2. Scope of the lactam-based cross-linking strategy at positions *i* and *i*+4.

As mentioned earlier, macrolactamisation is favoured with ring sizes containing at least seven residues.<sup>[115]</sup> Accordingly, for peptide stapling at positions  $i, i+4$ , a series of *N*-methyl-rich peptide bridges comprising two to four residues were inserted. Note that in all cases the ring size is comprised between seven and nine residues.

To start up with, evaluation of the ring size effect on the macrolactamisation extent was carried out with peptides **2.8**, **2.10** and **2.12** (see entries #1-3 in Table 2.2). Since macrolactamisation was foreseen challenging due to the steric hindrance provided by *N*-terminal *N*-methyl residues, strong coupling conditions were used at first. Thus, peptides **2.8**, **2.10** and **2.12** were treated with the HATU–HOAt–DIEA (3:3:6 eq) coupling system for 12 h. Unfortunately, cyclisation was not accomplished in any case. In an attempt to improve the macrolactamisation outcome, several reaction conditions were tested, including different coupling reagent systems (PyBOP–HOAt–DIEA and HATU–HOAt–DIEA), temperatures and reaction times. However, the same unfortunate results were observed. These results indicate that the ring size might not be responsible for the unfortunate cyclisation outcome.

At this stage we hypothesised that the *N*-terminal steric hindrance provided by the methyl substituent on the amine might account for the unfavourable macrolactamisation outcome. In order to confirm this theory, cyclisation of branched peptides **2.14** and **2.16** was tried (see entries #4-5 in Table 2.2). For that, several conditions were tested (including different coupling reagent systems, temperatures and reaction times), however, positive cyclisation outcomes were only observed with the HATU–HOAt–DIEA coupling system.

As expected, replacement of the original *N*-terminal *N*-MeAla residue by a more steric hindered residue, *N*-MePhe, resulted in complete failure towards the cyclic product generation (see entry #4 in Table 2.2).

Not surprisingly, replacement of that same fourth *N*-terminal residue by *N*-MeGly, which is less steric hindered and much more flexible, allowed cyclisation (see entry #5 in Table 2.2). However, only 30% of conversion was observed by HPLC-MS analysis (Figure 2.17). Although additional treatments with the same coupling system

were performed, the cyclisation rates could not be improved. Nevertheless, these results support the steric hindrance theory postulated earlier.

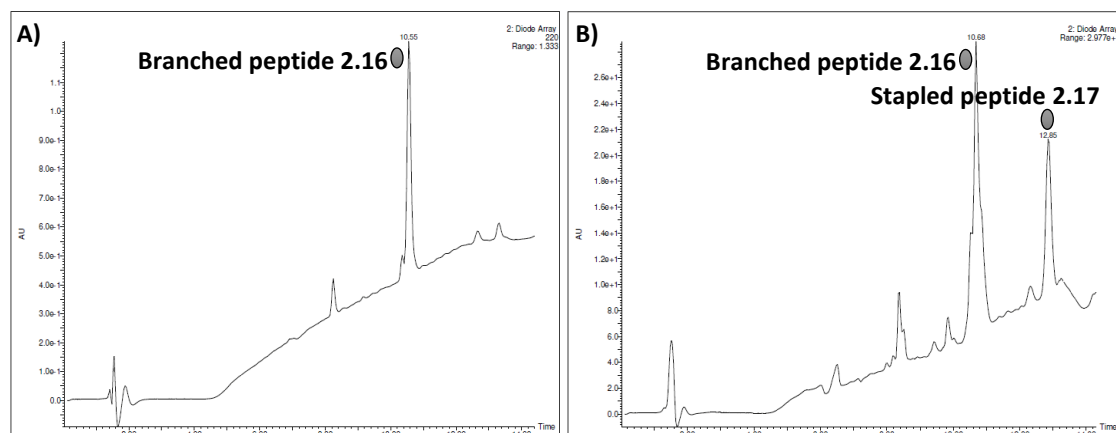
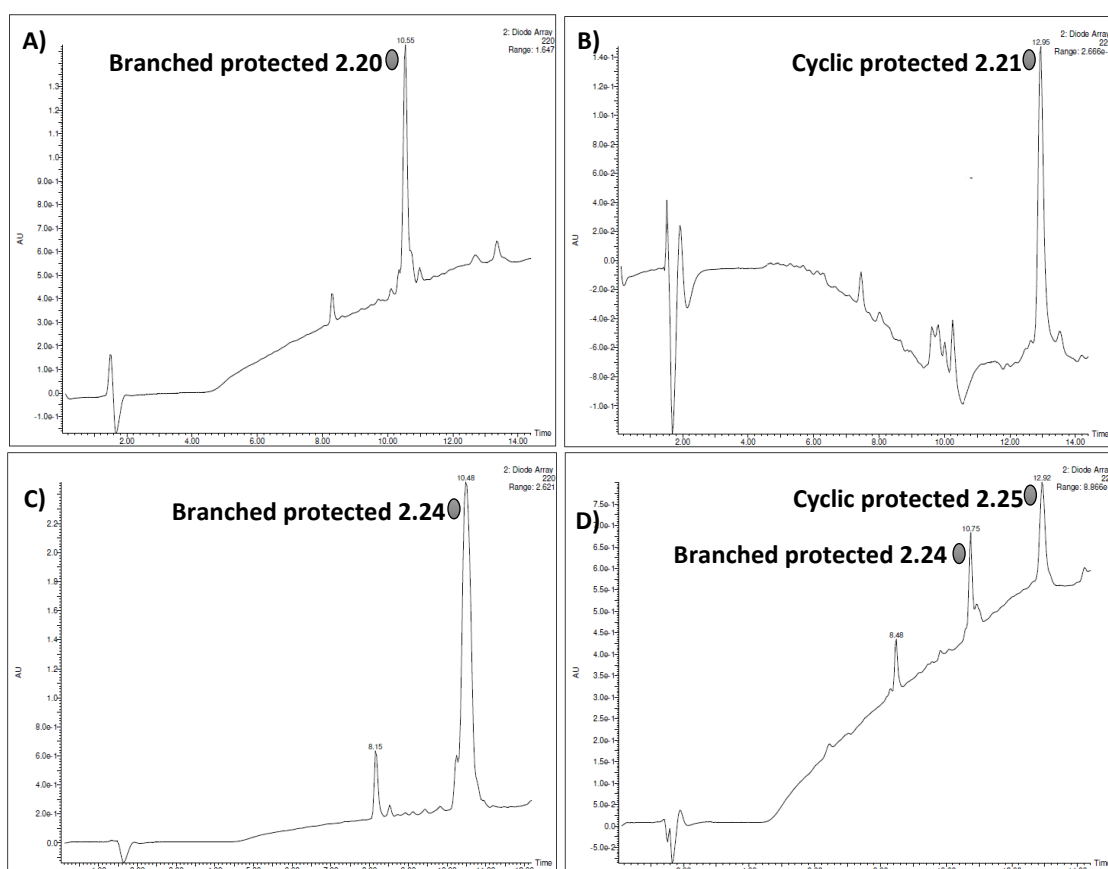


Figure 2.17. HPLC-MS chromatograms run at G20100t9T25 and processed at 220 nm. A) Branched peptide **2.16**; B) Cyclisation of branched peptide **2.16** to obtain cyclic peptide **2.17**.

In order to assess whether the staple sequence had an effect on the macrolactamisation extent, peptide **2.16** was modified by substituting one *N*-MeAla for Phe (see entry #6 in Table 2.2). Accordingly, cyclisation of **2.18** was attempted. The complete absence of the corresponding cyclic product (**2.19**) indicated that the staple sequence had indeed a pronounced effect on the cyclisation outcome. This particular subject was not further studied and was left on hold due to its complexity and level of experiments required to draw conclusions.

Finally, substitution of the staple *N*-terminal residue by non-*N*-methylated amino acids was assessed. Replacement of the *N*-terminal *N*-MeAla residue by the more reactive Ala residue resulted in successful peptide side-chain to side-chain macrolactamisation, where the corresponding cyclic derivative was obtained as the major product according to HPLC-MS analysis (see entry #7 in Table 2.2, and HPLC-MS chromatogram of branched peptide **2.20** and stapled peptide **2.21** in Figure 2.18). Whereas replacement of the *N*-terminal residue by the bulkier Phe residue resulted in no cyclisation, substitution by Gly afforded the desired product in a 55% HPLC yield (see entries #8-9 in Table 2.2, and HPLC-MS chromatogram of branched peptide **2.24** and stapled peptide **2.25** in Figure 2.18). Although additional treatments were carried out,

the cyclisation extent could not be improved. In the latter (see entry #9 in Table 2.2), the cyclisation outcome improvement compared to the *N*-MeGly analogue is not surprising, since the primary amine of Gly was expected to be more reactive due to its less hindered environment. However, it is quite surprising the fact that macrolactamisation with *N*-terminal Gly led to poorer results than the ones observed for *N*-terminal Ala. In fact, one would expect opposite results, since intrinsic flexibility of Gly is expected to favour the cyclisation rather than hamper it. Unfortunately, we were not capable of finding a plausible explanation for this fact.



**Figure 2.18.** HPLC-MS chromatograms run at G20100t9T25 and processed at 220 nm. A) Branched peptide **2.20**; B) Cyclisation of branched peptide **2.20** to obtain peptide **2.21**; C) Branched peptide **2.24**; D) Cyclisation of branched peptide **2.24** to obtain peptide **2.25**.

To sum up, several staple sequence combinations comprising *N*-methylated and non-*N*-methylated residues for cross-linking between positions  $i, i+4$  were tested, observing a poor cyclisation extent in most cases. In fact, peptide stapling between

relative positions  $i, i+4$  was only favoured when non-*N*-methylated residues such as Ala or Gly or less steric hindered *N*-MeGly were located at the staple *N*-terminal position.

In accordance to these results, steric hindrance either at the *N*-terminal residue or within the peptide staple sequence plays a key role in the macrolactamisation outcome. In this context, numerous experiments would be required for screening of the optimal peptide staple sequence. However, it is well known that peptides containing a high content of *N*-methylated residues are prone to undergo fragmentation upon cleavage and global deprotection. We wished to study peptide fragmentation of the three cyclised stapled peptides (**2.17**, **2.21** and **2.25**) before investing a considerable amount of time in the screening the optimal peptide staple sequence combination.

#### 2.3.1.4.4 Cleavage and global deprotection of highly *N*-methylated peptides studies

As mentioned earlier, highly *N*-methylated peptides are prone to undergo fragmentation upon acidic treatment. In order to study whether peptide fragmentation took place in the present system, several cleavage conditions for those compounds that could undergo complete or partial cyclisation, namely **2.17**, **2.21** and **2.25**, were tested and are summarised in Table 2.3.

| #  | Peptide     | Cleavage conditions                                      | Non-fragmented peptide (HPLC %)* |
|----|-------------|--|----------------------------------|
| 1  | <b>2.17</b> | HFIP-DCM (1:4 v/v), 1h                                   | 100                              |
| 2  | <b>2.17</b> | TFA-TIS-H <sub>2</sub> O (95:2.5:2.5 v/v), 30 min        | 6                                |
| 3  | <b>2.17</b> | TFA-TIS-H <sub>2</sub> O-DCM (50:2.5:2.5:45 v/v), 30 min | 6                                |
| 4  | <b>2.17</b> | TFA-TIS-H <sub>2</sub> O-DCM (20:2.5:2.5:75 v/v), 30 min | 6                                |
| 5  | <b>2.21</b> | HFIP-DCM (1:4 v/v), 1 h                                  | 100                              |
| 6  | <b>2.21</b> | TFA-TIS-H <sub>2</sub> O (95:2.5:2.5 v/v), 30 min        | 27                               |
| 7  | <b>2.21</b> | TFA-TIS-H <sub>2</sub> O-DCM (50:2.5:2.5:45 v/v), 30 min | 27                               |
| 8  | <b>2.21</b> | TFA-TIS-H <sub>2</sub> O-DCM (20:2.5:2.5:75 v/v), 30 min | 27                               |
| 9  | <b>2.25</b> | HFIP-DCM (1:4 v/v), 1h                                   | 100                              |
| 10 | <b>2.25</b> | TFA-TIS-H <sub>2</sub> O (95:2.5:2.5 v/v), 30 min        | 12                               |
| 11 | <b>2.25</b> | TFA-TIS-H <sub>2</sub> O-DCM (50:2.5:2.5:45 v/v), 30 min | 12                               |
| 12 | <b>2.25</b> | TFA-TIS-H <sub>2</sub> O-DCM (20:2.5:2.5:75 v/v), 30 min | 12                               |

Table 2.3. Tested cleavage and global deprotection for peptides **2.17**, **2.21** and **2.25**. \*For peptides **2.17** and **2.25**, the non-fragmented peptide HPLC percentage comprises the linear and cyclic peptides.

In all cases, the peptidyl resin was treated with the corresponding cleavage cocktail for 30 min, and the sample was subjected to HPLC-MS analysis to evaluate the deprotection outcome. Cleavage conditions without acid were used as a control to assess the crude HPLC purity before the anticipated fragmentations. Note that for all three peptides, peptide release from the resin under very mild conditions (HFIP–DCM (1:4 v/v)) rendered the cleaved and fully protected peptide, being no fragmentation observed by means of HPLC-MS analysis (see entries #1, #5 and #9 in Table 2.3).

Treatment of the peptidyl-resin **2.17** with the traditional TFA–TIS–H<sub>2</sub>O (95:2.5:2.5 v/v) cocktail mixture resulted in peptide fragmentation (see entry #2 in Table 2.3). Only 6% of the desired unprotected product **2.17** was obtained, and side-products arising from amide bond fragmentation between two consecutive *N*-MeAla residues or two consecutive *N*-MeAla and *N*-MeGly residues (by either *Path A*, *Path B* or *Path C*, see Scheme 2.16) and subsequent *N*-MeAla residue loss, respectively, were observed by HPLC-MS analysis (see HPLC chromatogram and product percentages in Table 2.5). Structure of the fragmented peptides are shown in Scheme 2.16.

Alongside, since complete cyclisation of **2.17** was not accomplished (see section 2.3.1.4.3), HPLC-MS analysis also showed fragmentation of the unreacted branched linear peptide (**2.16**). In fact, amide bond fragmentation between consecutive *N*-methylated residues resulted in *N*-MeGly, *N*-MeGly–*N*-MeAla and *N*-MeGly–*N*-MeAla–*N*-MeAla segment loss (see HPLC chromatogram and product percentages in Table 2.4 and structures of the linear peptide fragmented products in Scheme 2.17).

Additional efforts to avoid peptide fragmentation led to lowering the TFA percentage, and therefore the system stability upon milder acidic conditions was assessed. Neither treatment with a TFA–TIS–H<sub>2</sub>O–DCM (50:2.5:2.5:45 v/v) mixture, nor treatment with a TFA–TIS–H<sub>2</sub>O–DCM (20:2.5:2.5:75 v/v) cocktail proved effective to minimise peptide fragmentation (see entries #3-4 in Table 2.3). In fact, the exact same fragmentation pattern and fragmentation ratios were observed for all three treatments according to HPLC-MS analysis.

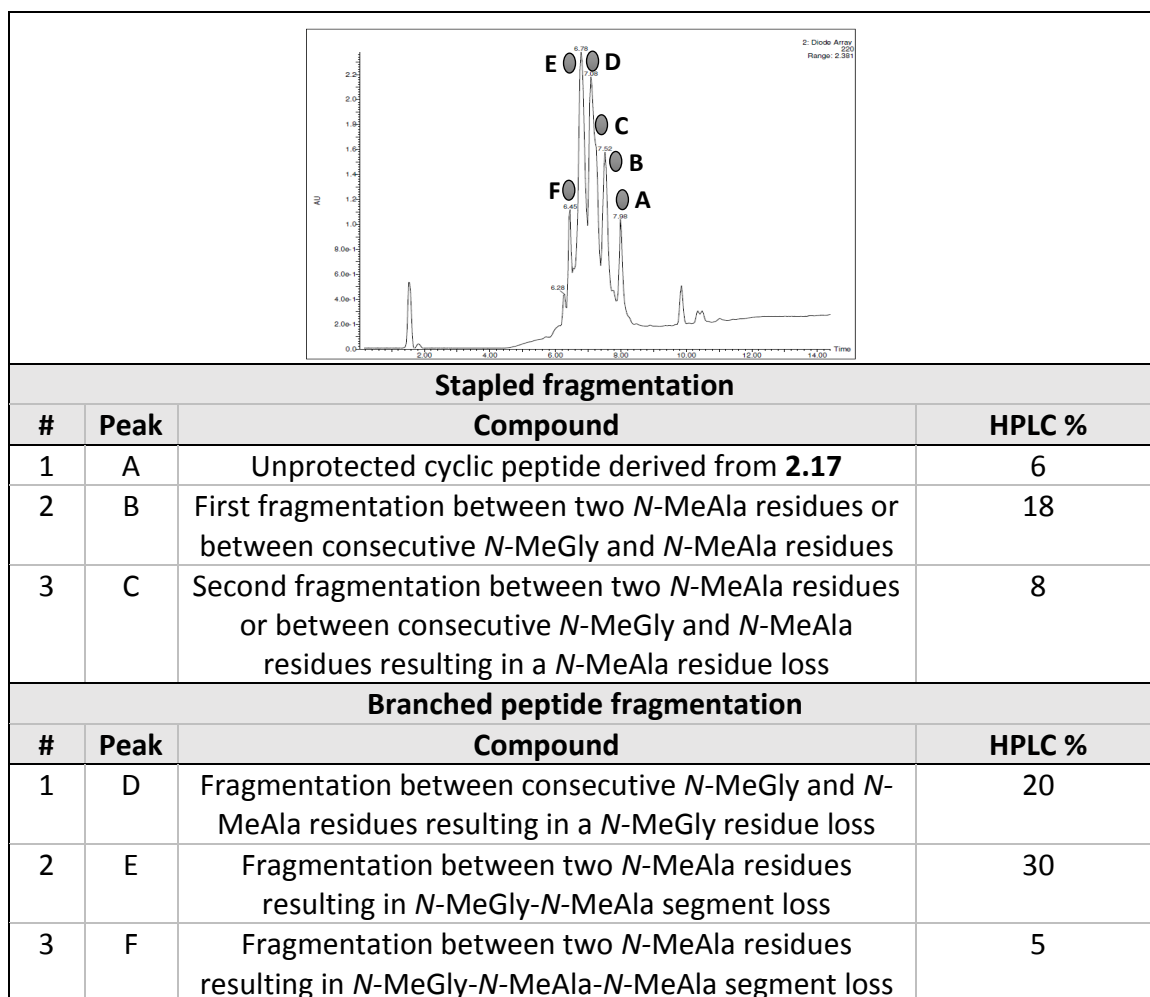
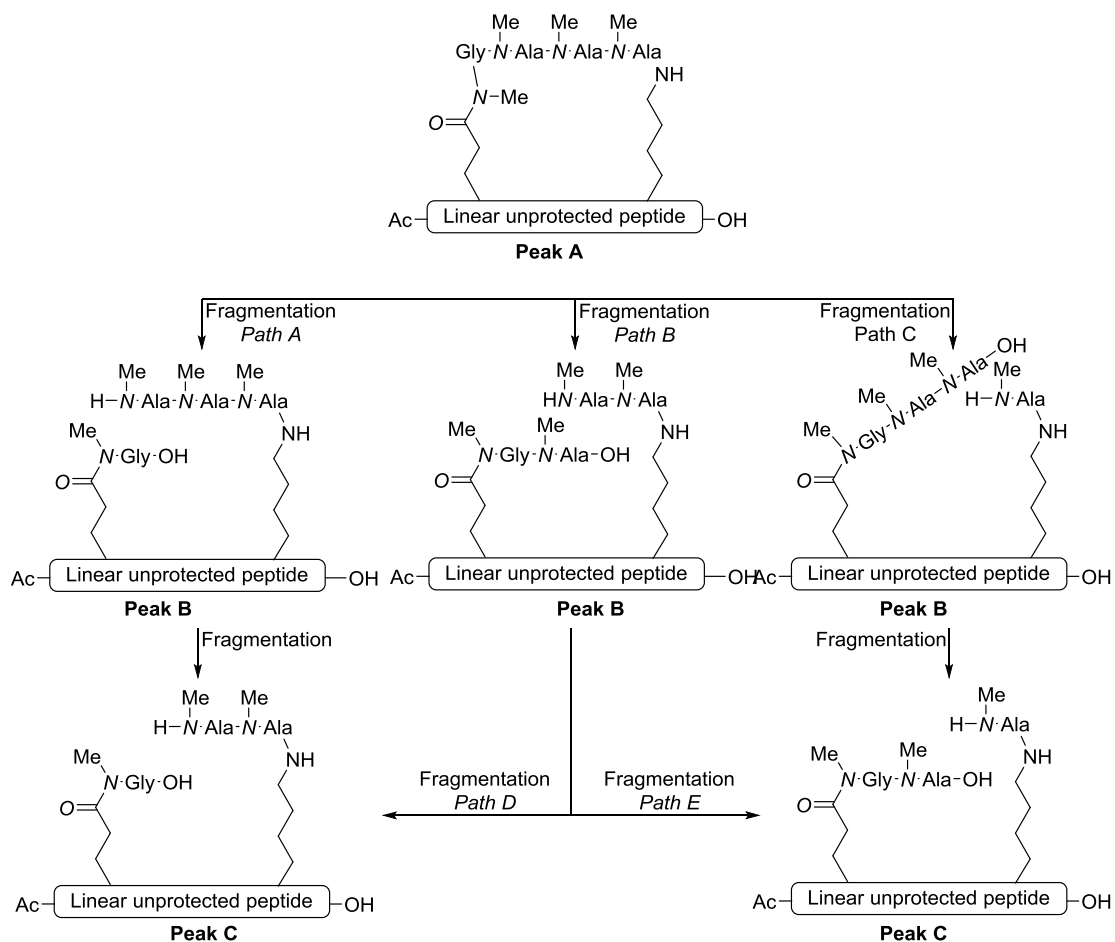
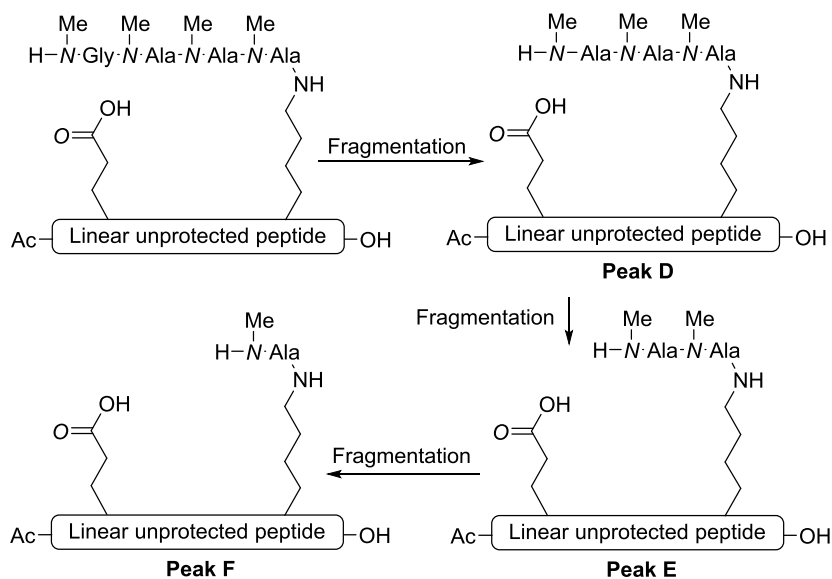


Table 2.4. HPLC-MS chromatogram run at G20100t9T25 and processed at 220 nm of peptide **2.17** fragmentation. The table encloses each peak identification and area.



Scheme 2.16. Fragmentation of cyclic **2.17** peptide upon acidic treatment. The indicated peaks correspond to those in Table 2.4.



Scheme 2.17. Fragmentation of branched **2.16** peptide upon acidic treatment

Evaluation of peptide **2.21** stability was also assessed. Thus, the peptidyl-resin **2.21** was treated with the previous 95%, 50% and 20% TFA mixtures (see entries #6-8 in Table 2.3). Not surprisingly, fragmentation was also observed. In this case, the desired unprotected peptide derived from **2.21** was obtained in a 27% HPLC yield, and side-products arising from amide bond fragmentation between two consecutive *N*-MeAla residues (by either *Path A* or *Path B*, see Scheme 2.18) and subsequent *N*-MeAla residue loss, respectively, were observed by HPLC-MS analysis (see HPLC chromatogram and product percentages in Table 2.5). Structures of the fragmented peptides are shown in Scheme 2.18.

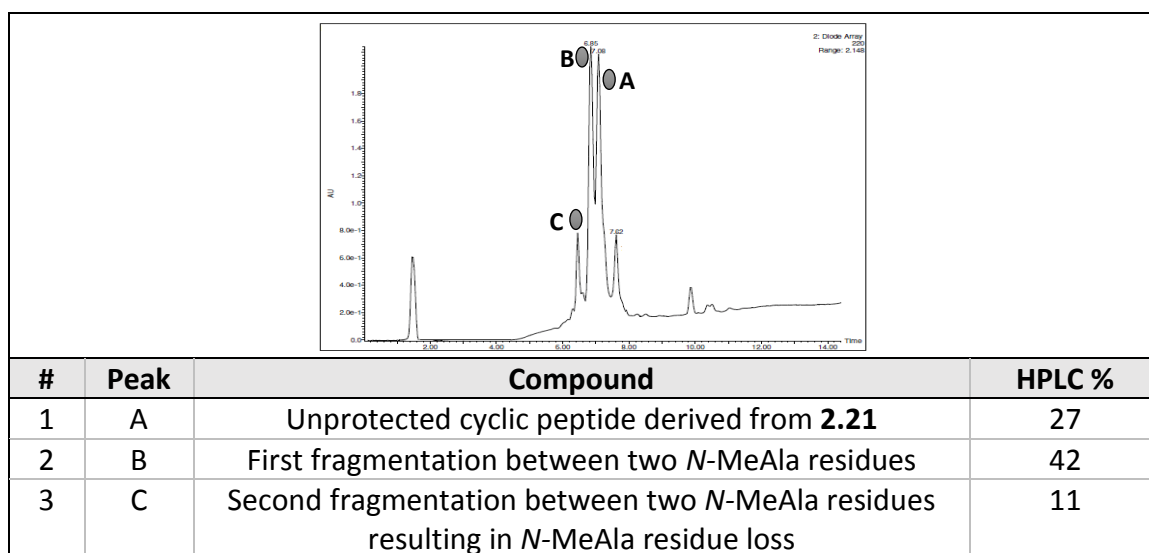
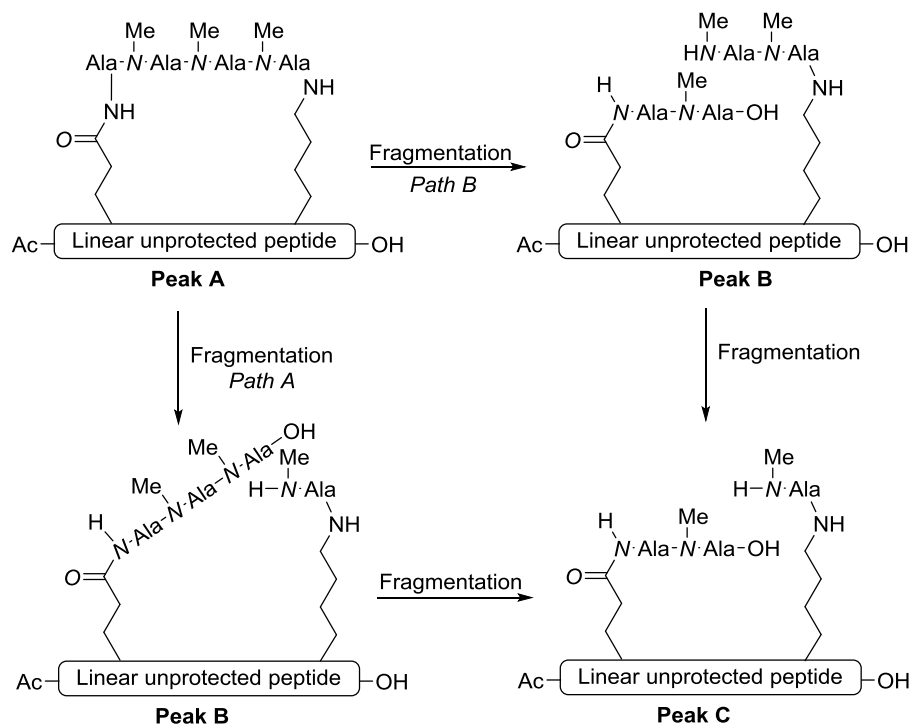


Table 2.5. HPLC-MS chromatogram run at G20100t9T25 and processed at 220 nm of peptide **2.21** fragmentation. The table encloses each peak identification and area.

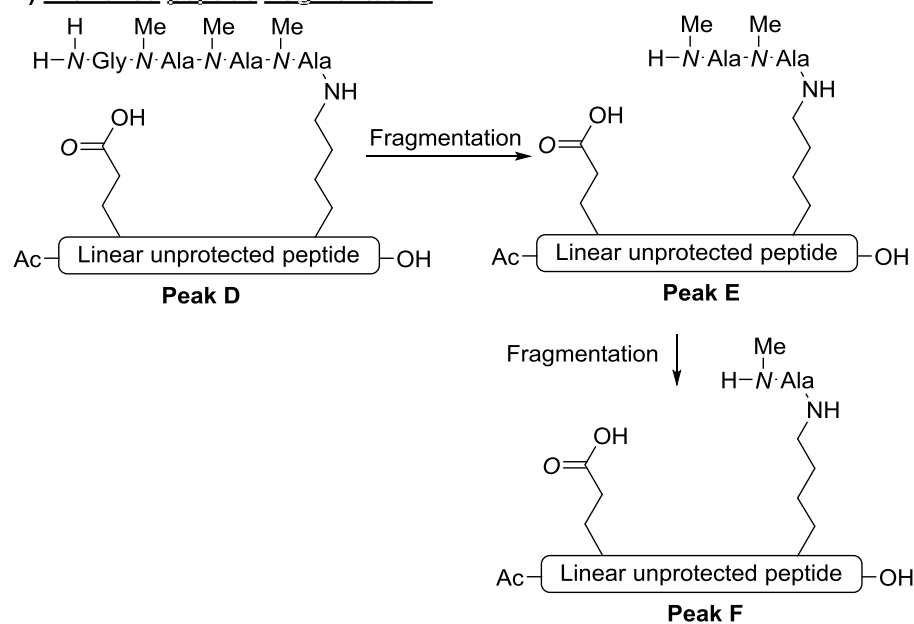
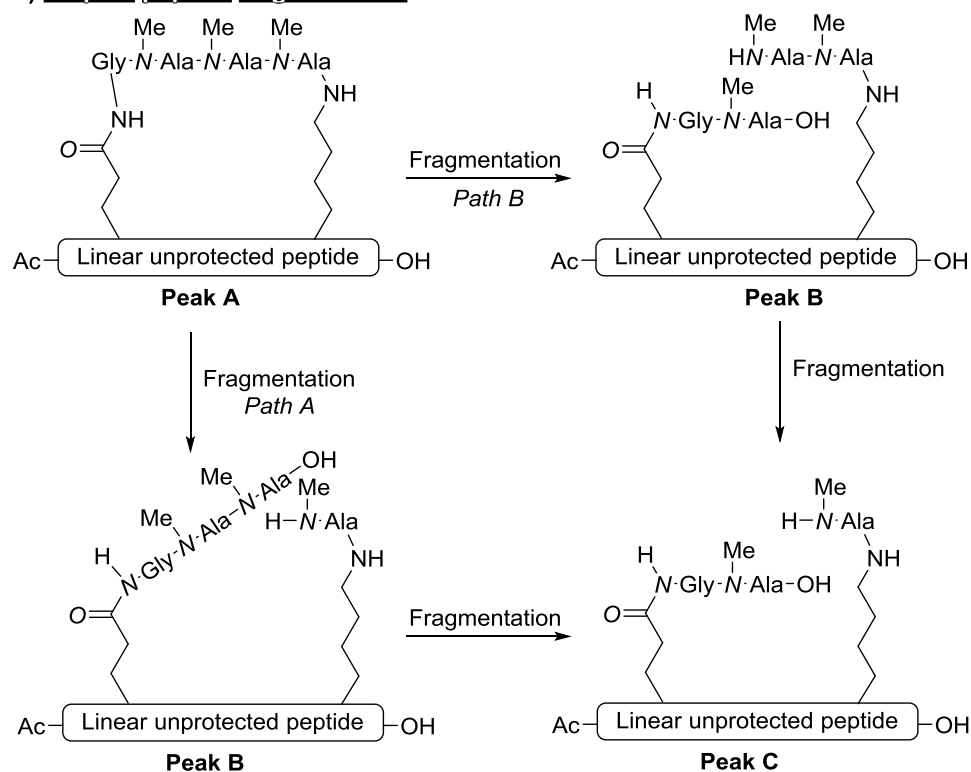
Peptide **2.25** cleavage and global deprotection did not give better results. In order to evaluate its stability upon acidic conditions, the same procedures as before were carried out (see entries #10-12 in Table 2.3). Unfortunately, the desired unprotected product derived from **2.25** was obtained in a 7% HPLC yield, and side-products arising from peptide fragmentation between two *N*-MeAla residues and subsequent *N*-MeAla residue loss were identified (see HPLC chromatogram and product percentages in Table 2.6 and structures of the fragmented peptides in Scheme 2.19B).



Scheme 2.18. Fragmentation of cyclic peptide **2.21** upon acidic treatment. The indicated peaks correspond to those in Table 2.5.

| Stapled peptide fragmentation  |      |  |        |
|--------------------------------|------|--|--------|
| #                              | Peak | Compound   | HPLC % |
| 1                              | A    | Unprotected cyclic peptide derived from <b>2.25</b>  | 7      |
| 2                              | B    | First fragmentation between two <i>N</i> -MeAla residues   | 11     |
| 3                              | C    | Second fragmentation between two <i>N</i> -MeAla residues resulting in a <i>N</i> -MeAla residue loss              | 28     |
| Branched peptide fragmentation |      |  |        |
| #                              | Peak | Compound   | HPLC   |
| 1                              | D    | Unprotected linear peptide derived from <b>2.24</b>  | 5      |
| 2                              | E    | Fragmentation between two <i>N</i> -MeAla residues resulting in Gly- <i>N</i> -MeAla segment loss                  | 34     |
| 3                              | F    | Fragmentation between two <i>N</i> -MeAla residues resulting in Gly- <i>N</i> -MeAla- <i>N</i> -MeAla segment loss | 5      |

Table 2.6. HPLC-MS chromatogram run at G20100t9T25 and processed at 220 nm of peptide **2.25** fragmentation. The table encloses each peak identification and area.

**A) Branched peptide fragmentation****B) Stapled peptide fragmentation**

Scheme 2.19. Fragmentation of cyclic peptide **2.14** upon acidic treatment. The indicated peaks correspond to those in Table 2.6.

Concurrently, since complete cyclisation of **2.25** was not accomplished (see section 2.3.1.4.3), fragmentation of the unreacted branched linear peptide also took place. Thus, the additional HPLC-MS peaks correspond to the linear unprotected peptide, segment Gly–N-MeAla loss due to fragmentation between two consecutive N-

MeAla residues (by either *Path A* or *Path B*, see Scheme 2.19B), and Gly–*N*-MeAla–*N*-MeAla segment loss due to fragmentation between two consecutive *N*-MeAla (see HPLC chromatogram and product percentages in Table 2.6 and structures of the cyclic fragmented peptide in Scheme 2.19A).

In sight of these results, we concluded that applicability of the lactam-based cross-linking methodology to prepare the target molecular architectures is rather limited. Both peptide cyclisation and global deprotection turned out very problematic. In fact, only a few of all the tested staple combinations could be cyclised, however, low-moderate cyclisation yields were observed in most of the cases. Furthermore, the deprotection outcome was not satisfactory, being the corresponding desired unprotected peptide not obtained or obtained as a minor product. Thus, at this point of the project, the lactam-based cross-link approach was discarded and a different peptide stapling technique was envisioned.

### 2.3.1.5 Thioether-based cross-linking

A thioether-cross link came up as a good alternative to prepare *N*-methyl-rich peptide bridges. Lys and Cys were selected as the stapling points (shown in bold in Figure 2.19). Given the unique properties of Cys, its derivatisation with a wide variety of electrophiles can be selectively performed under the presence of many functional groups. Thus, the thioether-based stapled peptide shown in Figure 2.19 was envisioned.

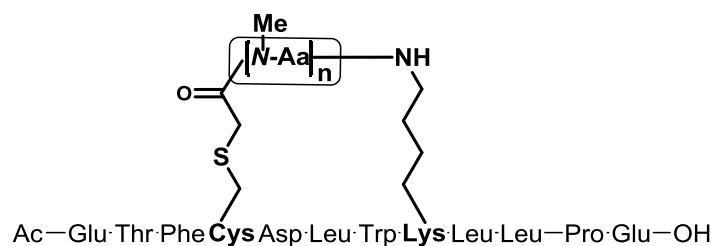
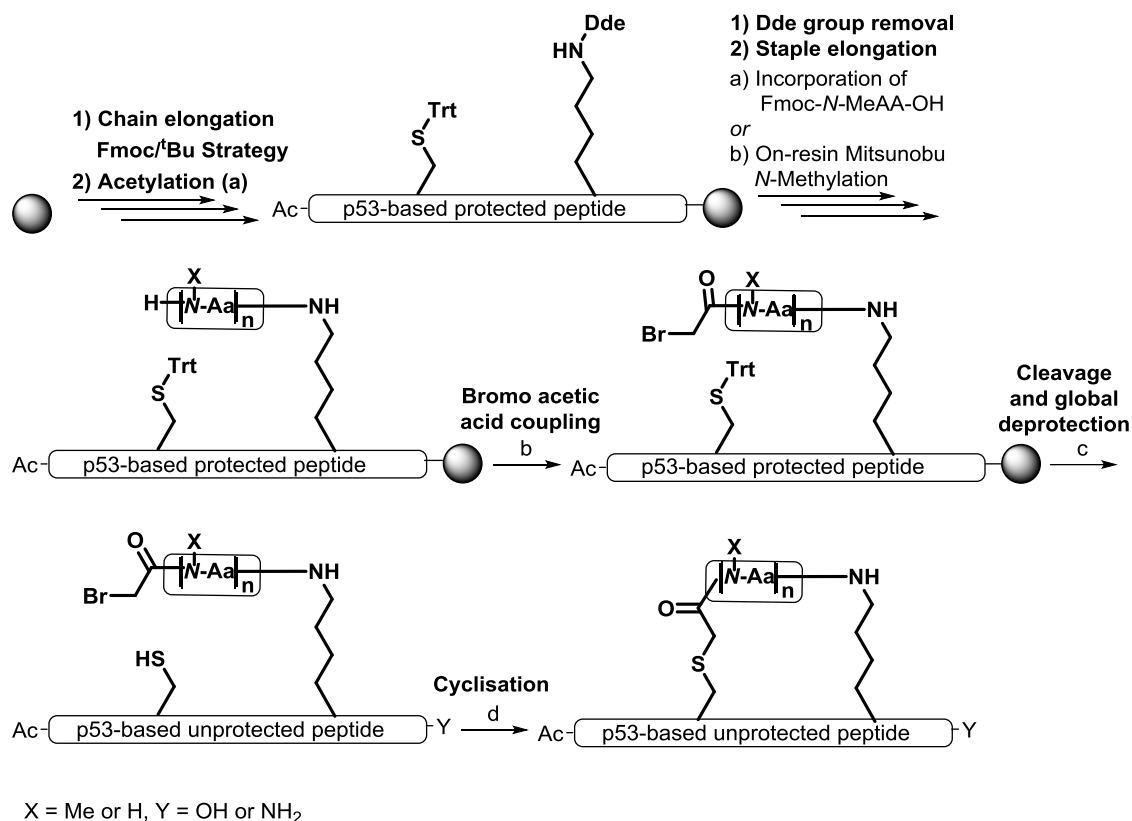


Figure 2.19. Thioether-based cross-link of HMSP.

#### 2.3.1.5.1 Synthetic methodology development for single staples

The same 12-mer peptide based on the p53 wild-type sequence that was employed in section 2.3.1.4.1, was used for the development of the synthetic methodology to prepare single HMSP based on a thioether cross-link. However, the Glu

residue was substituted by a Cys residues to provide the linear sequence with a thiol group. The peptide stapling points were located at relative  $i,i+4$  positions, and the strategy was developed as follows (Scheme 2.20).



*Scheme 2.20.* Synthetic methodology to prepare single “short” HMSP based on a thioether cross-link. **Chain elongation:** Couplings onto primary amines: Fmoc-AA(PG)-OH (3 eq), OxymaPure (3 eq), DIC (3 eq), DMF, 40 min; peptide couplings onto secondary amines: Fmoc-AA(PG)-OH (3 eq), HATU (3 eq) HOAt (3 eq), DIEA (3 eq), DMF, 1 h. **Staple elongation:** **Dde removal:** (Hydrazine–DMF (1:9 v/v) (1 x 1 min + 2 x 15 min)); **Strategy A:** repetitive cycles of 1) Fmoc-*N*-MeAla-OH (3 eq), HATU (3 eq) HOAt (3 eq), DIEA (3 eq), DMF, 1 h; and 2) piperidine–DMF (1:4 v/v) (1 x 1 min + 2 x 5 min)); or **Strategy B:** repetitive cycles of 1) Fmoc-Ala-OH (3 eq), HATU (3 eq) HOAt (3 eq), DIEA (3 eq), DMF, 1 h; 2) piperidine–DMF (1:4 v/v) (1 x 1 min + 2 x 5 min); 3) *o*-NBS (4 eq), DIEA (10 eq), DCM, 30 min; 4) MeOH (10 eq), PPh<sub>3</sub> (5 eq), DIAD (5 eq), THF<sub>dry</sub>, 1 h; 5) DBU (5 eq), HOCH<sub>2</sub>CH<sub>2</sub>SH (10 eq), DMF, (1 x 1 min + 2 x 10 min). a) **Acetylation:** Ac<sub>2</sub>O (3 eq), DIEA (9 eq), DCM, 20 min; b) Bromoacetic acid (5 eq), DIC (5 eq), DMF, 1 h; c) **Cleavage and global deprotection:** TFA–TIS–H<sub>2</sub>O (95:2.5:2.5 v/v), 1 h; d) **Cyclisation in solution:** aq. NH<sub>4</sub>HCO<sub>3</sub> (20 mM, pH = 7.9)/ACN (3:1).

For the linear chain elongation, the same approach as the one used for the development of lactam-based staples was followed (see section 2.3.1.4.1). Thus, a solid-phase approach combined with a Fmoc/<sup>t</sup>Bu strategy was pursued. Conveniently, the Rink Amide AM resin or the 2-CTC resin could be used, which rendered the amidated C-

terminal or the C-terminus as free carboxylic acid function, respectively. The loading of the resin was set up to 0.60 mmol/g resin. As in section 2.3.1.4.1, couplings onto primary amines were performed with the AA–OxymaPure–DIC (3:3:3 eq) coupling system and couplings onto secondary amines were carried out with the AA–HATU–HOAt–DIEA (3:3:3:6 eq) coupling mixture.

At position 5 starting from the C-terminus, a Lys residue was introduced, conveniently protected with the Dde group. Next, four positions further from the Lys residue, a Cys residue was placed and the synthesis was continued until the last residue. In order to avoid undesired elongation on the N-terminus upon construction of the staple, acetylation was carried out with the traditional Ac<sub>2</sub>O–DIEA (3:9 eq) mixture.

The starting point of the staple chain elongation was the Lys residue located at the fifth position starting from the C-terminus (Scheme 2.20). N-methylated linker elongation was accomplished by using either *Strategy A* or *Strategy B*. Once the staple chain was furnished, peptide coupling between the staple N-terminal position and bromoacetic acid was performed using DIC as coupling reagent. Monitoring of the reaction always indicated clean conversion according to HPLC-MS analysis. Peptide cleavage from the resin and global deprotection was carried out with the traditional TFA–TIS–H<sub>2</sub>O (95:2.5:2.5 v/v) cocktail, which furnished the unprotected cleaved peptide.

High nucleophilicity of the Cys residue thiol allowed thioether cross-linking in the presence of other functionalities displayed on the unprotected peptide. Cyclisation was accomplished in solution by treatment of the unprotected peptide with an aq. NH<sub>4</sub>CO<sub>3</sub> (20 mM, pH = 7.9)/ACN (3:1 v/v) solution for one hour. High dilution conditions ([1 mM]) were required to promote intramolecular cyclisation and prevent undesired polymerisation. According to HPLC-MS monitoring, reactions generally proceeded smoothly and full conversion was reached within an hour in most of the cases (see Figure 2.20 for a representative example).

In order to evaluate the scope of the developed methodology, numerous peptide staple combination sequences were designed for “short” and “large” HMSP, which involved diverse lengths and nature of N-methylated amino acids. In addition, the staple

length and nature effect on the secondary  $\alpha$ -helix structure was later on assessed by circular dichroism experiments (see section 2.3.2).

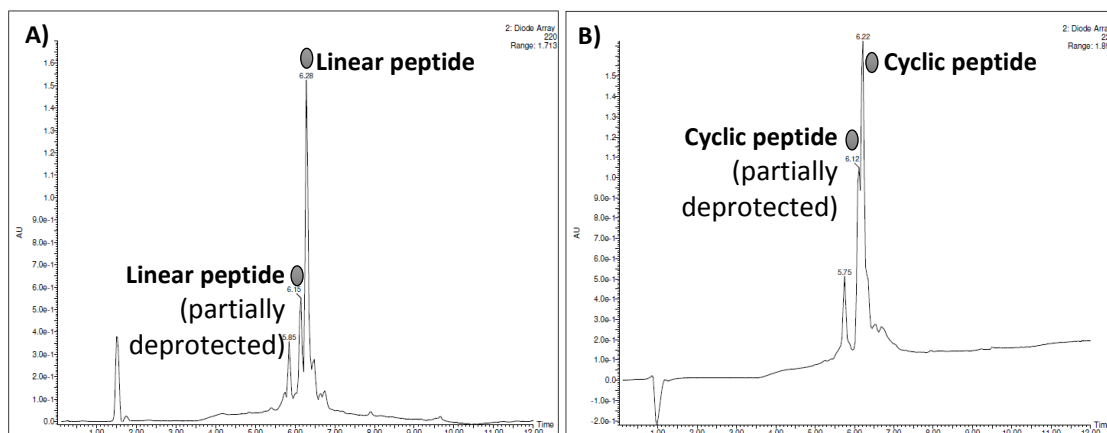


**Figure 2.20.** HPLC-MS chromatograms run at G20100t9T25 and processed at 220 nm. Representative HPLC analysis of the thioether-based cyclisation in solution (compound **2.26**). A) Chromatogram before cyclisation; B) Chromatogram after cyclisation through a thioether-based cross-link. Peak overlapping due to partial and complete Boc carbamate deprotection was observed.

#### 2.3.1.5.1.1 Preparation of “short” stapled peptides ( $i,i+4$ )

The developed synthetic methodology was applied to the preparation of short stapled peptides. Thus, insertion of several chemical bridges at relative positions  $i$  and  $i+4$  of the 12-mer p53-based peptide was carried out. In order to assess the staple length and nature role in the cyclisation outcome as well as in the secondary structure stabilisation, staple combinations ranged from one to three residues. Insertion of several residues such as *N*-MeAla, *N*-MePhe or Pro was pursued (Table 2.7). Whereas, insertion of the hydrophobic residues *N*-MeAla and *N*-MePhe allowed evaluation of the bulkiness effect on the cyclisation extent, introduction of Pro, which is known to be a helix breaker residue, allowed assessment of the residue impact on the helix secondary structure stabilisation.

In most cases, peptide chain elongation, staple construction and subsequent cyclisation in solution were accomplished without difficulty. Remarkably, in general peptide fragmentation upon cleavage did not take place, however, fragmentation of peptides **2.29** and **2.30** (see entries #4-5 in Table 2.7) could be detected by HPLC-MS

analysis (see section 2.3.1.4.4 for comments on this topic). Cleavage and global deprotection of **2.29** and **2.30** resulted in *N*-terminal *N*-MePhe residue loss and MeGly–*N*-MeAla segment loss, respectively. In both cases, the observed unprotected peptide/fragmented peptide ratio was 2:1.

| # | Peptide     | Staple sequence                                       | Cyclisation conversion (HPLC Yield) | Isolated yield (%)** |
|---|-------------|---|-------------------------------------|----------------------|
| 1 | <b>2.26</b> | – <i>N</i> -MeAla–                                    | Quantitative                        | 11                   |
| 2 | <b>2.27</b> | –Pro–Pro–   | Quantitative                        | 12                   |
| 3 | <b>2.28</b> | –Pro– <i>N</i> -MeAla–                                | Quantitative                        | 6                    |
| 4 | <b>2.29</b> | – <i>N</i> -MePhe– <i>N</i> -MeAla–*                  | Quantitative                        | -                    |
| 5 | <b>2.30</b> | – <i>N</i> -MeGly– <i>N</i> -MeAla– <i>N</i> -MeAla–* | Quantitative                        | -                    |

Table 2.7. Library of thioether-based stapled peptides cross-linked at positions *i* and *i*+4. \*Fragmentation upon cleavage of the linear peptide was observed. \*\*Isolated yields were determined after compound purification by HPLC.

HPLC purification of peptides **2.26**, **2.27**, and **2.28** was carried out (the obtained isolated yields ranged from 6-11%). The low-moderate isolation yields might be attributed to the synthetic complexity of these molecular architectures. Nevertheless, all three peptides were subjected to circular dichroism studies (see section 2.3.2). Unfortunately, the rather disappointing circular dichroism results suggested that the relative staple location positions did not favour the helical conformation. At this point of the project, we considered that isolation of peptides **2.29** and **2.30**, which was foreseen laborious, was not worth it and we moved onto the preparation of “large” stapled peptides.

#### 2.3.1.5.1.2 Preparation of “large” stapled peptides (*i*,*i*+7)

The synthetic methodology developed in section 2.3.1.5.1 was also applied for the preparation of “large” stapled peptides. In order to evaluate the effect of the overall peptide charge on the secondary structure stabilisation, two series of “large” stapled peptides were prepared, where the *C*-terminus was obtained as a free carboxylic acid

function or an amidated function. A 13-mer peptide based on the p-53 wild-type sequence was used for the preparation of the peptide library, being the key stapling residues located at relative positions  $i, i+7$ . In order to extensively study the staple length and nature of amino acids on both, the cyclisation outcome and the helical structure stabilisation, staple combinations ranged from one to three residues and contained several non-polar residues such as *N*-MeAla, *N*-MePhe, *N*-MeGly, Pro and hydrophilic residues, including *N*-MeLys, *N*-MeHis, *N*-MeGln (Table 2.8).

In regard to the cyclisation efficiency, similar results as the ones observed for the preparation of single “short” stapled peptides were obtained, where cyclisation was accomplished in quantitative HPLC yields in most of the cases. Surprisingly and in disagreement with the observed results for “short” thioether-based stapled peptides, fragmentation upon acidic treatment was not observed in any case. Based on these results, a plausible explanation was postulated. We hypothesised that the tendency of a certain peptide to undergo fragmentation might be related to the ring size, the overall content of *N*-methylated residues within the core ring and the nature of these residues. Probably, those combinations conferring more tension to the formed ring favoured hydrolysis and fragmentation of the peptide staple. Accordingly, peptides accounting for poorer stability, generally, presented a higher percentage of *N*-methylated residues within the core ring, which is the case for short peptides. In this context, the ring size of the prepared library of “short” stapled peptides varied from six to nine residues, whilst the ring size for “large” stapled peptides held from nine to twelve residues. On the other hand, nature of the *N*-methylated residues seems to play a key role in the overall peptide stability. Note that all peptides that so far underwent fragmentation (**2.16**, **2.17**, **2.21**, **2.24**, **2.25**, **2.29** and **2.30**) contain common *N*-MeAla residues. Consequently, we presumed that *N*-MeAla has a tendency to undergo fragmentation.

In general, synthesis of all peptides was satisfactorily accomplished (see entries #1-11 and #14 in Table 2.8), except for peptides **2.42** and **2.43**. Despite cyclisation of most of the  $i, i+7$  HMSP was successfully accomplished, poor isolation yields (1-11%) were obtained. Expected quantities of all final crude peptides were obtained and the HPLC-MS chromatograms of all the crude products were satisfactory. Thus, in this case

the low isolated yields were attributed to the limitations encountered during the purification process. The available HPLC equipment often led to product loss due to issues with the pumping system and leaking of the solvent lines. Additionally, the HPLC equipment required multiple injections to efficiently isolate the product (only 2-5 mg of the crude product could be injected per run), which ultimately led to an even higher percentage of product loss.

| #  | Peptide     | X               | Staple sequence       | Cyclisation conversion<br>HPLC Yield | Isolated yield (%)<br>*** |
|----|-------------|-----------------|-----------------------|--------------------------------------|---------------------------|
| 1  | <b>2.31</b> | OH              | –N-MeVal–             | Quantitative                         | 3                         |
| 2  | <b>2.32</b> | OH              | –N-MePhe–N-MeAla–     | Quantitative                         | 2                         |
| 3  | <b>2.33</b> | OH              | –N-MeGly–N-MeVal–     | Quantitative                         | 2                         |
| 4  | <b>2.34</b> | OH              | –N-MeLeu–Pro–         | Quantitative                         | 3                         |
| 5  | <b>2.35</b> | NH <sub>2</sub> | –N-MeVal–             | Quantitative                         | 11                        |
| 6  | <b>2.36</b> | NH <sub>2</sub> | –N-MePhe–N-MeAla–     | Quantitative                         | 2                         |
| 7  | <b>2.37</b> | NH <sub>2</sub> | –N-MeGly–N-MeVal–     | Quantitative                         | 5                         |
| 8  | <b>2.38</b> | NH <sub>2</sub> | –N-MeLeu–Pro–         | Quantitative                         | 5                         |
| 9  | <b>2.39</b> | NH <sub>2</sub> | –N-MeLys–N-MeGly–     | Quantitative                         | 3                         |
| 10 | <b>2.40</b> | NH <sub>2</sub> | –N-MeLys–N-MeLys–     | Quantitative                         | 3                         |
| 11 | <b>2.41</b> | NH <sub>2</sub> | –N-MeGly–N-MeLys–     | Quantitative                         | 3                         |
| 12 | <b>2.42</b> | NH <sub>2</sub> | –N-MeGln–N-MeVal–*    | Quantitative                         | 1                         |
| 13 | <b>2.43</b> | NH <sub>2</sub> | –N-MeHis–N-MeVal–**   | -                                    | -                         |
| 14 | <b>2.44</b> | NH <sub>2</sub> | –N-MeGly–N-MeVal–Pro– | Quantitative                         | 4                         |

*Table 2.8.* Library of thioether-based stapled peptides cross-linked at positions *i* and *i*+7. \*On-resin Mitsunobu *N*-methylation of the Gln residue was low yielding and cyclisation turned out troublesome. \*\* On-resin Mitsunobu *N*-methylation of the His residue was not accomplished. \*\*\*Isolated yields were determined after compound purification by HPLC.

However, synthesis of peptide **2.42** turned out troublesome (see entry #12 in Table 2.8), since many side-products derived from the on-resin Mitsunobu *N*-methylation were detected and the branched linear peptide was only obtained in a 18% HPLC yield. Identification of these side-products was not possible by HPLC-MS analysis. All these issues resulted in the formation of the desired stapled peptide **2.42** in small percentages. Nevertheless, the final crude peptide was subjected to HPLC purification

to be further studied by circular dichroism. On the other hand, preparation of peptide **2.43** (see entry #13 in Table 2.8) was not accomplished due to problems associated with the His on-resin Mitsunobu *N*-methylation. In fact, the mass of the desired peptide was not detected by HPLC-MS analysis and the formed side-products could not be identified. Nevertheless, all isolated pure peptides were subjected to circular dichroism studies (section 2.3.2).

### 2.3.1.5.2 Synthetic methodology development for double staples

After the success of the thioether-based stapling strategy for the preparation of single HMSP, we wished to explore the possibility of introducing double staples. A 17-mer peptide based on the p53 wild-type sequence was used for the development of the synthetic methodology to prepare double HMSP based on a thioether cross-link. The peptide stapling points were located at relative positions *i,i+4* and *i+8,i+12* positions (Figure 2.21).

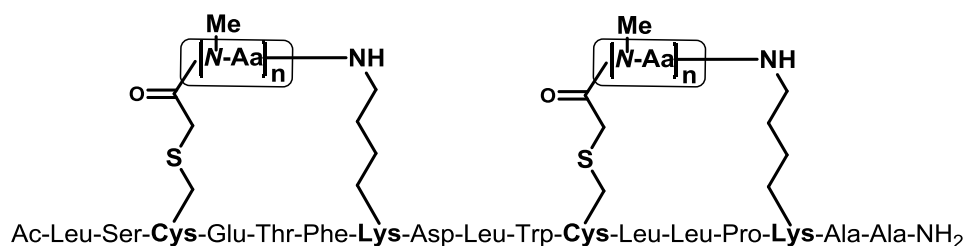


Figure 2.21. Double thioether-based cross-link.

The synthetic strategy was based on a partial synthesis of the p53-based peptide main chain and installation of the first staple on solid-phase. Following, elongation of the main chain until the *N*-terminus and final on-resin cyclisation furnished the double stapled peptide. Finally, the peptide was simultaneously unprotected and cleaved from the resin (Scheme 2.21).

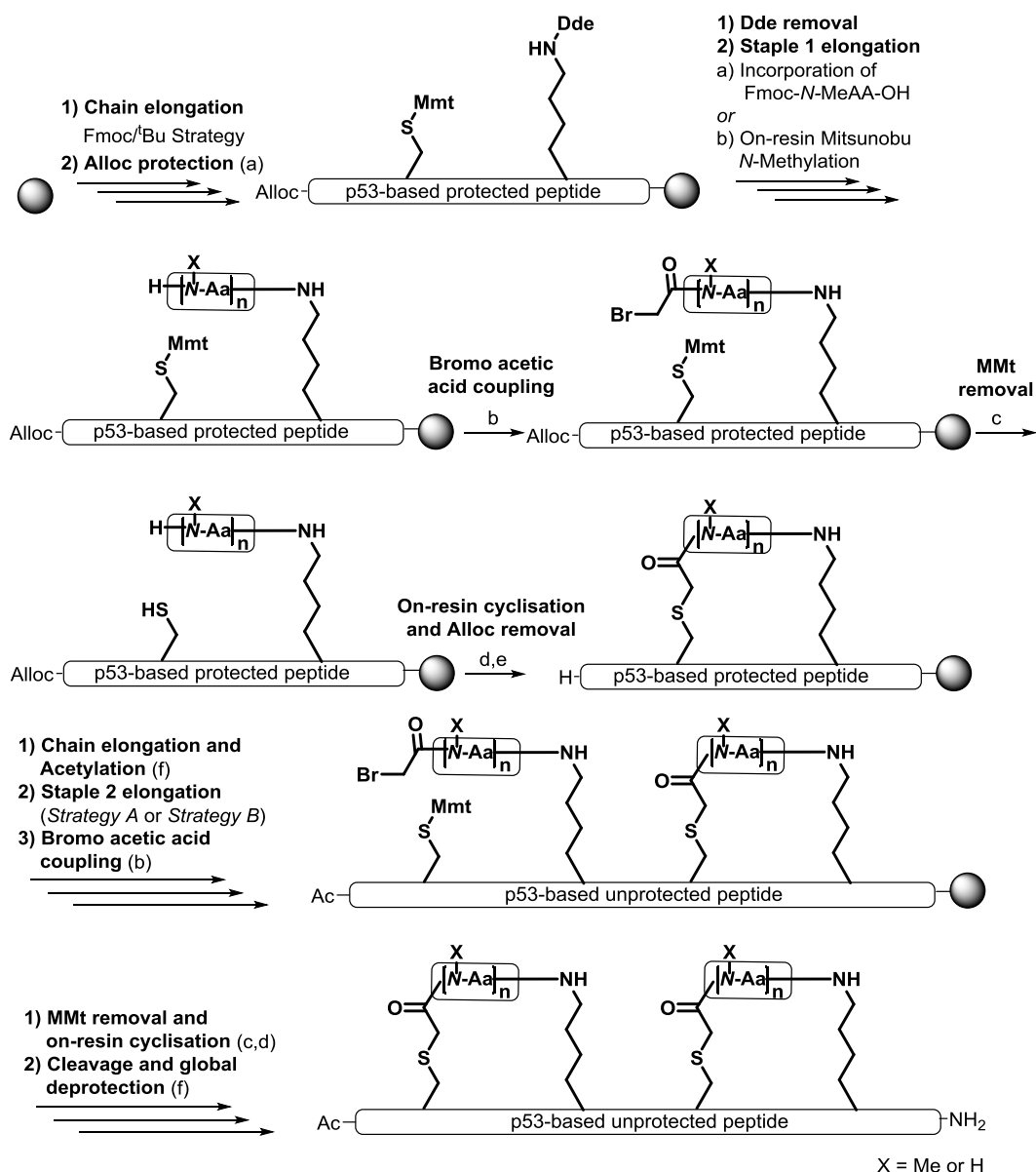
In more detail, a solid-phase approach based on the Fmoc/<sup>t</sup>Bu strategy was pursued, being the Rink Amide AM resin the polymeric support of choice. For the chain elongation, the same approach as the one used for the development of lactam-based staples was followed (see section 2.3.1.4.1). Since two on-resin cyclisation reactions were carried out at a later stage of the synthesis, the resin functionalisation was lowered

to 0.14 mmol/g resin to avoid undesired side-reactions. As for all this thesis, couplings onto primary amines were performed with the AA–OxymaPure–DIC (3:3:3 eq) coupling system, and couplings onto secondary amines were carried out with the AA–HATU–HOAt–DIEA (3:3:3:6 eq) coupling mixture. At position 3 starting from the C-terminus, a Lys residue was introduced, conveniently protected with the Dde group, which is orthogonal to the Fmoc group. Next, four positions further from the Lys residue, a Cys residue was placed, with the side-chain protected with the Mmt group, which is also orthogonal to the other protecting groups and can be selectively removed on solid-phase without causing peptide cleavage and deprotection of other functionalities. In order to avoid undesired elongation upon staple construction, the *N*-terminal amine of the Leu residue located at the ninth position starting from the C-terminus was protected with the Alloc group with Alloc-Cl–DIEA (3:9 eq).

The starting point of the first staple chain elongation was the Lys residue located at the third position starting from the C-terminus (Scheme 2.21). First, the Lys side-chain protecting group, Dde, was removed by treatment with hydrazine, and the corresponding staple1 was constructed using either *Strategy A* or *Strategy B* (see section 2.3.1.5.1).

Once the staple sequence was furnished, the Mmt group was removed by successive treatments with a TFA–TIS–DCM (3:5:92 v/v) mixture (3 x 15 min). Complete Mmt removal was monitored by addition of a few TFA drops to a small aliquot of the resin. No colouring of the resulting solution indicated full Mmt removal. Additional treatments were required if the solution turned into an orange colour. Once the Mmt group was completely removed, the remaining excess of acid was neutralised by treatment of the peptidyl-resin with a DIEA–DMF (1:99 v/v) solution (3 x 1 min).

Next, on-resin cyclisation was successfully accomplished by addition of a DIEA (5 eq) solution in DMF. We were happy to observe that the reaction proceeded smoothly. Moreover, full conversion was rapidly reached (within the first 30 min) according to HPLC-MS analysis (Figure 2.22A). Following, the *N*-terminal Alloc-protected residue was freed up to continue with the peptide chain elongation.



**Scheme 2.21.** Synthetic methodology to prepare double HMSF based on a thioether cross-link. **Chain elongation:** Couplings onto primary amines: Fmoc-AA(PG)-OH (3 eq), OxymaPure (3 eq), DIC (3 eq), DMF, 40 min; peptide couplings onto secondary amines: Fmoc-AA(PG)-OH (3 eq), HATU (3 eq) HOAt (3 eq), DIEA (3 eq), DMF, 1 h. **Staple elongation:** **Dde removal:** Hydrazine–DMF (1:9 v/v) (1 x 1 min + 2 x 15 min); and **Strategy A:** repetitive cycles of: 1) Fmoc-*N*-MeAla-OH (3 eq), HATU (3 eq) HOAt (3 eq), DIEA (3 eq), DMF, 1 h; and 2) piperidine–DMF (1:4 v/v) (1 x 1 min + 2 x 5 min) **or Strategy B:** repetitive cycles of 1) Fmoc-Ala-OH (3 eq), HATU (3 eq) HOAt (3 eq), DIEA (3 eq), DMF, 1 h; 2) piperidine–DMF (1:4 v/v) (1 x 1 min + 2 x 5 min); 3) *o*-NBS (4 eq), DIEA (10 eq), DCM, 30 min; 4) MeOH (10 eq), PPh<sub>3</sub> (5 eq), DIAD (5 eq), THF<sub>dry</sub>, 1 h; 5) DBU (5 eq), HOCH<sub>2</sub>CH<sub>2</sub>SH (10 eq), DMF, (1 x 1 min + 2 x 10 min)). a) **Alloc protection:** Alloc-Cl (3 eq), DIEA (9 eq), DCM, 30 min; b) **Bromoacetic acid** (5 eq), DIC (5 eq), DMF, 1 h; c) **Mmt removal:** TFA–TIS–DCM (3:5:92 v/v) (3 x 15 min); d) **Cyclisation:** DIEA (5 eq), DMF, 30 min; e) **Alloc removal:** Pd(PH<sub>3</sub>)<sub>4</sub> (0.1 eq), Phenylsilane (10 eq), DMF, (3 x 15 min); f) **Acetylation:** Ac<sub>2</sub>O (3 eq), DIEA (9 eq), DCM, 20 min; g) **Cleavage and global deprotection:** TFA–TIS–H<sub>2</sub>O (95:2.5:2.5 v/v), 1 h.

Once the full p53-like sequence was assembled, the *N*-terminal was acetylated to avoid undesired chain elongation upon construction of the second staple.

The same strategy as the one used for the first staple was applied to the preparation of the second bridge (Figure 2.22B). Again, thioether formation to render the second cycle was easily and rapidly accomplished by treatment of the resin with a basic DMF solution. Finally, peptide cleavage from the resin and global deprotection was carried out with the traditional TFA–TIS–H<sub>2</sub>O (95:2.5:2.5 v/v) cocktail, which rendered the cleaved unprotected peptide.

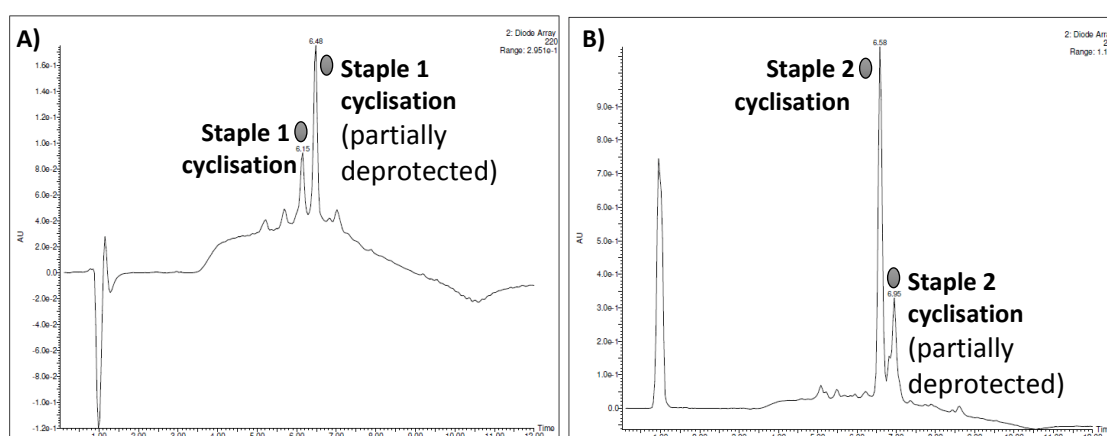
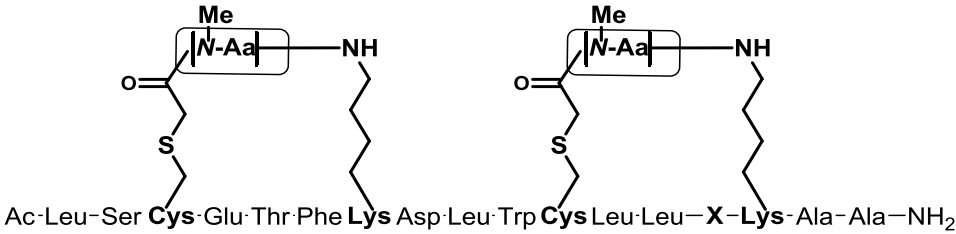


Figure 2.22. HPLC-MS chromatograms run at G20100t9T25 and processed at 220 nm. Representative HPLC analysis of both thioether-based on-resin cyclisation reactions (compound **2.46**). A) Cyclisation A for the construction of the first staple; B) Cyclisation B for the construction of the second staple. Peak overlapping due to partial and complete Boc carbamate deprotection was observed.

#### 2.3.1.5.2.1 Preparation of double stapled peptides ( $i,i+4$ and $i+8,i+12$ )

With this developed strategy in hands, a 17-mer p53-based peptide was used for the preparation of small library of double stapled peptides. Smart design of double HMSP was carried out as follows. First, in order to assess whether the designated stapling points were optimal to accommodate the  $\alpha$ -helical conformation, the staple lengths for staple1 and staple2 were set to one residue. Note that double stapled peptides present additional synthetic complexity, and therefore we considered that insertion of just one *N*-methylated residue on each staple was a good starting point. Next, screening of the *N*-methylated residues nature effect on the secondary structure

stabilisation was accomplished by preparing double stapled peptides displayed a Pro residue at both staple1 and staple2, an *N*-MeAla amino acid at both bridges and two *N*-MeLys residues at staple 1 and staple2. Additionally, a stapled peptide containing no amino acids within the staple sequence was prepared as a control peptide (Table 2.9).



| # | Peptide     | X   | Staple 1 sequence  | Staple 2 sequence  | Staple 1 Cyclisation conversion (HPLC yield) | Staple 2 Cyclisation conversion (HPLC yield) | Isolated yield (%)* |
|---|-------------|-----|--------------------|--------------------|--|--|---------------------|
| 1 | <b>2.45</b> | Lys | No AA              | No AA              | Quantitative                                 | Quantitative                                 | 1                   |
| 2 | <b>2.46</b> | Pro | -Pro-              | -Pro-              | Quantitative                                 | Quantitative                                 | 2                   |
| 3 | <b>2.47</b> | Lys | - <i>N</i> -MeAla- | - <i>N</i> -MeAla- | Quantitative                                 | Quantitative                                 | 1                   |
| 4 | <b>2.48</b> | Lys | - <i>N</i> -MeLys- | - <i>N</i> -MeLys- | Quantitative                                 | Quantitative                                 | 1                   |

Table 2.9. Library of double thioether-based stapled peptides cross-linked at positions  $i, i+4$ , and  $i+8, i+12$ . \*Isolated yields were determined after compound purification by HPLC.

In general, synthesis of all double HMSP was satisfactorily accomplished (see entries #1-4 in Table 2.9). Again, expected quantities of all final crude peptides were obtained, and the HPLC chromatograms of all the crude products were satisfactory. Thus, the low yields (1-2%) were attributed to product loss during HPLC purification.

In order to assess whether possible helicity of the double stapled peptides was conferred by staple1 or staple2, or whether it was a result of the synergy between both staples, peptides **2.49** and **2.50** were designed and prepared (Table 2.10). Again, expected quantities of all final crude peptides were obtained and the HPLC chromatograms of all the crude products were satisfactory. Thus, again the low isolated yields (2%) were attributed to the limitations encountered during the purification process.

| # | Peptide | Structure, cyclisation outcome and isolated yield          |
|---|---------|--|
| 1 | 2.49    | <p>Ac-LSQETFSDLW-Cys-Leu-Leu-Pro-Lys-AA-NH<sub>2</sub></p> |
|   |         | Quantitative cyclisation conversion (by HPLC)              |
|   |         | Isolation yield: 2% *                                      |
| 2 | 2.50    | <p>Ac-LS-Cys-Glu-Thr-Phe-Lys-DLWLLKAA-NH<sub>2</sub></p>   |
|   |         | Quantitative cyclisation conversion (by HPLC)              |
|   |         | Isolation yield: 2% *                                      |

Table 2.10. Library of double thioether-based stapled peptides cross-linked at positions i and i+4, and i+8 and i+12. \*Isolated yields were determined after compound purification by HPLC.

p53 wild-type linear analogues were prepared to serve as negative control for circular dichroism studies of single “short and “large” as well as double stapled peptides. Accordingly, 12-mer, 13-mer and 17-mer linear p53-based peptides were prepared with the amidated C-terminus (Table 2.11). Good-moderate isolation yields were obtained in all cases.

| # | Peptide | Length | Sequence                              | Isolated yield (%) * |
|---|---------|--------|---------------------------------------|----------------------|
| 1 | 2.51    | 12-mer | Ac-ETFESLWKLLPE-NH <sub>2</sub>       | 42                   |
| 2 | 2.52    | 13-mer | Ac-ETFSDLWKLLPEN- NH <sub>2</sub>     | 80                   |
| 3 | 2.53    | 17-mer | Ac-LSQETFSDLWKLLPEN-A-NH <sub>2</sub> | 54                   |

Table 2.11. Library of linear p53-based peptides. \*Isolated yields were determined after compound purification by HPLC.

### 2.3.2 Circular dichroism studies

Circular dichroism (CD) spectroscopy has been widely used for secondary structure characterisation of peptides and proteins. CD allows monitoring of conformational changes as well as estimation of the overall secondary structure content. In particular, random-coil,  $\alpha$ -helix, and parallel and antiparallel  $\beta$ -sheets secondary structures can be identified within the 260-190 nm wavelength range of a CD spectrum.<sup>[118]</sup> In this context, CD spectra of non-preorganised peptides (or peptides presenting a random-coil structure) show a characteristic intense minimum at 200 nm. CD spectra of helical conformations display a double minimum at 222 nm and 208 nm, and an intense maximum at 191 nm. Intensity of these three bands indicate the overall helical content. In fact, the extent of helix formation is most easily monitored by following the minimum at 222 nm ( $[\theta]_{222}$ ),<sup>[120]</sup> being the helicity percentage of a peptide or protein calculated as follows:

$$\text{Helicity \%} = \frac{[\theta]_{222}}{\max [\theta]_{222}} \cdot 100$$

$$[\theta]_{222} = \frac{\theta \cdot 100}{C \cdot n \cdot l}; \max [\theta]_{222} = (-4400 + 250 \cdot T)(1 - k/n)$$

Where:  $\theta$  (Ellipticity (m·deg)), C (concentration (mol·L<sup>-1</sup>)), n (number of residues); l (length of the cell (cm)), T (temperature (°C)), k (constant: k=3 for carboxy amidated peptides and k=4 for COOH terminated peptides).

The CD spectra of peptides and proteins is highly subjected to the environmental conditions, since the helical conformation is solvent- and pH- dependent. For instance, TFE is known to promote helix formation.<sup>[119]</sup> In addition, the helical structure is favoured in basic pH and destabilised at neutral pH.<sup>[119]</sup>

#### 2.3.2.1 CD studies of the HMSP library

In order to evaluate the intrinsic capacity of the prepared HMSP library to stabilise the helical conformation, CD studies were run in the absence of TFE and at a neutral pH (in a phosphate buffer of pH 7.4). Note that the helical conformation is least

stabilised upon these conditions,<sup>[119]</sup> thus these experiments indicate the actual impact of the peptide bridge nature and length on the helical conformation stabilisation. The obtained results are summarised in Table 2.12.

| #  | Peptide     | Staple type                 | Structure                        | %Helicity  |
|----|-------------|-----------------------------|----------------------------------|------------|
| 1  | <b>2.51</b> | Linear 12-mer               | Random coil                      | -          |
| 2  | <b>2.26</b> | (i,i+4)                     | Random coil                      | -          |
| 3  | <b>2.27</b> | (i,i+4)                     | Random coil                      | -          |
| 4  | <b>2.28</b> | (i,i+4)                     | Random coil                      | -          |
| 5  | <b>2.52</b> | Linear 13-mer               | Random coil                      | -          |
| 6  | <b>2.31</b> | (i,i+7)                     | $\alpha$ -helix                  | 33%        |
| 7  | <b>2.32</b> | (i,i+7)                     | $\alpha$ -helix                  | 39%        |
| 8  | <b>2.33</b> | (i,i+7)                     | $\alpha$ -helix                  | 31%        |
| 9  | <b>2.34</b> | (i,i+7)                     | $\alpha$ -helix                  | 35%        |
| 10 | <b>2.35</b> | (i,i+7)                     | $\alpha$ -helix                  | 19%        |
| 11 | <b>2.36</b> | (i,i+7)                     | $\alpha$ -helix                  | 38%        |
| 12 | <b>2.37</b> | (i,i+7)                     | $\alpha$ -helix                  | 26%        |
| 13 | <b>2.38</b> | (i,i+7)                     | $\alpha$ -helix                  | 20%        |
| 14 | <b>2.39</b> | (i,i+7)                     | $\alpha$ -helix                  | 32%        |
| 15 | <b>2.40</b> | <b>(i,i+7)</b>              | <b><math>\alpha</math>-helix</b> | <b>48%</b> |
| 16 | <b>2.41</b> | (i,i+7)                     | $\alpha$ -helix                  | 35%        |
| 17 | <b>2.42</b> | (i,i+7)                     | $\alpha$ -helix                  | 37%        |
| 18 | <b>2.44</b> | (i,i+7)                     | $\alpha$ -helix                  | 26%        |
| 19 | <b>2.53</b> | Linear 17-mer               | Random coil                      | -          |
| 20 | <b>2.45</b> | (i,i+7 and i+8,i+12)        | $\alpha$ -helix                  | 24%        |
| 21 | <b>2.46</b> | (i,i+7 and i+8,i+12)        | Random coil                      | -          |
| 22 | <b>2.47</b> | (i,i+7 and i+8,i+12)        | $\alpha$ -helix                  | 38%        |
| 23 | <b>2.48</b> | <b>(i,i+7 and i+8,i+12)</b> | <b><math>\alpha</math>-helix</b> | <b>46%</b> |
| 24 | <b>2.49</b> | (i,i+4)                     | $\alpha$ -helix                  | 21%        |
| 25 | <b>2.50</b> | (i,i+4)                     | $\alpha$ -helix                  | 22%        |

Table 2.12. CD studies of the HMSP library.

To start up with, the secondary structure of single “short” HMSP, where the staple was located between relative positions i,i+4, was evaluated and compared to the CD spectrum of the 12-mer linear p53-based peptide counterpart (see entries #1-4 in Table 2.12). In all cases, CD spectra showed an intense minimum at 200 nm, thus indicating the predominance of the random coil structure (Figure 2.23). In regards to the staple length impact on the secondary structure stabilisation, note that short peptide bridges ranging from one to two residues led to the same unfortunate results. Replacement of Pro, which is known to be a helix breaker residue, by Ala, that it is

expected to favour the helical conformation, did not have a positive impact on the  $\alpha$ -helix structure accommodation (see entries #2-4 in Table 2.12). Hence, these results suggested that the staple location within the peptide backbone and/or the distance between the stapling points (four residues) might not favour the helical secondary structure.

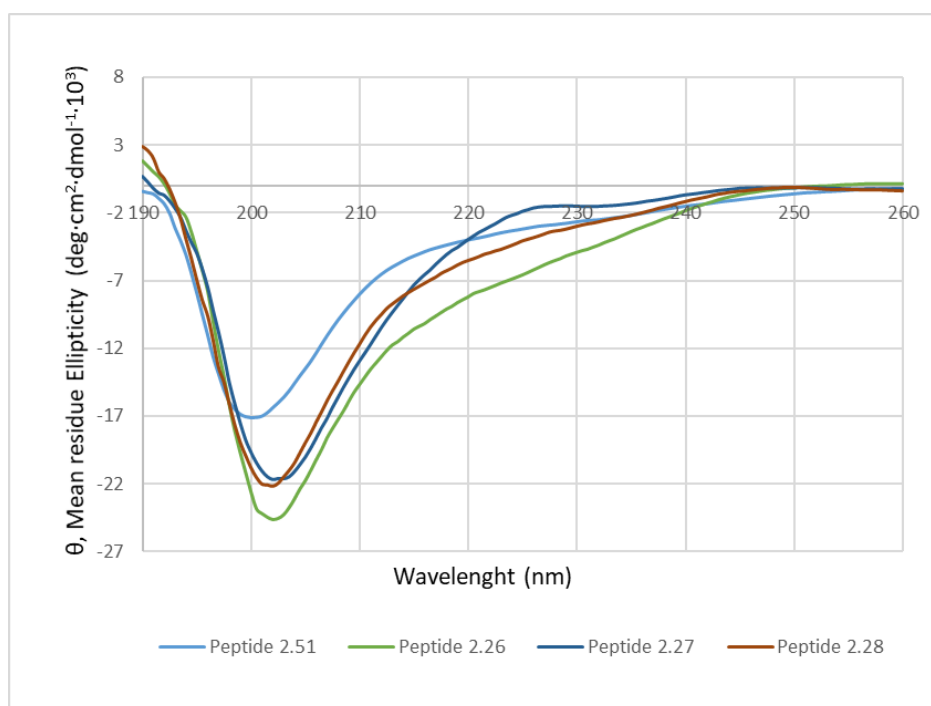


Figure 2.23. CD spectra of single “short” HMSP ( $i,i+4$ ).

Better results were obtained for single “large” HMSP, in which the chemical brace was placed between relative positions  $i,i+7$ . To the linear 13-mer p53-based peptide showing a random coil structure (see entry #5 in Table 2.12),  $\alpha$ -helix stabilisation was accomplished by insertion of thioether-based peptide bridges of diverse natures and lengths (see entries #6-18 in Table 2.12). In all cases, the CD spectra displayed a double minimum around 222 nm and 208 nm, and an intense maximum around 191 nm, suggesting that the selected stapling points were optimal to accommodate the helical conformation (Figure 2.24 and Figure 2.25). For all peptides, the helicity percentage was calculated following the minimum at 222 nm ( $[\theta]_{222}$ ), being the helicity percentages comprised within 19-48%.

First, synthesis of peptides **2.31**, **2.32**, **2.33** and **2.34**, which contain the unblocked C-terminus, was carried out and their CD spectra was assessed (see entries #6-9 in Table 2.12). Although in all cases helicity was promoted, peptide **2.32** gave the best results (38% of helical content) (see entry #7 in Table 2.12 and Figure 2.24). At this point of the project, we wished to evaluate whether the overall peptide charge had an impact on the helical structure accommodation. Note that positive charges enhance cellular uptake, and therefore peptides holding the amidated C-terminus were expected to present greater cellular permeability. With that purpose, preparation of a C-terminus amidated analogue of peptide **2.32**, which presents the greater helicity among and contains the staple sequence  $-N\text{-MePhe-}N\text{-MeAla-}$ , was carried out and both CD spectrum were compared (see entries #7 and #11 in Table 2.12 and Figure 2.24). Both peptides led to similar helicities (38% and 39%). Inspired by these positive CD results, a library of HMSP with the amidated C-terminus, where peptides were expected to present greater cellular uptake due to the additional positive charge, was designed and their corresponding CD was evaluated.

Based on the results obtained for the  $i,j+7$  HMSP library with both the unblocked or the amidated C-terminus (see entries #6-18 in Table 2.12, Figure 2.24 and Figure 2.25), conclusions on the optimal staple length to promote the helical secondary structure cannot be drawn. In fact, a general trend based on the staple dimensions (tested peptide staples varied from one to three *N*-methylated residues) could not be outlined. However, it is worth highlighting that all peptides containing *N*-MeLys residues, generally, present a rather high helical content. That is the case for peptides **2.39**, **2.40** and **2.41**, which display a 32%, 48% and 33% of helical content, respectively (see entries #14-16 in Table 2.12). We hypothesised that the ability of the free amine group (N-H) present in the Lys side chain might confer extra helical stability due to possible H-bonding with the peptide backbone. This plausible explanation complies with the obtained results, since a considerably higher helicity was observed for peptide **2.40**, which displayed two *N*-MeLys within the *N*-methyl-rich peptide bridge, compared to the helicity observed for peptides **2.39** and **2.41**.

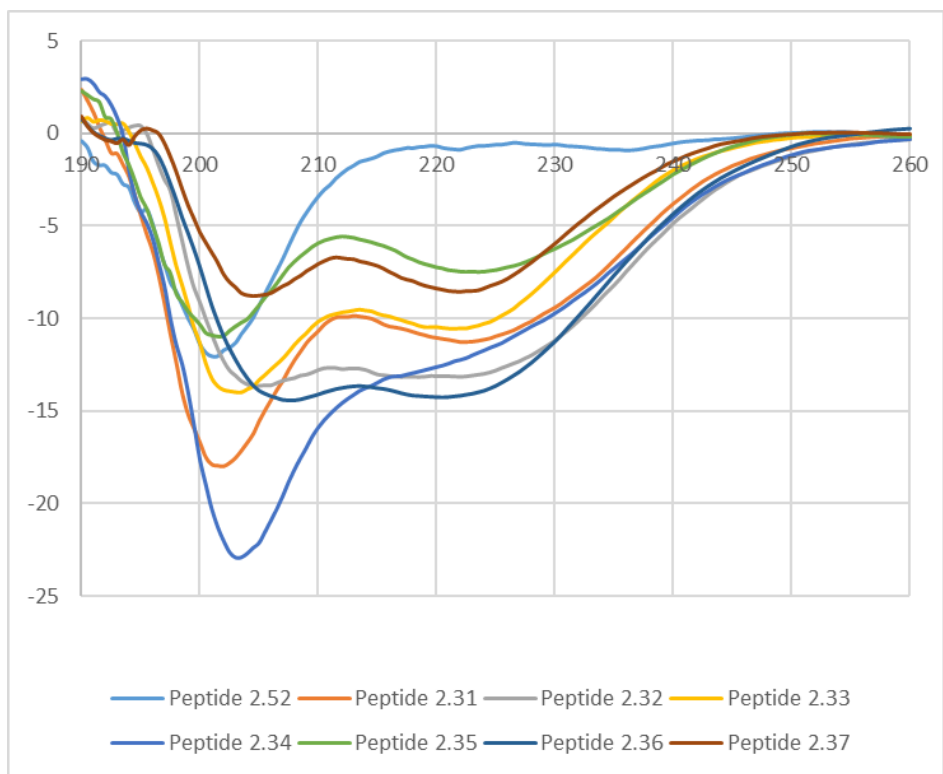


Figure 2.24. CD spectra of single "large" HMSP (i,i+7).

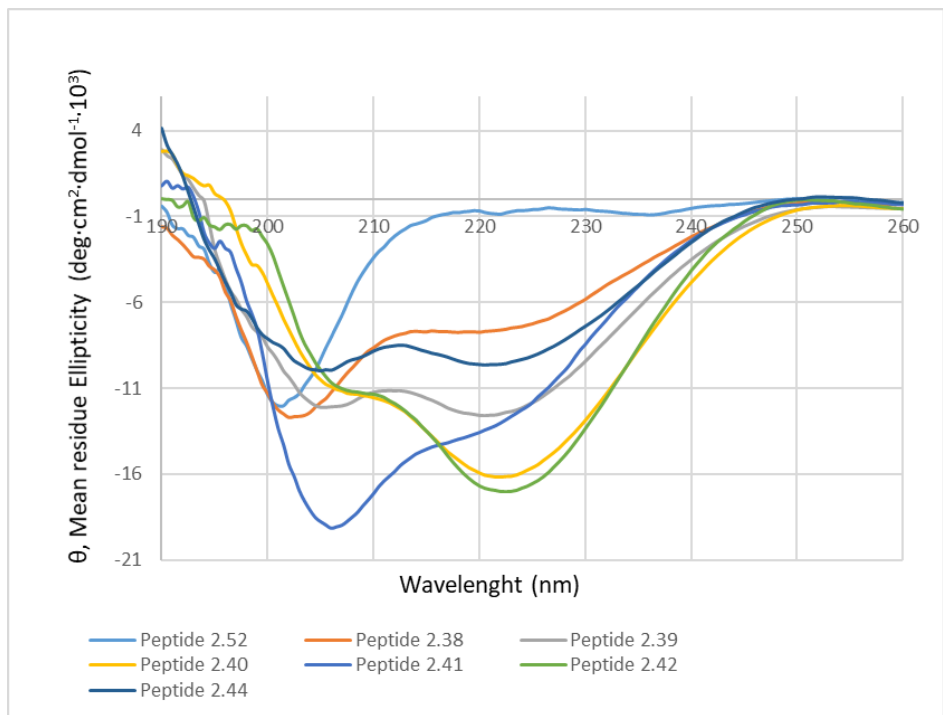


Figure 2.25. CD spectra of single "large" HMSP (i,i+7).

Interesting results were also obtained with double HMSP (Figure 2.26). Direct stapling between relative positions  $i,i+4$ , and  $i+8,i+12$  through a thioether-based bridge resulted in some helical conformation stabilisation (24%) (see entry #20 in Table 2.12). As expected, insertion of a Pro residue at both staple1 and staple2 positions, as well within the peptide backbone, resulted in destabilisation of the  $\alpha$ -helix structure, since peptide **2.46** presented a random coil structure (see entry #21 in Table 2.12). The Pro residue, which is known to break the helical stability, might account for these results. On the other hand, the 38% of helical content observed when placing a *N*-MeAla residue at staple1 and staple2 (see entry #22 in Table 2.12) indicates that insertion of one inert *N*-methylated residue results in considerable stabilisation of the helical conformation. In accordance with previous obtained results, insertion of a *N*-MeLys residue at staple1 and staple2 bridges resulted in the highest helicity observed for double stapled peptides (46%) (see entry #23 in Table 2.12). Thus, these experiments support the previously postulated theory, where the Lys side confers extra helical stability due H-bonding with the peptide backbone.

Inspired by these promising results, we wished to evaluate whether the greater helicity observed in peptide **2.48** was conferred by either staple1 or staple2, or whether it was a result of the synergy between both staples. With that purpose, the CD spectra of peptides **2.49** and **2.50** were evaluated (Figure 2.27). As a matter of fact, both individual staples located at relative positions  $i,i+4$  stabilised the helical conformation (21-22%) (see entries #24-25 in Table 2.12). On the basis of these results, the outstanding helical content of peptide **2.48** is a result of the addition effect of both staples. Concomitantly, these experiments confirm that complete failure of peptide staples **2.26**, **2.27** and **2.28** to accommodate the helical conformation is a matter of the staple location rather than the relative distance between the stapling points (see entries #2-4 in Table 2.12).

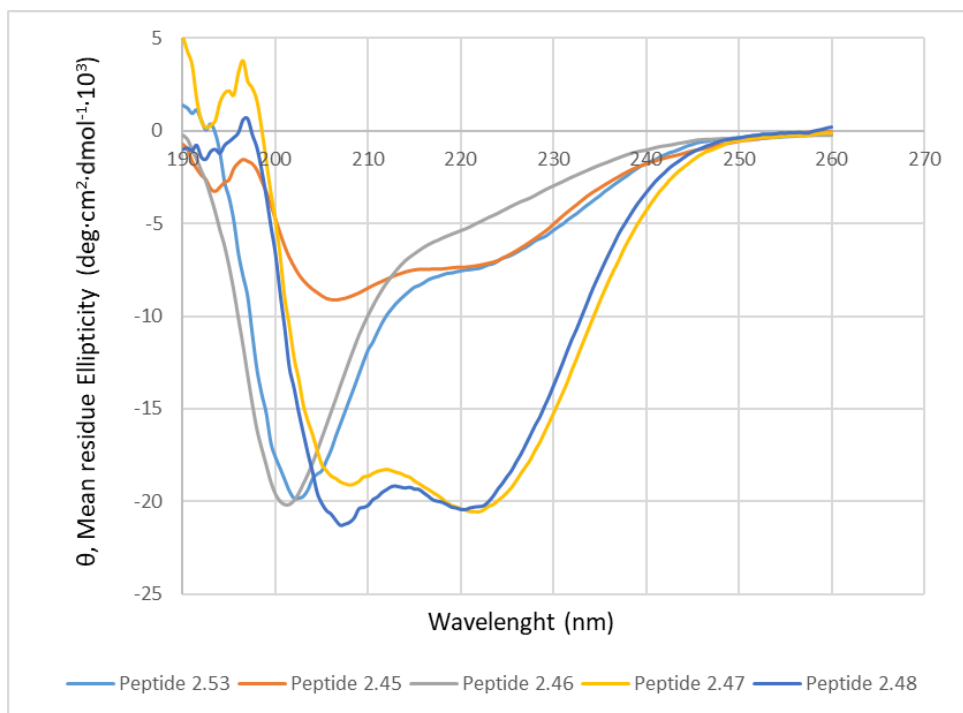


Figure 2.26. CD spectra of “double” HMSP (i,i+4 and i+8,i+12).

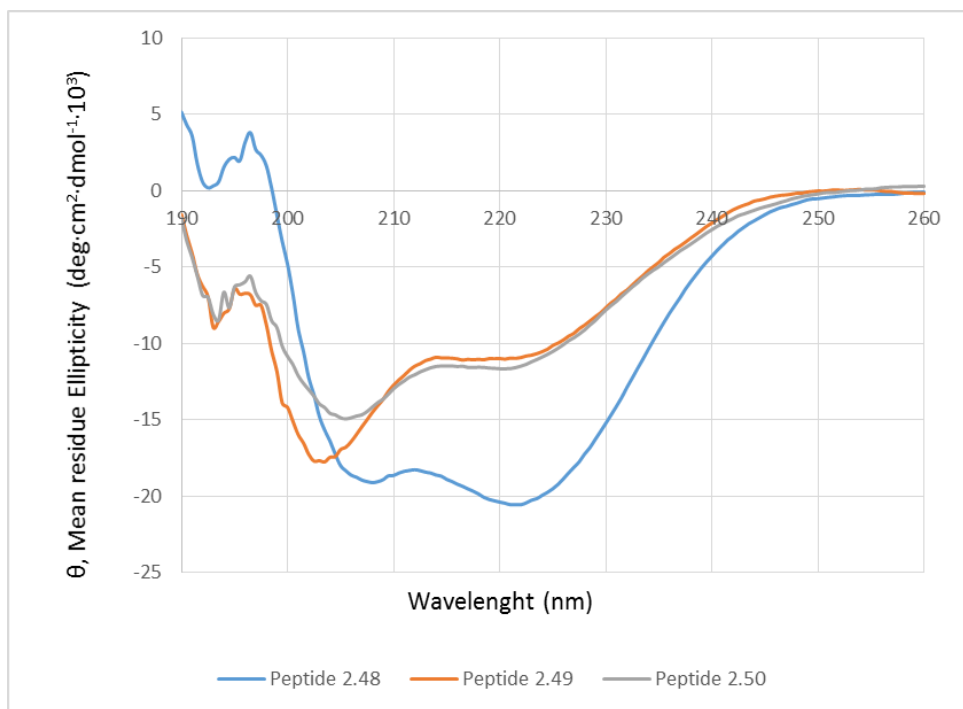


Figure 2.27. CD spectra of “single” HMSP (i,i+4).

To sum up, the novel developed molecular architectures, HMSP, allowed preparation of p53-based peptides with enhanced helical conformation. In this context, insertion of *N*-methyl-rich peptide bridges of different lengths (from one to three residues) and nature between positions  $i,i+7$  resulted in accommodation of the helical structure. Additionally, double HMSP, where two *N*-methyl-rich peptide bridges were inserted at relative positions  $i,i+4$  and  $i+8,i+12$ , also proved effective to stabilise the  $\alpha$ -helix secondary structure. Remarkably, in general insertion of *N*-MeLys residues accounts for additional helical stability due to H-bonding with the peptide backbone.

The synthetic methodologies developed in this study and the positive results obtained from the CD studies, together with the general trends outlined according to them, open the doors to an extensive staple screening with other *N*-methyl-rich peptide bridge combinations of various lengths and located at different positions, in order to draw final conclusions about the structural requirements of staples to induce helicity.

## 2.4 References

- [1] L. Nevola, E. Giralt, *Chem. Commun.* **2015**, 51, 3302–3315.
- [2] M. Pelay-Gimeno, A. Glas, O. Koch, T. N. Grossmann, *Angew. Chemie Int. Ed. Engl.* **2015**, 54, 8896–8927.
- [3] A. Glas, T. Grossmann, *Synlett* **2014**, 26, 1–5.
- [4] M. Gao, K. Cheng, H. Yin, *Biopolymers* **2015**, 104, 310–316.
- [5] N. London, B. Raveh, O. Schueler-Furman, *Curr. Opin. Chem. Biol.* **2013**, 17, 952–959.
- [6] N. Tsomaia, *Eur. J. Med. Chem.* **2015**, 94, 459–470.
- [7] A. M. Watkins, P. S. Arora, *Eur. J. Med. Chem.* **2015**, 94, 480–488.
- [8] D. R. Cary, M. Ohuchi, P. C. Reid, K. Masuya, *J. Synth. Org. Chem. Japan* **2017**, 75, 1171–1178.
- [9] T. A. Stone, C. M. Deber, *Biochim. Biophys. Acta Biomembr.* **2017**, 1859, 577–585.
- [10] T. Kieber-Emmons, R. Murali, M. I. Greene, *Curr. Opin. Biotechnol.* **1997**, 8, 435–441.
- [11] A. Grob, C. Hashimoto, H. Sticht, J. Eichler, *Front. Bioeng. Biotechnol.* **2016**, 3, 211–217.
- [12] P. Wójcik, Ł. Berlicki, *Bioorganic Med. Chem. Lett.* **2016**, 26, 707–713.
- [13] J. Deska, U. Kazmaier, *Curr. Org. Chem.* **2008**, 12, 355–385.
- [14] J. C. Phelan, N. J. Skelton, A. C. Braisted, R. S. McDowell, *J. Am. Chem. Soc.* **1997**, 119, 455–460.
- [15] M. N. Fodje, S. Al-Karadaghi, *Protein Eng.* **2002**, 15, 353–358.
- [16] A. L. Jochim, P. S. Arora, *ACS Chem. Biol.* **2010**, 5, 919–923.

- [17] A. Chakrabarty, R. L. Baldwin, *Adv. Protein Chem* **1995**, *46*, 141–176.
- [18] R. Schweitzer-Stenner, W. Gonzales, G. T. Bourne, J. A. Feng, G. R. Marshall, *J. Am. Chem. Soc.* **2007**, *129*, 13095–13109.
- [19] R. Banerjee, G. Basu, P. Chène, S. Roy, *J. Pept. Res.* **2002**, *60*, 88–94.
- [20] J. E. Donald, D. W. Kulp, W. F. Degrado, *Proteins* **2011**, *79*, 898–915.
- [21] S. Marqusee, R. L. Baldwin, *Proc. Natl. Acad. Sci. U.S.A.* **1987**, *84*, 8898–8902.
- [22] J. S. Albert, A. D. Hamilton, *Biochemistry* **1995**, *34*, 984–990.
- [23] Y. H. Lau, P. de Andrade, Y. Wu, D. R. Spring, *Chem. Soc. Rev.* **2015**, *44*, 91–102.
- [24] V. V. Iyer, *Curr. Med. Chem.* **2016**, *23*, 3025–3043.
- [25] G. L. Verdine, G. J. Hilinski, *Drug Discov. Today* **2012**, *9*, e41–e47.
- [26] X. Li, Y. Zou, H. G. Hu, *Chin. Chem. Lett.* **2018**, *29*, 1088–1092.
- [27] Q. Z. Zhang, Y. Tian, Y. Z. Lao, Z. G. Li, *Curr. Med. Chem.* **2014**, *21*, 2438–2452.
- [28] Y. Okamoto, *Proteins* **1994**, *19*, 14–23.
- [29] P. Pengo, L. Pasquato, S. Moro, A. Brigo, F. Fogolari, Q. B. Broxterman, B. Kaptein, P. Scrimin, *Angew. Chem. Int. Ed.* **2003**, *42*, 3388–3392.
- [30] M. Crisma, W. Bisson, F. Formaggio, Q. B. Broxterman, C. Toniolo, *Biopolymers* **2002**, *64*, 236–245.
- [31] M. Bellanda, S. Mammi, S. Geremia, N. Demitri, L. Randaccio, Q. B. Broxterman, B. Kaptein, P. Pengo, L. Pasquato, P. Scrimin, *Chem. Eur. J.* **2007**, *13*, 407–416.
- [32] R. Subiros-funosas, G. A. Acosta, A. El-faham, F. Albericio, *Tetrahedron Lett.* **2009**, *50*, 6200–6202.
- [33] L. A. Carpino, M. Beyermann, H. Wenschuh, M. Bienert, *Acc. Chem. Res.* **1996**, *29*, 268–274.

- [34] E. Benedetti, A. Bavoso, B. Di Blaso, V. Pavone, C. Pedone, C. Toniolot, G. M. Bonora, *Proc. Natl. Acad. Sci. U.S.A.* **1982**, *79*, 7951–7954.
- [35] H. Anke, *ChemBioChem* **2009**, *10*, 2266–2267.
- [36] R. Aurora, G. D. Rose, *Pept. Sci.* **1998**, *7*, 21–38.
- [37] J. S. Richardson, D. C. Richardson, *Science* **1988**, *240*, 1648–1652.
- [38] M. Scholtz, H. Qian, V. H. Robbins, R. L. Baldwin, *Biochemistry* **1993**, *32*, 9668–9676.
- [39] C. A. Hunter, J. K. M. Sanders, *J. Am. Chem. Soc.* **1990**, *112*, 5525–5534.
- [40] N. S. Robertson, A. G. Jamieson, *Reports Org. Chem.* **2015**, *2015:5*, 65–74.
- [41] J. C. Phelan, N. J. Skelton, A. C. Braisted, R. S. Mcdowell, *J. Am. Chem. Soc.* **1997**, *119*, 455–460.
- [42] H. Jo, N. Meinhardt, Y. Wu, S. Kulkarni, X. Hu, K. E. Low, P. L. Davies, W. F. Degrado, D. C. Greenbaum, *J. Am. Chem. Soc.* **2012**, *134*, 17704–17713.
- [43] A. M. Leduc, J. O. Trent, J. L. Wittliff, K. S. Bramlett, S. L. Briggs, N. Y. Chirgadze, Y. Wang, T. P. Burris, A. F. Spatola, *Proc. Natl. Acad. Sci. U.S.A.* **2003**, *100*, 11273–11278.
- [44] K. J. Skowron, T. E. Speltz, T. W. Moore, *Med. Res. Rev.* **2018**, *39*, 749–770.
- [45] Y. S. Tan, D. P. Lane, C. S. Verma, *Drug Discov. Today* **2016**, *21*, 1642–1653.
- [46] G. J. Hilinski, Y. Kim, J. Hong, P. S. Kutchukian, C. M. Crenshaw, S. S. Berkovitch, A. Chang, S. Ham, G. L. Verdine, *J. Am. Chem. Soc.* **2014**, *136*, 12314–12322.
- [47] G. H. Bird, N. Madani, A. F. Perry, A. M. Princiotto, J. G. Supko, X. He, E. Gavathiotis, J. G. Sodroski, L. D. Walensky, *Proc. Natl. Acad. Sci. U.S.A.* **2010**, *107*, 14093–14098.
- [48] Y. Lee, S. Han, Y. Lim, *Macromol. Rapid Commun.* **2016**, *37*, 1021–1026.

- [49] K. L. Keeling, O. Cho, D. B. Scanlon, G. W. Booker, A. D. Abell, K. L. Wegener, *Org. Biomol. Chem.* **2016**, *14*, 9731–9735.
- [50] G. L. Verdine, G. J. Hilinski, *Methods Enzymol.* **2012**, *503*, 3–33.
- [51] M. Chorev, E. Roubini, R. L. Mckee, S. W. Gibbons, M. E. Goldman, M. P. Caulfield, M. Rosenblatt, *Biochemistry* **1991**, *30*, 5968–5974.
- [52] H. C. Kolb, K. B. Sharpless, *Drug Discov. Today* **2003**, *8*, 1128–1137.
- [53] C. E. Schafmeister, J. Po, G. L. Verdine, *J. Am. Chem. Soc.* **2000**, *122*, 5891–5892.
- [54] Y. Kim, P. S. Kutchukian, G. L. Verdine, *Org. Lett.* **2010**, *12*, 3046–3049.
- [55] Y. Kim, G. L. Verdine, *Bioorg. Med. Chem. Lett.* **2009**, *19*, 2533–2536.
- [56] A. Glas, T. N. Grossmann, *Synlett* **2015**, *26*, 1–5.
- [57] G. H. Bird, C. W. Crannell, L. D. Walensky, *Curr. Protoc. Chem. Biol.* **2011**, *3*, 99–117.
- [58] G. H. Bird, F. Bernal, K. Pitter, L. D. Walensky, *Methods Enzymol.* **2008**, *446*, 369–386.
- [59] L. D. Walensky, A. L. Kung, I. Escher, T. J. Malia, R. D. Wright, G. Wagner, G. L. Verdine, S. J. Korsmeyer, *Science* **2004**, *305*, 1466–1470.
- [60] F. Bernal, A. F. Tyler, S. J. Korsmeyer, L. D. Walensky, G. L. Verdine, *J. Am. Chem. Soc.* **2007**, *129*, 2456–2457.
- [61] C. R. Braun, J. Mintseris, E. Gavathiotis, G. H. Bird, S. P. Gygi, L. D. Walensky, *Chem. Biol.* **2010**, *17*, 1325–1333.
- [62] E. Gavathiotis, M. Suzuki, M. L. Davis, K. Pitter, H. Bird, S. G. Katz, H. Tu, H. Kim, E. H. Cheng, N. Tjandra, L. D. Walensky, *Nature* **2008**, *455*, 1076–1081.
- [63] J. L. Labelle, S. G. Katz, G. H. Bird, E. Gavathiotis, M. L. Stewart, C. Lawrence, M. Godes, K. Pitter, A. L. Kung, L. D. Walensky, *J. Clin. Invest.* **2012**, *122*, 2018–2031.

- [64] R. M. Williams, M. N. Im, *J. Am. Chem. Soc.* **1991**, *113*, 9276–9286.
- [65] Y. N. Belokon, V. I. Tararov, V. I. Maleev, T. F. Savel'eva, M. G. Ryzhov, *Tetrahedron Asymmetry* **1998**, *9*, 4249–4252.
- [66] W. Qiu, V. Soloshonok, C. Cai, X. Tang, V. J. Hruby, *Tetrahedron* **2000**, *56*, 2577–2582.
- [67] D. Migoń, D. Neubauer, W. Kamysz, *Protein J.* **2018**, *37*, 2–12.
- [68] P. M. Cromm, J. Spiegel, T. N. Grossmann, *ACS Chem. Biol.* **2015**, *10*, 1362–1375.
- [69] L. D. Walensky, G. H. Bird, *J. Med. Chem.* **2014**, *57*, 6275–6288.
- [70] D. Y. Jackson, D. S. King, J. Chmielewski, S. Singh, P. G. Schultz, *J. Am. Chem. Soc.* **1991**, *113*, 9391–9392.
- [71] H. Jo, N. Meinhardt, Y. Wu, S. Kulkarni, X. Hu, K. E. Low, P. L. Davies, W. F. Degrado, D. C. Greenbaum, *J. Am. Chem. Soc.* **2012**, *134*, 17704–17713.
- [72] F. M. Brunel, P. E. Dawson, *Chem. Commun.* **2005**, *28*, 2552–2554.
- [73] Y. Wang, D. H. Chou, *Angew. Chem. Int. Ed. Engl.* **2015**, *54*, 10931–10934.
- [74] A. M. Spokoyny, Y. Zou, J. J. Ling, H. Yu, Y. Lin, B. L. Pentelute, *J. Am. Chem. Soc.* **2013**, *135*, 5946–5949.
- [75] A. J. Rojas, C. Zhang, E. V Vinogradova, N. H. Buchwald, J. Reilly, L. Pentelute, S. L. Buchwald, *Chem. Sci.* **2017**, *8*, 4257–4263.
- [76] E. V Vinogradova, C. Zhang, A. M. Spokoyny, B. L. Pentelute, S. L. Buchwald, *Nature* **2015**, *526*, 687–691.
- [77] A. M. Felix, E. P. Heimer, C. T. Wang, T. J. Lambros, A. Fournier, T. F. Mowles, S. Maines, R. M. Campbell, B. B. Wegrzynski, V. Toome, D. Fry, V. S. Madison, *Int. J. Pept. Protein Res.* **1988**, *32*, 441–454.
- [78] M. Chorev, E. Roubini, R. L. Mckee, S. W. Gibbons, M. E. Goldman, M. P. Caulfield,

- M. Rosenblatt, *Biochemistry* **1991**, *30*, 5968–5974.
- [79] R. S. Harrison, N. E. Shepherd, H. N. Hoang, G. Ruiz-Gómez, T. a Hill, R. W. Driver, V. S. Desai, P. R. Young, G. Abbenante, D. P. Fairlie, *Proc. Natl. Acad. Sci. U.S.A.* **2010**, *107*, 11686–11691.
- [80] V. V Rostovtsev, L. G. Green, V. V Fokin, K. B. Sharpless, *Angew. Chem. Int. Ed. Engl.* **2002**, *41*, 2596–2599.
- [81] S. Cantel, A. Le, C. Isaad, M. Scrima, J. J. Levy, R. D. Dimarchi, P. Rovero, J. A. Halperin, A. M. D'Ursi, A. M. Papini, M. Chorev, *J. Org. Chem.* **2008**, *73*, 5663–5674.
- [82] Y. H. Lau, P. De Andrade, S. T. Quah, M. Rossmann, L. Laraia, N. Sköld, T. J. Sum, P. J. E. Rowling, T. L. Joseph, C. Verma, M. Hyvönen, L. S. Itzhaki, A. R. Venkitaraman, C. J. Brown, D. P. Lane, D. R. Spring, *Chem. Sci.* **2014**, *5*, 1804–1809.
- [83] M. Scrima, A. Le Chevalier-Isaad, P. Rovero, A. M. Papini, M. Chorev, A. M. D'Ursi, *European J. Org. Chem.* **2010**, *2010*, 446–457.
- [84] Y. H. Lau, P. De Andrade, N. Sköld, G. J. Mckenzie, A. R. Venkitaraman, C. Verma, D. P. Lane, D. R. Spring, *Org. Biomol. Chem.* **2014**, *12*, 4074–4077.
- [85] S. Kneissl, E. J. Loveridge, C. Williams, M. P. Crump, R. K. Allemann, *ChemBioChem* **2008**, *9*, 3046–3054.
- [86] C. M. Haney, M. T. Loch, W. S. Horne, *Chem. Commun.* **2011**, *47*, 10915–10917.
- [87] P. A. Cistrone, A. P. Silvestri, J. C. J. Hintzen, P. E. Dawson, *ChemBioChem* **2018**, *19*, 1031–1035.
- [88] Y. Demizu, S. Nagoya, M. Shirakawa, M. Kawamura, N. Yamagata, Y. Sato, M. Doi, M. Kurihara, *Bioorg. Med. Chem. Lett.* **2013**, *23*, 4292–4296.
- [89] T. Okamoto, K. Zobel, A. Fedorova, C. Quan, H. Yang, W. J. Fairbrother, D. C. S. Huang, B. J. Smith, K. Deshayes, P. E. Czabotar, *ACS Chem. Biol.* **2012**, *8*, 297–302.

- [90] G. H. Bird, E. Gavathiotis, J. L. Labelle, S. G. Katz, L. D. Walensky, *ACS Chem. Biol.* **2014**, *9*, 831–837.
- [91] F. Giordanetto, D. Revell, L. Knerr, M. Hostettler, A. Paunovic, C. Priest, A. Janefeldt, A. Gill, *ACS Med. Chem. Lett.* **2013**, *4*, 1163–1168.
- [92] J. Chatterjee, C. Gilon, A. Hoffman, H. Kessler, *Acc. Chem. Res.* **2008**, *41*, 1331–1342.
- [93] M. Teixidó, F. Albericio, E. Giralt, *J. Pept. Res.* **2005**, *65*, 153–166.
- [94] W. M. Hewitt, S. F. L. Leung, C. R. Pye, A. R. Ponkey, M. Bednarek, M. P. Jacobson, R. S. Lokey, *J. Am. Chem. Soc.* **2015**, *137*, 715–721.
- [95] J. Chatterjee, B. Laufer, H. Kessler, *Nat. Protoc.* **2012**, *7*, 432–444.
- [96] P. Kussie, S. Gorina, V. Marechal, B. Elenbaas, J. Moreau, A. Levine, N. Pavletich, *Science* **1996**, *274*, 948–953.
- [97] K. G. Mclure, P. W. K. Lee, *EMBO J.* **1998**, *17*, 3342–3350.
- [98] A. Huart, T. R. Hupp, *Biodiscovery* **2013**, *5*, 1–15.
- [99] L. A. Carpino, *J. Am. Chem. Soc.* **1993**, *115*, 4397–4398.
- [100] Y. Nishiyama, M. Tanaka, S. Saito, S. Ishizuka, T. Mori, K. Kurita, *Chem. Pharm. Bull.* **1999**, *47*, 576–578.
- [101] A. El-Faham, F. Albericio, *Chem. Rev.* **2011**, *111*, 6557–6602.
- [102] L. A. Carpino, D. Ionescu, A. El-Faham, *J. Org. Chem.* **1996**, *61*, 2460–2465.
- [103] R. B. Merrifield, A. R. Mitchell, J. E. Clarke, *J. Org. Chem.* **1974**, *39*, 660–668.
- [104] M. Stawikowski, G. B. Fields, in *Curr. Protoc. Protein Sci.*, **2002**, p. Chapter 18, Unit 18.1.
- [105] J. D. Wade, J. Bedford, R. C. Sheppard, G. W. Tregear, *Pept. Res.* **1991**, *4*, 194–199.

- [106] S. Capasso, A. Vergara, L. Mazzarella, *J. Am. Chem. Soc.* **1998**, *120*, 1990–1995.
- [107] F. Albericio, *Curr. Opin. Chem. Biol.* **2004**, *8*, 211–221.
- [108] M. J. Martin, R. Rodriguez-Acebes, Y. Garcia-Ramos, V. Martinez, C. Murcia, I. Digon, I. Marco, M. Pelay-Gimeno, R. Fernández, F. Reyes, A. M. Francesch, S. Munt, J. Tulla-Puche, F. Albericio, C. Cuevas, *J. Am. Chem. Soc.* **2014**, *18*, 6754–6762.
- [109] J. D. Wade, M. N. Mathieu, M. Macris, G. W. Tregear, *Lett. Pept. Sci.* **2000**, *7*, 107–112.
- [110] I. Coin, M. Beerbaum, P. Schmieder, M. Bienert, M. Beyermann, *Org. Lett.* **2008**, *10*, 3857–3860.
- [111] J. A. N. Urban, T. Vaisar, R. Shen, M. S. Lee, *Int. J. Pept. Res. Ther.* **1996**, *47*, 182–189.
- [112] C. Van der Auwera, M. J. O. Anteunis, *Eur. J. Allergy Clin. Immunol.* **1988**, *31*, 186–191.
- [113] C. J. Brown, S. T. Quah, J. Jong, A. M. Goh, P. C. Chiam, K. H. Khoo, M. L. Choong, M. A. Lee, L. Yurlova, K. Zolghadr, T. L. Joseph, C. S. Verma, D. P. Lane, *ACS Chem. Biol.* **2013**, *8*, 506–512.
- [114] K. L. Morrison, G. A. Weiss, *Curr. Opin. Chem. Biol.* **2001**, *5*, 302–307.
- [115] C. J. White, A. K. Yudin, *Nat. Chem.* **2011**, *3*, 509–524.
- [116] D. Ben-ishai, *J. Am. Chem. Soc.* **1957**, *79*, 5736–5738.
- [117] R. M. Freidinger, J. S. Hinkle, D. S. Perlow, B. H. Arison, *J. Org. Chem.* **1983**, *48*, 77–81.
- [118] S. C. Miller, T. S. Scanlan, *J. Am. Chem. Soc.* **1997**, *119*, 2301–2302.
- [119] S. Marqusee, V. H. Robbins, R. L. Baldwin, *Proc. Natl. Acad. Sci. U.S.A.* **1989**, *86*,

5286–5290.

[120] K. Bakshi, M. R. Liyanage, D. B. Volkin, C. R. Middaugh, *Methods Mol. Biol.* **2014**, *1088*, 247-253.

[121] M. Zhang, T. Yuan, H. J. Vogel, *Protein Sci.* **1993**, *2*, 1931–1937.

## **CONCLUSIONS**



## Conclusions

### Conclusions for CHAPTER 1 are:

1. A robust Fmoc-based stepwise methodology for the preparation of complex cyclodepsipeptides that are composed of  $\beta$ -branched residues and contain consecutive and multiple ester bonds was successfully developed. In this context, the drawbacks commonly encountered in depsipeptide synthesis, namely (i) problematic Fmoc protecting group removal due to DKP formation and  $\alpha,\beta$ -elimination side-reactions, and (ii) selection of the appropriate protecting group scheme for residue incorporation, were extensively studied and solved.
2. Fmoc removal of the second residue with the traditional piperidine–DMF (1:4 v/v) (2 x 1 min) mixture led to DKP formation (18%). Lower DKP formation rates were observed when replacing the piperidine–DMF (1:4 v/v) system by the DBU–DMF (2:98 v/v) cocktail, and most importantly, when adding small percentages of the HOBt organic acid to the deprotection mixture. Among all tested

conditions, the optimal treatment to minimise DKP formation was found to be the following: 0.1 M HOBt in DBU–DMF (2:98 v/v) (2 x 1 min).

3. Assembly of Fmoc-protected residues at the amine function *via* ester bond formation turned out problematic due to undesired racemisation,  $\alpha,\beta$ -elimination side-reactions and residue loss. In all cases, an improvement in the Fmoc removal step was observed when replacing the traditional piperidine–based mixture by the DBU–DMF (2:98 v/v) cocktail. For the first time, addition of small percentages of organic acids (HOBt or OxymaPure) to the Fmoc removal cocktail generally led to better deprotection outcomes. The organic acid concentration had an effect on the Fmoc elimination step, whereas addition of HOBt or OxymaPure in a 0.1 M concentration usually improved the Fmoc removal outcome, addition of higher percentages of both organic acids (in a 0.2 M concentration) accounted for poorer results, probably due to partial or complete base neutralisation.
4. The residue incorporation success to form ester linkages highly depended on the  $N^\alpha$ -protecting group.
  - a. *First ester linkage*: insertion of the Ac-Thr(OH)-OH residue with the amine function protected with Ac and Alloc protecting groups led to no residue incorporation. The until now unreactive Ac-Thr(OH)-OH derivative could be finally introduced in a stepwise manner as Fmoc-Thr(TBDMS)-OH. The Fmoc and TBDMS groups were simultaneously removed by treatment with TBAF, and the  $\alpha,\beta$ -elimination side-product formation was fully prevented.
  - b. *Second ester linkage*: esterification of the *N,O*-Me<sub>2</sub>Thr-OH residue can be accomplished with both the Alloc and the Fmoc protected *N,O*-Me<sub>2</sub>Thr-OH residues. However, 22-23% of racemisation was observed in both cases. *N*-alkylated amino acids are more susceptible to epimerisation at the  $\alpha$ -carbon upon amino acid activation, and racemisation might be attributed to this moiety. Additional efforts to prevent racemisation gave the same unfavourable results. Fmoc removal at this point of the synthesis with a DBU–DMF (2:98) solution successfully afforded the desired product in a

57% HPLC conversion, being formation of the undesired  $\alpha,\beta$ -elimination side-product significantly minimised. Although Fmoc removal leads to lower yields compared to Alloc, the Fmoc protecting group might be very useful for the rapid preparation of a series of synthetic analogues.

- c. *Third ester linkage*: insertion of the Ac-Thr(<sup>t</sup>Bu)-OH residue with the N<sup>α</sup> position protected with Ac and Alloc resulted in no residue incorporation. Introduction of the residue was accomplished with commercially available Fmoc-Thr(<sup>t</sup>Bu)-OH, and complete formation of the undesired  $\alpha,\beta$ -elimination side-product upon Fmoc removal conditions was circumvented by treatment with a 0.1 M HOBt in DBU–DMF (2:98) solution.
5. Evaluation of the fully stepwise efficiency was carried out by comparison with two synthetic strategies containing one and two depsipeptide building block segment condensations for the preparation of the target molecule. Remarkably, all three strategies account for comparable yields after HPLC purification (24–26%). It is worth highlighting that the fully Fmoc-based stepwise strategy presents some advantages over segment condensation strategies. Preparation of didepsipeptides building blocks, which often comprise several reaction and purification steps can be avoided. Moreover, the Fmoc-based stepwise strategy becomes a valuable tool for the rapid generation of many synthetic analogues.

Conclusions for CHAPTER 2 are:

6. A novel class of stapled peptides, namely HMSP, were designed and successfully developed, in which a short *N*-methyl-rich peptide bridge was inserted at key stapling positions to promote the helical conformation.
7. Incorporation of the *N*-methyl-rich peptide bridge was successfully accomplished by either stepwise incorporation of Fmoc-protected *N*-methylated residues previously synthesised in solution (*Strategy A*) or sequential Fmoc-AA-OH residue assembly and subsequent on-resin Mitsunobu *N*-Methylation (*Strategy B*). Both approaches turned out efficient for the elongation of the *N*-methyl-rich

- peptide staples. Conveniently, either method can be used based on the staple length and nature of the amino acids
8. Applicability of a lactam-based cross-linking methodology to prepare the target molecular architectures is rather limited. Both, peptide cyclisation and global deprotection steps turned out very problematic. In fact, only a few of all the tested staple combinations could be cyclised, however, low to moderate cyclisation rates were observed in most of the cases. In this context, macrolactamisation was only accomplished for “short” stapled peptides when *N*-MeGly, Ala or Gly were located at the staple *N*-terminal position. Furthermore, the deprotection outcome was not satisfactory, being the corresponding desired unprotected peptide not obtained or obtained as a minor product. Thus, the lactam-based cross-link approach was discarded for the preparation of HMSP.
  9. A thioether-based cross-linking methodology was successfully developed for the preparation of single and double HMSP. Scope of the developed methodology was evaluated by insertion of numerous peptide bridge combination sequences to key stapling positions, which involved diverse lengths and nature of *N*-methylated amino acids. In fact, good to excellent cyclisation rates were observed in most of the cases and the thioether-based cross-linking approach circumvented peptide fragmentation upon cleavage and global deprotection. These results confirmed the efficiency of this strategy for the preparation of HMSP.
  10. The staple length and nature effect on the secondary  $\alpha$ -helix structure was assessed by circular dichroism experiments. For peptide stapling at positions *i,i+4*, the helical secondary structure was only promoted when the staple was located at specific stapling positions. On the other hand, peptide stapling between positions *i,i+7*, as well as double peptide stapling resulted in accommodation of the helical structure. Remarkably, the HMSP compounds exhibiting the highest helical conformation were a “large” stapled peptide holding two *N*-MeLys residues at the stapling entity and a double stapled peptide that incorporated a *N*-MeLys residues at both staple 1 and staple 2. The *N*-MeLys

free amine capacity to form H-bonds with the peptide backbone might account for additional helical stability.

11. These novel molecular architectures are highly versatile, since the length and flexibility of the staple can be modulated to screen the optimal HMSP combination in seek of an enhanced pharmacological profile.
12. The thioether-based cross-linking methodology turns into a convenient methodology to generate cyclic *N*-methylated peptides in a straightforward manner.





## **EXPERIMENTAL SECTION**



### 3.1 Materials and methods

#### 3.1.1 Solvents and reagents

##### 3.1.1.1 Solvents

All solvents were purchased to the suppliers Panreac, Scharlau, SDS, Sigma-Aldrich.

##### 3.1.1.1.1 Anhydrous solvents

- DCM: was distilled from CaH<sub>2</sub> under N<sub>2</sub> atmosphere.
- THF: a sodium wire and benzophenone were added to a volume of THF and refluxed under N<sub>2</sub> atmosphere.
- DMF was stored with 4 Å activated molecular sieves.

##### 3.1.1.2 Reagents

All the reagents were purchased to the suppliers Acros Organics, AlfaAesar, Bachem, Fluka, Fluorochem, Iris Biotech GmbH, MerckMillipore, Novabiochem, Sigma-Aldrich, TCI.

#### 3.1.2 Instrumentation

##### 3.1.2.1 General basic instrumentation

|                                 |  |
|---------------------------------|--|
| <b>BALANCES</b>                 | METTLER TOLEDO AG245<br>METTLER TOLEDO ME204<br>METTLER TOLEDO NEWCLASSIC MS |
| <b>Digital Heat Block</b>       | Thermo Scientific  |
| <b>Lyophilisers</b>             | Labcono<br>CHRIST Alpha 2-4 LD plus  |
| <b>Orbital shaker</b>           | HEIDOLPH Unimax 1010   |
| <b>Rotatory evaporators</b>     | HEIDOLPH Labrota 4003 Control  |
| <b>Vortex mixer</b>             | VELP Scientifica   |
| <b>Ultrasonic bath</b>          | Branson 3510   |
| <b>UV-Vis Spectrophotometer</b> | SEGONAM Uvikon XS  |

### 3.1.2.2 Chromatography

#### 3.1.2.2.1 Thin layer chromatography (TLC)

TLC was performed on an aluminium foil sheet, which was coated with a thin silica gel layer (stationary phase). The sample was applied on the plate and an appropriate solvent mixture (mobile phase) was eluted. Separation was accomplished due to different polarity of the compounds. A UV-Vis spectrophotometer was used to visualise the spots that absorbed UV light at 254 nm, and TLC staining solutions were used to visualise compounds that did not absorb UV light.

TLC staining solutions:

- Basic KMnO<sub>4</sub>: 40 g of K<sub>2</sub>CO<sub>3</sub> + 6 g of KMnO<sub>4</sub> in 600 mL of water, then 5 mL of 10% NaOH were added. The staining solution oxidises compounds containing diols, C=C, reactive methylenes, phenols, thiols, phosphines etc.
- Ninhydrin: 20 g of ninhydrin in 600 mL of ethanol. Primary amines produce blue spots at room temperature. Boc-protected primary amines produce spots on heating. Secondary amines are sometimes detected but the stain is weak.

#### 3.1.2.2.2 Column chromatography on silica gel

Column chromatography was performed using flash chromatography with Acros silica gel (35 – 70 µm).

#### 3.1.2.2.3 High performance liquid chromatography (HPLC)

##### 3.1.2.2.3.1 Analytical HPLC

Analytical HPLC was performed on a Waters instrument comprising a Waters 2695 (Waters, MA, USA) separation module, an automatic injector, a photodiode array detector (Waters 996 or Waters 2998) and a Millennium login system controller. The following columns were used: a Xbridge™ C18 reversed-phase analytical column (2.5 µm x 4.6 mm x 75 mm) and a SunFire™ C18 reversed-phase analytical column (3.5 µm x 4.6 mm x 100 mm). The analyses were run with linear gradients of H<sub>2</sub>O (0.045% TFA)

and ACN (0.036% TFA) over 8 min. UV detection was set at 220 nm and the system run at a flow rate of 1.0 mL/min.

Analytical HPLC was also performed on a Shimadzu instrument comprising a two solvent delivery pumps (Shimadzu LC-10AD), a degasser (Shimadzu DGU-14A), an automatic injector (Shimadzu SIL-10A XL), a Shimadzu dual wavelength detector (Shimadzu SPD-M10AVP), and a prominence communications bus module (Shimadzu CBM-20A). The column used was a XBridge™ C18 reversed-phase column (3.5 µm x 4.6 mm x 42 mm). Linear gradients of H<sub>2</sub>O (0.045% TFA) and ACN (0.036% TFA) over 15 min were used. The UV detection was set at 220 and 254 nm and the system run at a flow rate of 1.0 mL/min.

#### *3.1.2.2.3.2 Semi-analytical HPLC*

Semi-analytical HPLC was performed on a Shimadzu instrument comprising a two solvent delivery pumps (Shimadzu LC-10AD), a degasser (Shimadzu DGU-14A), an automatic injector (Shimadzu SIL-10A XL), a Shimadzu dual wavelength detector (Shimadzu SPD-M10AVP), and a prominence communications bus module (Shimadzu CBM-20A). The column used was a XBridge™ Peptide BEH C18 Prep reversed-phase 130Å column (5 µm x 10 mm x 100 mm). Linear gradients of H<sub>2</sub>O (0.045% TFA) and ACN (0.036% TFA) over 20 min were used. The UV detection was set at 220 and 254 nm and the system run at a flow rate of 2.0 mL/min.

#### *3.1.2.2.3.3 HPLC-MS*

HPLC-MS was performed on a Waters instrument comprising a Waters 2695 separation module, an automatic injector, a Waters 2996 photodiode array detector, a Waters ESI-MS Micromass ZQ 4000 spectrometer, and a Masslynx v4.1 system controller. HPLC-MS was also performed on a Waters instrument comprising a Waters 2795 separation module, an automatic injector, a Waters 2996 photodiode array detector, a Waters ESI-MS Micromass ZQ 2000 spectrometer and a Masslynx v4.1 system controller. The following columns were used: a Sunfire™ C18 reversed-phase analytical column (3.5 µm x 4.6 mm x 75 mm), and a XBridge™ C18 reversed-phase column (3.5 µm x 4.6 mm x 42 mm). The analyses were run with linear gradients of H<sub>2</sub>O

(0.1% HCOOH) and ACN (0.07% HCOOH) over 9 min. UV detection was set at 220 nm and the system run at a flow rate of 0.3 mL/min.

### 3.1.2.3 MALDI-TOF

Mass spectra were recorded on a MALDI-TOF Applied Biosystem 4700 with a N<sub>2</sub> laser of 337 nm using ACH matrix (10 mg/mL of ACH in ACN–H<sub>2</sub>O–TFA (1:1:0.1 v/v)).

Sample preparation: a mixture of sample solution (1 μL) and matrix (1 μL) was prepared, placed on a MALDI-TOF plate and dried by air.

### 3.1.2.4 Nuclear Magnetic Resonance (NMR)

<sup>1</sup>H and <sup>13</sup>C spectra were recorded on a Varian MERCURY 400 or a Bruker 400 MHz Avance III spectrometer for organic small molecules. Chemical shifts (δ) are expressed in parts per million downfield from tetramethylsilyl chloride. Coupling constants are expressed in Hertz.

### 3.1.2.5 Circular dichroism spectroscopy

Circular dichroism experiments were carried out in spectro-polarimeter (Jasco Inc., Easton MD USA and Spectra Manager version 1.53.01 (Jasco). The following parameter were used: sensitivity (standar (100 m·deg)), start (260 nm), end (190 nm), data pitch (0.5 nm), scanning mode (immediately), scanning speed (20 nm/min), response (1 sec), band width (1.0 nm) and accumulation (3).

## 3.1.3 Solid-Phase Peptide Synthesis (SPPS)

### 3.1.3.1 General considerations

Solid-phase synthesis was carried out manually in polypropylene syringes fitted with two polyethylene filter discs. All soluble reagents were removed by suction. Washings between deprotection and coupling were carried out with DMF (3 x 1 min) and DCM (3 x 1 min) using 4 mL solvent/g resin for each wash. When not specified all the transformations were performed at 25 °C. Short treatments were carried out with

manual stirring while longer transformations took place in orbital shakers. All the peptides were synthesised using the Fmoc/<sup>t</sup>Bu protection strategy.

### 3.1.3.2 Colorimetric test

#### 3.1.3.2.1 Kaiser test

The Kaiser or ninhydrin test is a colorimetric test that enables the qualitative detection of primary amines. It is commonly used in SPPS to monitor coupling and deprotection treatments. The peptide resin was washed with DCM and the solvents removed by suction. A few beads of the resin were placed on a glass tube and 6 drops of solution A and 2 drops of solution B were added. The tube was incubated at 110 °C for 3 minutes. A dark blue colour reveals the presence of free primary amines while a yellow coloration ensures 99 % of coupling rate.

- Solution A: A solution of phenol (400 g) in absolute EtOH (100 mL) was prepared. Some heating was needed to achieve complete dissolution of the phenol. 20 mL of a 10 mM aqueous KCN solution (65 mg of KCN in 100 mL of H<sub>2</sub>O) was added to freshly distilled pyridine (1000 mL). The two solutions were stirred with the ion exchange resin Amberlite MB-3 (40 g) for 45 minutes, then filtered and combined to obtain Solution A for Kaiser test.
- Solution B: Ninhydrin (2.5 g) was dissolved in absolute EtOH (50 mL). The ninhydrine reagent is light sensitive, thus, Solution B was kept in a flask protected from light.

#### 3.1.3.2.2 Chloranil test

The chloranil test is a colorimetric test used in SPPS that enables qualitative detection of free secondary amines. It is commonly used to monitor couplings onto proline or *N*-alkyl residues.

The peptide-resin was washed with DCM and the solvent was removed by suction. A few beads were transferred to a glass tube and 5 drops of a saturated chloranil solution in toluene were added. 20 drops of acetone were then added and the mixture

was shaken in a vortex mixer for 5 minutes at room temperature. The resin beads staining green indicate the presence of free secondary amines.

### **3.1.3.3 Conditioning of the resin and first amino acid incorporation**

The Rink Amide Aminomethyl resin and the 2-Chlorotrityl chloride resin were the resins of choice to carry out solid-phase peptide synthesis in the present thesis.

#### **3.1.3.3.1 Rink Amide Aminomethyl resin (Rink Amide AM)**

*Conditioning* of the resin consisted of washes with DMF (5 x 1 min) and DCM (5 x 1 min) to obtain an optimal swelling of the resin before incorporation of the first amino acid.

*Incorporation* of the first amino acid onto the Rink Amide AM resin is achieved through a peptide coupling between the corresponding Fmoc-protected amino acid and the free primary amine present in the resin. The loading of commercially available Rink Amide AM resin is often comprised between 0.1 – 0.7 mmol/g resin. The amine functionality of the resin is Fmoc-protected, hence Fmoc group removal is required prior to the first amino acid incorporation. The Fmoc group was removed by treatment with a solution of piperidine in DMF (1:4 v/v) (1 x 1 min + 1 x 5 min + 1 x 10 min). The resin was washed with DMF (3 x 1 min), DCM (3 x 1 min) and DMF (3 x 1 min). A solution of Fmoc-AA(PG)-OH–DIC–OxymaPure (5:5:5 eq) in DMF was added to the resin and shaken for one hour. A Kaiser test was carried out to check coupling completion. If necessary, more coupling cycles were performed until complete incorporation was accomplished.

#### **3.1.3.3.2 2-Chlorotrityl chloride resin (2-CTC)**

*Conditioning* of the resin consisted of washes with DMF (5 x 1 min) to eliminate hydrochloric acid traces, and with DCM (5 x 1 min) to obtain an optimal swelling of the resin before incorporation of the first amino acid.

*Incorporation* of the first amino acid onto the 2-CTC resin is achieved through a nucleophilic attack of the carboxylate form of the corresponding Fmoc-protected amino acid to form an ester bond. The loading of commercial 2-CTC is rather high (1.6 mmol/g resin), therefore aggregation may take place. Thus, a lower loading (0.3 – 0.8 mmol/g)

was achieved by the addition of a solution of the Fmoc-protected amino acid (0.3 – 0.8 equivalents) and DIEA (3 eq) in DCM onto the resin. After 10 minutes, more DIEA (7 eq) was added and the reaction mixture was shaken for 40 minutes. In order to terminate the excess of reactive positions, 800  $\mu$ L of MeOH/g resin were added and the reaction was shaken for 10 minutes. Then, the solvents were removed by suction, and the resin was washed with DCM (3 x 1 min), DMF (3 x 1 min) and DCM (3 x 1 min).

#### 3.1.3.3.2.1 Fmoc quantification and real loading determination

The loading capacity of the resin can be evaluated by quantifying the Fmoc-dibenzofulvene adduct formed during Fmoc removal of the first amino acid. Thus, while carrying out deprotection treatments and washes, all the fractions were collected in a volumetric flask and the UV absorbance at 290 nm of the resulting mixture was measured. The loading capacity was calculated as follows:

$$Real\ loading = \frac{A \cdot X}{\epsilon \cdot \gamma \cdot l}$$

Where: A (Absorbance), X (Volume of the solvent (mL)),  $\epsilon$  (Molar absorbance coefficient (5800 L  $\cdot$  mol<sup>-1</sup>  $\cdot$  cm<sup>-1</sup>)),  $\gamma$  (Resin weight (g)), l (Length of the cell (cm)).

#### 3.1.3.4 Cleavage from the resin and global deprotection protocols

Cleavage and global deprotection from either resin used in the present thesis (the Rink Amide AM or the 2-CTC resin) can be achieved by treatment of the peptidyl-resin with TFA and the appropriate scavenger mixture. According to the side chain groups present in the peptide sequence, a different cleavage cocktail is considered to be the most suitable for the system (Table 1).

| Side chain PG                   | Cleavage cocktail                         |
|---------------------------------|---|
| None                            | TFA                                       |
| <sup>t</sup> Bu and/or Boc      | TFA–H <sub>2</sub> O (95:5 v/v)           |
| Trt                             | TFA–TIS (95:5 v/v)                        |
| Trt, <sup>t</sup> Bu and/or Boc | TFA–H <sub>2</sub> O–TIS (95:2.5:2.5 v/v) |

Table 1. Cleavage cocktail mixture according to the side-chain protecting groups.

#### 3.1.3.4.1 Rink Amide Aminomethyl resin

Cleavage of the peptide from the Rink Amide AM resin provides the peptide with an amide function at the C-terminus. Cleavage can only be achieved by treatment of the resin upon strong acidic conditions, thus furnishing the peptide with all the free side-chain functionalities.

- Protocol Cle1 (*Cleavage from the resin and global deprotection*): After washes with DCM (3 x 1 min), the resin was treated with the most suitable cocktail mixture for one hour (10 mL/g resin). The mixture was collected in a falcon containing cold TBDME, in which the peptide precipitated. The precipitate was washed three times with cold TBDME. A mixture of H<sub>2</sub>O–ACN (1:1 v/v) was added and the resulting mixture was lyophilised.

#### 3.1.3.4.2 2-Chlorotrityl chloride resin

Cleavage of the peptide from the 2-CTC resin provides the peptide with the acid function at the C-terminus, therefore enabling cyclisation in solution. *Protocol Cle2* was used to obtain the fully unprotected cleaved peptide. *Protocol Cle3* and *Protocol Cle4* afforded the cleaved peptide furnished with all the side-chain protecting group functionalities. *Protocol Cle5* was the procedure of choice when cleavage and global deprotection under anhydrous conditions were required.

- Protocol Cle2 (*Cleavage from the resin and global deprotection*): After washes with DCM (3 x 1 min), the resin was treated with the most suitable cocktail mixture (see Table 1) (1 x 1 min + 2 x 5 min) (10 mL/g resin). The mixture fractions were collected in a round bottom flask and let to stir for 50 minutes to achieve full deprotection. The solvent was removed under reduced pressure until a small volume was left. The resulting volume was then transferred to a falcon containing cold TBDME, in which the peptide precipitated. The precipitate was washed three times with cold TBDME. A mixture of H<sub>2</sub>O–ACN (1:1 v/v) was added and the resulting mixture was lyophilised.
- Protocol Cle3 (*Cleavage from the resin*): Cleavage from the resin was achieved by treatment with a TFA–DCM (2:98 v/v) (1 x 1 min + 2 x 5 min) (10 mL/g resin)

mixture. The resin was then washed with DCM until the colour of the resin changed from red to original yellow. All the fractions were collected in a round-bottomed flask containing H<sub>2</sub>O (15 mL/0.2 g resin). A N<sub>2</sub> flow was bubbled through to evaporate the TFA and the DCM present in the mixture. The resulting mixture was freeze-dried.

- **Protocol *Cle4* (Cleavage from the resin):** After washes with DCM (3 x 1 min), the resin was treated with a HFIP–DCM (1:4 v/v) (10 mL/ g resin) (60 min) solution and washed with DCM until the colour of the resin changed from red to original yellow. All the fractions were collected in a round-bottomed flask and the solvent was removed under a N<sub>2</sub> flow. The crude product was dissolved in a H<sub>2</sub>O–ACN (1:1 v/v) mixture and lyophilised.
- **Protocol *Cle5* (Cleavage and global deprotection under anhydrous conditions):** Cleavage from the resin and global deprotection was achieved by treatment of the peptide-resin with a TFA–TIS–dry DCM (90:5:5 v/v) (1 x 1 min + 2 x 5 min) (10 mL/ g resin) mixture under anhydrous conditions. All the fractions were collected in a round-bottomed flask and let to stir for 30 min to achieve full removal of the protecting groups. A N<sub>2</sub> flow was bubbled through the reaction mixture to evaporate the solvents. The crude product was lyophilised.

#### **3.1.3.4.3 Peptide “mini-cleavage” to monitor reaction conversion**

- **Protocol *MC*:** To evaluate reaction conversion when performing a reaction on solid-phase, a small aliquot of the peptidyl-resin was treated with the appropriate cleavage cocktail. A N<sub>2</sub> flow was bubbled through to remove all the solvent, followed by the addition of a H<sub>2</sub>O/ACN (1:1 v/v) mixture. The sample was then analysed by HPLC-MS.

### **3.1.4 Peptide purification**

#### **3.1.4.1 Semi-analytical reversed-phase equipment**

Most peptides were purified using a HPLC-reversed phase equipment. Semi-analytical HPLC was performed on a Shimadzu instrument comprising a two solvent delivery pumps (Shimadzu LC-10AD), a degasser (Shimadzu DGU-14A), an automatic

injector (Shimadzu SIL-10A XL), a Shimadzu dual wavelength detector (Shimadzu SPD-M10AVP), and a prominence communications bus module (Shimadzu CBM-20A). The column used was a XBridge™ Peptide BEH C18 Prep reversed-phase 130Å column (5 µm x 10 mm x 100 mm). Linear gradients of H<sub>2</sub>O (0.045% TFA) and ACN (0.036% TFA) over 20 min were used. The UV detection was set at 220 and 254 nm and the system run at a flow rate of 2.0 mL/min

Sample preparation: the peptide crude was dissolved in the minimal amount of a H<sub>2</sub>O–ACN solution, in which the ACN percentage depended on the sample nature. The resulting solution was filtered through a 0.45 mm nylon filter and the optimal HPLC binary gradient was chosen according to the sample complexity. The collected fractions were analysed by HPLC-MS and the combined pure fractions were freeze-dried.

#### **3.1.4.2 Porapak™ Rxn Cartridges**

Peptide and/or small polar molecules purification using reversed-phase Porapak™ Rxn Cartridges turns out convenient if the purification is foreseen facile or salts need to be removed from a sample. The cartridge sorbents are available in fritted syringe-barrels devices in 6cc, 20cc and 60cc volumes. The cartridge size was chosen according to the amount of crude product.

Sample preparation and purification: the crude product was dissolved in the minimal amount of a H<sub>2</sub>O–ACN solution, in which the ACN percentage depended on the sample nature. The cartridge was first conditioned with MeOH, followed by the sample loading. The sample was eluted with a gradient of H<sub>2</sub>O–ACN. The binary gradient was chosen according to the sample complexity. The collected fractions were analysed by HPLC-MS and the combined pure fractions were freeze-dried.

#### **3.1.5 Peptide characterisation**

Peptide characterisation was performed by HPLC-MS, MALDI-TOF and/or HRMS analysis. HPLC-PDA analysis was employed to confirm peptide purity.

## 3.2 Chapter 1

### 3.2.1 General protocols

#### 3.2.1.1 Solid-phase synthesis protocols

##### 3.2.1.1.1 Peptide coupling protocols

The peptide chain elongation can be accomplished by using several protocols. Herein described the ones used in the present thesis. All the coupling treatments were performed at 25 °C unless stated otherwise. After one minute of manual stirring, the reaction mixture was shaken in an orbital shaker. Coupling conversion was checked by means of the appropriate colorimetric test and re-coupling was carried out if required.

- Protocol Pep1: was used when coupling onto primary amines.

| Step | Treatment         | Conditions   |
|------|-------------------|--|
| 1    | Washes            | DMF (3 x 1 min) + DCM (3 x 1 min) + DMF (3 x 1 min)          |
| 2    | Deprotection      | Piperidine–DMF (1:4 v/v) (1 x 1 min + 2 x 5 min)             |
| 3    | Washes            | DMF (3 x 1 min) + DCM (3 x 1 min) + DMF (3 x 1 min)          |
| 4    | Coupling*         | Fmoc-AA(PG)-OH–OxymaPure–DIC (3:3:3 eq)<br>in DMF for 40 min |
| 5    | Washes            | DMF (3 x 1 min) + DCM (3 x 1 min)                            |
| 6    | Colorimetric test | Kaiser test  |

\*To prevent racemisation, the amino acid was pre-activated with the coupling reagent (DIC) and the additive (OxymaPure) for 5 minutes before addition of the pre-activated solution to the resin-bound.

- Protocol Pep2: was used when coupling onto secondary amines.

| Step | Treatment         | Conditions   |
|------|-------------------|--|
| 1    | Washes            | DMF (3 x 1 min) + DCM (3 x 1 min) + DMF (3 x 1 min)          |
| 2    | Deprotection      | Piperidine–DMF (1:4 v/v) (1 x 1 min + 2 x 10 min)            |
| 3    | Washes            | DMF (3 x 1 min) + DCM (3 x 1 min) + DMF (3 x 1 min)          |
| 4    | Coupling*         | Fmoc-AA(PG)-OH–HATU–HOAt–DIEA (3:3:3:6 eq)<br>in DMF for 1 h |
| 5    | Washes            | DMF (3 x 1 min) + DCM (3 x 1 min)                            |
| 6    | Colorimetric test | Chloranil test   |

### 3.2.1.1.2 On-resin Steglich esterification

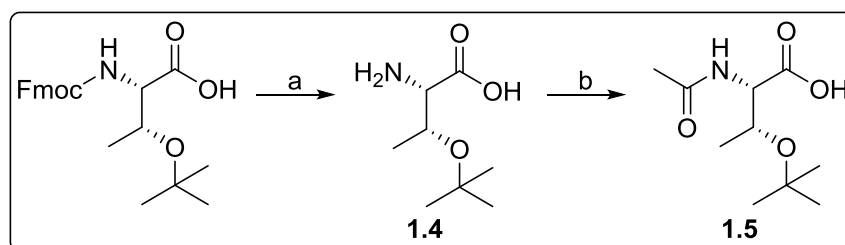
On-resin Steglich esterification allows the activation of the amino acid with a carbodiimide, *via* the traditional *O*-acylurea mechanism (DIC/AA, 1:1) or the anhydride intermediate formation (DIC/AA, 2:1). The activated specie reacts with the free alcohol in the presence of catalytic DMAP, which enhances the nucleophilicity of the hydroxyl moiety.

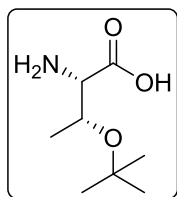
In the present thesis, esterification was accomplished through the *O*-acylurea mechanism. The reagents and solvents ratio used are described as follows: AA–DIC–DMAP (8:8:0.5 eq) in dry DCM/DMF (9:1 v/v).

- Protocol Est: The peptidyl-resin was washed with dry DCM (3 x 1 min) and it was dried under *vacuum* for 20 minutes. The peptide-resin was transferred to a pyrex® culture tube provided with a magnetic stirrer. A solution containing AA–DIC (8:8 eq) in dry DCM was pre-activated for 5 minutes before it is added to the tube. A solution of DMAP (0.5 eq) in dry DMF was also added to the tube and reacted for 2 hours and 30 minutes at 35 °C. The reaction mixture was cooled to rt, transferred to a polypropylene syringe fitted with two polyethylene discs and washed with dry DCM (3 x 1 min), DMF (3 x 1 min) and DCM (3 x 1 min). Reaction completion was monitored by HPLC-MS.

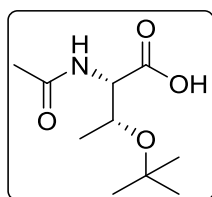
## 3.2.2 Preparation of the building blocks

### 3.2.2.1 Synthesis of 1.5



**Compound 1.4** (*O*-(*tert*-butyl)-*L*-threonine)

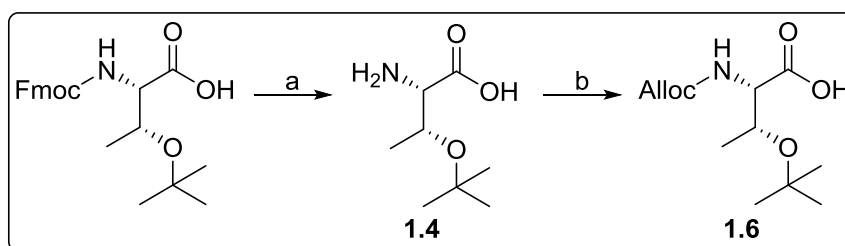
Fmoc-Thr(*t*Bu)-OH (740 mg, 1.86 mmol, 1.0 eq) was dissolved in dry DCM (6 mL), and Et<sub>2</sub>N (1.9 mL) was added. The yellow solution was let to stir at rt for 4 h. The solvent was removed under reduced pressure. DCM (40 mL) and an aqueous NaHCO<sub>3</sub> solution (40 mL) were added, and the aqueous layer was washed with DCM (2 x 30 mL). The pH was brought to 4–5, and the aqueous phase was extracted with DCM (3 x 40 mL). The combined organic layers were dried over MgSO<sub>4</sub> and filtered off. The solvent was removed under *vacuum* to afford **1.4** (277 mg, 85%) as a white solid. The crude product was used without further purification. <sup>1</sup>H NMR (400 MHz, CD<sub>3</sub>OD) δ 4.41 – 4.34 (m, 1H), 3.81 (d, *J* = 1.9 Hz, 1H), 1.31 (d, *J* = 6.5 Hz, 3H), 1.19 (s, 9H). <sup>13</sup>C NMR (101 MHz, CD<sub>3</sub>OD) δ 170.8, 75.9, 66.9, 60.0, 28.7, 21.4. ESI(+)**MS** *m/z* calculated for C<sub>8</sub>H<sub>17</sub>NO<sub>3</sub> 176.1, found [M + H]<sup>+</sup> 177.9.

**Compound 1.5** (*N*-acetyl-*O*-(*tert*-butyl)-*L*-threonine)

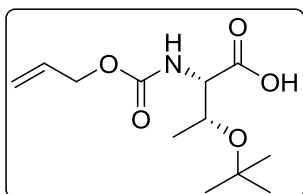
AcOH (90 μL, 1.59 mmol, 1.0 eq), EDC·HCl (305 mg, 1.59 mmol, 1.0 eq) and DIEA (276 μL, 1.59 mmol, 1.0 eq) were placed in a round bottom flask and DCM (8 mL) was added. After 5 min, a solution of **1.4** (277, 1.59 mmol, 1.0 eq) in dry DCM (3 mL) was added to the reaction mixture, followed by addition of a DMAP (19 mg, 0.60 mmol, 0.1 eq) solution in DMF (1 mL). After 3 h and 30 min, the organic layer was washed with an aqueous 10% NH<sub>4</sub>Cl solution (3 x 10 mL), with brine (10 mL), dried over MgSO<sub>4</sub>, and filtered off. The solvent was removed under *vacuum* to afford **1.5** (137 mg, 100%) as a

yellow oil. The crude product was used without further purification.  $^1\text{H NMR}$  (400 MHz,  $\text{CDCl}_3$ )  $\delta$  6.73 (d,  $J = 6.5$  Hz, 1H), 4.54 – 4.47 (m, 1H), 4.38 – 4.29 (m, 1H), 2.13 (s, 3H), 1.24 (s, 9H), 1.14 (d,  $J = 6.4$  Hz, 3H).  $^{13}\text{C NMR}$  (101 MHz,  $\text{CDCl}_3$ )  $\delta$  172.8, 172.7, 76.6, 66.5, 57.8, 28.2, 22.7, 18.9. **ESI(+)**MS  $m/z$  calculated for  $\text{C}_{10}\text{H}_{19}\text{NO}_4$  217.1, found  $[\text{M} + \text{H}]^+$  218.1.

### 3.2.2.2 Synthesis of 1.6



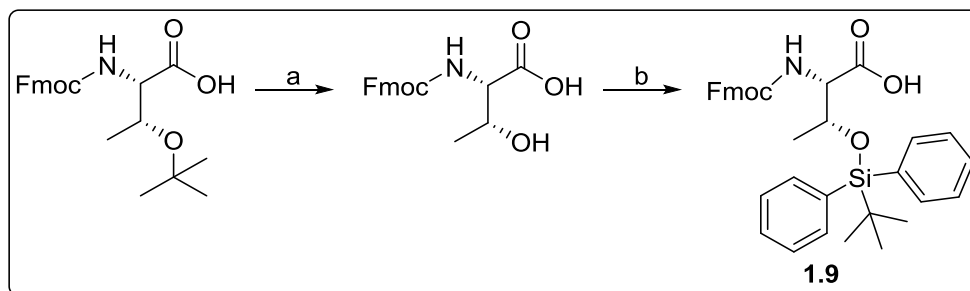
#### Compound 1.6 (*N*-((allyloxy)carbonyl)-*O*-(*tert*-butyl)-*L*-threonine)



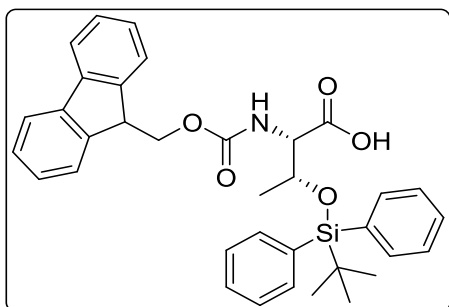
Allyl chloroformate (152  $\mu\text{L}$ , 1.43 mmol, 1.0 eq) was dissolved in dioxane (734  $\mu\text{L}$ ) and a solution of  $\text{NaN}_3$  (93 mg, 1.72 mmol, 1.2 eq) in water (470  $\mu\text{L}$ ) was added. The emulsion was let to stir for 2 h. The reaction was monitored by TLC ( $R_{\text{f}}^{\text{Alloc-azide}}$  (DCM) = 0.73). **1.4** (250 mg, 1.43 mmol, 1.0 eq) was dissolved in a 2% aqueous  $\text{Na}_2\text{CO}_3$ -dioxane (1:1 v/v, 2.3 mL) solution and added to the reaction mixture. The pH was adjusted to 9–10 by dropwise addition of a saturated aqueous solution of  $\text{NaOH}$  until pH 7, and an aqueous saturated solution of  $\text{Na}_2\text{CO}_3$  until the desired pH was reached. The reaction was monitored by TLC. After 6 h, the aqueous phase was washed with TBDME (3 x 15 mL) and the pH was dropped to 4–5 by dropwise addition of a 1 M  $\text{HCl}$  aqueous solution. The aqueous phase was extracted with  $\text{EtOAc}$  (3 x 15 mL), and the combined organic layers were dried over  $\text{MgSO}_4$  and filtered off. The solvent was removed under *vacuo* to afford the crude product **1.6** (371 mg, 100%) as yellow oil.  $^1\text{H NMR}$  (400 MHz,  $\text{CDCl}_3$ )  $\delta$

8.69 (bs, 1H), 5.98 – 5.86 (m, 1H), 5.70 (d,  $J = 6.1$  Hz, 1H), 5.28 (dd,  $J = 35.5, 13.8$  Hz, 2H), 4.59 (d,  $J = 4.8$  Hz, 2H), 4.35 – 4.25 (m, 1H), 1.26 (s, 9H), 1.17 (d,  $J = 6.2$  Hz, 3H).  $^{13}\text{C}$  NMR (101 MHz,  $\text{CDCl}_3$ )  $\delta$  173.0, 156.5, 132.4, 118.2, 76.7, 66.9, 66.3, 58.7, 28.2, 18.4. HRMS-ESI(-)  $m/z$  calculated for  $\text{C}_{12}\text{H}_{21}\text{NO}_5$  259.1341, found  $[\text{M} - \text{H}]^-$  258.1352.

### 3.2.2.3 Synthesis of 1.9



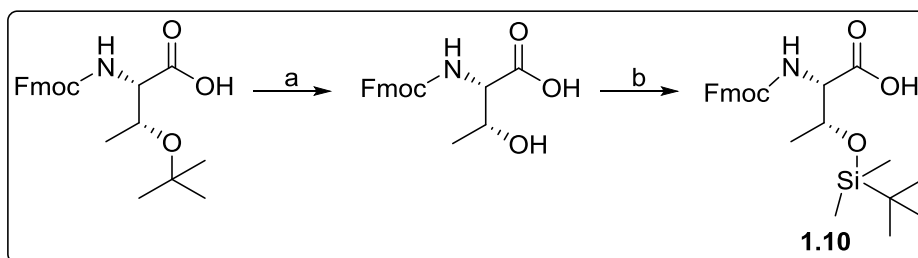
**Compound 1.9** (*N*-(((9H-fluoren-9-yl)methoxy)carbonyl)-*O*-(*tert*-butyldiphenylsilyl)-*L*-threonine)



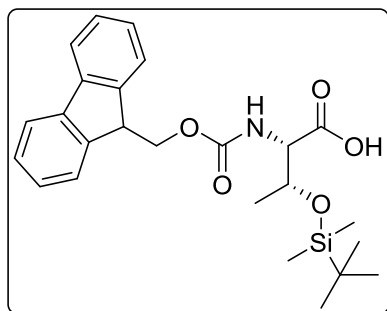
Fmoc-Thr(*t*Bu)-OH (2.000 g, 5.00 mmol, 1.0 eq) was dissolved in a TFA–DCM (9:1 v/v, 40 mL) mixture and let to stir at rt. After 1 h, the solvent was removed under reduced pressure and co-evaporated with DCM (3 x 20 mL), toluene (3 x 20 mL) and  $\text{Et}_2\text{O}$  (3 x 20 mL) to afford Fmoc-Thr-OH (1.707 g, 100%) as white solid. TBDPS-Cl (300  $\mu\text{L}$ , 1.16 mmol, 1.5 eq) was dissolved in ACN (10 mL) and the reaction mixture was cooled to 0 °C with an ice bath. A solution of Fmoc-Thr-OH (261 mg, 0.77 mmol, 1.0 eq) in ACN (10 mL) was added, followed by dropwise addition of DBU (173  $\mu\text{L}$ , 1.16 mmol, 1.5 eq). The reaction mixture was brought to rt and let to stir for 20 h. The crude product was purified by flash chromatography on silica gel (DCM/MeOH, 1:0  $\rightarrow$  9:1) to afford **1.9** (53 mg,

12%) as white solid.  $^1\text{H NMR}$  (400 MHz, DMSO)  $\delta$  7.89 (d,  $J = 7.5$  Hz, 2H), 7.74 (d,  $J = 7.4$  Hz, 2H), 7.70 – 7.67 (m, 3H), 7.45 – 7.29 (m, 11H), 7.04 (d,  $J = 8.8$  Hz, 1H), 4.32 – 4.22 (m, 3H), 4.11 – 4.06 (m, 1H), 3.97 – 3.93 (m, 1H), 1.09 (d,  $J = 6.3$  Hz, 3H), 0.95 (s, 9H).  $^{13}\text{C NMR}$  (101 MHz, DMSO)  $\delta$  172.4, 156.4, 143.9, 143.8, 140.7, 140.7, 136.4, 134.5, 129.2, 127.7, 127.5, 127.1, 125.4, 125.3, 120.1, 66.4, 65.8, 59.9, 46.7, 26.6, 20.3, 18.7. **HRMS-ESI(+)**  $m/z$  calculated for  $\text{C}_{35}\text{H}_{37}\text{NO}_5\text{Si}$  579.2441, found  $[\text{M} + \text{Na}]^+$  602.2340.

### 3.2.2.4 Synthesis of 1.10



**Compound 1.10** (*N*-(((9H-fluoren-9-yl)methoxy)carbonyl)-*O*-(*tert*-butyldimethylsilyl)-*L*-threonine)

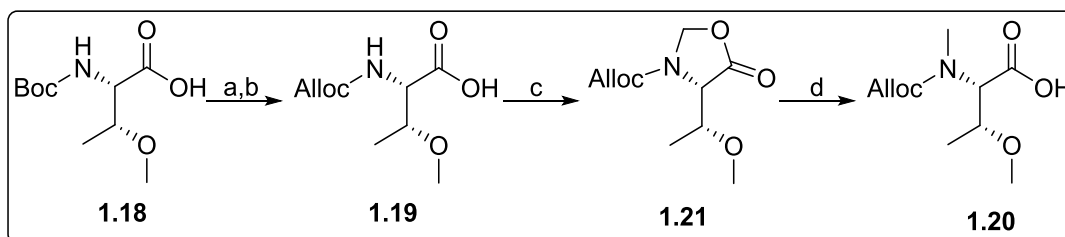


Fmoc-Thr(*t*Bu)-OH (2.000 g, 5.00 mmol, 1.0 eq) was dissolved in a TFA–DCM (9:1 v/v, 40 mL) mixture and let to stir at rt. After 1 h, the solvent was removed under reduced pressure and co-evaporated with DCM (3 x 20 mL), toluene (3 x 20 mL) and Et<sub>2</sub>O (3 x 20 mL) to afford Fmoc-Thr-OH (1.707 g, 100%) as white solid.

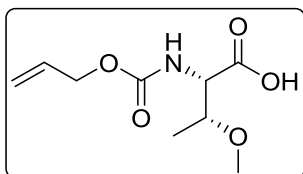
Fmoc-Thr-OH (860 mg, 2.52 mmol, 1.0 eq) was dissolved in dry DCM (50 mL) and imidazole (686 mg, 10.08 mmol, 4.0 eq) was added. The reaction mixture was cooled to 0 °C with an ice bath, followed by addition of TBDMS-Cl (2.137 g, 7.58 mmol, 3.0 eq).

The suspension was brought to rt and it was let to stir for 24 h under N<sub>2</sub> atmosphere. The solvent was removed under reduced pressure and the crude product was purified by flash chromatography on silica gel (DCM/MeOH, 1:0 → 8:2) to afford **1.10** (616 mg, 54%) as white solid. <sup>1</sup>H NMR (400 MHz, CDCl<sub>3</sub>) δ 7.77 (d, J = 7.5 Hz, 2H), 7.62 (d, J = 5.0 Hz, 1H), 7.60 (d, J = 4.6 Hz, 1H), 7.40 (t, J = 7.4 Hz, 2H), 7.32 (t, J = 7.4 Hz, 2H), 5.58 (d, J = 7.6 Hz, 1H), 4.48 – 4.37 (m, 3H), 4.33 (dd, J = 7.7, 2.8 Hz, 1H), 4.26 (t, J = 7.1 Hz, 1H), 1.21 (d, J = 6.3 Hz, 3H), 0.91 (s, 9H), 0.13 (d, J = 3.3 Hz, 6H). <sup>13</sup>C NMR (101 MHz, CDCl<sub>3</sub>) δ 175.1, 156.6, 144.0, 143.8, 141.5, 141.4, 127.9, 127.2, 125.3, 125.3, 120.1, 68.7, 67.4, 59.5, 47.3, 25.8, 20.1, 18.0, -4.4, -5.0. ESI(+)**MS** m/z calculated for C<sub>25</sub>H<sub>33</sub>NO<sub>5</sub>Si 455.2, found [M + Na]<sup>+</sup> 478.1.

### 3.2.2.5 Synthesis of 1.20



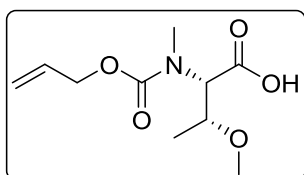
**Compound 1.19** (*N*-((allyloxy)carbonyl)-*O*-methyl-*L*-threonine)



Boc-Thr(Me)-OH (1.003 g, 4.30 mmol, 1.0 eq) was treated with a mixture of TFA–DCM (4:6 v/v, 40 mL). After 2 h, the solvent was evaporated under reduced pressure and co-evaporated with DCM (3 x 10 mL), toluene (3 x 10 mL) and Et<sub>2</sub>O (3 x 10 mL). The resulting crude product **1.18** (572 mg, 100%) was obtained as yellow oil and it was reacted without further purification. ESI(+)**MS** m/z calculated for C<sub>5</sub>H<sub>12</sub>NO<sub>3</sub> 133.1, found [M+H]<sup>+</sup> 133.9

In parallel, allyl chloroformate (456  $\mu\text{L}$ , 4.29 mmol, 1.0 eq) was dissolved in dioxane (2.2 mL) and a solution of  $\text{NaN}_3$  (279 mg, 5.15 mmol, 1.2 eq) in water (1.4 mL) was added. The emulsion was let to stir for 2 h. The reaction was monitored by TLC ( $R_{\text{f}}^{\text{Alloc-azide}}$  (DCM) = 0.73). **1.18** (572 mg, 4.29 mmol, 1.0 eq) was dissolved in a 2% aqueous  $\text{Na}_2\text{CO}_3$ -dioxane (1:1, 7 mL) solution and added to the reaction mixture. The pH was adjusted to 9–10 by dropwise addition of a saturated aqueous solution of NaOH until pH 7, and an aqueous saturated solution of  $\text{Na}_2\text{CO}_3$  until the desired pH was reached. The reaction was monitored by TLC. After 6 h, the aqueous phase was washed with TBDME (3 x 40 mL) and the pH was dropped to 1.5 by dropwise addition of a 1 M HCl aqueous solution. The aqueous phase was extracted with EtOAc (3 x 50 mL), and the combined organic layers were dried over  $\text{MgSO}_4$  and filtered off. The solvent was removed under *vacuo* to afford the crude product **1.19** (907 mg, 97%) as brown oil.  $^1\text{H}$  NMR (400 MHz,  $\text{CDCl}_3$ )  $\delta$  = 6.01 – 5.76 (m, 1H), 5.62 (d,  $J$  = 8.5 Hz, 1H), 5.39 – 5.15 (m, 2H), 4.60 (d,  $J$  = 5.5 Hz, 2H), 4.38 (dd,  $J$  = 8.9, 2.2 Hz, 1H), 4.02 - 4.00 (m, 1H), 3.34 (s, 3H), 1.23 (d,  $J$  = 6.3 Hz, 3H), 1.22 (s, 1H).  $^{13}\text{C}$  NMR ( $\text{CDCl}_3$ , 400 MHz)  $\delta$  = 175.0, 156.7, 132.4, 117.9, 76.1, 66.1, 58.1, 56.9, 15.3. ESI(+)-MS  $m/z$  calculated for  $\text{C}_9\text{H}_{15}\text{NO}_5$  217.1, found  $[\text{M} + \text{H}]^+$  217.9.

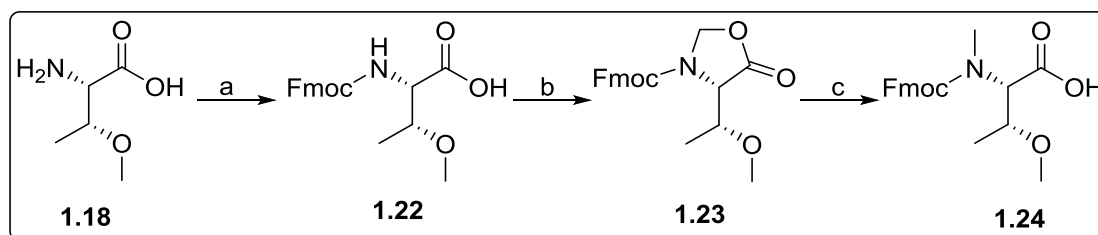
**Compound 1.20** (*N*-((allyloxy)carbonyl)-*N,O*-dimethyl-*L*-threonine)



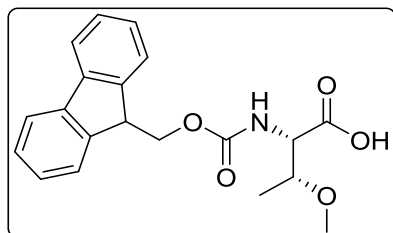
*p*-TsOH (110 mg, 0.55 mmol, 0.1 eq) and *p*-formaldehyde (152 mg, 5.06 mmol, 1.1 eq) were placed in a 2-neck round bottom flask and dissolved in dry toluene (8 mL). A solution of **1.19** (1.000 g, 4.60 mmol, 1.0 eq) in toluene (5 mL) was added dropwise, and the yellow suspension was brought to reflux. A Dean stark trap was used to remove the water formed during the reaction. After 3 h, EtOAc (150 mL) and a 5% aqueous  $\text{Na}_2\text{CO}_3$  solution (150 mL) were added. The organic layer was washed with a 5% aqueous  $\text{Na}_2\text{CO}_3$  solution (2 x 150 mL),  $\text{H}_2\text{O}$  (2 x 150 mL), brine (150 mL), dried over  $\text{MgSO}_4$ , and filtered off. The solvent was removed under *vacuum* to afford **1.21** (940 mg, 89%) as a

yellow oil. **ESI(+)**MS  $m/z$  calculated for  $C_{10}H_{15}NO_5$  229.1, found  $[M + 2H]^+$  231.8. The crude product was used without further. **1.21** (141 mg, 0.62 mmol, 1.0 eq) was dissolved in dry DCM (4.0 mL) and TIS (508  $\mu$ L, 2.48 mmol, 4.0 eq) was added, followed by addition of TFA (3.6 mL). The yellow solution was stirred for 14 h under  $N_2$  atmosphere. The solvent was removed under *vacuo* and the crude product was subjected to flash chromatography on silica gel (DCM/MeOH, 1:0  $\rightarrow$  9:1) to afford pure **1.20** (138 mg, 82%) as yellow oil.  **$^1H$  NMR** (400 MHz,  $CDCl_3$ )  $\delta$  6.01 – 5.85 (m, 1H), 5.36 – 5.17 (m, 2H), 4.95 (d,  $J = 4.7$  Hz, 1H), 4.65 – 4.58 (m,  $J = 9.9, 5.8$  Hz, 2H), 4.10 – 3.98 (m, 1H), 3.33 (s, 3H), 3.04 (s, 3H), 1.20 (d,  $J = 6.3$  Hz, 3H).  **$^{13}C$  NMR** (101 MHz,  $CDCl_3$ )  $\delta$  174.7, 157.8, 132.9, 117.5, 76.6, 66.8, 63.3, 57.4, 33.3, 15.4. **HRMS-ESI(-)**  $m/z$  calculated for  $C_{10}H_{17}NO_5$  231.2400, found  $[M - H]^-$  230.1037.

### 3.2.2.6 Synthesis of 1.24



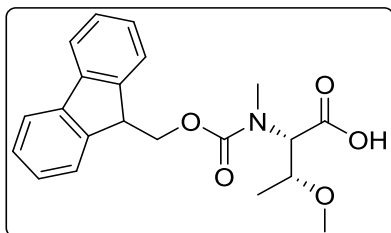
**Compound 1.22** (*N*-(((9H-fluoren-9-yl)methoxy)carbonyl)-*O*-methyl-*L*-threonine)



Boc-Thr(Me)-OH (1.003 g, 4.30 mmol, 1.0 eq) was treated with a mixture of TFA–DCM (4:6 v/v, 40 mL). After 2 h, the solvent was evaporated under reduced pressure and co-evaporated with DCM (3 x 10 mL), toluene (3 x 10 mL) and  $Et_2O$  (3 x 10 mL). The resulting crude product **1.18** (572 mg, 100%) was obtained as yellow oil and it was reacted without further purification. **1.18** (572 mg, 4.29 mmol, 1.0 eq) was dissolved in

dioxane (13 mL) and a 10% aqueous  $\text{Na}_2\text{CO}_3$  (19 mL) solution was added. A solution of Fmoc-OSu (1.838 g, 5.59 mmol, 1.3 eq) in dioxane (12 mL) was added dropwise and the suspension was let to stir for 22 h.  $\text{H}_2\text{O}$  (20 mL) was added and the aqueous layer was washed with  $\text{Et}_2\text{O}$  (2 x 15 mL) and acidified to pH 4–5 by addition of a 1.0 M HCl solution. The aqueous layer was extracted with EtOAc (3 x 30 mL) and the crude product was subjected to flash chromatography on silica gel (DCM/MeOH, 1:0  $\rightarrow$  9:1) to afford pure **1.22** (917 mg, 60%) as white solid.  $^1\text{H NMR}$  (400 MHz,  $\text{CDCl}_3$ )  $\delta$  7.77 (d,  $J = 7.5$  Hz, 2H), 7.61 (m, 2H), 7.40 (t,  $J = 7.5$  Hz, 2H), 7.33 (dd,  $J = 7.4, 0.8$  Hz, 2H), 5.56 (d,  $J = 8.0$  Hz, 1H), 4.42 (t,  $J = 7.9$  Hz, 3H), 4.24 (t,  $J = 7.0$  Hz, 1H), 4.04 – 3.98 (m, 1H), 3.41 (s, 3H), 1.22 (d,  $J = 6.3$  Hz, 3H).  $^{13}\text{C NMR}$  (101 MHz,  $\text{CDCl}_3$ )  $\delta$  143.8, 141.5, 127.9, 127.2, 125.3, 120.2, 102.8, 76.1, 67.5, 57.9, 47.3, 15.1. **ESI(+)**MS  $m/z$  calculated for  $\text{C}_{20}\text{H}_{21}\text{NO}_5$  355.1, found  $[\text{M} + \text{H}]^+$  356.3.

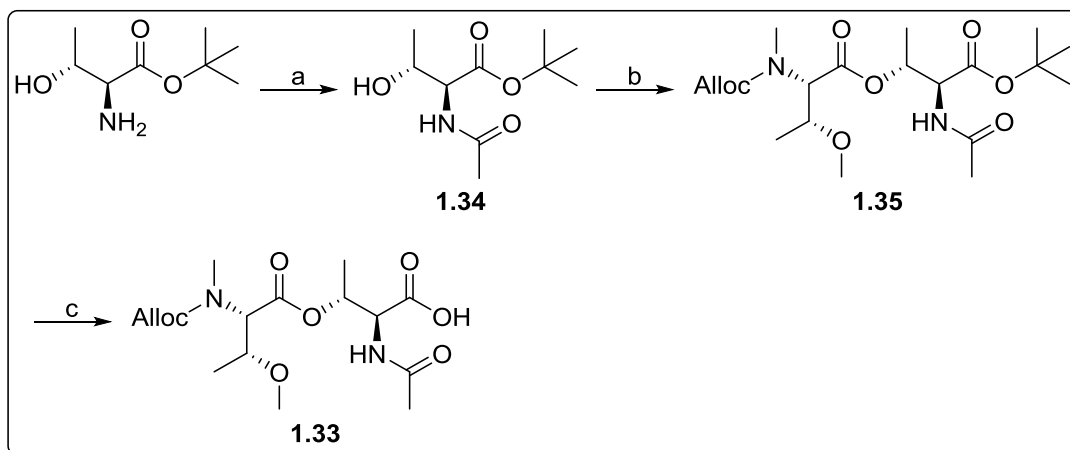
**Compound 1.24** (*N*-(((9H-fluoren-9-yl)methoxy)carbonyl)-*N,O*-dimethyl-*L*-threonine)



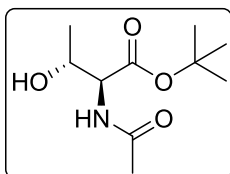
*p*-TsOH (62 mg, 0.31 mmol, 0.1 eq) and *p*-formaldehyde (85 mg, 2.84 mmol, 1.1 eq) were placed in a 2-neck round bottom flask and dissolved in dry toluene (4.5 mL). A solution of **1.22** (917 mg, 2.58 mmol, 1.0 eq) in toluene (3 mL) was added dropwise, and the yellow suspension was brought to reflux. A Dean stark trap was used to remove the water formed during the reaction. After 3 h, EtOAc (80 mL) and a 5% aqueous  $\text{Na}_2\text{CO}_3$  solution (80 mL) were added. The organic layer was washed with a 5% aqueous  $\text{Na}_2\text{CO}_3$  solution (2 x 80 mL),  $\text{H}_2\text{O}$  (2 x 80 mL), brine (80 mL), dried over  $\text{MgSO}_4$ , and filtered off. The solvent was removed under *vacuum* to afford **1.23** (531 mg, 56%) as a yellow oil. **ESI(+)**MS  $m/z$  calculated for  $\text{C}_{21}\text{H}_{21}\text{NO}_5$  367.1, found  $[\text{M} + \text{H}]^+$  368.3. The crude product was used without further purification. **1.23** (531 mg, 2.32 mmol, 1.0 eq) was dissolved in dry DCM (9.3 mL) and TIS (1179  $\mu\text{L}$ , 5.75 mmol, 4.0 eq) was added, followed by the addition of TFA (8.4 mL). The yellow solution was stirred for 14 h under  $\text{N}_2$  atmosphere.

The solvent was removed under *vacuo* and the crude product was subjected to flash chromatography on silica gel (DCM/MeOH, 1:0 → 9:1) to afford pure **1.24** (781 mg, 82%) as white solid.  $^1\text{H NMR}$  (400 MHz,  $\text{CDCl}_3$ , rotamers)  $\delta$  7.80 – 7.72 (m, 2H), 7.65 – 7.51 (m, 2H), 7.43 – 7.28 (m, 4H), 4.94 (d,  $J = 4.9$  Hz, 1H), 4.55 – 4.42 (m, 2H), 4.33 – 4.21 (m, 1H), 4.12 – 4.01 (m, 1H), 3.34 + 3.27 (s, 3H), 3.07 + 2.99 (s, 3H), 1.19 + 1.04 (d,  $J = 6.3$  Hz, 3H).  $^{13}\text{C NMR}$  (101 MHz,  $\text{CDCl}_3$ , rotamers)  $\delta$  179.7, 157.9, 141.5, 132.9, 127.9, 127.2, 125.2, 120.2, 77.3, 76.7, 68.2, 57.4, 47.4 (47.4), 34.0 (33.6), 15.5 (15.4). **HRMS-ESI(+)**  $m/z$  calculated for  $\text{C}_{21}\text{H}_{23}\text{NO}_5$  369.1654, found  $[\text{M} + \text{H}]^+$  370.1649.

### 3.2.2.7 Synthesis of 1.33



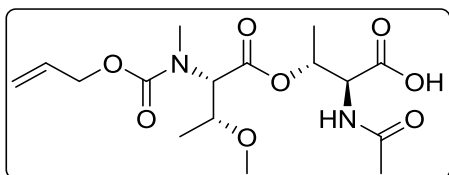
#### Compound 1.34 (*tert*-butyl acetyl-L-threoninate)



H-Thr-OtBu-HCl (500 mg, 2.36 mmol, 1.0 eq) was dissolved in dry DCM (15 mL) and DIEA (413  $\mu\text{L}$ , 2.36 mmol, 1.0 eq) was added. A mixture of AcOH (163  $\mu\text{L}$ , 2.85 mmol, 1.2 eq) and DIC (444  $\mu\text{L}$ , 2.85 mmol, 1.2 eq) in dry DCM (5.0 mL) was let to react for 5 min before it was added to the reaction mixture. Finally, DMAP (29 mg, 0.24 mmol, 0.1 eq) was dissolved in DMF (2 mL) and added to the reaction mixture. After 3 h 30 min the reaction mixture was diluted with EtOAc (50 mL) and washed with an aqueous 10%

solution of citric acid (40 mL). The water layer was extracted with EtOAc (35 mL), and the combined organic layers were washed with an aqueous 10% citric acid solution (2 x 50 mL), water (2 x 50 mL), brine (50 mL), dried over MgSO<sub>4</sub> and filtered off. The solvent was removed under reduced pressure to afford **1.34** (600 mg, 97%) as white solid. Compound **1.34** was used without further purification. <sup>1</sup>H NMR (400 MHz, CDCl<sub>3</sub>) δ = 4.49 (dd, J = 8.7, 2.8 Hz, 1H), 4.31 – 4.23 (m, J = 6.4, 3.2 Hz, 1H), 2.08 (s, 3H), 1.49 – 1.47 (m, 9H), 1.22 (d, J = 6.4 Hz, 3H). <sup>13</sup>C NMR (CDCl<sub>3</sub>, 400 MHz) δ = 170.7, 170.2, 82.5, 68.4, 57.8, 28.0, 23.1, 20.0. ESI(+)**MS** m/z calculated for C<sub>10</sub>H<sub>19</sub>NO<sub>4</sub> 217.1, found [M + H]<sup>+</sup> 218.1.

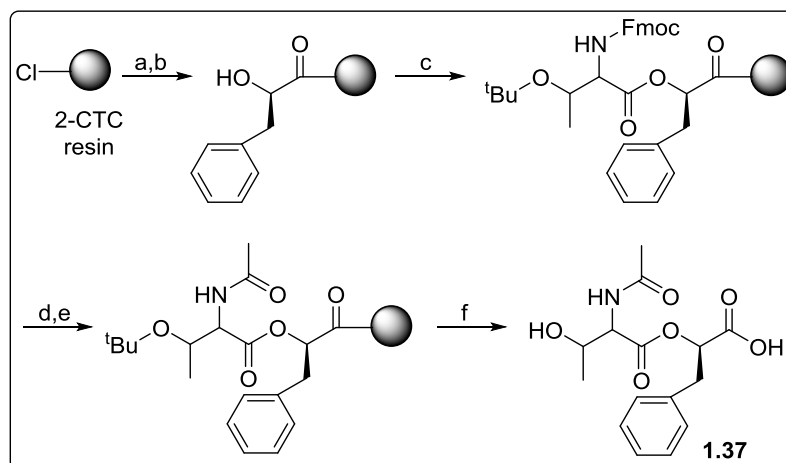
**Compound 1.33** (*N*-acetyl-*O*-(*N*-((allyloxy)carbonyl)-*N*,*O*-dimethyl-*L*-threonyl)-*L*-threonine)



Carboxylic acid **1.20** (135 mg, 0.59 mmol, 1.5 eq) was dissolved in dry DCM (1 mL) and the solution was cooled to 0 °C with an ice bath, followed by addition of DIC (91 μL, 0.59 mmol, 1.5 eq). After 5 min, a solution of compound **1.34** (85 mg, 0.39 mmol, 1.0 eq) in dry DCM (500 μL) was added dropwise, followed by addition of a DMAP (10 mg, 0.08 mmol, 0.2 eq) solution in DMF (150 μL). After 24 h, the solvent was removed under *vacuo* to afford the crude product **1.35** as yellow oil. ESI(+)**MS** m/z calculated for C<sub>20</sub>H<sub>34</sub>N<sub>2</sub>NaO<sub>8</sub> [M + Na]<sup>+</sup> 453.2, found 423.2. The crude product was used without further purification. The crude product **1.35** was dissolved in a TFA/DCM (9:1 v/v, 1 mL) mixture and it was let to stir for 2 h under N<sub>2</sub> atmosphere. The solvent was removed under reduced pressure, and the product was freeze-dried and purified using a C18 reversed-phase Porapak<sup>TM</sup> Rxn Cartridge (H<sub>2</sub>O/ACN, 1:0 → 6:4) to afford pure **1.33** (68 mg, 100%) as yellow oil. <sup>1</sup>H NMR (400 MHz, CDCl<sub>3</sub>, rotamers) δ 7.19 (d, J = 8.9 Hz, 2H), 7.02 (d, J = 8.8 Hz, 1H), 5.96 – 5.85 (m, 1H), 5.60 – 5.46 (m, 1H), 5.34 – 5.17 (m, 2H), 4.96 – 4.80 (m, 2H), 4.70 – 4.50 (m, 2H), 4.02 – 3.83 (m, 1H), 3.29 + 3.27 (d, 3H), 3.01 + 2.85 (s, 3H), 2.12 (s, 3H), 1.30 + 1.25 (d, J = 6.5 Hz, 7H), 1.16 + 1.14 (d, J = 6.6 Hz, 1H). <sup>13</sup>C NMR (101 MHz,

$\text{CDCl}_3$ , rotamers)  $\delta$  172.9, 168.8, 168.5, 158.2, 132.4, 117.8, 76.4, 71.4, 67.1, 62.8, 57.3 (57.1), 55.8, 32.7 (32.7), 22.6, 17.3 (16.9), 15.7 (15.0). **HRMS-ESI(+)**  $m/z$  calculated for  $\text{C}_{16}\text{H}_{26}\text{N}_2\text{O}_8$  374.1689, found  $[\text{M} + \text{Na}]^+$  397.1575.

### 3.2.2.8 Synthesis of **1.37**

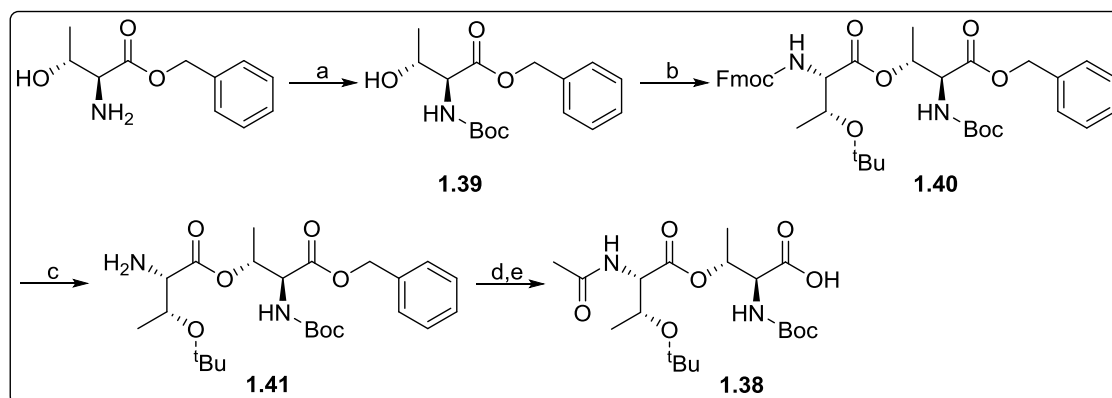


#### Compound **1.37** ((*R*)-2-((acetyl-*L*-threonyl)oxy)-3-phenylpropanoic acid)

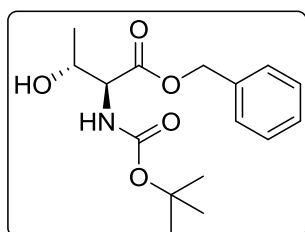
2-CTC resin (500 mg, 1.60 mmol/g resin) was placed in a 10 mL polypropylene syringe fitted with two polyethylene filter discs. The resin was conditioned and D-(+)-3-phenyllactic acid (66 mg, 0.40 mmol, 1.0 eq) was incorporated following the general procedure described above. Fmoc-Thr(tBu)-OH (1.271 g, 3.20 mmol, 8.0 eq) was dissolved in dry DCM (2.7 mL) and DIC (496  $\mu\text{L}$ , 3.20 mmol, 8.0 eq) was added. After 5 min, the mixture was added to the peptidyl-resin, followed by addition of a DMAP (24 mg, 0.20 mmol, 0.5 eq) solution in DMF (300  $\mu\text{L}$ ). The reaction mixture was shaken for 2 h 30 min. The Fmoc group was removed by treatment with a piperidine–DMF (1:4 v/v) (2 x 1 min) solution. Acetylation of the free amine was performed as follows: the peptidyl-resin was treated with AcOH–OxymaPure–DIC (3:3:3 eq) for 20 min, being the Kaiser test used to monitor reaction conversion. Cleavage and global deprotection was achieved by following *Protocol Cle5*. The crude product was purified using a C18 reversed-phase Porapak<sup>TM</sup> Rxn Cartridge ( $\text{H}_2\text{O}/\text{ACN}$ , 1:0  $\rightarrow$  7:3) to afford pure **1.37** (38 mg, 31% over 5 steps) as white solid. <sup>1</sup>H NMR (400 MHz,  $\text{CD}_3\text{OD}$ )  $\delta$  7.32 – 7.20 (m, 5H), 5.24 (dd,  $J = 8.2, 4.4$  Hz, 1H, ), 4.46 (d,  $J = 3.6$  Hz, 1H), 4.22 – 4.12 (m, 1H), 3.22 (dd,  $J$

= 14.4, 4.4 Hz, 1H), 3.14 (dd,  $J$  = 14.4, 8.2 Hz, 1H), 2.00 (s, 3H), 1.13 (d,  $J$  = 6.4 Hz, 3H).  $^{13}\text{C}$  NMR (101 MHz,  $\text{CD}_3\text{OD}$ )  $\delta$  173.6, 172.7, 171.4, 137.5, 130.5, 129.5, 128.0, 74.9, 68.3, 59.6, 38.2, 22.4, 20.1. HRMS-ESI(+)  $m/z$  calculated for  $\text{C}_{15}\text{H}_{19}\text{NO}_6$  309.1291, found  $[\text{M} + \text{H}]^+$  310.1299.

### 3.2.2.9 Synthesis of 1.38



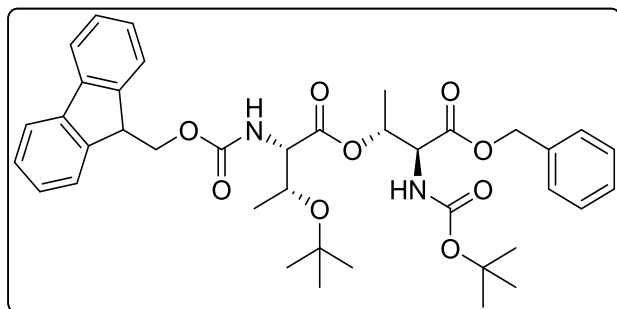
#### Compound 1.39 (benzyl (tert-butoxycarbonyl)-L-threoninate)



H-Thr-OBzl-oxalate (1.900 g, 6.35 mmol, 1.0 eq) was dissolved in DCM (20 mL), followed by the addition of  $\text{Et}_3\text{N}$  (1859  $\mu\text{L}$ , 13.34 mmol, 2.1 eq) and di-*tert*-butyl-dicarbamate (1603  $\mu\text{L}$ , 6.98 mmol, 1.1 eq). The reaction mixture was stirred for 16 h until all the starting material was consumed. The solvent was removed under reduced pressure, and the crude product was purified by flash chromatography on silica gel (Hexane/EtOAc, 8:2  $\rightarrow$  6:4) to afford **1.39** (1.091 g, 56%) as yellow oil.  $^1\text{H}$  NMR (400 MHz,  $\text{CDCl}_3$ )  $\delta$  7.36 (s, 5H), 5.32 (bs, 1H), 5.21 (q,  $J$  = 12.3 Hz, 2H), 4.31 (bs, 2H), 1.44 (s, 9H), 1.24 (d,  $J$  = 6.4 Hz, 3H).  $^{13}\text{C}$  NMR (101 MHz,  $\text{CDCl}_3$ )  $\delta$  171.5, 156.3, 135.4, 128.8, 128.6,

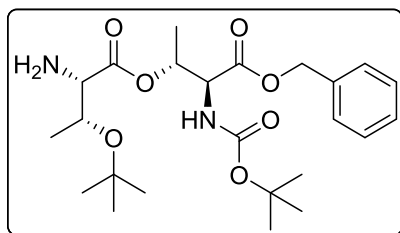
128.5, 80.3, 68.3, 67.4, 58.9, 28.4, 20.1. **ESI(+)**MS  $m/z$  calculated for  $C_{16}H_{23}NO_5$  309.2, found  $[M + H]^+$  310.2.

**Compound 1.40** (benzyl *O*-(*N*-(((9H-fluoren-9-yl)methoxy)carbonyl)-*O*-(*tert*-butyl)-*L*-threonyl)-*N*-(*tert*-butoxycarbonyl)-*L*-threoninate)



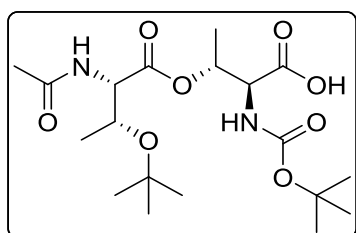
Fmoc-Thr(*t*Bu)-OH (1.682 g, 4.24 mmol, 1.2 eq) was dissolved in dry DCM (10 mL) and the solution was cooled to 0 °C with an ice bath, followed by addition of DIC (656  $\mu$ L, 4.24 mmol, 1.2 eq). After 5 min, a solution of **1.39** (1.091 g, 3.53 mmol, 1.0 eq) in dry DCM (5 mL) was added dropwise, followed by addition of a DMAP (86 mg, 0.71 mmol, 0.2 eq) solution in DMF (1 mL). After 2 h, the reaction mixture was brought to rt and let to stir for 18 more hours. The solvent was removed under *vacuo* and the crude product was purified by flash chromatography on silica gel (Hexane/EtOAc, 1:0  $\rightarrow$  8:2) to afford **1.40** (2.428 g, 100%) as yellow oil.  **$^1H$  NMR** (400 MHz,  $CDCl_3$ )  $\delta$  7.75 (d,  $J = 7.5$  Hz, 2H), 7.60 (dd,  $J = 11.2, 7.5$  Hz, 2H), 7.39 (t,  $J = 7.3$  Hz, 2H), 7.32 – 7.24 (m, 7H), 5.56 (d,  $J = 8.8$  Hz, 1H), 5.49 – 5.41 (m, 1H), 5.31 (d,  $J = 9.6$  Hz, 1H), 5.15 (s, 2H), 4.49 (dd,  $J = 9.6, 2.1$  Hz, 1H), 4.37 (dd,  $J = 7.2, 2.7$  Hz, 2H), 4.24 (t,  $J = 7.3$  Hz, 1H), 1.43 (s, 9H), 1.33 (d,  $J = 6.4$  Hz, 3H), 1.19 (d,  $J = 6.5$  Hz, 3H), 1.17 (s, 9H).  **$^{13}C$  NMR** (101 MHz,  $CDCl_3$ )  $\delta$  170.1, 169.8, 156.5, 156.0, 144.0, 143.9, 141.4, 135.2, 128.6, 128.5, 127.8, 127.2, 125.3, 120.0, 80.3, 74.2, 72.3, 67.8, 67.3, 67.0, 59.7, 57.4, 47.2, 28.6, 28.3. **ESI(+)**MS  $m/z$  calculated for  $C_{39}H_{48}N_2O_9$  688.3, found  $[M + H]^+$  689.4.

**Compound 1.41** (benzyl *N*-(*tert*-butoxycarbonyl)-*O*-(*O*-(*tert*-butyl)-*L*-threonyl)-*L*-threoninate)



**1.40** (2.428 g, 3.53 mmol, 1.0 eq) was dissolved in dry DCM (12 mL), and Et<sub>2</sub>N (3.5 mL) was added. The yellow solution was let to stir at rt for 4 h. The solvent was removed under reduced pressure, and the crude product was purified by flash chromatography on silica gel (Hexane/EtOAc, 9:1 → 7:3) to afford **1.41** (781 mg, 46%) as yellow oil. <sup>1</sup>H NMR (400 MHz, CDCl<sub>3</sub>) δ 7.35 (s, 5H), 5.45 – 5.37 (m, 1H), 5.30 – 5.22 (m, 1H), 5.15 (t, *J* = 10.0 Hz, 2H), 4.47 (dd, *J* = 9.6, 2.3 Hz, 1H), 3.89 – 3.81 (m, 1H), 3.05 (d, *J* = 3.9 Hz, 1H), 1.45 (s, 9H), 1.31 (d, *J* = 6.5 Hz, 3H), 1.16 (d, *J* = 6.2 Hz, 3H), 1.13 (s, 9H). <sup>13</sup>C NMR (101 MHz, CDCl<sub>3</sub>) δ 173.7, 170.2, 156.0, 135.3, 128.7, 128.7, 80.4, 73.8, 71.4, 68.6, 67.7, 60.5, 57.4, 28.7, 28.4, 20.1, 17.1. ESI(+)**MS** *m/z* calculated for C<sub>24</sub>H<sub>38</sub>N<sub>2</sub>O<sub>7</sub> 466.3, found [M + H]<sup>+</sup> 467.1.

**Compound 1.38** (*O*-(*N*-acetyl-*O*-(*tert*-butyl)-*L*-threonyl)-*N*-(*tert*-butoxycarbonyl)-*L*-threonine)



**1.41** (781 mg, 1.68 mmol, 1.0 eq) was dissolved in dry DCM (10 mL) and Et<sub>3</sub>N (328 μL, 2.36 mmol, 1.4 eq) was added. The reaction mixture was cooled to 0 °C with an ice bath, and acetyl chloride (144 μL, 2.02 mmol, 1.2 eq) was added dropwise. After 20 min, the reaction mixture was brought to rt and it was let to stir for an extra 40 min until all the starting material was consumed. DCM (10 mL) was added, and the organic layer

was washed with brine (15 mL), dried over MgSO<sub>4</sub>, filtered off and concentrated in *vacuo*. The crude product was dissolved in MeOH (10 mL), followed by addition of palladium on carbon (51 mg, 10% w/w). H<sub>2</sub> was bubbled through the back suspension for 15 min until all the starting material disappeared according to TLC analysis. The reaction mixture was filtered over Celite®, washed with MeOH (2 x 5 mL), and concentrated in *vacuum*. Flash chromatography purification on silica gel (DCM/MeOH, 1:0 → 95:5) afforded **1.38** (331 mg, 47% over two steps) as white solid. <sup>1</sup>H NMR (400 MHz, CDCl<sub>3</sub>) δ 6.45 (d, *J* = 8.8 Hz, 1H), 5.50 – 5.44 (m, 1H), 5.38 (d, *J* = 9.1 Hz, 1H), 4.50 (dd, *J* = 9.3, 2.1 Hz, 1H), 4.38 (dd, *J* = 8.8, 1.9 Hz, 1H), 4.19 – 4.13 (m, 1H), 2.08 (s, 3H), 1.47 (s, 9H), 1.32 (d, *J* = 6.5 Hz, 3H), 1.17 (d, *J* = 6.2 Hz, 3H), 1.14 (s, 9H). <sup>13</sup>C NMR (101 MHz, CDCl<sub>3</sub>) δ 172.2, 171.6, 169.7, 156.2, 80.3, 74.6, 72.7, 67.0, 58.1, 57.2, 28.6, 28.4, 22.9, 21.0, 16.8. HRMS-ESI(+) *m/z* calculated for C<sub>19</sub>H<sub>34</sub>N<sub>2</sub>O<sub>8</sub> 418.2315, found [M + Na]<sup>+</sup> 441.2207.

### 3.2.3 Study of the optimal Fmoc removal conditions to minimise DKP formation

#### Determination of the DKP formation percentage:

DKP formation was assessed by comparison of the loading level after the first and the third amino acid incorporation. The following formula was used to calculate the DKP formation percentage for all six tested conditions.

$$DKP \text{ formation} = \frac{\text{Loading first amino acid} - \text{Loading third amino acid}}{\text{Loading first amino acid}} \cdot 100$$

Where: Loading first amino acid (loading of the resin after the first amino acid incorporation (mmol/g resin)); Loading third amino acid (loading of the resin after the third amino acid incorporation (mmol/g)).

#### General protocol to evaluate DKP formation:

The resin conditioning and incorporation of the first amino acid, Fmoc-MeAla-OH, were accomplished by standard means. The real loading after the first residue incorporation was determined by Fmoc UV quantification of the dibenzofulvene-piperidine adduct formed during Fmoc removal at λ = 290 nm. Incorporation of the

second residue, Fmoc-Ala-OH, was achieved following *Protocol Pep2*. Fmoc removal was accomplished with a short treatment of the peptidyl-resin with the corresponding deprotection cocktail (2 x 1 min) (see all six tested Fmoc removal conditions in Table 2). The resin was washed with DMF (3 x 1 min), DCM (3 x 1 min) and DMF (3 x 1 min). Quickly after, the third residue, Fmoc-Pro-OH, was assembled following standard *Protocol Pep1*. A Kaiser test was run to ensure full residue assembly. Finally, the real loading at this stage was determined by Fmoc UV quantification of the dibenzofulvene-piperidine adduct formed during Fmoc removal at  $\lambda = 290$  nm.

- DKP formation results:

In total, six conditions for Fmoc removal of the second residue incorporation were tested and are summarised in Table 2.

| # | Fmoc removal conditions of the second residue           | Loading (1 <sup>st</sup> AA Fmoc quantification) | Loading (3 <sup>rd</sup> AA Fmoc quantification) | DKP formation (%) |
|---|---|--|--|-------------------|
| 1 | Piperidine–DMF (1:4 v/v) (2 x 1 min)                    | 0.65 mmol/g                                      | 0.57 mmol/g                                      | 18                |
| 2 | DBU–DMF (2:98 v/v) (2 x 1 min)                          | 0.66 mmol/g                                      | 0.59 mmol/g                                      | 11                |
| 3 | 0.1 M HOBT in Piperidine–DMF (1:4 v/v) (2 x 1 min)      | 0.67 mmol/g                                      | 0.57 mmol/g                                      | 15                |
| 4 | 0.1 M OxymaPure in Piperidine–DMF (1:4 v/v) (2 x 1 min) | 0.66 mmol/g                                      | 0.51 mmol/g                                      | 23                |
| 5 | 0.1 M HOBT in DBU–DMF (2:98 v/v) (2 x 1 min)            | 0.62 mmol/g                                      | 0.59 mmol/g                                      | 5                 |
| 6 | 0.1 M OxymaPure in DBU–DMF (2:98 v/v) (2 x 1 min)       | 0.62 mmol/g                                      | 0.53 mmol/g                                      | 15                |

Table 2. Fmoc removal studies to minimise DKP formation.

### 3.2.4 Ester bond formation studies by evaluation of the amino acid optimal protecting group scheme

The optimal protecting group scheme for residue incorporation *via* on-resin Steglich incorporation was evaluated for all three ester linkages.

On-resin esterification of the corresponding residue was carried out following *Protocol Est*. In order to evaluate the esterification outcome, a small aliquot of the peptidyl-resin was subjected to *Protocol MC*, and the esterification conversion was determined by HPLC-MS.

The obtained results for the first, second and third ester linkages are summarised in Table 3, Table 4 and Table 5, for the first, second and third ester, respectively.

#### - First ester linkage: protection scheme

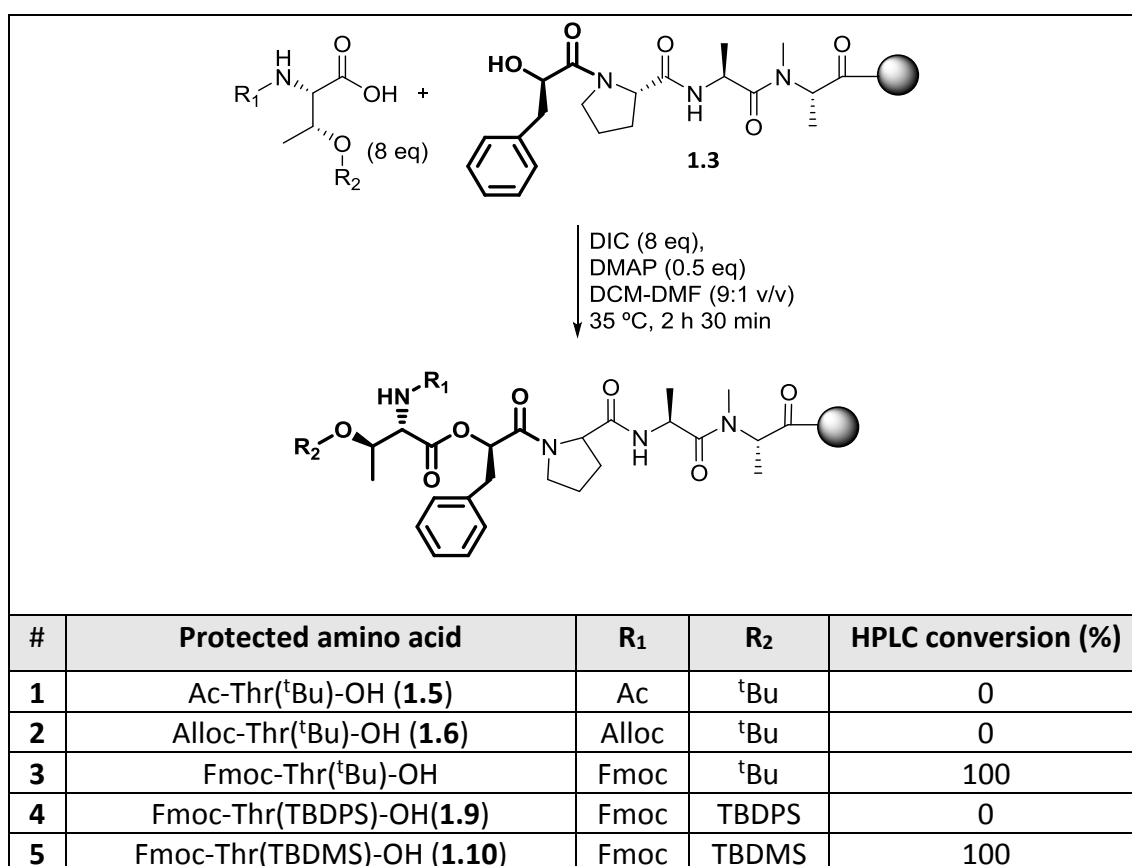
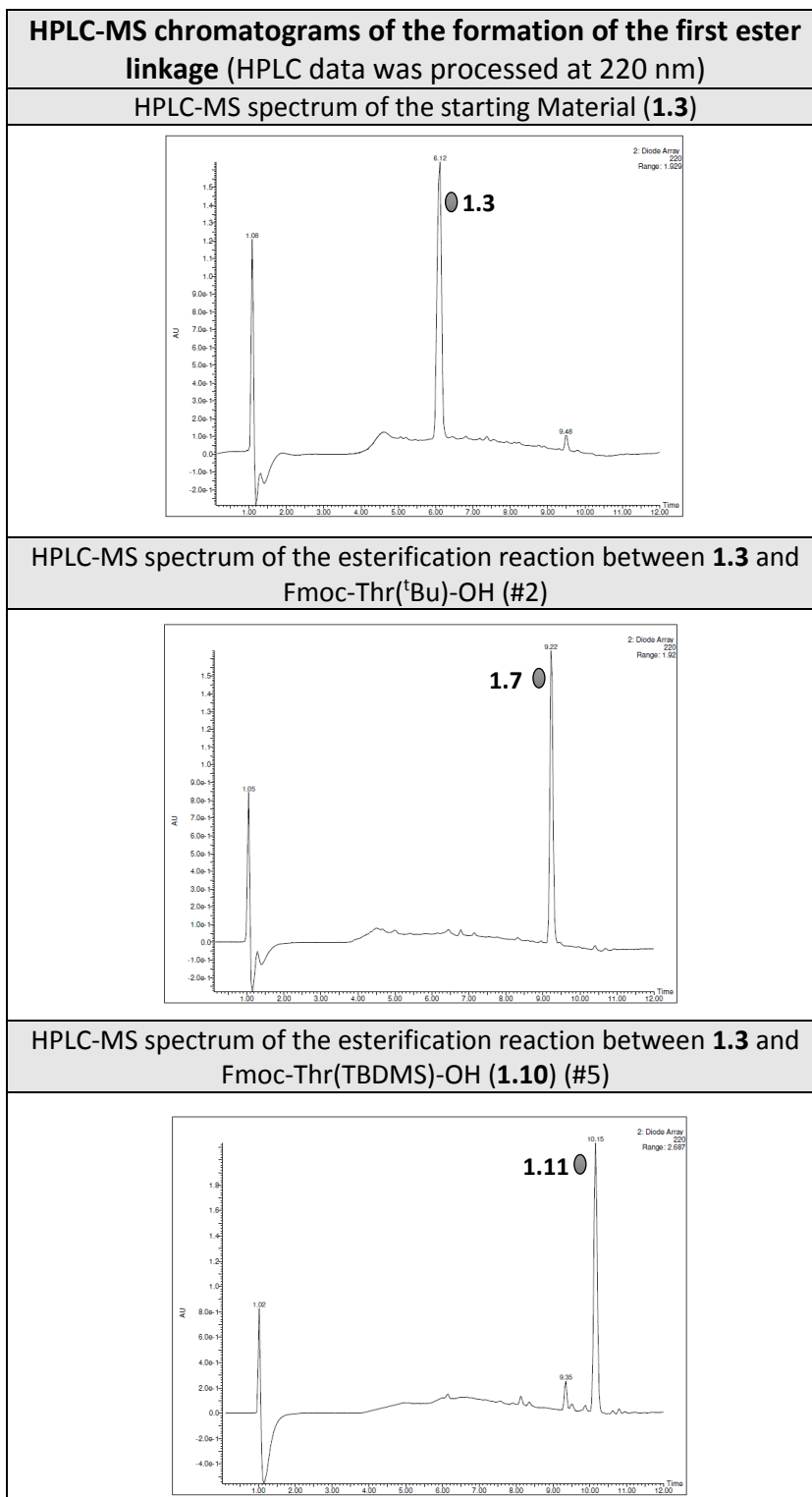


*Table 3.* First ester linkage: Study of the esterification rates by incorporation of several R<sub>1</sub>-Thr(R<sub>2</sub>)-OH derivatives. Esterification conversion was determined by HPLC-MS analysis. HPLC data was processed at 220 nm.

HPLC-MS chromatograms of the formation of the first ester linkage with several  $R_1$ -Thr( $R_2$ )-OH derivatives are shown as follows. Chromatograms of entries #1-2 and #4 are not shown, since only the unreacted starting material was detected in all cases (see spectrum of the starting material **1.3** below).



- Second ester linkage: protection scheme

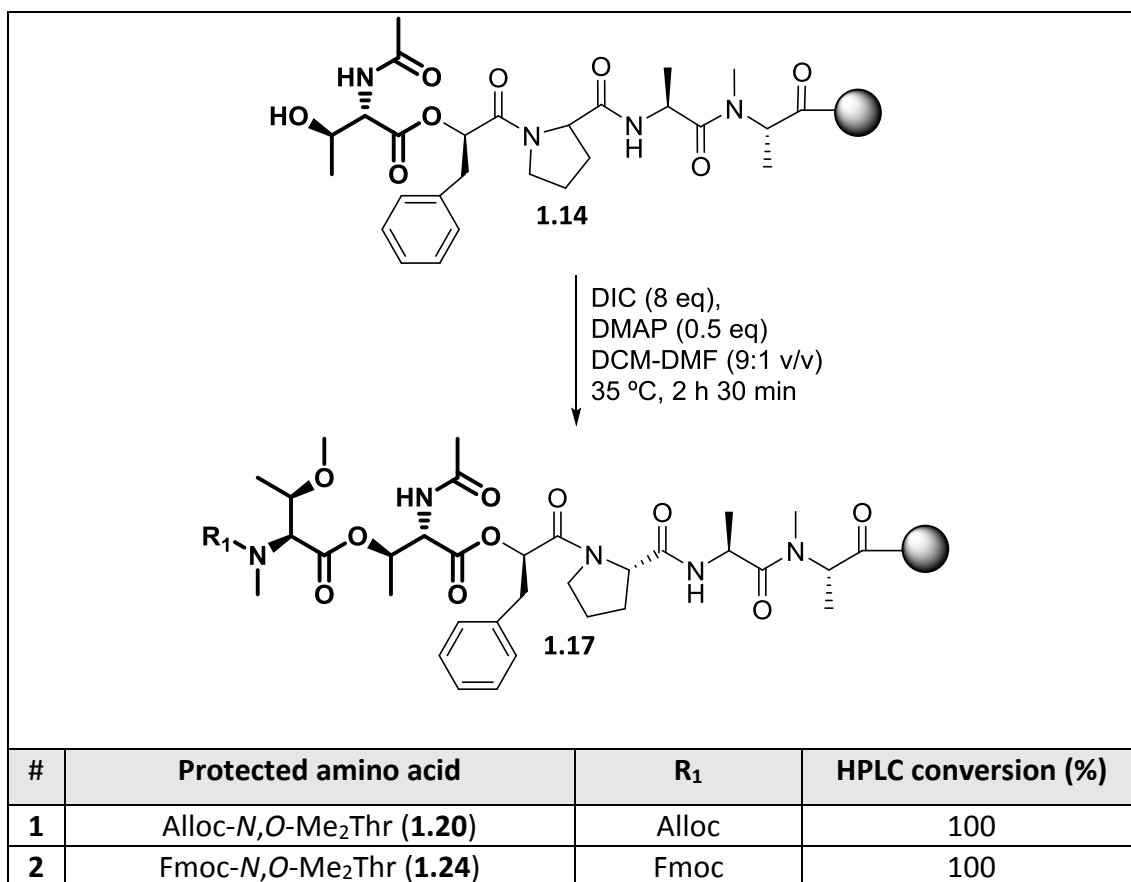
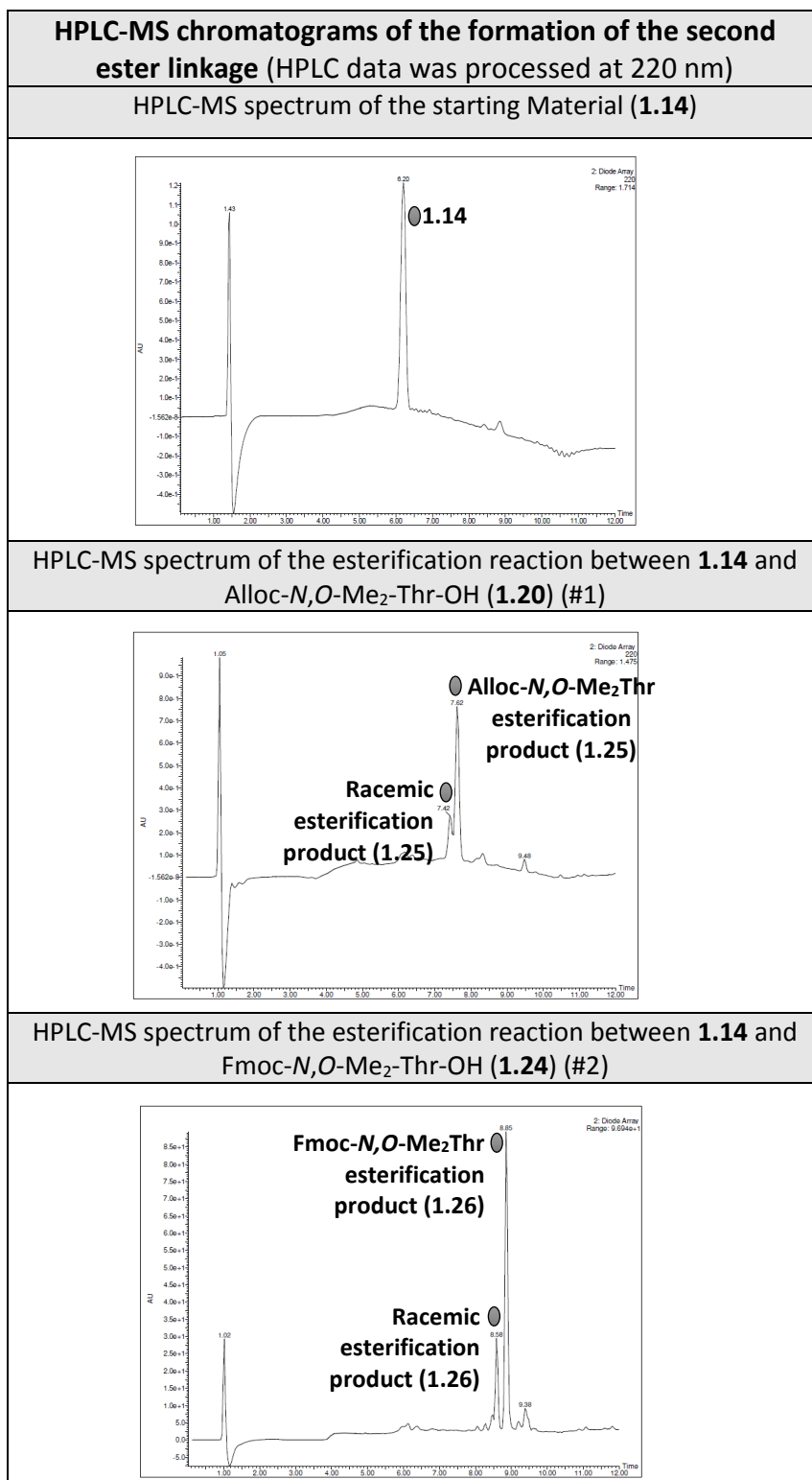
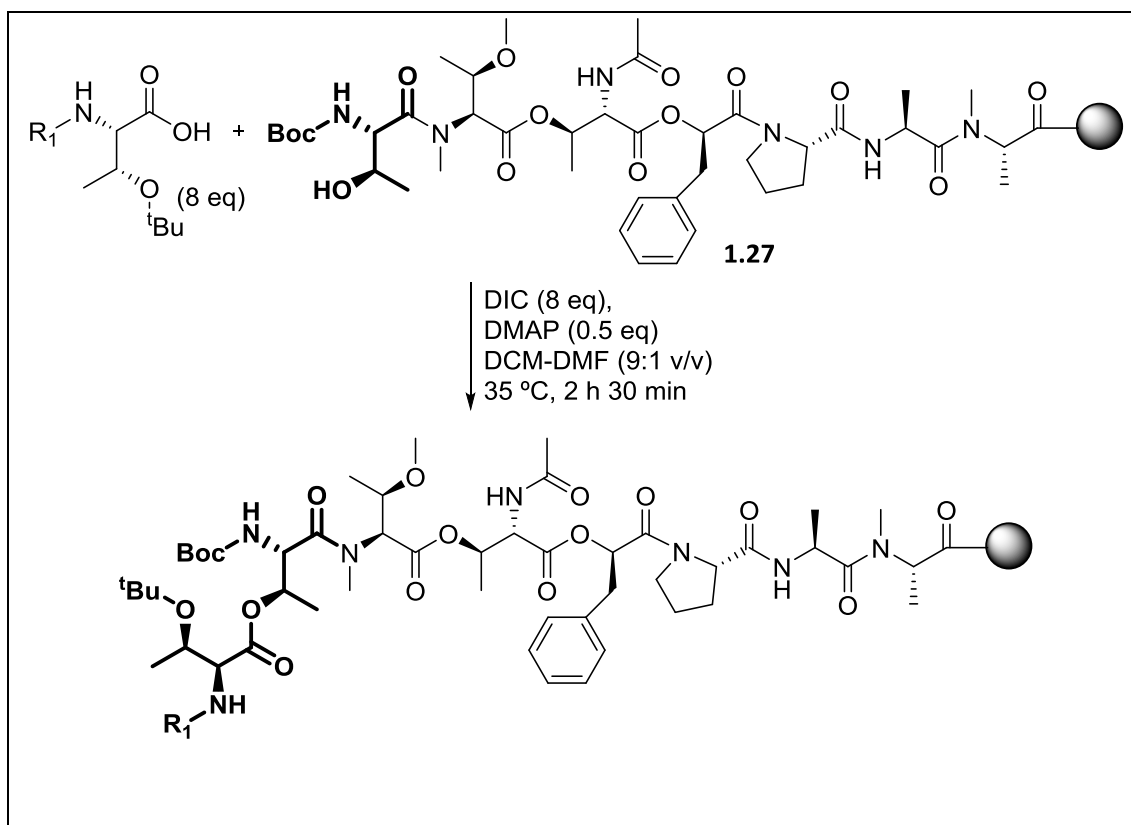


*Table 4.* Second ester linkage: Study of the esterification rates by incorporation of several R<sub>1</sub>-*N,O*-Me<sub>2</sub>-Thr-OH derivatives. Esterification conversion was evaluated by HPLC-MS analysis. HPLC data was processed at 220 nm.

HPLC-MS chromatograms of the formation of the second ester linkage with R<sub>1</sub>-Thr(Me)-OH derivatives are shown as follows.



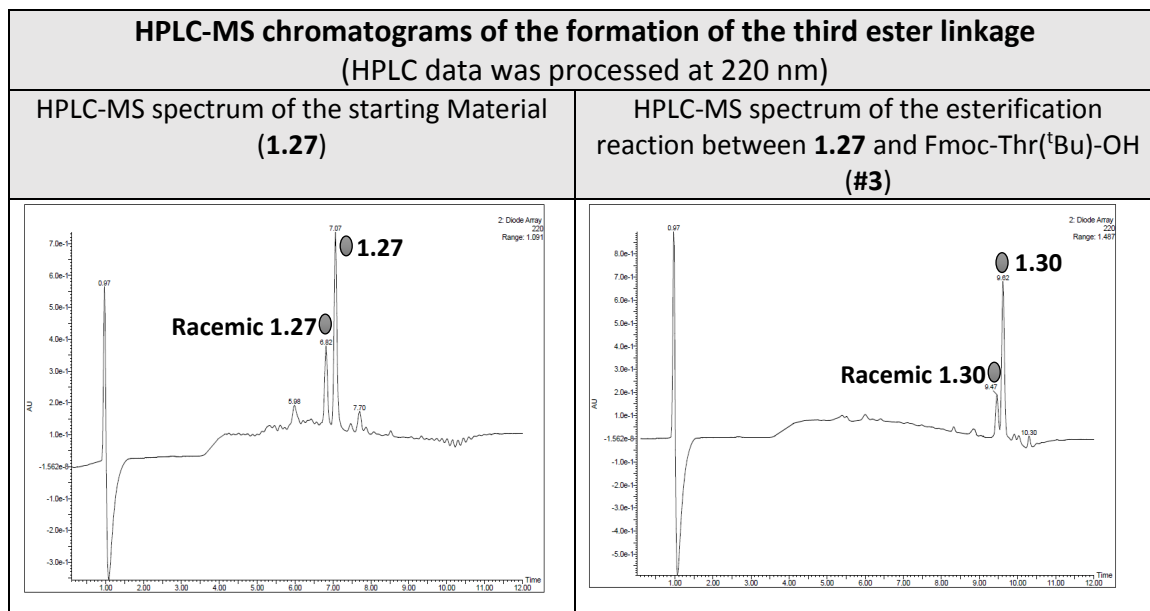
- Third ester linkage: protection scheme



| # | Protected amino acid               | $R_1$ | HPLC conversion (%) |
|---|------------------------------------|-------|---------------------|
| 1 | Ac-Thr( $t\text{Bu}$ )-OH (1.5)    | Ac    | 0                   |
| 2 | Alloc-Thr( $t\text{Bu}$ )-OH (1.6) | Alloc | 0                   |
| 3 | Fmoc-Thr( $t\text{Bu}$ )-OH        | Fmoc  | 100                 |

Table 5. Third ester linkage: Study of the esterification rates by incorporation of several  $R_1$ -Thr( $t\text{Bu}$ )-OH derivatives. Esterification conversion was evaluated by HPLC-MS analysis. HPLC data was processed at 220 nm.

HPLC-MS chromatograms of the formation of the third ester linkage with several R<sub>1</sub>-Thr(<sup>t</sup>Bu)-OH derivatives are shown as follows. Chromatograms of entries #1-2 are not shown, since only the unreacted starting material was detected in all cases (see spectrum of the starting material **1.27** below).



### 3.2.5 Fmoc removal studies after formation of the three ester linkages

The optimal Fmoc removal conditions after formation of the three ester linkages were evaluated. In all cases, a short treatment (1 x 1 min) of the peptidyl-resin with the corresponding deprotection cocktail was performed after formation of the ester linkage. Quickly after Fmoc removal, the resin was washed with DMF (3 x 1 min) and DCM (3 x 1 min). In order to evaluate the deprotection outcome, a small aliquot of the peptidyl-resin was subjected to *Protocol MC*, and the deprotection outcome was analysed by HPLC-MS. The obtained results for Fmoc removal after the first, second and third ester linkages formation are summarised in Table 6, Table 7 and Table 8, respectively. Additionally, the HPLC chromatograms are shown below.

- Tested Fmoc removal conditions after the first ester linkage formation

1.7

Fmoc removal assessment

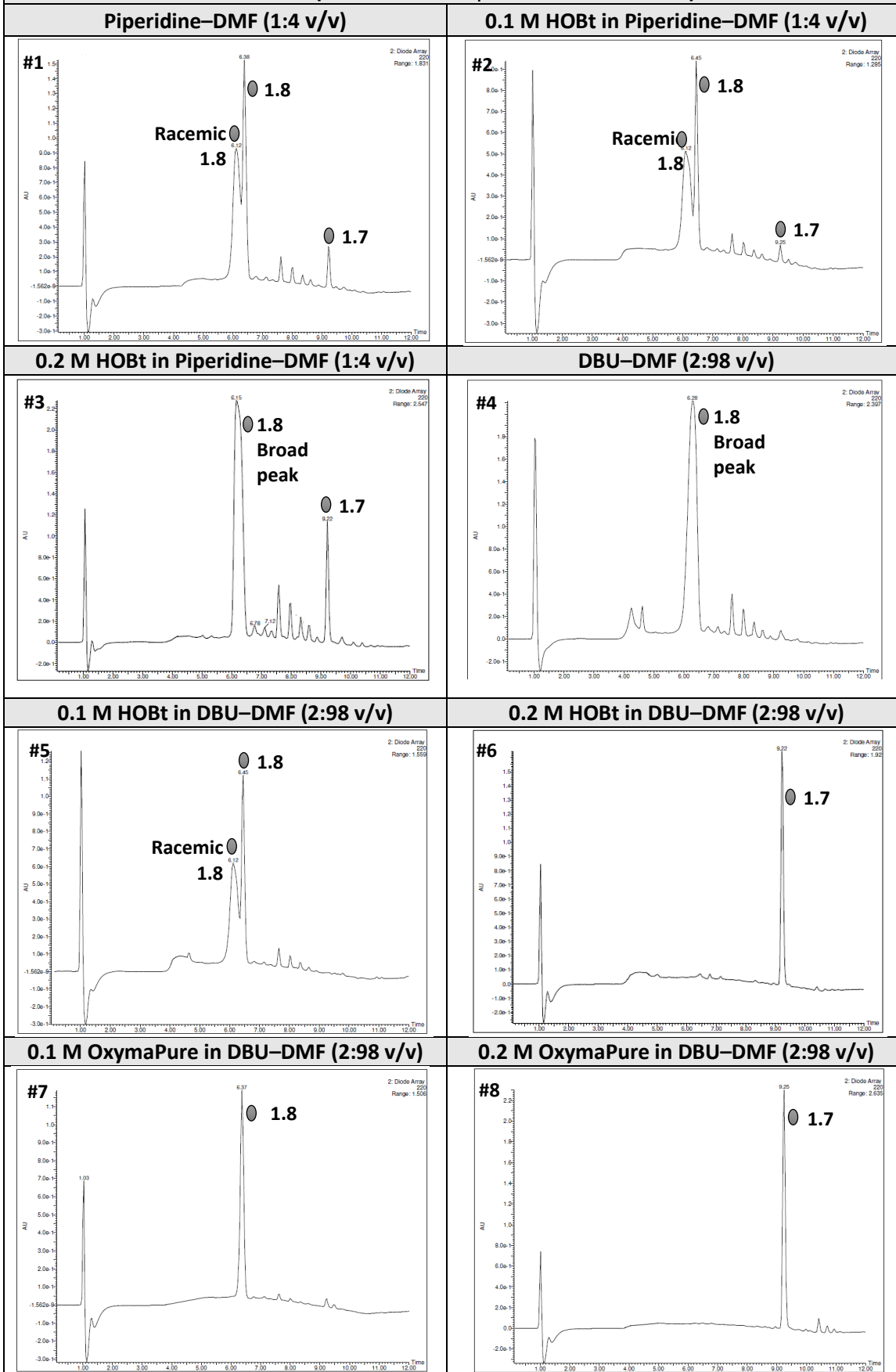
1.8

| # | Fmoc removal conditions                            | Product/SM ratio        | Racemisation    |
|---|--|-------------------------|-----------------|
| 1 | Piperidine–DMF (1:4 v/v) (1 x 1 min)               | <b>1.8/1.7</b><br>95:5  | 54%             |
| 2 | 0.1 M HOBt in Piperidine–DMF (1:4 v/v) (1 x 1 min) | <b>1.8/1.7</b><br>95:5  | 60%             |
| 3 | 0.2 M HOBt in Piperidine–DMF (1:4 v/v) (1 x 1 min) | <b>1.8/1.7</b><br>87:13 | Broad peak      |
| 4 | DBU–DMF (2:98 v/v) (1 x 1 min)                     | <b>1.8/1.7</b><br>100:0 | Broad peak      |
| 5 | 0.1 M HOBt in DBU–DMF (2:98 v/v) (1 x 1 min)       | <b>1.8/1.7</b><br>100:0 | 56%             |
| 6 | 0.2 M HOBt in DBU–DMF (2:98 v/v) (1 x 1 min)       | <b>1.8/1.7</b><br>0:100 | No Fmoc removal |
| 7 | 0.1 M OxymaPure in DBU–DMF (2:98 v/v) (1 x 1 min)  | <b>1.8/1.7</b><br>100:0 | 0%              |
| 8 | 0.2 M OxymaPure in DBU–DMF (2:98 v/v) (1 x 1 min)  | <b>1.8/1.7</b><br>0:100 | No Fmoc removal |

*Table 6.* Study of the optimal Fmoc removal conditions after formation of the first ester linkage. Racemisation was determined by HPLC-MS analysis. HPLC data was processed at 220 nm.

HPLC-MS chromatograms of the Fmoc removal studies after formation of the first ester linkage between **1.3** and Fmoc-Thr(<sup>t</sup>Bu)-OH to afford **1.7** are shown as follows.

HPLC-MS chromatograms of the Fmoc removal studies after the first ester linkage formation (HPLC data was processed at 220 nm)



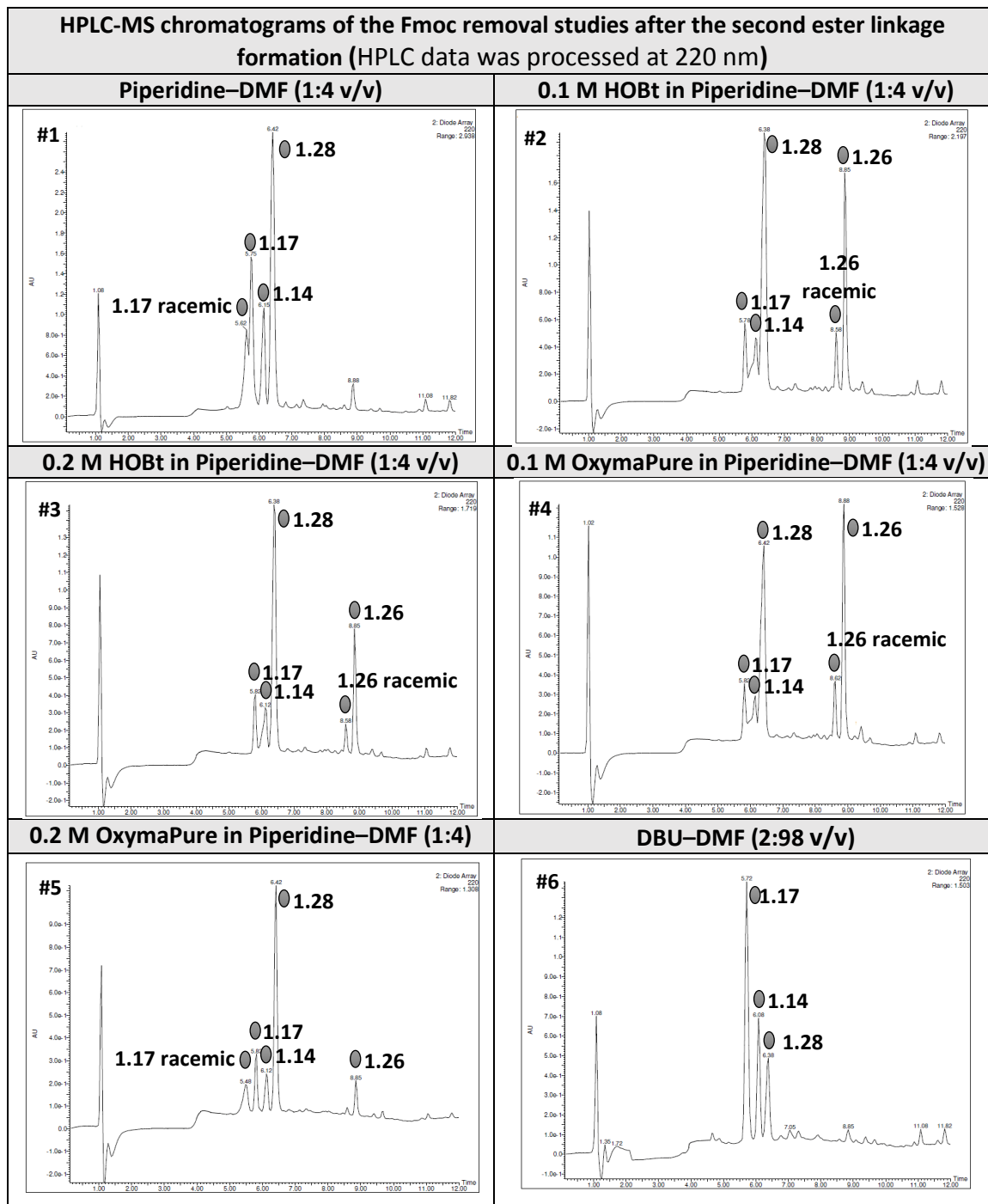
- Tested Fmoc removal conditions after the second ester linkage formation

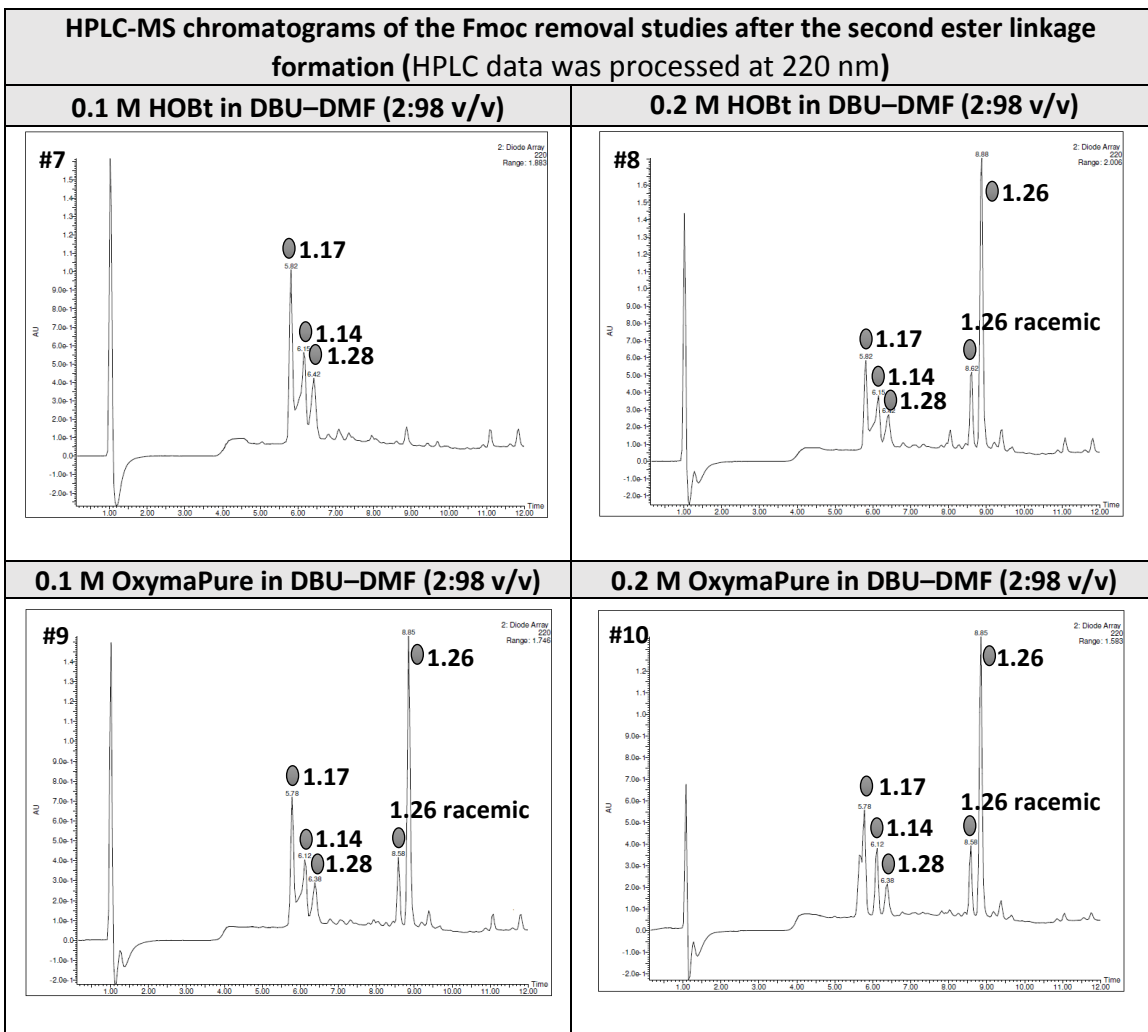
The diagram illustrates the Fmoc removal of compound 1.26. The starting material 1.26 has an Fmoc group on the nitrogen of the first amino acid residue. Upon removal, three products are formed: 1.17 (the desired product with a free amine), 1.14 (a product with a hydroxyl group, labeled as residue loss), and 1.28 (a product with an enone system, labeled as α,β-elimination).

| #  | Fmoc removal conditions                                 | 1.26 (%) | 1.17 (%) | 1.14 (%) | 1.28 (%) |
|----|---|----------|----------|----------|----------|
| 1  | Piperidine–DMF (1:4 v/v) (1 x 1 min)                    | 0        | 37       | 15       | 48       |
| 2  | 0.1 M HOBT in Piperidine–DMF (1:4 v/v) (1 x 1 min)      | 32       | 8        | 11       | 49       |
| 3  | 0.2 M HOBT in Piperidine–DMF (1:4 v/v) (1 x 1 min)      | 26       | 9        | 10       | 57       |
| 4  | 0.1 M OxymaPure in Piperidine–DMF (1:4 v/v) (1 x 1 min) | 38       | 9        | 10       | 43       |
| 5  | 0.2 M OxymaPure in Piperidine–DMF (1:4 v/v) (1 x 1 min) | 8        | 25       | 10       | 57       |
| 6  | DBU–DMF (2:98) (1 x 1 min)                              | 0        | 57       | 23       | 19       |
| 7  | 0.1 M HOBT in DBU–DMF (2:98 v/v) (1 x 1 min)            | 0        | 43       | 36       | 21       |
| 8  | 0.2 M HOBT in DBU–DMF (2:98 v/v) (1 x 1 min)            | 60       | 16       | 16       | 8        |
| 9  | 0.1 M OxymaPure in DBU–DMF (2:98 v/v) (1 x 1 min)       | 51       | 22       | 18       | 9        |
| 10 | 0.2 M OxymaPure in DBU–DMF (2:98 v/v) (1 x 1 min)       | 54       | 30       | 11       | 5        |

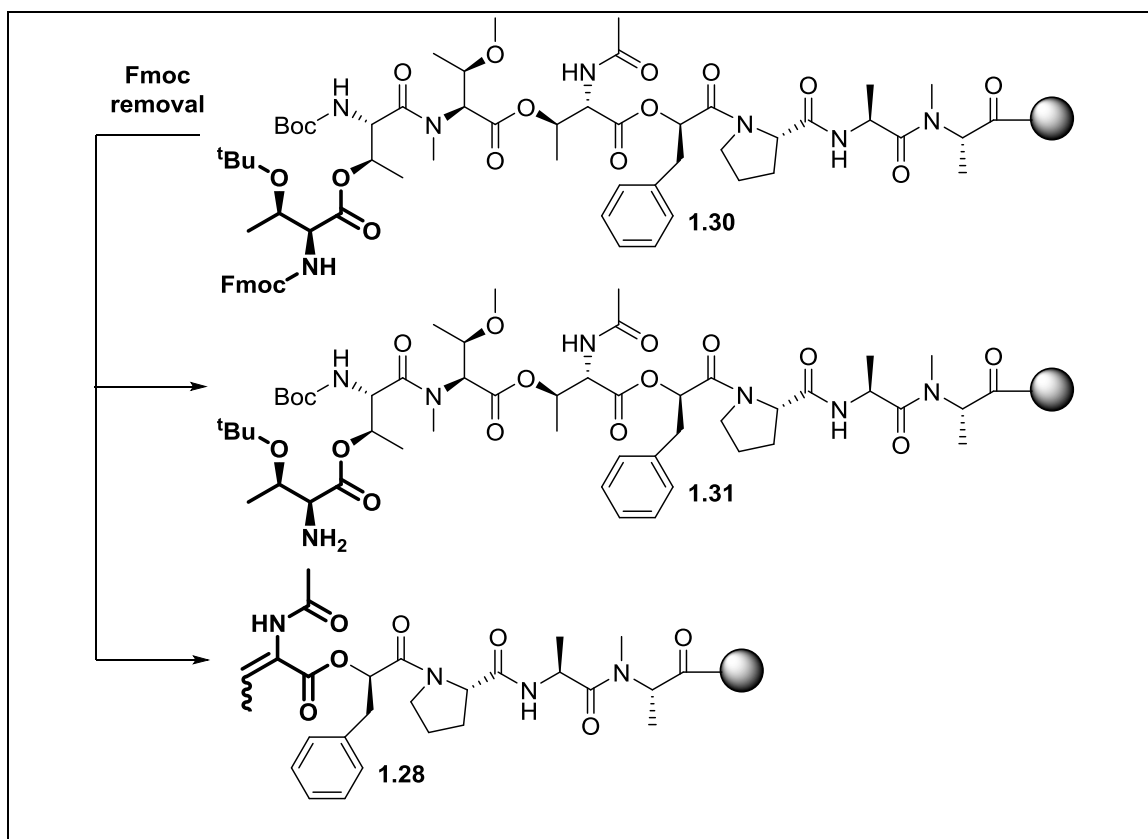
Table 7. Study of the optimal Fmoc removal conditions after formation of the second ester linkage. Formation percentages of the desired product and undesired side-products were determined by HPLC-MS analysis. HPLC data was processed at 220 nm.

HPLC-MS chromatograms of the Fmoc removal studies after formation of the second ester linkage between **1.14** and Fmoc-*N,O*-Me<sub>2</sub>-Thr(*t*Bu)-OH (**1.24**) are shown as follows.





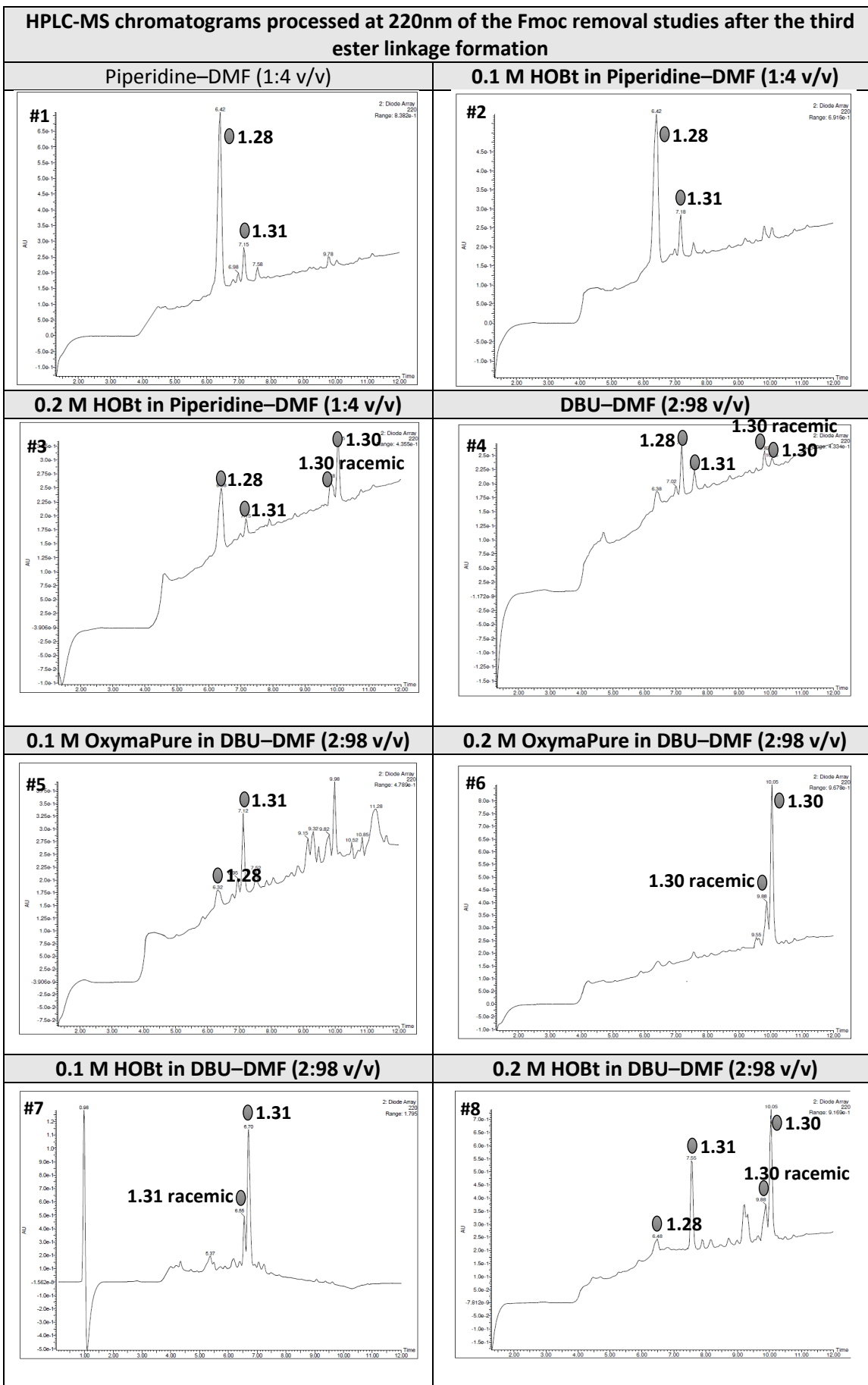
- Tested Fmoc removal conditions after the third ester linkage formation



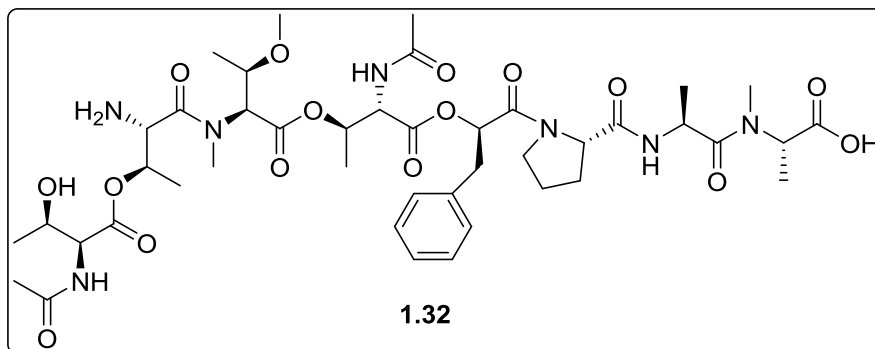
| # | Fmoc removal conditions                            | 1.30 (%) | 1.31 (%) | 1.28 (%) |
|---|--|----------|----------|----------|
| 1 | Piperidine–DMF (1:4 v/v) (1 x 1 min)               | 0        | 10       | 90       |
| 2 | 0.1 M HOBT in Piperidine–DMF (1:4 v/v) (1 x 1 min) | 0        | 12       | 88       |
| 3 | 0.2 M HOBT in Piperidine–DMF (1:4 v/v) (1 x 1 min) | 41       | 44       | 15       |
| 4 | DBU–DMF (2:98 v/v) (1 x 1 min)                     | 15       | 45       | 22       |
| 5 | 0.1 M OxymaPure in DBU–DMF (2:98 v/v) (1 x 1 min)  | 30       | 26       | 9        |
| 6 | 0.2 M OxymaPure in DBU–DMF (2:98 v/v) (1 x 1 min)  | 100      | 0        | 0        |
| 7 | 0.1 M HOBT in DBU–DMF (2:98 v/v) (1 x 1 min)       | 0        | 100      | 0        |
| 8 | 0.2 M HOBT in DBU–DMF (2:98 v/v) (1 x 1 min)       | 63       | 32       | 5        |

*Table 8.* Study of the optimal Fmoc removal conditions after formation of the third ester linkage. Formation percentages of the desired product and undesired side-products were determined by HPLC-MS analysis. HPLC data was processed at 220 nm.

HPLC-MS chromatograms of the Fmoc removal studies after formation of the third ester linkage between **1.27** and Fmoc-Thr(<sup>t</sup>Bu)-OH are shown as follows.



### 3.2.6 Assembly of linear depsipeptide 1.32



#### 3.2.6.1 Synthesis of 1.32 using a fully stepwise strategy

The 2-CTC resin (25 mg, 1.6 mmol/g resin) was placed in a 2 mL-polypropylene syringe fitted with two polyethylene filter discs. The conditioning of the resin and incorporation of the first amino acid, Fmoc-MeAla-OH (6 mg, 0.02 mmol, 1.0 eq), was carried out by standard means. The Fmoc group was removed by treatment with a piperidine–DMF solution (1:4 v/v) (1 x 1 min + 2 x 10 min). The peptidyl-resin was washed with DMF (3 x 1 min), DCM (3 x 1 min) and DMF (3 x 1 min), and a solution of Fmoc-Ala-OH\*H<sub>2</sub>O (17 mg, 0.05 mmol, 3.0 eq), HATU (20 mg, 0.05 mmol, 3.0 eq), HOAt (7 mg, 0.05 mmol, 3.0 eq) and DIEA (18  $\mu$ L, 0.11 mmol, 6.0 eq) in DMF (500  $\mu$ L) was added to the peptidyl-resin according to *Protocol Pep2*, which is used for residue incorporation onto secondary amines. In order to minimise diketopiperazine formation, the Fmoc group of the second residue was eliminated by treatment with a 0.1 M OxymaPure in DBU–DMF (2:98 v/v) solution (2 x 1 min). A mixture of Fmoc-Pro-OH (18 mg, 0.05 mmol, 3.0 eq), OxymaPure (8 mg, 0.05 mmol, 3.0 eq) and DIC (8  $\mu$ L, 0.05 mmol, 3.0 eq) in DMF (500  $\mu$ L) was added to the peptide-bound employing *Protocol Pep1*, and the Fmoc group was subsequently removed by treatment with a piperidine–DMF (1:4 v/v) (1 x 1 min + 2 x 5 min) solution. A mixture of D-(+)-phenyllactic (9 mg, 0.05 mmol, 3.0 eq), HATU (20 mg, 0.05 mmol, 3.0 eq), HOAt (7 mg, 0.05 mmol, 3.0 eq) and DIEA (18  $\mu$ L, 0.11 mmol, 6.0 eq) in DMF (500  $\mu$ L) was added to the resin following *Protocol Pep2*.

The Steglich esterification was selected for the incorporation of the fifth residue. **1.10** (Fmoc-Thr(TBDMS)-OH) (64 mg, 0.14 mmol, 8.0 eq), DIC (22  $\mu$ L, 0.14 mmol, 8.0 eq)

and DMAP (1 mg, 0.01 mmol, 0.5 eq) were added to the peptidyl-resin following *Protocol Est*. The TBDMS and Fmoc groups were simultaneously removed by treatment with a 1.0 M TBAF (36  $\mu$ L, 0.02 mmol, 1.0 eq) (2 x 10 min) solution in THF (500  $\mu$ L) under  $N_2$  atmosphere. The resin was washed with dry THF (3 x 1 min), DCM (3 x 1 min) and DMF (3 x 1 min), and the corresponding free amine was acetylated by treatment with a solution of AcOH (2  $\mu$ L, 0.05 mmol, 3.0 eq), OxymaPure (8 mg, 0.05 mmol, 3.0 eq) and DIC (8  $\mu$ L, 0.05 mmol, 3.0 eq) in DMF (500  $\mu$ L) for 40 minutes.

The peptidyl-resin was washed with dry DCM (3 x 1 min), dried under *vacuum* for 20 minutes and transferred to a pyrex<sup>®</sup> culture tube provided with a magnetic stirrer. Steglich esterification of the fifth residue was achieved through either *Method A*) or *Method B*). *Method A* **1.20** (Alloc-*N,O*-Me<sub>2</sub>Thr-OH) (32 mg, 0.14 mmol, 8.0 eq), DIC (22  $\mu$ L, 0.14 mmol, 8.0 eq) and DMAP (1 mg, 0.01 mmol, 0.5 eq) were added to the peptidyl-resin following *Protocol Est*. Alloc removal was achieved by treatment with a solution of Pd(PPh<sub>3</sub>)<sub>4</sub> (2 mg, 1.75·10<sup>-3</sup> mmol, 0.1 eq) and phenylsilane (22  $\mu$ L, 0.18 mmol, 10.0 eq) (1 x 15 min) in DCM (500  $\mu$ L) under anhydrous conditions. *Method B* **1.24** (Fmoc-*N,O*-Me<sub>2</sub>Thr-OH) (52 mg, 0.14 mmol, 8.0 eq), DIC (22  $\mu$ L, 0.14 mmol, 8.0 eq) and DMAP (1 mg, 0.01 mmol, 0.5 eq) were added to the peptidyl-resin following *Protocol Est*. Fmoc removal was achieved by treatment with a DBU–DMF (2:98 v/v) (1 x 1 min) solution. The peptidyl-resin was washed with DMF (3 x 1 min), DCM (3 x 1 min) and DMF (3 x 1 min).

A mixture of Boc-Thr-OH (12 mg, 0.05 mmol, 3.0 eq), HATU (20 mg, 0.05 mmol, 3.0 eq), HOAt (7 mg, 0.05 mmol, 3.0 eq) and DIEA (18  $\mu$ L, 0.11 mmol, 6.0 eq) in DMF (500  $\mu$ L) was added to the resin through an amidation reaction using *Protocol Pep2* conditions. In this case, re-coupling was required to accomplish full incorporation of the Thr derivative.

Incorporation of the last amino acid was achieved *via* a Steglich esterification reaction. Fmoc-Thr(<sup>t</sup>Bu)-OH (56 mg, 0.14 mmol, 8.0 eq), DIC (22  $\mu$ L, 0.14 mmol, 8.0 eq) and DMAP (1 mg, 0.01 mmol, 0.5 eq) were added to the peptidyl-resin following *Protocol Est*. Fmoc removal was achieved by treatment with a solution of 0.1 M HOBt in DBU–DMF (2:98 v/v) (1 x 1 min). The peptide resin was washed with DMF (3 x 1 min), DCM (3 x 1 min) and DMF (3 x 1 min). The peptidyl-resin was washed with DMF (3 x 1 min), DCM

(3 x 1 min) and DMF (3 x 1 min), and the corresponding free amine was acetylated by treatment with a solution of AcOH (2  $\mu$ L, 0.05 mmol, 3.0 eq), OxymaPure (8 mg, 0.05 mmol, 3.0 eq) and DIC (8  $\mu$ L, 0.05 mmol, 3.0 eq) in DMF (500  $\mu$ L) for 40 minutes. The peptide resin was washed with DMF (3 x 1 min), DCM (3 x 1 min) and DMF (3 x 1 min). Treatment of the peptidyl-resin with a TFA–TIS–DCM (90:5:5 v/v) over 30 min furnished the crude linear depsipeptide. The lyophilised crude linear peptide was purified by HPLC using a XBridge™ C18 reversed-phase column (3.5  $\mu$ m x 4.6 mm x 42 mm) (purification gradient: C18 G0100t20T25) to afford pure **1.32** (4.0 mg, 25% over 16 steps) as white solid.

### **3.2.6.2 Synthesis of 1.32 using a synthetic strategy containing one depsipeptide building block segment condensation**

The 2-CTC resin (25 mg, 1.6 mmol/g resin) was placed in a 2 mL-polypropylene syringe fitted with two polyethylene filter discs. The conditioning of the resin and incorporation of the first amino acid, Fmoc-MeAla-OH (6 mg, 0.02 mmol, 1.0 eq), was carried out by standard means. The Fmoc group was removed by treatment with a piperidine–DMF solution (1:4 v/v) (1 x 1 min + 2 x 10 min). The peptidyl-resin was washed with DMF (3 x 1 min), DCM (3 x 1 min) and DMF (3 x 1 min), and a solution of Fmoc-Ala-OH\*H<sub>2</sub>O (17 mg, 0.05 mmol, 3.0 eq), HATU (20 mg, 0.05 mmol, 3.0 eq), HOAt (7 mg, 0.05 mmol, 3.0 eq) and DIEA (18  $\mu$ L, 0.11 mmol, 6.0 eq) in DMF (500  $\mu$ L) was added to the peptidyl-resin according to *Protocol Pep2*, which is used for the incorporation of a residue onto a secondary amine. In order to minimise diketopiperazine formation, the Fmoc group of the second residue was removed by treatment with a 0.1 M OxymaPure in DBU–DMF (2:98 v/v) solution (2 x 1 min). A mixture of Fmoc-Pro-OH (18 mg, 0.05 mmol, 3.0 eq), OxymaPure (8 mg, 0.05 mmol, 3.0 eq) and DIC (8  $\mu$ L, 0.05 mmol, 3.0 eq) in DMF (500  $\mu$ L) was added to the peptide-bound employing *Protocol Pep1*, and the Fmoc group was subsequently removed by treatment with a piperidine–DMF (1:4 v/v) (1 x 1 min + 2 x 5 min) solution. The peptidyl-resin was washed with DMF (3 x 1 min), DCM (3 x 1 min) and DMF (3 x 1 min).

Segment condensation of **1.37** was performed as follows. A mixture of building block **1.37** (16 mg, 0.05 mmol, 3.0 eq), PyBOP (mg, 0.05 mmol, 3.0 eq), HOAt (7 mg, 0.05 mmol, 3.0 eq) and DIEA (18  $\mu$ L, 0.11 mmol, 6.0 eq) in DMF (500  $\mu$ L) was added to the resin and shaken for 24 hours. The resin was washed with DMF (3 x 1 min), DCM (3 x 1 min) and DMF (3 x 1 min).

The peptidyl-resin was washed with dry DCM (3 x 1 min), dried under *vacuum* for 20 minutes and transferred to a pyrex<sup>®</sup> culture tube provided with a magnetic stirrer. Steglich esterification of the fifth residue was achieved through either *Method A*) or *Method B*). *Method A* **1.20** (Alloc-*N,O*-Me<sub>2</sub>Thr-OH) (32 mg, 0.14 mmol, 8.0 eq), DIC (22  $\mu$ L, 0.14 mmol, 8.0 eq) and DMAP (1 mg, 0.01 mmol, 0.5 eq) were added to the peptidyl-resin following *Protocol Est*. Alloc removal was achieved by treatment with a solution of Pd(PPh<sub>3</sub>)<sub>4</sub> (2 mg, 1.75·10<sup>-3</sup>mmol, 0.1 eq) and phenylsilane (22  $\mu$ L, 0.18 mmol, 10.0 eq) (1 x 15 min) in DCM (500  $\mu$ L) under anhydrous conditions. *Method B* **1.24** (Fmoc-*N,O*-Me<sub>2</sub>Thr-OH) (52 mg, 0.14 mmol, 8.0 eq), DIC (22  $\mu$ L, 0.14 mmol, 8.0 eq) and DMAP (1 mg, 0.01 mmol, 0.5 eq) were added to the peptidyl-resin following *Protocol Est*. Fmoc removal was achieved by treatment with a DBU–DMF (2:98 v/v) (1 x 1 min) solution. The peptide resin was washed with DMF (3 x 1 min), DCM (3 x 1 min) and DMF (3 x 1 min).

A mixture of Boc-Thr-OH (12 mg, 0.05 mmol, 3.0 eq), HATU (20 mg, 0.05 mmol, 3.0 eq), HOAt (7 mg, 0.05 mmol, 3.0 eq) and DIEA (18  $\mu$ L, 0.11 mmol, 6.0 eq) in DMF (500  $\mu$ L) was added to the resin through an amidation reaction using *Protocol Pep2* conditions. In this case, re-coupling was required to accomplish full incorporation of the Thr derivative.

Incorporation of the last amino acid was achieved *via* a Steglich esterification reaction. Fmoc-Thr(<sup>t</sup>Bu)-OH (56 mg, 0.14 mmol, 8.0 eq), DIC (22  $\mu$ L, 0.14 mmol, 8.0 eq) and DMAP (1 mg, 0.01 mmol, 0.5 eq) were added to the peptidyl-resin following *Protocol Est*. Fmoc removal was achieved by treatment with a solution of 0.1 M HOBt in DBU–DMF (2:98 v/v) (1 x 1 min). The peptide resin was washed with DMF (3 x 1 min), DCM (3 x 1 min) and DMF (3 x 1 min). The peptidyl-resin was washed with DMF (3 x 1 min), DCM (3 x 1 min) and DMF (3 x 1 min), and the corresponding free amine was acetylated by treatment with a solution of AcOH (2  $\mu$ L, 0.05 mmol, 3.0 eq), OxymaPure (8 mg, 0.05

mmol, 3.0 eq) and DIC (8  $\mu$ L, 0.05 mmol, 3.0 eq) in DMF (500  $\mu$ L) for 40 minutes. The peptide resin was washed with DMF (3 x 1 min), DCM (3 x 1 min) and DMF (3 x 1 min). Treatment of the peptidyl-resin with a TFA–TIS–DCM (90:5:5 v/v) over 30 min furnished the crude linear depsipeptide. The lyophilised crude linear peptide was purified by HPLC using a XBridge™ C18 reversed-phase column (3.5  $\mu$ m x 4.6 mm x 42 mm) (purification gradient: C18 G0100t20T25) to afford pure **1.32** (3.9 mg, 24% over 14 steps) as white solid.

### 3.2.6.3 Synthesis of **1.32** by using a synthetic strategy containing two depsipeptide building block segment condensations

The 2-CTC resin (25 mg, 1.6 mmol/g resin) was placed in a 2 mL-polypropylene syringe fitted with two polyethylene filter discs. The conditioning of the resin and incorporation of the first amino acid, Fmoc-MeAla-OH (6 mg, 0.02 mmol, 1.0 eq), was carried out by standard means. The Fmoc group was removed by treatment with a piperidine–DMF solution (1:4 v/v) (1 x 1 min + 2 x 10 min). The peptidyl-resin was washed with DMF (3 x 1 min), DCM (3 x 1 min) and DMF (3 x 1 min), and a solution of Fmoc-Ala-OH\*H<sub>2</sub>O (17 mg, 0.05 mmol, 3.0 eq), HATU (20 mg, 0.05 mmol, 3.0 eq), HOAt (7 mg, 0.05 mmol, 3.0 eq) and DIEA (18  $\mu$ L, 0.11 mmol, 6.0 eq) in DMF (500  $\mu$ L) was added to the peptidyl-resin according to *Protocol Pep2*, which is used for the incorporation of a residue onto a secondary amine. In order to minimise diketopiperazine formation, the Fmoc group of the second residue was removed by treatment with a 0.1 M OxymaPure in DBU–DMF (2:98 v/v) solution (2 x 1 min). A mixture of Fmoc-Pro-OH (18 mg, 0.05 mmol, 3.0 eq), OxymaPure (8 mg, 0.05 mmol, 3.0 eq) and DIC (8  $\mu$ L, 0.05 mmol, 3.0 eq) in DMF (500  $\mu$ L) was added to the peptide-bound employing *Protocol Pep1*, and the Fmoc group was subsequently removed by treatment with a piperidine–DMF (1:4 v/v) (1 x 1 min + 2 x 5 min) solution. The peptidyl-resin was washed with DMF (3 x 1 min), DCM (3 x 1 min) and DMF (3 x 1 min).

Segment condensation of **1.37** was performed as follows. A mixture of building block **1.37** (16 mg, 0.05 mmol, 3.0 eq), PyBOP (mg, 0.05 mmol, 3.0 eq), HOAt (7 mg, 0.05 mmol, 3.0 eq) and DIEA (18  $\mu$ L, 0.11 mmol, 6.0 eq) in DMF (500  $\mu$ L) was added to the

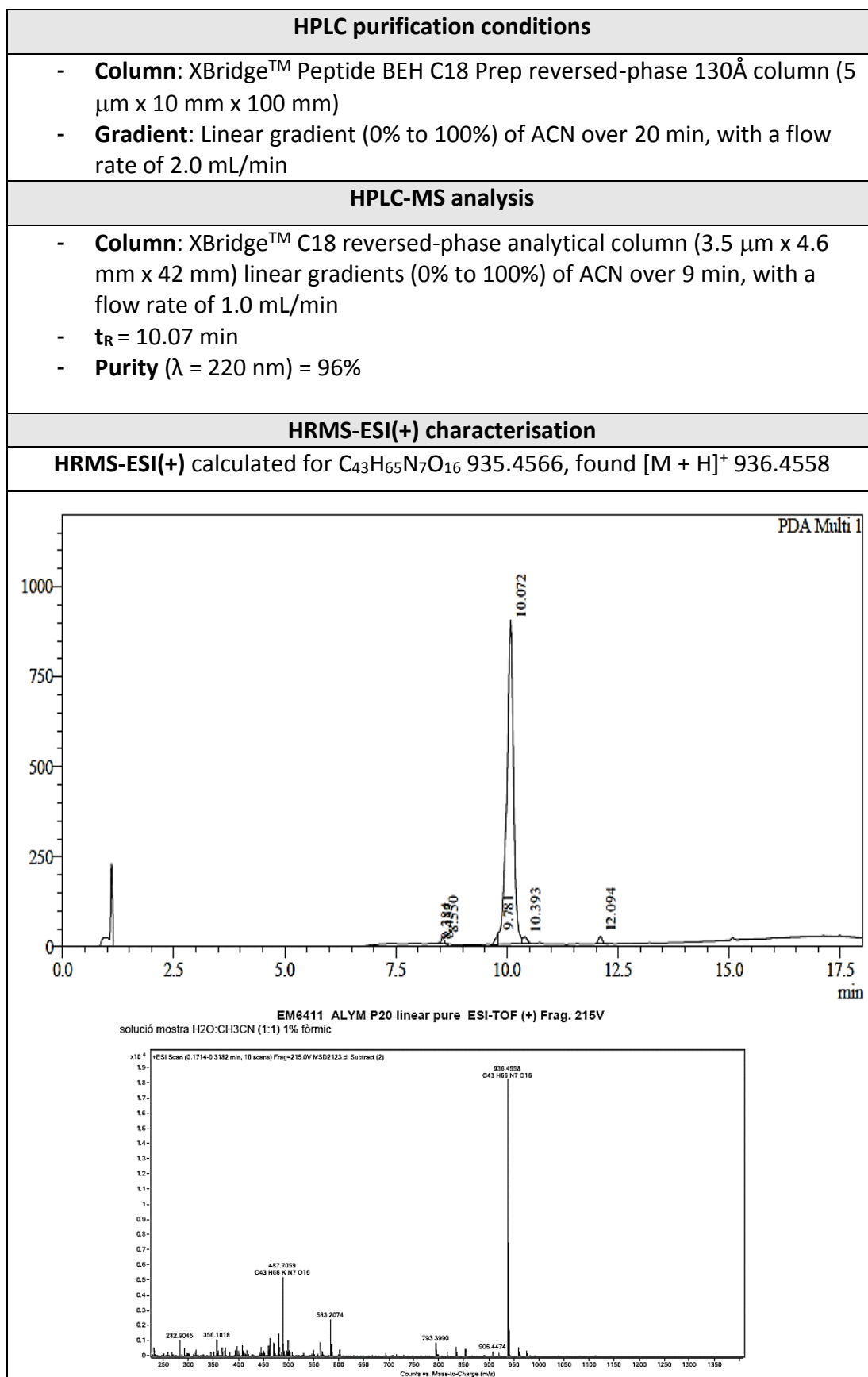
resin and shaken for 24 hours. The resin was washed with DMF (3 x 1 min), DCM (3 x 1 min) and DMF (3 x 1 min).

Steglich esterification of the fifth residue was achieved through either *Method A*) or *Method B*). *Method A* **1.20** (Alloc-*N,O*-Me<sub>2</sub>Thr-OH) (32 mg, 0.14 mmol, 8.0 eq), DIC (22 μL, 0.14 mmol, 8.0 eq) and DMAP (1 mg, 0.01 mmol, 0.5 eq) were added to the peptidyl-resin following *Protocol Est*. Alloc removal was achieved by treatment with a solution of Pd(PPh<sub>3</sub>)<sub>4</sub> (2 mg, 1.75·10<sup>-3</sup>mmol, 0.1 eq) and phenylsilane (22 μL, 0.18 mmol, 10.0 eq) (1 x 15 min) in DCM (500 μL) under anhydrous conditions. *Method B* **1.24** (Fmoc-*N,O*-Me<sub>2</sub>Thr-OH) (52 mg, 0.14 mmol, 8.0 eq), DIC (22 μL, 0.14 mmol, 8.0 eq) and DMAP (1 mg, 0.01 mmol, 0.5 eq) were added to the peptidyl-resin following *Protocol Est*. Fmoc removal was achieved by treatment with a DBU–DMF (2:98 v/v) (1 x 1 min) solution. The peptide resin was washed with DMF (3 x 1 min), DCM (3 x 1 min) and DMF (3 x 1 min).

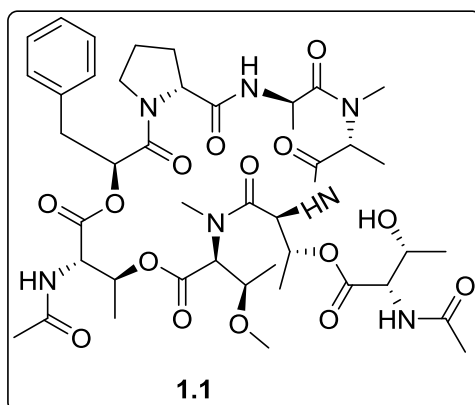
Segment condensation of **1.38** was performed as follows. A mixture of building block **1.38** (21 mg, 0.05 mmol, 3.0 eq), HATU (19 mg, 0.05 mmol, 3.0 eq) and collidine (14 μL, 0.11 mmol, 6.0 eq) in DMF (500 μL) was added to the resin and shaken for 2 hours. The resin was washed with DMF (3 x 1 min), DCM (3 x 1 min) and DMF (3 x 1 min).

The peptide resin was washed with DMF (3 x 1 min), DCM (3 x 1 min) and DMF (3 x 1 min). Treatment of the peptidyl-resin with a TFA–TIS–DCM (90:5:5 v/v) over 30 min furnished the crude linear depsipeptide. The lyophilised crude linear peptide was purified by HPLC using a XBridge™ Peptide BEH C18 Prep reversed-phase 130Å column (5 μm x 10 mm x 100 mm) (purification gradient: C18 G0100t20T25) to afford pure **1.32** (4.3 mg, 26% over 11 steps) as white solid.

## 3.2.6.4 1.32 characterisation



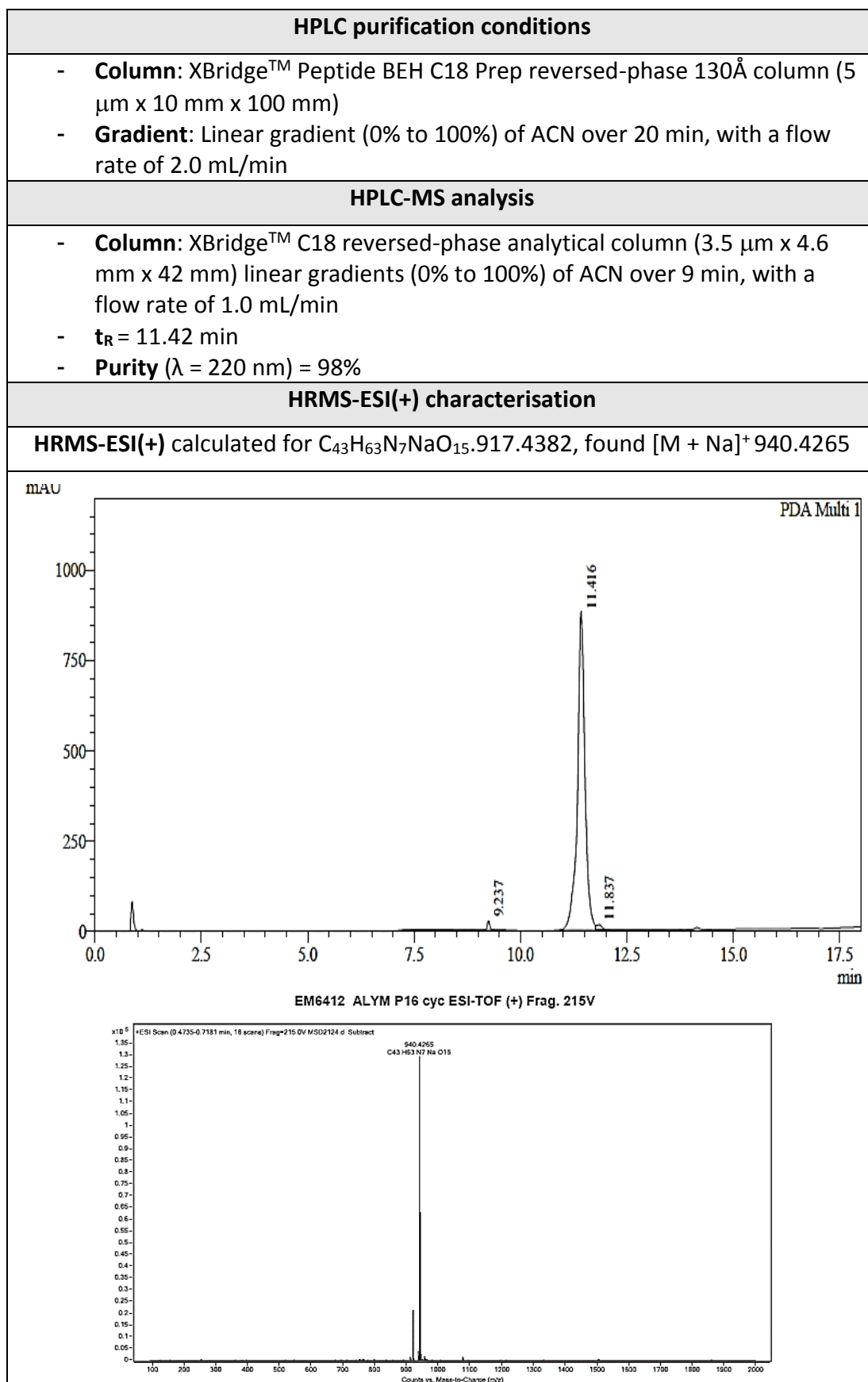
### 3.2.7 Macrolactamisation of **1.32** to obtain cyclic depsipeptide **1.1**



#### 3.2.7.1 Cyclisation of **1.32**

**1.32** (2.9 mg,  $3.10 \cdot 10^{-3}$  mmol, 1.0 eq) was dissolved in DMF (3.10 mL) and 2,4,6-collidine (1.2  $\mu$ L,  $9.30 \cdot 10^{-3}$  mmol, 3.0 eq) and HATU (1.2 mg,  $3.10 \cdot 10^{-3}$  mmol, 1.0 eq) were added. The reaction mixture was let to stir for 2 hours until full consumption of the starting material was observed by HPLC analysis. The solvent was removed under reduced pressure, and the crude cyclic peptide was purified by HPLC using a XBridge<sup>TM</sup> Peptide BEH C18 Prep reversed-phase 130Å column (5  $\mu$ m x 10 mm x 100 mm) (purification gradient: C18 G0100t20T25) to afford pure **1.1** (1 mg, 22%) as white solid.

## 3.2.7.2 1.1 characterisation



## 3.3 Chapter 2

### 3.3.1 General protocols

#### 3.3.1.1 Solid-phase synthesis protocols

##### 3.3.1.1.1 Peptide coupling protocols

The peptide chain elongation can be accomplished by using several protocols. Herein described the ones used in the present thesis. All the coupling treatments were performed at 25 °C unless stated otherwise. After one minute of manual stirring, the reaction mixture was shaken in an orbital shaker. Coupling conversion was checked by means of the appropriate colorimetric test and re-coupling was carried out if required.

- Protocol Pep1: was used when coupling onto primary amines.

| Step | Treatment         | Conditions   |
|------|-------------------|--|
| 1    | Washes            | DMF (3 x 1 min) + DCM (3 x 1 min) + DMF (3 x 1 min)          |
| 2    | Deprotection      | Piperidine–DMF (1:4 v/v) (1 x 1 min + 2 x 5 min)             |
| 3    | Washes            | DMF (3 x 1 min) + DCM (3 x 1 min) + DMF (3 x 1 min)          |
| 4    | Coupling*         | Fmoc-AA(PG)-OH–OxymaPure–DIC (3:3:3 eq)<br>in DMF for 40 min |
| 5    | Washes            | DMF (3 x 1 min) + DCM (3 x 1 min)                            |
| 6    | Colorimetric test | Kaiser test  |

\*To prevent racemisation, the amino acid was pre-activated with the coupling reagent (DIC) and the additive (OxymaPure) over 5 minutes.

- Protocol Pep2: was used when coupling onto secondary amines.

| Step | Treatment         | Conditions   |
|------|-------------------|--|
| 1    | Washes            | DMF (3 x 1 min) + DCM (3 x 1 min) + DMF (3 x 1 min)          |
| 2    | Deprotection      | Piperidine–DMF (1:4 v/v) (1 x 1 min + 2 x 10 min)            |
| 3    | Washes            | DMF (3 x 1 min) + DCM (3 x 1 min) + DMF (3 x 1 min)          |
| 4    | Coupling*         | Fmoc-AA(PG)-OH–HATU–HOAt–DIEA (3:3:3:6 eq)<br>in DMF for 1 h |
| 5    | Washes            | DMF (3 x 1 min) + DCM (3 x 1 min)                            |
| 6    | Colorimetric test | Chloranil test   |

### 3.3.1.1.2 Bromoacetic acid coupling protocol

- Protocol Pep3: Commercially available Bromoacetic acid (5 eq) was dissolved in DMF and DIC (5 eq) was added. The resulting solution was added to the peptide-resin and shaken in an orbital shaker for 30 minutes. A “mini-cleavage” was performed and the sample was analysed by HPLC-MS to confirm reaction completion.

### 3.3.1.1.3 Fmoc removal protocol

The Fmoc group is removed by treatment of the peptidyl-resin with a basic solution.

- Protocol Fmoc1: The peptide-resin was treated with a piperidine–DMF (1:4 v/v) (1 x 1 min + 2 x 5 min) solution. The peptidyl resin was washed with DMF (3 x 1 min), DCM (3 x 1 min) and DMF (3 x 1 min).

### 3.3.1.1.4 Dde removal protocol

The Dde group can be orthogonally removed upon treatment with hydrazine.

- Protocol Dde: The resin bound was treated with a hydrazine–DMF (1:9 v/v) (1 x 1 min + 2 x 15 min) solution. The peptidyl-resin was washed with DMF (3 x 1 min), DCM (3 x 1 min) and DMF (3 x 1 min).

### 3.3.1.1.5 Allyl and Alloc removal protocols

The Allyl and Alloc groups are removed under neutral conditions by treatment of the peptide-bound with catalytic Pd(PPh<sub>3</sub>)<sub>4</sub> and phenylsilane, which serves as scavenger. Herein described the employed procedures. *Protocol All1* was generally used in the present work unless stated otherwise. *Protocol All2* was used when the system required anhydrous conditions.

- Protocol All: The peptide-resin was washed with DCM (3 x 1 min) and treated with a solution of catalytic Pd(PPh<sub>3</sub>)<sub>4</sub>–Phenylsilane (0.1:10 eq) in DCM (3 x 15 min). The resin was washed with DCM (3 x 1 min), DMF (3 x 1 min) and DCM (3 x 1 min).

#### 3.3.1.1.6 Mmt removal protocol

Occasionally, the side chain of the cysteine residue is protected with the Mmt group. The Mmt group can be removed under very mild acidic conditions, thus ensuring orthogonality with other common protecting groups such as <sup>t</sup>Bu, Boc, among others.

- Protocol Mmt: The Mmt group was selectively removed on solid-phase by treatment of the peptide-bound with TFA–TIS–DCM (5:5:90 v/v) (3 x 15 min). The resin was washed with DCM (3 x 1 min), DMF (3 x 1 min) and a solution of DIEA in DMF (1:99) (3 x 1 min) to neutralise all the leftover acid. Full Mmt removal was assessed by addition of a few drops of TFA to a small aliquot of the peptide resin. Orange colouring of the resin indicates the presence of the Mmt group, and therefore more removal cycles are required.

#### 3.3.1.1.7 Acetylation protocols

*Protocol Ac1* was used for acetylation of primary amines, and *Protocol Ac2* was employed for the acetylation of secondary amines *via* an amidation reaction using strong coupling conditions.

- Protocol Ac1: Acetylation of primary amines was accomplished by treatment of the peptide-resin with a solution of Ac<sub>2</sub>O–DIEA (3:9 eq) in DCM (1 x 20 min). The resin was washed with DCM (3 x 1 min), DMF (3 x 1 min) and DMF (3 x 1 min). A Kaiser test was used to monitor reaction conversion.
- Protocol Ac2: A mixture of AcOH–HATU–HOAt–DIEA (3:3:3:6 eq) in DMF was added to the resin and it was shaken for one hour. The resin was washed with DMF (3 x 1 min) and DCM (3 x 1 min). The appropriate colorimetric test was run to monitor reaction conversion.

#### 3.3.1.1.8 Three-step Mitsunobu *N*-methylation protocol

The three-step Mitsunobu *N*-methylation allows the *N*-methylation of primary amines under mild conditions. First, the amine is protected and activated with the *o*-nitrobenzenesulfonyl group (*o*-NBS), followed by the *N*-methylation. Once the *N*-methylation is accomplished, the *o*-NBS group is removed.

- **Protocol *Mit***: A solution of *o*-NBS-Cl–DIEA (4:10 eq) in DCM was added to the peptide-resin and shaken for 90 minutes. The Kaiser test was performed to ensure all primary amines had been protected. If otherwise, the same treatment was repeated. The resin was washed with DCM (3 x 1 min), DMF (3 x 1 min) and dry THF (3 x 1 min). *N*-methylation was achieved by adding a solution of PPh<sub>3</sub>–MEOH (5:10 eq) in anhydrous THF to the peptidyl-resin. After one minute of manual stirring, a solution of DIAD (5 eq) in dry THF was added dropwise over 10 minutes and shaken for 20 more minutes. The *N*-methylation step was repeated until full reaction completion was accomplished (reaction monitored by HPLC-MS). The *o*-NBS group was removed by treatment of the peptidyl-resin with a solution of DBU (5 eq) and 2-mercaptoethanol (10 eq) in DMF (1 x 1 min + 2 x 15 min). The resin was then washed with DMF (3 x 1 min), DCM (3 x 1 min) and DMF (3 x 1 min).

#### 3.3.1.1.9 Alloc protection protocol

- **Protocol *Pro***: Alloc protection on solid-phase was accomplished by treatment of the peptide-resin with a solution of Alloc-Cl–DIEA (3:9 eq) in DCM for 30 minutes. A Kaiser test was run to monitor reaction conversion.

#### 3.3.1.1.10 Cyclisation through thioether cross-linking

On-resin side-chain to side-chain cyclisation to form a thioether bond takes place through the nucleophilic attack of a sulphur group of a cysteine residue to the bromomethylene moiety present in the peptide sequence. Two steps are required, including selective removal of the cysteine residue and nucleophilic displacement to form the thioether bond.

- **Protocol *Cyc1***: First, the Mmt group of the cysteine residue was selectively removed following *Protocol Mmt*. Nucleophilic attack of the sulphur moiety to form the thioether bond took place by addition of a DIEA (5 eq) solution in DMF. The reaction was shaken for 30 minutes and reaction completion was monitored by HPLC-MS.

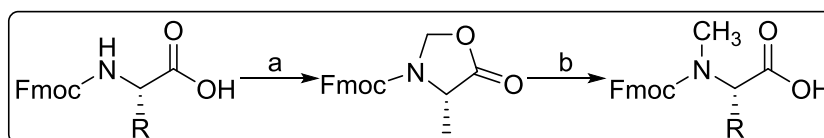
### 3.3.1.2 Solution phase synthesis protocols

#### 3.3.1.2.1 Peptide cyclisation in solution through thioether cross-linking

Side-chain to side-chain cyclisation to form a thioether bond between a cysteine residue and a bromomethylene group can be selectively performed in solution in the presence of other functionalities. The nucleophilic substitution of the sulphur group of a cysteine residue to a bromomethylene group takes place under slightly basic conditions (pH = 7.9).

- Protocol Cyc2: The cleaved unprotected peptide crude product was dissolved in a mixture of  $\text{NH}_4\text{HCO}_3(\text{aq})$  (20 mM, pH = 7.9)–ACN (3:1 v/v) (5 mM), and it was let to stir for 30 minutes. The reaction was monitored by HPLC-MS. After full conversion was reached, the reaction mixture was lyophilised to afford the crude product.

### 3.3.2 Preparation of Fmoc-*N*-Me-amino acids

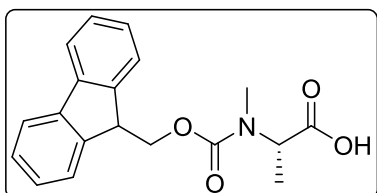


#### General protocol for the preparation of Fmoc-*N*-Me-amino acids

*p*-TsOH (0.1 eq) and *p*-formaldehyde (1.1 eq) were placed in a 2-neck round bottom flask and dissolved in dry toluene (8 mL per each 5.00 mmol of *p*-formaldehyde). A solution of the corresponding commercially available Fmoc-AA-OH (1.0 eq) in toluene (5 mL per each 4.60 mmol of Fmoc-AA-OH) was added dropwise, and the yellow suspension was brought to reflux. A Dean stark trap was used to remove the water formed during the reaction. After 3 h, EtOAc and a 5% aqueous  $\text{Na}_2\text{CO}_3$  solution were added. The organic layer was washed with a 5% aqueous  $\text{Na}_2\text{CO}_3$  solution (2 x),  $\text{H}_2\text{O}$  (2 x), brine, dried over  $\text{MgSO}_4$ , and filtered off. The solvent was removed under *vacuum* to afford the corresponding 5-oxazolidine intermediate crude product. The crude product was used without further purification. The 5-oxazolidine was dissolved in dry DCM (30 mL per each 4.60 mmol of Fmoc-AA-OH) and TIS (4.0 eq) was added, followed by the

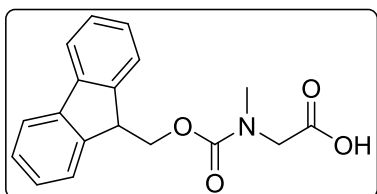
addition of TFA (27 mL per each 4.60 mmol of Fmoc-AA-OH). The yellow solution was stirred for 14 h under N<sub>2</sub> atmosphere, and the solvent was removed under *vacuo* and the crude product was subjected to flash chromatography on silica gel.

**Compound 2.1** (*N*-(((9*H*-fluoren-9-yl)methoxy)carbonyl)-*N*-methyl-*L*-alanine)



Fmoc-Ala-OH (1.039 g, 3.33 mmol, 1.0 eq) was subjected to the general protocol for the preparation Fmoc-*N*-Me-amino acids. The crude product was subjected to flash chromatography on silica gel (DCM/MeOH, 1:0 → 9:1) to afford pure **2.1** (1.325 g, 82% over two steps) as white solid. <sup>1</sup>H NMR (400 MHz, CDCl<sub>3</sub>, rotamers) δ 7.77 (d, *J* = 7.5 Hz, 2H), 7.63 – 7.53 (m, 2H), 7.42 – 7.31 (m, 4H), 4.95 – 4.86 + 4.68 – 4.58 (m, 1H), 4.55 – 4.36 (m, 2H), 4.32 – 4.20 (m, 1H), 2.92 (s, 3H), 1.47 + 1.38 (d, *J* = 7.3 Hz, 3H). <sup>13</sup>C NMR (101 MHz, CDCl<sub>3</sub>, rotamers) δ 177.2, 157.0, 144.0, 141.5, 127.8, 127.2, 125.2, 120.1, 68.1, 54.4 (54.0), 47.4, 30.7, 14.7. ESI(+)**MS** *m/z* calculated for C<sub>19</sub>H<sub>19</sub>NO<sub>4</sub> 325.1 found [M + H]<sup>+</sup> 326.2.

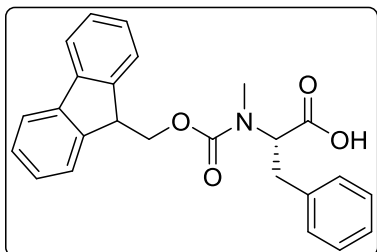
**Compound 2.2** (*N*-(((9*H*-fluoren-9-yl)methoxy)carbonyl)-*N*-methylglycine)



Fmoc-Gly-OH (1.000 g, 3.37 mmol, 1.0 eq) was subjected to the general protocol for the preparation Fmoc-*N*-Me-amino acids. The crude product was subjected to flash chromatography on silica gel (DCM/MeOH, 1:0 → 9:1) to afford pure **2.2** (755 mg, 72% over two steps) as white solid. <sup>1</sup>H NMR (400 MHz, CDCl<sub>3</sub>, rotamers) δ 7.79 – 7.71 (m, 2H), 7.56 (dd, *J* = 27.6, 7.4 Hz, 2H), 7.43 – 7.34 (m, 2H), 7.33 – 7.27 (m, 2H), 4.47 – 4.38

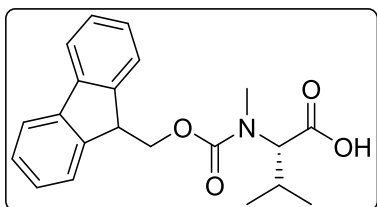
(m, 2H), 4.24 (dt,  $J = 12.7, 6.7$  Hz, 1H), 4.08 (s, 1H), 3.93 (s, 1H), 3.03 + 2.98 (s, 3H).  $^{13}\text{C}$  NMR (101 MHz,  $\text{CDCl}_3$ , rotamers)  $\delta$  173.7, 156.8, 143.6, 141.1, 127.6, 127.5, 126.9, 126.8, 124.7, 119.8, 67.7 (67.6), 50.4, 49.9, 47.0, 35.8, 35.3. ESI(+)MS  $m/z$  calculated for  $\text{C}_{18}\text{H}_{17}\text{NO}_4$  311.1, found  $[\text{M} + \text{H}]^+$  312.1.

**Compound 2.3** (*N*-(((9*H*-fluoren-9-yl)methoxy)carbonyl)-*N*-methyl-*L*-phenylalanine)



Fmoc-Phe-OH (1.020 g, 2.64 mmol, 1.0 eq) was subjected to the general protocol for the preparation Fmoc-*N*-Me-amino acids. The crude product was subjected to flash chromatography on silica gel (DCM/MeOH, 1:0  $\rightarrow$  9:1) to afford pure **2.3** (962 mg, 91% over two steps) as white solid.  $^1\text{H}$  NMR (400 MHz,  $\text{CDCl}_3$ , rotamers)  $\delta$  7.75 (d,  $J = 7.4$  Hz, 2H), 7.54 – 7.26 (m, 8H), 7.24 – 7.19 (m, 3H), 4.88 (dd,  $J = 11.1, 5.0$  Hz, 1H), 4.55 (dd,  $J = 10.8, 5.7$  Hz, 1H), 4.37 (dd,  $J = 7.1, 2.7$  Hz, 1H), 4.21 (t,  $J = 7.1$  Hz, 1H), 3.38 (dd,  $J = 14.3, 4.8$  Hz, 1H), 3.14 (m, 1H), 2.79 + 2.77 (s, 3H).  $^{13}\text{C}$  NMR (101 MHz,  $\text{CDCl}_3$ , rotamers)  $\delta$  175.7, 156.9, 144.0, 141.4, 137.0, 129.0, 128.8, 128.7, 127.8, 127.2, 125.1, 120.1, 68.0 (67.5), 61.0, 47.2, 34.8, 32.6. ESI(+)MS  $m/z$  calculated for  $\text{C}_{25}\text{H}_{23}\text{NO}_4$  401.2, found  $[\text{M} + \text{H}]^+$  402.2.

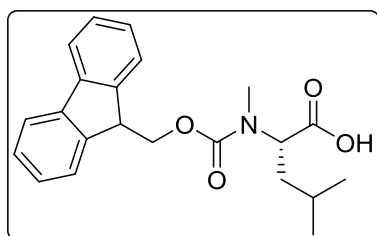
**Compound 2.4** (*N*-(((9*H*-fluoren-9-yl)methoxy)carbonyl)-*N*-methyl-*L*-valine)



Fmoc-Val-OH (1.130 g, 3.33 mmol, 1.0 eq) was subjected to the general protocol for the preparation Fmoc-*N*-Me-amino acids. The crude product was subjected to flash

chromatography on silica gel (DCM/MeOH, 1:0 → 9:1) to afford pure **2.4** (965 mg, 82% over two steps) as white solid.  $^1\text{H NMR}$  (400 MHz, DMSO, rotamers)  $\delta$  12.74 (s, 1H), 7.89 (d,  $J = 7.2$  Hz, 2H), 7.68 – 7.62 (m, 2H), 7.44 – 7.39 (m, 2H), 7.35 – 7.28 (m, 2H), 4.47 – 4.26 (m, 3H), 4.17 + 3.86 (d,  $J = 10.3$  Hz, 1H), 2.73 + 2.70 (s, 3H), 2.18 – 1.89 (m, 1H), 0.93 + 0.81 (d,  $J = 6.5$  Hz, 3H), 0.74 + 0.58 (d,  $J = 6.6$  Hz, 3H).  $^{13}\text{C NMR}$  (101 MHz,  $\text{CDCl}_3$ , rotamers)  $\delta$  174.9, 160.3, 144.0, 141.5, 127.9, 127.2, 125.1, 120.2, 68.1 (67.9), 65.6, 64.2, 47.4, 27.6, 19.9, 19.2 (19.0). **ESI(+)**MS  $m/z$  calculated for  $\text{C}_{21}\text{H}_{23}\text{NO}_4$  353.2, found  $[\text{M} + \text{H}]^+$  354.2.

**Compound 2.5** (*N*-(((9*H*-fluoren-9-yl)methoxy)carbonyl)-*N*-methyl-*L*-leucine)



Fmoc-Leu-OH (1.202 g, 3.40 mmol, 1.0 eq) was subjected to the general protocol for the preparation Fmoc-*N*-Me-amino acids. The crude product was subjected to flash chromatography on silica gel (DCM/MeOH, 1:0 → 9:1) to afford pure **2.5** (1.098 g, 88% over two steps) as white solid. **ESI(+)**MS  $m/z$  calculated for  $\text{C}_{22}\text{H}_{25}\text{NO}_4$  367.2, found  $[\text{M} + \text{H}]^+$  368.2.  $^1\text{H NMR}$  (400 MHz,  $\text{CDCl}_3$ , rotamers)  $\delta$  7.80 – 7.71 (m, 2H), 7.63 – 7.53 (m, 2H), 7.44 – 7.26 (m, 4H), 4.96 – 4.89 (t,  $J = 7.9$  Hz, 1H), 4.53 – 4.39 (m, 2H), 4.25 (dt,  $J = 11.6, 6.4$  Hz, 1H), 2.87 + 2.85 (s, 3H), 1.79 – 1.72 (m, 1H), 1.71 – 1.42 (m, 2H), 0.97 + 0.88 (d,  $J = 6.7$  Hz, 3H), 0.95 + 0.75 (d,  $J = 6.5$  Hz, 3H).  $^{13}\text{C NMR}$  (101 MHz,  $\text{cdcl}_3$ )  $\delta$  177.7, 157.3, 156.6, 144.1, 144.0, 141.5, 127.8, 127.2, 125.2, 125.1, 124.8, 120.1, 67.9, 56.9, 47.4, 37.3, 30.5, 25.0 (24.8), 23.4 (23.2), 21.4 (21.1). **ESI(+)**MS  $m/z$  calculated for  $\text{C}_{22}\text{H}_{25}\text{NO}_4$  367.2, found  $[\text{M} + \text{H}]^+$  368.1.

### 3.3.3 Chain elongation of a p53-based linear peptide

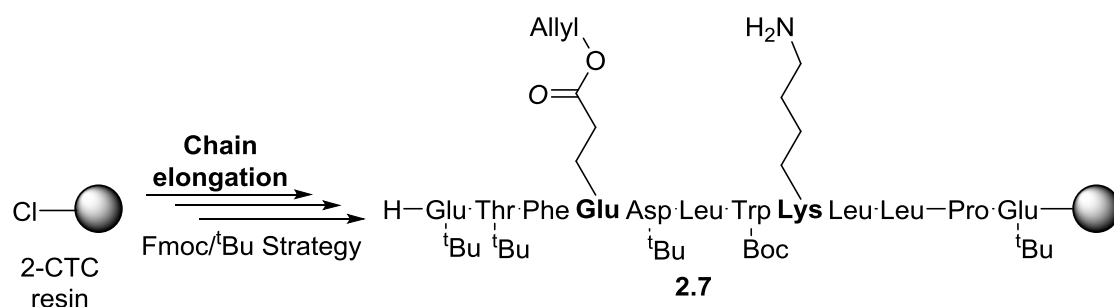
Linear chain elongation to furnish peptides with the unblocked C-terminus: The 2-CTC resin (300 mg, 1.6 mmol/g resin) was placed in a 2 mL-polypropylene syringe fitted

with two polyethylene filter discs. The conditioning of the resin and incorporation of the first amino acid, Fmoc-Glu(<sup>t</sup>Bu)-OH (38 mg, 0.019 mmol, 1.0 eq), was carried out by standard means. Generally, *Protocol Pep1* and *Protocol Pep2* were used for peptide couplings onto primary and secondary amines, respectively. Fmoc removal was accomplished following *Protocol Fmoc1*. *N*-terminal amine acetylation was accomplished following *Protocol Ac1*. Next, the Dde group removal was achieved following *Protocol Dde*.

Linear chain elongation to furnish peptides with the amidated C-terminus: The Rink Amide AM resin (300 mg, 0.14 mmol/g resin) was placed in a 2 mL-polypropylene syringe fitted with two polyethylene filter discs. The conditioning of the resin and incorporation of the first amino acid, Fmoc-Glu(<sup>t</sup>Bu)-OH (53 mg, 0.126 mmol, 3.0 eq), was carried out by standard means. Generally, *Protocol Pep1* and *Protocol Pep2* were used for peptide couplings onto primary and secondary amines, respectively. Fmoc removal was accomplished following *Protocol Fmoc1*. *N*-terminal amine acetylation was accomplished following *Protocol Ac1*. Next, the Dde group removal was achieved following *Protocol Dde*.

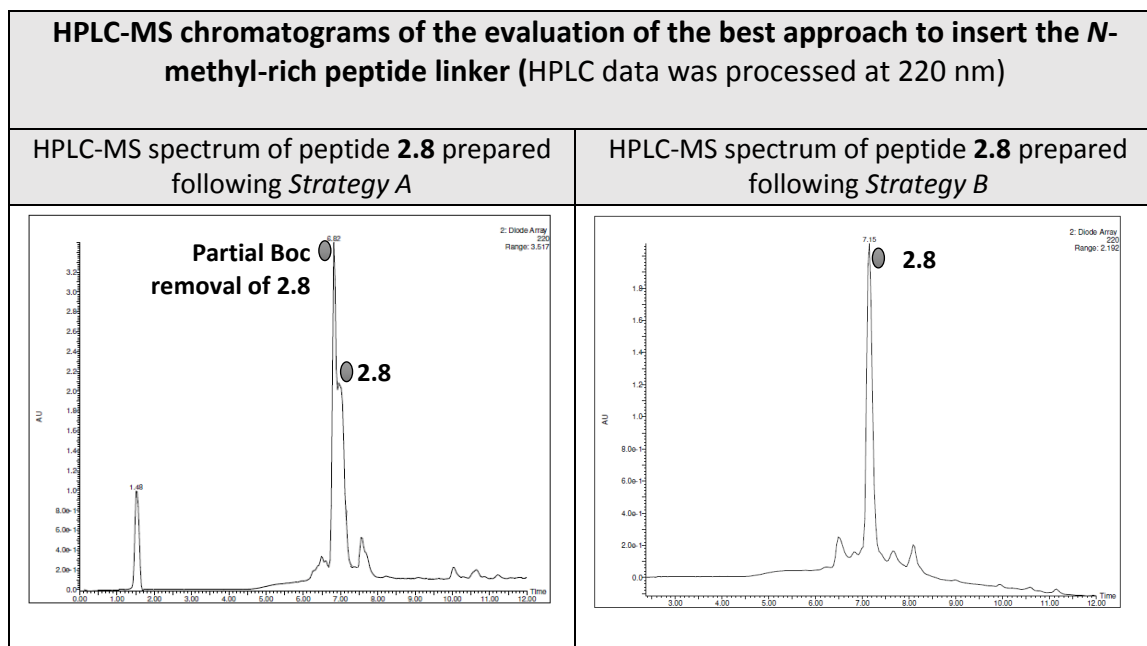
### 3.3.4 Evaluation of the best approach to insert the *N*-methyl-rich peptide linker

The linear chain elongation of a 12-mer peptide containing the following linear sequence (**2.7**) was carried out according to the general protocol described in section 3.3.3.



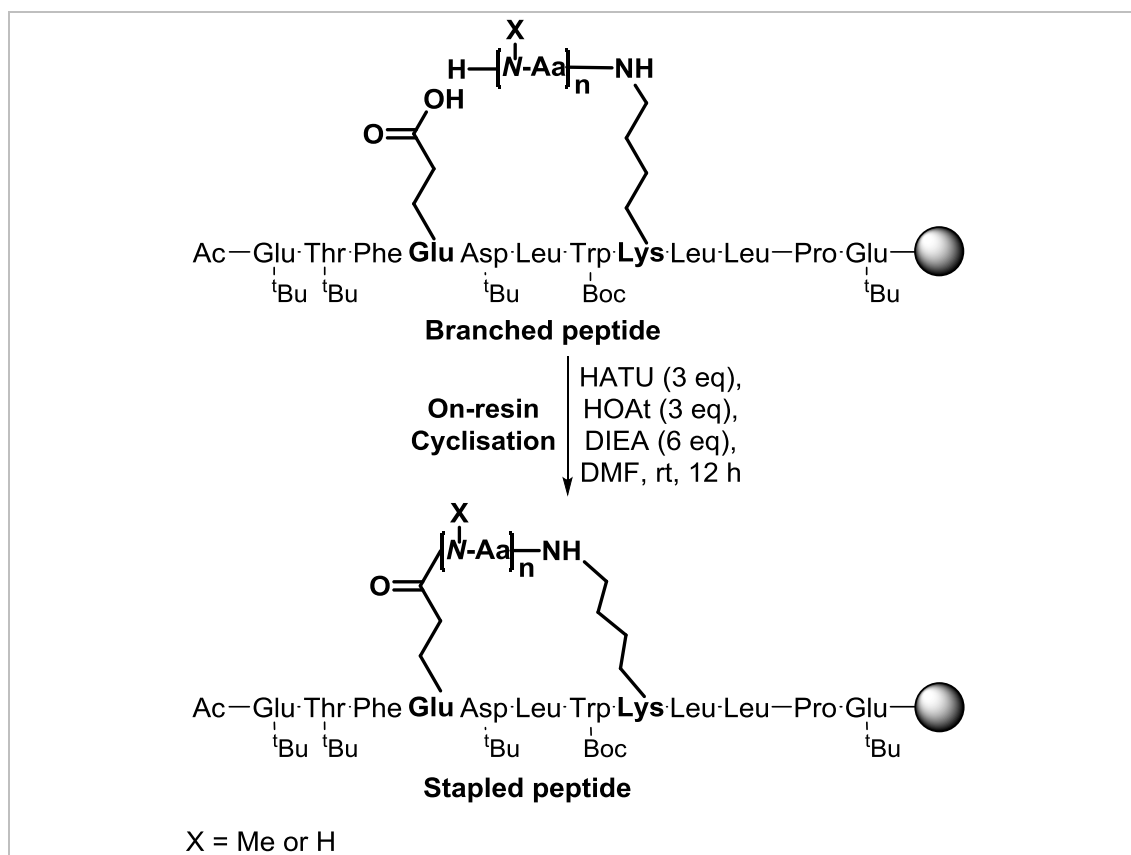
After Dde removal, two strategies were developed for the insertion of a tetrapeptide bridge containing four *N*-MeAla residues (**2.8**). A small aliquot of the





### 3.3.5 Scope of the lactam-based cross-link: Macrolactamisation studies

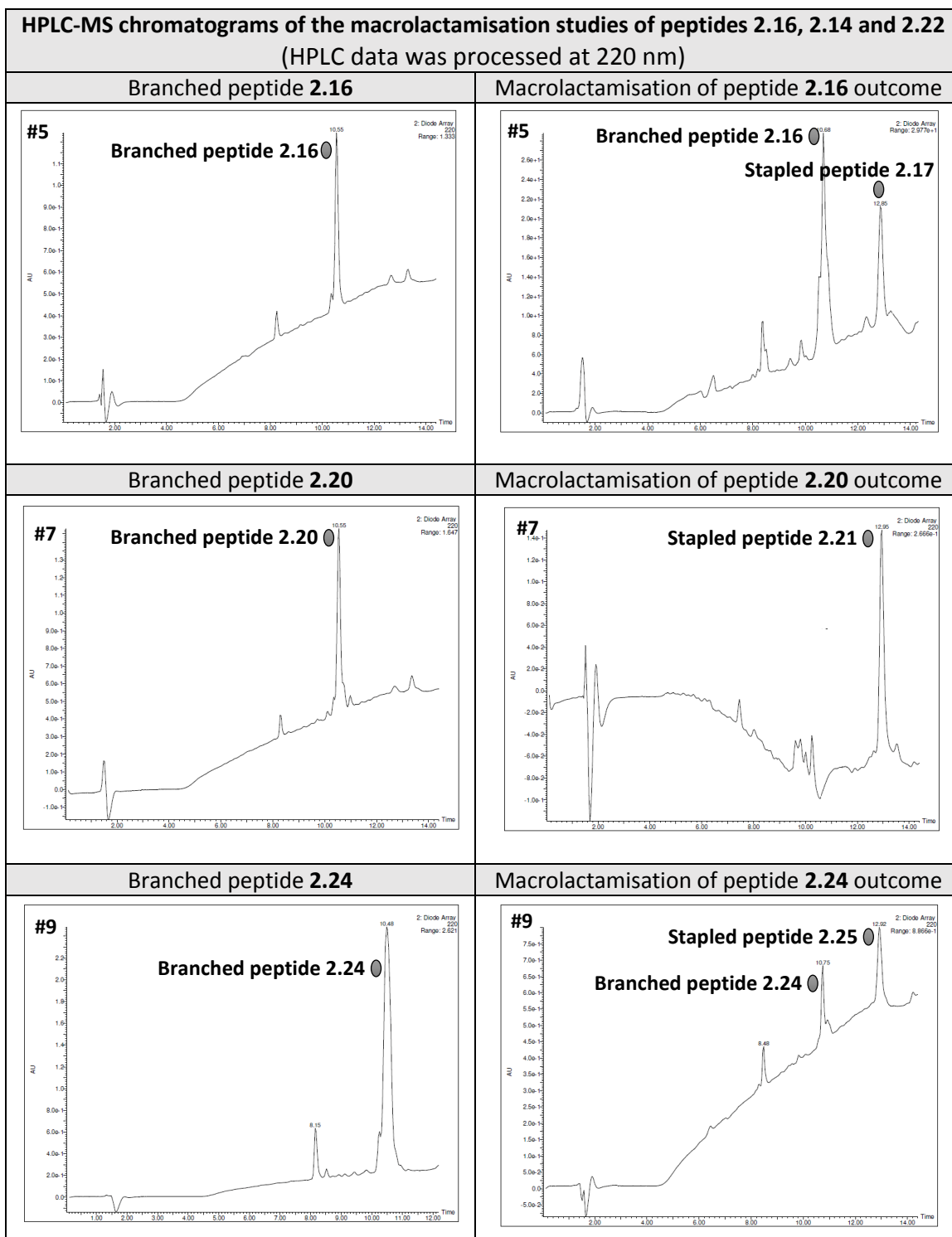
Scope of the lactam-based cross-linking approach was evaluated with different staple sequence combinations. In all cases, Alloc removal was first accomplished using *Protocol All*, followed by elongation of the corresponding branched region (see section 3.3.4) at the first stapling position (i). Next, the corresponding branched linear peptidyl-resin was treated with a solution of HATU–HOAt–DIEA (3:3:6 eq) in DMF for 12 h. A small aliquot of the peptidyl-resin was subjected to *Protocol MC* to analyse the macrolactamisation outcome by HPLC-MS (see section 1.1.3.5.3). A 12-mer peptide was used for preparation of a library single “short” stapled peptides, where the stapling points were located at relative positions  $i, i+4$ . All the staple sequence combinations as well as the macrolactamisation outcome are summarised Table 9.



| # | Branched peptide | Stapled peptide | Staple sequence                   | On-resin cyclisation (% HPLC conversion) |
|---|------------------|-----------------|-----------------------------------|--|
| 1 | <b>2.8</b>       | <b>2.9</b>      | –N-MeAla–N-MeAla–N-MeAla–N-MeAla– | 0  |
| 2 | <b>2.10</b>      | <b>2.11</b>     | –N-MeAla–N-MeAla–N-MeAla–         | 0  |
| 3 | <b>2.12</b>      | <b>2.13</b>     | –N-MeAla–N-MeAla–                 | 0  |
| 4 | <b>2.14</b>      | <b>2.15</b>     | –N-MePhe–N-MeAla–N-MeAla–N-MeAla– | 0  |
| 5 | <b>2.16</b>      | <b>2.17</b>     | –N-MeGly–N-MeAla–N-MeAla–N-MeAla– | 30                                       |
| 6 | <b>2.18</b>      | <b>2.19</b>     | –N-MeGly–Phe–N-MeAla–N-MeAla–     | 0  |
| 7 | <b>2.20</b>      | <b>2.21</b>     | –Ala–N-MeAla–N-MeAla–N-MeAla–     | 100                                      |
| 8 | <b>2.22</b>      | <b>2.23</b>     | –Phe–N-MeAla–N-MeAla–N-MeAla–     | 0  |
| 9 | <b>2.24</b>      | <b>2.25</b>     | –Gly–N-MeAla–N-MeAla–N-MeAla–     | 55                                       |

Table 9. Scope of the lactam-based cross-linking strategy at positions *i* and *i*+4.

HPLC-MS chromatograms of peptide macrolactamisation that resulted in actual product formation are shown below. Chromatograms of entries #1-4, #6 and #8 are not shown, since only the unreacted starting material was detected in all cases.



### 3.3.6 Cleavage and global deprotection of highly *N*-methylated peptides studies

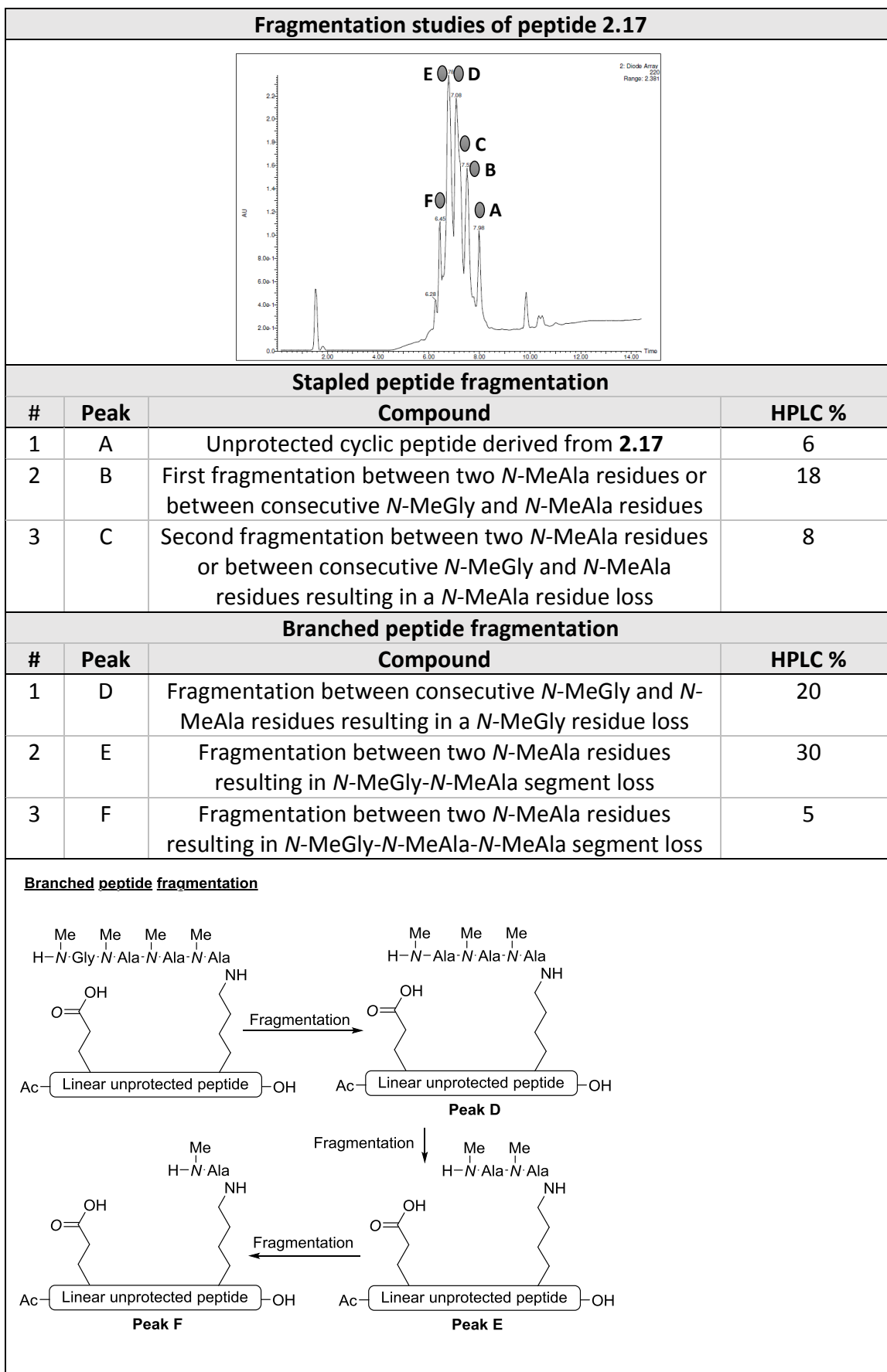
Whereas *Protocol Cle4* was followed for peptide cleavage with the HFIP mixture, *Protocol Cle2* was followed for peptide cleavage with the TFA cocktail.

In all cases, the resulting peptidyl-resin cleavage crude was subjected to HPLC-MS analysis to assess the cleavage and deprotection outcome. The obtained results are summarised in Table 10.

| #  | Peptide     | Cleavage conditions                                      | Non-fragmented peptide (HPLC %) |
|----|-------------|--|---------------------------------|
| 1  | <b>2.17</b> | HFIP-DCM (1:4 v/v), 1h                                   | 100                             |
| 2  | <b>2.17</b> | TFA-TIS-H <sub>2</sub> O (95:2.5:2.5 v/v), 30 min        | 6                               |
| 3  | <b>2.17</b> | TFA-TIS-H <sub>2</sub> O-DCM (50:2.5:2.5:45 v/v), 30 min | 6                               |
| 4  | <b>2.17</b> | TFA-TIS-H <sub>2</sub> O-DCM (20:2.5:2.5:75 v/v), 30 min | 6                               |
| 5  | <b>2.21</b> | HFIP-DCM (1:4 v/v), 1 h                                  | 100                             |
| 6  | <b>2.21</b> | TFA-TIS-H <sub>2</sub> O (95:2.5:2.5 v/v), 30 min        | 27                              |
| 7  | <b>2.21</b> | TFA-TIS-H <sub>2</sub> O-DCM (50:2.5:2.5:45 v/v), 30 min | 27                              |
| 8  | <b>2.21</b> | TFA-TIS-H <sub>2</sub> O-DCM (20:2.5:2.5:75 v/v), 30 min | 27                              |
| 9  | <b>2.25</b> | HFIP-DCM (1:4 v/v), 1h                                   | 100                             |
| 10 | <b>2.25</b> | TFA-TIS-H <sub>2</sub> O (95:2.5:2.5 v/v), 30 min        | 12                              |
| 11 | <b>2.25</b> | TFA-TIS-H <sub>2</sub> O-DCM (50:2.5:2.5:45 v/v), 30 min | 12                              |
| 12 | <b>2.25</b> | TFA-TIS-H <sub>2</sub> O-DCM (20:2.5:2.5:75 v/v), 30 min | 12                              |

Table 10. Tested cleavage and global deprotection for compounds **2.17**, **2.21** and **2.25**.

Following, the chromatograms of all three peptidyl-resin cleavage crudes by treatment with the TFA mixtures are shown. Since peptide fragmentation upon cleavage with TFA was detected in all three cases (**2.17**, **2.21** and **2.25**), further efforts to identify all peptide fragments were carried out and are summarised in Table 11,



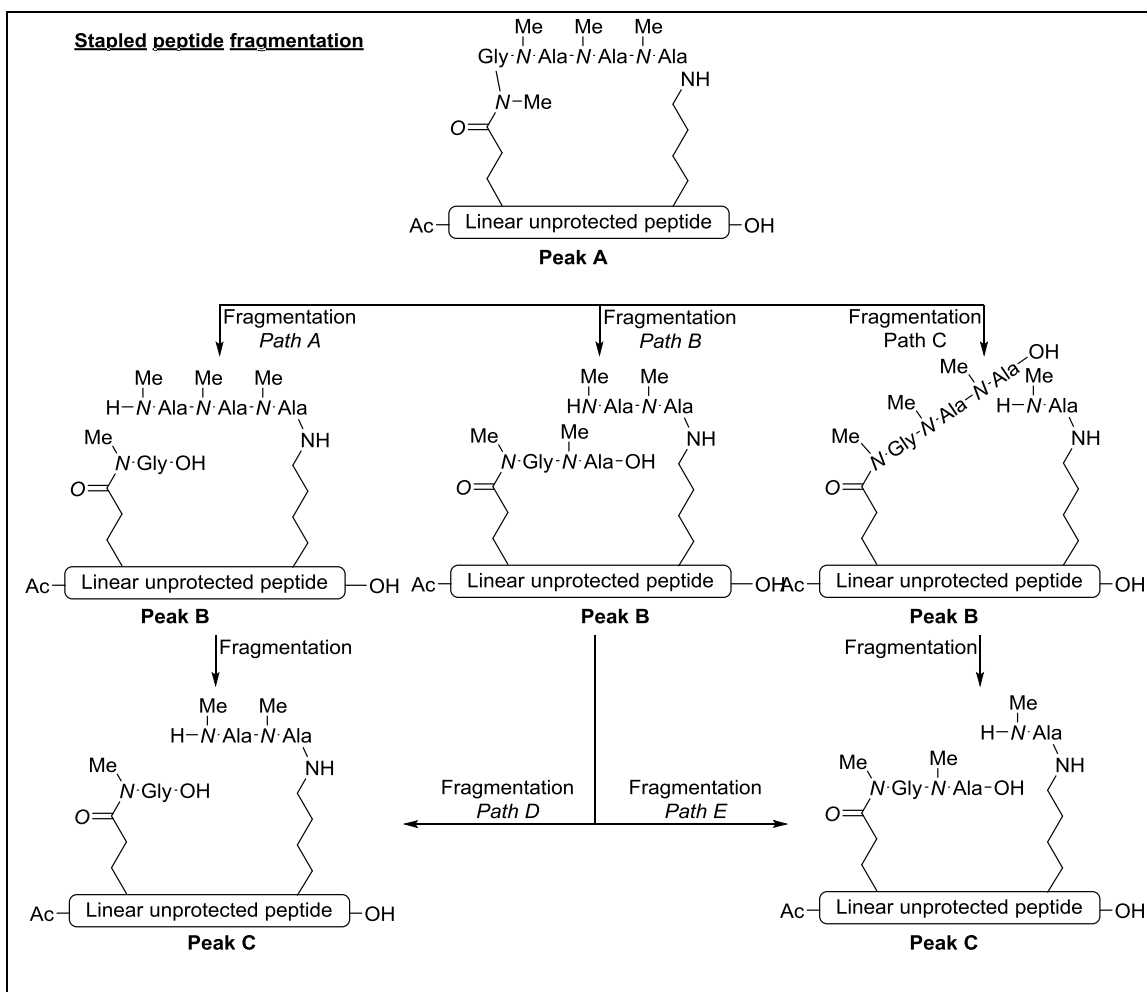
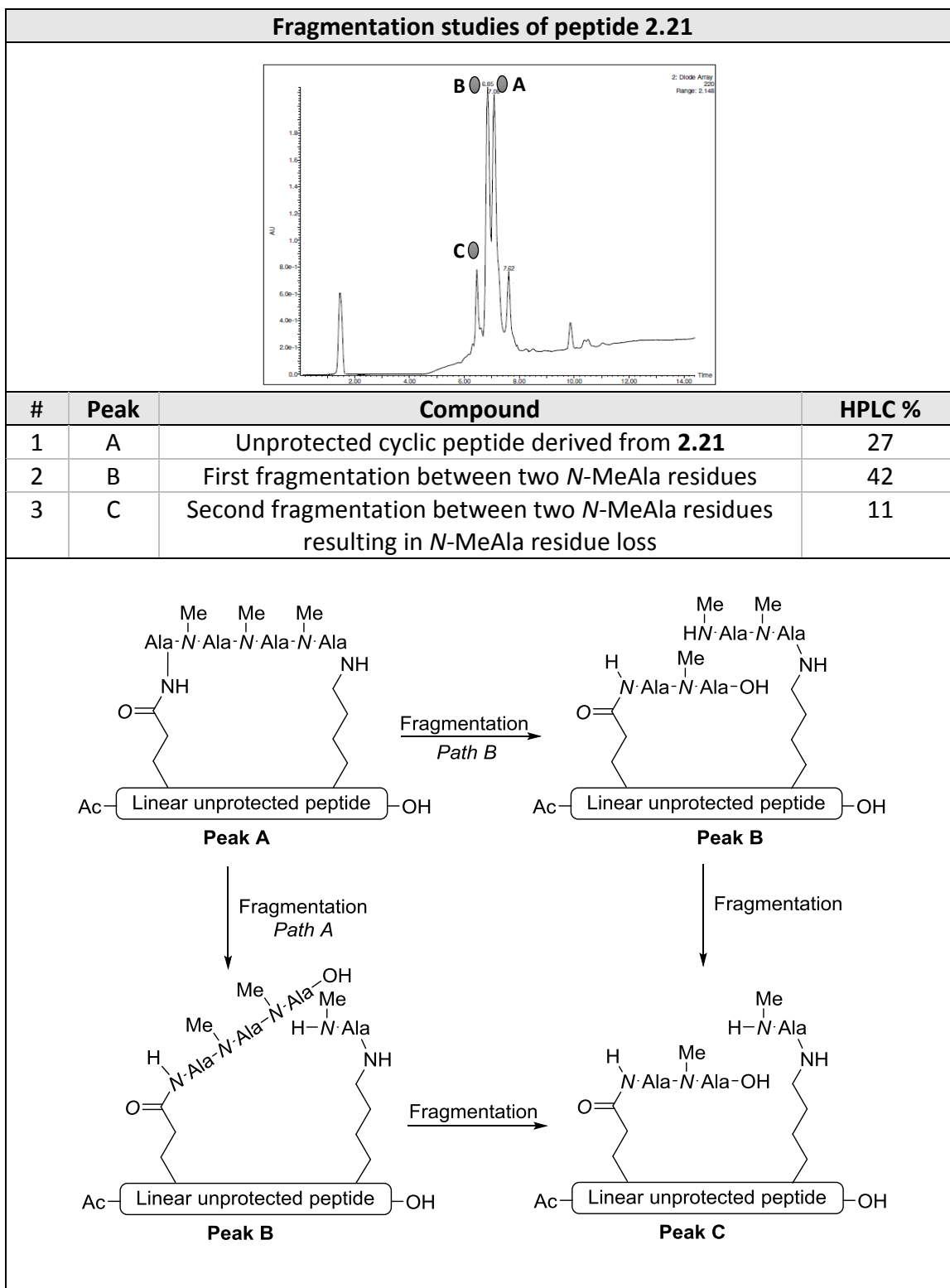
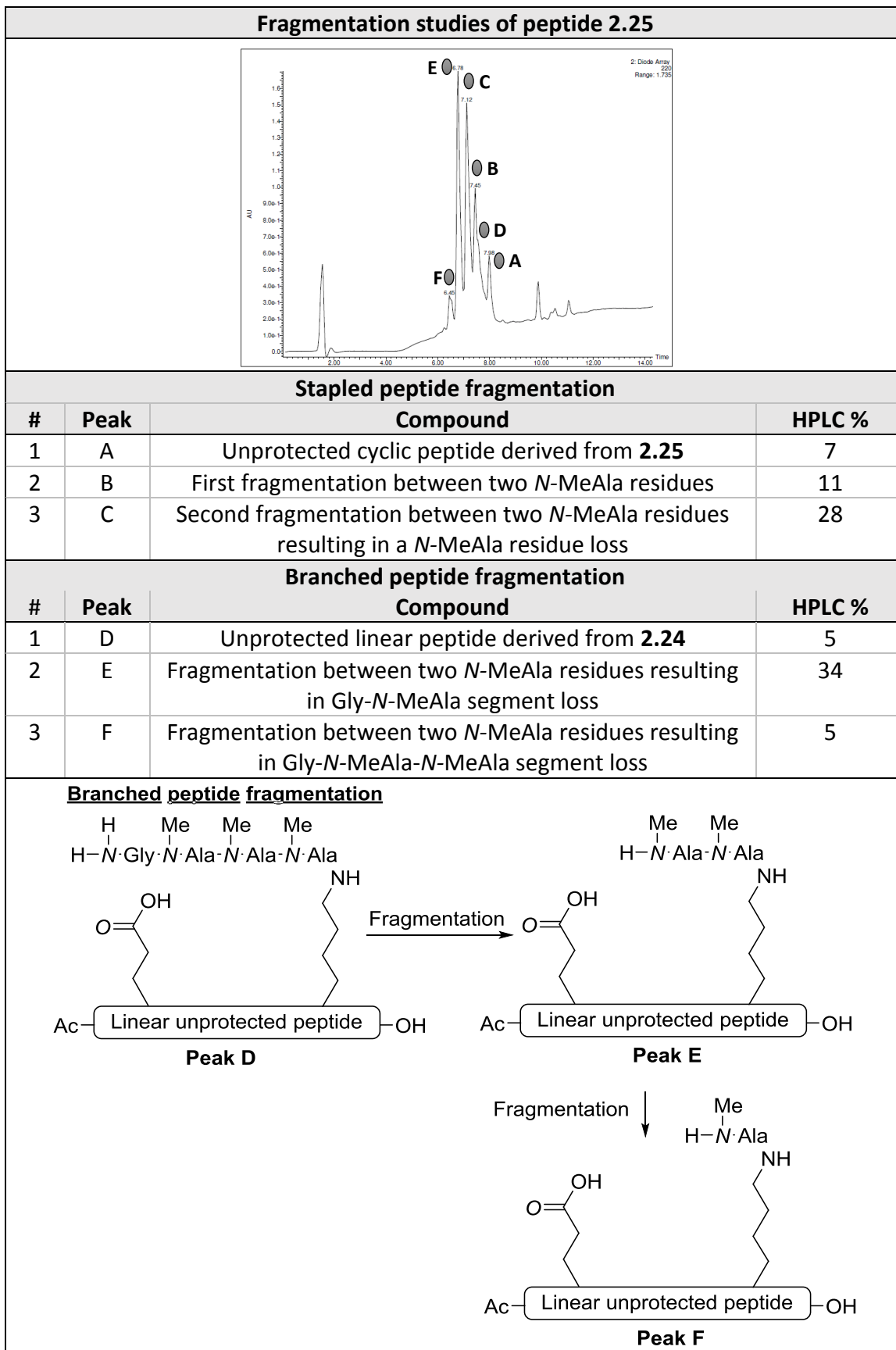


Table 11. Fragmentation of stapled peptide **2.17** upon cleavage.





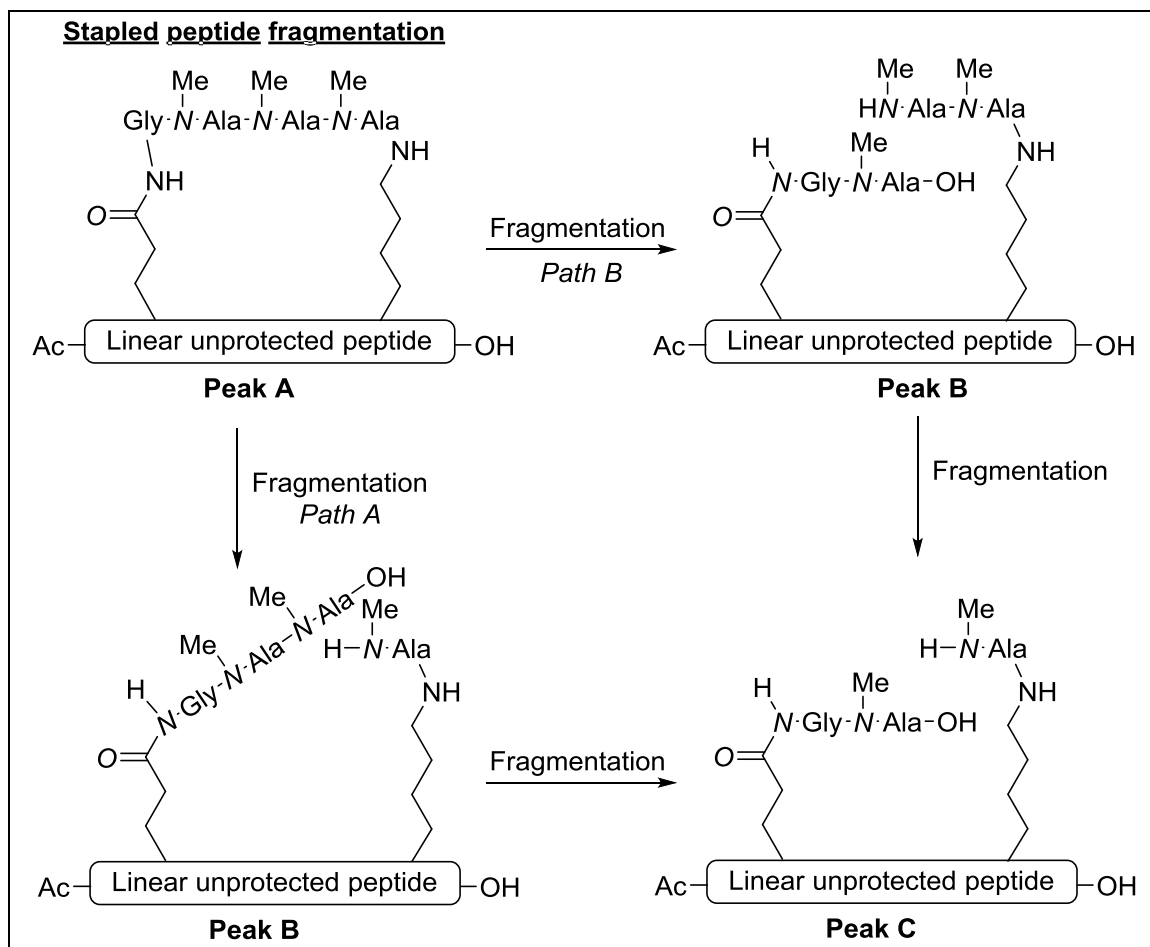


Table 13. Fragmentation of peptide **2.25** upon cleavage.

### 3.3.7 Preparation of the peptide library

#### 3.3.7.1 Preparation of single “short” HMSP (i,i+4) with the unblocked C-terminus

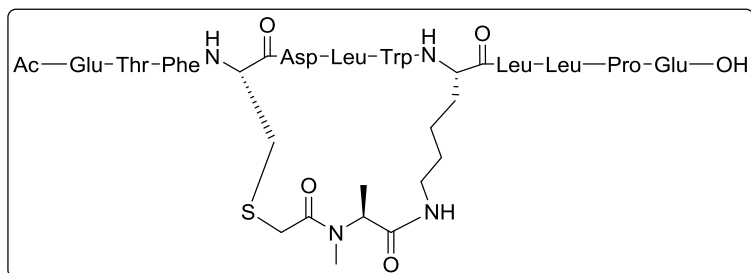
##### Synthetic protocol

The 2-CTC resin (commercial functionalisation: 1.6 mmol/g resin) was placed in a 2 mL-polypropylene syringe fitted with two polyethylene filter discs. *Conditioning* of the resin and *incorporation of the first amino acid* was carried out by standard means, being the loading level set up to 0.30 mmol/g. Generally, *Protocol Pep1* and *Protocol Pep2* were used for peptide couplings onto primary and secondary amines, respectively. Fmoc removal was accomplished following *Protocol Fmoc1*. At position 5 starting from the C-terminus, a Lys residue was introduced, conveniently protected with the Dde group, which is orthogonal to the Fmoc group. Four positions further from the Lys residue, a Cys residue was placed. After the linear chain elongation was furnished, N-terminal amine acetylation was accomplished following *Protocol Ac1*. Next, Dde group removal was achieved following *Protocol Dde*.

*Construction of the N-methyl-rich peptide bridge* was carried out following *Strategy A* (section 3.3.4). Thus, the general method consisted of successive cycles of the corresponding Fmoc-N-methylated-amino acid coupling and deprotection steps. Next, bromoacetic acid was incorporated following *Protocol Pep3*.

*Peptide cleavage and global deprotection* was accomplished following *Protocol Cle2*. *Cyclisation in solution* through a thioether-based cross-linking approach was accomplished following *Protocol Cyc2*. Finally, the crude peptide was subjected to HPLC purification.

## Peptide 2.26

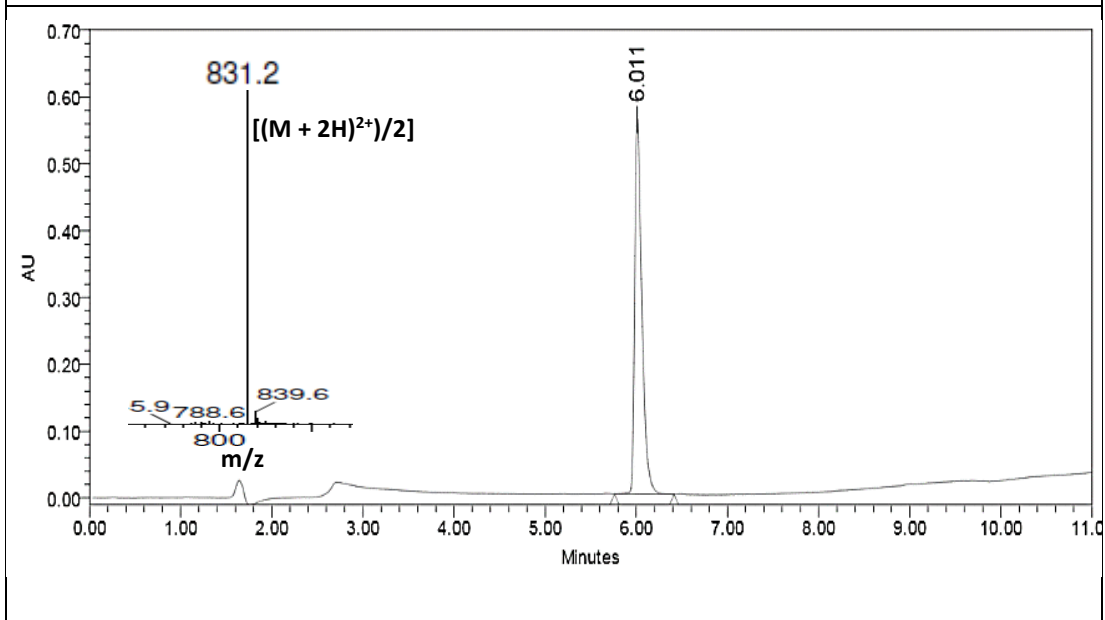


### HPLC purification conditions and yield

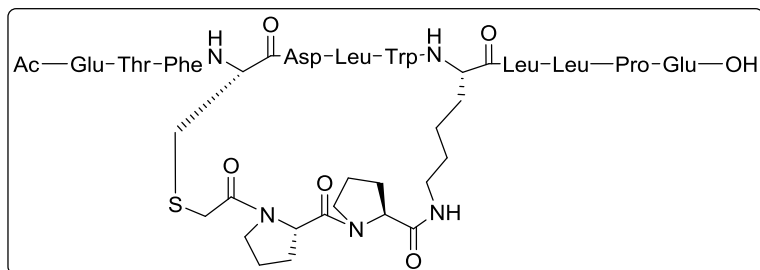
- **Column:** XBridge™ Peptide BEH C18 Prep reversed-phase 130Å column (5 μm x 10 mm x 100 mm).
- **Gradient:** Linear gradient (5% to 30% over 2 min and 30% to 55% over 15 min) of ACN, with a flow rate of 2.0 mL/min.
- **Quantity:** 22 mg.
- **Yield:** 11%.

### HPLC-PDA and ESI(+)-MS characterisation

- **Column:** SunFire™ C18 reversed-phase analytical column (3.5 μm x 4.6 mm x 100 mm) linear gradients (0% to 100%) of ACN over 8 min, with a flow rate of 1.0 mL/min.
- **t<sub>R</sub>** = 6.01 min.
- **Purity** (λ = 220 nm) = 100%.
- **ESI(+)-MS** calculated for C<sub>78</sub>H<sub>113</sub>N<sub>15</sub>O<sub>23</sub>S 1659.8, found [((M + 2H)<sup>2+</sup>)/2] 831.2.



## Peptide 2.27

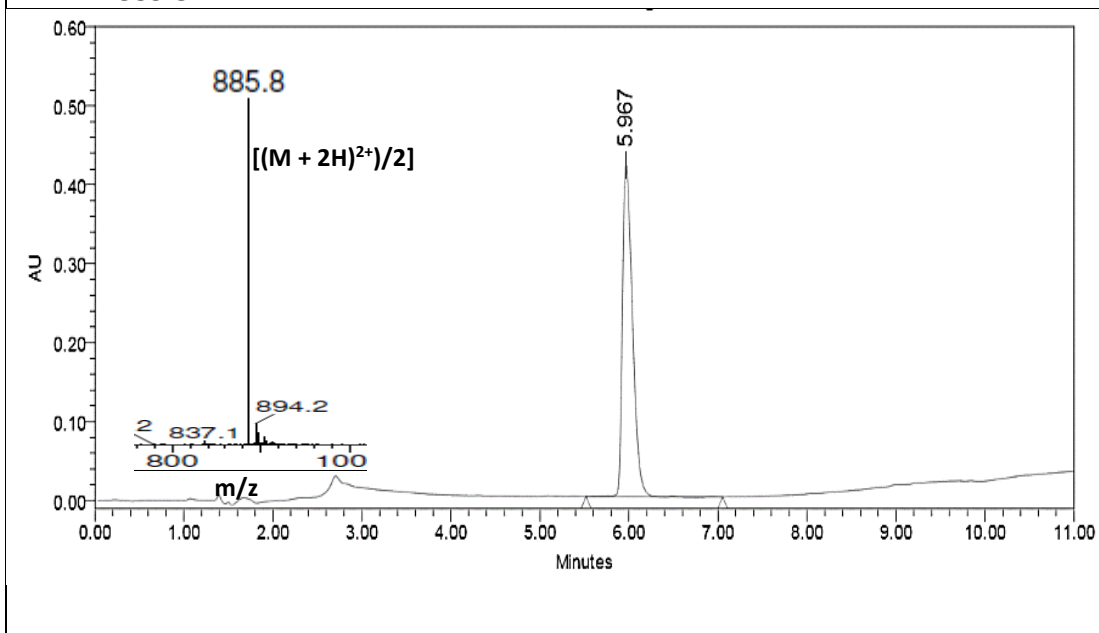


## HPLC purification conditions and yield

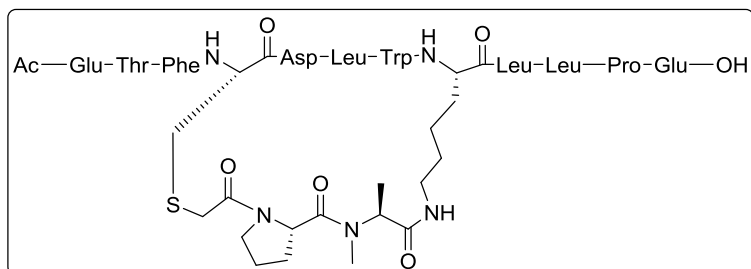
- **Column:** XBridge™ Peptide BEH C18 Prep reversed-phase 130Å column (5 μm x 10 mm x 100 mm).
- **Gradient:** Linear gradient (20% to 40% over 2 min and 40% to 60% over 15 min) of ACN, with a flow rate of 2.0 mL/min.
- **Quantity:** 24 mg.
- **Yield:** 12%.

## HPLC-PDA and ESI(+)-MS characterisation

- **Column:** SunFire™ C18 reversed-phase analytical column (3.5 μm x 4.6 mm x 100 mm) linear gradients (0% to 100%) of ACN over 8 min, with a flow rate of 1.0 mL/min.
- **t<sub>R</sub>** = 5.97 min.
- **Purity** (λ = 220 nm) = 100%.
- **ESI(+)-MS** calculated for C<sub>84</sub>H<sub>120</sub>N<sub>16</sub>O<sub>24</sub>S 1768.8, found [((M + 2H)<sup>2+</sup>)/2] 885.8.



## Peptide 2.28

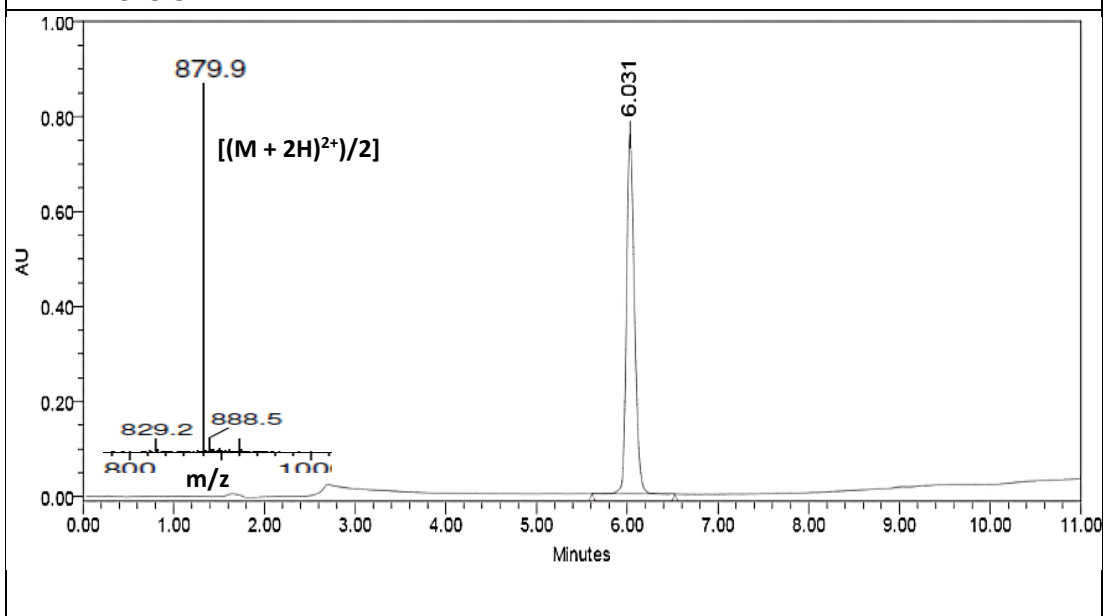


### HPLC purification conditions and yield

- **Column:** XBridge™ Peptide BEH C18 Prep reversed-phase 130Å column (5 μm x 10 mm x 100 mm).
- **Gradient:** Linear gradient (20% to 40% over 2 min and 40% to 60% over 15 min) of ACN, with a flow rate of 2.0 mL/min.
- **Quantity:** 6 mg.
- **Yield:** 6%.

### HPLC-PDA and ESI(+)-MS characterisation

- **Column:** SunFire™ C18 reversed-phase analytical column (3.5 μm x 4.6 mm x 100 mm) linear gradients (0% to 100%) of ACN over 8 min, with a flow rate of 1.0 mL/min.
- **t<sub>R</sub>** = 6.03 min.
- **Purity** (λ = 220 nm) = 100%.
- **ESI(+)-MS** calculated for C<sub>83</sub>H<sub>120</sub>N<sub>16</sub>O<sub>24</sub>S 1756.8, found [((M + 2H)<sup>2+</sup>)/2] 879.9.



### 3.3.7.2 Preparation of single “large” HMSP (i,i+7) with the unblocked C-terminus

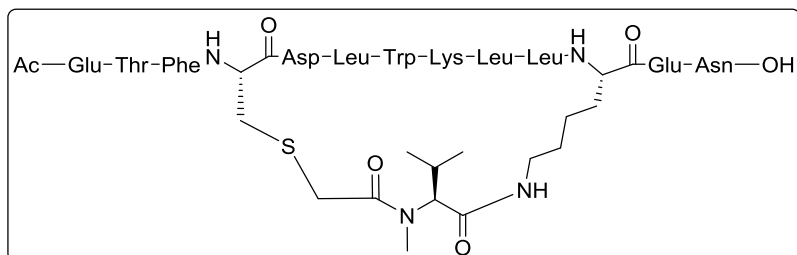
#### Synthetic protocol

The 2-CTC resin (commercial functionalisation: 1.6 mmol/g resin) was placed in a 2 mL-polypropylene syringe fitted with two polyethylene filter discs. *Conditioning of the resin and incorporation of the first amino acid* was carried out by standard means, being the loading level set up to 0.30 mmol/g. Generally, *Protocol Pep1 and Protocol Pep2* were used for peptide couplings onto primary and secondary amines, respectively. Fmoc removal was accomplished following *Protocol Fmoc1*. At position 3 starting from the C-terminus, a Lys residue was introduced, conveniently protected with the Dde group, which is orthogonal to the Fmoc group. Four positions further from the Lys residue, a Cys residue was placed. After the linear chain elongation was furnished, N-terminal amine acetylation was accomplished following *Protocol Ac1*. Next, Dde group removal was achieved following *Protocol Dde*.

*Construction of the N-methyl-rich peptide bridge* was carried out following *Strategy A* (section 3.3.4). Thus, the general method consisted of successive cycles of the corresponding Fmoc-N-methylated-amino acid coupling and deprotection steps. Next, bromoacetic acid was incorporated following *Protocol Pep3*

*Peptide cleavage and global deprotection* was accomplished following *Protocol Cle2*. *Cyclisation in solution* through a thioether-based cross-linking approach was accomplished following *Protocol Cyc2*. Finally, the crude peptide was subjected to HPLC purification.

**Peptide 2.31**

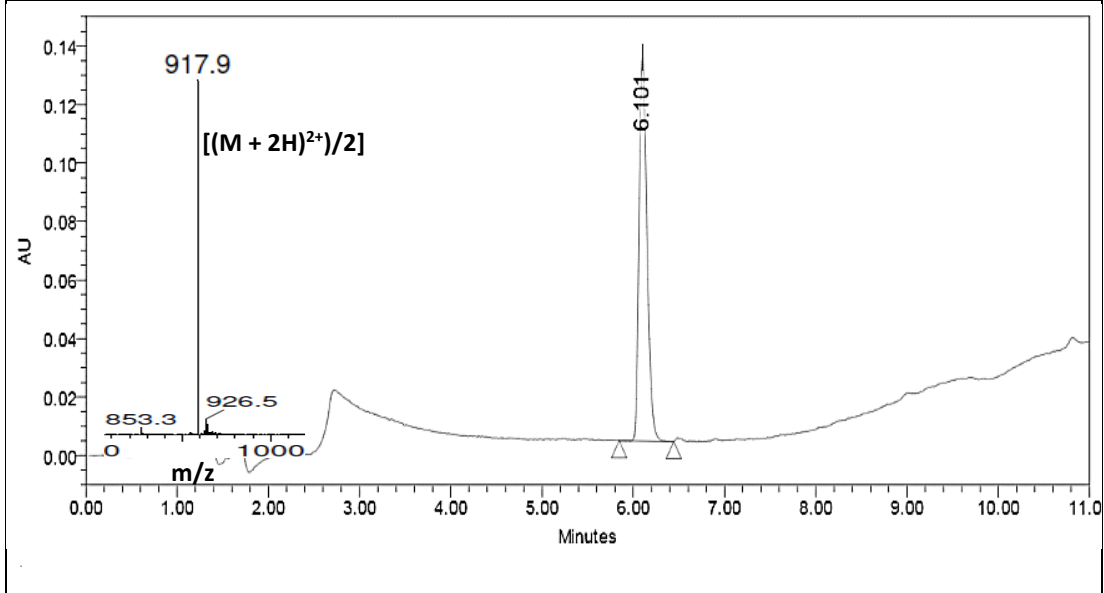


**HPLC purification conditions and yield**

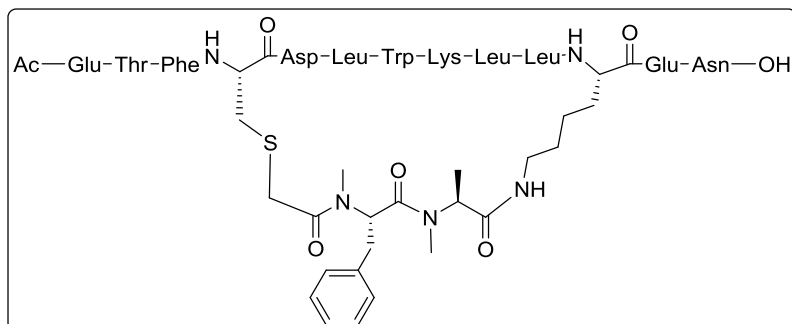
- **Column:** XBridge™ Peptide BEH C18 Prep reversed-phase 130Å column (5 μm x 10 mm x 100 mm).
- **Gradient:** Linear gradient (20% to 40% over 5 min and 40% to 50% over 15 min) of ACN, with a flow rate of 2.0 mL/min.
- **Quantity:** 3 mg.
- **Yield:** 3%.

**HPLC-PDA and ESI(+)-MS characterisation**

- **Column:** SunFire™ C18 reversed-phase analytical column (3.5 μm x 4.6 mm x 100 mm) linear gradients (0% to 100%) of ACN over 8 min, with a flow rate of 1.0 mL/min.
- **t<sub>R</sub>** = 6.10 min.
- **Purity** (λ = 220 nm) = 100%.
- **ESI(+)-MS** calculated for C<sub>85</sub>H<sub>128</sub>N<sub>18</sub>O<sub>25</sub>S 1832.9, found [((M + 2H)<sup>2+</sup>)/2] 917.9.



## Peptide 2.32

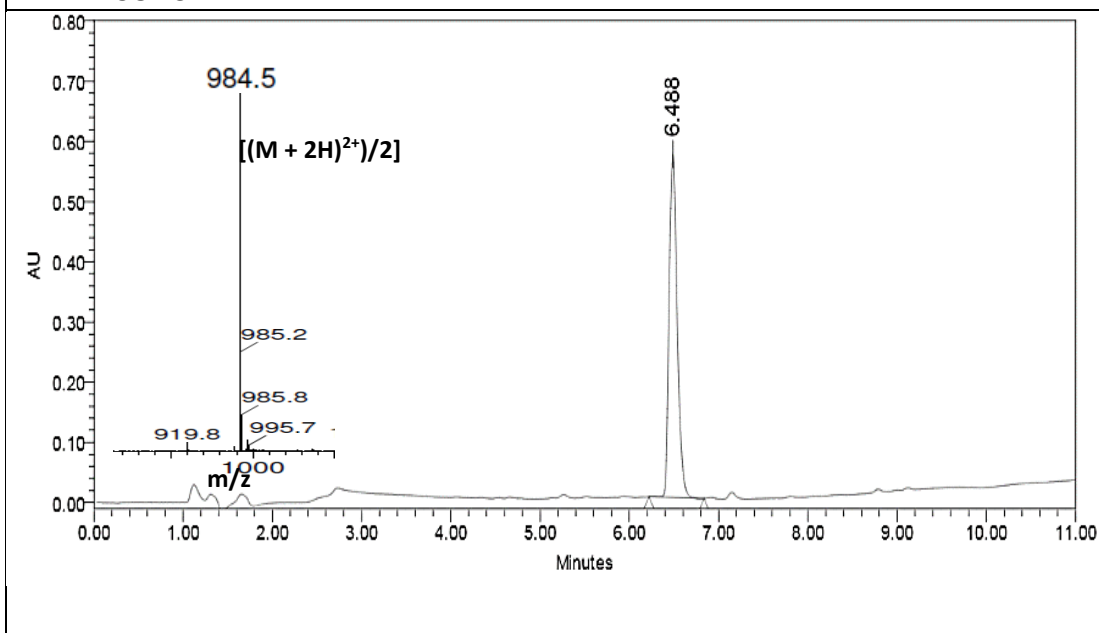


## HPLC purification conditions and yield

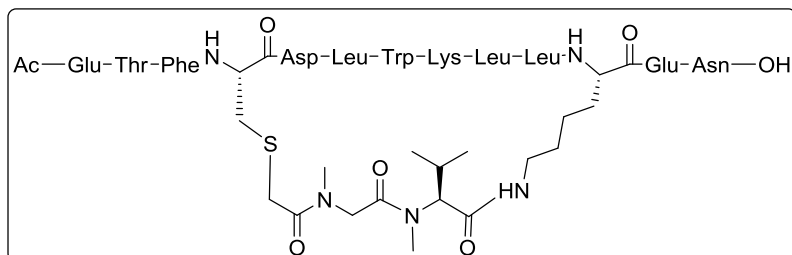
- **Column:** XBridge™ Peptide BEH C18 Prep reversed-phase 130Å column (5 μm x 10 mm x 100 mm).
- **Gradient:** Linear gradient (20% to 40% over 5 min and 40% to 60% over 15 min) of ACN, with a flow rate of 2.0 mL/min.
- **Quantity:** 2 mg.
- **Yield:** 2%.

## HPLC-PDA and ESI(+)-MS characterisation

- **Column:** SunFire™ C18 reversed-phase analytical column (3.5 μm x 4.6 mm x 100 mm) linear gradients (0% to 100%) of ACN over 8 min, with a flow rate of 1.0 mL/min.
- **t<sub>R</sub>** = 6.49 min.
- **Purity** (λ = 220 nm) = 100%.
- **ESI(+)-MS** calculated for C<sub>93</sub>H<sub>135</sub>N<sub>19</sub>O<sub>26</sub>S 1967.0, found [((M + 2H)<sup>2+</sup>)/2] 984.5.



### Peptide 2.33

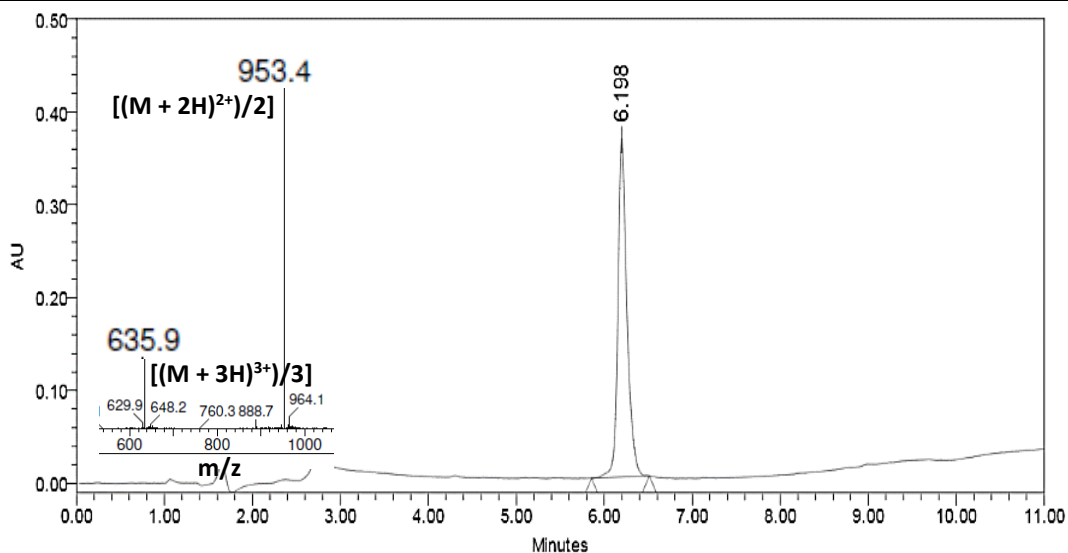


#### HPLC purification conditions and yield

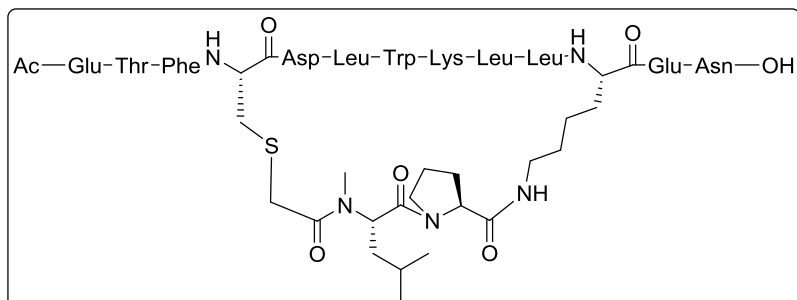
- **Column:** XBridge™ Peptide BEH C18 Prep reversed-phase 130Å column (5 μm x 10 mm x 100 mm).
- **Gradient:** Linear gradient (20% to 40% over 5 min and 40% to 60% over 15 min) of ACN, with a flow rate of 2.0 mL/min.
- **Quantity:** 1 mg.
- **Yield:** 2%.

#### HPLC-PDA and ESI(+)-MS characterisation

- **Column:** SunFire™ C18 reversed-phase analytical column (3.5 μm x 4.6 mm x 100 mm) linear gradients (0% to 100%) of ACN over 8 min, with a flow rate of 1.0 mL/min.
- **t<sub>R</sub>** = 6.20 min.
- **Purity** (λ = 220 nm) = 100%.
- **ESI(+)-MS** calculated for C<sub>88</sub>H<sub>133</sub>N<sub>19</sub>O<sub>26</sub>S 1903.9, found [((M + 2H)<sup>2+</sup>)/2] 953.4 and [((M + 3H)<sup>3+</sup>)/2] 635.9.



## Peptide 2.34

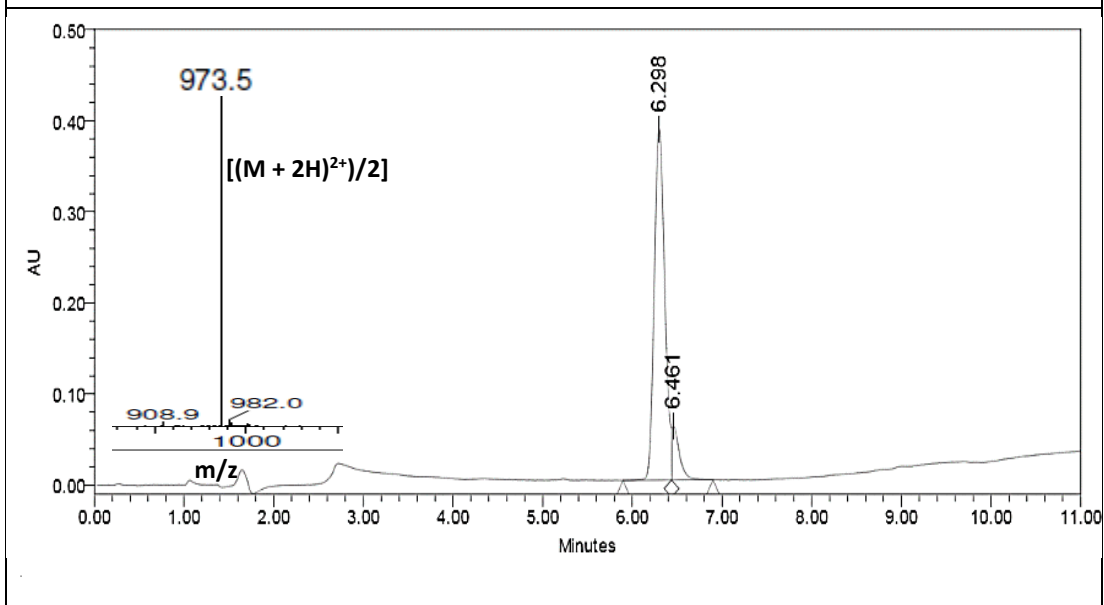


## HPLC purification conditions and yield

- **Column:** XBridge™ Peptide BEH C18 Prep reversed-phase 130Å column (5 μm x 10 mm x 100 mm).
- **Gradient:** Linear gradient (20% to 40% over 5 min and 40% to 60% over 15 min) of ACN, with a flow rate of 2.0 mL/min.
- **Quantity:** 4 mg.
- **Yield:** 3%.

## HPLC-PDA and ESI(+)-MS characterisation

- **Column:** SunFire™ C18 reversed-phase analytical column (3.5 μm x 4.6 mm x 100 mm) linear gradients (0% to 100%) of ACN over 8 min, with a flow rate of 1.0 mL/min..
- **t<sub>R</sub>** = 6.30 min.
- **Purity** (λ = 220 nm) = 90%.
- **ESI(+)-MS** calculated for C<sub>91</sub>H<sub>137</sub>N<sub>19</sub>O<sub>26</sub>S 1944.0, found [((M + 2H)<sup>2+</sup>)/2] 973.5.



### 3.3.7.3 Preparation of single “large” HMSP (i,i+7) with the amidated C-terminus

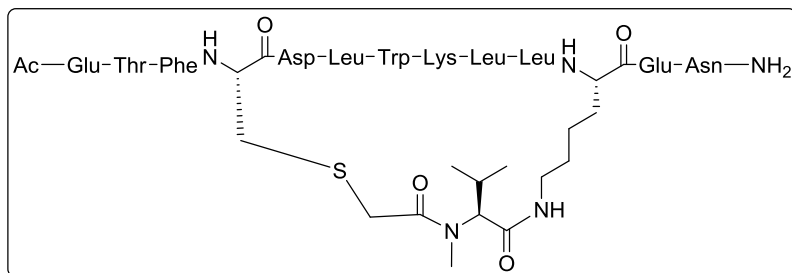
#### Synthetic protocol

The Rink amide AM resin (commercial functionalisation: 0.14 mmol/g resin) was placed in a 2 mL-polypropylene syringe fitted with two polyethylene filter discs. *Conditioning* of the resin and *incorporation of the first amino acid* was carried out by standard means. Generally, *Protocol Pep1* and *Protocol Pep2* were used for peptide couplings onto primary and secondary amines, respectively. Fmoc removal was accomplished following *Protocol Fmoc1*. At position 3 starting from the C-terminus, a Lys residue was introduced, conveniently protected with the Dde group, which is orthogonal to the Fmoc group. Four positions further from the Lys residue, a Cys residue was placed. After the linear chain elongation was furnished, *N*-terminal amine acetylation was accomplished following *Protocol Ac1*. Next, Dde group removal was achieved following *Protocol Dde*.

*Construction of the N-methyl-rich peptide bridge* was carried out following a combination of *Strategy A* and *Strategy B* (section 3.3.4). Whereas *Strategy A* was used for incorporation of Pro, *N*-MeAla, *N*-MeGly, *N*-MePhe, *N*-MeVal, *N*-MeLeu, *Strategy B* was used for incorporation of *N*-MeLys, *N*-MeGln and *N*-MeHis. Next, bromoacetic acid was incorporated following *Protocol Pep3*.

*Peptide cleavage and global deprotection* was accomplished following *Protocol Cle2*. *Cyclisation in solution* through a thioether-based cross-linking approach was accomplished following *Protocol Cyc2*. Finally, the crude peptide was subjected to HPLC purification.

## Peptide 2.35

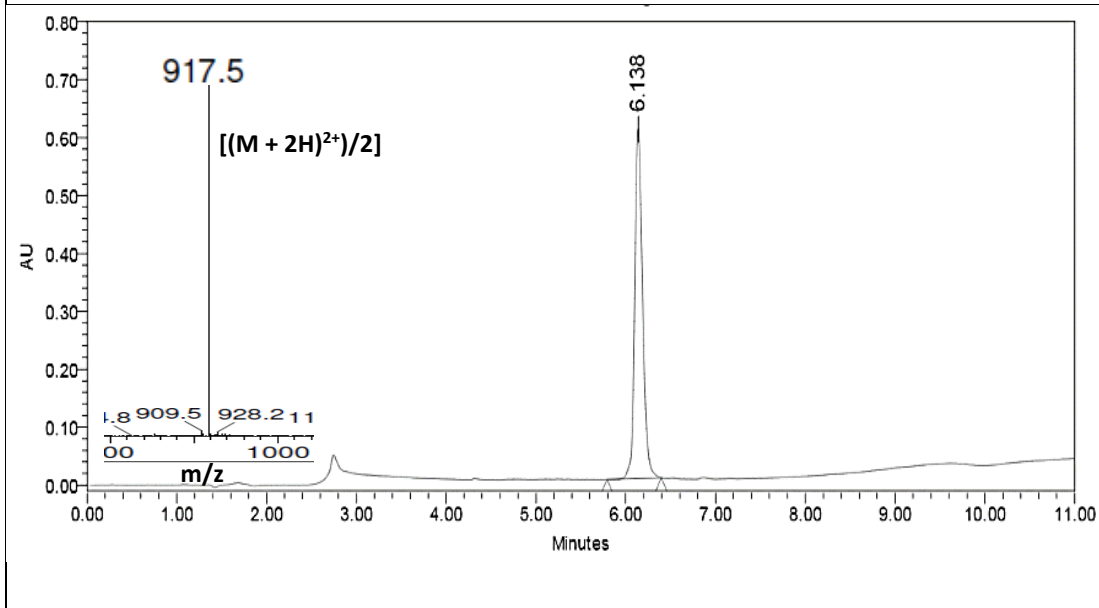


## HPLC purification conditions and yield

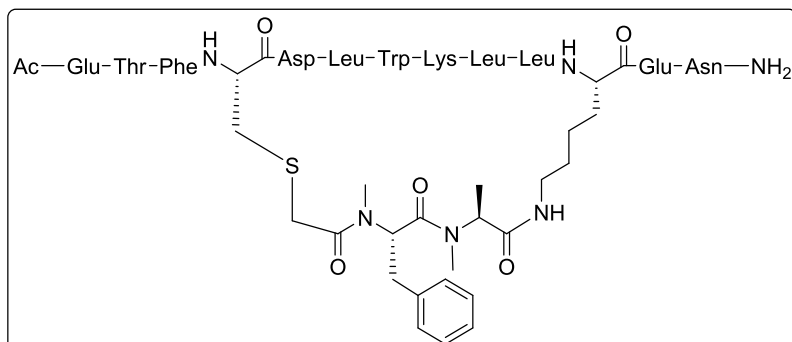
- **Column:** XBridge™ Peptide BEH C18 Prep reversed-phase 130Å column (5 μm x 10 mm x 100 mm).
- **Gradient:** Linear gradient (20% to 40% over 5 min and 40% to 50% over 15 min) of ACN, with a flow rate of 2.0 mL/min.
- **Quantity:** 15 mg.
- **Yield:** 11%.

## HPLC-PDA and ESI(+)-MS characterisation

- **Column:** SunFire™ C18 reversed-phase analytical column (3.5 μm x 4.6 mm x 100 mm) linear gradients (0% to 100%) of ACN over 8 min, with a flow rate of 1.0 mL/min.
- **t<sub>R</sub>** = 6.14 min.
- **Purity** (λ = 220 nm) = 100%.
- **ESI(+)-MS** calculated for C<sub>85</sub>H<sub>128</sub>N<sub>18</sub>O<sub>25</sub>S 1832.9, found [((M + 2H)<sup>2+</sup>)/2] 917.5.



**Peptide 2.36**

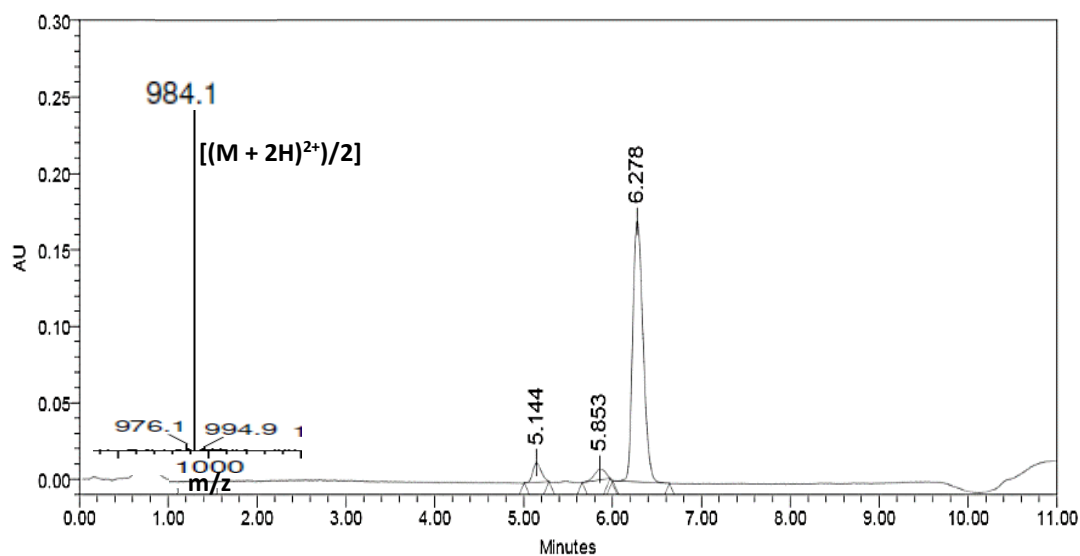


**HPLC PURIFICATION CONDITIONS AND YIELD**

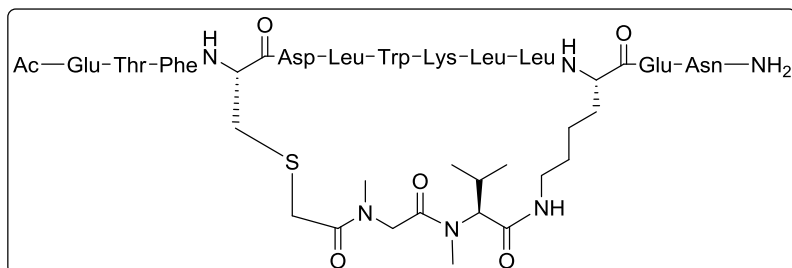
- **Column:** XBridge™ Peptide BEH C18 Prep reversed-phase 130Å column (5 μm x 10 mm x 100 mm).
- **Gradient:** Linear gradient (20% to 40% over 5 min and 40% to 50% over 15 min) of ACN, with a flow rate of 2.0 mL/min.
- **Quantity:** 3 mg.
- **Yield:** 2%.

**HPLC-PDA and ESI(+)-MS characterisation**

- **Column:** SunFire™ C18 reversed-phase analytical column (3.5 μm x 4.6 mm x 100 mm) linear gradients (0% to 100%) of ACN over 8 min, with a flow rate of 1.0 mL/min.
- **t<sub>R</sub>** = 6.28 min.
- **Purity** (λ = 220 nm) = 91%.
- **ESI(+)-MS** calculated for C<sub>93</sub>H<sub>135</sub>N<sub>19</sub>O<sub>26</sub>S 1967.0, found  $[(M + 2H)^{2+}]/2$  984.1.



## Peptide 2.37

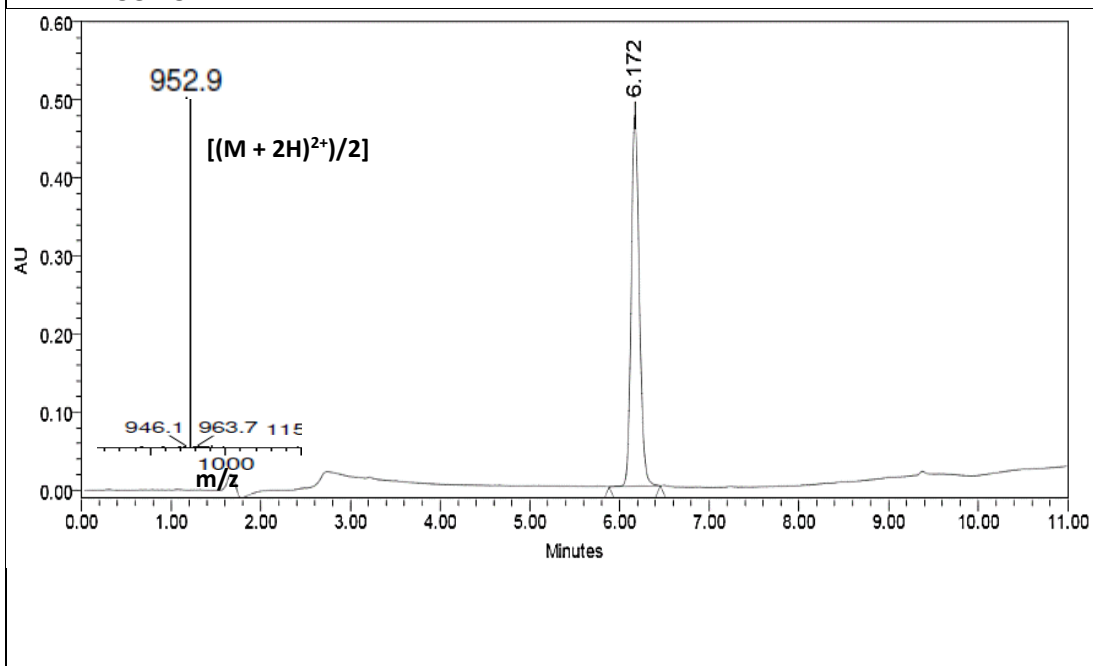


## HPLC purification conditions and yield

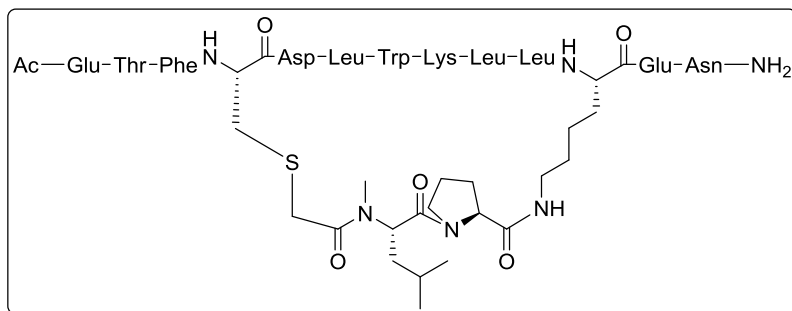
- **Column:** XBridge™ Peptide BEH C18 Prep reversed-phase 130Å column (5 μm x 10 mm x 100 mm).
- **Gradient:** Linear gradient (20% to 40% over 5 min and 40% to 45% over 15 min) of ACN, with a flow rate of 2.0 mL/min.
- **Quantity:** 7 mg.
- **Yield:** 5%.

## HPLC-PDA and ESI(+)-MS characterisation

- **Column:** SunFire™ C18 reversed-phase analytical column (3.5 μm x 4.6 mm x 100 mm) linear gradients (0% to 100%) of ACN over 8 min, with a flow rate of 1.0 mL/min.
- **t<sub>R</sub>** = 6.17 min.
- **Purity** (λ = 220 nm) = 100%.
- **ESI(+)-MS** calculated for C<sub>88</sub>H<sub>134</sub>N<sub>20</sub>O<sub>25</sub>S 1903.0, found [((M + 2H)<sup>2+</sup>)/2] 952.9.



**Peptide 2.38**

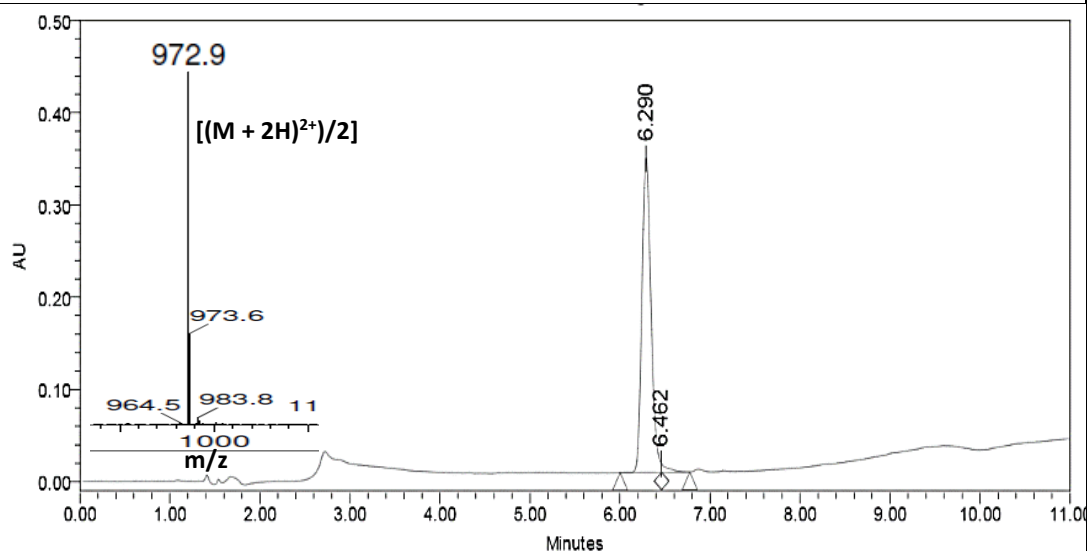


**HPLC purification conditions and yield**

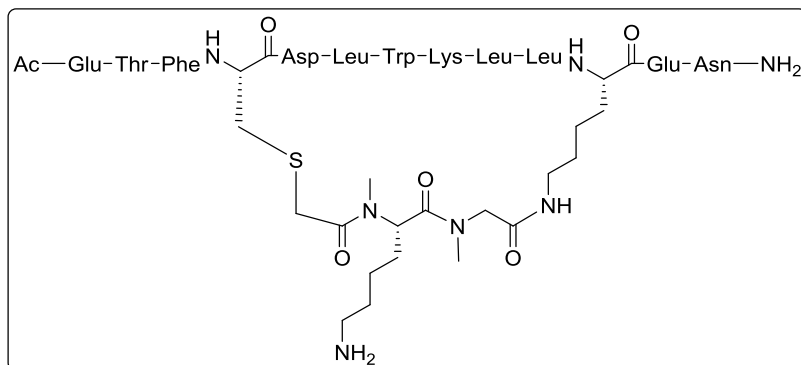
- **Column:** XBridge™ Peptide BEH C18 Prep reversed-phase 130Å column (5 μm x 10 mm x 100 mm).
- **Gradient:** Linear gradient (20% to 45% over 5 min and 45% to 45% over 15 min) of ACN, with a flow rate of 2.0 mL/min.
- **Quantity:** 6 mg.
- **Yield:** 5%.

**HPLC-PDA and ESI(+)-MS characterisation**

- **Column:** SunFire™ C18 reversed-phase analytical column (3.5 μm x 4.6 mm x 100 mm) linear gradients (0% to 100%) of ACN over 8 min, with a flow rate of 1.0 mL/min.
- **t<sub>R</sub>** = 6.29 min.
- **Purity** (λ = 220 nm) = 98%.
- **ESI(+)-MS** calculated for C<sub>91</sub>H<sub>138</sub>N<sub>20</sub>O<sub>25</sub>S 1943.0, found [((M + 2H)<sup>2+</sup>)/2] 972.9.



## Peptide 2.39

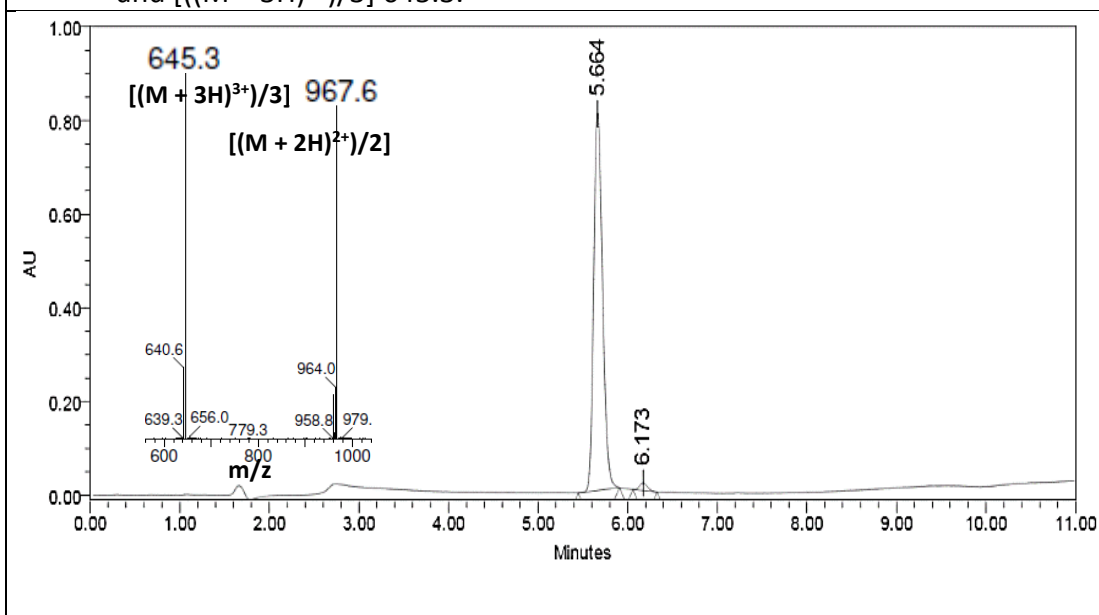


## HPLC purification conditions and yield

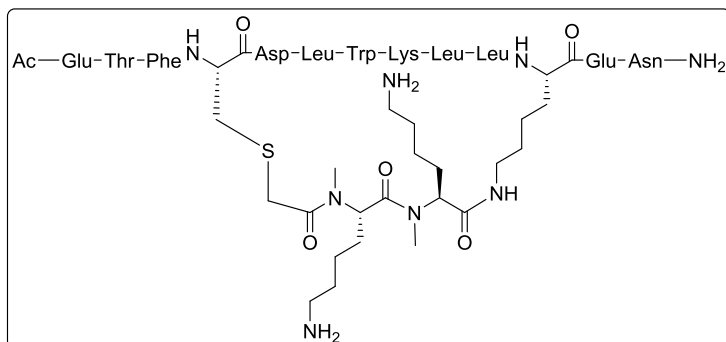
- **Column:** XBridge™ Peptide BEH C18 Prep reversed-phase 130Å column (5 μm x 10 mm x 100 mm).
- **Gradient:** Linear gradient (0% to 20% over 5 min and 20% to 50% over 15 min) of ACN, with a flow rate of 2.0 mL/min.
- **Quantity:** 4 mg.
- **Yield:** 3%.

## HPLC-PDA and ESI(+)-MS characterisation

- **Column:** SunFire™ C18 reversed-phase analytical column (3.5 μm x 4.6 mm x 100 mm) linear gradients (0% to 100%) of ACN over 8 min, with a flow rate of 1.0 mL/min.
- **t<sub>R</sub>** = 5.66 min.
- **Purity** (λ = 220 nm) = 98%.
- **ESI(+)-MS** calculated for C<sub>89</sub>H<sub>137</sub>N<sub>21</sub>O<sub>25</sub>S 1932.0, found [((M + 2H)<sup>2+</sup>)/2] 967.6 and [((M + 3H)<sup>3+</sup>)/3] 645.3.



### Peptide 2.40

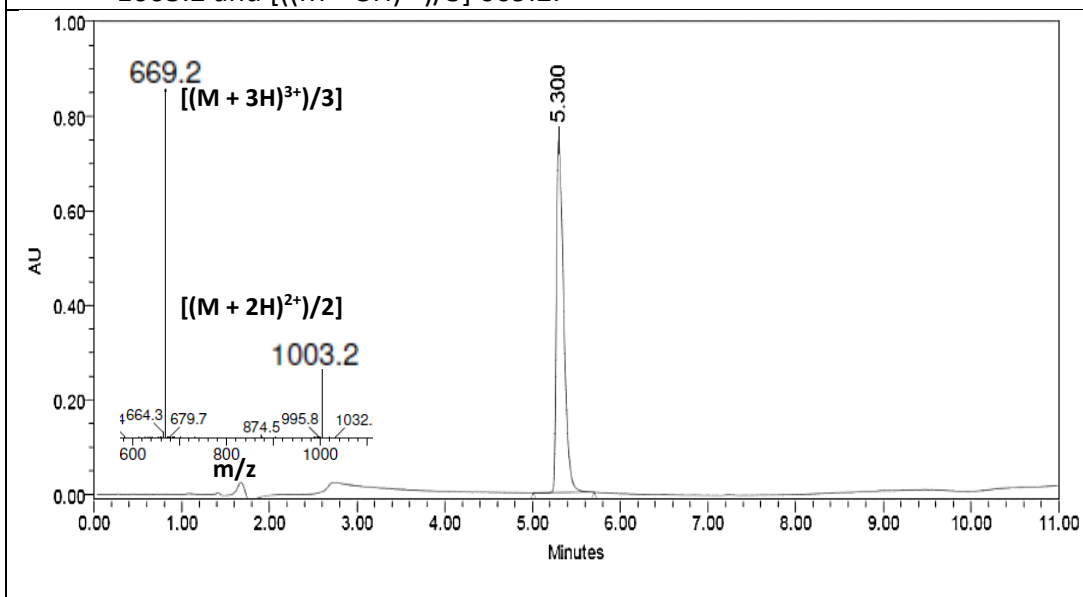


#### HPLC purification conditions and yield

- **Column:** XBridge™ Peptide BEH C18 Prep reversed-phase 130Å column (5 μm x 10 mm x 100 mm).
- **Gradient:** Linear gradient (20% to 30% over 5 min and 30% to 35% over 15 min) of ACN, with a flow rate of 2.0 mL/min.
- **Quantity:** 5 mg.
- **Yield:** 3%.

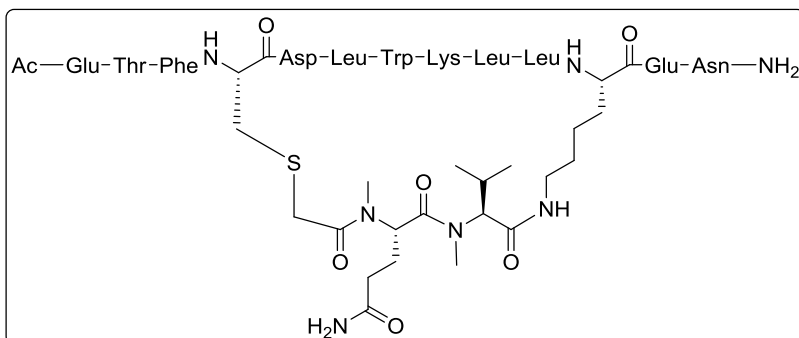
#### HPLC-PDA and ESI(+)-MS characterisation

- **Column:** SunFire™ C18 reversed-phase analytical column (3.5 μm x 4.6 mm x 100 mm) linear gradients (0% to 100%) of ACN over 8 min, with a flow rate of 1.0 mL/min.
- **t<sub>R</sub>** = 5.30 min.
- **Purity** (λ = 220 nm) = 100%.
- **ESI(+)-MS** calculated for C<sub>93</sub>H<sub>146</sub>N<sub>22</sub>O<sub>25</sub>S 2004.1, found [((M + 2H)<sup>2+</sup>)/2] 1003.2 and [((M + 3H)<sup>3+</sup>)/3] 669.2.





**Peptide 2.42**

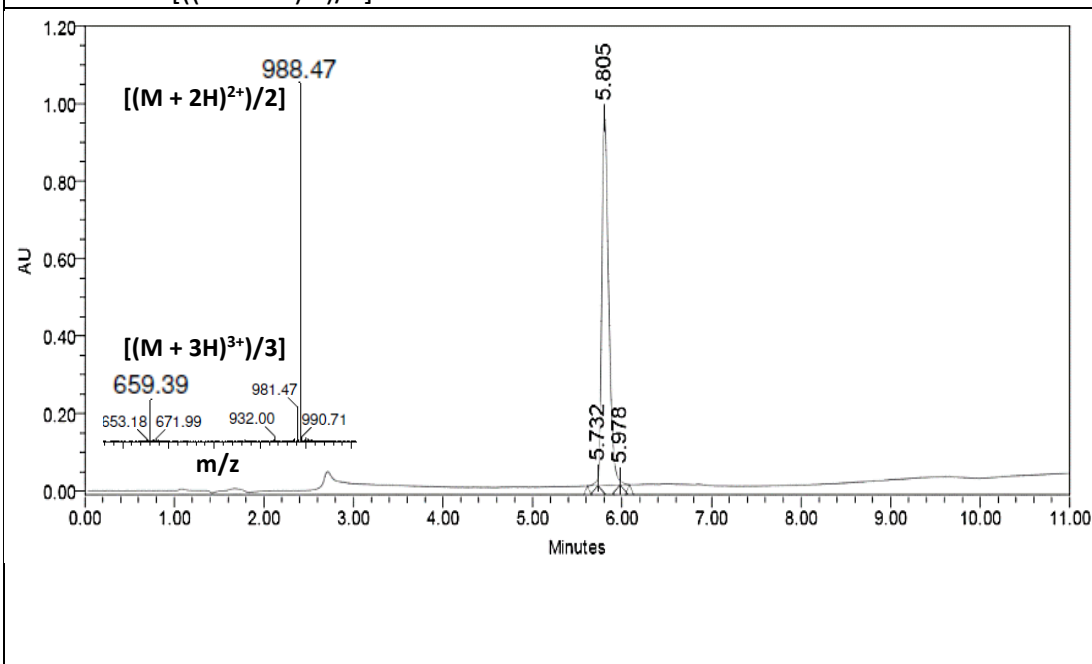


**HPLC purification conditions and yield**

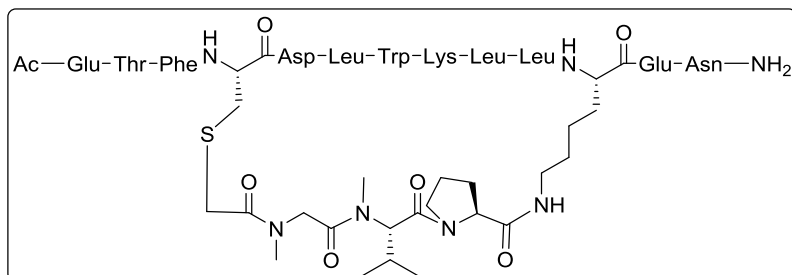
- **Column:** XBridge™ Peptide BEH C18 Prep reversed-phase 130Å column (5 μm x 10 mm x 100 mm).
- **Gradient:** Linear gradient (20% to 35% over 5 min and 35% to 50% over 15 min) of ACN, with a flow rate of 2.0 mL/min.
- **Quantity:** 1 mg. Yield: 1%.

**HPLC-PDA and ESI(+)-MS characterisation**

- **Column:** SunFire™ C18 reversed-phase analytical column (3.5 μm x 4.6 mm x 100 mm) linear gradients (0% to 100%) of ACN over 8 min, with a flow rate of 1.0 mL/min.
- **t<sub>R</sub>** = 5.81 min.
- **Purity** (λ = 220 nm) = 99%.
- **ESI(+)-MS** calculated for C<sub>91</sub>H<sub>139</sub>N<sub>21</sub>O<sub>26</sub>S 1974.0, found [((M + 2H)<sup>2+</sup>)/2] 988.5 and [((M + 3H)<sup>3+</sup>)/3] 659.4.



## Peptide 2.44

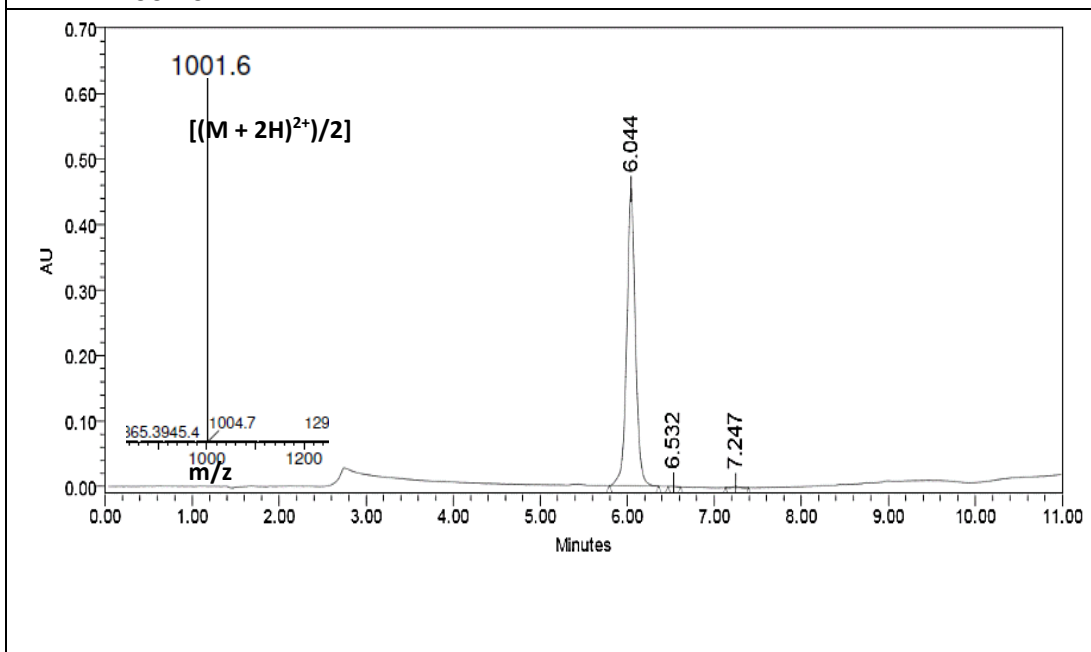


## HPLC purification conditions and yield

- **Column:** XBridge™ Peptide BEH C18 Prep reversed-phase 130Å column (5 μm x 10 mm x 100 mm).
- **Gradient:** Linear gradient (20% to 40% over 5 min and 40% to 50% over 15 min) of ACN, with a flow rate of 2.0 mL/min.
- **Quantity:** 6 mg.
- **Yield:** 4%.

## HPLC-PDA and ESI(+)-MS characterisation

- **Column:** SunFire™ C18 reversed-phase analytical column (3.5 μm x 4.6 mm x 100 mm) linear gradients (0% to 100%) of ACN over 8 min, with a flow rate of 1.0 mL/min.
- **t<sub>R</sub>** = 6.04 min.
- **Purity** (λ = 220 nm) = 99%.
- **ESI(+)-MS** calculated for C<sub>93</sub>H<sub>141</sub>N<sub>21</sub>O<sub>26</sub>S 2001.0, found  $[(M + 2H)^{2+}]/2$  1001.6.



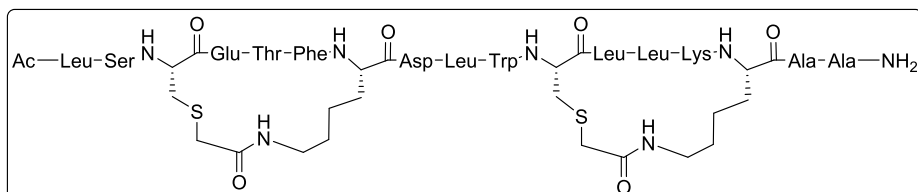
### 3.3.7.4 Preparation of double HMSP (i,i+4, and i+8,i+12) with the amidated C-terminus

#### Synthetic protocol

The Rink amide AM resin (commercial functionalisation: 0.14 mmol/g resin) was placed in a 2 mL-polypropylene syringe fitted with two polyethylene filter discs. *Conditioning* of the resin and *incorporation of the first amino acid* was carried out by standard means. Generally, *Protocol Pep1* and *Protocol Pep2* were used for peptide couplings onto primary and secondary amines, respectively. Fmoc removal was accomplished following *Protocol Fmoc1*. At position 3 starting from the C-terminus, a Lys residue was introduced, conveniently protected with the Dde group, which is orthogonal to the Fmoc group. Four positions further from the Lys residue, a Cys residue protected with the orthogonal Mmt protecting group was placed. The linear chain elongation was carried out until the Leu ninth residue. The Fmoc group removed by standard means, and the N-terminal function was protected with the Alloc group by using *Protocol Pro*. Next, Dde group removal was achieved following *Protocol Dde*. *Construction of the first N-methyl-rich peptide bridge* was carried out following a combination of *Strategy A* and *Strategy B* (section 3.3.4). Whereas *Strategy A* was used for incorporation of Pro and N-MeAla, *Strategy B* was used for incorporation of N-MeLys. Next, bromoacetic acid was incorporated following *Protocol Pep3*. *On-resin side-chain to side-chain cyclisation* through a thioether-based cross-linking approach to incorporate *Staple1* was carried out as follows. First, the Mmt group was selectively eliminated using *Protocol Mmt*, followed by *Protocol Cyc1*, in which a nucleophilic displacement took place to furnish the cyclic product. Next, *complete linear chain elongation* was undertaken. For that, the Alloc group was removed by using *Protocol All*, and the full peptide linear chain was synthesised following the same strategy as the one used for the insertion of the first nine residues. Next, N-terminal amine acetylation was accomplished following *Protocol Ac1*. The same procedures as the ones used for *Staple1*, were used for the *construction of the second N-methyl-rich peptide bridge* and subsequent *on-resin side-chain to side-chain cyclisation*. *Peptide cleavage and global*

deprotection was accomplished following *Protocol Cle2*, and the crude peptide was subjected to HPLC purification

### Peptide 2.45

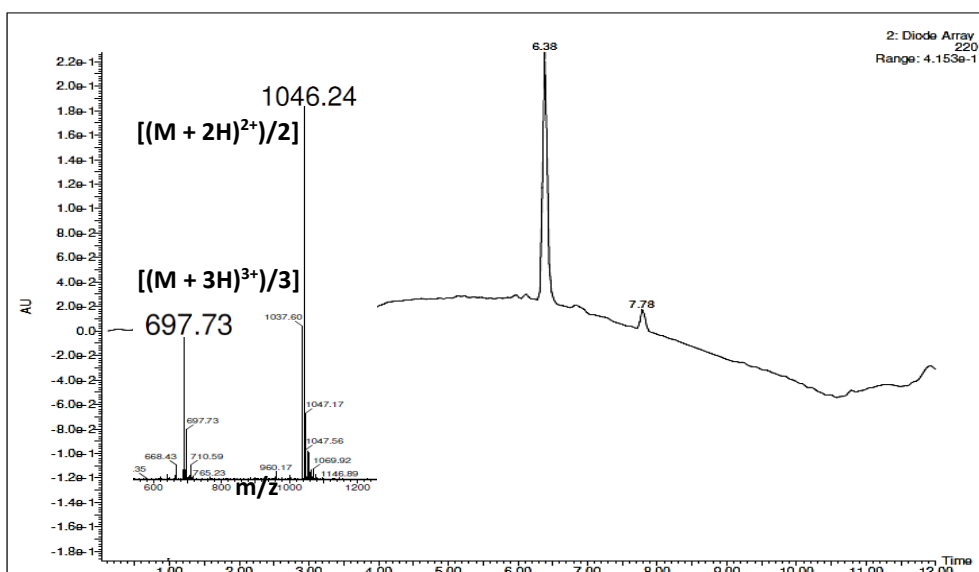


#### HPLC purification conditions and yield

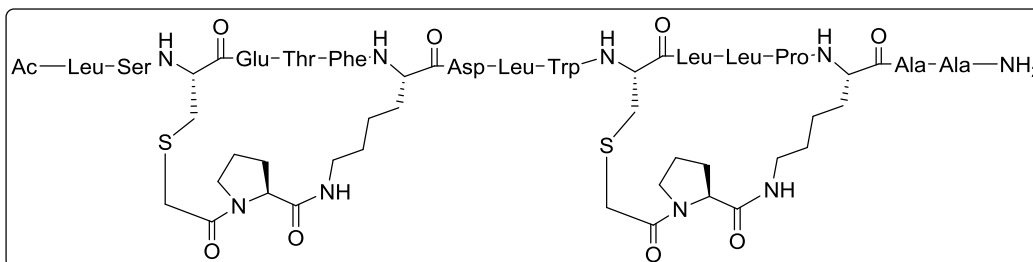
- **Column:** XBridge™ Peptide BEH C18 Prep reversed-phase 130Å column (5 μm x 10 mm x 100 mm).
- **Gradient:** Linear gradient (20% to 40% over 5 min and 40% to 45% over 15 min) of ACN, with a flow rate of 2.0 mL/min.
- **Quantity:** 1 mg.
- **Yield:** 1%.

#### HPLC-PDA and ESI(+)/MS characterisation

- **Column:** XBridge™ C18 reversed-phase analytical column (3.5 μm x 4.6 mm x 42 mm) linear gradients (0% to 100%) of ACN over 8 min, with a flow rate of 1.0 mL/min.
- **t<sub>R</sub>** = 6.38 min.
- **Purity** (λ = 220 nm) = 92%.
- **ESI(+)/MS** calculated for C<sub>96</sub>H<sub>148</sub>N<sub>22</sub>O<sub>26</sub>S<sub>2</sub> 2090.0, found  $[(M + 2H)^{2+}]/2$  1046.3 and  $[(M + 3H)^{3+}]/3$  697.7.



**Peptide 2.46**

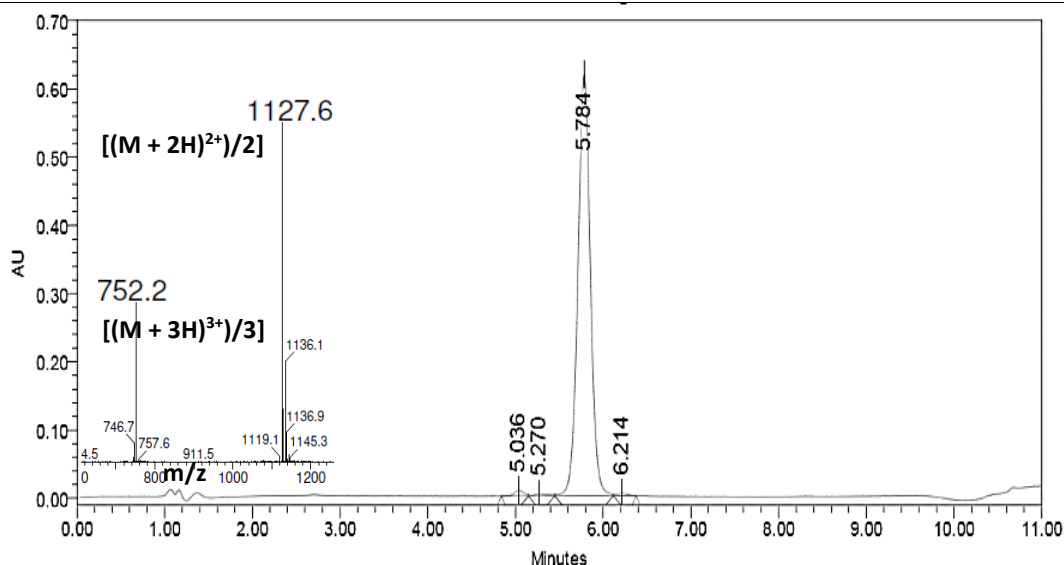


**HPLC purification conditions and yield**

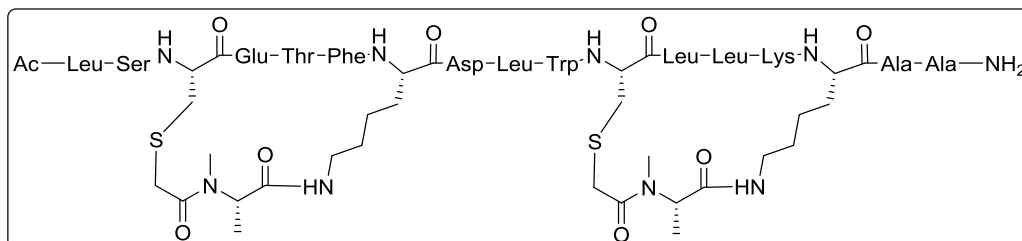
- **Column:** XBridge™ Peptide BEH C18 Prep reversed-phase 130Å column (5 μm x 10 mm x 100 mm).
- **Gradient:** Linear gradient (20% to 45% over 5 min and 45% to 50% over 15 min) of ACN, with a flow rate of 2.0 mL/min.
- **Quantity:** 4 mg.
- **Yield:** 2%.

**HPLC-PDA and ESI(+)-MS characterisation**

- **Column:** SunFire™ C18 reversed-phase analytical column (3.5 μm x 4.6 mm x 100 mm) linear gradients (0% to 100%) of ACN over 8 min, with a flow rate of 1.0 mL/min.
- **t<sub>R</sub>** = 5.78 min.
- **Purity** (λ = 220 nm) = 98%.
- **ESI(+)-MS** calculated for C<sub>105</sub>H<sub>156</sub>N<sub>22</sub>O<sub>29</sub>S<sub>2</sub> 2254.1, found  $[(M + 2H)^{2+}]/2$  1127.6 and  $[(M + 3H)^{3+}]/3$  752.2.



## Peptide 2.47

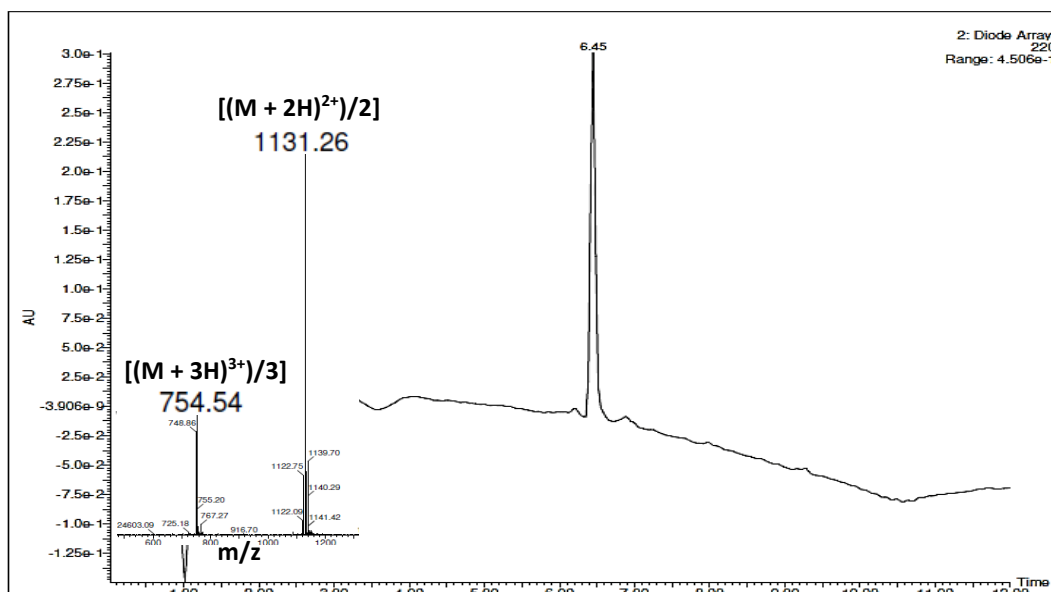


## HPLC purification conditions and yield

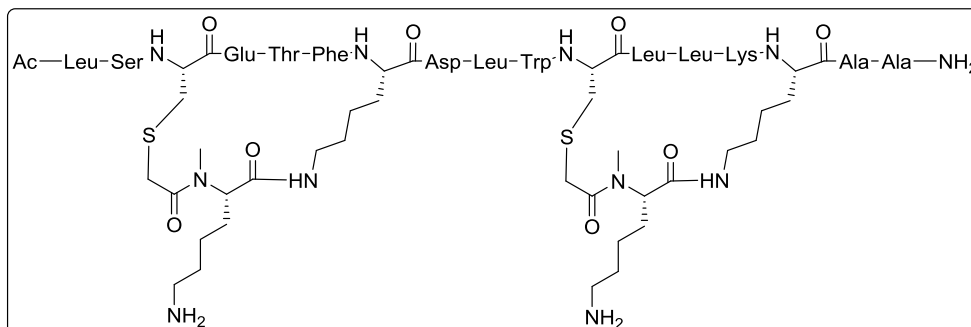
- **Column:** XBridge™ Peptide BEH C18 Prep reversed-phase 130Å column (5 μm x 10 mm x 100 mm).
- **Gradient:** Linear gradient (20% to 45% over 5 min and 45% to 50% over 15 min) of ACN, with a flow rate of 2.0 mL/min.
- **Quantity:** 1 mg.
- **Yield:** 1%.

## HPLC-PDA and ESI(+)-MS characterisation

- **Column:** XBridge™ C18 reversed-phase analytical column (3.5 μm x 4.6 mm x 42 mm) linear gradients (0% to 100%) of ACN over 8 min, with a flow rate of 1.0 mL/min.
- **t<sub>R</sub>** = 6.45 min.
- **Purity** (λ = 220 nm) = 96%.
- **ESI(+)-MS** calculated for C<sub>106</sub>H<sub>161</sub>N<sub>23</sub>O<sub>29</sub>S<sub>2</sub> 2261.1, found  $[(M + 2H)^{2+}]/2$  1131.3 and  $[(M + 3H)^{3+}]/3$  754.5.



**Peptide 2.48**

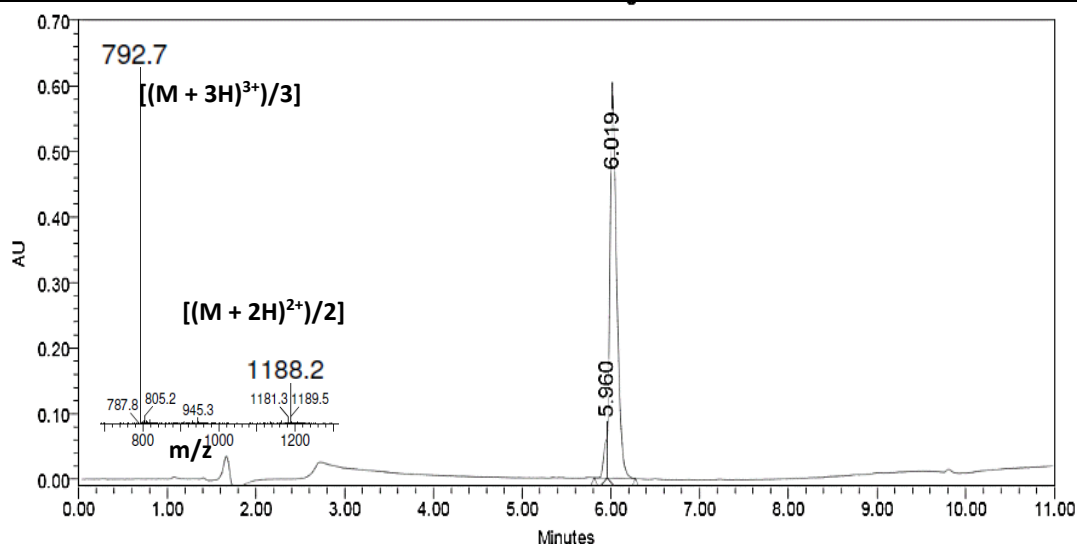


**HPLC purification conditions and yield**

- **Column:** XBridge™ Peptide BEH C18 Prep reversed-phase 130Å column (5 μm x 10 mm x 100 mm).
- **Gradient:** Linear gradient (20% to 35% over 5 min and 35% to 45% over 15 min) of ACN, with a flow rate of 2.0 mL/min.
- **Quantity:** 1 mg.
- **Yield:** 1%.

**HPLC-PDA and ESI(+)-MS characterisation**

- **Column:** SunFire™ C18 reversed-phase analytical column (3.5 μm x 4.6 mm x 100 mm) linear gradients (0% to 100%) of ACN over 8 min, with a flow rate of 1.0 mL/min.
- **t<sub>R</sub>** = 6.02 min.
- **Purity** (λ = 220 nm) = 95%.
- **ESI(+)-MS** calculated for C<sub>110</sub>H<sub>176</sub>N<sub>26</sub>O<sub>28</sub>S<sub>2</sub> 2374.3, found [((M + 2H)<sup>2+</sup>)/2] 1188.2 and [((M + 3H)<sup>3+</sup>)/3] 792.7.



### 3.3.7.5 Preparation of single HMSP (i,i+4) with the amidated C-terminus

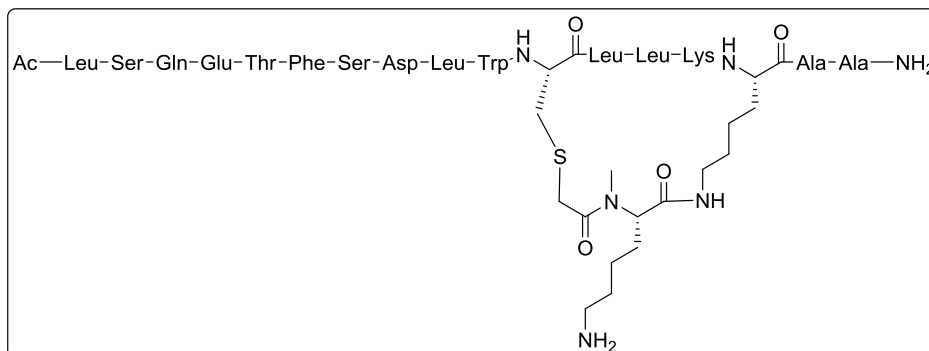
#### Synthetic protocol

The Rink amide AM resin (commercial functionalisation: 0.14 mmol/g resin) was placed in a 2 mL-polypropylene syringe fitted with two polyethylene filter discs. *Conditioning* of the resin and *incorporation of the first amino acid* was carried out by standard means. Generally, *Protocol Pep1* and *Protocol Pep2* were used for peptide couplings onto primary and secondary amines, respectively. Fmoc removal was accomplished following *Protocol Fmoc1*. A Lys residue was introduced at relative position *i*, conveniently protected with the Dde group, which is orthogonal to the Fmoc group. Four positions further from the Lys residue, a Cys residue was placed. After the linear chain elongation was furnished, *N*-terminal amine acetylation was accomplished following *Protocol Ac1*. Next, Dde group removal was achieved following *Protocol Dde*.

*Construction of the N-methyl-rich peptide bridge* was carried out following *Strategy B* (section 3.3.4). Next, bromoacetic acid was incorporated following *Protocol Pep3*.

*Peptide cleavage and global deprotection* was accomplished following *Protocol Cle2*. *Cyclisation in solution* through a thioether-based cross-linking approach was accomplished following *Protocol Cyc2*. Finally, the crude peptide was subjected to HPLC purification.

**Peptide 2.49**

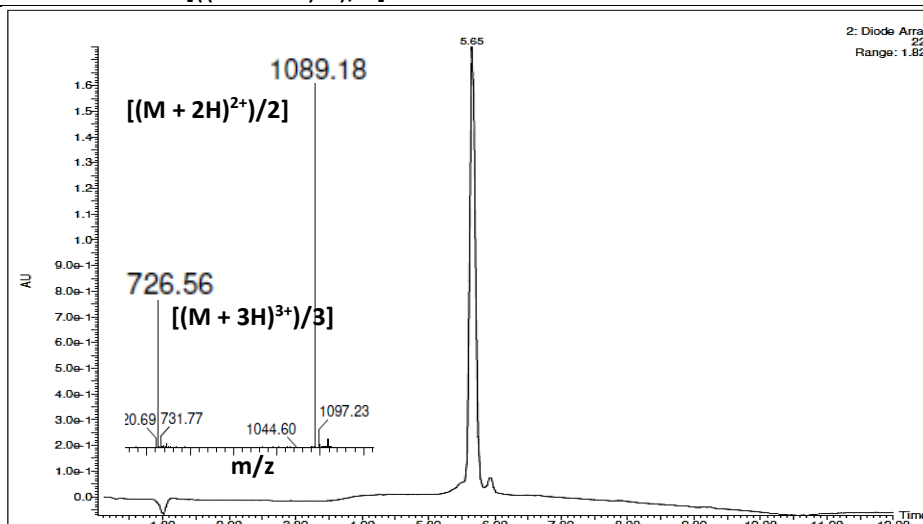


**HPLC purification conditions and yield**

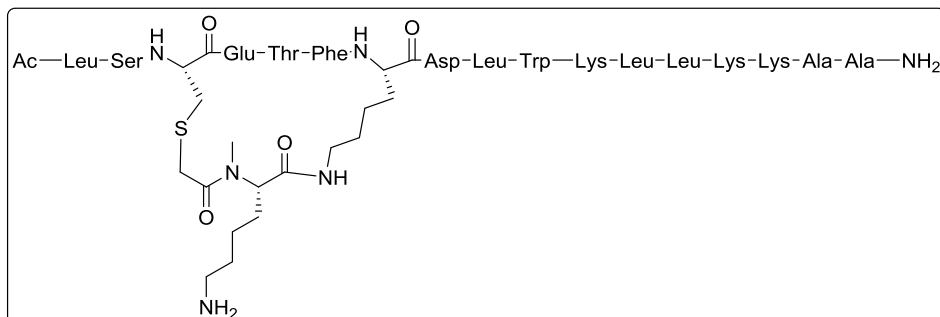
- **Column:** XBridge™ Peptide BEH C18 Prep reversed-phase 130Å column (5 µm x 10 mm x 100 mm).
- **Gradient:** Linear gradient (20% to 40% over 5 min and 40% to 45% over 15 min) of ACN, with a flow rate of 2.0 mL/min.
- **Quantity:** 3 mg.
- **Yield:** 2%.

**HPLC-PDA and ESI(+)-MS characterisation**

- **Column:** XBridge™ C18 reversed-phase analytical column (3.5 µm x 4.6 mm x 42 mm) linear gradients (0% to 100%) of ACN over 8 min, with a flow rate of 1.0 mL/min.
- **t<sub>R</sub>** = 5.65 min.
- **Purity** (λ = 220 nm) = 93%.
- **ESI(+)-MS** calculated for C<sub>100</sub>H<sub>158</sub>N<sub>24</sub>O<sub>28</sub>S 2176.1, found [((M + 2H)<sup>2+</sup>)/2] 1089.2 and [((M + 3H)<sup>3+</sup>)/3] 726.6.



## Peptide 2.50

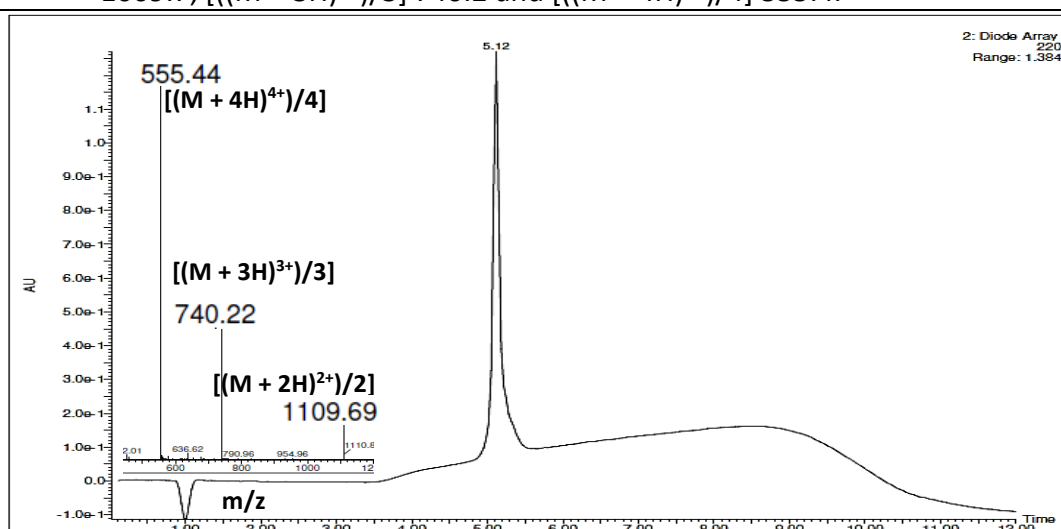


## HPLC purification conditions and yield

- **Column:** XBridge™ Peptide BEH C18 Prep reversed-phase 130Å column (5 μm x 10 mm x 100 mm).
- **Gradient:** Linear gradient (20% to 40% over 5 min and 40% to 50% over 15 min) of ACN, with a flow rate of 2.0 mL/min.
- **Quantity:** 3 mg.
- **Yield:** 2%.

## HPLC-PDA and ESI(+)-MS characterisation

- **Column:** XBridge™ C18 reversed-phase analytical column (3.5 μm x 4.6 mm x 42 mm) linear gradients (0% to 100%) of ACN over 8 min, with a flow rate of 1.0 mL/min.
- **t<sub>R</sub>** = 5.12 min.
- **Purity** (λ = 220 nm) = 96%.
- **ESI(+)-MS** calculated for C<sub>104</sub>H<sub>169</sub>N<sub>25</sub>O<sub>26</sub>S 2217.2, found [((M + 2H)<sup>2+</sup>)/2] 1109.7, [((M + 3H)<sup>3+</sup>)/3] 740.2 and [((M + 4H)<sup>4+</sup>)/4] 555.4.



### 3.3.7.6 Preparation of linear p53-based peptides

The Rink amide AM resin (commercial functionalisation: 0.74 mmol/g resin) was placed in a 2 mL-polypropylene syringe fitted with two polyethylene filter discs. *Conditioning* of the resin and *incorporation of the first amino acid* was carried out by standard means.

Generally, *Protocol Pep1 and Protocol Pep2* were used for peptide couplings onto primary and secondary amines, respectively. Fmoc removal was accomplished following *Protocol Fmoc1*. After the linear chain elongation was furnished, *N-terminal amine acetylation* was accomplished following *Protocol Ac1*.

*Peptide cleavage and global deprotection* was accomplished following *Protocol Cle2*, and the crude peptide was subjected to HPLC purification.

## Peptide 2.51

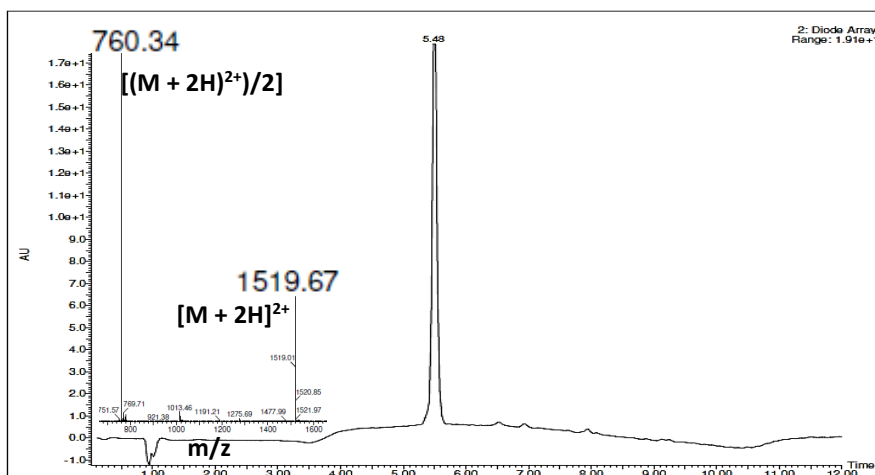
Ac–Glu–Thr–Phe–Ser–Asp–Leu–Trp–Lys–Leu–Leu–Pro–Glu–NH<sub>2</sub>

### HPLC purification conditions and yield

- **Column:** XBridge™ Peptide BEH C18 Prep reversed-phase 130Å column (5 μm x 10 mm x 100 mm).
- **Gradient:** Linear gradient (20% to 40% over 5 min and 40% to 50% over 15 min) of ACN, with a flow rate of 2.0 mL/min.
- **Quantity:** 16 mg.
- **Yield:** 42%.

### HPLC-PDA and ESI(+)-MS characterisation

- **Column:** XBridge™ C18 reversed-phase analytical column (3.5 μm x 4.6 mm x 42 mm) linear gradients (0% to 100%) of ACN over 8 min, with a flow rate of 1.0 mL/min.
- **t<sub>R</sub>** = 5.48 min.
- **Purity** (λ = 220 nm) = 97%.
- **ESI(+)-MS** calculated for C<sub>72</sub>H<sub>107</sub>N<sub>15</sub>O<sub>21</sub> 1517.8, found [(M + 2H)]<sup>2+</sup> 1519.7 and [((M + 2H)<sup>2+</sup>)/2] 760.3.



**Peptide 2.52**



| HPLC purification conditions and yield  |
|---|
| <ul style="list-style-type: none"> <li>- <b>Column:</b> XBridge™ Peptide BEH C18 Prep reversed-phase 130Å column (5 µm x 10 mm x 100 mm).</li> <li>- <b>Gradient:</b> Linear gradient (20% to 40% over 5 min and 40% to 45% over 15 min) of ACN, with a flow rate of 2.0 mL/min.</li> <li>- <b>Quantity:</b> 45 mg.</li> <li>- <b>Yield:</b> 80%.</li> </ul>  |
| HPLC-PDA and ESI(+)-MS characterisation   |
| <ul style="list-style-type: none"> <li>- <b>Column:</b> XBridge™ C18 reversed-phase analytical column (3.5 µm x 4.6 mm x 42 mm) linear gradients (0% to 100%) of ACN over 8 min, with a flow rate of 1.0 mL/min.</li> <li>- <b>t<sub>R</sub></b> = 5.35 min.</li> <li>- <b>Purity</b> (λ = 220 nm) = 100%.</li> <li>- <b>ESI(+)-MS</b> calculated for C<sub>76</sub>H<sub>113</sub>N<sub>17</sub>O<sub>23</sub> 1631.8, found [M + 2H]<sup>2+</sup> 1633.8 and <math>[(M + 2H)^{2+}]/2</math> 817.4.</li> </ul> |
|   |

## Peptide 2.53

Ac-Leu-Ser-Gln-Glu-Thr-Phe-Ser-Asp-Leu-Trp-Lys-Leu-Leu-Pro-Glu-Asn-Ala-NH<sub>2</sub>

## HPLC purification conditions and yield

- **Column:** XBridge™ Peptide BEH C18 Prep reversed-phase 130Å column (5 μm x 10 mm x 100 mm).
- **Gradient:** Linear gradient (20% to 40% over 5 min and 40% to 45% over 15 min) of ACN, with a flow rate of 2.0 mL/min.
- **Quantity:** 36 mg.
- **Yield:** 54%.

## HPLC-PDA and ESI(+)-MS characterisation

- **Column:** XBridge™ C18 reversed-phase analytical column (3.5 μm x 4.6 mm x 42 mm) linear gradients (0% to 100%) of ACN over 8 min, with a flow rate of 1.0 mL/min.
- **t<sub>R</sub>** = 5.52 min.
- **Purity** (λ = 220 nm) = 100%.
- **ESI(+)-MS** calculated for C<sub>93</sub>H<sub>142</sub>N<sub>22</sub>O<sub>29</sub> 2032.1, found [((M + 2H)<sup>2+</sup>)/2] 1017.0 and [((M + 3H)<sup>3+</sup>)/3] 678.4.

